Synthese modifizierter Thiostannate: Integration von Übergangsmetallkationen durch Verwendung aromatischer und cyclischer Aminmoleküle

Sowie die Entwicklung alternativer Synthesewege

zur Darstellung von Thiostannaten

bei Raumtemperatur

Kumulative Dissertation

zur Erlangung des Doktorgrades

der Mathematisch-Naturwissenschaftlichen Fakultät

der Christian-Albrechts-Universität

zu Kiel

vorgelegt von

Jessica Hilbert

Kiel

2016

Referent: Prof. Dr. Wolfgang Bensch

Korreferent: Prof. Dr. Christian Näther

Tag der mündlichen Prüfung: 07.12.2016

Zum Druck genehmigt: Kiel, 07.12.2016

Prof. Dr. N. Oppelt, Dekanin

Synthese modifizierter Thiostannate: Integration von Übergangsmetallkationen durch Verwendung aromatischer und cyclischer Aminmoleküle

Sowie die Entwicklung alternativer Synthesewege zur Darstellung von Thiostannaten bei Raumtemperatur

Die wesentlichen Ziele dieser Arbeit waren die Darstellung und Charakterisierung neuer übergangsmetallhaltiger Thiostannate, in denen eine kovalente Bindung zwischen dem ladungsneutralisierenden Übergangsmetallkomplex und dem Thiostannat vorliegt. Aromatische und cyclische Aminmoleküle wie 1,10-Phenanthrolin (phen), 2,2-Bipyridin (2,2'-bipy) oder 1,4,8,11-Tetraazacyclotetradecan (cyclam) wurden ausgewählt, da diese spezielle Molekülstrukturen und elektronische Eigenschaften aufweisen, die eine kovalente Bindung zwischen dem Übergangsmetallkation und dem Thiostannation ermöglichen sollten. Diese Amine sind Feststoffe, so dass eine Modifizierung der üblichen solvothermalen Syntheseroute erforderlich war. Bei einer neuen Syntheseroute wurde schwach koordinierendes Methylamin als „Hilfsamin" eingesetzt. Mit dieser Syntheseroute konnten vierzehn neue Verbindungen erhalten werden, in deren Strukturen das Übergangsmetallkation kovalent an die Thiostannateinheit gebunden ist. Mit 1,10-Phenanthrolin konnten dreizehn neue Verbindungen synthetisiert werden. Acht dieser Verbindungen mit der allgemeinen Formel $\{[TM(phen)_2]_2[Sn_2S_6]\}\cdot x$phen$\cdot x H_2O$ (TM = Mn, Fe, Co; x = 0 bzw. 1) weisen in den Strukturen $\pi-\pi$-Wechselwirkungen zwischen den aromatischen Liganden auf, was zu einer Stabilisierung der Anordnung der Baueinheiten führt. Das $[Sn_2S_6]^{4-}$-Anion fungiert als verbrückende Einheit, bei der alle vier terminalen S^{2-}-Anionen in Bindungen involviert sind und zwei TM(II)-Komplexe verknüpfen. Dieser spezielle Bindungsmodus des $[Sn_2S_6]^{4-}$-Anions wurde in diesen Verbindungen zum ersten Mal beobachtet. In der Verbindung $\{[Mn(phen)_2]_2[Mn(phen)]_2[SnS_4]_2]\}$ wird das seltenere $[SnS_4]^{4-}$-Anion gefunden, welches mit seinen vier S^{2-}-Anionen in Bindungen zu drei Mn^{2+} Zentren involviert ist. Dies ist ein Bindungsmodus der bisher noch nie beobachtet wurde. Verbindungen mit Ni^{2+} konnten erst mit aromatischen Additiven wie 2,2'-Bipyridin, 4,4'-Biypridin oder Biphenyl, synthetisiert werden. Mit dem cyclischen Molekül cyclam konnte mit $\{[Ni(cyclam)]_2[SnS_2S_6]\}_n\cdot n H_2O$ eine der wenigen zweidimensionalen Verbindungen dieser Verbindungsklasse kristallisiert und charakterisiert werden.

Die Verbindung $\{[Ni(tren)]_2[Sn_2S_6]\}_n$ (tren = Tris(2-aminoethyl)amin) hat sich als geeigneter Precursor für die Synthese von weiteren Thiostannaten erwiesen. Ein ungewöhnliches strukturelles Merkmal stellt ein $Ni_2N_8S_4$-Bioktaeder dar, dessen Ni-S-Bindungen unterschiedlich stark sind und bei der Zugabe eines Amins geöffnet werden. Die freien Koordinationsstellen am Ni^{2+}-Kation werden durch N-Donoratome besetzt. Mit diesem Precursor konnten vier neue Verbindungen mit der allgemeinen Formel $[Ni(tren)(Amin)]_2[Sn_2S_6]\cdot x H_2O$ sowie zwei weiteren Verbindungen mit der allgemeinen Formel

$[Ni(Amin)_3]_2[Sn_2S_6]\cdot xH_2O$ synthetisiert werden. Besonders hervorzuheben ist, dass die Synthesen bei Raumtemperatur durchgeführt wurden.

Als Precursoren wurden auch (wasser)lösliche Verbindungen wie $[Ni(tren)(H_2O)Cl]Cl$ bzw. Komplexe der allgemeinen Formel $[Ni(Amin)_3]^{2+}$ (Amin = bidentates Amin) sowie $Na_4SnS_4\cdot 14H_2O$ verwendet. Mit diesen Edukten konnte eine Syntheseroute entwickelt werden, mit der Thiostannate bei Raumtemperatur in wässriger Lösung darstellbar sind. Diese neue Syntheseroute verringert den experimentellen Aufwand, es steht eine Art Baukastensystem zur Darstellung neuer Verbindungen zu Verfügung. Mit diesem synthetischen Vorgehen konnten sieben neue Verbindungen mit der allgemeinen Formel $[Ni(tren)(Amin)]_2[Sn_2S_6]\cdot xH_2O$ bzw. $[Ni(Amin)_3]_2[Sn_2S_6]\cdot xH_2O$ sowie fünf weitere, bereits bekannte Verbindungen erhalten werden. Alle Verbindungen kristallisierten bei Raumtemperatur innerhalb von 1-3 Tagen.

Synthesis of Modified Thiostannates: Integration of Transition Metal Cations by Usage of Aromatic and Cyclic Amine Molecules

Together with the Development of an Alternative Synthesis Route for the Formation of Thiostannates at Room Temperature

The principal aims of this work were the preparation and characterization of new transition metal containing thiostannates, which exhibit a covalent bond between the cation of the charge compensating complex and the thiostannate unit. Aromatic and cyclic amines like 1,10-phenathroline (phen), 2,2'-bipyridine (2,2'-bipy) or 1,4,8,11-tetraazacyclotetradecane (cyclam) were chosen, because of their special molecular structure and electronic properties, which should enable a covalent bond between the transition metal cation and the thiostannate ion. These amines are solids and therefore a modification of the standard solvothermal synthesis route was necessary. For establishing a new synthesis route the weak coordinating methylamine was applied as "supporting amine". With this synthesis route fourteen new compounds could be obtained. In all crystal structures the transition metal cation is covalently joined to the thiostannate unit. Applying the 1,10-phenanthroline, thirteen new compounds could be synthesized. Eight of these compounds with the general formula $\{[TM(phen)_2]_2[Sn_2S_6]\}\cdot x\text{phen}\cdot x H_2O$ (TM = Mn, Fe, Co; x = 0 or 1) feature π-π interactions between the aromatic ligands in the structures, which stabilize the arrangement of the building units. The $[Sn_2S_6]^{4-}$ anion acts as a bridging unit, whereat all terminal S^{2-} anions are involved in bonds and linking two TM(II) complexes. This special connection mode of the $[Sn_2S_6]^{4-}$ unit has been observed in these compounds for the first time. The compound $\{[Mn(phen)_2]_2[Mn(phen)]_2[SnS_4]_2]\}$ features the less common $[SnS_4]^{4-}$ anion, which is involved with the four S^{2-} anions in bonds towards three Mn^{2+} centers. This is also a connection mode never observed before. Compounds with Ni^{2+} could only be synthesized by the usage of aromatic additives like 2,2'-bipyridine, 4,4'-bipyridine or biphenyl. By applying the cyclic molecule cyclam the compound $\{[Ni(cyclam)]_2[Sn_2S_6]\}_n\cdot n H_2O$ crystallized, exhibiting a rare two dimensional structure.

The compound $\{[Ni(tren)]_2[Sn_2S_6]\}_n$ (tren = tris(2-aminoethyl)amine) proved to be a suitable precursor for the formation of further thiostannates. An uncommon structural characteristic is the presence of a $Ni_2N_8S_4$ bi-octahedron, with Ni-S bonds differing in strength and these bonds are opened by addition of a further amine molecules. The free coordination sites at the Ni^{2+} cation are occupied by N donor atoms. With this precursor four new compounds with the general formula $[Ni(tren)(amine)]_2[Sn_2S_6]\cdot x H_2O$ as well as two further compounds with the general formula $[Ni(amine)_3]_2[Sn_2S_6]\cdot x H_2O$ could be obtained. Remarkable in this case is, that all syntheses were performed at room temperature.

In further syntheses, (water)soluble compounds like $[Ni(tren)(H_2O)Cl]Cl$ or complexes with the general formula $[Ni(amine)_3]^{2+}$ (amine = bidentate amine) and $Na_4SnS_4\cdot 14H_2O$ were applied. With the use of these educts a new synthesis route was developed for the formation of thiostannates at room temperature in aqueous solution. This new synthesis route reduces the

experimental efforts and delivers a construction kit for the formation of new compounds. Following this approach seven new compounds with the general formula $[Ni(tren)(amine)]_2[Sn_2S_6]\cdot xH_2O$ or $[Ni(amine)_3]_2[Sn_2S_6]\cdot xH_2O$ and five further, already known, compounds could be obtained. All compounds crystallized at room temperature within 1-3 days.

Inhaltsverzeichnis

1. Einleitung 1
1.1 Motivation 1
1.2 Wissenschaftlicher Hintergrund 2
1.2.1 Thiostannate 2
1.2.2 Solvothermalsynthese 6
1.3 Zielsetzungen der Arbeit 7
1.3.1 Verwendung aromatischer und cyclischer Amine 7
1.3.2 Verwendung vorgefertigter Baueinheiten 8
1.3.3 Alternative Syntheserouten 8
2. Experimenteller Teil 10
2.1 Synthesemethoden 10
2.1.1 Solvothermale Synthesen 10
2.1.2 Synthesen bei Raumtemperatur 10
2.2 Verwendete Chemikalien und Abkürzungen 12
2.3 Synthese der TM-Amin-Komplexe und $Na_4SnS_4 \cdot 14H_2O$ 14
2.4 Verwendete Untersuchungsmethoden 15
3. Ergebnisse & Diskussion 16
3.1 Publikationen der solvothermalen Synthese übergangsmetallhaltiger Zinn-Schwefel-Verbindungen (kumulativer Hauptteil, Teil 1) 16
3.1.1 Solvothermale Synthese fünf manganhaltiger Thiostannate mit 1,10-Phenanthrolin: Untersuchung des Einflusses verschiedener Reaktionsparameter auf die Produktbildung. 17
3.1.2 Synthese der Verbindungen $\{[TM(phen)_2]_2[Sn_2S_6]\}$ und $\{[TM(phen)_2]_2[Sn_2S_6]\} \cdot phen \cdot H_2O$ (TM = Fe, Co) unter solvothermalen Bedingungen. 31
3.1.3 Solvothermale Synthese der Verbindungen $\{[Ni(phen)_2]_2[Sn_2S_6]\}$·2,2'-bipy und $\{[Ni(phen)_2]_2[Sn_2S_6]\}$·4,4'-bipy ½$H_2O$ 38
3.1.4 Erfolgreiche Verknüpfung von TM-Amin-Komplexen mit dem Thiostannatanion durch Verwendung ausgewählter Aminmoleküle *(accepted 24.10.16)* 48
3.1.5 $\{[Ni(1,2\text{-dach})(ma)]_4[Sn_{10}S_{20}O_4]\}$, Synthese der seltenen $[Sn_{10}S_{20}O_4]^{8-}$-Einheit mit direkter Verknüpfung zum ladungsausgleichenden Komplex. *(submitted 10.10.16)* 56
3.2 Publikationen zur Synthese übergangsmetallhaltiger Thiostannate mit Precursoren bei Raumtemperatur (kumulativer Hauptteil, Teil 2) 64
3.2.1 Verwendung der Verbindung $\{[Ni(tren)]_2[Sn_2S_6]\}_n$ als Precursor zur Darstellung von Thiostannaten bei Raumtemperatur 65
3.2.2 Reaktion von $\{[Ni(tren)]_2[Sn_2S_6]\}_n$ mit tren und 2amp bei RT zu zwei weiteren Thiostannaten: Untersuchung der temperaturabhängigen Stabilität des Precursors und der Verbindungen $[Ni(tren)_2]_2[Sn_2S_6] \cdot 8H_2O$ und $[Ni(tren)(2amp)]_2[Sn_2S_6]$. *(submitted 03.11.16)* 73

3.3 weitere Ergebnisse – Synthesen mit vorgefertigten Komplexen und Thiostannat-Einheiten 94

3.3.1 Systematische Untersuchungen der chemischen Reaktivität von $Na_4SnS_4 \cdot 14H_2O$ und $[Mn(phen)_3][ClO_4]_2$ und der Synthesen mit diesen Edukten 96

3.3.1.1 Untersuchungen zum Verhalten von $Na_4SnS_4 \cdot 14H_2O$ in wässriger Lösung bei Zugabe von HCl. 96

3.3.1.2 Löslichkeitsversuche mit $[Mn(phen)_3][ClO_4]_2$ und $Na_4SnS_4 \cdot 14H_2O$ 98

3.3.1.3 Synthesen mit $[Mn(phen)_3][ClO_4]_2$ und $Na_4SnS_4 \cdot 14H_2O$ 98

3.3.2 Synthesen von Thiostannaten bei RT bei Verwendung von $[Ni(Amin)_3]^{2+}$-Komplexen und $Na_4SnS_4 \cdot 14H_2O$ 100

3.3.2.1 Die neuen Verbindungen $[Ni(tren)(en)]_2[Sn_2S_6] \cdot xH_2O$ (x =2 bzw. 6) 101

3.3.2.2 Die neuen Verbindungen $[Ni(tren)(1,2\text{-dach})]_2[Sn_2S_6] \cdot xH_2O$ (x =3 bzw. 4) 103

3.3.2.3 Die neue Verbindung $[Ni(tren)(1,2\text{-dap})]_2[Sn_2S_6] \cdot 4H_2O$ 105

3.3.2.4 Die neue Verbindung $[Ni(tren)(2amp)]_2[Sn_2S_6] \cdot 10H_2O$ 106

3.3.2.5 Spektroskopische Untersuchungen der neuen Verbindungen 107

3.3.3 Synthesen mit weiteren $[TM(Amin)_n]Cl_2$- bzw. $[TM(Amin)_n][ClO_4]_2$- Komplexen und Na_4SnS_4 $14H_2O$ bei RT 109

3.3.3.1 Die neue Verbindung $[Ni(2amp)_3]_2[Sn_2S_6] \cdot 9.5H_2O$ 110

4. Zusammenfassung und Ausblick 115

4.1 Solvothermale Synthesen mit festen Aminen unter Verwendung von Hilfsaminen ... 115

4.2 Synthesen mit dem Precursor $\{[Ni(tren)]_2[Sn_2S_6]\}_n$ bei Raumtemperatur 117

4.3 Synthesen mit $[TM(Amin)_n]Cl_2$ bzw. $[TM(Amin)_n][ClO_4]_2$ und Na_4SnS_4 $14H_2O$ bei Raumtemperatur 117

5. Anhang 118

5.1 Publikationsliste 118

5.1.1 Publikationen 118

5.1.2 Posterbeiträge und Präsentationen 119

5.2 Supporting Information (SI) 120

5.2.1 SI für die Publikation: “Influence of the Synthesis Parameters onto Nucleation and Crystallization of Five New Tin-Sulfur Containing Compounds” 120

5.2.2 SI für die Publikation: “Utilization of Mixtures of Aromatic N-donor Ligands of Different Coordination Ability for the Solvothermal Synthesis of Thiostannate Containing Molecules” .. 137

5.2.3 SI für die Publikation:“ Room temperature synthesis of thiostannates from $\{[Ni(tren)]_2[Sn_2S_6]\}_n$” 144

5.2.4 SI für die Publikation: “Transition Metal Complexes with Linkage to the Thiostannate Units Forced by Suitable Amine Molecules” 162

5.2.5 SI für die Publikation: “$\{[Ni(1,2\text{-dach})_2(ma)]_4[Sn_{10}S_{20}O_4]\}$ – An Example of the Rare Tin-Oxo-Sulfide Cluster with Uncommon Connection Mode Towards a Charge Compensating Ni(II) Complex” 185

5.2.6 SI für die Publikation: “Studies of the Reactivity of {[Ni(tren)]$_2$[Sn_2S_6]}$_n$: Synthesis and Crystal Structure of two New Thiostannates at Room Temperature” 191
5.3 Strukturdaten / Messprotokolle 212
5.3.1 Messprotokoll der Verbindung {[Mn(phen)$_2$]$_2$[Sn_2S_6]} 212
5.3.2 Messprotokoll der Verbindung {[Mn(phen)$_2$]$_2$[Sn_2S_6]} 218
5.3.3 Messprotokoll der Verbindung {[Mn(phen)$_2$]$_2$[Sn_2S_6]}·phen 223
5.3.4 Messprotokoll der Verbindung {[Mn(phen)$_2$]$_2$[Sn_2S_6]}·phen·H_2O 230
5.3.5 Messprotokoll der Verbindung {[Mn(phen)$_2$]$_2$[SnS_4]$_2$[Mn(phen)$_2$}·H_2O 236
5.3.6 Messprotokoll der Verbindung {[Fe(phen)$_2$]$_2$[Sn_2S_6]} 243
5.3.7 Messprotokoll der Verbindung {[Fe(phen)$_2$]$_2$[Sn_2S_6]}·phen·H_2O 248
5.3.8 Messprotokoll der Verbindung {[Co(phen)$_2$]$_2$[Sn_2S_6]} 254
5.3.9 Messprotokoll der Verbindung {[Co(phen)$_2$]$_2$[Sn_2S_6]}·phen·H_2O 259
5.3.10 Messprotokoll der Verbindung {[Ni(phen)$_2$]$_2$[Sn_2S_6]}·2,2’-bipy 265
5.3.11 Messprotokoll der Verbindung {[Ni(phen)$_2$]$_2$[Sn_2S_6]}·4,4’bipy·½H_2O 271
5.3.12 Messprotokoll der Verbindung [Ni(tren)(ma)(H_2O)]$_2$[Sn_2S_6]·4H_2O 277
5.3.13 Messprotokoll der Verbindung [Ni(1,2dap)(tren)]$_2$[Sn_2S_6]·2H_2O 281
5.3.14 Messprotokoll der Verbindung {[Ni(phen)$_2$]$_2$[Sn_2S_6]}·biph 287
5.3.15 Messprotokoll der Verbindung {[Ni(phen)$_2$]$_2$[Sn_2S_6]}·phen·H_2O 293
5.3.16 Messprotokoll der Verbindung {[Ni(cyclam)]$_2$[Sn_2S_6]}$_n$·2*n*H_2O 299
5.3.17 Messprotokoll der Verbindung {[Mn(bipy)$_2$]$_2$[Sn_2S_6]} 304
5.3.18 Messprotokoll der Verbindung {[Ni(1,2dach)$_2$(ma)]$_4$[$Sn_{10}S_{20}O_4$]} 309
5.3.19 Messprotokoll der Verbindung [Ni(tren)$_2$]$_2$[Sn_2S_6]·8H_2O 315
5.3.20 Messprotokoll der Verbindung [Ni(2amp)(tren)]$_2$[Sn_2S_6] 321
5.3.21 Messprotokoll der Verbindung [Ni(en)(tren)]$_2$[Sn_2S_6]·2H_2O 328
5.3.22 Messprotokoll der Verbindung [Ni(en)(tren)]$_2$[Sn_2S_6]·6H_2O 333
5.3.23 Messprotokoll der Verbindung [Ni(1,2dach)(tren)]$_2$[Sn_2S_6]·3H_2O 339
5.3.24 Messprotokoll der Verbindung [Ni(1,2dach)(tren)]$_2$[Sn_2S_6]·4H_2O 345
5.3.25 Messprotokoll der Verbindung [Ni(1,2dap)(tren)]$_2$[Sn_2S_6]·4H_2O 352
5.3.26 Messprotokoll der Verbindung [Ni(2amp)(tren)]$_2$[Sn_2S_6]·10H_2O 358
5.3.27 Messprotokoll der Verbindung [Ni(2amp)$_3$]$_2$[Sn_2S_6]·9½ H_2O 364
5.4 Hintergrundinformationen zu Kap. 3.3.1 373
5.5 Hintergrundinformationen zu Kap. 3.3.2 375
5.6 Hintergrundinformationen zu Kap. 3.3.3 381
5.7 Acta E Publikationen 384
5.7.1 Crystal structure of tris(N-methylsalicylaldiminato-κ^2N,O)vanadium(III) 384
5.7.2 Crystal structure of tris(N-methylsalicylaldiminato-κ^2N,O)chromium(III) 393

6. Danksagung 403
7. Eidesstattliche Erklärung 404
8. Literaturverzeichnis 405

1. Einleitung

1.1 Motivation

1989 postulierte die Arbeitsgruppe um Bedard et. al., dass die Zukunft der kristallinen mikroporösen Materialien auf Hauptgruppenmetallsulfiden basieren wird.[1] Ausgang für diese Annahme war die Synthese von Germanium(IV)- bzw. Zinn(IV)sulfid Netzwerkstrukturen unter hydrothermalen Bedingungen in Anwesenheit von organischen strukturdirigierenden Molekülen.[1] Alle vorher beschriebenen mikroporösen Materialien basierten auf oxidischen Baueinheiten, hauptsächlich mit den Elementen Si und Al.[1] Eine wenig zur Kenntnis genommene Beobachtung ist, dass natürliche sulfidische Mineralien sowohl bei der chemischen Zusammensetzung als auch bei der Koordinationschemie gegenüber den Oxiden eine deutlich größere Vielfalt aufweisen. Sowohl Hauptgruppen- als auch Übergangsmetallionen (transition metal = TM) werden oft mit Sulfidanionen in tetraedrischer Umgebung gefunden. Tetraeder stellen die Grundbaueinheit der mikroporösen Strukturen in Feststoffen dar, werden aber auch in Lösung gefunden.[1,2] Die Koordinationsgeometrie der Sulfide unterscheidet sich deutlich von der der Oxide: Ein typischer M-S-M (M = Metall) Winkel liegt in dem schmalen Bereich von 105-115° und ist deutlich näher am idealen Tetraederwinkel von 109°, während M-O-M Winkel mit 140-150° eine signifikante Abweichung aufweisen.[3–5] Die beiden Ionen Ge^{4+} und Sn^{4+} liegen in sulfidischer Umgebung oft tetraedrisch vor und könnten in mikroporösen Materialien Al^{3+} bzw. Si^{4+} ersetzen. Mikroporöse Materialien auf Basis von Ge/Sn könnten dann die typischen (Ionen)austausch- und katalytischen Eigenschaften der Zeolithe mit den Halbleitereigenschaften der Chalkogenide vereinen.[6,7] Letztlich sollte damit die Struktur- und Eigenschaftsvielfalt und somit auch die Einsatzmöglichkeiten sulfidbasierender mikroporöser Materialien deutlich größer sein.[1,6,7] Der Einsatz organischer Moleküle sowie das Einbringen von Übergangsmetallen in das anorganische Netzwerk sollten dazu beitragen diese Vielfalt zu erweitern.[6] Die Hydrothermalsynthese sollte die optimale Syntheseroute darstellen, da die sulfidischen Baueinheiten auch in (wässrigen) Lösungen gebildet werden und unter diesen Bedingungen kristalline Materialien guter Qualität erhalten werden können.[1,2,8]

Seit diese Überlegungen publiziert wurden sind über 25 Jahre vergangen, Zeit zu rekapitulieren, welche Fortschritte erzielt wurden und in welche Richtung sich die Forschung auf dem Gebiet mikroporöser sulfidischer Verbindungen entwickelt hat.

Die Hydrothermal- oder allg. Solvothermalsynthese hat sich tatsächlich als Methode der Wahl erwiesen: Es konnte eine Vielzahl an sulfidbasierten Verbindungen dargestellt und sowohl organische Moleküle als auch Übergangsmetalle erfolgreich in die anorganischen Netzwerke integriert werden, wie in zahlreichen Übersichtsartikeln zusammengefasst wurde.[2,6,7,9–16] Allerdings wird der Reaktionsverlauf unter solvothermalen Bedingungen von einer Vielzahl von Reaktionsparametern beeinflusst (s. Abschnitt 1.2.2).[8,17–19] Dieser Umstand macht es bisher unmöglich das Ergebnis eines Experimentes vorherzusagen. Neue Verbindungen werden in der Regel auf der Grundlage von Erfahrungswerten, daraus resultierenden

Richtlinien sowie nach dem Prinzip „Versuch-und-Irrtum“ erhalten.[11–15] Besonders nachteilig ist, dass bei den potentiell porösen Netzwerkstrukturen, welche mit Hilfe von strukturdirigierenden organischen Molekülen erhalten wurden, die Strukturdirektoren nicht ohne Kollaps der gesamten Struktur entfernt werden können.[6] Nichts desto trotz konnten Verbindungen mit herausragenden Eigenschaften hergestellt werden. Exemplarisch seien hier $[Sn_3S_7]_n \cdot 2n(NMe_4) \cdot nH_2O$ [20], $[Sn_3S_7]_n \cdot 1.33n(Me_2NH_2) \cdot 0.66n(Me_3NH)$ [21] (Ionenaustausch), $[Sn_3S_7]_n \cdot 2n(dabcoH)$ [22] (Katalyse) und $Na_4In_7Cu_3S_{35} \cdot xH_2O$ [23] (lichtinduzierte Wasserstoffgenerierung) genannt.

Inwieweit besteht noch Forschungsbedarf? Wie bereits erwähnt ist es bisher nicht möglich Produkte einer Solvothermalsynthese vorherzusagen oder Aussagen über die Struktureigenschaftsbeziehungen der erhaltenen Verbindungen zu treffen. Auf diesen Gebieten besteht erheblicher Forschungsbedarf. Das finale Ziel muss sein, Verbindungen geplant und mit bestimmten Eigenschaften darzustellen. Um dieses Ziel zu erreichen, muss die Zahl der umfänglich charakterisierten Verbindungen deutlich vergrößert werden. Aus der Kenntnis der Syntheseparameter, der Kristallstrukturen, chemischen Zusammensetzung und der resultierenden Eigenschaften können eventuell verlässliche Regel abgeleitet werden, welche Produkt- und Eigenschaftsvorhersage erlauben. Allerdings ist es sinnvoll neben der Solvothermalsynthese neue Syntheserouten zu entwickeln und zu verfolgen[11,14,15], da über diese neuen Routen Verbindungen zugänglich sind, welche sonst nicht hergestellt werden können.

1.2 Wissenschaftlicher Hintergrund

1.2.1 Thiostannate

Die Bezeichnung „Thiostannate“ umfasst eine Gruppe von Verbindungen mit der allg. Formel $[A]_x^{m+}[Sn_ySz]^{m-}$ (A = ladungsausgleichende kationische Komponente).[2] Nach der Definition von Krebs ist dieser Begriff auf Verbindungen anwendbar, bei denen „diskrete (auch polymere) $[Sn_yS_z]^{m-}$-Struktureinheiten identifizierbar sind; Kriterien sind signifikant stärkere (und meist stärker kovalente) Sn-S-Bindungen relativ zu (stärker heteropolaren) schwächeren A···S-Bindungen.“[2]

Wie zuvor beschrieben liegt der Vorteil von sulfidischen Verbindungen in der Möglichkeit der Bildung von Tetraedern mit einer Vielzahl an Hauptgruppen- und Übergangsmetallen.[1,2] Durch Kombination von Schwefel mit Ge oder Sn unter solvothermalen Bedingungen sollten so die Eigenschaften von Zeolithen und Hauptgruppenchalkogeniden vereinigt werden können.[6]

Der Vorteil von Thiostannaten gegenüber anderen Thiometallaten liegt in der vielseitigen Koordinationsmöglichkeit der Zinnkationen.[6,17] Eine rein formale Betrachtung des PSE lässt für Sn die Schlussfolgerung zu, dass Koordinationszahlen (coordination number CN) 2 - 9 im Bereich des Möglichen liegen.[6,17] Beobachtet werden bei den Thiostannaten in der Regel CN 4 - 6, größere CN sind möglich, allerdings oft nur durch HT-Synthesen (HT = Hochtemperatur) zugänglich.[2,6] Zusätzlich wird die strukturelle Vielfalt durch die verschiedenen

Oxidationsstufen Sn(II) und Sn(IV) erweitert,[6,17] wobei die höhere Oxidationsstufe in Thiostannaten deutlich häufiger beobachtet wird.[13] Sn(II) weist ein einsames Elektronenpaar auf und ist in der Regel trigonal pyramidal (CN 3) koordiniert, wobei das freie Elektronenpaar die vierte Ecke eines Pseudo-Tetraeders bildet.[9] Für Sn(IV) wird typischerweise CN 4 - 6 gefunden und ist tetraedrisch (CN 4), trigonal bipyramidal (CN 5) sowie oktaedrisch (CN 6) von Schwefelanionen umgeben.[7,17] Die kleinste daraus resultierende Einheit für Sn(IV) ist der $[SnS_4]^{4-}$-Tetraeder. Diese primäre Baueinheit weist eine ausgeprägte Tendenz zur Kondensation auf und durch Verknüpfung über Ecken und Kanten erfolgt die Bildung größerer Einheiten bis hin zu Ketten oder Schichten.[2,12,13] Mit abnehmendem pH-Wert nimmt der Kondensationsgrad kontinuierlich zu.[2,6] Die am häufigsten beobachtete Baueinheit ist der durch Kantenverknüpfung gebildete $[Sn_2S_6]^{4-}$-Bi-Tetraeder.[13] Bekannt sind jedoch auch größerer Baugruppen, wie $[Sn_3S_7]^{2-}$,[22,24–26] $[Sn_4S_9]^{2-}$,[26,27] $[Sn_5S_{12}]^{4-}$,[22,24] $[Sn_3S_9]^{6-}$ [28] oder $[Sn_4S_{10}]^{4-}$ [29] (Abb. 1).

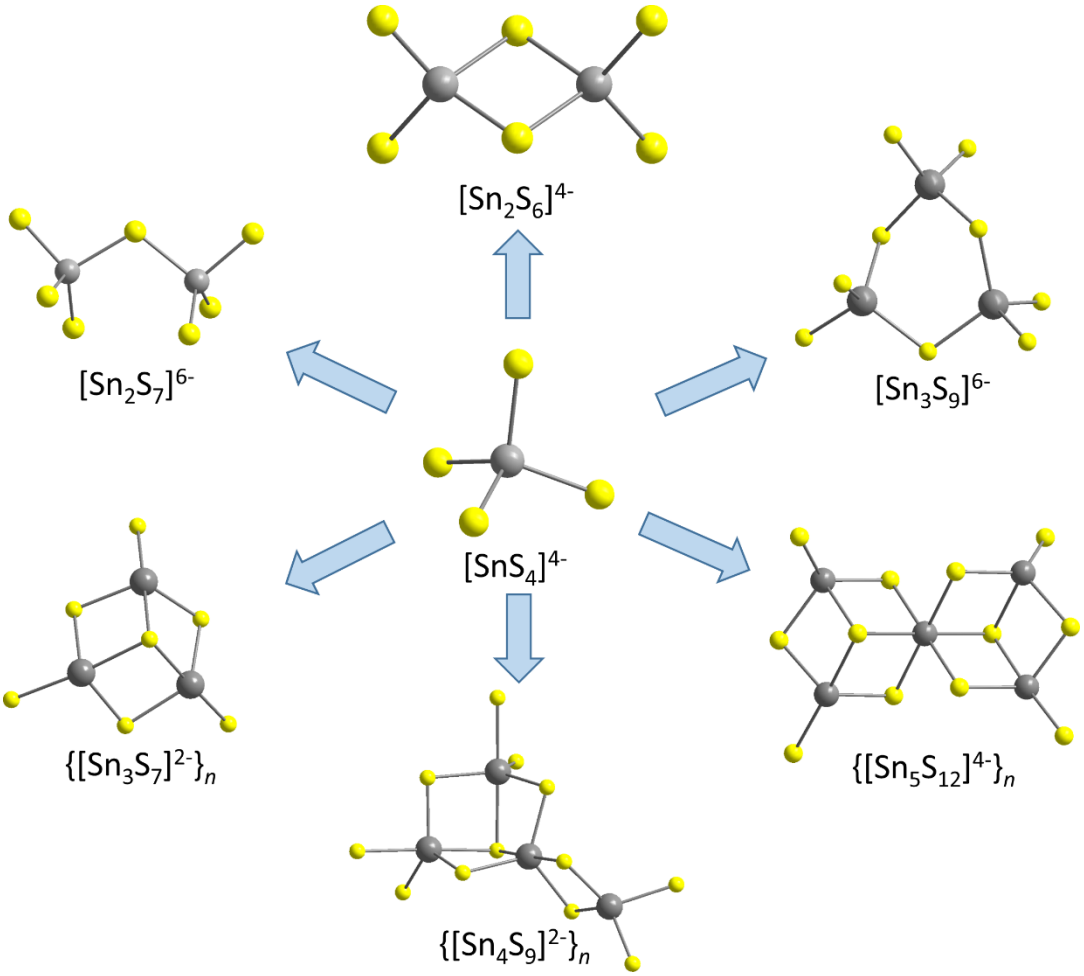

Abbildung 1: Schematische Darstellung der Verknüpfung des $[SnS_4]^{4-}$-Tetraeders zu ausgewählten Thiostannateinheiten.

Größere Baueinheiten sind für Thiostannate nicht bekannt, da mit zunehmender Größe, also steigendem Kondensationsgrad, ebenso die CN des Anions zunimmt.[10] Dies hat zur Folge, dass ein Ladungsausgleich zwischen Anion und Kation, in diesem Fall S(-II) und Sn(IV), nicht ausreichend gewährleistet ist und die entsprechenden Strukturen nicht ausreichend stabil

sind (Pauling's 2. Regel „electrostatic valence rule“).[10] Größere Einheiten mit Sn und S sind so genannte „gefüllte Cluster“ („stuffed clusters“), wie das $[Sn_{10}S_{20}O_4]^{8-}$-Ion, dessen zusätzliche Sauerstoffanionen zum Ladungsausgleich beitragen.[10]

Thiostannate lassen sich je nach Gegenion und weiteren strukturellen Bestandteilen in vier Gruppen einteilen: a) rein anorganische Verbindungen mit anorganischen Kationen, b) anorganisch-organische Hybrid-Verbindungen mit protonierten Aminen als Gegenionen, c) Verbindungen mit integrierten Übergangsmetallkationen und protonierten Aminen als Gegenionen und d) Verbindungen mit $[TM(Amin)_n]^{m+}$ bzw. $[La(Amin)_n]^{m+}$ Komplexen als Gegenionen.[6,7,9,11–13,16] In letzterem Fall können diskrete Anionen und Kationen oder eine direkte Verknüpfung zwischen Übergangsmetallkomplex und Thiostannat-Einheit vorliegen.[13] Bei einer direkten Verknüpfung von Anion und Kation können diese Verbindungen streng genommen nicht mehr als Thiostannate bezeichnet werden (s. Definition oben). Korrekter ist hier die Bezeichnung „übergangsmetallhaltige Zinn-Schwefel-Verbindungen“.[2]

Die ersten Thiostannate waren rein anorganischer Natur. Durch Variation des Kations konnten je nach Größe und Ladung unterschiedliche Strukturen und Tendenzen zur Bildung bestimmter Strukturtypen abgeleitet werden.[6]

Zur Erweiterung der strukturellen Vielfalt wurden Amine eingesetzt, welche in protonierter Form als ladungsausgleichende Komponente [25] und/oder als strukturdirigierendes Molekül agieren.[17] Die Palette der Verbindungen konnte durch Verwendung von Aminmolekülen deutlich erweitert werden, allerdings konnten keine klaren Regeln zur Bildung bestimmter Strukturtypen festgestellt werden: Ein Aminmolekül führt manchmal zu Bildung verschiedener anionischer Strukturen, während eine bestimmte anionische Struktur bei Einsatz verschiedener Amine erhalten wird.[17,30] Diese Verbindungen, wie z.B. $[Et_4N]_{2n}[Sn_3S_7]_n$,[25] $[dabcoH]_{2n}[Sn_3S_7]_n$,[25] $[Me_2NH_2]_{4/3n}[Me_3NH]_{2/3n}[Sn_3S_7]_n \cdot 1.25H_2O$,[21,31] weisen weitere Eigenschaften auf, wie gezielte Adsorption bestimmter Moleküle (CO_2, H_2O, Ar),[25,32] oder die Entfernung von Schwermetallionen (Cs^+, Sr^+, Cd^{2+}, Pb^{2+}, UO_2^{2+}) aus wässrigen Lösungen.[21,31,33] Daher kommen diese Verbindungen u.a. als potentielle Gassensoren sowie mögliche chemoselektive Transistoren in Betracht.[32]

Um die physikalischen Eigenschaften von Thiostannaten zu modifizieren, wurden Übergangsmetallkationen in die Netzwerke integriert. Damit sollten z.B. Ferromagnetismus, Magnetwiderstand, Ferroelektrizität, kombinierte Ionen- und elektrische Leitfähigkeit, sowie Supraleitfähigkeit erzeugt werden.[9] Die Kombination der Thiostannatgerüste mit Übergangsmetallkomplexen (TM-Komplexen) sollte schließlich zu einer Erweiterung der Eigenschaften um elektrische, optische und magnetische Komponenten führen.[12]

Im Folgenden soll auf die letzte Gruppe von Verbindungen näher eingegangen werden. Die Herausforderung bei der Kombination von TM-Komplexen und Thiostannat-Einheiten besteht in der direkten Verknüpfung dieser beiden Bausteine, also einer kovalenten Bindung zwischen dem Übergangsmetallkation und Schwefelanionen. Häufig liegen jedoch diskrete Thiostannate und TM-Komplexkationen vor.[13] Die Analyse dieser Verbindungen erlaubt

einige Tendenzen in Bezug auf das verwendete TM und/oder Aminmolekül abzuleiten, bei denen eine direkte Bindung wahrscheinlicher ist (Tab. 1).

Tabelle 1: Auflistung der Verbindungen mit TM-Komplexen, sortiert nach Übergangsmetall, Aminmolekül und erfolgreicher Integration.

TM	Amine: direkte Bindung	∑	Amine: diskreten Ionen	∑
Mn	en (2x)[34,35], tepa (1x)[36], phen (6x)[37,38], 1,2-dap (2x)[39,40], tren (1x)[41], trien (2x)[42,43], 1,2-dach (2x)[44], 2,2'-bipy (1x)[45]	17	en (2x)[46,47], dien (2x)[39,47]	4
Fe	tepa (1x)[48], 1,2-dach (1x)[45], phen (2x)[49]	3	---	0
Co	tren (1x)[50], tepa (1x)[48], cyclam (1x)[51], phen (2x)[49]	5	en (2x)[46,52], dien (2x)[43,53]	4
Ni	tren (1x)[54], tepa (2x)[43,48], phen (3x)[45,55], cyclam (1x)[45], cyclen (1x)[56], 1,2-dach&ma (1x)[57]	9	en (1x)[50,58], dien (1x)[58], 1,2-dap (1x)[50], 1,2-dach (1x)[43], peha (1x)[43], aepa (1x)[43], tren (1x)[59], tren&ma (1x)[54], tren&en (2x)[60], tren&1,2-dap (2x)[54,60], 2amp (1x)[60], tren&1,2-dach (2x)[60], tren&2amp (2x)[59,60]	17
Cu	---	0	---	0
Zn	tren (1x)[53]	1	en (1x)[46]	1

Aus dieser Auflistung lassen sich folgende Schlussfolgerungen ziehen:
1) Verbindungen mit Mn^{2+} und Ni^{2+} sind deutlich häufiger vertreten als Verbindungen mit Fe^{2+}, Co^{2+} oder Zn^{2+}. Verbindungen mit $Cu^{+/2+}$ sind in dieser Verbindungsklasse nicht bekannt. Dies lässt sich anhand der entscheidend unterschiedlichen Tendenzen der hier aufgeführten Übergangsmetallkationen erklären: a) Mn^{2+} besitzt eine vergleichbare Affinität sowohl zu S^{2-} als auch zu N-Donoren.[11–13,37,61–64] Dabei scheint die Affinität zu N-Donoren deutlich weniger ausgeprägt zu sein als bei den anderen aufgeführten Übergangsmetallkationen.[65–68] Daher ist eine kovalente Bindung eines Mn-Komplexes an die Thiostannat-Einheit wahrscheinlicher. b) Ni^{2+} hat eine deutlich ausgeprägtere Tendenz an N-Donoren als an S^{2-} zu binden und stabile Komplexe zu bilden im Vergleich zu Mn^{2+}, Fe^{2+}, Co^{2+} oder Zn^{2+}.[65,66,69,70] Folglich ist die Bildung isolierter Ni^{2+}-Komplexkationen und Thiostannat-Anionen wahrscheinlicher. c) Bei der Betrachtung der Cu-Komplexe muss die Umgebung berücksichtigt werden: Cu^{2+} bildet theoretisch stabilere Amin-Komplexe als Ni^{2+} [65,66,70,71], in sulfidischer Umgebung wird jedoch nur Cu^{+} beobachtet. Daher muss zwischen Cu^{+}/Cu^{2+}-Komplexen unterschieden werden. Cu^{+} ist deutlich chalkophiler als die anderen TM-Kationen – daher erfolgt hier bevorzugt eine Bindung an Sulfidanionen.[11–13] Daher wird mit Ag^{+} sowie Cu^{+} eine Integration des TM-Kations in die Thiostannat-Einheit beobachtet und (protonierte) Amine liegen als isolierte Einheiten vor.[72–76]

2) Nicht nur das Übergangsmetallkation, sondern auch das Aminmolekül hat einen Einfluss auf eine Bindung des TM-Komplexes an S^{2-}: a) Bei der Verwendung von tetra- oder pentadentaten Aminmolekülen (z.B. tren (= Tris-(2-Aminoethyl)amin), tepa (= Tetraethylenpentamin), cyclam (= 1,4,8,11-Tetraazacylotetradecan) oder cyclen (= 1,4,7,10-Tetraazacyclodecan)), welche die Koordinationssphäre am Übergangsmetallkation nicht vollständig sättigen können, ist eine Besetzung der freien Koordinationsstellen durch kovalente Bindung an S^{2-} der Thiostannat-Einheit sehr wahrscheinlich.[43,45,48,50,51,56] Bei der Verwendung von Ni^{2+} kann allerdings die Tendenz, der Bindung zu N-Donoren, so ausgeprägt sein, dass bei Überschuss des Amins (z.B. tren) die vollständige Absättigung der Koordinationssphäre durch N-Atome bevorzugt gegenüber einer Bindung zu S^{2-} ist, auch wenn dies zur Folge hat, dass nicht alle funktionellen Gruppen des Aminmoleküls an das Übergangsmetallkation koordinieren können.[59] b) In einigen Verbindungen liegt eine Bindung zwischen TM-Komplex und Thiostannat-Einheit vor, obwohl bidentate Aminliganden (phen (= 1,10-Phenanthrolin), 1,2-dach (= 1,2-Diaminocyclohexan), 2,2'-bipy (= 2,2'-Bipyridin)) eingesetzt wurden.[45,49,55] Diese Aminmoleküle sind durch Mehrfachkoordination in der Lage, die Koordinationsstellen an den Übergangsmetallkationen vollständig zu besetzen. Damit dennoch TM-S-Bindungen gebildet werden können, müssen weitere Stabilisierungsmechanismen wie etwa π-π-Wechselwirkungen zwischen den aromatischen Liganden eine Rolle spielen.[37,38,49]

Bisher finden sich in dieser Verbindungsklasse nur $[Sn_2S_6]^{4-}$- und deutlich seltener $[SnS_4]^{4-}$-Einheiten. Größere Thiostannat-Anionen ($[Sn_3S_7]^{2-}$,[22,24–26] $[Sn_4S_9]^{2-}$,[26,27] $[Sn_5S_{12}]^{4-}$,[22,24] $[Sn_3S_9]^{6-}$ [28]oder $[Sn_4S_{10}]^{4-}$ [29]) wurden bisher nur bei den Verbindungen mit organischen Aminmolekülen oder TM-freien anorganisch-organischen Hybridverbindungen beobachtet. Ausnahmen bilden durch Sauerstoff erweiterte Einheiten, sogenannte gefüllte Cluster oder Zinn-Oxid-Verbindungen, aber auch hier ist die Anzahl auf zwei bekannte Verbindungen beschränkt.[56,57]

Das $[SnS_4]^{4-}$-Anion wurde bisher nur in Verbindung mit Mn und als verbrückender Ligand beobachtet.[37,38,42,43] Das $[Sn_2S_6]^{4-}$-Ion liegt hingegen als isoliertes Anion vor oder ist über einen der drei folgen Verknüpfungsmodi mit dem TM-Komplex verbunden: a) nur zwei, gegenüberliegende (*trans*) terminale S^{2-}-Anionen gehen eine Bindung ein, b) alle vier terminalen S^{2-}-Anionen sind in Bindungen involviert und binden an zwei TM-Komplexe oder c) die Thiostannat-Einheit verknüpft vier Komplexe miteinander.[12,45]

1.2.2 Solvothermalsynthese

Die Methode der Wahl zur Darstellung von Thiostannaten ist bisher die Solvothermalsynthese.[2,7,11–13,17] Synthesen unter solvothermalen Bedingungen werden in abgeschlossen Reaktionsgefäßen und überhitzen Lösungsmitteln (100-250°C) unter autogenen Drücken durchgeführt, wodurch die Eigenschaften des Lösungsmittels entscheidend verändert werden.[8,17–19] Typische Lösungsmittel sind Wasser, Amine und Alkohole sowie Mischungen dieser Lösungsmittel.[12,13]

Bei Einsatz von TM, Sn, S in (wässrigen) Aminlösungen beruht die Bildung von Thiostannaten auf der Generierung von Polysulfiden unter basischen Bedingungen.[13,17] Diese reaktiven Spezies reagieren mit den Edukten und bilden Zwischenprodukte sowie letztlich die finalen Produkte.[77] Die Aminmoleküle fungieren nicht nur als Lösungsmittel, sondern auch als Strukturdirektoren, in protonierter Form als ladungsausgleichende Komponente und generieren den basischen pH-Wert für die Bildung der Polysulfide.[13,17,25] TM-Amin-Komplexe werden in der Regel *in-situ* gebildet.[13] Erst seit kurzer Zeit werden vorgefertigte TM-Amin-Komplexe als Edukte verwendet.[45,51,78–80]
Der Vorteil der Solvothermalsynthese ist die vergleichsweise milde Reaktionsführung in stark polaren Lösungen, bei denen organische Moleküle sowie größere Strukturen (Ketten und Ringe) intakt bleiben.[13,17] Oft können metastabile Verbindungen erhalten werden[8,14,17,18], welche mit anderen synthetischen Methoden nicht zugänglich sind. Allerdings handelt es sich bei Solvothermalsynthesen um komplexe heterogene Reaktionen mit einer Vielzahl an Gleichgewichten und Einflussparameter[8,13]: z.B. Temperatur, pH-Wert, Edukte, Größe, Form und Ladung der Kationen, Redox-Potentiale, Siedepunkt, Viskosität, Polarität der Lösungsmittel sowie Mineralisatoren beeinflussen den Reaktionsverlauf.[8,13] Erfolgreiche Synthesen neuer Verbindungen basieren in der Regel auf Variationen anhand von Erfahrungswerten und nicht auf allgemein gültigen Regeln bzw. Vorschriften.[11,13,15]

1.3 Zielsetzungen der Arbeit

Die Solvothermalsynthese ermöglicht bisher noch keine gezielte Synthese von Thiostannaten mit bestimmten Strukturen und Eigenschaften.[13–15,30] Alle Erkenntnisse, welche auf der Basis der Analyse vieler Synthesen gezogen werden können, geben nur Hinweise über ein bestimmtes Reaktionsverhalten, aber ermöglichen keine zuverlässige Produktvorhersage.[30] Welche Variation von Syntheseparametern bewirkt welche Änderung bei der Produktbildung? Welche (weiteren) Aminmoleküle forcieren eine kovalente Bindung des TM-Komplexes an die Thiostannat-Einheit? Des Weiteren sind nur Tendenzen über das Wechselspiel zwischen Struktur und Eigenschaften der entsprechenden Verbindungen bekannt.[13–15] Wie beeinflusst die Kristallstruktur die Eigenschaften? Für ein tiefer gehendes Verständnis des Zusammenspiels verschiedener Parameter bedarf es der Synthese weiterer Verbindungen und deren eingehender Untersuchung. Dafür ist es zum einen erforderlich bereits etablierten Synthesemethoden weiterzuentwickeln, zum anderen ist es erforderlich jenseits der üblichen Pfade neue Synthesewege zu entwickeln und zu verfolgen.[11,14,15]

1.3.1 Verwendung aromatischer und cyclischer Amine

Der Einsatz von aromatischen bzw. cyclischen Aminen wie 1,10-Phenanthrolin (phen), 2,2‘-Bipyridin (2,2‘-bipy) und 1,4,8,11-Tetraazacyclotetradecan (cyclam) sollte zu neuen Strukturmotiven führen. Aufgrund der ausgeprägten Tendenz aromatischer Aminmoleküle zur Ausbildung stabilisierender π-π-Wechselwirkungen wurden Synthesen mit phen und 2,2‘-bipy durchgeführt.[81–84] Zu Beginn der Doktorarbeit war nur eine Zinn-Schwefel-Verbindung

mit phen bekannt.[37] Im Gegensatz dazu gibt es eine ganze Reihe an Übergangsmetallkomplexen mit phen und 2,2‘-bipy. Eine weitere Überlegung war, ob die besonderen optischen Eigenschaften dieser Aminmoleküle auf die resultierenden Verbindungen übertragen werden. Cyclam wurde als tetradentater Ligand ausgewählt, welcher aufgrund seiner Struktur die Koordinationssphäre von Übergangsmetallkationen nicht vollständig sättigen kann, so dass über den zweiten oder dritten Bindungsmodus $[Sn_2S_6]^{4-}$ kovalent an das Übergangsmetallzentrum gebunden werden könnte. Durch diese Art der Anbindung wird die Bildung einer Ketten- oder sogar Schichtstruktur ermöglicht.[44,51]
Da es sich bei diesen drei Aminmolekülen (phen, 2,2‘-bipy, cyclam) um nur gering wasserlösliche Feststoffe handelt, diese daher weder als Lösungsmittel fungieren noch für einen ausreichenden basischen pH-Wert sorgen können, ist eine Modifizierung der bisherigen solvothermalen Vorgehensweise erforderlich. Zur Generierung eines basischen Reaktionsmilieus wird ein weiteres Amin benötigt, ein sogenanntes Hilfsamin, welches allerdings keine Konkurrenz bei der Komplexierung von Übergangsmetallkationen zu dem eigentlich zu integrierendem Aminmolekül darstellen darf. Bei den Thiostannaten bieten sich monodentate Aminmoleküle wie z.B. Methylamin an: einerseits kann Methylamin in protonierter Form aufgrund der hohen Ladungsdichte der Thiostannateinheiten alleine keine Stabilisierung des Thiostannatgerüstes bewirken (im Gegensatz z.B. zu den Thioantimonaten);[13,64,85] andererseits ist die Bildung von TM-Komplexen mit monodentaten Aminmolekülen in Anwesenheit der zuvor genannten Aminmolekülen sehr unwahrscheinlich.[66,69–71]

1.3.2 Verwendung vorgefertigter Baueinheiten

Bei der solvothermalen Synthese werden die Thiostannationen sowie die Übergangsmetallkomplexe in der Regel *in-situ* gebildet und sind verschiedenen thermodynamischen Gleichgewichten unterworfen.[13,15] Daher war ein weiterer Ausgangspunkt für die Entwicklung neuer Synthesewege der Einsatz vorgefertigter Baueinheiten. Der Vorteil liegt darin, dass die *in-situ* Bildung dieser Einheiten wegfallen würde und daher die Zahl der Reaktionsparameter verringert wird, was zu einer Vereinfachung der Reaktionen beitragen kann. Dadurch werden die Reaktionen überschaubarer und können eventuell schneller „entschlüsselt“ werden. D.h. zwischen den eingesetzten Edukten und den Produkten können leichter „Beziehungen“ hergestellt werden, so dass nachfolgende Synthesen besser planbar sind. Im Idealfall könnte ein Baukastenprinzip entwickelt und gezielt Verbindungen synthetisiert werden, vorausgesetzt die entsprechenden vorgefertigten Baueinheiten stehen zu Verfügung und sind in dem entsprechenden Lösungsmittel stabil.

1.3.3 Alternative Syntheserouten

Besonders attraktiv sind bei Raumtemperatur (RT) lösliche Edukte, so dass die Reaktion unter Normaldruck durchgeführt werden kann. Damit werden die Zahl der Reaktionsparameter sowie der Syntheseaufwand reduziert. Im Hinblick auf mögliche Anwendungen und damit auch Herstellung im Großmaßstab wären solche Reaktionen ideal. Allerdings ist die

Umstellung der Synthesen auf RT mit einer deutlichen Verlangsamung der Reaktion verbunden, sodass bisher die Synthese kristalliner Thiostannate mehrere Monate in Anspruch genommen hat.[28,86] Die Herausforderung besteht darin reaktive, ausreichend (wasser)lösliche Edukte zu identifizieren, welche nicht sofort zu unerwünschten (Neben)Produkten wie binären Sulfiden, sondern in einem angemessen Zeitraum zu der angestrebten Verbindung reagieren. Allerdings muss beachtet werden, dass hingegen die Übersättigung nicht zu schnell erreicht wird, so dass Kristalle ausreichender Größe gebildet werden können.[87]

Ziele dieser Arbeit waren die Synthese und Charakterisierung neuer Thiostannate/Zinn-Schwefel-Verbindungen, sowie die Etablierung neuer Synthesewege. Um diese Ziele zu erreichen, wurden aromatische (phen, 2,2'-bipy) und cyclische (cyclam) Aminmoleküle eingesetzt sowie vorgefertigte Baueinheiten. Als Edukte wurden $Na_4SnS_4 \cdot 14H_2O$,[88] sowie verschiedene $[Ni(Amin)_3]^{2+}$-Komplexe (Amin = en, 1,2-dach, 1,2-dap, 1,3-dap, 2amp) verwendet, mit denen eine geeignete Methode zur Synthese von Thiostannaten bei RT untersucht wurde.

2. Experimenteller Teil

2.1 Synthesemethoden

2.1.1 Solvothermale Synthesen

Die solvothermalen Synthesen wurden überwiegend in 11 mL DURAN© Kulturröhrchen durchgeführt. Diese wurden mit Polytetrafluorethylen (PFTE) abgedichteten Schraubverschlüssen aus Polybutylenterephtalat (PBT) versehen und für die Reaktion in Stahlblöcke mit passender Bohrung und Schutzhaube gestellt. Die Verwendung der Gläser ermöglichte die visuelle Kontrolle des Reaktionsfortschritts, sowie das schnellere Testen von Reaktionsparametern aufgrund der geringeren Einwaage (Chemikalienverbrauch). Da die Gläser nicht für alle Variationen der Syntheseparameter ausreichend stabil waren (zu hohe Temperatur, zu hoher Druck), wurden einige Synthesen im Stahlautoklav mit schwimmenden Tefloneinsatz (Innenvolumen ~33 mL) mit entsprechend angepassten Einwaagen durchgeführt.

Die Synthesen wurden entweder unter statischen oder dynamischen (rührenden) Bedingungen durchgeführt. Statische Synthesen wurden in der Regel zur Züchtung von Einkristallen genutzt. Der Vorteil der dynamischen Synthesen liegt in den deutlich verkürzten Reaktionszeiten, so dass Synthesen in wenigen Stunden abgeschlossen waren. Das erlaubt in kürzerer Zeit einen größeren Parameterraum zu untersuchen. Wenn die Produkte auf diese Weise phasenrein erhalten werden, können in kürzere Zeit größere Mengen für Untersuchungen dargestellt werden. Allerdings bilden sich nicht alle Verbindungen unter dynamischen Bedingungen, welche unter statischen Bedingungen zugänglich waren. Synthesen mit Eisen und Cobalt z.B. ergaben unter dynamischen Bedingungen diverse Sulfide von Co bzw. Fe.

Die Chemikalien (TM oder TM-Chloride, Sn und S sowie in einigen Fällen feste Amine) wurden auf 0.2 mg genau eingewogen, in das Reaktionsgefäß überführt und mit Amin und dest. Wasser versetzt. Nach Verschluss der Reaktionsgefäße wurden diese für eine definierte Zeit bei Temperaturen zwischen 100-150°C getempert. In der Regel wurden die Gefäße nach Ablauf der Reaktionszeit aus dem Ofen genommen und unkontrolliert auf RT abgekühlt. Bei einigen Versuchen wurde langsam mit einem Temperaturprogramm auf RT abgekühlt, um eine Verbesserung der Kristallqualität zu ermöglichen. Schnelles Abschrecken von Proben wurde angewendet, um eine Umwandlung der Produkte bei längeren Abkühlzeiten zu verhindern. Anschließend wurden alle Proben abgesaugt, mit dest. Wasser und EtOH gewaschen und im Exsikkator über Kieselgel getrocknet.

2.1.2 Synthesen bei Raumtemperatur

Diese Synthesen wurden in handelsüblichen 5 mL Schnappdeckelgläschen durchgeführt. Die verwendeten Chemikalien (TM-Amin-Komplexe und $Na_4SnS_4 \cdot 14H_2O$) wurden auf 0.2 mg genau eingewogen, in das Schnappdeckelglas überführt und mit Amin und dest. Wasser versetzt. Zu beachten ist hierbei, dass die Aminzugabe vor der Wasserzugabe erfolgt. Ansonsten erfolgte eine Zersetzung des Na_4SnS_4 $14H_2O$ mit anschließender Reaktion mit den

Übergangsmetallkationen zu bei RT stabilen TM_xS_y-Spezies. Nach Zugabe des Lösungsmittels wurden die Gefäß verschlossen, etwa eine Minute kräftig geschüttelt und anschließend bei RT stehen gelassen. Nach Ablauf der Reaktionszeit wurde die Mutterlauge abgenommen, aufbewahrt, der Feststoff abgesaugt und das Produkt vorsichtig mit dest. Wasser gewaschen. Beobachtungen legten nahe, dass einige der erhaltenen Produkte empfindlich mit EtOH reagieren, daher wurden die Produkte nicht mehr mit diesem LM gewaschen. Die Proben wurden anschließend im Exsikkator über Kieselgel getrocknet.

2.2 Verwendete Chemikalien und Abkürzungen

Die verwendeten Chemikalien, deren Reinheitsgrad, Hersteller sowie deren in dieser Arbeit verwendeten Abkürzungen sind in Tabelle 1 aufgelistet. Des Weiteren sind allgemeine in dieser Arbeit genutzte Abkürzungen (Tab. 2), sowie Abkürzungen weiterer Chemikalien aufgeführt (Tab. 3).

Tabelle 2: Auflistung der verwendeten Chemikalien, deren Abkürzung, Reinheitsgrad und Hersteller.

Chemikalien – allgemein	**Abkürzung**	**Reinheitsgrad**	**Hersteller**
Anthracen, $C_{14}H_{10}$	anthra	≥ 99%	Merck
Biphenyl, $C_{12}H_{10}$	biph	99%	Acros Organics
Cobalt	Co	≥ 99 %	Merck
Cobalt(II)chlorid Hexahydrat	$CoCl_2 \cdot 6H_2O$	≥ 98%	Sigma Aldrich
Cobalt(II)perchlorat Hexahydrat	$Co(ClO_4)_2 \cdot 6H_2O$	98%	abcr
Eisen	Fe	≥ 99%	Merck
Eisen(II)chlorid Tetrahydrat	$FeCl_2 \cdot 4H_2O$	≥ 99%	Sigma Aldrich
Eisen(II)perchlorat Hexahydrat	$Fe(ClO_4)_2 \cdot 6H_2O$	99%	abcr
Glyoxal	---	40%, in Wasser	abcr
Mangan	Mn	99.9%	Alfa Aesar
Mangan(II)chlorid Tetrahydrat	$MnCl_2 \cdot 4H_2O$	≥ 99%	Merck
Mangan(II)perchlorat Hexahydrat	$Mn(ClO_4)_2 \cdot 6H_2O$	99%	abcr
Naphthalen, $C_{10}H_8$	naph	99%	abcr
Natriumsulfid Nonahydrat	$Na_2S \cdot 9H_2O$	≥ 98%	Fisher Scientific
Natriumtetrahydroborat	$NaBH_4$	98%	abcr
Nickel	Ni	≥ 99%	Merck
Nickel(II)chlorid Hexahydrat	$NiCl_2 \cdot 6H_2O$	99%	Merck
Nickel(II)perchlorat Hexahydrat	$Ni(ClO_4)_2 \cdot 6H_2O$	99%	abcr
Phenanthren, $C_{14}H_{10}$	phenan	98%	abcr
p-Terphenyl, $C_{18}H_{14}$	*p*-terp	99%	abcr
Schwefel	S	99.9%	Alfa Aesar
Zinn	Sn	99.5%	Alfa Aesar
Zinn(IV)chlorid Pentahydrat	$SnCl_4 \cdot 5H_2O$	98%	Sigma Aldrich
Chemikalien – Amine	**Abkürzung**	**Reinheitsgrad**	**Hersteller**
1,10-Phenanthrolin, $C_{12}H_8N_2$	phen	99%	abcr
1,2-Diaminopropan, $C_3H_{10}N_2$	1,2-dap	99%	Alfa Aesar
1,3-Diaminopropan, $C_3H_{10}N_2$	1,3-dap	98%	Alfa Aesar
1,4,8,11-Tetraazacyclotetradecan, $C_{10}H_{24}N_4$	cyclam	98%	abcr
1,5,8,12-Tetraazadodecan, $C_8H_{22}N_4$	---	94%	Aldrich
2,2‘-Bipyridin, $C_{10}H_8N_2$	2,2‘-bipy	99%	abcr
2-Aminomethylpyridin, $C_6H_8N_2$	2amp	99%	abcr
4,4‘-Bipyridin, $C_{10}H_8N_2$	4,4‘-bipy	98%	abcr
Diethylentriamin, $C_4H_{13}N_3$	dien	99%	Sigma Aldrich
Ethylendiamin, $C_2H_8N_2$	en	99%	Grüssing
Ethylamin, C_2H_7N	ea	70%, in Wasser	Fluka

Chemikalien – Amine	Abkürzung	Reinheitsgrad	Hersteller
Methylamin, CH_5N	ma	40%, in Wasser	abcr
n-Butylamin, $C_4H_{11}N$	ba	≥ 98%	Fluka
n-Propylamin, C_3H_9N	npa	99%	Merck
trans-1,2-Diaminocyclohexan, $C_6H_{14}N_2$	1,2-dach	99%	Sigma Aldrich
Tris(2-aminoethyl)amin, $C_6H_{18}N_4$	tren	96%	Aldrich
Chemikalien - Lösungsmittel	**Abkürzung**	**Reinheitsgrad**	**Hersteller**
2-Propanol, C_3H_7OH	---	rein	Walter (Händler)
Aceton, C_3H_6O	---	chem. rein	Walter (Händler)
Acetonitril, C_2H_3N	---	Chromos solvent	Walter (Händler)
n-Butanol, C_4H_9OH	---	reinst	Merck
Chloroform, $CHCl_3$	---	99-99.4%	Sigma Aldrich
Cyclohexan, C_6H_{12}	---	rein	Walter (Händler)
Dichlormethan, CH_2Cl_2	---	Amylen stabilisiert	Walter (Händler)
Diethylether, $C_4H_{10}O$	---	≥ 99.8%	Sigma Aldrich
Ethanol, C_2H_5OH	EtOH	99.9% vergällt	Walter (Händler)
Methanol, CH_3OH	MeOH	rein	BASF
n-Hexan, C_6H_{14}	---	95%	Walter (Händler)
Toluol, C_7H_8	---	rein	Walter (Händler)

Tabelle 3: Auflistung allgemeiner Abkürzungen.

Sonstige	Abkürzungen	sonstige	Abkürzungen
Abbildung	Abb.	Lösung	Lsg.
allgemein	allg.	Lösungsmittel	LM
beziehungsweise	bzw.	Minuten	Min.
destilliert	dest.	Raumtemperatur	RT
Hochtemperatur	HT	siehe *xy*	s. *xy*
Kapitel	Kap.	Stunde	h
konzentriert	konz.	Tabelle	Tab.
Koordinationszahl (coordination number)	CN	Übergangsmetall (transition metal)	TM

Tabelle 4: Auflistung der Abkürzungen weiterer Chemikalien.

weitere Chemikalien	Abkürzungen
1,4,7,10-Tetraazacyclodecan, $C_8H_{20}N_4$	cyclen
1,4-Diazabicyclo[2.2.2]octan, $C_6H_{12}N_2$	dabco
N-2-Aminoethyl-1,3-propandiamin, $C_5H_{15}N_3$	aepa
Pentaethylenhexamin, $C_{10}H_{28}N_6$	peha
Tetraethylenpentamin, $C_8H_{23}N_5$	tepa
Triethylentetramin, $C_6H_{18}N_4$	trien

2.3 Synthese der TM-Amin-Komplexe und $Na_4SnS_4 \cdot 14H_2O$

In der nachfolgenden Tabelle sind die in dieser Arbeit verwendeten TM-Amin-Komplexe, deren Produktfarbe sowie deren Synthesebedingungen mit Ausbeute aufgelistet. Gleiches ist für $Na_4SnS_4 \cdot 14H_2O$ aufgeführt.

Tabelle 5: Auflistung der verwendeten Komplexe mit Farbe, Synthesebedingungen und Ausbeuten.

Komplex	Farbe	Synthese	Ausbeute
$[Mn(phen)_3][ClO_4]_2$	gelb	5 mmol des entsprechenden $TM(ClO_4)_2 \cdot 6H_2O$ Salzes sowie 15 mmol phen bzw. 2,2'-bipy wurden getrennt in EtOH gelöst. Anschließend wurden die Lösungen unter Rühren vereint, die Reaktionslösung etwa 20 Min bei RT gerührt, der entstandene Feststoff abgesaugt und an der Luft getrocknet.[a]	95-99%
$[Mn(2,2'\text{-bipy})_3][ClO_4]_2$	gelb		
$[Fe(phen)_3][ClO_4]_2$	dunkelrot		
$[Fe(2,2'\text{-bipy})_3][ClO_4]_2$	dunkelrot		
$[Co(phen)_3][ClO_4]_2$	gelblich		
$[Co(2,2'\text{-bipy})_3][ClO_4]_2$	gelblich		
$[Ni(phen)_3][ClO_4]_2$	rosa		
$[Ni(2,2'\text{-bipy})_3][ClO_4]_2$	rosa		
$[Cu(phen)_3][ClO_4]_2$	hellblau		
$[Cu(2,2'\text{-bipy}][ClO_4]_2$	hellblau		
$[Ni(en)_3]Cl_2 \cdot 2H_2O$	rosaviolett	5 mmol des entsprechenden $TMCl_2 \cdot xH_2O$ oder $TM(ClO_4)_2 \cdot 6H_2O$ Salzes wurden in EtOH gelöst und unter Rühren mit 15 mmol des entsprechenden Amins versetzt. Die Reaktionslösung wurde etwa 20 Min. bei RT gerührt, der entstandene Feststoff abgesaugt und an der Luft getrocknet.[a]	95-99%
$[Ni(1,2\text{-dach})_3]Cl_2 \cdot 2H_2O$	violett		
$[Ni(1,2\text{-dap})_3]Cl_2 \cdot 2H_2O$	violett		
$[Ni1,3\text{-dap})_3]Cl_2 \cdot 2H_2O$	violett		
$[Ni(2amp)_3][ClO_4]_2$	violett		
$[Ni(tren)(H_2O)Cl]Cl \cdot H_2O$	hellblau	5 mmol $NiCl_2 \cdot 6H_2O$ wurden in EtOH gelöst unter Rühren mit 5 mmol tren versetzt und weitere 20 Min. gerührt. Anschließend wurde durch langsame Zugabe von Diethylether ein hellblauer Feststoff ausgefällt, welcher abfiltriert und getrocknet wurde.[89]	80%
$[Ni(cyclam)][ClO_4]_2$	orange	15 mmol $Ni(ClO_4)_2 \cdot 6H_2O$ wurden in 40 mL H_2O gelöst und mit 15 mmol 1,5,8,12-Tetra-azadodecan versetzt. Unter Kühlung (5°C) wurde die rot-braune Reaktionsmischung mit 3 mL Glyoxal versetzt. Nach 24 h bei RT wurde die violette Reaktionsmischung erneut gekühlt (5°C) und langsam (1 h) mit 30 mmol $NaBH_4$ versetzt. Die schwarze Lösung wurde 20 Min. auf 90°C erhitzt, heiß filtriert und das Filtrat mit 5 mL konz. Perchlorsäure versetzt. Der beim Abkühlen erhaltene orangefarbener Feststoff wurde abfiltriert, mit EtOH sowie Diethylether gewaschen und getrocknet.[90,91]	35%

Thiostannat-Einheit	Farbe	Synthese	Ausbeute
$Na_4SnS_4 \cdot 14H_2O$	farblos	Unter Rühren wurde zu einer $Na_2S \cdot 9H_2O$ Lösung (60 mmol in 40 mL H_2O) tropfenweise eine $SnCl_4 \cdot 5H_2O$ Lösung (15 mmol in 20 mL) gegeben. Die Reaktionslösung wurde für 8 h bei 45°C gerührt, anschließend in 300 mL MeOH geben und über Nacht gekühlt. Der entstandene farblose Feststoff wurde abgesaugt, mit EtOH gewaschen und getrocknet.[92]	90%

[a] Die Originalvorschrift von Ruis-Pérez et. al für $[Ni(2,2'\text{-bipy})_3]Cl_2$ [93] wurde entsprechend für die anderen Komplexe angepasst. Die Vorschrift konnte ohne Probleme hochskaliert werden.

2.4 Verwendete Untersuchungsmethoden

In der nachfolgenden Tabelle sind die zur Charakterisierung der Produkte verwendeten Methoden und Geräte aufgelistet.

Tabelle 6: Zur Charakterisierung der Produkte verwendete Methoden und Geräte sowie dazugehörigen Kenndaten.

Methode	Gerät (Hersteller)	Geräteparameter
Pulverdiffraktometrie	Stadi-P (STOE)	Transmissionsgeometrie, Cu-$K_{\alpha 1}$ (1.540598 Å); Germanium-Monochromator, Detektor: IP-PSD (STOE), linear PSD (STOE) bzw. MYTHEN 1K (DECTRIS)
Einkristallstrukturanalyse	IPDS (STOE)	Mo-K_α (0.71073 Å), Graphit-Monochromator
IR-Spektroskopie	ATR-IR-Spektrometer (Bruker Alpha P)	400-4000 cm^{-1}; Diamant aus ATR-Kristall, Auflösung: 4 cm^{-1}
UV/vis-Spektroskopie, diffuse Reflektion	Cary5Varian (TechtronPty. Darmstadt)	250-2000 nm, Referenzmaterial: $BaSO_4$
Raman-Spektroskopie	ISF66/FRA106 FT Raman (Bruker AXS)	100-3500 cm^{-1}; Nd: YAG Laser (λ = 1064 nm); Auflösung: 2 cm^{-1}
Elementaranalyse, CHNS-Analyse	EuroEA Element Analyzer (EURO VECTOR)	He-Trägergas, Verbrennung in O_2 (1010°C); Detektion über Wärmeleitzelle
SEM /EDX	ESEM XL 30 (Philips)	Rasterelektronenmikroskop mit EDX-Aufsatz der Fa. EDAX
Differenzthermoanalyse/ Thermogravimetrie (DTA/TG)	STA 409 CD (Netzsch)	Pt-Pt/Rh-Thermoelement; Gasstrom N_2 mit 75 cm^3/min; Heizrate: 4 bzw. 1 K/min
Magnetmessungen	PPMS Model 600 (Quantum Design)	Temperaturbereich 2-325 K;

3. Ergebnisse & Diskussion

3.1 Publikationen der solvothermalen Synthese übergangsmetallhaltiger Zinn-Schwefel-Verbindungen (kumulativer Hauptteil, Teil 1)

Mit den ausgewählten aromatischen (phen, 2,2‘-bipy) und cyclischen (cyclam) Aminmolekülen konnten unter solvothermalen Bedingungen fünfzehn neue Zinn-Schwefel-Verbindungen dargestellt und charakterisiert werden.

Mit Phenanthrolin und Mn^{2+} wurden fünf neue Verbindungen erhalten, von denen vier $\{[Mn(phen)_2]_2[Sn_2S_6]\}$ als Strukturmotiv aufweisen. Die fünfte Verbindung enthält die seltenere $[SnS_4]^{4-}$-Einheit. Auf die Strukturen sowie den Einfluss verschiedener Syntheseparameter wird in der Veröffentlichung in Abschnitt 3.1.1 eingegangen. Mit Fe^{2+} und Co^{2+} konnten jeweils zwei untereinander und zu Mn^{2+}-haltigen Verbindungen isostrukturelle Verbindungen erhalten werden (s. Kap. 3.1.2). Die Stabilisierung einer mit Ni^{2+} analogen $\{[TM(phen)_2]_2[Sn_2S_6]\}$ Einheit gelang erst mit Zusatz cokristallisierender weiterer aromatischer Moleküle, wie 2,2‘-bipy, 4,4‘-bipy und biph (s. Kap. 3.1.3 und 3.1.4).

Die Synthesen mit 2,2‘-Bipyridin waren deutlich anspruchsvoller als jene mit Phenanthrolin: erst nach Entwicklung einer alternativen Syntheseroute konnte eine Verbindung mit Mn^{2+} erhalten werden. Dies gelang durch den Einsatz vorgefertigter Komplexe und Thiostannat-Einheit (Precursoren) sowie der Einstellung des pH-Wertes (s. Kap. 3.1.4).

Mit cyclam konnte mit Ni^{2+} eine der wenigen zweidimensionalen Zinn-Schwefel-Verbindungen dargestellt werden. Diese Verbindung konnte sowohl mit der „klassischen“ Syntheseroute ausgehend von den Elementen mit Methylamin als Hilfsamin als auch bei der Verwendung vorgefertigter Precursoren erhalten werden. (s. Kap. 3.1.4)

3.1.1 Solvothermale Synthese fünf manganhaltiger Thiostannate mit 1,10-Phenanthrolin: Untersuchung des Einflusses verschiedener Reaktionsparameter auf die Produktbildung.

Zusammenfassung der Publikation „Influence of the Synthesis Parameters onto Nucleation and Crystallization of Five New Tin-Sulfur Containing Compound".

Durch die systematische Untersuchung ausgewählter Syntheseparameter (Temperatur, pH-Wert, Einwaageverhältnisse, Amin-Konzentration und Reaktionszeit) konnten die fünf Verbindungen $\{[Mn(phen)_2]_2[Sn_2S_6]\}$ (zwei Polymorphe: A: $P2_1/n$, Z = 2, B: $C2/c$ Z = 4), $\{[Mn(phen)_2]_2[Sn_2S_6]\}\cdot phen$ ($P\bar{1}$, Z = 1), $\{[Mn(phen)_2]_2[Sn_2S_6]\}\cdot phen\cdot H_2O$ ($P\bar{1}$, Z = 1) und $\{[Mn(phen)_2]_2[Mn(phen)]_2[SnS_4]_2\}\cdot H_2O$ ($P\bar{1}$, Z = 1) synthetisiert werden.

Einkristalle der Verbindungen wurden unter statischen Bedingungen bei der Reaktion von $MnCl_2\cdot 4H_2O$, Sn, S, phen im mmol Verhältnis 1:1:3:2 bzw. 2:1:4:1 in 30% Methylaminlösung erhalten. Bei einem Einwaageverhältnis von 1:1:3:2 (in mmol) kristallisierten die Verbindungen $\{[Mn(phen)_2]_2[Sn_2S_6]\}$ (A & B) und $\{[Mn(phen)_2]_2[Sn_2S_6]\}\cdot phen\cdot H_2O$ nacheinander über einen Zeitraum von 30 Tagen. Die Verbindung $\{[Mn(phen)_2]_2[Sn_2S_6]\}\cdot phen$ konnte nur bei Reaktionen im Kulturröhrchen bei einem pH-Wert von 11 erhalten werden. $\{[Mn(phen)_2]_2[Mn(phen)]_2[SnS_4]_2\}\cdot H_2O$ kristallisierte dagegen nur bei einem Einwaageverhältnis von 2:1:4:1 (in mmol) im Tefloneinsatz und nur unter statischen Bedingungen.

In vier der Verbindungen sind $[Mn(phen)_2]^{2+}$-Komplexe direkt mit dem $[Sn_2S_6]^{4-}$-Ion über Mn-S-Bindungen verbunden. Das Thiostannatanion fungiert als verbrückende Einheit: alle vier terminalen S^{2-}-Anionen sind in Bindungen involviert und verknüpfen zwei Mn(II)-Komplexe. Dies führt zur Bildung von neutralen $\{[Mn(phen)_2]_2[Sn_2S_6]\}$-Molekülen. Dieser Bindungsmodus wurde bei Thiostannaten zum ersten Mal beobachtet. In den Strukturen werden verschiedene π-π-Wechselwirkungen zwischen den aromatischen Liganden beobachtet. Die Energie dieser Wechselwirkungen wurde exemplarisch für eines der Polymorphe von $\{[Mn(phen)_2]_2[Sn_2S_6]\}$ berechnet und lag im Bereich um 10-14 kcal/mol.

In $\{[Mn(phen)_2]_2[Mn(phen)]_2[SnS_4]_2\}\cdot H_2O$ liegen MnN_4S_2-Oktaeder und MnN_2S_3 trigonale Bipyramiden vor. In der trigonalen Bipyramide agiert das $[SnS_4]^{4-}$-Anion als tridentater Ligand, ein Bindungsmodus der hier zum ersten Mal beobachtet wurde.

Unter dynamischen Bedingungen wurden der Einfluss der Temperatur, der Amin-Konzentration, des pH-Wertes und des LM-Volumens auf die Produktbildung in Abhängigkeit der Reaktionszeit untersucht.

Die Experimente zum Einfluss der Aminkonzentration (10%, 20%, 30% & 40%) und der Reaktionstemperatur (120°C, 140°C & 150°C) haben ergeben, dass zunächst mit abnehmender Konzentration und steigender Temperatur die Produktvielfalt zunimmt: Bei Aminkonzentrationen von 30% und 40% wurde bei allen drei Temperaturen lediglich eines der Polymorphe von $\{[Mn(phen)_2]_2[Sn_2S_6]\}$ (A) beobachtet. Nur bei Synthesen mit 20% Amin

(140°C & 150°C) konnten alle vier Verbindungen nacheinander beobachtet werden. Bei einer Aminkonzentration von 10% nahm die Produktvielfalt wieder ab.

Der Einfluss des LM-Volumens (1-2 mL, 30% Amin) in Abhängigkeit von der Reaktionszeit (15h und 20h) bei 150°C untermauert die Annahme, dass bei höheren Drücken die Bildung einiger Verbindungen unterdrückt wird: Nur bei LM-Volumen unterhalb von 1.4 mL konnte z.B. die Verbindung $\{[Mn(phen)_2]_2[Sn_2S_6]\}\cdot phen\cdot H_2O$ beobachtet werden.

Der Einfluss des pH-Wertes (pH = 11, 12, 13, 14) in Kombination mit der Temperatur (120°C, 140°C, 150°C) führte zu dem Ergebnis, dass mit abnehmendem pH-Wert und zunehmender Temperatur die Produktvielfalt zunimmt. Bei einem pH-Wert von 13 und 14 wurde bei allen drei Temperaturen nur $\{[Mn(phen)_2]_2[Sn_2S_6]\}$ (A) erhalten. Erst bei pH-Werten von 11 und 12, konnte u.a. bei 150°C eine Umwandlung zu $\{[Mn(phen)_2]_2[Sn_2S_6]\}$ (B) beobachtet werden.

Inorganic Chemistry

Article

pubs.acs.org/IC

Influence of the Synthesis Parameters onto Nucleation and Crystallization of Five New Tin−Sulfur Containing Compounds

Jessica Hilbert, Christian Näther, and Wolfgang Bensch*

Institute of Inorganic Chemistry, Christian-Albrechts-University of Kiel, Max-Eyth-Str. 2, Kiel 24118, Germany

Supporting Information

ABSTRACT: The distinct control of the synthesis parameters achieved crystallization of five new inorganic−organic hybrid tin sulfides with 1,10-phenanthroline (phen) as the organic component: $\{[Mn(phen)_2]_2(\mu_2\text{-}Sn_2S_6)\}$ (**1**, **3**), $\{[Mn(phen)_2]_2(\mu_2\text{-}Sn_2S_6)\}\cdot phen$ (**2**), $\{[Mn(phen)_2]_2(\mu_2\text{-}Sn_2S_6)\}\cdot phen\cdot H_2O$ (**4**), and $\{[Mn(phen)_2]_2[\mu\text{-}\eta^2\text{-}\eta^2\text{-}SnS_4]_2[Mn(phen)]_2\}\cdot H_2O$ (**5**). Compounds **1**, **3**, and **4** occur successively under static conditions by increasing the reaction time up to 8 weeks. Stirring the reaction mixtures and keeping the educt ratio constant allow preparation of distinct phase pure samples within very short reaction times. At higher autogenous pressure, crystallization and conversion of several compounds are suppressed, and only **1** crystallized. Compound **2** could only be obtained in glass tubes at low pH value of the reaction mixture or at low amine concentration. Adjusting the pH value of the solution, the concentration, and the volume of the solvent, compounds **1**−**4** crystallize sequentially and were successively converted into each other. Results of thermal stability experiments and solubility studies suggest that compounds **1** and **3** are polymorphs following the density rule. Compounds **2** and **4** may be viewed as pseudopolymorphs of **1** and **3**.

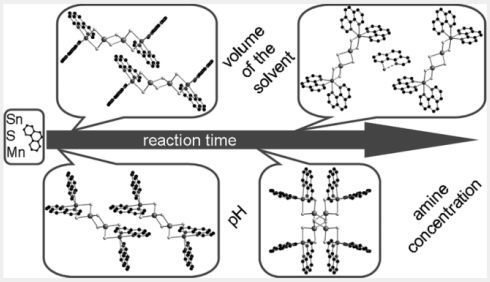

■ INTRODUCTION

During the last decades, a huge variety of thiometalate compounds were prepared by the solvothermal route, and the intriguing chemistry of these compounds has been discussed in various review articles.[1−5] Thiostannates are an attractive group of compounds among the main group thiometalates, and they are promising candidates for catalysis, sensors, absorbers, and ion exchangers.[6−9] Alteration of physicochemical properties of thiostannates can be achieved by integration of transition metal cations (TMCs) into the networks.[10] In most cases, the syntheses are performed under solvothermal conditions,[11−14] and due to the multidimensional parameter space, controlling product formation is a challenging task. Many parameters, for example, kind of educts, reaction time and temperature, concentration of the solvent, type of solvent, pH value, redox potential, autogenous pressure, and viscosity of the solvent, influence the product formation. In addition, changing only one parameter alters others in a not well-controlled way. Another drawback of solvothermal syntheses done under static conditions (no stirring of the mixture) is the development of strong concentration gradients that may lead to the nucleation and growth of different phases. On the other hand, crystals are obtained under these conditions that are suitable for single-crystal X-ray work. A critical review of the synthesis conditions reported in a large number of papers reveals that, in the overwhelming cases, reaction times were chosen between 3 and about 7 days. Keeping in mind that the reaction conditions of solvothermal syntheses are mild enough to obtain metastable or kinetically stabilized products, one can expect that the least stable compound crystallizes first followed by the more stable compound(s) (Ostwald's rule). The energetic difference between the different compounds is often small and can be overcome by extending the reaction time. This approach was demonstrated by us to be successful in the thioantimonate chemistry.[15] Because solvothermal syntheses are often performed in steel autoclaves, an optical control of reaction progress as a function of time is not possible, but also, reactions undertaken in glass tubes do not allow online identifying crystallization of different compounds as a function of the reaction time. However, the occurrence of crystalline intermediates/metastable compounds, their interconversion, and their crystal growth can be studied using suitable *in situ* techniques like X-ray diffraction performed with synchrotron radiation sources.[16,17a−e] Disadvantages of such experiments are the time restriction and the large experimental effort. Until now, several hybrid thiostannates have been synthesized with predominantly TMCs coordinated by aliphatic amine molecules. Using π-conjugated ligands for TMC complexation, specific photochemical and electrochemical properties can be expected.[18] A promising ligand is 1,10-phenanthroline (phen) that was used for the generation of new thiostannates.[19]

Received: February 17, 2014
Published: May 20, 2014

   dx.doi.org/10.1021/ic500369m | *Inorg. Chem.* 2014, 53, 5619−5630

Table 1. Selected Details of the Data Collection and Structure Refinement Results

	1	3	2	4	5
crystal system	monoclinic	monoclinic	triclinic	triclinic	triclinic
space group	$P2_1/n$	$C2/c$	$P\bar{1}$	$P\bar{1}$	$P\bar{1}$
M (g/mol)	1260.44	1260.44	1440.64	1458.66	1812.86
a (Å)	10.8230(4)	25.6736(7)	10.0642(9)	11.3203(7)	10.8703(5)
b (Å)	9.8940(2)	11.1006(4)	10.6249(9)	12.1436(7)	12.5183(6)
c (Å)	24.8107(10)	18.0647(5)	13.6927(12)	12.7586(7)	14.9644(6)
α (deg)	90.0	90.0	71.700(7)	113.200(4)	103.381(3)
β (deg)	91.356(3)	98.164(2)	81.458(7)	90.908(5)	108.390(3)
γ (deg)	90.0	90.0	84.346(7)	111.974(4)	101.636(4)
V (Å^3)	2656.05(15)	5096.1(3)	1372.6(2)	1479.92(15)	1794.71(14)
Z	4	4	1	1	1
$D_{calculated}$ (g/cm^3)	1.576	1.643	1.743	1.637	1.677
μ (mm^{-1})	1.670	1.741	1.629	1.513	1.654
scan range (deg)	$1.64 \le \theta \le 24.62$	$2.00 \le \theta \le 27.00$	$1.58 \le \theta \le 22.78$	$1.77 \le \theta \le 27.00$	$1.51 \le \theta \le 27.00$
reflections collected	28 044	22 159	11 651	13 856	18 641
independent reflections	4454	5496	11 661	6406	7768
observed reflections	3840	4972	8029	4952	6507
goodness-of-fit on F^2	1.373	1.095	1.027	0.938	1.079
final R indices ($I > 2\sigma(I)$)	$R1$ = 0.0428	$R1$ = 0.0264	$R1$ = 0.0634	$R1$ = 0.0284	$R1$ = 0.0412
	$wR2$ = 0.1045	$wR2$ = 0.0574	$wR2$ = 0.1115	$wR2$ = 0.696	$wR2$ = 0.1039
R indices (all data)	$R1$ = 0.0517	$R1$ = 0.0322	$R1$ = 0.1046	$R1$ = 0.0432	$R1$ = 0.0534
	$wR2$ = 0.1078	$wR2$ = 0.0593	$wR2$ = 0.1242	$wR2$ = 0.0731	$wR2$ = 0.1084
res. elec. dens. (e/Å^3)	0.566 and −0.681	0.301 and −0.326	0.971 and −0.876	0.653 and −0.660	0.972 and −0.720

In the present contribution, we report results of the investigation of the Mn/Sn/S/phen system and synthesized four new inorganic−organic hybrid compounds under static conditions with the $[Sn_2S_6]^{4-}$ anion connecting Mn^{2+} centered complex cations into the $\{[Mn(phen)_2]_2(Sn_2S_6)\}$ unit as the main structural motif. Three of these compounds ($\{[Mn(phen)_2]_2(Sn_2S_6)\}$ (**1** and **3**) and $\{[Mn(phen)_2]_2(Sn_2S_6)\}\cdot phen\cdot H_2O$ (**4**)) were discovered by increasing the reaction time from 5 days to 8 weeks. The occurrence of **1** and **3** as a function of reaction time is a nice example for Ostwald's rule.[20,21] Compound **5**, $\{[Mn(phen)_2]_2(SnS_4)_2[Mn(phen)]_2\}\cdot H_2O$, features a tetradentate acting $[SnS_4]^{4-}$ ion exhibiting a hitherto not observed binding mode and could only be isolated applying static reaction conditions. We then performed solvothermal reactions under dynamic conditions (stirring of the reaction slurries) applying always identical educt ratios of the Mn, Sn, and S sources and varying the reaction conditions. Under these conditions $\{[Mn(phen)_2]_2(Sn_2S_6)\}\cdot phen$ (**2**) crystallized at a lower pH value using a glass tube as the reaction container. Interestingly, compounds **1**−**4** were obtained within a few hours as phase pure materials adjusting the amine concentration, reaction time, temperature, autogenous pressure, and/or pH value, while compound **5** did not crystallize under these conditions.

■ EXPERIMENTAL SECTION

Synthesis. *General.* All chemicals were purchased and used without further purifications. All compounds were prepared under solvothermal conditions in glass tubes (inner volume 11 mL) or Teflon-lined steel autoclaves (inner volume 30 mL) using $MnCl_2\cdot 4H_2O$, Sn, S, and phen. Further details of the syntheses are summarized in Tables S1 and S2 (Supporting Information). The crystalline products were filtered off after the reactions, washed with water and ethanol, and dried in vacuum. The reaction products were separated manually, and the homogeneity was checked by X-ray powder diffraction (XRPD) and elemental analysis. Experimental and calculated XRPD patterns are shown in Figure S1 (Supporting Information). For the dynamic syntheses, the products were not separated, but the composition of product mixture was evaluated by XRPD.

Reactions in Teflon-Lined Steel Autoclaves under Static Conditions. A 1.57 (0.79) mmol of $MnCl_2\cdot 4H_2O$, 0.79 (0.79) mmol of Sn, 3.14 (2.37) mmol of S, and 0.79 (1.58) mmol of phen were reacted with 6.28 mL of solvent under static conditions at 120 and 150 °C. Solvent compositions in detail: methylamine (ma) (30%): 3.96 mL of ma (40%, aqueous solution, abcr) and 1.32 mL of deionized water; butylamine (ba) (100%): 6.28 mL of ba (≥98%, Fluka); and ba (50%): 2.64 mL of ba (≥98%, Fluka) and 2.64 mL of deionized water.

Reactions in Glass Tubes under Static Conditions. A 0.5 (0.25) mmol of $MnCl_2\cdot 4H_2O$, 0.25 (0.25) mmol of Sn, 1.0 (0.75) mmol of S, and 0.25 (0.5) mmol of phen were reacted with 2 mL of solvent under static conditions at 120 °C. The synthesis could not be carried out at 150 °C because the screw caps were not stable at this temperature. Solvent compositions in detail: ma (30%): 1.5 mL of ma (40%, aqueous solution, abcr) and 0.5 mL of deionized water; ethylamine (ea) (50%): 1.42 mL of ea (70%, aqueous solution Fluka) and 0.58 mL of deionized water; *n*-propylamine (npa) (100%): 2 mL of npa (99% Merck−Suchardt); npa (50%): 1 mL of npa (99% Merck−Suchardt) and 1 mL of deionized water; ba (100%); and ba (50%): 1 mL of ba and 1 mL of deionized water. A short overview of the reaction conditions of the syntheses performed under static conditions can be found in Table S1 (Supporting Information).

Dynamic Syntheses in Glass Tubes. A 0.2 mmol of $MnCl_2\cdot 4H_2O$, 0.2 mmol of Sn, 0.6 mmol of S, and 0.4 mmol of phen with methylamine solution (ma; 40%, aqueous solution, abcr) were reacted in a 7 mL glass tube under stirring conditions (magnetic stirrer) at T = 120, 140, and 150 °C up to 20 h. An overview of the used solvent mixtures and their resulting pH values are given in Table S2 (Supporting Information). To exclude any influence of the stirring speed on nucleation and crystal growth, in all experiments, the same magnetic stirrer was used with a fixed stirring speed.

Single-Crystal Structure Determination. The intensity data for the compounds were collected using a STOE IPDS-1 (Imaging Plate Diffraction System) with Mo Kα radiation (λ = 0.07107 Å) at room temperature. The structures were solved with direct methods using the program SHELXS-97[22], and the refinements were done against F^2 with SHELXL-97.[23]

dx.doi.org/10.1021/ic500369m | *Inorg. Chem.* 2014, 53, 5619−5630

All non-hydrogen atoms except those of the disordered uncoordinated phen ligand in compound **2** were refined anisotropic. The C−H hydrogen atoms were positioned with idealized geometry and refined isotropic using a riding model. For all compounds, a numerical absorption correction was performed. All crystals investigated for compound **2** where nonmerohedral twinned. This twinning unfortunately leads to reflections along the *c* axis, which cannot be resolved. Therefore, data were measured to only $2\theta = 45°$, and the structure was refined using the HKLF-5 option. Unfortunately, by using this procedure, the equivalent reflections cannot be merged, and therefore, the number of independent reflections is artificially too large. If the overlapping reflections are omitted, the completeness is less than 60% which is inacceptable. The structure can easily be solved in space groups *P*1 and $P\bar{1}$. In space group *P*1, the displacement factors of several atoms are nonpositive defined, and the Flack *x* parameter is always about 0.5. Large correlations of the parameters are observed indicating the presence of a center of symmetry. Even if the uncoordinated phen ligand seems to be ordered in *P*1, Platon immediately suggest space group $P\bar{1}$ in which this ligand is disordered around a center of inversion. Therefore, space group $P\bar{1}$ was selected for the final refinements. In compound **4**, the water H atoms were not located but considered in the formula. One phen ligand is disordered around a center of inversion, in which also one water molecule is involved. Both of them were refined with half occupancy. The disorder remains if the structure refinement is performed in space group $P\bar{1}$, where all atoms are located in general positions. After structure refinement for compound **5**, there was one remaining small electron density maximum to which a half-occupied water molecule was assigned. Additional residual electron density peaks were located, which can be assigned to the water H atoms. The O−H H distances were set to ideal values and finally the H atoms were refined using a riding model.

Selected refinement results are summarized in Table 1. Structural data have been deposited in the Cambridge Crystallographic Data Centre as publication nos. CCDC 999247 (**1**), CCDC 999248 (**2**), CCDC 999249 (**3**), CCDC 999250 (**4**), and CCDC 999251 (**5**). Copies of the data can be obtained, free of charge, on application to CCDC, 12 Union Road, Cambridge CB2 1 EZ, UK (deposit@ccdc.ca.ac.uk).

X-ray Powder Diffractometry. The XRPD patterns were recorded on a STOE Stadi-P powder diffractometer (Cu Kα_1 radiation, λ = 1.540598 Å, Ge monochromator) in transmission geometry.

Investigation of the samples during heating was done by *in situ* X-ray diffractometry (PANalytical X'Pert Pro diffractometry, Cu Kα radiation, Göbel mirror at the incident beam, PIXel detector, step size 0.03). The *in situ* measurements were carried out in a high-temperature chamber (HTC, Anton Paar HTK 1200N) under helium atmosphere with a heating rate of 4 °C/min and held at constant temperature during the measurement.

Energy Dispersive X-ray Experiments. Scanning electron microscopy investigations and energy dispersive X-ray (EDX) analyses were done with a Philips environmental scanning electron microscope ESEM XL30 equipped with an EDAX detector.

Spectroscopic Properties. *UV/visible Spectroscopy.* UV/visible (UV/vis) spectroscopic investigations were carried out at room temperature using an UV/vis/NIR two-channel spectrometer Cary 5 from Varian Techtron Pty., Darmstadt. The optical properties of compounds **1**−**5** were investigated by analyzing the UV/vis reflectance spectra of the powdered samples (with $BaSO_4$ powder used as reference material). The absorption data were calculated applying the Kubelka−Munk relation for diffuse reflectance data (see Figure S2, Supporting Information).

Infrared Spectroscopy. MIR spectra (400−3500 cm^{-1}) were recorded with an ATI Mattson Genesis spectrometer (see Figure S3 and Table S3, Supporting Information).

Raman Spectroscopy. Raman spectra were recorded with a Bruker IFS 66 Fourier transform spectrometer (wavelength: 541.5 nm) in the range from 100 to 3500 cm^{-1} (see Table S4 and Figure S4, Supporting Information).

Atomic Absorption Spectroscopy. Atomic absorption spectroscopy (AAS) was performed with a PerkinElmer Analyst 3000 system.

■ RESULTS AND DISCUSSION

Synthetic Aspects. The five new compounds were obtained during a systematic investigation of the influence of the synthesis parameters onto product formation applying static conditions. The reproducibility of the results was verified by performing each synthesis several times. Only compounds **1**, **3**, **4**, and **5** could be obtained in Teflon-lined autoclaves under static conditions. Compound **1** could be identified up to 21 days of reaction time, compounds **3** and **4** crystallized between 21 and 30 days, and for even longer reaction times, only **4** could be observed. Remarkably, besides **1**, **3**, and **4**, another compound (**2**) crystallized at T = 120 °C using glass tubes as a reaction container and adjusting the pH value to 11. There are two remarkable differences between the two types of containers: the volume and the roughness of the surface. While the surface of the glass tubes is relatively smooth, that of the Teflon-liner is rough and porous. These two factors may be important for nucleation and crystallization of a distinct compound. One can only speculate whether heterogeneous nucleation is favored using Teflon as the container and homogeneous nucleation occurs in the glass tubes. In this context, it is noted that, in all investigations, always new Teflon-liner were used to avoid any cross-contamination. Indeed the Teflon-liners are used several times but only for the same chemical system. Another interesting result obtained during the studies is that several compounds transform into others as a function of the reaction time.

In the following, we first present the crystal structures of the new compounds grouped according to the different structural building units. Compound **5** does not contain the $[Sn_2S_6]^{4-}$ anion but was obtained during our systematic study, and therefore, we include the structure in our discussion. In the next section, we then discuss the results of the syntheses performed under dynamic conditions.

Crystal Structures of Compounds 1−4. In the structures of **1**−**4**, the $[Mn(phen)_2]^{2+}$ complex is a central structural motif. The Mn^{2+} ion has two bonds to S atoms of the $[Sn_2S_6]^{4-}$ anion and four bonds to N atoms of the phen ligands, thus forming distorted $[MnN_4S_2]^{2+}$ octahedra. The geometric parameters of the complexes such as Mn−N and Mn−S bond lengths as well as the angles around Mn^{2+} (Table S5, Supporting Information) are very similar in **1**−**4**, and match well with literature data.[10,19,24−26] The $[Sn_2S_6]^{4-}$ bitetrahedron is very common in thiostannates[10,25−36] and is formed by two edge-sharing SnS_4 tetrahedra. The geometric parameters of the $[Sn_2S_6]^{4-}$ anions in **1**−**4** display the typical bonding pattern with longer bridging Sn−S bonds and shorter bonds to the S atoms that are also bonded to Mn^{2+} (see Table S5, Supporting Information). Interestingly, the bond formation to Mn^{2+} does not significantly affect the Sn−S bonding pattern compared to the free $[Sn_2S_6]^{4-}$ anion as exemplified by comparison of the geometric parameters for compounds **1** and **3** with data of $Na_4Sn_2S_6{\cdot}14\ H_2O$ (see Table S6, Supporting Information).

In all compounds, all terminal S atoms of the $[Sn_2S_6]^{4-}$ anion have bonds to the Mn^{2+} centered complex. We note that, in most cases, this moiety is found as a discrete anion[37,38] or is acting as a bidentate ligand using the *trans* terminal S atoms.[10,37,38] The tetradentate bonding mode observed in **1**−**4** for the $[Sn_2S_6]^{4-}$ anion was never observed before and has been found so far only in the related class of selenidostannates

dx.doi.org/10.1021/ic500369m | *Inorg. Chem.* 2014, 53, 5619−5630

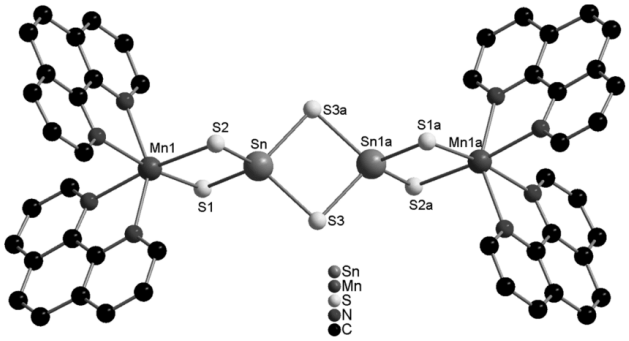

Figure 1. Structure of the $\{[Mn(phen)_2]_2(\mu_2\text{-}Sn_2S_6)\}$ moiety observed in compounds **1**−**4**. The hydrogen atoms are omitted for clarity.

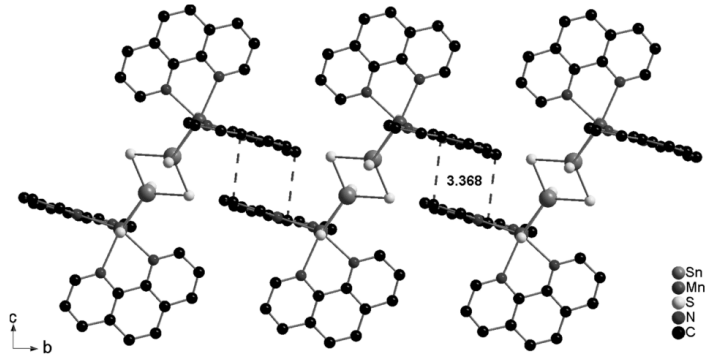

Figure 2. Parallel arrangement of the molecules in **1** along *b*, assembled by off-center parallel stacking (blue dashed lines) along *c*. Hydrogen atoms are omitted for clarity.

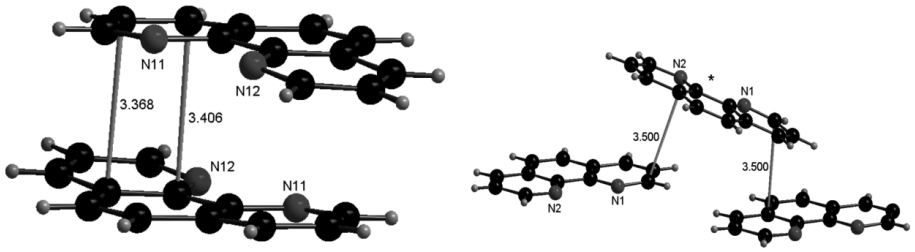

Figure 3. Two different arrangements of the phen molecules in the structure of **1**. The red lines with the numbers show the shortest intermolecular distances in Å.

where only few examples were reported.[14,39] Hence, in the structures of **1**−**4**, $\{[Mn(phen)_2]_2(\mu_2\text{-}Sn_2S_6)\}$ moieties are observed (Figure 1), and the different structures result from different packing of the constituents due to different stacking arrangements of the phen ligands. The dihedral angles between the phenantroline ligands are listed in Table S7 (Supporting Information). These values scatter around 90° by about ±10°.

Compound **1** (monoclinic, space group $P2_1/n$, $Z = 2$) is isostructural to $\{[Mn(phen)_2]_2(\mu_2\text{-}Sn_2Se_6)\}$[18] whereas compound **3** (monoclinic, space group $C2/c$, $Z = 4$) is isostructural to $\{[Fe(phen)_2]_2(\mu_2\text{-}Sn_2Se_6)\}$.[14]

In compound **1**, each $\{[Mn(phen)_2]_2(\mu_2\text{-}Sn_2S_6)\}$ unit interacts with adjacent molecules through off-center parallel stacking[40] between the phen ligands (3.369 Å) along the *c* axis (Figure 2). The molecules proceed along [100] and [010] (Figure 2 and Figure S5, Supporting Information) leading to formation of a two-dimensional (2D) layerlike arrangement within the *ab* plane. A three-dimensional (3D) network is generated by an off-center parallel arrangement along [001] (Figure S5, Supporting Information).

The energy involved in the stacking of the phen ligands was exemplarily calculated for compound **1**.[41−44] The two different

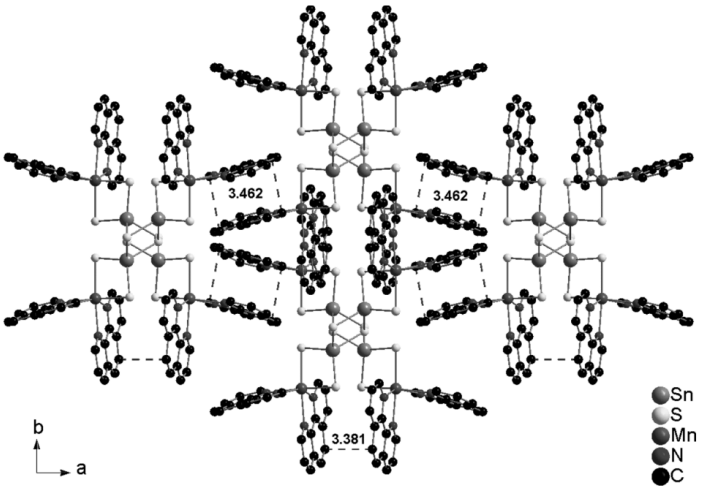

Figure 4. Antiparallel stacking of the layers along *c*; off-center parallel stacking (blue dashed lines) in **3** along the *a* and *b* axes. Hydrogen atoms are omitted for clarity.

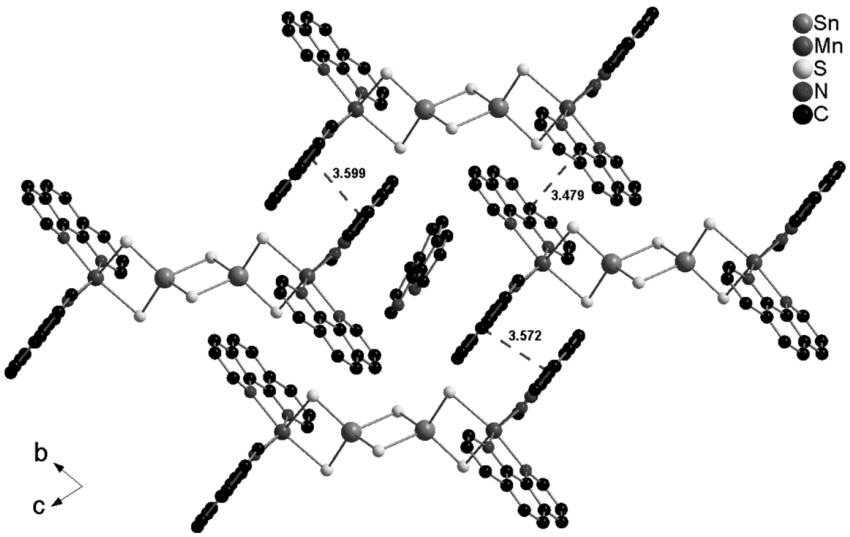

Figure 5. Arrangement of the molecules in **2** with off-center parallel orientation of the phen ligands (blue dashed lines) along *b* and *c*. Hydrogen atoms are omitted for clarity. Only one position of the disordered free phen molecule is displayed.

arrangements of the phen molecules were cut-out of the structure of **1** for the calculations (see Figure S5, Supporting Information). The energy obtained for the arrangement on the left in Figure 3 is 10.4 kcal/mol while the interaction energy of the phen ligand marked with an asterisk (Figure 3, right) with the two molecules below is about 13.4 kcal/mol. These values are in the typical range reported in the literature (e.g., see ref 42b). We note that the separations of the phen molecules in compounds **2**–**5** are in the same range observed for **1**, and therefore, it can be assumed that the interaction energies are also in the range calculated for this compound.

In compound **3**, each $\{[Mn(phen)_2]_2(\mu_2\text{-}Sn_2S_6)\}$ unit interacts also with adjacent molecules by two different off-center parallel stacking along [100] (3.381 Å) and along [010] (3.462 Å) leading to the formation of a layerlike arrangement within the (001) plane (Figure 4). The layers are antiparallel oriented along [001] and are joined by off-center parallel stacking along [100] (Figure 4).

dx.doi.org/10.1021/ic500369m | *Inorg. Chem.* 2014, 53, 5619−5630

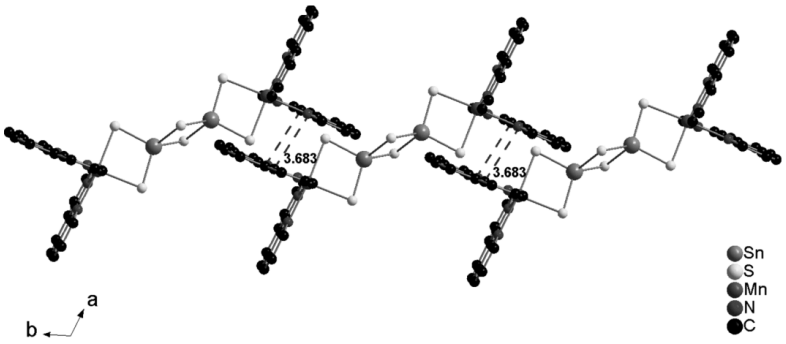

Figure 6. Chainlike arrangement of the $\{[Mn(phen)_2]_2(\mu_2\text{-}Sn_2S_6)\}$ units along the *b* axis. Hydrogen atoms are omitted for clarity.

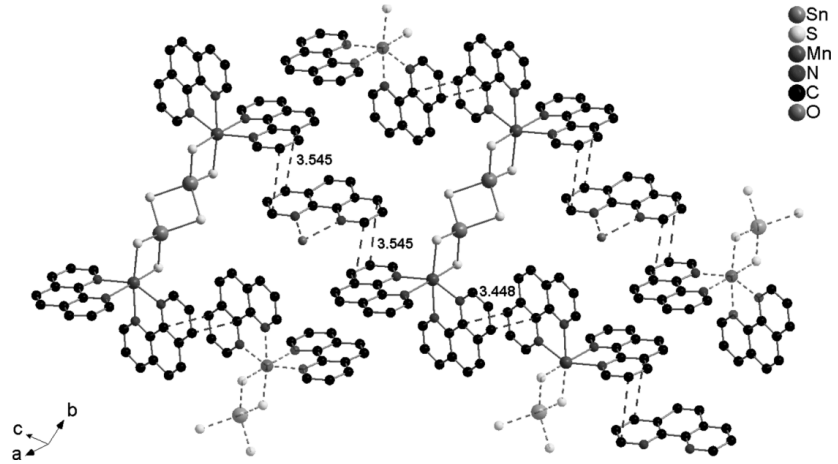

Figure 7. 3D arrangement of the molecules in **4** showing the off-center parallel stacking (blue dashed lines). Hydrogen atoms are omitted for clarity. The dashed lines between O and N atoms indicate hydrogen-bonding interactions.

Compounds **2** and **4** (triclinic, space group $P\bar{1}$, $Z = 1$, Table 1) contain an additional phen molecule (**2**) or a phen molecule and a lattice water molecule (**4**). In the structure of **2**, the $\{[Mn(phen)_2]_2(\mu_2\text{-}Sn_2S_6)\}$ units are joined via off-center parallel stacking interactions along the two different directions [010] (3.599 and 3.572 Å) and [001] (3.479 Å) (Figure 5). The interaction along [001] occurs between slightly staggered molecules (Figure S6, Supporting Information), generating a 3D arrangement with tunnels running along [100]. The tunnels are occupied by phen molecules (Figure S7, Supporting Information) that are disordered over two positions.

A chainlike arrangement of the $\{[Mn(phen)_2]_2(\mu_2\text{-}Sn_2S_6)\}$ moieties along [010] is observed in the structure of compound **4** initiated by off-center parallel stacking arrangement (3.683 Å) along [100] (Figure 6). The not coordinated phen molecule is involved in off-center parallel stacking (3.545 Å) bridging two $\{[Mn(phen)_2]_2(\mu_2\text{-}Sn_2S_6)\}$ moieties in a parallel displaced way developing a 3D arrangement of the constituents (Figure 7). The H_2O molecule seems to interact with the phen molecule via hydrogen bonds, but because the position of the H atoms could not be determined, no further details can be reported.

Compound **5**, $\{[Mn(phen)_2]_2(\mu\text{-}\eta^2\text{-}\eta^2\text{-}SnS_4)_2[Mn(phen)]_2\}\cdot H_2O$, crystallizes in the triclinic space group $P\bar{1}$ with one formula unit in the unit cell. The two crystallographically independent Mn^{2+} ions are in different environments. The Mn1 atom is chelated by two phen molecules and is further coordinated by two S atoms from the $[SnS_4]^{4-}$ anion forming a distorted octahedron. However, the Mn2 atom is coordinated by two N atoms of one phen and three S atoms of two $[SnS_4]^{4-}$ anions in a distorted $[MnN_2S_3]$ trigonal bipyramidal coordination geometry (Figure 8). Two symmetry related trigonal bipyramids share a common edge forming a $[Mn_2S_4N_4]$ dimer with a Mn···Mn separation of 3.262 Å that is shorter than in comparable dimers with Mn···Mn distances between 3.3655 and 3.5984 Å.[45−48] Two $[SnS_4]^{4-}$ anions bridge this dimer with two $[Mn1(phen)_2]^{2+}$ cations via three μ_2-S atoms and one μ_3-S atom forming the neutral molecule (Figure 8). To the best of our knowledge, this is the first example for a $[SnQ_4]^{4-}$ anion (Q = S, Se) connecting two different types of TM^{n+} complex cations in the modes observed here.

The different binding modes of the S atoms influence both the Sn−S bond lengths and S−Sn−S bond angles: The Sn1−S1

dx.doi.org/10.1021/ic500369m | *Inorg. Chem.* 2014, 53, 5619−5630

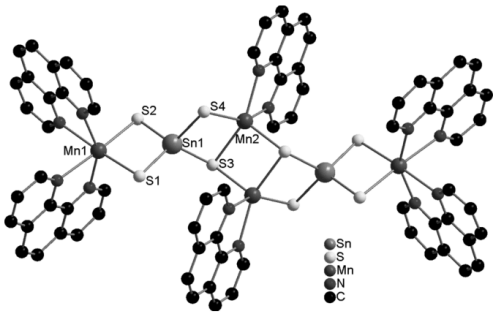

Figure 8. Molecular structure of compound **5**. The hydrogen atoms are omitted for clarity. Only selected atoms are labeled.

and Sn1−S2 bonds are slightly shorter, the Sn−S4 bond is similar, and the Sn1-μ_3-S3 distance is distinctly longer compared to the discrete $[SnS_4]^{4-}$ anion (see Table S8, Supporting Information). The S−Sn−S angles range from 102.17(4)° to 116.12(4)° indicating a severe deviation from the ideal geometry, while discrete $[SnS_4]^{4-}$ thiostannate anions exhibit only small distortions of tetrahedral geometry.[49] Comparable distorted $[SnS_4]^{4-}$ anions were also observed in some thiostannates.[19,24]

In **5**, the units are arranged in chains along the *a* axis and interact via off-center parallel stacking interactions between the central $Mn_2S_4N_4$ moieties (Figure 9). These chains are further connected within the *ac* plane by off-center parallel stacking of the phen molecules of the octahedra $Mn1S_2N_4$ at the periphery of the molecules (Figure 9). The structure analysis gave no hints for a significant interaction between the lattice water molecules and the 2D supramolecular layers.

In comparison to the $[Sn_2S_6]^{4-}$ bitetrahedron, the examples of thiostannates containing the $[SnS_4]^{4-}$ tetrahedron are limited.[19,24,50−52] In addition, the only compound exhibiting a similar bridging function has been observed in the $_\infty{}^1[MnSnS_4]$ chains of $(1,4\text{-dabH})_2MnSnS_4$, but the ammonium molecules act only as charge balancing ions.[51] Examples for a $[SnQ_4]^{4-}$ anion (Q = S, Se) acting as a tetradentate μ_2-η^2-η^2-ligand bridging two TM^{n+} amine complex cations has been observed in the related class of chalkogenidoarsenates.[53,54]

Variation of the Synthesis Parameters. The successful isolation and characterization of the title compounds as well as the observation that several compounds are transformed with increasing reaction time encouraged us to investigate the compound formation in more detail. Therefore, after isolation of the first compound $\{[Mn(phen)_2]_2(\mu_2\text{-}Sn_2S_6)\}$ (**1**), the reaction time was gradually increased up to finally 8 weeks. In this time window, compound **1** converts within about 3 weeks into $\{[Mn(phen)_2]_2(\mu_2\text{-}Sn_2S_6)\}$ (**3**) that is further converted into $\{[Mn(phen)_2]_2(\mu_2\text{-}Sn_2S_6)\}\cdot phen\cdot H_2O$ (**4**) within 40 days. Obviously, the long reaction times needed to obtain compounds **3** and **4** precluded experiments under static conditions. Hence, we first investigated whether compounds **1**−**4** can be obtained under stirring conditions applying the molar ratio of 1:1:3:2 for the starting materials (compare Table S1, Supporting Information). The advantage of this synthesis route is that the reaction times can be significantly reduced and often the desired products are already obtained after a few hours. In addition, the method is particularly suited to study the influence of various reaction parameters onto product formation within a reasonable time period. But, one should note that sometimes not all compounds nucleate and crystallize under stirring conditions and single crystals cannot be obtained. In the present study, selected reaction parameters such as temperature, pH value, solvent volume, amine concentration,

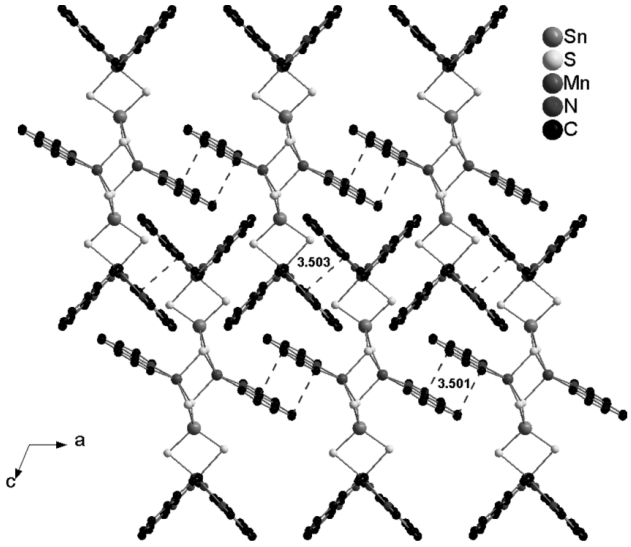

Figure 9. Off-center parallel stacking (blue dashed lines, numbers are the distances between adjacent phen molecules) of the $\{[Mn(phen)_2]_2[\mu_2\text{-}\eta^2\text{-}\eta^2\text{-}SnS_4]_2[Mn(phen)]_2\}\cdot H_2O$ units within the *ac* plane. Hydrogen atoms are omitted for clarity.

dx.doi.org/10.1021/ic500369m | *Inorg. Chem.* 2014, 53, 5619−5630

Table 2. Compounds that are Obtained if $MnCl_2 \cdot 4H_2O$, Sn, and S are Reacted with Phen at Different Temperatures Using Varying Amine Concentrations[a]

temp	40%	30%	20%	10%
150 °C	1	1	1 + 2 → 3 + 4 → 4	1 → 2 → 4
140 °C	1	1	1 + 2 → 2 → 2 + 3 + 4 → 4	2 → 4
120 °C	1	1	2	2

[a]Note that the pH value for these concentrations is ∼14.

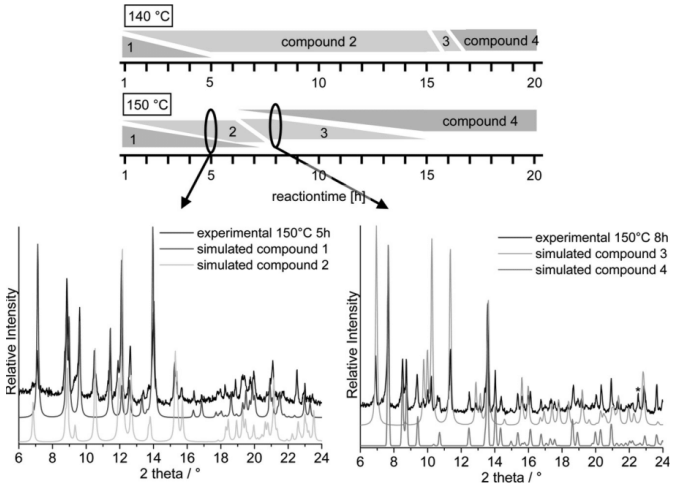

Figure 10. Top: Summary of the formation of the distinct products at an amine concentration of 20% as a function of time at 140 °C (top) and 150 °C (bottom). The pH value was ∼14. Bottom: Selected XRPD pattern of the reaction products after a reaction time of 5 h (left) and 8 h (right) at 150 °C. For further XRPD patterns, see Figures S8 and S9 (Supporting Information).

and reaction time were systematically varied. In the following, the results obtained varying these parameters are discussed.

Influence of Reaction Temperature and Concentration of the Solvent Amine. An increase of the reaction temperature increases the concentration of dissolved species, which has a direct influence on the reaction rate and crystal growth.[55] The temperature does not only affect the kinetics of the reaction but also results in a change of the autogenous pressure,[56] rate of diffusion,[56] viscosity, and dielectric constant of the solvent.[56,57] The latter will also influence the pH of the solution of strong protic solvents.[56] Applying the elements in the syntheses of thiometalates requires the usage of an amine to generate a strong alkaline medium. Elemental sulfur reacts at high pH values to form, for example, polysulfide species, that dissolve the metallic elements.[58−60] Because phen does not provide the necessary pH value, a liquid amine must be supplied. To prevent complex formation with the generated transition metal ions, a monodentate amine, for example, methylamine, is most suitable. Obviously, the pH value of the solution as well as the pressure in the reaction vessel depends on this amine concentration.

As can be seen from Table 2, only compound **1** could be synthesized with the highest amine concentrations (30−40%) independent from the reaction temperature and reaction time. By reducing the amine concentration, a clear effect of the temperature could be observed. At T = 120 °C and amine concentrations of 10% and 20%, only compound **2** is formed for reaction times of 20 h. By increasing the temperature to 140 °C (amine concentration: 20%), a mixture of compounds **1** and **2** is observed for several hours, and **1** disappears after about 5 h (Figure 10). After 16 h, **2**−**4** coexist for about 0.5 h, compounds **2** and **3** disappear, and only **4** is observed as final product. The situation is different at T = 150 °C, where **1** and **2** are simultaneously present up to about 7 h, and for a very short time period, **1**−**4** coexist followed by disappearance of **1** and **2**. Up to about 15 h reaction time, **3** and **4** could be identified in the reaction product, and for t > 15 h, only **4** was observed. The situation is quite different for 10% amine concentration where only compound **2** was observed at T = 120 °C and a conversion of compound **2** into **4** occurs at T = 140 °C. For the highest temperature of 150 °C, compound **1** is observed first for a short time, and then, **2** and **4** are successively formed with increasing reaction time. At this amine concentration, compound **3** was never observed.

As mentioned above, the concentration of the amine in aqueous solution does not only alter the pH value but the pressure in the reaction vessel. Hence, we studied the effect of the pressure onto product formation by gradually reducing the volume of the 30% methylamine solution at T = 150 °C and reaction times t = 15 and 20 h. As can be seen in Table 2, at this concentration and 2 mL of solvent, only **1** could be obtained in the selected time window. For t = 15 h for 1.6−2.0 mL, only **1** crystallized, and at 1.3−1.5 mL, a mixture of **1** and **3** occurs. Further reduction to 1.0−1.2 mL, yielded only compound **3** as reaction product (Figure 11). By increasing the reaction time to 20 h, a mixture of **1** and **3** was observed for a volume of 1.5−1.8

dx.doi.org/10.1021/ic500369m | Inorg. Chem. 2014, 53, 5619−5630

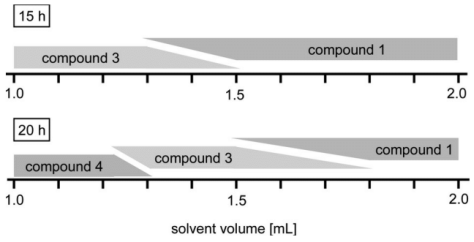

Figure 11. Summary of the formation of the individual products as a function of solvent volume at 15 h (top) and 20 h (bottom). The pH value was ~14. XRPD patterns of the reaction products are displayed in Figures S10 and S11 (Supporting Information).

mL (Figure 10). A further reduction to 1.4 mL achieved only crystallization of **3** while at 1−1.1 mL solution only **4** crystallized. These observations suggest that the conversion of the different compounds is inhibited by higher pressures. Moreover, this series of experiments shows that **2** is only obtained from an amine concentration less than or equal to 20%. But, we cannot exclude that only the pressure is the compound determining factor because a change in concentration of the reactants in solution may also influence the product formation. To verify this, the syntheses were carried out with reduced solvent volume and simultaneously adjusted sample weight. Because these syntheses yield identical results, our hypothesis that the pressure plays the most important role seems to be justified.

It is well documented that $[SnS_4]^{4-}$ tetrahedra are able to condensate to oligomeric anions with the general formula $[Sn_mS_n]^{(2n-4m)-}$,[61a,b] that is, $[Sn_2S_7]^{6-}$, $[Sn_2S_6]^{4-}$, and polymeric $[SnS_3]^{2-}_{\infty}$ species, as well as the adamantane-like $[Sn_4S_{10}]^{4-}$ anion are formed when the pH is reduced.[62] To investigate whether new compounds are formed at lower pH values, further syntheses were carried out keeping the volume of the solvent constant. Interestingly, down to pH = 11, no new compound was formed, but a clear influence on product crystallization of the title compounds was observed (Table 3).

Table 3. Summary of the Observed Compounds in the Variation of the pH Value at Different Temperatures, Constant Volume of 2 mL, and Reaction Times of 5−20 h

temp	pH 14	pH 13	pH 12	pH 11
150 °C	1	1	1 → 3	1 → 3
140 °C	1	1	1	1 → 2
120 °C	1	1	1	2

Regardless of the temperature, only compound **1** was obtained at pH = 13−14. At lower pH values (11−12), however, a significant influence of the temperature is seen. At 150 °C, first compound **1** is formed that then is transformed into **3** after 20 h (pH = 12), while the conversion at a pH = 11 took place about 5 h earlier than at pH = 12. Compound **2** could not be detected for pH = 12−14 at all temperatures. By adjusting the pH value to 11, compound **2** was the only reaction product at T = 120 °C within the selected reaction time range. For the same pH value, a conversion of **1** to **2** occurs at T = 140 °C, and for T = 150 °C, this compound could not be observed but rather the occurrence of **1** followed by conversion into **3**. These observations are in agreement with the results of the concentration studies, in which at low temperatures, also, no conversions were observed and depending on the concentration of the amine compounds **1** and **2** represented the most stable forms. However, compound **4** was not observed under the present reaction conditions.

Investigations on the Thermal Properties and the Transition Behavior. The thermal properties of {[Mn(phen)$_2$]$_2$(μ_2-Sn$_2$S$_6$)}·phen·H$_2$O (**4**) were investigated by simultaneous differential thermoanalysis and thermogravimetry (DTA-TG). In this case, it might be expected that, on heating, water is removed in the first step leading to the formation of {[Mn(phen)$_2$]$_2$(μ_2-Sn$_2$S$_6$)}·phen (**2**). On further heating, phen may be emitted, and a transformation into compounds **1** or **3** might be observed. On heating compound **4** with 4 °C/min, three distinct mass steps are observed in the TG curve that are accompanied by three endothermic events in the DTA curve (Figure 12). The experimental mass losses of 1.9% and 12.4%

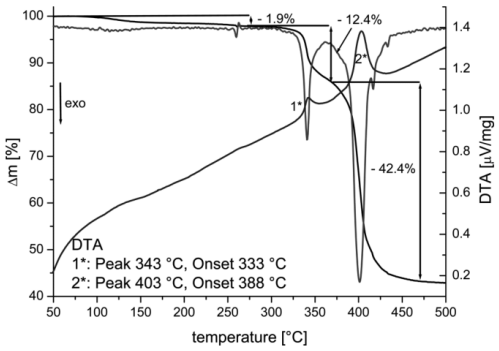

Figure 12. DTA, TG, and DTG curves of compound **4** at 4 °C/min measured in nitrogen atmosphere.

are in reasonable agreement with that calculated for the removal of water in the first and phen in the second TG step (Δm_{calc}(−H$_2$O = 1.2% and Δm_{calc}(−phen) = 12.4%). In contrast, the mass loss in the third TG step of 42.4% is only in rough agreement with that expected for the removal of the remaining four phen ligands Δm_{calc}(−4 phen) = 49.3%.

However, from the DTG curve, it is obvious that all mass steps are not well resolved, and therefore, heating rate dependent DTA-TG measurements were performed with 1, 8, and 16 °C/min (see Figure S12, Supporting Information). These investigations clearly demonstrated that the best resolution is obtained with 4 °C/min. In further investigations, additional DTA-TG measurements were performed, and the residues obtained after the first and second TG step at 260 and 360 °C were isolated and investigated by XRPD (Figure 13 and Figure S13, left, Supporting Information). Surprisingly, the X-ray powder pattern of the residue obtained after the first step corresponds to that calculated for **4**. However, the powder pattern of residue isolated after the second TG step at 360 °C corresponds to that calculated for **3** (Figure 13). It is noted that an additional reflection is observed at about 8.9°, which does not correspond to one of the reflections of the second modification **1**, and at the moment, we have no explanation for this observation. However, as mentioned above, the powder pattern of the residue obtained after the first TG step is similar to that of the pristine material **4**. To investigate if compound **2**

dx.doi.org/10.1021/ic500369m | Inorg. Chem. 2014, 53, 5619−5630

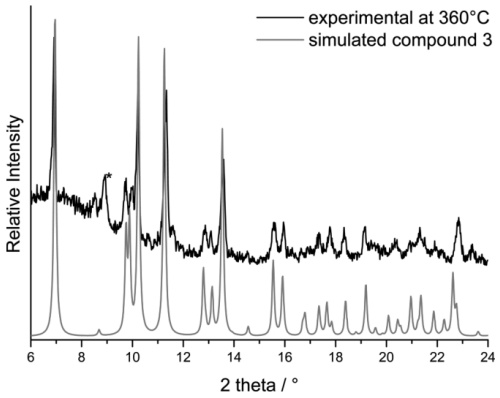

Figure 13. Experimental X-ray powder pattern of the residue obtained after the second TG step at 360 °C and simulated pattern for compound **3** calculated from single-crystal data. The additional reflection that cannot be assigned to one of compounds **1** or **3** is indicated by a star.

can be obtained at higher temperatures, a second TG run was performed and stopped at 340 °C. Comparison of the experimental X-ray powder pattern of this residue with those calculated for all compounds clearly shows that a mixture of compounds **4** and **3** is obtained (Figure S13, right, Supporting Information). Therefore, it can be assumed that the water is removed from **4** without significant structural changes leading to a compound of the same composition as **2**, which in this case represents a further modification.

To gain further knowledge on the thermal behavior of compound **4**, measurements using temperature-dependent XRPD were performed (Figures S14 and S15, Supporting Information). In this case, all reflections of compound **4** disappear at about 315 °C, indicating the formation of an amorphous phase, which does not crystallize on further heating. The discrepancy between the DTA-TG and temperature-dependent XRPD experiments is not surprising because they are performed under different experimental conditions and it is well known that the outcome of a thermal decomposition depends on a number of parameters, for example, the heating rate and the atmosphere used in the measurement.

Investigations on the Stability of Compounds 1 and 3. As mentioned above, thermal decomposition of compound **4** leads to the formation of compound **3** as an intermediate, which exhibits the same composition as compound **1**. Whether they truly represent polymorphic modifications is difficult to decide because the structure of **1** contains small cavities in which no electron density could be located indicating that they are empty (see the Single-Crystal Structure Determination section). In contrast, in **3**, some residual electron density was found in the cavities indicative for the presence of disordered solvent. However, one must keep in mind that **3** can be isolated at 360 °C by thermal decomposition of compound **4**, and hence, it is practically impossible that the cavities are filled with some solvent. Therefore, even if **3** contains some residual solvent, it can be assumed that it can be removed without collapse of the structure, and therefore, it is highly likely that **1** and **3** represent polymorphic modifications. In any case, the question rises which of the two compounds is more stable at room temperature. To answer this question, a solvent-mediated conversion experiment was performed in which a mixture of both forms was stirred in a saturated solution in water with an excess of the solid material. After 2 days, the residue was filtered off and investigated by XRPD measurements, which clearly proves that the mixture is still present (see Figure S16, Supporting Information). This might be traced back to a low solubility of compounds **1** and **3** in water that prevents a transformation into the more stable compound. To determine the solubility of **1** and **3**, a solution of each of the compounds with an excess of solid was stirred for only 1 day in water to exclude any transformation into the more stable compound. Afterward, a distinct volume of the clear solution was

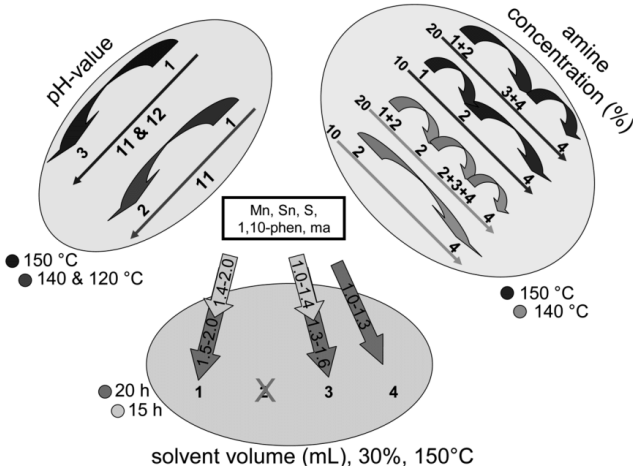

Figure 14. Overview of the results of the investigation of the influence of selected synthesis parameters on the formation of compounds **1**–**4** (see text).

dx.doi.org/10.1021/ic500369m | *Inorg. Chem.* 2014, 53, 5619−5630

investigated by AAS (Table S9, Supporting Information). The result clearly shows that compound **3** is less soluble and therefore should be more stable at room temperature than **1**.

■ CONCLUSIONS

In the structures of **1**−**4**, a central $[Sn_2S_6]^{4-}$ bitetrahedron bridges two unsaturated $[Mn(phen)_2]^{2+}$ complex cations by the four terminal S atoms to form neutral $\{[Mn(phen)_2]_2(\mu_2\text{-}Sn_2S_6)\}$ moieties, a connection mode never observed for the $[Sn_2S_6]^{4-}$ anion. Compound **5** belongs to the group of less common compounds with a $[SnS_4]^{4-}$ unit acting as a bridging ligand. In addition, in this compound, the $[SnS_4]$ unit exhibits a unique coordination mode.

The results of the systematic study of the influence of synthesis parameters onto product formation are schematically summarized in Figure 14. At high amine concentrations (30−40%) affording high pH values (solvent volume constant of 2 mL), only compound **1** crystallized at T = 120−150 °C. Lowering the concentration to 10−20%, phase pure **2** is obtained at the lowest temperature, while a more complex behavior of occurrence and conversion of the samples are found at higher temperatures and 10−20% amine concentrations. It is remarkable that compound **3** could not be observed under these reaction conditions. The solvent volume also strongly affects nucleation and growth of the individual compounds (t = 20 h). Compound **4** is formed at the lowest volume while **1** is observed at the highest volume. It seems that a high pressure in the reaction vessel suppresses conversion of **1** into the other compounds with time as observed for low amine concentrations and a constant volume of 2 mL. Finally, crystallization of a distinct compound can be controlled by adjusting the pH value. For T = 120 °C and pH = 11, compound **2** crystallized as phase pure material while for T = 140 °C first compound **1** occurs that is then transformed into **2**. The final reaction product at T = 150 °C and pH = 11−12 is compound **3** that appears after **1** disappeared.

The results obtained during the studies are remarkable with respect to several points. Stirring the reaction slurry allows a relatively fast screening of the parameter space of solvothermal syntheses compared to traditional reactions performed for several days. In addition, new compounds can be discovered within reasonable time frames that require long time periods if static conditions are applied. Under stirring conditions, the formation of concentration gradients within the reaction mixtures is avoided yielding phase pure materials if the synthesis parameters are appropriately adjusted. Finally, the results demonstrate the complexity of the solvothermal approach, and only a systematic variation of the synthesis conditions leads to a better understanding of these reactions. The mechanism of the conversion or transformation of the different compounds cannot be deduced from the experiments. Two further interesting results should be shortly highlighted. Compound **5** was only observed in low yield using a Teflon-lined steel autoclave while compound **2** crystallized only in glass tubes. These observations indicate that the surface of the reaction vessel plays an important but yet not understood role for the nucleation of distinct compounds.

The two compounds **1** and **3** are presumably polymorphs and follow the density rule, that is, the density of **3** is larger than that of **1** suggesting that **3** is thermodynamically stable at low temperatures. The compounds **2** and **4** may be viewed as pseudopolymorphs of **1** and **3**.

■ ASSOCIATED CONTENT

Supporting Information

Experimental and simulated XRPD patterns of **1**−**5** (Figure S1); results of the UV/vis, IR, and Raman measurements of **1**−**5** (Figures S2−S4); illustration of the arrangement of the molecules in the structures **1** and **2** (Figures S5−S7); selected XRPD patterns for the series of time-dependent formation experiments at 140 and 150 °C (Figures S8 and S9, respectively); selected XRPD patterns for the series of solvent volume-dependent formation after 15 and 20 h (Figures S10 and S11, respectively); thermogravimetric curves of compound **4** for different heating rates (Figure S12); powder pattern of the decomposition of **4** at 260 and 340 °C (Figure S13); illustration of an overview of the temperature-dependent XRPD experiments (Figures S14 and S15); powder pattern before and after solvent-mediated conversion experiments of **1** and **3** (Figure S16); an overview of the reaction conditions, an overview of the solvent mixtures, the absorptions of the IR spectra, and data of the signals in the Raman spectra (Tables S1−S4); selected bond length and angles of **1**−**5**, selected bond length and angles of **1** and **3** compared to $Na_4Sn_2S_6{\cdot}14H_2O$, dihedral angles between the phenanthroline moieties for compounds **1**−**5**, and selected bond length and angles of compound **5** compared to $Na_4SnS_4{\cdot}14H_2O$ (Tables S5−S8); results of the solubility measurement of AAS (Table S9) This material is available free of charge via the Internet at http://pubs.acs.org. Structural data have been deposited in the Cambridge Crystallographic Data Centre as publication nos. CCDC 999247 (**1**), CCDC 999248 (**2**), CCDC 999249 (**3**), CCDC 99250 (**4**), and CCDC 999251 (**5**). Copies of the data can be obtained, free of charge, on application to CCDC, 12 Union Road, Cambridge CB2 1 EZ, UK (deposit@ccdc.ca.ac.uk).

■ AUTHOR INFORMATION

Corresponding Author

*Phone: +49 431 880-2419; fax: +49 431 880-1520; e-mail: wbensch@ac.uni-kiel.de.

Notes

The authors declare no competing financial interest.

■ ACKNOWLEDGMENTS

Financial support by the State of Schleswig-Holstein is gratefully acknowledged.

■ REFERENCES

(1) Sheldrick, W. S.; Wachhold, M. *Coord. Chem. Rev.* **1998**, *176*, 211−322.
(2) Sheldrick, W. S. *J. Chem. Soc., Dalton Trans.* **2000**, 3041−3052.
(3) Bu, X. H.; Zheng, N. F.; Feng, P. Y. *Chem.—Eur. J.* **2004**, *10*, 3356−3362.
(4) Feng, P. Y.; Bu, X. H.; Zheng, N. F. *Acc. Chem. Res.* **2005**, *38*, 293−303.
(5) Dehnen, S.; Melullis, M. *Coord. Chem. Rev.* **2007**, *251*, 1259−1280.
(6) Jiang, T.; Lough, A.; Ozin, G. A. *Adv. Mater.* **1998**, *10*, 42−46.
(7) Ahari, H.; Ozin, G. A.; Bedard, R. L.; Petrov, S.; Young, D. *Adv. Mater.* **1995**, *7*, 370−374.
(8) Enzel, P.; Henderson, G. S.; Ozin, G. A.; Bedard, R. L. *Adv. Mater.* **1995**, *7*, 64−68.
(9) Parise, J. B.; Ko, Y. H.; Rijssenbeek, J.; Nellis, D. M.; Tan, K. M.; Koch, S. *J. Chem. Soc., Chem. Commun.* **1994**, 527.
(10) Pienack, N.; Schinkel, D.; Puls, A.; Ordolff, M.-E.; Lühmann, H.; Näther, C.; Bensch, W. *Z. Naturforsch.* **2012**, *67b*, 1098−1106.

(11) Park, Y.; Liao, J. H.; Kim, K. W.; Kanatzidis, M. G. *Inorg. Organomet. Oligomers Polym., Proc. IUPAC Symp. Macromol.* **1991**, *33*, 263−276.
(12) Manos, M. J.; Kanatzidis, M. G. *Inorg. Chem.* **2009**, *48*, 4658−4660.
(13) Sheldrick, W. S. *Z. Anorg. Allg. Chem.* **1988**, *562*, 23−30.
(14) Sheldrick, W. S.; Schaaf, B. *Z. Anorg. Allg. Chem.* **1994**, *620*, 1041−1045.
(15) Schaefer, M.; Kurowski, D.; Pfitzner, A.; Näther, C.; Rejai, Z.; Müller, K.; Ziegler, N.; Bensch, W. *Inorg. Chem.* **2006**, *45*, 3726−3731.
(16) Seidlhofer, B.; Antonova, E.; Wang, J.; Schinkel, D.; Bensch, W. *Z. Anorg. Allg. Chem.* **2012**, *638*, 2555−2564.
(17) (a) Engelke, L.; Schaefer, M.; Schur, M.; Bensch, W. *Chem. Mater.* **2001**, *13*, 1383−1390. (b) Michailovski, A.; Kiebach, R.; Bensch, W.; Grunwaldt, J.-D.; Baiker, A.; Komarneni, S.; Patzke, G. R. *Chem. Mater.* **2007**, *19*, 185−197. (c) Engelke, L.; Schaefer, M.; Porsch, F.; Bensch, W. *Eur. J. Inorg. Chem.* **2003**, 506−513. (d) Antonova, E.; Seidlhofer, B.; Wang, J.; Hinz, M.; Bensch, W. *Chem.—Eur. J.* **2012**, *18*, 15316−15322. (e) Kiebach, R.; Pienack, N.; Ordolff, M.-E.; Studt, F.; Bensch, W. *Chem. Mater.* **2006**, *18*, 1196−1205.
(18) Liu, G.-N.; Guo, G.-C.; Zhang, M.-J.; Guo, J.-S.; Zeng, H. Y.; Huang, J.-S. *Inorg. Chem.* **2011**, *50*, 9660−9669.
(19) Liu, G.-N.; Guo, G.-C.; Chen, F.; Guo, S.-P.; Jiang, X.-M.; Yang, C.; Wang, M. S.; Wu, M. F.; Huang, J. S. *CrystEngComm* **2010**, *12*, 4035−4037.
(20) van Santen, R. A. *J. Phys. Chem.* **1984**, *88*, 5768−5769.
(21) Ostwald, W. *Z. Phys. Chem.* **1897**, *22*, 289.
(22) Sheldrick, G. M. *SHELXS-97, Program for the Solution of Crystal Structures*; University of Göttingen: Göttingen, Germany, 1997.
(23) Sheldrick, G. M. *SHELXL-97, Program for the Refinement of Crystal Structures*; University of Göttingen: Göttingen, Germany, 1997.
(24) Pienack, N.; Näther, C.; Bensch, W. *Eur. J. Inorg. Chem.* **2009**, 1575−1577.
(25) Pienack, N.; Näther, C.; Bensch, W. *Z. Naturforsch.* **2008**, *63b*, 1243−1251.
(26) Zhou, J.; Bian, G.-Q.; Dai, J.; Zhang, Y.; Tang, A.; Q.-Y. Zhu, Q.-Y. *Inorg. Chem.* **2007**, *46*, 1541−1543.
(27) Pienack, N.; Puls, A.; Näther, C.; Bensch, W. *Inorg. Chem.* **2008**, *47*, 9606−9611.
(28) Pienack, N.; Lehmann, S.; Lühmann, H.; El-Madani, M.; Näther, C.; Bensch, W. *Z. Anorg. Allg. Chem.* **2008**, *634*, 2323−2329.
(29) Behrens, M.; Scherb, S.; Näther, C.; Bensch, W. *Z. Anorg. Allg. Chem.* **2003**, *629*, 1367−1373.
(30) Jia, D.-X.; Zhang, Y.; Dai, J.; Zhu, Q.-Y.; Gu, X.-M. *Z. Anorg. Allg. Chem.* **2004**, *630*, 313−318.
(31) Fu, M.-L.; Guo, G.-C.; Liu, B.; Wu, A.-Q.; Huang, J.-S. *Chin. J. Inorg. Chem.* **2005**, *21*, 25−29.
(32) Gu, X.-M.; Dai, J.; Jia, D.-X.; Zhang, Y.; Zhu, Q.-Y. *Cryst. Growth Des.* **2005**, *5*, 1845−1848.
(33) Jia, D.-X.; Dai, J.; Zhu, Q.-Y.; Zhang, Y.; Gu, X. M. *Polyhedron* **2004**, *23*, 937−942.
(34) Zhou, J.; Liu, X.; Chen, G.-Q.; Zhang, F.; Li, L.-R. *Z. Naturforsch.* **2010**, *65b*, 1229−1234.
(35) Wang, Z.; Xu, G.; Bi, Y.; Wang, C. *CrystEng. Comm.* **2010**, *12*, 3703−3707.
(36) Krebs, B.; Pohl, S.; Schiwy, W. *Z. Anorg. Allg. Chem.* **1972**, *393*, 241−252.
(37) Seidlhofer, B.; Pienack, N.; Bensch, W. *Z. Naturforsch.* **2010**, *65b*, 937−975.
(38) Zhou, J.; Liu, X.; Chen, G.-Q.; Zhang, F.; Li, L. R. *Z. Naturforsch.* **2010**, *65b*, 1229−1234.
(39) Kromm, A.; Sheldrick, W. S. *Z. Anorg. Allg. Chem.* **2008**, *634*, 1005−1010.
(40) Martinez, C. R.; Iverson, B. L. *Chem. Sci.* **2012**, *3*, 2191.
(41) Grimme, S. . University of Bonn, Germany. Private communication, TPSS-D3/def2-TZVP method; accuracy of energies calculated with the method is about 5−10%.
(42) (a) Goerigk, L.; Kruse, H.; Grimme, S. *ChemPhysChem* **2011**, *12*, 3421−3433. (b) Grimme, S. *Angew. Chem., Int. Ed.* **2008**, *47*, 3430−3434.
(43) Grimme, S. *WIREs Comput. Mol. Sci.* **2011**, *1*, 211−228.
(44) Grimme, S.; Antony, J.; Ehrlich, S.; Krieg, H. *J. Chem. Phys.* **2010**, *132*, 154104.
(45) Seela, J. L.; Folting, K.; Wang, R.-J.; Huffmann, J. C. G.; Cristou, G. *Inorg. Chem.* **1985**, *24*, 4454−4456.
(46) Seela, J. L.; Knapp, M. J.; Kolack, K. S.; Chang, H.-R.; Huffman, J. C.; Hendrickson, D. N.; G. Christou, G. *Inorg. Chem.* **1998**, *37*, 516−525.
(47) Lin, C.-H.; Chen, C.-G.; Tsai, M.-L.; Lee, G.-H.; Liaw, W.-F. *Inorg. Chem.* **2008**, *47*, 11435−11443.
(48) Tamura, H.; Tanaka, S.; Matsubayashi, G.; Mori, W. *Inorg. Chim. Acta* **1995**, *232*, 51−55.
(49) Schiwy, W.; Pohl, S.; Krebs, B. *Z. Anorg. Allg. Chem.* **1973**, *402*, 77−86.
(50) Pienack, N.; Näther, C.; Bensch, W. *Solid States Sci.* **2007**, *9*, 100−107.
(51) Pienack, N.; Bensch, W. *Z. Anorg. Allg. Chem.* **2006**, *632*, 1733−1736.
(52) Pienack, N.; Möller, K.; Näther, C.; Bensch, W. *Solid States Sci.* **2007**, *9*, 1110−1114.
(53) Liu, G.-N.; Guo, G.-C.; Chen, F.; Wang, S.-H.; Sun, J.; Huang, J.-S. *Inorg. Chem.* **2012**, *51*, 472−482.
(54) Jia, D.; Zhao, J.; Pan, Y.; Tang, W.; Wu, B.; Zhang, Y. *Inorg. Chem.* **2011**, *50*, 7195−7201.
(55) Demazeau, G. *J. Mater. Sci.* **2008**, *43*, 2104−2114.
(56) Rabenau, A. *Angew. Chem.* **1985**, *97*, 1017−1032; *Angew. Chem., Int. Ed. Engl.* **1985**, *24*, 1026−1040.
(57) Schur, M. Dissertation. Johann-Wolfgang-Goethe-Universität, Frankfurt am Main, 1999.
(58) Jiang, T.; Lough, A.; Ozin, G. A.; Bedard, R. L. *J. Mater. Chem.* **1998**, *8*, 733−741.
(59) Schur, M.; Bensch, W. *Z. Kristallogr.* **1997**, *212*, 305−307.
(60) Schur, M.; Bensch, W. *Z. Anorg. Allg. Chem.* **1998**, *624*, 310−314.
(61) (a) Sheldrick, W. S.; Wachhold, M. *Angew. Chem.* **1997**, *109*, 214−234. (b) *Angew. Chem., Int. Ed. Engl.* **1997**, *36*, 206−224.
(62) Krebs, B. *Angew. Chem.* **1983**, *95*, 113−134; *Angew. Chem., Int. Ed. Engl.* **1983**, *22*, 113−134.

3.1.2 Synthese der Verbindungen {[TM(phen)$_2$]$_2$[Sn$_2$S$_6$]} und {[TM(phen)$_2$]$_2$[Sn$_2$S$_6$]}·phen·H$_2$O (TM = Fe, Co) unter solvothermalen Bedingungen.

Zusammenfassung der Veröffentlichung „The [Sn$_2$S$_6$]$^{4-}$ Anion as Tetradentate Linker: Solvothermal Synthesis and Selected Properties of {[TM(phen)$_2$]$_2$[Sn$_2$S$_6$]} and {[TM(phen)$_2$[Sn$_2$S$_6$]}·phen·H$_2$O (TM = Co, Fe).

Die Fe- und Co-haltigen Zinn-Schwefel-Verbindungen mit der allgemeinen Formel {[TM(phen)$_2$]$_2$[Sn$_2$S$_6$]} ($P2_1/n$, Z=2) und {[TM(phen)$_2$]$_2$[Sn$_2$S$_6$]}·phen·H$_2$O ($P\bar{1}$, Z=1) wurden unter solvothermalen Bedingungen erhalten. Die eisenhaltigen Verbindungen wurden aus Fe, Sn, S und phen (1:1:1:2) in wässriger Methylaminlösung bei 120°C hergestellt. Entscheidend für die unterschiedliche Kristallisation dieser Verbindungen war die Reaktionszeit: Nach drei Tagen wurde die Verbindung {[Fe(phen)$_2$]$_2$[Sn$_2$S$_6$]} erhalten, welche sich mit zunehmender Reaktionszeit in das Pseudopolymorph {[Fe(phen)$_2$]$_2$[Sn$_2$S$_6$]}·phen·H$_2$O umwandelte. Die cobalthaltigen Verbindungen wurden mit Co bzw. CoCl$_2$·6H$_2$O sowie Sn, S und phen (1:1:3:2) in wässriger Methylaminlösung (120°C, 5d) synthetisiert. Bei diesen Verbindungen war nicht die Reaktionszeit, sondern die Co-Quelle für die Kristallisation der verschiedenen Verbindungen entscheidend: Bei der Verwendung von CoCl$_2$·6H$_2$O wurde {[Co(phen)$_2$]$_2$[Sn$_2$S$_6$]} erhalten, mit elementarem Co kristallisierte das Pseudopolymorph {[Co(phen)$_2$]$_2$[Sn$_2$S$_6$]}·phen·H$_2$O.

In der Struktur sind zwei [TM(phen)$_2$]$^{2+}$-Komplexe über eine verbrückende [Sn$_2$S$_6$]$^{4-}$-Einheit miteinander verbunden. Die Anordnung der Moleküle wird durch π-π Wechselwirkungen stabilisiert.

Die Strukturen dieser Verbindungen sind insofern bemerkenswert, da zum einen sehr wenige eisen- und cobalthaltige Verbindungen bekannt waren.[43,46,48,51,76] Zum anderen diese wenigen Beispiele in nur einem Fall isostrukturell zueinander waren.[48]

ARTICLE

DOI: 10.1002/zaac.201400369

The $[Sn_2S_6]^{4-}$ Anion Acting as Tetradentate Linker: Solvothermal Synthesis and Selected Properties of $\{[TM(phen)_2]_2Sn_2S_6\}$ and $\{[TM(phen)_2]_2Sn_2S_6\}\cdot phen\cdot H_2O$ (*TM* = Fe, Co)

Jessica Hilbert,[a] Christian Näther,[a] and Wolfgang Bensch*[a]

Dedicated to Professor Martin Jansen on the Occasion of His 70th Birthday

Keywords: Tin; Sulfur; Solvothermal syntheses; Crystal structure; Spectroscopic properties; Hirshfeld surface analysis

Abstract. Four new compounds with the $[Sn_2S_6]^{4-}$ anion acting as tetradentate ligand to metal cations of $[TM(phen)_2]^{2+}$ complexes (*TM* = Fe, Co; phen = 1,10-phenanthroline) were synthesized under solvothermal conditions. The compounds are rare cases where Fe^{2+}/Co^{2+} cations form bonds to sulfide anions of a thiometallate anion. In the structures of the compounds the $\{[TM(phen)_2]_2Sn_2S_6\}$ molecule is the main structural motif. The phen ligands of neighboring molecules are oriented in a way that off-center parallel stacking results leading to weak intermolecular interactions. In two of the four compounds a free phen molecule is trapped between adjacent $\{[TM(phen)_2]_2Sn_2S_6\}$ moieties and an additional H_2O molecule is located near the two nitrogen atoms of the free phen molecule. The Hirshfeld surface analysis yields a variety of weak intermolecular interactions which may be regarded as essential for the packing arrangement of the different constituents and the stability of the compounds.

Dedicated Cluster

Introduction

Thiometallate compounds are mainly prepared by the solvothermal route and many of these materials exhibit fascinating structural features and interesting properties as discussed in several review articles.[1–6] In the past few years it was demonstrated that the physico-chemical properties of such compounds can be altered by integration of transition metal cations (TMCs) into the networks.[7] The most often observed SnS_x building units are the $[SnS_4]^{4-}$ tetrahedron[8–13] and the $[Sn_2S_6]^{4-}$ bi-tetrahedron.[14–25] Less-common species are e.g. the $[Sn_2S_7]^{6-}$ building unit[26] or the polymeric $[SnS_3]_\infty^{2-}$, anion which are formed by condensation of the $[SnS_4]^{4-}$ moiety yielding a series with the general formula $[Sn_mS_n]^{(2n-4m)-}$ [27] as well as the adamantane-like $[Sn_4S_{10}]^{4-}$ anion.[28] More complex SnS_x entities were also reported like Sn_4S_6 or Sn_8S_{12} cores in thiostannate derivatives.[29] The $[Sn_2S_6]^{4-}$ anion mostly occurs as isolated entity,[30–37] or is acting as bidentate ligand to a metal cations using the *trans* terminal sulfur atoms.[17,38,39] A tridentate binding mode of the $[Sn_2S_6]^{4-}$ anion was also reported in literature.[40] Among the compounds with transition metal cations bonded to a thiostannate anion via *TM*–S bond only one example is known for Fe^{2+} [17] and three were reported for Co^{2+}.[17,18,40] In these compounds multidentate amine molecules were applied leaving binding sites free at the transition metal cations for bond formation to the $[Sn_2S_6]^{4-}$ anion. But Fe^{2+}/Co^{2+}–S bond formation in the presence of a bidentate amine molecule was never observed. Recently, we systematically studied the formation of Mn^{2+} containing thiostannates in the system Mn/Sn/S/1,10-phenanthroline (phen) by varying the reaction parameters. We were able to isolate and characterize four new compounds featuring the $[Sn_2S_6]^{4-}$ anion acting as tetradentate ligand and one compound with the $[SnS_4]^{4-}$ anion exhibiting an unusual coordination mode.[41]

To investigate the influence of the metal cation into more detail we now extended the synthetic experiments to Fe^{2+} and Co^{2+}. Within these investigations we prepared four new compounds of composition $\{[TM(C_{12}H_8N_2)_2]_2Sn_2S_6\}$ and $\{[TM(C_{12}H_8N_2)_2]_2Sn_2S_6\}\cdot C_{12}H_8N_2\cdot H_2O$ (*TM* = Fe, Co. $C_{12}H_8N_2$ = phen). Herein we report the solvothermal syntheses and selected properties of these compounds.

Experimental Section

General: All chemicals were purchased and used without further purifications. All compounds were prepared under solvothermal conditions in glass tubes (inner volume 11 mL) using Fe, Co, $CoCl_2\cdot 6H_2O$, tin, sulfur and 1,10-phenanthroline (phen, $C_{12}H_8N_2$). The crystalline products were filtered off after the reactions, washed with water and ethanol or acetone and dried in vacuo. The reaction products were separated manually and the homogeneity of the crystalline part was checked by X-ray powder diffraction and elemental analysis.

Synthesis of $\{[Fe(C_{12}H_8N_2)_2]_2Sn_2S_6\}$ (I): Fe (14.0 mg, 0.25 mmol), Sn (29.7 mg, 0.25 mmol), S (24.1 mg, 0.75 mmol), and phen (90.1 mg,

* Prof. Dr. W. Bensch
Fax: +49-431-880-1520
E-Mail: wbensch@ac.uni-kiel.de
[a] Institute of Inorganic Chemistry
Christian-Albrechts-University of Kiel
Max-Eyth-Str. 2
24118 Kiel, Germany

Zeitschrift für anorganische und allgemeine Chemie ZAAC Journal of Inorganic and General Chemistry

0.5 mmol) with methylamine (1.5 mL, 40 %, aqueous solution, abcr) and water (0.5 mL) were reacted in a glass tube. The mixture was heated at 120 °C for 3 d. Black crystals located on greyish-black chunks were manually separated giving a yield of about 15 % based on tin. According to EDX-analysis the greyish-black materials contained Fe, Sn, and S but no reflections could be detected in the X-ray powder pattern, suggesting the presence of amorphous Fe/Sn sulfides. Elemental analysis: calcd. C 45.7, H 2.6, N 8.9 %; found: C 45.3, H 2.4, N 8.6 %.

Synthesis of $\{[Fe(C_{12}H_8N_2)_2]_2Sn_2S_6\}\cdot C_{12}H_8N_2\cdot H_2O$ (II): Fe (14.0 mg, 0.25 mmol), Sn (29.7 mg, 0.25 mmol), S (24.1 mg, 0.75 mmol), and phen (90.1 mg, 0.5 mmol, $C_{12}H_8N_2$) with methylamine (1.5 mL, 40 %, aqueous solution, abcr) and water (0.5 mL) were reacted in a glass tube at 120 °C for 9 d. The black crystals of **II** with a yield of app. 25 % (based on Sn) were located on the surface of a dark grey powder. Like for **I** no reflections were seen in the X-ray powder pattern of this powder indicating the presence of amorphous sulfides. Elemental analysis: calcd. C 49.3, H 2.9, N 9.6 %; found: C 48.9, H 2.9, N 9.6 %.

Synthesis of $\{[Co(C_{12}H_8N_2)_2]_2Sn_2S_6\}$ (III): $CoCl_2\cdot 6H_2O$ (59.5 mg, 0.25 mmol), Sn (29.7 mg, 0.25 mmol), S (24.1 mg, 0.75 mmol), and phen (90.1 mg, 0.5 mmol, $C_{12}H_8N_2$) with methylamine (1.5 mL, 40 %, aqueous solution, abcr) and water (0.5 mL) were reacted in a glass tube. The mixture was heated at 120 °C for 5 d. The yield of the dark red crystals was only about 1 % (based on Sn). The main product consists of X-ray amorphous sulfides. Elemental analysis: calcd. C 45.5, H 2.5, N 8.8 %; found: C 45.1, H 2.4, N 8.5 %.

Synthesis of $\{[Co(C_{12}H_8N_2)_2]_2Sn_2S_6\}\cdot C_{12}H_8N_2\cdot H_2O$ (IV): Co (14.5 mg, 0.25 mmol), Sn (29.7 mg, 0.25 mmol), S (24.1 mg, 0.75 mmol), and phen (90.1 mg, 0.5 mmol, $C_{12}H_8N_2$) with methylamine (1.5 mL, 40 %, aqueous solution, abcr) and water (0.5 mL) were reacted in a glass tube. The mixture was heated at 120 °C for 5 d. The major product seems to consist of X-ray amorphous sulfides. The yield of the dark red crystals was ca. 20 % based on tin. Elemental analysis: calcd. C 49.1, H 2.9, N 9.6 %; found: C 48.7, H 2.8, N 9.4 %.

Structure Determination: The intensity data for the compounds were collected using a STOE IPDS-1 (Imaging Plate Diffraction System) with Mo-K_α radiation at room temperature. The structures were solved with direct methods using the program SHELXS-97 and the refinements were done against F^2 with SHELXL-97.[42] For all non-hydrogen atoms anisotropic displacement parameters were used. The hydrogen atoms were positioned with idealized geometry and were refined using a riding model. In compound **II** and **IV**, the O–H hydrogen atoms could not be located in the difference map, but were considered in the formula. One phen ligand was disordered around a center of inversion. This ligand seems to interact with one water molecule. Both of them were refined with half occupancy. The disorder remains constant if the structure refinement is performed in space group $P1$, where all atoms are located in general positions. There are also no hints for super structure reflections.

Selected refinement results are summarized in Table 1.

Crystallographic data (excluding structure factors) for the structures in this paper have been deposited with the Cambridge Crystallographic Data Centre, CCDC, 12 Union Road, Cambridge CB21EZ, UK. Copies of the data can be obtained free of charge on quoting the depository numbers CCDC-1018578 (**I**), CCDC-1018579 (**II**), CCDC-1018580 (**III**), and CCDC-1018581 (**IV**) (Fax: +44-1223-336-033; E-Mail: deposit@ccdc.cam.ac.uk, http://www.ccdc.cam.ac.uk).

X-ray Powder Diffractometry: The X-ray powder diffraction patterns were recorded with a STOE Stadi-P powder diffractometer (Cu-$K_{\alpha 1}$ radiation, λ = 1.540598 Å, Ge monochromator) in transmission geometry.

EDX Experiments: Scanning electron microscopy investigations and energy dispersive X-ray analyses (EDX) were done with a Philips En-

Table 1. Selected details of the data collection and structure refinement results for compounds **I–IV**.

	$\{[Fe(phen)_2]_2Sn_2S_6\}$ (**I**)	$\{[Fe(phen)_2]_2Sn_2S_6\}\cdot$phen H_2O (**II**)	$\{[Co(phen)_2]_2Sn_2S_6\}$ (**III**)	$\{[Co(phen)_2]_2Sn_2S_6\}$ phen H_2O (**IV**)
Crystal system	monoclinic	triclinic	monoclinic	triclinic
Space group	$P2_1/n$	$P\bar{1}$	$P2_1/n$	$P\bar{1}$
M /g·mol^{-1}	1262.26	1460.48	1268.42	1466.64
a /Å	10.7112(3)	11.2219(5)	10.7234(4)	11.1548(11)
b /Å	9.9266(4)	12.1407(6)	9.8026(2)	12.1375(11)
c /Å	25.3421(8)	12.7130(6)	24.8913(10)	12.6701(11)
α /°	90	113.956(4)	90	114.481(10)
β /°	93.194(3)	89.821(4)	94.046(3)	88.891(11)
γ /°	90	110.318(4)	90	110.404(10)
V /Å^3	2690.33(16)	1465.02(12)	2609.98(15)	1447.0(2)
Temperature /K	293(2)	293(2)	293(2)	200(2)
Z	2	1	2	1
$D_{calculated}$ /g·cm^{-3}	1.558	1.655	1.614	1.683
μ /mm^{-1}	1.719	1.593	1.851	1.685
Scan range /°	$2.03 \le \theta \le 24.62$	$1.78 \le \theta \le 27.00$	$1.64 \le \theta \le 24.60$	$2.21 \le \theta \le 27.00$
Reflections collected	18892	15811	23024	20374
Independent reflections	4463	6390	4378	6188
Observed reflections	3924	5063	3758	5056
Goodness-of-fit on F^2	1.218	1.128	1.187	1.022
R values [$I > 2\sigma(I)$]	R_1 = 0.0648 wR_2 = 0.1629	R_1 = 0.0404, wR_2 = 0.0832	R_1 = 0.0405 wR_2 = 0.1061	R_1 = 0.0370 wR_2 = 0.0952
R values (all data)	R_1 = 0.0732 wR_2 = 0.1661	R_1 = 0.0597, wR_2 = 0.0886	R_1 = 0.0498 wR_2 = 0.1098	R_1 = 0.0455 wR_2 = 0.0989
Res. elec. dens. /e·Å^3	0.624 and 0.653	0.846 and 0.618	0.572 and 0.356	1.291 and 1.378

vironmental Scanning Electron Microscope ESEM XL30 equipped with an EDAX detector.

Raman Spectroscopy: Raman spectra were recorded with a Bruker IFS 66 Fourier transform Raman spectrometer (wavelength: 541.5 nm) in the region from 100 to 3500 cm^{-1}.

Infrared Spectroscopy: MIR spectra (450–3000 cm^{-1}) were recorded with an ATI Mattson Genesis spectrometer.

Results and Discussion

Synthetic Aspects

In our previous study of the system Mn/Sn/S/1,10-phenanthroline five different compounds could be isolated.[41] These compounds were obtained whilst stirring conditions of the reaction slurry varying the time, temperature and amount of solvent. All attempts to synthesize the analogous Fe/Co compounds applying identical reaction conditions failed. One can only speculate about the reason but the comparable affinity of Mn^{2+} to form bonds to both S and N may be a key difference to Fe^{2+}/Co^{2+}, which normally prefer bonding to only N ligands or sulfide anions. Under stirring conditions tin as well as the transition metals may react very fast with the in-situ formed sulfide species and only X-ray amorphous products were formed. Applying static reaction conditions a concentration gradient may be present producing the species in solution necessary for nucleation and crystallization of the title compounds, besides amorphous products. This scenario may explain the low yield observed, while in the Mn^{2+} system four compounds could be prepared as phase pure products. At the moment no explanation is at hand why the reaction with $CoCl_2 \cdot 6H_2O$ afforded crystallization of **III**, while elemental Co results in a mixture of **III** and **IV** after the first day and only **IV** could be identified after 5 d reaction time. Extending the reaction time of the slurries with $CoCl_2 \cdot 6H_2O$ beyond 5 d resulted in a mixture of **III** and **IV**. The mixture for the synthesis of **III** contains slightly more water than that used for the preparation of **IV**. There is no simple explanation why the latter compound crystallized with a water molecule and **III** without a H_2O molecule. One should keep in mind that solvothermal reactions are complex and variation of one synthesis parameters affects others in a not well understood way often preventing an explanation why a compound is formed or not.

Crystal Structures

$[Fe(phen)_2]_2Sn_2S_6$ (**I**) and its Co^{2+} containing counterpart $[Co(phen)_2]_2Sn_2S_6$ (**III**) are isotypic and crystallize in the monoclinic space group $P2_1/n$ with two formula units in the unit cell. In contrast, $[Fe(phen)_2]_2Sn_2S_6 \cdot phen \cdot H_2O$ (**II**) and $[Co(phen)_2]_2Sn_2S_6 \cdot phen \cdot H_2O$ (**IV**) crystallize in the triclinic space group $P\bar{1}$ with one formula unit in the unit cell. In all compounds the atoms are located on general positions.

In the structures of **I**–**IV** all terminal sulfur atoms of the $[Sn_2S_6]^{4-}$ anion have bonds to the TM^{2+} cation of the $[TM(phen)_2]^{2+}$ entities forming discrete complexes with the general formula $\{[TM(phen)_2]_2Sn_2S_6\}$ (Figure 1). In comparison to the discrete $[Sn_2S_6]^{4-}$ anion,[43] the Sn–S bond lengths observed in the title compounds differ not significantly, but the bond angles are affected (Table 2). These angles scatter around 92.56–93.32° (S_3–Sn–S_{3a}), 86.68–87.47° (Sn–S_3–Sn), and 99.57–119.62° (S_1–Sn–S_2, S_1–Sn–S_3) (see Table 2), indicating a deviation from the ideal tetrahedral arrangement, but are comparable to literature data.[17,18,38–41] The Fe^{2+}/Co^{2+}-S/N bonds are in the range reported for tin-sulfur compounds containing these cations.[17,18,40]

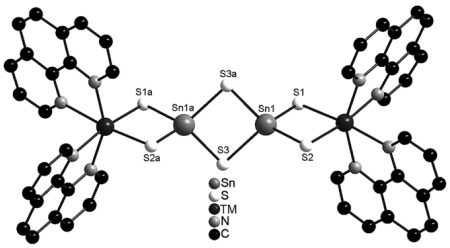

Figure 1. Structure of the $\{[TM(phen)_2]_2Sn_2S_6\}$ moieties. The hydrogen atoms are omitted for clarity.

Table 2. Selected bond lengths /Å and angles /° of compounds **I**–**IV**.

	I	II	III	IV
Sn–S1	2.344(2)	2.3351(10)	2.3366(14)	2.3404(8)
Sn–S2	2.359(2)	2.3531(10)	2.3528(14)	2.35533(8)
Sn–S3	2.457(3)	2.4401(9)	2.4522(15)	2.4459(8)
Sn–S3[a]	2.443(2)	2.4508(10)	2.4414(13)	2.4514(8)
S1–Sn–S2	100.10(9)	101.22(3)	99.57(5)	100.90(3)
S1–Sn–S3	119.62(9)	117.87(4)	119.13(5)	118.05(3)
S2–Sn–S3	113.64(9)	113.82(4)	113.93(5)	113.76(3)
S1–Sn–S3[a]	114.00(9)	116.32(4)	116.73(5)	116.34(3)
S2–Sn–S3[a]	118.22(9)	115.23(4)	116.73(5)	115.63(3)
S3–Sn–S3[a]	92.56(8)	93.32(3)	92.53(5)	93.16(2)
Sn–S3–Sn[a]	87.44(8)	86.68(3)	87.47(5)	86.84(2)
*TM*1–N1	2.305(8)	2.191(3)	2.250(4)	2.159(2)
*TM*1–N2	2.202(8)	2.247(3)	2.164(4)	2.222(2)
*TM*1–N3	2.194(8)	2.181(3)	2.152(5)	2.134(2)
*TM*1–N4	2.219(8)	2.248(3)	2.201(4)	2.211(3)
*TM*1–S1	2.523(3)	2.4841(11)	2.4907(16)	2.4647(9)
*TM*1–S2	2.498(3)	2.5313(11)	2.4699(15)	2.5256(9)

Symmetry transformations used to generate equivalent atoms: a: $-x+1, -y+1, -z$.

The values of the dihedral angles between the phen ligands scatter around 90° by about ± 10° (Table 3).

In compounds **I** and **III**, which are isostructural to one of the two polymorphs of $\{[Mn(phen)_2]_2Sn_2S_6\}$,[41] each molecule interacts with adjacent molecules via off-center parallel stacking between the phen ligands [3.372–3.479 Å (**I**) and 3.374–3.508 Å (**III**)] along the *c* axis (Figure 2). Along the *a* axis the phen molecules also interact in a twisted way (**I**: 3.334 and 3.577 Å; **III**: 3.340 and 3.657 Å). It was reported in literature for simpler aromatic systems like benzene and derivatives that a slightly twisted arrangement seems to be energetically favorable.[42] Calculations of the interaction energies for the

Zeitschrift für anorganische und allgemeine Chemie ZAAC Journal of Inorganic and General Chemistry

Table 3. Dihedral angles between the phen moieties for compounds **I–IV**.

	Angles		Angles	
I	N(12)–Fe(1)–N(1)–C(1)	–92.14 (0.87)	N(12)–Fe(1)–N(2)–C(10)	93.17 (0.89)
	N(12)–Fe(1)–N(1)–C(12)	93.09 (0.68)	N(12)–Fe(1)–N(2)–C(11)	–92.58 (0.69)
II	N(22)–Fe(1)–N(1)–C(1)	–91.20 (0.34)	N(22)–Fe(1)–N(2)–C(10)	96.04 (0.32)
	N(22)–Fe(1)–N(1)–C(12)	85.37 (0.27)	N(22)–Fe(1)–N(2)–C(11)	–85.22 (0.25)
III	N(12)–Co(1)–N(1)–C(1)	–96.40 (0.50)	N(12)–Co(1)–N(2)–C(10)	90.94 (0.51)
	N(12)–Co(1)–N(1)–C(12)	85.86 (0.37)	N(12)–Co(1)–N(2)–C(11)	–89.77 (0.38)
IV	N(22)–Co(1)–N(1)–C(1)	–90.14 (0.26)	N(22)–Co(1)–N(2)–C(10)	96.10 (0.25)
	N(22)–Co(1)–N(1)–C(12)	86.81 (0.21)	N(22)–Co(1)–N(2)–C(11)	–84.89 (0.20)

two types of stacking performed for the isostructural Mn^{2+} compound exhibiting very similar intermolecular distances yielded about 10 kcal·mol^{-1} for the former and about 13 kcal·mol^{-1} for the latter arrangement[41] being in the typical range of literature data.[45]

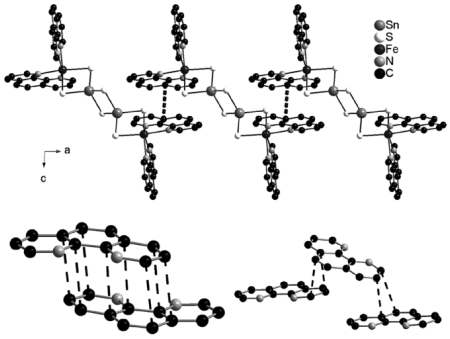

Figure 2. (top) Parallel arrangement of the molecules in **I** along [110], assembled by off-center parallel stacking (dashed lines). Only the shortest intermolecular contact is indicated. (bottom) The two types of interactions (dashed lines) between phen molecules in the structure of **I**. Hydrogen atoms are omitted for clarity.

The arrangement of the molecules along [010] and [110] (Figure 3) leads to a two-dimensional (2D) layer-like arrangement within the *ab* plane. A three-dimensional (3D) network is generated by an off-center parallel arrangement along [001] (Figure 3).

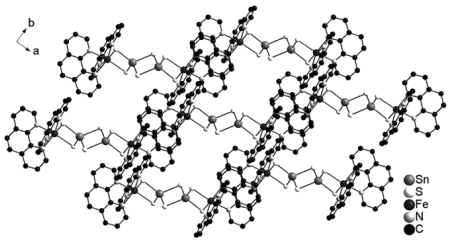

Figure 3. Parallel arrangement of the molecules within the *ab* plane. Hydrogen atoms are omitted for clarity.

In the structures of **II** and **IV** being isostructural to $\{[Mn(phen)_2]_2Sn_2S_6\}$·phen·$H_2O$[41] an additional free phen molecule, without covalent bonding to adjacent molecules, is disordered around a center of inversion. A chainlike arrangement of the $\{[TM(phen)_2]_2Sn_2S_6\}$ moieties is observed with off-center parallel stacking arrangement [3.471–3.647 Å (**II**) and 3.419–3.683 Å (**IV**), respectively] along [100] (Figure 4). The non-coordinating phen molecule is involved in off-center parallel stacking [3.348–3.655 Å (**II**) and 3.311–3.526 Å (**IV**), respectively] bridging two $\{[TM(phen)_2]_2Sn_2S_6\}_n$ chain-like arrangements along [010] leading to the 3D arrangement (Figure 4). Hydrogen bonding interactions between the phen and the water molecules are expected but could not be confirmed because the hydrogen atoms of the water molecule could not be located in the Fourier difference map.

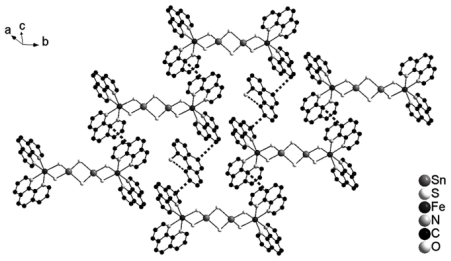

Figure 4. Arrangement of the molecules in **II** showing the off-center parallel stacking (thick dashed lines). Hydrogen atoms are omitted for clarity. Only one position of the disordered free phen molecule is displayed. The dashed lines between O and N atoms indicate hydrogen bonding interactions.

The Hirshfeld surface analysis yields a comprehensive picture about the three-dimensional intermolecular interactions and was calculated using CrystalExplorer 3.1.[46–51] In Figure 5 (top) is shown the d_{norm} surface of a molecule in compound **I** in one orientation together with three further molecules having contacts to the former molecule. The dark areas on the Hirshfeld surface indicates intermolecular interactions and a detailed analysis of these contacts using the finger print plot reveals that S···H bonds present 26% (**III**: 25.8%), N···H contacts 2.4% (**III**: 2.3%), C···H interactions 12.3% (**III**: 13.6%), and H···H contacts 32% (**III**: 34.1%) of all intermolecular interactions (note: contacts with $< 1\%$ are neglected). The volume of the molecule was obtained as 1328 Å^3 (**III**:

1289 Å^3). Because the free phen molecule in **II** and **IV** is disordered, which cannot be properly handled by the program, the structure was transformed to space group $P\bar{1}$ with one ordered free phen molecule (Figure 5, bottom).

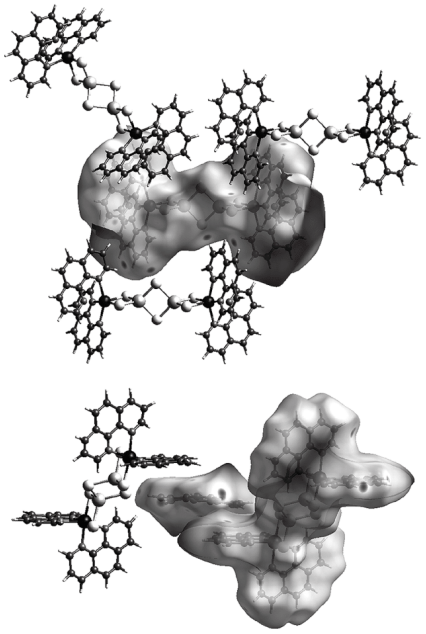

Figure 5. (top) View of the Hirshfeld surface of one molecule of compound **I** (mapped with d_{norm}). (bottom) The phen molecule and the complex in compound **III** together with a further complex in the vicinity. The closest contacts are shown as dark areas.

In the drawing it can nicely be seen that the shape of the surface of the free phen molecule adopts the shape of the neighboring phen ligand of the complex, and vice versa. Like for compounds **I** and **III** the intermolecular H···H interactions dominate (**II**: 32 %; **IV**: 32.1 %) followed by C···H (**II**: 22.8 %; **IV**: 23.3 %) and S···H bonding interactions (**II** and **IV**: 20.1 %). While S···C contacts in **I** and **III** are much less than 1 %, for **II** and **IV** they cannot be neglected (**II** and **IV**: 3 %). Finally, N···H interactions (**II**: 2.5 %; **IV**: 2.4 %) and O···H contacts (**II**: 2.6 %; **IV**: 2.4 %) complete the intermolecular contacts. From this analysis it is obvious that taking into account weak intermolecular interactions gives a more detailed picture about the arrangement of the molecules in the structure.

Raman Spectroscopy

For thiostannates the interesting region of the Raman spectra ranges from 400 to 100 cm^{-1} where the Sn–S modes are located. Especially for the $[Sn_2S_6]^{4-}$ anion the data are well documented.[14,40,44] The assignment of the modes was done on the basis of these data and they are listed for **I** and **II** serving as examples (Table 4).

Table 4. Data of the signals /cm^{-1} in the Raman spectra of $Na_4Sn_2S_6{\cdot}14H_2O$[44] and compounds **I** and **II**.

$Na_4Sn_2S_6{\cdot}14H_2O$	**I**	**II**
377	375	375
341	342	342
281	284	285
190	182	182
151	158	158
136	133	131

The resonances of the symmetric Sn–S_t stretching modes are found around 380 cm^{-1}, while the Sn–S_b vibrations are located at lower wave numbers at about 340 cm^{-1} (**I**). The mode at 280 cm^{-1} is caused by a Sn_2S_2 ring vibration. The small energetic differences between the resonances of the title compounds and those reported for $Na_4Sn_2S_6{\cdot}14H_2O$ are caused by slightly differing bond lengths and angles. Deformation vibrations occur below 200 cm^{-1}, but a detailed assignment is not unambiguous due to resonances for lattice vibrations.

The absorptions in the IR spectra for the compounds **I**, **II**, and **IV** can be assigned to 1,10-phenanthroline as well as the *TM*–N stretching vibration at ca. 420 cm^{-1} [52,41] (Table 5). The absorption at about 1030 cm^{-1} of compounds **II** and **IV** are caused by the additional 1,10-phenanthroline molecule in the structure. The weak absorption above 3000 cm^{-1} in **II** and **IV** can be assigned to water. The low yield of **III** and the fact that the crystals were partially intergrown with the X-ray amorphous phase prevented collection of enough material for recording an IR spectrum.

Table 5. Absorption of the IR spectra /cm^{-1} of compounds **I**, **II**, and **IV** (w = weak, m = medium, s = strong).

Phen [4]	**I**	**II**	**IV**	Assignment
–	–	~3370	~3360	w, ν (O–H)
3033	3040	3031	3034	m, ν (C–H)
1616	1616	1620	1622	m, ν (C=C)
1560	1575	1584	1575	m, ν (C=C)
1502	1508	1507	1507	m, ν (C=C)
1493	1493	1492	1494	m, ν (C=C)
1421	1420	1414	1415	s, combined
1344	1340	1340	1341	m, ν (C=C)
1216	1205	1217	1219	m, ν (C=C)
1337	1135	1138	1137	m, δ (C=C–H)
–	1092	1089	1089	m, ν (C–N) bonded phen
1035	–	1032	1032	m, ν (C–N) free phen
853	840	851	851	s, δ (C=C=C)
839	–	837	836	s, δ (C=C=C)
779	–	777	778	m, δ (C–H)
–	765	–	760	m, δ (C–H)
738	–	737	–	δ (C–H),
721	721	721	722	s, δ (C–H)
637	635	635	636	m, δ (C–H)
625	–	620	621	m, δ (C–H)
–	–	418	419	m, ν (*TM*–N)

Zeitschrift für anorganische und allgemeine Chemie ZAAC Journal of Inorganic and General Chemistry

Conclusions

We were able to synthesize and characterize four new compounds consisting of the tetradentate acting $[Sn_2S_6]^{4-}$ anion and Fe^{2+}/Co^{2+} centered complexes. All compounds are isostructural to recently reported Mn^{2+} containing compounds. An unanswered question is why five compounds could be isolated applying Mn^{2+} and only two each for Fe^{2+} and Co^{2+} despite using very similar synthesis conditions. On the other hand, the presented result supports our findings that Mn^{2+} is much easier integrated into thiometallate networks, while synthetic tricks like application of multidentate N donor ligands must be applied using Fe^{2+}/Co^{2+} yielding coordinately unsaturated Fe^{2+}/Co^{2+} centered complexes, which then form bonds to the sulfur atoms of the thiostannate anion. Therefore, the title compounds are rare examples because the bidentate phen ligand was applied and the special reaction conditions suppressed formation of the stable $[TM(phen)_3]^{2+}$ complexes.

Acknowledgements

Financial support by the State of Schleswig-Holstein and the DFG is gratefully acknowledged.

References

[1] W. S. Sheldrick, M. Wachhold, *Coord. Chem. Rev.* **1998**, *176*, 211.
[2] W. S. Sheldrick, *J. Chem. Soc. Dalton Trans.* **2000**, 3041.
[3] X. H. Bu, N. F. Zheng, P. Y. Feng, *Chem. Eur. J.* **2004**, *10*, 3356.
[4] P. Y. Feng, X. H. Bu, N. F. Zheng, *Acc. Chem. Res.* **2005**, *38*, 293.
[5] S. Dehnen, M. Melullis, *Coord. Chem. Rev.* **2007**, *251*, 1259.
[6] B. Seidlhofer, N. Pienack, W. Bensch, *Z. Naturforsch. B* **2010**, *65*, 937.
[7] N. Pienack, D. Schinkel, A. Puls, M. E. Ordolff, H. Lühmann, C. Näther, W. Bensch, *Z. Naturforsch. B* **2012**, *67*, 1098.
[8] E. Ruzin, S. Jakobi, S. Dehnen, *Z. Anorg. Allg. Chem.* **2008**, 634, 995.
[9] G.-N. Liu, G.-C. Guo, F. Chen, S.-P. Guo, X.-M. Jiang, C. Yang, M. S. Wang, M. F. Wu, J. S. Huang, *CrystEngComm* **2010**, *12*, 4035.
[10] N. Pienack, C. Näther, W. Bensch, *Eur. J. Inorg. Chem.* **2009**, 1575.
[11] N. Pienack, C. Näther, W. Bensch, *Solid State Sci.* **2007**, *9*, 100.
[12] N. Pienack, W. Bensch, *Z. Anorg. Allg. Chem.* **2006**, *632*, 1733.
[13] N. Pienack, K. Möller, C. Näther, W. Bensch, *Solid State Sci.* **2007**, *9*, 1110.
[14] N. Pienack, C. Näther, W. Bensch, *Z. Naturforsch. B* **2008**, *63*, 1243.
[15] J. Zhou, G.-Q. Bian, J. Dai, Y. Zhang, A. Tang, Q.-Y. Zhu, *Inorg. Chem.* **2007**, *46*, 1541.
[16] N. Pienack, A. Puls, C. Näther, W. Bensch, *Inorg. Chem.* **2008**, *47*, 9606.
[17] N. Pienack, S. Lehmann, H. Lühmann, M. El-Madani, C. Näther, W. Bensch, *Z. Anorg. Allg. Chem.* **2008**, *634*, 2323.
[18] M. Behrens, S. Scherb, C. Näther, W. Bensch, *Z. Anorg. Allg. Chem.* **2003**, *629*, 1367.
[19] D.-X. Jia, Y. Zhang, J. Dai, Q.-Y. Zhu, X.-M. Gu, *Z. Anorg. Allg. Chem.* **2004**, *630*, 313.
[20] M.-L. Fu, G.-C. Guo, B. Liu, A.-Q. Wu, J.-S. Huang, *Chin. J. Inorg. Chem.* **2005**, *21*, 25.
[21] X.-M. Gu, J. Dai, D.-X. Jia, Y. Zhang, Q.-Y. Zhu, *Cryst. Growth Des.* **2005**, *5*, 1845.
[22] D.-X. Jia, J. Dai, Q.-Y. Zhu, Y. Zhang, X.-M. Gu, *Polyhedron* **2004**, *23*, 937–942.
[23] J. Zhou, X. Liu, G.-Q. Chen, F. Zhang, L.-R. Li, *Z. Naturforsch. B* **2010**, *65*, 1229.
[24] Z. Wang, G. Xu, Y. Bi, C. Wang, *CrystEngComm* **2010**, *12*, 3703.
[25] B. Krebs, S. Pohl, W. Schiwy, *Z. Anorg. Allg. Chem.* **1972**, *393*, 241.
[26] W. S. Sheldrick, B. Schaaf, *Z. Anorg. Allg. Chem.* **1994**, *620*, 1041.
[27] W. S. Sheldrick, M. Wachhold, *Angew. Chem.* **1997**, *109*, 214; *Angew. Chem. Int. Ed. Engl.* **1997**, *36*, 206.
[28] B. Krebs, *Angew. Chem.* **1983**, *95*, 113; *Angew. Chem. Int. Ed. Engl.* **1983**, *22*, 113.
[29] Z. H. Fard, C. Müller, T. Harmening, R. Pöttgen, S. Dehnen, *Angew. Chem.* **2009**, *121*, 4507.
[30] J. Li, B. Marler, H. Kessler, M. Soulard, S. Kallus, *Inorg. Chem.* **1997**, *36*, 4697.
[31] J. Zhou, X. Liu, G.-Q. Chen, F. Zhang, L. R. Li, *Z. Naturforsch. B* **2010**, *65*, 1229.
[32] D.-X. Jia, Y. Zhang, J. Dai, Q.-Y. Zhu, X.-M. Gu, *Z. Anorg. Allg. Chem.* **2004**, *630*, 313.
[33] D.-X. Jia, A.-M. Zhu, J. Deng, Y. Zhang, *Z. Anorg. Allg. Chem.* **2007**, *633*, 1246.
[34] Q. Zhao, D.-X. Jia, Y. Zhang, L. Song, J. Dai, *Inorg. Chim. Acta* **2007**, *360*, 1895.
[35] X.-H. Lu, J.-J. Liang, J. Zhao, Y. Zhang, D.-X. Jia, *J. Chem. Crystallogr.* **2011**, *41*, 557.
[36] S. Dehnen, C. Zimmermann, *Z. Anorg. Allg. Chem.* **2002**, *628*, 2463.
[37] D. B. Mitzi, L. L. Kosbar, C. E. Murray, M. Copel, A. Afzal, *Nature* **2004**, *428*, 299.
[38] Y. Zhang, J. Zhou, A.-B. Tang, G.-Q. Bian, J. Dai, *J. Chem. Crystallogr.* **2010**, *40*, 496.
[39] X.-M. Gu, J. Dai, D.-X. Jia, Y. Zhang, Q.-Y. Zhu, *Cryst. Growth Des.* **2005**, *5*, 1845.
[40] C. Zeisler, C. Näther, W. Bensch, *CrystEngComm* **2013**, *15*, 8874.
[41] J. Hilbert, C. Näther, W. Bensch, *Inorg. Chem.* **2014**, *53*, 5619.
[42] E. C. Lee, D. Kim, P. Jurecka, P. Tarekeshwar, P. Hobza, K. S. Kim, *J. Phys. Chem. A* **2007**, *111*, 3446–3457.
[43] G. M. Sheldrick, *SHELXS-97*, Program for the Solution of Crystal Structures, University of Göttingen, Göttingen, Germany **1997**; G. M. Sheldrick, *SHELXL-97*, Program for the Refinement of Crystal Structures, University of Göttingen, Göttingen, Germany **1997**.
[44] B. Krebs, S. Pohl, W. Schiwy, *Angew. Chem. Int. Ed. Engl.* **1970**, *9*, 897.
[45] S. Grimme, *Angew. Chem. Int. Ed.* **2008**, *47*, 3430.
[46] M. A. Spackman, D. Jayatilaka, *CrystEngComm* **2009**, *11*, 19.
[47] M. A. Spackman, J. J. McKinnon, *CrystEngComm* **2002**, *4*, 378.
[48] J. J. McKinnon, M. A. Spackman, A. S. Mitchell, *Acta Crystallogr., Sect. B* **2004**, *60*, 627.
[49] J. J. McKinnon, D. Jayatilaka, M. A. Spackman, *Chem. Commun.* **2007**, 3814.
[50] M. A. Spackman, J. J. McKinnon, D. Jayatilaka, *CrystEngComm* **2008**, *10*, 377.
[51] M. J. Turner, J. J. McKinnon, D. Jayatilaka, M. A. Spackman, *CrystEngComm* **2011**, *13*, 1804.
[52] M. S. Atanassova, G. D. Dimitrov, *Spectrochim. Acta Part A* **2003**, *59*, 1655.

Received: August 3, 2014
Published Online: October 20, 2014

3.1.3 Solvothermale Synthese der Verbindungen {[Ni(phen)$_2$]$_2$[Sn$_2$S$_6$]}·2,2'-bipy und {[Ni(phen)$_2$]$_2$[Sn$_2$S$_6$]}·4,4'-bipy ½H$_2$O

Zusammenfassung der Publikation „Utilization of mixtures of aromatic N-donor ligands of different coordination ability for the solvothermal synthesis of thiostannate containing molecules".

Die Verbindungen {[Ni(phen)$_2$]$_2$[Sn$_2$S$_6$]}·2,2'-bipy (*P*2$_1$/*n*, Z = 2) und {[Ni(phen)$_2$]$_2$[Sn$_2$S$_6$]}·4,4'-bipy·½H$_2$O (*C*2/*c*, Z=4) wurden unter solvothermalen Bedingungen (120°C, 7d) mit NiCl$_2$·6H$_2$O, Sn, S, phen und 2,2'-bipy (bzw. 4,4'-bipy) in wässriger Methylaminlösung synthetisiert.

Die Struktur von {[Ni(phen)$_2$]$_2$[Sn$_2$S$_6$]} ist analog zu den in Abschnitt 3.1.1 und 3.1.2 aufgeführten Verbindungen mit Mn, Fe und Co aufgebaut. Im Gegensatz zu diesen Verbindungen war für die Kristallisation der nickelhaltigen Verbindungen der Zusatz eines weiteren aromatischen Aminmoleküls (2,2'-bipy bzw. 4,4'bipy) notwendig. Ni^{2+} bildet mit phen deutlich stabilere Komplexe als Mn^{2+}, Fe^{2+} oder Co^{2+}.[65] Um eine Ni-S-Bindung zu erzwingen, mussten schwächer koordinierende, aromatische Amine hinzugesetzt werden, welche durch π-π-Wechselwirkungen zu einer Stabilisierung der {[Ni(phen)$_2$]$_2$[Sn$_2$S$_6$]} Einheit beitragen.

Dalton Transactions

PAPER

Cite this: *Dalton Trans.*, 2015, **44**, 11542

Utilization of mixtures of aromatic N-donor ligands of different coordination ability for the solvothermal synthesis of thiostannate containing molecules†

J. Hilbert, C. Näther and W. Bensch*

Received 23rd March 2015,
Accepted 22nd May 2015

DOI: 10.1039/c5dt01145k

www.rsc.org/dalton

Utilization of mixtures of differently coordinating aromatic N-donor ligands leads to the formation of the two new compounds {[Ni(phen)$_2$]$_2$Sn$_2$S$_6$}·4,4′-bipy·$\frac{1}{2}$H$_2$O **I** and {[Ni(phen)$_2$]$_2$Sn$_2$S$_6$}·2,2′-bipy **II** that could be prepared under solvothermal conditions (4,4′-bipy = 4,4′-bipyridine, $C_{10}H_8N_2$; phen = 1,10-phenanthroline, $C_{12}H_8N_2$; 2,2′-bipy = 2,2′-bipyridine, $C_{10}H_8N_2$). In the structures of both compounds Ni–S bond formation is observed which is highly unusual when only bidentate N-donor ligands are applied in the reaction mixture. The detailed analysis of the crystal structure indicates that the presence of 4,4′-bipy and 2,2′-bipy molecules are essential for the stabilization of the arrangement of the constituents. The main structural motif {[Ni(phen)$_2$]$_2$Sn$_2$S$_6$} is arranged generating off center parallel stacking of the phen ligands. The empty spaces between the {[Ni(phen)$_2$]$_2$Sn$_2$S$_6$} moieties are occupied by either 2,2′-bipy (**I**) or 4,4′-bipy (**II**) molecules which are oriented towards the phen ligands to form intermolecular π–π interactions.

1 Introduction

Compounds containing thiostannate building blocks may be classified according to different criteria. One group of thiostannates are pure inorganic compounds containing *e.g.* metal cations and thiostannate anions like in $Na_4Sn_2S_6·14H_2O$,[1] $Rb_6Sn_2S_7$,[2] $Cs_2Sn_4S_9$,[3] $Cs_2Sn_2S_6$ or $K_2Sn_2S_5$,[4] $(Rb_4(H_2O)_4)[SnS_4]$,[5] $K_{10}M_4Sn_4S_{17}$ (M = Mn, Fe, Co, Zn)[6] and $(NH_4)_4[Sn_2S_6]·3H_2O$[7] to mention just a few. In these compounds the cations and anions are held together by mainly electrostatic interactions. The examples demonstrate the structural variability with thiostannate ions displaying different Sn : S ratios and therefore different structural motifs. Another group of compounds is composed of organic cations and thiostannate anions, like *e.g.* (TMA)$[Sn_3S_7]·2H_2O$ (TMA = tetramethylammonium),[8] (DABCOH)$_2[Sn_3S_7]·H_2O$ (DABCO = 1,4-diazabicyclo[2.2.2]octane),[9] $(enH)_4[Sn_2S_6]$ (en = ethylenediamine),[10] or $(tmdpH_2)[Sn_3S_7]$ (tmdp = 4,4′-trimethylenedipiperidine).[11] Charge compensation may be also achieved by transition metal or lanthanoide cation centered complexes like in $(M(en)_3)_2[Sn_2S_6]$ (M = Mn, Co, Ni, Zn),[12–14] $(M(dien)_2)_2[Sn_2S_6]$ (M = Mn, Co, Ni; dien = diethylentriamine),[14–16] $(Nd(dien)_3)_2[Sn_2S_6]Cl_2$, $(Nd(dien)_3)_2[Sn_2S_6]·(SH)_2$,[17] $(Y_2(dien)_2(OH)_2)[Sn_2S_6]$,[18] $(Ni(1,2\text{-dap})_3)_2[Sn_2S_6]·2H_2O$ (1,2-dap = 1,2-diaminopropane),[12] $(Ni(1,2\text{-dach})_3)_2[Sn_2S_6]·4H_2O$ (1,2-dach = 1,2-diaminocyclohexane), $(Ni(peha)_2)[Sn_2S_6]·H_2O$ (peha = pentaethylenehexamine) or $(Ni(aepa)_2)_2[Sn_2S_6]$ (aepa = N-2-aminoethyl-1,3-propandiamine).[16]

Another class of compounds is characterized by M–S bonds between the thiostannate ion and transition metal cations which are further surrounded by N donor atoms from amine ligands. In such compounds the $[Sn_2S_6]^{4-}$ and $[SnS_4]^{4-}$ anion, respectively, acts as bidentate ligand like in {[Mn(1,2-dach)$_2$(H$_2$O)]$_2$[Sn$_2$S$_6$]},[19] $\{[Mn(en)_2]_2[Sn_2S_6]\}_n$,[20] $\{[Mn(1,2\text{-dap})_2]_2[Sn_2S_6]\}_n$,[21] {[M(tepa)]$_2$[Sn$_2S_6$]} (M = Mn, Fe, Co, Ni; tepa = tetraethylenepentamine),[22,23] $\{[Mn(trien)]_2[SnS_4]\}_n·4nH_2O$ (trien = triethylenetetramine),[24] $\{[M(tren)]_2[Sn_2S_6]\}$[12,25] (M = Mn, Co; tren = tris(2-aminoethyl-)amine), $\{[Co(cyclam)]_2[Sn_2S_6]\}_n·2nH_2O$[26] (cyclam = 1,4,8,11-tetraaza-cyclotetradecane), *o*-{[Ni(tepa)]$_2$[Sn$_2$S$_6$]}, $\{[Mn(trien)]_2[SnS_4]\}_n$[16] or in a tetradentate fashion as observed for *e.g.* $\{[Mn(phen)_2]_2[Sn_2S_6]\}$,[27] $\{[TM(phen)_2]_2[Sn_2S_6]\}$[28] (M = Fe, Co) or $\{[Mn(phen)]_2[SnS_4]\}_n·nH_2O$.[29]

Finally metal cations may be integrated into the thiostannate unit as observed for $(1,4\text{-dabH})_2MnSnS_4$[30] (1,4-dab = 1,4-diaminobutane), (DBUH)$CuSnS_3$ (DBU = 1,8-diaza-bicyclo-[5.4.0]undec-7-ene) and $(1,4\text{-dabH}_2)Cu_2SnS_4$,[31] $(1,4\text{-dabH}_2)Ag_2SnS_4$,[32] $(enH)_3Cu_7Sn_4S_{12}$,[33] $(DBNH)_2Cu_6Sn_2S_8$[34] (DBN = 1,5-diazabicyclo[4.3.0]non-5-ene), $(dienH_2)Cu_2Sn_2S_6$,[35] $(NH_4)_2$-

Institute of Inorganic Chemistry, Christian-Albrechts-University of Kiel, Max-Eyth-Str. 2, 24118 Kiel, Germany. E-mail: wbensch@ac.uni-kiel.de; Fax: +49 431 880–1520; Tel: +49 431 880–2419

†Electronic supplementary information (ESI) available: PXRD pattern, selected angles of the octahedral Ni^{2+} enivironment, IR- and Raman spectra. CCDC 1054460 and 1054461. For ESI and crystallographic data in CIF or other electronic format see DOI: 10.1039/c5dt01145k

$Ag_6Sn_3S_{10}$,[36] $(enH_2)Ag_2SnS_4$,[37] $(enH_2)HgSnS_4$,[38] $(enH_2)_2Cu_8Sn_3S_{12}$ [39] and $[Mn(dien)_2]MnSnS_4$.[21]

Many of the above-mentioned compounds were obtained under solvothermal conditions and state-of-art of the chemistry of thiostannates and other thiometallates was reviewed in several articles highlighting the synthetic approaches, the structural variability and flexibility of the anions.[40] Analyzing the structures of thiometallate compounds with transition metal cations having bonds to S atoms of the anions, the Mn^{2+} ion can be easily integrated in the anions independent from the amine applied, whereas Fe^{2+}, Co^{2+}, Ni^{2+}, or Zn^{2+} prefer bond formation to the N atoms of the amine molecules and M–S bond formation must be forced by applying multidentate amine molecules (tetra- or pentadentate) in the synthesis mixture which do not satisfy the coordination requirements of the cations. Mn^{2+} seems to have a comparable affinity to both S and N atoms as can be seen from the thiostannate examples presented above but a similar observation was also made for *e.g.* thioantimonates.[41]

During a systematic study of the Mn/phen/Sn/S system we prepared $\{[Mn(phen)_2]_2(\mu_2\text{-}Sn_2S_6)\}\cdot phen$ and $\{[Mn(phen)_2]_2(\mu_2\text{-}Sn_2S_6)\}\cdot phen\cdot H_2O$ containing co-crystallized phen molecules which are arranged with respect to phen ligands of the Mn^{2+} centered complexes to achieve attractive so-called π–π interactions.[27] The energy involved in these interactions is between *ca.* 10 and 13 kcal mol^{-1}.[42–45] While the interaction energy between stacked phen molecules is low compared to that of covalent or ionic bonds, it seems to be large enough to stabilize frequently observed arrangements of aromatic molecules with respect to each other, like *e.g.* face-to-face, off-center, slipped or edge-to-face. Modifying the synthesis conditions originally applied for the preparation of $\{[Mn(phen)_2]_2(\mu_2\text{-}Sn_2S_6)\}\cdot phen$ and using Co, Fe instead of Mn we were able to crystallize $\{[TM(phen)_2]_2Sn_2S_6\}\cdot phen\cdot H_2O$ (TM = Co, Fe) with similar arrangements of the phen molecules found for the analogous Mn compound.[28] This was a surprising result because Co^{2+}/Fe^{2+} have a strong preference for N donor atoms yielding normally isolated $[TM(L)_n]^{2+}$ (L = bidentate or tridentate ligands) complexes and thiometallate anions.[13,16,46–49] All thiometallate compounds displaying a Co–S/Fe–S bond were obtained in the presence of a tetradentate or pentadentate ligand like tren,[12,48–50] tepa[23] and cyclam,[26] with one exception where 1,2-dach (1,2-dach = 1,2 diaminocyclohexane) was used as amine.[51]

In our ongoing synthetic work all attempts to synthesize the analogous Ni^{2+} containing compounds failed despite varying the reaction conditions reported in.[27–29] One possible reason is the high stability of the $[Ni(phen)_3]^{2+}$ complex, which is *in situ* formed under the solvothermal reaction conditions. Hence, we developed a new synthetic strategy applying mixtures of aromatic N-donor ligands which are either strong (phen), medium (2,2′-bipyridine), weak/monodentate coordinating (4,4′-bipyridine) which should lead to the solely coordination of Ni^{2+} by phen and the other molecule-donor ligands might act as structural stabilizers *via* intermolecular π–π-interactions.

During the experiments we were able to prepare and characterize the two new compounds $\{[Ni(phen)_2]_2Sn_2S_6\}\cdot 4,4'\text{-bipy}\cdot\frac{1}{2}H_2O$ (**I**) and $\{[Ni(phen)_2]_2Sn_2S_6\}\cdot 2,2'\text{-bipy}$ (**II**). Here we report the syntheses, crystal structures and spectroscopic data of these compounds.

2 Results and discussion

Synthetic aspects

For the synthesis of thiometallates applying elemental Sn and S a very weak coordinating amine like methylamine is necessary which generates the basic conditions for production of polysulfide anions which attack Sn to form the thiostannate ion.

In our previous investigations of the TM/Sn/S/phen systems (TM = Mn, Fe, Co, Ni) we demonstrated that Mn^{2+} easily forms bonds to thiostannate anions and five compounds with compositions $\{[Mn(phen)_2]_2Sn_2S_6\}$, $\{[Mn(phen)_2]_2Sn_2S_6\}\cdot phen$, $\{[Mn(phen)_2]_2Sn_2S_6\}\cdot phen\cdot H_2O$ and $\{[Mn(phen)_2]_2[SnS_4]_2\text{-}[Mn(phen)]_2\}\cdot H_2O$ could be prepared of which four were accessible even under stirring conditions.[27] The syntheses with Fe and Co yielded only two compounds ($\{[M(phen)_2]_2Sn_2S_6\}$ and $\{[M(phen)_2]_2Sn_2S_6\}\cdot phen\cdot H_2O$, M = Fe, Co) and only under static conditions.[28] Applying the synthesis conditions used for TM = Mn, Fe, and Co no compounds were accessible with Ni and the reaction products only contained the crystallized $[Ni(phen)_3]^{2+}$ complex (counter ion: Cl^-) and X-ray amorphous sulfides. One reason may be the differing stabilities of the $[TM(phen)_3]^{2+}$ complexes with log β (TM): Mn: 10.5, Fe: 21.2, Co: 19.9, Ni: 24.3.[52] To force bond formation between Ni^{2+} and the thiostannate anion syntheses were performed with mixtures of aromatic bidentate N-donor ligands which have different coordination abilities. The bidentate amine phen is a strong coordinating ligand,[52] while 2,2′-bipy has a weak/medium coordination tendency[52] and 4,4′-bipy can only act as a monodentate ligand to one Ni^{2+} center. Both 4,4′-bipy and 2,2′-bipy may act as stabilizing molecules *via* π–π interactions and both are not strong competitors for phen. During the explorative synthetic work we observed that the ratio phen : bipy is an important parameter. Compound **I** containing co-crystallized 4,4′-bipy was only obtained when the amount of 4,4′-bipy was between 20–65% of the total amount of amine. The highest yield was observed for a Ni : phen : 4,4′-bipy molar ratio of 1 : 1 : 1. Applying mixtures of phen and 2,2′-bipy compound **II** crystallized only applying 20–50% 2,2′-bipy of the total amount of amine. For compound **II** the highest yield was obtained at a molar ratio of 1 : 2 : 1 for Ni : phen : 2.2′-bipy. When the syntheses were carried out using the analogue cobalt and iron salts ($CoCl_2\cdot 6H_2O$ or $FeCl_2\cdot 4H_2O$) under the conditions mentioned above, the known compounds $\{[Co(phen)_2]_2Sn_2S_6\}$[28] and $\{[Fe(phen)_2]_2Sn_2S_6\}$,[28] were obtained.

Crystal structures

The compound $\{[Ni(phen)_2]_2Sn_2S_6\}\cdot 4,4'\text{-bipy}\cdot\frac{1}{2}H_2O$ (**I**) crystallizes in the monoclinic space group *C*2/*c* with four formula

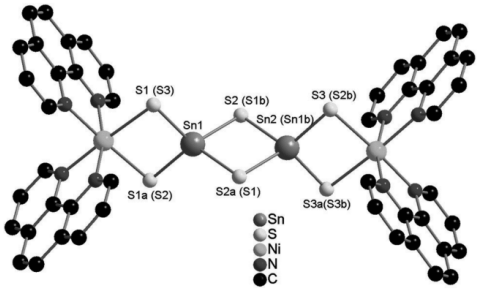

Fig. 1 Structure of the $\{[Ni(phen)_2]_2Sn_2S_6\}$ moieties in **I** as a representative. Labelling of the atoms for **II** are given in parentheses. The hydrogen atoms are omitted for clarity.

units in the unit cell with all atoms on general positions except the two unique Ni and Sn atoms. $\{[Ni(phen)_2]_2Sn_2S_6\}\cdot$2,2′-bipy (**II**) crystallizes in the monoclinic space group $P2_1/n$ with two formula units in the unit cell and all atoms are located on general sites.

Both structures feature the $[Sn_2S_6]^{4-}$ anion and charge compensating Ni^{2+} centered complexes. The Ni^{2+} cations of the $[Ni(phen)_2]^{2+}$ complexes have two Ni–S bonds leading to the formation of discrete molecules (Fig. 1).

The Ni–S bond lengths (2.4960 Å–2.5047 Å) as well as the Ni–N bonds (2.083 Å–2.124 Å) are within the range reported in literature.[12–14,16,23] (Table 1).

The angles around Ni^{2+} scatter between 78.64(13)° and 175.86(9)° (**I**) and between 77.38(11)° and 172.28(9)° (**II**), respectively, indicative for a severe distortion of the octahedra, but still in the range of literature data.[16] The distortion is caused by the fixed position of the N-atoms in the phen-

Table 1 Selected bond lengths (Å) and angles (°) of compounds **I** and **II**[a]

	I		**II**
Sn1–S1	2.3366(10)	Sn–S3	2.3296(9)
Sn1–S1[a]	2.3382(10)	Sn–S2	2.3475(9)
Sn1–S2	2.4532(9)	Sn–S1[b]	2.4488(9)
Sn1–S2[a]	2.4630(9)	Sn–S1	2.4524(9)
S1–Sn–S1[a]	100.59(5)	S2–Sn–S3	100.43(3)
S2–Sn–S2[a]	92.78(4)	S1–Sn–S1[b]	92.46(3)
S1–Sn–S2[a]	117.27(4)	S1–Sn–S3	120.84(3)
S1[a]–Sn–S2[a]	115.02(3)	S1–Sn–S2	113.00(3)
S2–Sn–S3	117.28(4)	S2–Sn–S1[b]	118.10(3)
S2[a]–Sn–S3	114.57(3)	S3–Sn–S1[b]	113.30(3)
Sn1–S1–Sn2	87.46(3)	Sn–S1–Sn[b]	87.54(3)
Ni1–N1	2.103(3)	Ni1–N1	2.120(3)
Ni1–N2	2.122(3)	Ni1–N2	2.161(3)
Ni1–N21	2.083(3)	Ni1–N21	2.106(3)
Ni1–N22	2.124(3)	Ni1–N22	2.112(3)
Ni1–S1	2.4960(11)	Ni1–S2	2.4946(10)
Ni1–S3	2.5047(11)	Ni1–S3	2.4984(10)

[a] Symmetry transformations used to generate equivalent atoms: *a*: $-x+1$, y, $-z+1/2$; *b*: $-x+1$, $-y+1$, $-z$.

molecule leading to acute angles around the Ni^{2+} cations (**I**: N1–Ni1–N2: 78.64(13), N21–Ni1–N22: 79.03(13); **II**: N1–Ni1–N2: 77.38(11), N21–Ni1–N22: 78.25(12)) (Table S1†). The values of the dihedral angles between the phen ligands are around 90° ± 10° (Table S2†) and they are comparable with literature data.[27,28] The $[Sn_2S_6]^{4-}$ ion which is generated by edge-sharing of two SnS_4 tetrahedra exhibits the typical Sn–S bonding pattern of short Sn–S_t (t = terminal) and longer Sn–S_b (b = bridging) bonds. Comparing the geometric parameters of the thiostannate ion of the title compounds with those of the discrete anion $[Sn_2S_6]^{4-}$(ref. 1,12–16,46) the Sn–S bond lengths do not differ significantly (Table 1). Different, however, are the bond angles which cover a wide range from 87.46 to 117.27° in **I** and they are between 87.54° and 120.84° in **II** evidencing a strong deviation from ideal tetrahedral geometry, a phenomenon also observed previously.[12,23,26–28,53]

Besides the $\{[Ni(phen)_2]_2Sn_2S_6\}$ moiety, the structure of **I** contains an additional 4,4′-bipy and a water molecule, which is disordered over two half occupied positions. The $\{[Ni(phen)_2]_2Sn_2S_6\}$ units are arranged as rods in all three crystallographic directions (Fig. 2). The 4,4′-bipy molecules are assembled in a chain-like fashion along [100] and [001] (Fig. 2). The water molecule is located between adjacent

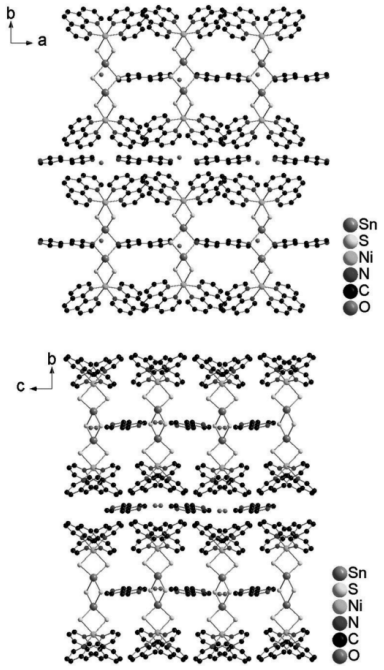

Fig. 2 Parallel arrangement of the molecules in **I** within the *ab*-plane (top) and *bc*-plane (bottom), respectively. Hydrogen atoms are omitted for clarity.

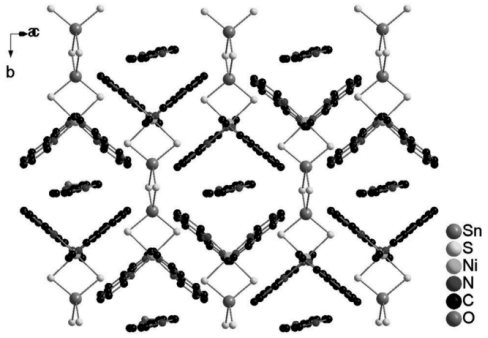

Fig. 3 Arrangement of the molecules in **I** viewed along [10−1]. The 4,4′-bipy molecules are located in the free spaces between the $\{[Ni(phen)_2]_2Sn_2S_6\}$ moieties. Hydrogen atoms are omitted for clarity.

4,4′-bipy molecules and the N···O separation of 2.922 Å indicates hydrogen bonding interaction.

The arrangement of the constituents for optimal intermolecular interactions in **I** becomes clear viewing along [10−1]: The $\{[Ni(phen)_2]_2Sn_2S_6\}$ moieties are interlaced along [101] and the 4,4′-bipy molecules are located in the thus generated voids (Fig. 3).

The phen ligands of neighbored complexes exhibit a short intermolecular distance of 3.489 Å and two even shorter separations are observed between phen and co-crystallized 4,4′-bipy molecules at 3.343–3.455 Å. Such short distances between off-centered parallel stacked aromatic molecules indicate π–π interactions (Fig. 4 and 5).[42–45,54,55]

In the structure of **II** the $\{[Ni(phen)_2]_2Sn_2S_6\}$ moieties are lined-up along a and c, respectively (Fig. 6). The 2,2′-bipy molecules are located between two adjacent $\{[Ni(phen)_2]_2Sn_2S_6\}$ units yielding a sequence AAB along [100] where A stands for the phen Ligand and B for the 2,2′-bipy molecule.

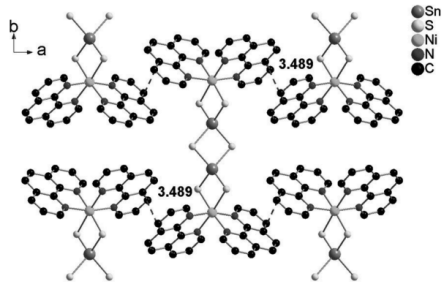

Fig. 4 Off-center parallel orientation of the phen ligands in **I** within the *ab*-plane. The purple dashed lines indicate the shortest intermolecular distances. Hydrogen atoms are omitted for clarity.

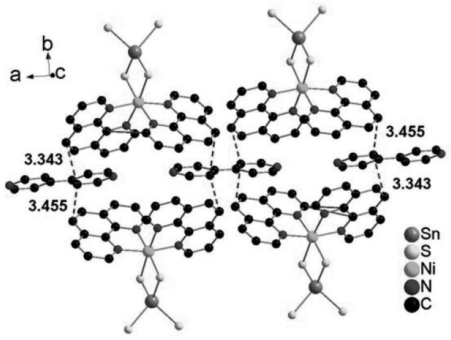

Fig. 5 Off-center parallel orientation of the phen ligands as well as 4,4′-bipy molecules in **I** along [101]. The purple dashed lines indicate the shortest intermolecular distances. Hydrogen atoms are omitted for clarity.

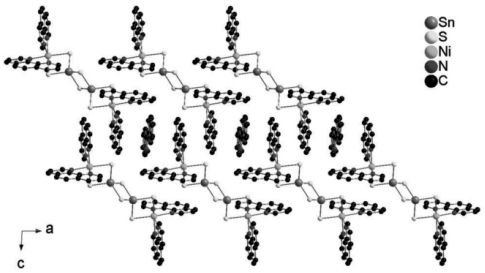

Fig. 6 Arrangement of the molecules in **II** within the *ac*-plane. The 2,2′-bipy molecules are disordered over two positions between two pairs of phen ligands of the $\{[Ni(phen)_2]_2Sn_2S_6\}$ moieties. Hydrogen atoms are omitted for clarity.

Like in compound **I** the aromatic components adopt orientations which allow attractive intermolecular interactions. Along [010] all molecules are arranged in rows, while along [101] the phen ligands are staggered. The 2,2′-bipy molecules can now be aligned parallel to the upper and the lower phen ligand of adjacent rows (Fig. 7, top) leading either to a parallel arrangement or a staggered arrangement (Fig. 7, bottom). The intermolecular distances for these orientations between the 2,2′-bipy molecule and the phen ligands are almost identical with 3.279–3.826 Å for the parallel and 3.335–3.921 Å and 3.396–4.059 Å for the staggered orientations. As discussed above and in agreement with literature data such distances can be regarded as π–π interactions.[54,55]

Physcial properties

The Sn–S modes in the Raman spectra of thiostannates are located in the region of 400 to 100 cm^{-1}. The assignment of

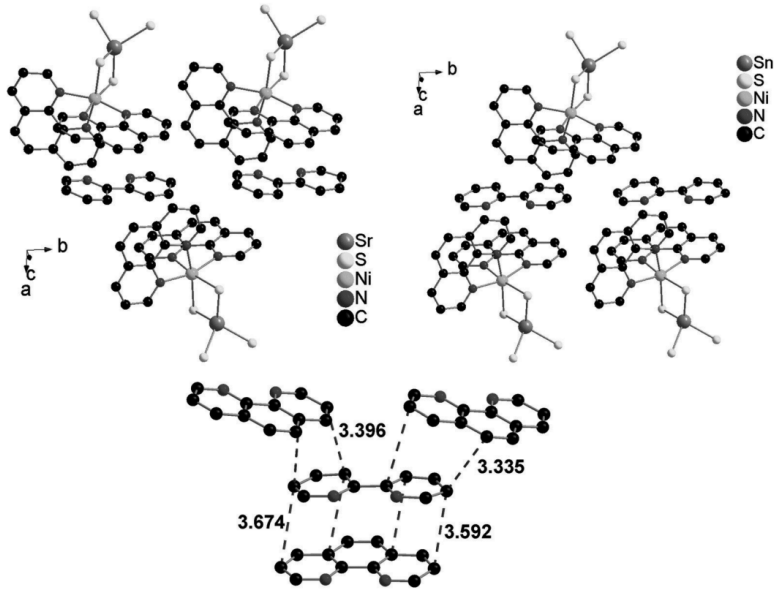

Fig. 7 Arrangement of the 2,2′-bipy molecules between the $\{[Ni(phen)_2]_2Sn_2S_6\}$ moieties (top) in the structure of **II**. The shortest intermolecular distances are shown (purple dashed lines, distances in Å, bottom). For reasons of clarity only one arrangement of the 2,2′-bipy molecule is shown. Hydrogen atoms and part of the $\{[Ni(phen)_2]_2Sn_2S_6\}$ moieties as well as hydrogen atoms are omitted.

the modes for compounds **I** and **II** was done on the basis of the data documented for the $[Sn_2S_6]^{4-}$ anion[1,56,57] and NiS_2 [58] (Table 2).

The resonance of the symmetric Sn–S_t stretching mode is found around 390 cm^{-1} in the discrete anion. In the title compounds the $[Sn_2S_6]^{4-}$ unit has bonds to Ni^{2+} resulting in slightly shorter Sn–S bonds leading to a shift of the signal to higher wave numbers. The Sn–S–Sn vibrations are located at lower wave numbers at about 340 cm^{-1}. The mode at 280 cm^{-1} could be caused by a Sn_2S_2 ring vibration, the energetic differences between the resonances of **I** and **II** and those reported for $Na_4Sn_2S_6{\cdot}14H_2O$ could be generated by slightly differing bond lengths and angles. But since the Ni–S vibrations are located in this region as well, a detailed assignment is not possible.

Table 2 Data of the signals in the Raman spectra of $Na_4Sn_2S_6{\cdot}14H_2O$[1] and compounds **I** and **II** compared to the $[Sn_2S_6]^{4-}$ anion[1,56,57] and NiS_2 [58] in cm^{-1}

$[Sn_2S_6]^{4-}$	NiS_2	**I**	**II**
391		394	399
341		336	340
	301	298	298
281	283	273	276
	222	219	212
190	181		180

In the IR spectra, the absorptions can be assigned to phen[59–61], the Ni–N stretching vibration at ≈ 420 cm^{-1} (ref. 27 and 28) and to one of the bipy molecules[62–65] (Table 3). The absorptions of the 4,4′-bipy molecule are mostly overlapping with the absorptions of phen, but for example at *ca.* 800 cm^{-1} only 4,4′-bipy causes a signal, which therefore can only be observed in compound **I**. For 2,2′-bipy (**II**) this absorption is shifted to slightly higher wavenumbers (818/819 cm^{-1}) due the different position of the N-atoms in the aromatic ring.

In the UV/vis spectra of both compounds three bands are observed (see Fig. S4 and S5†). The first two absorptions (**I**: ~2.48 eV and ~3.32 eV; **II**: ~2.55 eV and ~3.16 eV) can be assigned to the Ni^{2+} d–d transition $^3A_{2g} \rightarrow {}^3T(^3F)$ and $^3A_{2g} \rightarrow {}^3T(^3P)$.[66] The third band (**I**: 4.63 eV; **II**: 4.59 eV) might probably be traced back to the $\pi \rightarrow \pi^*$ transition of the aromatic amines.[59]

The thermal properties of both compounds were investigated by simultaneously differential thermoanalysis and thermogravimetry. On heating compound **I** at 4 °C min^{-1} one mass step of 40.8% is observed in the TG curve that is accompanied with an endothermic peak in the DTA curve at about 340 °C (Fig. S6†). On further heating a second much smaller mass step is observed and in the following the samples mass decreases continuously. The experimental mass loss observed in each step are not in agreement with those calculated for a stepwise removal of the organic ligands.

Table 3 Absorptions in the IR-spectra of compounds I and II compared to 1,10-phen[59–61], 4,4′-bipy[62,63] and 2,2′-bipy[64,65]

1,10-phen	4,4′-bipy	2,2′-bipy	I	II	Assignment
3035	3023	—	3042	3035w	ν(C–H)
—	—	2982	—	2979w	ν(C–H)
—	—	2916	—	2922w	ν(C–H)
1616	1604	—	1624	1620	ν(C=C)
—	—	1595	—	1598	ν(C–C) + ν(C–N)
1586	1585	—	1587	—	ν(C=C)
—	—	1579	—	1578	ν(C=C)
1560	—	1555	—	1557	ν(C=C)
1516	—	1517	1510	1510	ν(C=C)
1494	1491	—	1494	1491	ν(C=C)
—	—	1458	—	1456	δ(C=C–H)
1421	1416	—	1419	1416	Combination band
1344	—	—	1342	1344	ν(C=C)
—	—	1253	—	1255	ν(C=C)
1216	1218	—	1218	1222	ν(C=C)
—	—	1210	—	1206	δ(C=C–H)
1137	1133	1238	1136	1134	δ(C=C–H)
1092	—	—	1096	1096	ν (C=C)
—	1068	—	1065	—	Ring breathing
1035	—	1038	—	1036	ν(C–N)
996	992	—	991	—	δ(C=C–H)
987	—	—	—	985	δ(C=C–H)
869	—	—	866	—	ν(ring)
853	—	—	—	858	δ(C=C=C)
848	—	—	844	846	δ(C=C=C)
—	—	818	—	819	δ(C=C–H)
—	800	—	802	—	δ(C=C–H)
779	—	—	780	779	δ(C–H)
—	—	758	—	753	δ(C=C–H)
721	724	—	724	722	δ(C–H)
643	—	—	640	637	ν(ring)
625	—	616	—	620	δ(C–H)
606	607	—	609	—	δ(C=C=C)
478	—	—	476	—	ν(ring)
—	—	—	422	422	ν(Ni–N)

Therefore, this reaction seems to be more complex. For compound **II** several poorly resolved mass steps are observed, all of them accompanied with endothermic events in the DTA curve, indicating that the organic ligands are stepwise removed.

Both compounds exhibit paramagnetic behaviour (see Fig. S8 and S9†). The value for the Weiss constant is near zero demonstrating that the Ni^{2+} cations are magnetically isolated. The effective magnetic moment for Ni^{2+} amounts to 2.88 μ_B which is near the spin only value.

3 Experimental section

Synthesis

General. All chemicals were used as purchased without further purifications. The compounds were prepared under solvothermal conditions in glass tubes (inner volume 11 mL) using $NiCl_2{\cdot}6H_2O$, Sn, sulfur, phen, 4,4′-bipy and 2,2′-bipy, respectively. The reaction products were filtered off after reaction, washed with water and ethanol and dried *in vacuo*. Afterwards crystals in the products were separated manually. The homogeneity of the separated samples was checked by X-ray powder diffraction and elemental analysis.

Synthesis of $\{[Ni(C_{12}H_8N_2)_2]_2Sn_2S_6\}\cdot C_{10}H_8N_2\cdot\frac{1}{2}H_2O$ (I). 59.5 mg (0.25 mmol) $NiCl_2{\cdot}6H_2O$, 29.7 mg (0.25 mmol) Sn, 24.1 mg (0.75 mmol) S, 45.1 mg (0.25 mmol) phen ($C_{12}H_8N_2$) and 39.0 mg (0.25 mmol) 4,4′-bipy ($C_{10}H_8N_2$) with 1.5 mL methylamine (40%, aqueous solution, abcr) and 0.5 mL water (pH ≈ 14) were reacted at 120 °C for 7 days. The product consisted of dark red-brown crystals of **I** and black to brown powder and crumbs. The yield of the manually separated crystals was app. 15% (based on tin). According to EDX analysis the brownish-black product contains Ni, Sn and S in varying composition. However, the X-ray powder diffraction pattern did not show reflections and one can only assume that these are X-ray amorphous Ni/Sn sulfides. When the synthesis is carried out under stirring conditions, a brownish powder of **I** is obtained after five hours with a yield being about more than twice as high as under static conditions (appr. 45%, based on tin). Elemental analysis, results in %: found: C 48.47, H 2.71, N 9.54, calculated: C 48.61, H 2.88, N 9.77.

Synthesis of $\{[Ni(C_{12}H_8N_2)_2]_2Sn_2S_6\}\cdot C_{10}H_8N_2$ (II). 59.5 mg (0.25 mmol) $NiCl_2{\cdot}6H_2O$, 29.7 mg (0.25 mmol) Sn, 24.1 mg (0.75 mmol) S, 90.1 mg (0.5 mmol) phen ($C_{12}H_8N_2$) and 39.0 mg (0.25 mmol) 2,2′-bipy ($C_{10}H_8N_2$) with 1.5 mL methylamine (40%, aqueous solution, abcr) and 0.5 mL water were reacted in a glass tube (pH ≈ 14). The mixture was heated at 120 °C for 7 days. The product contained deep red crystals of **II** and greyish-black powder and crumbs. The yield of the crystals was app. 20–25% (based on tin). The yield could be increased significantly under stirring conditions (appr. 65%, based on tin). The byproduct is X-ray amorphous and according to EDX data contains Ni, Sn and S. Elemental analysis, results in %: found: C 48.65, H 2.79, N 9.73, calculated: C 48.91, H 2.83, N 9.83.

Structure determination

The intensity data for the compounds were collected using a STOE IPDS-1 (Imaging Plate Diffraction System) with Mo-K_α radiation. The structures were solved with direct methods using the program SHELXS-97 [67] and the refinements were done against F^2 with SHELXL-97.[68] For all non-hydrogen atoms anisotropic displacement parameters were used. The hydrogen atoms were positioned with idealized geometry and were refined using a riding model. In compound **I** the O–H hydrogen atoms were located in the difference Fourier map, their bond lengths set to ideal values and refined using a riding model. The water molecule is disordered over two half occupied positions and was refined using a split model. The structure contains additional non-coordinating 4,4′-bipy molecules that are located on centres of inversion. In compound **II**, the non-coordinating 2,2′-bipy molecule is disordered and was refined using a split model with restraints for bond lengths and angles.

Selected refinement results are summarized in Table 4. Structural data have been deposited in the Cambridge Crystallographic Data Centre as publication no. CCDC 1054460 (**I**), CCDC 1054461 (**II**).

Table 4 Selected details of the data collection and structure refinement results

	{[Ni(phen)$_2$]$_2$Sn$_2$S$_6$}·4,4′-bipy·$\frac{1}{2}$H$_2$O	{[Ni(phen)$_2$]$_2$Sn$_2$S$_6$}·2,2′-bipy
Crystal system	Monoclinic	Monoclinic
Space group	$C2/c$	$P2_1/n$
M (g mol^{-1})	1442.18	1424.16
a (Å)	18.3431(6)	10.5715(2)
b (Å)	19.4475(6)	9.9086(2)
c (Å)	15.0835(5)	24.9960(4)
α (°)	90	90
β (°)	95.556(2)	92.8000(10)
γ (°)	90	90
V (Å^3)	5355.4(3)	2615.17(8)
Temperature (K)	200(2)	200(2)
Z	4	2
$D_{calculated}$ (g cm^{-3})	1.789	1.809
μ (mm^{-1})	1.9.03	1.946
Scan range (°)	$1.53 \leq \theta \leq 28.00$	$1.63 \leq \theta \leq 27.93$
Reflections collected	31 723	44 107
Independent reflections	6419	6238
Observed reflections	5042	5617
Goodness-of-fit on F^2	1.084	1.059
R values ($I > 2\sigma(I)$)	R_1 = 0.0466	R_1 = 0.0480
	wR_2 = 0.1038	wR_2 = 0.1274
R values (all data)	R_1 = 0.0641	R_1 = 0.0520
	wR_2 = 0.1113	wR_2 = 0.1307
Res. elec. dens. (e Å^{-3})	0.706 and −0.801	1.024 and −0.770

X-ray powder diffractometry

The X-ray powder diffraction patterns were recorded on a STOE Stadi-P powder diffractometer (Cu-K$_{\alpha1}$ radiation, λ = 1.540598 Å, Ge monochromator) in transmission geometry.

SEM and EDX

Scanning electron microscopy investigations and energy dispersive X-ray analyses (EDX) were done with a Philips Environmental Scanning Electron Microscope ESEM XL30 equipped with an EDAX detector.

Raman spectroscopy

Raman spectra were recorded with a Bruker IFS 66 Fourier transform Raman spectrometer (wavelength: 541.5 nm) in the region from 100 to 3500 cm^{-1}.

Infrared spectroscopy

MIR spectra (400–4000 cm^{-1}) were recorded with a Bruker Alpha P spectrometer.

UV/visible spectroscopy

UV/vis spectra were recorded with an UV-vis-NIR two channel spectrometer Cary 5 from Varian Techtron Pty., Darnstadt at room temperature of powdered samples with $BaSO_4$ powder as reference material. The absorption data were calculated applying the Kubelka–Munk relation for diffuse reflectance data.

Thermal properties

DTA-TG measurements were performed using a Netzsch STA 409 CD under a nitrogen flow of 75 mL min^{-1} and at a heating rate of 4 K min^{-1}. The instrument was calibrated using standard reference materials.

Magnetic properties

The magnetic properties were investigated using a physical properties measurement system (PPMS) Model 600 from Quantum Design at H = 100 Oe in the temperature range 1.9–325 K.

4 Conclusions

In the manuscript we presented a new synthesis strategy based on the observation of different coordination abilities of aromatic N-donor ligands towards Ni^{2+}. Applying suitable mixtures of the aromatic amine molecules with the proper ratio between Ni^{2+} and the strong coordinating phen ligand, products crystallized where the medium/weak or non-resp. monodentate aromatic amine molecule acts as stabilizer of the structures *via* π–π-interactions. Currently we experimentally investigate whether this is a new general concept, which can be applied to other transition metals opening new opportunities for the generation of hitherto not accessible thiostannates.

Acknowledgements

Financial support by the State of Schleswig-Holstein and the DFG is gratefully acknowledged.

Notes and references

1 B. Krebs, S. Pohl and W. Schiwy, *Angew. Chem., Int. Ed. Engl.*, 1970, **9**, 897–898.
2 (*a*) K. O. Klepp and F. Fabian, *Z. Naturforsch., B: Chem. Sci.*, 1999, **54**, 1505–1509; (*b*) Klepp, O. Kurt and F. Fabian, *Z. Naturforsch., B: Chem. Sci.*, 1999, **54**, 1505–1509.
3 G. A. Marking, M. Evain, V. Petricek and M. G. Kanatzidis, *J. Solid State Chem.*, 1998, **141**, 17–28.
4 J.-H. Liao, C. Varotsis and M. G. Kanatzidis, *Inorg. Chem.*, 1993, **32**, 2453–2462.
5 E. Ruzin, S. Jakobi and S. Dehnen, *Z. Anorg. Allg. Chem.*, 2008, **634**, 995–1001.
6 O. Palchik, R. G. Iyer, J. H. Liao and M. G. Kanatzidis, *Inorg. Chem.*, 2003, **42**, 5052–5054.
7 P. Nørby, J. Overgaard, P. S. Christensen, B. Richter, X. Song, M. Dong, A. Han, J. Skibsted, B. B. Iversen and S. Johnsen, *Chem. Mater.*, 2014, **26**, 4494–4504.
8 J. B. Parise, Y. Ko, J. Rijssenbeek, D. M. Nellis, K. Tan and S. Koch, *J. Chem. Soc., Chem. Commun.*, 1994, 527.
9 T. Jiang, A. Lough and G. A. Ozin, *Adv. Mater.*, 1998, **10**, 42–46.
10 H. Pada Nayek, Z. Lin and S. Dehnen, *Z. Anorg. Allg. Chem.*, 2009, **635**, 1737–1740.
11 X. Wang, T.-L. Sheng, S.-C. Xiang, S.-M. Hu, R.-B. Fu and X.-T. Wu, *Chin. J. Struct. Chem.*, 2010, **29**, 260–264.

12 M. Behrens, S. Scherb, C. Näther and W. Bensch, *Z. Anorg. Allg. Chem.*, 2003, **629**, 1367–1373.
13 D.-X. Jia, Y. Zhang, J. Dai, Q.-Y. Zhu and X.-M. Gu, *Z. Anorg. Allg. Chem.*, 2004, **630**, 313–318.
14 D.-X. Jia, J. Dai, Q.-Y. Zhu, Y. Zhang and X.-M. Gu, *Polyhedron*, 2004, **23**, 937–942.
15 M.-L. Fu, G.-C. Guo, B. Liu, A.-Q. Wu and J.-S. Huang, *Chin. J. Inorg. Chem.*, 2005, **21**, 25–29.
16 N. Pienack, H. Lühmann, B. Seidlhofer, J. Ammermann, C. Zeisler, F. Danker, C. Näther and W. Bensch, *Solid State Sci.*, 2014, **33**, 67–72.
17 X.-H. Lu, J.-J. Liang, J. Zhao, Y. Zhang and D.-X. Jia, *J. Chem. Crystallogr.*, 2011, **41**, 557–562.
18 J. Zhou, X. Liu, L. An, F. Hu, W. Yan and Y. Zhang, *Inorg. Chem.*, 2012, **51**, 2283–2290.
19 N. Pienack, C. Näther and W. Bensch, *Z. Naturforsch., B: Chem. Sci.*, 2008, **63**, 1243–1251.
20 Z. Wang, G. Xu, Y. Bi and C. Wang, *CrystEngComm*, 2010, **12**, 3703.
21 C.-Y. Yue, X.-W. Lei, L. Yin, X.-R. Zhai, Z.-R. Ba, Y.-Q. Niu and Y.-P. Li, *CrystEngComm*, 2015, **17**, 814–823.
22 J. Zhou, G.-Q. Bian, J. Dai, Y. Zhang, A.-B. Tang and Q.-Y. Zhu, *Inorg. Chem.*, 2007, **46**, 1541–1543.
23 N. Pienack, S. Lehmann, H. Lühmann, M. El-Madani, C. Näther and W. Bensch, *Z. Anorg. Allg. Chem.*, 2008, **634**, 2323–2329.
24 N. Pienack, C. Näther and W. Bensch, *Eur. J. Inorg. Chem.*, 2009, 1575–1577.
25 N. Pienack, D. Schinkel, A. Puls, M.-E. Ordolff, H. Lühmann, C. Näther and W. Bensch, *Z. Naturforsch., B: Chem. Sci.*, 2012, **67**, 1098–1106.
26 C. Zeisler, C. Näther and W. Bensch, *CrystEngComm*, 2013, **15**, 8874.
27 J. Hilbert, C. Näther and W. Bensch, *Inorg. Chem.*, 2014, **53**, 5619–5630.
28 J. Hilbert, C. Näther and W. Bensch, *Z. Anorg. Allg. Chem.*, 2014, **640**, 2858–2863.
29 G.-N. Liu, G.-C. Guo, F. Chen, S.-P. Guo, X.-M. Jiang, C. Yang, M.-S. Wang, M.-F. Wu and J.-S. Huang, *CrystEngComm*, 2010, **12**, 4035.
30 N. Pienack, K. Möller, C. Näther and W. Bensch, *Solid State Sci.*, 2007, **9**, 1110–1114.
31 N. Pienack, C. Näther and W. Bensch, *Solid State Sci.*, 2007, **9**, 100–107.
32 N. Pienack and W. Bensch, *Z. Anorg. Allg. Chem.*, 2006, **632**, 1733–1736.
33 M. Behrens, M.-E. Ordolff, C. Näther, W. Bensch, K.-D. Becker, C. Guillot-Deudon, A. Lafond and J. A. Cody, *Inorg. Chem.*, 2010, **49**, 8305–8309.
34 N. Pienack, C. Näther and W. Bensch, *Eur. J. Inorg. Chem.*, 2009, 937–946.
35 N. Pienack, A. Puls, C. Näther and W. Bensch, *Inorg. Chem.*, 2008, **47**, 9606–9611.
36 M. BaiYin, L. Ye, Y. An, X. Liu, C. Jia and G. Ning, *Bull. Chem. Soc. Jpn.*, 2005, **78**, 1283–1284.
37 Y. An, B. Menghe, L. Ye, M. Ji, X. Liu and G. Ning, *Inorg. Chem. Commun.*, 2005, **8**, 301–303.
38 Y. Wang, M. BaiYin, S. Ji, X. Liu, Y. An and G. Ning, *Chem. Res. Chin. Univ.*, 2006, **22**, 411–414.
39 R.-C. Zhang, H.-G. Yao, S.-H. Ji, M.-C. Liu, M. Ji and Y.-L. An, *Chem. Commun.*, 2010, **46**, 4550–4552.
40 (*a*) A. Rabenau, *Angew. Chem., Int. Ed. Engl.*, 1985, **97**, 1017–1032; (*b*) W. S. Sheldrick and M. Wachhold, *Angew. Chem., Int. Ed. Engl.*, 1997, **36**, 206–224; (*c*) W. S. Sheldrick and M. Wachhold, *Coord. Chem. Rev.*, 1998, **176**, 211–322; (*d*) S. Dehnen and M. Melullis, *Coord. Chem. Rev.*, 2007, **251**, 1259–1280; (*e*) G. Demazeau, *J. Mater. Sci.*, 2008, **43**, 2104–2114; (*f*) W. S. Sheldrick, *J. Chem. Soc., Dalton Trans.*, 2000, 3041–3052; (*g*) X. Bu, N. Zheng and P. Feng, *Chem. – Eur. J.*, 2004, **10**, 3356–3362; (*h*) B. Seidlhofer, N. Pienack and W. Bensch, *Z. Naturforsch., B: Chem. Sci.*, 2010, **65**, 937–975; (*i*) W.-W. Xiong, G. Zhang and Q. Zhang, *Inorg. Chem. Front.*, 2014, **1**, 292.
41 (*a*) W. Bensch and M. Schur, *Eur. J. Solid State Inorg. Chem.*, 1996, **33**, 1149–1160; (*b*) W. Bensch and M. Schur, *Z. Naturforsch., B: Chem. Sci.*, 1997, **52**, 405–409; (*c*) M. Schur, C. Näther and W. Bensch, *Z. Naturforsch., B: Chem. Sci.*, 2001, **56**, 79–84; (*d*) A. Puls, C. Näther and W. Bensch, *Z. Anorg. Allg. Chem.*, 2006, **632**, 1239–1243.
42 L. Goerigk, H. Kruse and S. Grimme, *ChemPhysChem*, 2011, **12**, 3421–3433.
43 S. Grimme, *Angew. Chem., Int. Ed.*, 2008, **47**, 3430–3434.
44 S. Grimme, *WIREs Comput. Mol. Sci.*, 2011, **1**, 211–228.
45 S. Grimme, J. Antony, S. Ehrlich and H. Krieg, *J. Chem. Phys.*, 2010, **132**, 154104.
46 J. Zhou, X. Liu, G.-Q. Chen, F. Zhang and L.-R. Li, *Z. Naturforsch., B: Chem. Sci.*, 2010, **65**, 1229–1234.
47 (*a*) C.-Y. Yue, X.-W. Lei, Y.-X. Ma, N. Sheng, Y.-D. Yang, G.-D. Liu and X.-R. Zhai, *Cryst. Growth Des.*, 2014, **14**, 101–109; (*b*) R. J. Lees, A. V. Powell and A. M. Chippindale, *Polyhedron*, 2005, **24**, 1941–1948; (*c*) H.-O. Stephan and M. G. Kanatzidis, *Inorg. Chem.*, 1997, **36**, 6050–6057; (*d*) H. Lühmann, Z. Rejai, K. Möller, P. Leisner, M.-E. Ordolff, C. Näther and W. Bensch, *Z. Anorg. Allg. Chem.*, 2008, **634**, 1687–1695; (*e*) R. Stähler, C. Näther and W. Bensch, *Eur. J. Inorg. Chem.*, 2001, 1835–1840; (*f*) R. Kiebach, W. Bensch, R.-D. Hoffmann and R. Pöttgen, *Z. Anorg. Allg. Chem.*, 2003, **629**, 532–538; (*g*) C. Anderer, N. Delwa de Alarcon, C. Näther and W. Bensch, *Chem. – Eur. J.*, 2014, **20**, 16953–16959; (*h*) J. Zhou and L. An, *CrystEngComm*, 2011, **13**, 5924–5928; (*i*) J. Zhou, L. An, X. Liu, L. Huang and X. Huang, *Dalton Trans.*, 2011, **40**, 11419–11424; (*j*) M.-L. Feng, W.-W. Xiong, D. Ye, J.-R. Li and X.-Y. Huang, *Chem. – Asian J.*, 2010, **5**, 1817–1823; (*k*) J. Zhou, L. An and F. Zhang, *Inorg. Chem.*, 2011, **50**, 415–417; (*l*) X. Liu, *Inorg. Chem. Commun.*, 2011, **14**, 437–439; (*m*) W. Tang, C. Tang, F. Wang, R. Chen, Y. Zhang and D. Jia, *J. Solid State Chem.*, 2013, **199**, 287–294; (*n*) P. Vaqueiro, A. M. Chippindale and A. V. Powell, *Inorg. Chem.*, 2004, **43**, 7963–7965; (*o*) H.-O. Stephan and

M. G. Kanatzidis, *J. Am. Chem. Soc.*, 1996, **118**, 12226–12227; (*p*) X. Liu and J. Zhou, *Inorg. Chem. Commun.*, 2011, **14**, 1286–1289; (*q*) M.-F. Wang, C.-Y. Yue, Z.-D. Yuan and X.-W. Lei, *Acta Crystallogr., Sect. C: Cryst. Struct. Commun.*, 2013, **69**, 855–858; (*r*) P. Vaqueiro, D. P. Darlow, A. V. Powell and A. M. Chippindale, *Solid State Ionics*, 2004, **172**, 601–605; (*s*) R. J. Lees, A. V. Powell and A. M. Chippindale, *J. Phys. Chem. Solids*, 2007, **68**, 1215–1219; (*t*) L. Engelke, C. Näther, P. Leisner and W. Bensch, *Z. Anorg. Allg. Chem.*, 2008, **634**, 2959–2965.

48 C.-Y. Yue, X.-W. Lei, R.-Q. Liu, H.-P. Zhang, X.-R. Zhai, W.-P. Li, M. Zhou, Z.-F. Zhao, Y.-X. Ma and Y.-D. Yang, *Cryst. Growth Des.*, 2014, **14**, 2411–2421.

49 J. Zhou, G.-Q. Bian, Y. Zhang, J. Dai and N. Cheng, *Z. Anorg. Allg. Chem.*, 2007, **633**, 2701–2705.

50 (*a*) R. Stähler and W. Bensch, *J. Chem. Soc., Dalton Trans.*, 2001, 2518–2522; (*b*) M. Schaefer, R. Stähler, W.-R. Kiebach, C. Näther and W. Bensch, *Z. Anorg. Allg. Chem.*, 2004, **630**, 1816–1822; (*c*) J. Lichte, H. Lühmann, C. Näther and W. Bensch, *Z. Anorg. Allg. Chem.*, 2009, **635**, 2021–2026; (*d*) J. Zhou, X. Liu, L. An, F. Hu, Y. Kan, R. Li and Z. Shen, *Dalton Trans.*, 2013, **42**, 1735–1742.

51 R. Kiebach, R. Warratz, C. Näther and W. Bensch, *Z. Anorg. Allg. Chem.*, 2009, **635**, 988–994.

52 H. Irving and J. Mellor, *J. Chem. Soc.*, 1962, 5222–5237.

53 (*a*) Y. Zhang, J. Zhou, A.-B. Tang, G.-Q. Bian and J. Dai, *J. Chem. Crystallogr.*, 2010, **40**, 496–500; (*b*) X.-M. Gu, J. Dai, D.-X. Jia, Y. Zhang and Q.-Y. Zhu, *Cryst. Growth Des.*, 2005, **5**, 1845–1848.

54 E. C. Lee, D. Kim, P. Jurecka, P. Tarakeshwar, P. Hobza and K. S. Kim, *J. Phys. Chem. A*, 2007, **111**, 3446–3457.

55 C. R. Martinez and B. L. Iverson, *Chem. Sci.*, 2012, **3**, 2191.

56 B. Krebs and W. Schiwy, *Z. Anorg. Allg. Chem.*, 1973, **398**, 63–71.

57 W. Schiwy, C. Blutau, D. Gäthje and B. Krebs, *Z. Anorg. Allg. Chem.*, 1975, **412**, 1–10.

58 D. W. Bishop, P. S. Thomas and A. S. Ray, *Mater. Res. Bull.*, 1998, **33**, 1303–1306.

59 M. S. Atanassova and G. D. Dimitrov, *Spectrochim. Acta, Part A*, 2003, **59**, 1655–1662.

60 M. Reiher, G. Brehm and S. Schneider, *J. Phys. Chem. A*, 2004, **108**, 734–742.

61 D. A. Thornton and G. M. Watkins, *J. Coord. Chem.*, 1992, **25**, 299–315.

62 R. Podgajny, M. Bałanda, M. Sikora, M. Borowiec, L. Spałek, C. Kapusta and B. Sieklucka, *Dalton Trans.*, 2006, 2801–2809.

63 J. G. Contreras and C. J. Díz, *J. Coord. Chem.*, 2007, **16**, 245–249.

64 E. Castellucci, L. Angeloni, N. Neto and G. Sbrana, *Chem. Phys.*, 1979, **43**, 365–373.

65 M. L. Niven and G. C. Percy, *Transition Met. Chem.*, 1978, **3**, 267–271.

66 S. P. Roe, J. O. Hill and R. J. Magee, *Monatsh. Chem.*, 1991, **122**, 467–478.

67 G. M. Sheldrick, *SHELXS-97, Program for the Solution of Crystal Structures*, University of Göttingen, Göttingen (Germany), 1997.

68 G. M. Sheldrick, *SHELXS-97, Program for the Solution of Crystal Structures*, University of Göttingen, Göttingen (Germany), 1997.

3.1.4 Erfolgreiche Verknüpfung von TM-Amin-Komplexen mit dem Thiostannatanion durch Verwendung ausgewählter Aminmoleküle *(accepted 24.10.16)*

Zusammenfassung der Veröffentlichung „Transition Metal Complexes with Linkage to the Thiostannate Units Forced by Suitable Amine Molecules“.

Die Verbindungen, in denen TM-S-Bindungen ein charakteristisches Merkmal darstellen, wurden durch Verwendung ausgewählter Aminmoleküle (phen, 2,2‘-bipy, 1,2-dach, cyclam) erhalten. Die Verbindungen $\{[Ni(phen)_2]_2[Sn_2S_6]\}\cdot$biph ($P2_1/n$, Z=2) und $\{[Ni(phen)_2]_2[Sn_2S_6]\}\cdot phen\cdot H_2O$ ($P\bar{1}$, Z=1) sind isostrukturell zu den in Kap. 3.1.1 bzw. 3.1.3 diskutierten Verbindungen. Für die Synthese wurde das unter Abschnitt 3.1.3 vorgestellte Konzept zusätzlicher aromatischer Aminmoleküle erweitert. Die Ergebnisse der Synthesen mit biph (Integration), Naphthalin, Anthracen, Phenanthren oder *p*-Terphenyl (keine Integration in die Kristallstruktur) legen nahe, dass nicht nur allein der aromatische Charakter des Additives, sondern auch dessen Form und Größe entscheidend für die Ausbildung von π–π-Wechselwirkungen und daher für eine Integration in die Kristallstruktur ist. Trotzdem war die Anwesenheit von einem der Aminmoleküle wie Naphthalin, Anthracen, Phenanthren oder *p*-Terphenyl notwendig für die Kristallisation von $\{[Ni(phen)_2]_2[Sn_2S_6]\}\cdot phen\cdot H_2O$.

Die Verbindung $\{[Fe(1,2\text{-dach})_2][Sn_2S_6]\}_n\cdot 2n$1,2-dachH ($P\bar{1}$, Z=1) ist ein seltenes Beispiel einer eisenhaltigen Zinn-Schwefel-Verbindung und wurde unter solvothermalen Bedingungen mit Fe, Sn, S (1:1:4) in 1,2-dach im Stahlautoklav mit Tefloneinsatz (130°C, 4d) hergestellt. Wie alle bisherigen eisenhaltigen Verbindungen, weist auch diese Verbindung ein manganhaltiges Pendant auf.[44] Dies ist ein Hinweis darauf, dass Fe^{2+} zwar deutlich schwieriger zu einer Fe-S-Bindung gezwungen werden kann, bei geeigneten Bedingungen allerdings ein vergleichbares Verhalten wie Mangan aufweist.[36,44,48]

$\{[Ni(cyclam)]_2[Sn_2S_6]\}_n\cdot 2nH_2O$ ($P\bar{1}$, Z=1) ist erst das zweite Beispiel für eine zweidimensionale Zinn-Schwefel-Verbindung: Jedes der terminalen S Atome des $[Sn_2S_6]^{4-}$-Anions bindet an einen anderen $[Ni(cyclam)]^{2+}$-Komplex und führt zur Ausbildung von Schichten, welche über Wasserstoffbrücken der Wassermoleküle miteinander verknüpft sind. Die Verbindung konnte sowohl mit $NiCl_2\cdot 6H_2O$, Sn, S und cyclam (1:1:3:1) in wässriger Methylaminlösung (120°C, 7d), als auch mit $[Ni(cyclam)][ClO_4]_2$ und $Na_4SnS_4\cdot 14H_2O$ in Wasser (120°C, 5d) hergestellt werden. Der zweite Syntheseweg stellt eine neue Route dar, bei der (wasser)lösliche Precursoren zur Synthese von Zinn-Schwefel-Verbindungen eingesetzt wurden.

Die Verbindung $\{[Mn(2,2'\text{-bipy})_2]_2[Sn_2S_6]\}$ ($P2_1/n$, Z=2) konnte nur bei der Reaktion von $[Mn(2,2'\text{-bipy})_3][ClO_4]_2$ und $Na_4SnS_4\cdot 14H_2O$ (1:1) bei pH ~10 (120°C, 7d) synthetisiert werden. Alle anderen Versuche (siehe Kap. 3.1.1) waren erfolglos. In der Struktur sind die Moleküle so angeordnet, dass π-π-Wechselwirkungen auftreten können.

ARTICLE WILEY-VCH

Transition Metal Complexes with Linkage to the Thiostannate Units Forced by Suitable Amine Molecules

Jessica Hilbert,[a] Nicole Pienack, [a] Henning Lühmann, [a] Christian Näther[a] and Wolfgang Bensch*[a]

Abstract: Using the solvothermal approach five new tin-sulfur compounds were synthesized. All compounds exhibit a direct covalent bond between the thiostannate unit and the charge compensating transition metal TM^{2+} ion, leading to the formation of discrete neutral molecules, chains or layered structures. In the structures, the $[Sn_2S_6]^{4-}$ anion is connected to the TM^{2+} cations in three different ways: a) only two and opposite terminal S atoms are involved in bonding; b) the four terminal S atoms connect two different complexes and c) the four terminal S atoms link four complexes. The compounds are: $\{[Ni(phen)_2]_2[Sn_2S_6]\}\cdot$biph (**1**), $\{[Ni(phen)_2]_2[Sn_2S_6]\}\cdot phen\cdot H_2O$ (**2**), $\{[Fe(1,2\text{-dach})_2][Sn_2S_6]\}_n\cdot 2n$ 1,2-dachH (**3**), $\{[Ni(cyclam)]_2[Sn_2S_6]\}_n\cdot 2n\ H_2O$ (**4**) and $\{[Mn(2,2'\text{-bipy})_2]_2[Sn_2S_6]\}$ (**5**). Compounds **1**-**3** were prepared from elements/chlorides, whereas for the preparation of compounds **4** and **5** a new synthesis strategy was developed using $Na_4SnS_4\cdot 14H_2O$ and TM^{2+} centered complexes as precursor. Under solvothermal conditions *in situ* condensation reaction of the $[SnS_4]^{4-}$ anions leads to the formation of the $[Sn_2S_6]^{4-}$ moiety.

Keywords: Crystal Structures, Solvothermal Syntheses, Spectroscopic Properties, Tin, Sulfur

Introduction

Thiostannates and tin-sulfur compounds exhibit a large variety of chemical compositions and crystal structures. The charge compensation in these compounds can be achieved in different ways: a) inorganic cations, b) inorganic-organic hybrid compounds with protonated amine molecules as counterions, c) compounds with integrated transition metal ions (TM) in the thiostannate unit and protonated amines as counterions and finally d) compounds containing $[TM(amine)_n]^{m+}$ or $[Ln(amine)_n]^{m+}$ complexes for charge compensation as summarized in several review articles.[1,2,3] In the latter group mainly the $[Sn_2S_6]^{4-}$ unit is observed, whereas the $[SnS_4]^{4-}$ anion is less common.[1,3,4,5–11] Other thiostannate ions like for example $[Sn_3S_7]^{2-}$,[12,13,14] $[Sn_4S_9]^{2-}$,[13,15] $[Sn_5S_{12}]^{4-}$,[14] $[Sn_3S_9]^{6-}$ [16] or $[Sn_4S_{10}]^{4-}$ [17] are only found in pure inorganic or inorganic-organic hybrid compounds so far. The $[Sn_4S_{10}]^{4-}$ anion seems to be largest ion and it is assumed that for larger units the charge at the cation sites (Sn^{4+}) is too high to satisfy the coordination environment of the resulting tri-coordinated anion sites (S^{2-}).[18] The main challenge during the synthesis of $[TM(amine)_n]^{m+}$ containing tin-sulfur compounds is the covalent linkage of the cation of the complexes to the thiostannate units (Tab. 1). In most compounds only discrete anions and cations are observed. Compounds exhibiting discrete molecules (0D), chain (1D) or layer (2D) structures generated by TM^{2+}-S bonds are less often observed (see Tab. 1). Hence, it is a synthetic challenge to force the formation of bonds between the $[TM(amine)_n]^{m+}$ complexes and different thiostannate anions. Regarding the chemical nature of Mn^{2+}, Fe^{2+}, Co^{2+}, Ni^{2+} or Zn^{2+} ions, Mn^{2+} exhibits a very different behavior with a significantly larger number of compounds with both Mn-N and Mn-S bonds (Tab. 1).

Table 1. The numbers of thiostannate/tin-sulfur compounds with $[TM(amine)_n]^{m+}$ complexes as charge compensating units and the dimensionality.

TM	Discrete ions	0D	1D	2D
Mn	2 [19,20]	9 [6,21,22]	7 [5,11,22,23,24]	---
Fe	---	3 [7,25]	---	---
Co	3 [11,19,26]	4 [7,25,27]	---	1 [10]
Ni	10 [9,11,27,28]	4 [8,11,25]	1 [9]	---
Zn	1 [19]	1 [26]	---	---
TM	16	21	8	1

Therefore, Mn^{2+} seems to have a comparable affinity towards N and S atoms. The remaining cations mentioned above exhibit an obviously higher affinity towards N, and bond formation to S atom(s) has to be enforced by synthetic tricks, e.g. using amines like tetraethylenepentamine (tepa) in $\{[Ni(tepa)]_2[Sn_2S_6]\}$ [11,25] or tris(2-aminoethyl)amine (tren) in $\{[Ni(tren)]_2[Sn_2S_6]\}_n$ [9], which cannot saturate the coordination sphere of the metal center. Aromatic or cyclic amines with rigid positions of the amine groups like 1,10-phenanthroline (phen) in $\{[TM(phen)_2]_2[Sn_2S_6]\}\cdot$(TM = Fe, Co) [7,8] and $\{[Ni(phen)_2]_2[Sn_2S_6]\}\cdot$amine (amine = 2,2'-bipyridine (2,2'-bipy), 4,4'-bipyridine (4,4'-bipy)) [8] and 1,2-diaminocyclohexane (1,2-dach) in the related class of thioantimonates in $\{[Fe(1,2\text{-dach})_2][Sb_6S_{10}]\}$ [29] seem to be exceptions: in principal these amine ligands could satisfy the coordination requirements of the TM^{2+} centers, but interestingly TM-S bonds have been observed, even with Fe^{2+} and Co^{2+} which normally prefer bonds to N donor ligands. A further observation is that only few $[TM(amine)_n]^{2+}$ containing tin-sulfur compounds exhibit a dimensionality larger than zero. Among these, compounds with Mn^{2+} are the most frequent, which might be explained by the circumstance that Mn(II) do not favor a special coordination geometry, as exemplified by a variety of thiometalate compounds.[24,30] However, the only known two dimensional $[TM(amine)_n]^{2+}$ containing tin-sulfur compound is $\{[Co(cyclam)_2[Sn_2S_6]\}_n\cdot 2nH_2O$

* Prof. Dr. W. Bensch
E-Mail: wbensch@ac.uni-kiel.de
[a] Institute of Inorganic Chemistry
Christian-Albrechts-University of Kiel
Max-Eyth-Str. 2, 24118 Kiel, Germany

Supporting information for this article is given via a link at the end of the document.

(cyclam = 1,4,8,11-tetraazacyclotetradecane),[10] again a ligand with quite rigid positions of the amine groups.

In our ongoing work we performed further syntheses with the amine molecules 1,2-dach, phen, cyclam and 2,2'-bipy. The experiments afforded five new tin-sulfur compounds: $\{[Ni(phen)_2]_2[Sn_2S_6]\}\cdot biph$ (**1**) (biph = biphenyl), $\{[Ni(phen)_2]_2[Sn_2S_6]\}\cdot phen\cdot H_2O$ (**2**), $\{[Fe(1,2\text{-dach})_2][Sn_2S_6]\}_n \cdot 2n$ 1,2-dachH (**3**), $\{[Ni(cyclam)]_2[Sn_2S_6]\}_n\cdot 2n\, H_2O$ (**4**) and $\{[Mn(2,2'\text{-bipy})_2]_2[Sn_2S_6]\}$ (**5**), all featuring a direct connection between the thiostannate units and the charge compensating $[TM(amine)_n]^{2+}$ complexes. Moreover, for the compounds **3** (1D) und **4** (2D) higher dimensionalities of the structures are observed.

Experimental Section

General: The following chemicals were used as purchased without further purification: $NiCl_2\cdot 6H_2O$ (pure, Merck); Fe (≥ 99%, Merck); Sn (99.5%, Alfa Aesar); S (99.5% Alfa Aesar), 1,10-phenanthroline (phen, $C_{12}H_8N_2$, 99%, abcr); biphenyl (biph, $C_{12}H_8$, 99%, Acros Organics); methylamine solution (ma, in water 40%, abcr); *trans*-1,2-diaminocyclohexane (1,2-dach, $C_6H_{14}N_2$, 99% Aldrich); 1,4,8,11-tetraazacyclotetradecane (cyclam, $C_{10}H_{24}N_4$, 98%, abcr). $Na_4SnS_4\cdot 14H_2O$, $[Ni(cyclam)][ClO_4]_2$ and $[Mn(2,2'\text{-bipy})_3][ClO_4]$ were synthesized applying literature procedure.[31] The reaction products were filtered off, washed with water and ethanol and dried over silica gel. The crystalline products were separated manually, and the homogeneity was checked by X-ray powder diffraction (XRPD) and elemental analysis. CAUTION: Salts containing perchlorates are potentially explosive when heated.

Synthesis of $\{[Ni(phen)_2]_2[Sn_2S_6]\}\cdot biph$ (1): 59.5 mg (0.25 mmol) $NiCl_2\cdot 6H_2O$, 29.7 mg (0.25 mmol) Sn, 24.1 mg (0.75 mmol) S, 45.1 mg (0.25 mmol) phen and 38.6 mg (0.25 mmol) biph were reacted in a glass tube (inner volume 11 mL) with 1.5 mL ma and 0.5 mL H_2O at 120°C for 7 d. The product contained dark red crystals of **1** in a yield of about 10%, based on tin, and black powder, which could not be identified. Elemental analysis, results in %: found: C 50.3, H 2.6, N 7.6, calculated: C 50.7, H 2.8, N 7.9.

Synthesis of $\{[Ni(phen)_2]_2[Sn_2S_6]\}\cdot phen\cdot H_2O$ (2): 59.5 mg (0.25 mmol) $NiCl_2\cdot 6H_2O$, 29.7 mg (0.25 mmol) Sn, 24.1 mg (0.75 mmol) S, 450 mg (2.5 mmol) phen and 2 mL 30% ma were mixed in a glass tube (inner volume 11 mL) and heated at 120°C for 7 d. The product consisted of dark red crystals of **2**, X-ray amorphous brownish red crumbs and powder (yield: ~ 25%, based on tin). Elemental analysis, results in %: found: C 49.4, H 2.8, N 9.8, calculated: C 49.2, H 2.9, N 9.6.

Synthesis of $\{[Fe(1,2\text{-dach})_2][Sn_2S_6]\}_n\cdot 2n$1,2-dachH (3): 56.2 mg (1.01 mmol) Fe, 118.7 mg (1.00 mmol) Sn and 128.9 (4.02 mmol) S with 4 mL 1,2-dach were heated in a Teflon-lined steel autoclave at 130°C for 4 d. The yield of the yellow needles was about 15 - 20% (based on tin). Elemental analysis, results in %: found: C 29.8, H 6.0, N 11.8; calculated: C 30.5, H6.2, N 11.9.

Synthesis of $\{[Ni(cyclam)]_2[Sn_2S_6]\}_n\cdot 2nH_2O$ (4): 59.5 mg (0.25 mmol) $NiCl_2\cdot 6H_2O$, 29.7 mg (0.25 mmol) Sn, 24.1 mg (0.75 mmol) S and 55.1 mg (0.25 mmol) cyclam were reacted with 2 mL 30% ma in a glass tube (inner volume 11 mL) at 120°C for 7 d. The compound could also be obtained by reacting 114 mg (0.25 mmol) $[Ni(cyclam)][ClO_4]_2$ and 296 mg (0.5 mmol) $Na_4SnS_4\cdot 14H_2O$ with 2 mL H_2O in a glass tube at 120°C for 5d. The product consisted of orange needles/blocks (yield: ~ 40%, based on tin) as well as fawn powder. Elemental analysis, results in %: found: C 24.5, H 5.4, N 11.1, calculated: C 24.4, H 5.3, N 11.4.

Synthesis of $\{[Mn(2,2'\text{-bipy})_2]_2[Sn_2S_6]\}$ (5): 118.2 mg (0.20 mmol) $Na_4SnS_4\cdot 14H_2O$ and 144.5 mg (0.20 mmol) $[Mn(2,2'\text{-bipy})_3][ClO_4]_2$ were reacted in 2 mL H_2O with an adjusted pH value of 10 (approx. 50 µL 0.2 m HCl) in a glass tube (inner volume 11 mL) at 120°C for 7 d. The product consists of red crystals of **5** in app. 35 % yield (based on tin), and X-ray amorphous black crumbs. Elemental analysis, results in %: found: C 41.2, H 2.8, N 9.8, calculated: C 41.3, H 2.8, N 9.6.

Crystal Structure determination: The intensity data were collected using a STOE IPDS-1 (Imaging Plate Diffraction System) with Mo-K_α radiation at 170(2), 200(2) and 293(2) K (Tab. 2). The structures were solved with direct methods using the program Shelxs-97 [32] and the refinements were done against F^2 with Shelxl-97 [33] and Shelxl-2014 [34], respectively. All non-hydrogen atoms were refined anisotropic. The C-H hydrogen atoms were positioned with idealized geometry and were refined isotropic with $U_{iso}(H) = 1.2\ U_{eq}(C)$ using a riding model. In compound **1** the biphenyl molecule is disordered and was refined with half occupancy and restraints for bond lengths and bond angles. In compound **2** the H_2O hydrogen atoms could not be located but were considered in the calculation of the formula and the molecular weight. One phen ligand is disordered around a center of inversion, in which also one water molecule is involved. Both of them were refined with half occupancy. The disorder remains constant if the structure refinement is performed in space group *P*1, where all atoms are located in general positions. For compound **3** the N-H hydrogen atoms were positioned with idealized geometry and refined isotropic using a riding model, except those at N4 which were located in the difference map. Their bond lengths were set to an ideal value, and finally they were refined by using a riding model. For compound **4** the water hydrogen atoms were located in difference map, their bond lengths were set to ideal values and finally they were refined isotropic with $U_{iso}(H) = 1.5\ U_{eq}(O)$ using a riding model. For compound **5** one of the 2,2'-bipy ligands is disordered in two orientations and was refined using restraints for the geometry (SAME) and for the anisotropic displacement parameters (SIMU/DELU).

Selected refinement results are summarized in Tab. 2. Structural data have been deposited in the Cambridge Crystallographic Data Centre as publication no. CCDC 1502618 (**1**) to CCDC 1502622 (**5**). Copies of the data can be obtained, free of charge, on application to CCDC, 12 Union Road, Cambridge CB2 1 EZ, UK (mail: deposit@ccdc.ca.ac.uk).

X-ray Powder Diffractometry: The X-ray powder diffraction patterns were measured on a STOE Stadi-P powder diffractometer (Cu-K_α1 radiation, λ = 1.540598 Å, Ge monochromator) in transmission geometry with a MYTHEN 1K detector (DECTRIS) or a STOE linear PSD (compound **3**) (Supporting Information, Fig. S1).

Infrared Spectroscopy: MIR spectra (400-4000 cm^{-1}) were collected with an ATI Mattson Genesis spectrometer or a Bruker Alpha P spectrometer (Supporting Information, Fig. S2-4 and Tab. S1-3).

Raman spectroscopy: Raman spectra were recorded with a Bruker IFS 66 Fourier transform Raman spectrometer (wavelength: 541.5 nm) in the region from 100 to 3500 cm^{-1} (Supporting Information, Fig. S5 and Tab. S4).

Ultraviolet-Visible Spectroscopy: UV/visible (UV/vis) spectroscopic investigations were carried out at room temperature using an UV/Vis/NIR two-channel spectrometer Cary 5 from Varian Techtron Pty., Darmstadt (200-3000 cm^{-1}). The optical properties of the compounds were investigated by analyzing the UV/Vis reflectance spectra of the powdered samples (with $BaSO_4$ powder used as reference material) (Supporting Information Fig. S6)

Elemental Analysis: CHN analyses were done with a EURO EA Elemental Analyzer, fabricated by EURO VECTOR Instruments and Software.

Energy Dispersive X-ray Spectroscopy: Scanning electron microscopy investigations and EDX analyses were done using a Philips Environmental Scanning Electron Microscope ESEM XL30 equipped with an EDAX detector.

Table 2: Selected details of the data collection and structure refinement results.

	1	2	3	4	5
crystal system	monoclinic	triclinic	triclinic	triclinic	monoclinic
space group	$P2_1/n$	$P\bar{1}$	$P\bar{1}$	$P\bar{1}$	$P2_1/n$
M (g/ mol)	1422.17	1466.19	944.44	983.86	1164.35
a (Å)	10.5704(3)	11.0469(4)	7.2867(3)	9.0689(4)	8.7695(3)
b (Å)	9.9312(2)	12.0833(5)	11.1149(5)	9.8368(4)	20.5296(6)
c (Å)	25.1118(8)	12.6141(5)	13.1459(6)	10.1537(4)	12.3761(4)
α (°)	90	115.055(3)	76.927(4)	97.227(3)	90
β (°)	93.041(3)	88.190(3)	74.900(4)	94.227(3)	95.791(3)
γ (°)	90	110.349(3)	82.578(4)	104.107(3)	90
V (Å3)	2632.44(12)	1416.81(10)	998.50	866.36(6)	2216.75
temperature (K)	170(2)	170(2)	293(2)	200(2)	200(2)
Z	2	1	1	1	2
$D_{calculated}$ (g/ cm^3)	1.794	1.718	1.571	1.886	1.744
μ (mm^{-1})	1.932	1.800	1.940	2.890	1.993
scan range (deg)	1.624≤ θ ≤27.004	1.799≤ θ ≤27.004	1.64≤ θ ≤29.18	2.03≤ θ ≤27.92	1.929≤ θ ≤26.798
reflections collected	18437	12598	19083	13721	18518
independent reflections	5764	6107	5377	4135	4691
observed reflections	4751	4756	3632	3686	4143
goodness-of-fit on F^2	1.030	0.988	1.392	1.047	1.048
R values (I > 2σ(I))	R1 = 0.0381 wR2 = 0.0947	R1 = 0.0409 wR2 = 0.1005	R1 = 0.0294 wR2 = 0.0717	R1 = 0.0337 wR2 = 0.0844	R1 = 0.0348 wR2 = 0.0910
R values (all data)	R1 = 0.0496 wR2 = 0.0997	R1 = 0.0567 wR2 = 0.1074	R1 = 0.0356 wR2 = 0.0730	R1 = 0.0380 wR2 = 0.0859	R1 = 0.0408 wR2 = 0.0944
res. elec. dens. (e/Å^3)	0.746 and -0.807	0.847 and -0.933	0.841 and -0.822	0.912 and -0.988	0.426 and -0.373

Results and Discussion

Synthetic Aspects

Despite all efforts there are no general rules for predictions of the outcome of a solvothermal synthesis. There are some hints available based on experiences obtained by "trial-and-error" syntheses.[35] Starting from known compounds stepwise variations were done until a crystalline product is obtained, followed by synthesis optimization for improving the crystal quality and the yield. Two approaches were applied to prepare the title compounds: in one approach TM or $TMCl_2$, Sn, S and amines in aqueous solutions were applied. The resulting thiostannate unit and TM(II) complexes are then formed *in-situ.* Normally these reactions take place in a strong basic milieu (pH 12-14), ideal for the formation of reactive polysulfides necessary for further reactions with other educts, intermediates or products.[1,36] On the other hand the compounds could be crystallized applying preformed $[TM(amine)_n][ClO_4]_2$ complexes and $Na_4SnS_4 \cdot 14H_2O$ in water at pH 10-12 (Fig. 1).

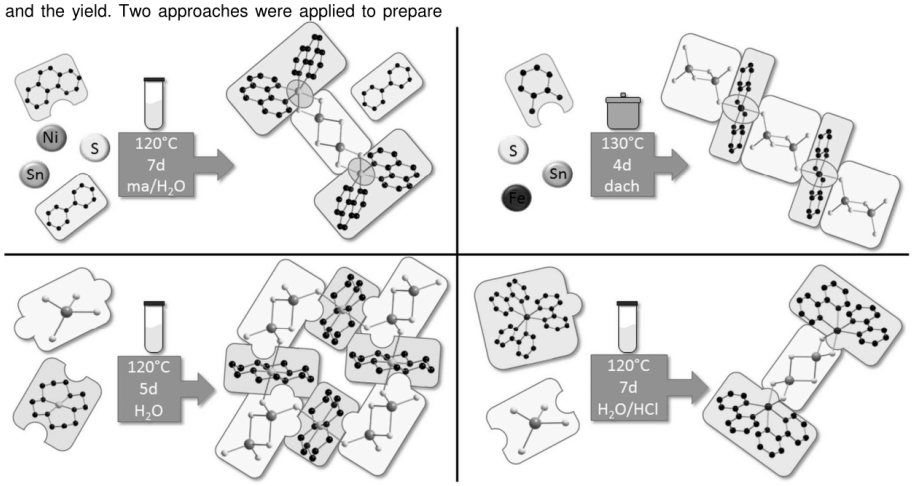

Figure 1: Graphical overview of the different synthesis routes and resulting compound.

$[Ni(phen)_2]_2[Sn_2S_6]$}·biph (**1**) was synthesized analogous to the compounds {$[Ni(phen)_2]_2[Sn_2S_6]$}·2,2'-bipy and {$[Ni(phen)_2]_2[Sn_2S_6]$}·4,4'-bipy·½H_2O.[8] In the latter two compounds the aromatic amines 2,2'-bipy and 4,4'-bipy were added for stabilization of the structure of {$[Ni(phen)_2]_2[Sn_2S_6]$} via π-π bonding interactions. Syntheses without these amine molecules led to formation of $[Ni(phen)_2]Cl_2$ complexes.[8] Therefore, the concept of stabilizing thiostannate containing compounds by addition of an aromatic amine molecule could be verified by applying biphenyl during the syntheses of **1**. But syntheses with naphthalene, anthracene, phenanthrene or *p*-terphenyl did not lead to the formation of compounds containing any of these molecules. Hence, it seems that other factors play also an important role for crystallization of compounds containing these aromatic molecules. One may speculate that the size matching is essential for generation of π-π interactions and if the aromatic molecules are too large or exhibit the 'wrong' shape these are not integrated into a crystalline product. Nevertheless compound **2** {$[Ni(phen)_2]_2[Sn_2S_6]$}·phen·H_2O crystallized in the presence of naphthalene, anthracene, phenanthrene or *p*-terphenyl and the analogous syntheses with Mn, Fe, Co lead to the formation of {$[TM(phen)_2]_2[Sn_2S_6]$} and {$[TM(phen)_2]_2[Sn_2S_6]$}·phen·H_2O (TM = Mn, Fe, Co).[6,7]

{$[Ni(phen)_2]_2[Sn_2S_6]$}·phen·H_2O (**2**) was initially obtained by applying similar conditions as described for **1**, but adding naphthalene, anthracene, phenanthrene or *p*-terphenyl instead of biph. Although these aromatic molecules are not part of the structure of **2**, they are essential for the formation of **2**: without these 'additives' a $[Ni(phen)_3]Cl_2$ complex and X-ray amorphous dark crumbs and powders were obtained. Only if the 'additives' or phen are applied in a distinct excess crystals of **2** are formed.

In contrast to **1** and **2**, {$[Fe(1,2\text{-dach})_2]_n[Sn_2S_6]_n$·2*n*1,2-dachH (**3**) crystallized as a chain structure. However Mn and Fe seem to behave similar because the isostructural compound {$[Mn(1,2\text{-dach})_2][Sn_2S_6]_n$·2*n*1,2-dachH was reported recently. [22]

The synthesis conditions for {$[Ni(cyclam)]_2[Sn_2S_6]_n$·2*n*$H_2O$ (**4**) are comparatively robust: compound **4** could be obtained applying $Ni/NiCl_2·6H_2O$, Sn, S, cyclam in aqueous ma solution as well as using $[Ni(cyclam)]^{2+}$ complexes and $Na_4SnS_4·14H_2O$ in water. The pH value of the first reaction mixture was 12-13, the latter a pH value of 11 was measured, i.e., compound **4** is formed in this range of the pH values.

Compound **5** ({$[Mn(2,2'\text{-bipy})_2]_2[Sn_2S_6]$}) could only be obtained by applying $[Mn(2,2'\text{-bipy})_3][ClO_4]_2$ and $Na_4SnS_4·14H_2O$ in aqueous solutions. Initially the reaction mixture exhibits a pH value of ~12 which has to be lowered for the formation of compound **5**. In contrast to the synthesis of **4**, the adjustment of the pH value is crucial for a successful synthesis. Only with a pH range from 8.5 – 11 compound **5** is formed, otherwise only X-ray amorphous crumbs are obtained. The highest yield is received at pH ~ 10. Experiments synthesizing this compound applying other Mn, Sn or S sources were not successful.

Crystal Structures

Compounds **1** and **5** crystallize in the monoclinic space group $P2_1/n$ (Z = 2) and compound **2**, **3** as well as **4** crystallize in the triclinic space group $P\bar{1}$ (Z = 1). All compounds feature the $[Sn_2S_6]^{4-}$ anion (Fig. 2) with the anionic unit linked to the charge compensating $[TM(amine)_n]^{2+}$ complexes via TM^{2+}-S bonds to the terminal sulfur atoms. The $[Sn_2S_6]^{4-}$ unit, composed of two edge-sharing SnS_4 tetrahedra, feature the typical Sn-S bonding pattern of short Sn-S_{term} and longer Sn-(μ-S) bonds.

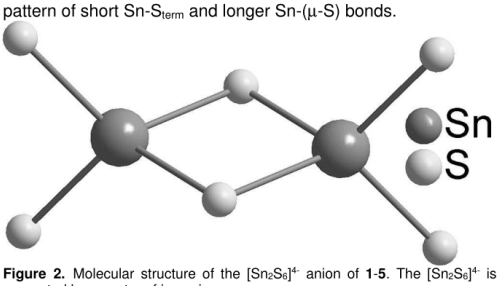

Figure 2. Molecular structure of the $[Sn_2S_6]^{4-}$ anion of **1**-**5**. The $[Sn_2S_6]^{4-}$ is generated by a center of inversion.

For **1** - **5** these units feature almost identical bond lengths (Sn-S_{term}: 2.3221(11) – 2.3461(9) Å; Sn-(μ-S): 2.4369(9) – 2.4569(11) Å) and the geometric parameters are similar to literature data of for instance the discrete ion in $Na_4Sn_2S_6·14H_2O$.[37] (Supporting Information, Tab. S5). Especially the S_{term}-Sn-S_{term} angles in compounds **1**, **2** and **5** show deviations up to 10° from ideal tetrahedral ge ometry of a free $[Sn_2S_6]^{4-}$ ion (S_{term}-Sn-S_{term}: 100.25(3) – 103.69(9)°; S_{term}-Sn-(μ-S): 113.31(3) – 120.43(3)°; (μ-S)-Sn-(μ-S): 92.15(3) – 92.89(3)°), while the anions in **3** and **4** are less distorted (S_{term}-Sn-S_{term}: 113.44(3) - 117.28(2)°; S_{term}-Sn-(μ-S): 110.54(3) – 114.03(3)°; (μ-S)-Sn-(μ-S): 93.17(3) - 93.83(2)°). The distinct deviation of these angles in compounds **1**, **2** and **5** is caused by the fixed position of the terminal S atoms by the bonds to the bridging TM^{2+} cation, but all values are still comparable to literature data of similar compounds.[6,7]

The distorted octahedral environment of all TM^{2+} ion is composed of four N donor atoms of the respective amine ligands and two S atoms of the $[Sn_2S_6]^{4-}$ unit. In all compounds the TM-S bonds are significantly longer (2.5016(10) - 2.6188(7) Å) compared to the TM-N bonds (2.108(3) - 2.351(6) Å) without a noticeable influence of the position of the S atoms in the complex (*trans* or *cis*). In compounds **1**, **2** and **5** the S atoms are located in *cis* position. The rigid positions of the biting angles of the N-donor atoms of the amine ligands (phen or 2,2'-bipy) and the $[Sn_2S_6]^{4-}$ unit causes a distinct distortion of the ideal octahedral geometry (N-TM-N/N-TM-S: 71.25(12) – 95.23(8)°; 153.4(2) - 173.95(10)°) (Supporting Information, Ta b. S6 and S7), comparable to literature data for similar compounds.[6–8] In compounds **3** and **4** the S atoms are located in *trans* position in the octahedron and the TM ions are on special positions leading to ideal angles (N-TM-N/S-TM-S: 180.00(17) – 180.00(3)°), while the *cis* angles significantly deviate from ideal values (80.21(8) - 99.79(8)°) (Supporting Information, Tab . S8), as observed in similar compounds. [22]

The compounds {$[Ni(phen)_2]_2[Sn_2S_6]$}·biph (**1**) and {$[Ni(phen)_2]_2[Sn_2S_6]$}·phen·H_2O (**2**) consist both of {$[Ni(phen)_2]_2[Sn_2S_6]$} complexes and additional organic molecules. The structure of {$[TM(phen)_2]_2[Sn_2S_6]$} is constructed by the linkage of two $[Ni(phen)_2]^{2+}$ complexes with a bridging [μ-$Sn_2S_6]^{4-}$ unit (Fig. 3), and do not significantly differ from compounds with this motif [6–8] or compounds with its selenium analogous[38] and will not be discussed here in detail. The biphenyl molecule (**1**) and the additional phen molecule (**2**) is arranged to generate extended π–π interactions with phen

ligands of the TM^{2+} centered complex. Such interactions are weak but might be important for the stability of the compound.

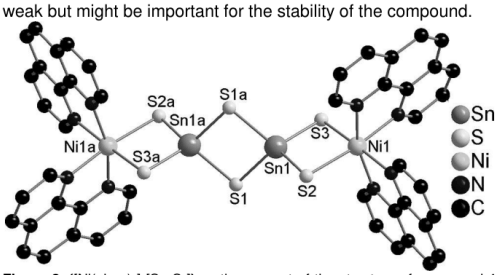

Figure 3. {[Ni(phen)$_2$]$_2$[Sn_2S_6]} motive as part of the structure of compound **1** and **2**. Only selected atoms are labeled. Symmetry transformations used to generate equivalent atoms: compound 1: -x, 1-y, -z; compound 2: 1-x, 1-y, 1-z. Hydrogen atoms are omitted for clarity.

The structure of **1** ({[Ni(phen)$_2$]$_2$[Sn_2S_6]}·biph) is related to that of {[Ni(phen)$_2$]$_2$[Sn_2S_6]}·2,2'-bipy [8] with the biphenyl molecule located in a very similar position like in the latter compound. The {[Ni(phen)$_2$]$_2$[Sn_2S_6]} (A) and biph (B) moieties are stacked in an AABAAB sequence within the *ac* plane along the *a* axis (Supporting Information, Fig. S7) and the biph molecules are disordered over two positions in rows along the *b* axis (Supporting Information, Fig. S8). In **1** and {[Ni(phen)$_2$]$_2$[Sn_2S_6]}·2,2'-bipy the aromatic molecules determine the structure: several off-center parallel π–π interactions are observed leading to the final arrangements of the constituents (Supporting Information, Fig. S9; **1**: 3.296 - 3.444 Å; {[Ni(phen)$_2$]$_2$[Sn_2S_6]}·2,2'-bipy: 3.335 - 3.674 Å [8]).[39] Regarding the compound {[Ni(phen)$_2$]$_2$[Sn_2S_6]}·4,4'-bipy·½H_2O [8] the amine influences the crystal structure by hydrogen bonding interactions between the 4,4'-bipy molecules with crystal water arranged in rows between the {[Ni(phen)$_2$]$_2$[Sn_2S_6]}·moieties.

Compound **2** ({[Ni(phen)$_2$]$_2$[Sn_2S_6]}·phen·H_2O) is isostructural to the compounds {[TM(phen)$_2$]$_2$[Sn_2S_6]}·phen·H_2O (TM = Mn, Fe, Co) reported in literature.[6,7] The {[Ni(phen)$_2$]$_2$[Sn_2S_6]}·complexes and additional phen molecules are interwoven within the *ab* plane and stacked along the *c* axis (Supporting Information, Fig. S10). Again off-center parallel stacking of the free phen molecules and the phen ligands is observed (Supporting Information, Fig. S11; **2**: 3.523-3.662 Å; {[Mn(phen)$_2$]$_2$[Sn_2S_6]}·phen·H_2O: 3.448-3.545 Å [6]). The crystal water is located in direct neighborhood of the free phen molecule and displays hydrogen bonding interactions (O···N:3.096 Å) which seem to be important for the stabilization of the compound.

{[Fe(1,2-dach)$_2$][Sn_2S_6]}$_n$·2*n*1,2-dachH (**3**) is isostructural to the compound {[Mn(1,2-dach)2][Sn_2S_6]}$_n$·2*n*1,2-dachH.[22] In these compounds a different connection mode of the [Sn_2S_6]$^{4-}$ anion with the [TM(amine)$_n$]$^{2+}$ complex compared to **1** and **2** is observed. In **3** only two of the four terminal S atoms of the anion in *trans* position have bonds to Fe^{2+}. The connection mode generates chains along the *b* axis with Fe^{2+} centered complexes as nodes and the anions as linkers (Fig. 4)

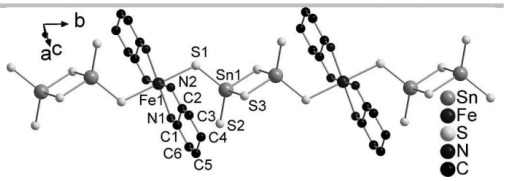

Figure 4. Direct linkage of the [Sn_2S_6]$^{4-}$ anions and [Fe(1,2-dach)$_2$]$^{2+}$ complexes leading to chains in compound **3**. Atoms of the asymmetric unit are labeled. H atoms are omitted for clarity.

The octahedral environment of the Fe^{2+} cation is composed of four N atoms of opposite 1,2-dach molecules and two terminal S atoms of two [Sn_2S_6]$^{4-}$ units in *trans* position. All angles around Fe^{2+} indicate a moderate distortion of the octahedron (Supporting Information, Tab. S8). The Fe-N bonds at 2.183(2) - 2.201(2) Å are in the range of literature data. [7,25] The Fe-S bond at 2.6138(7) is slightly longer compared to data for Fe containing thiostannates, but comparable to a compound with the same connection mode like observed here.[22] The anionic chains are stacked alternatingly with charge compensating [1,2-dachH]$^+$ cations along the *a* axis (Supporting Information, Fig. S12). Hydrogen bonding interactions between the non-bonded terminal S atoms of the anions and the (NH_3) groups of the [1,2-dachH]$^+$ ions lead to the formation of layers within the *ab* plane.(Supporting Information, Tab. S9 and Fig. S13).

{[Ni(cyclam)]$_2$[Sn_2S_6]}$_n$·2*n*H_2O (**4**) is a rare example of a two-dimensional [TM(amine)$_n$]$^{m+}$ complexes containing tin-sulfur compound. The only other know two-dimensional compound is the isostructural {[Co(cyclam)]$_2$[Sn_2S_6]}$_n$·2*n*H_2O [10]. In these compounds another connection mode of the [Sn_2S_6]$^{4-}$ anion is observed: all four terminal S atoms are involved in bonds to the TM^{2+} cation, but each S_{term} connects different TM^{2+} centered complexes, resulting in the formation of layers within the *bc* plane (Fig. 5).

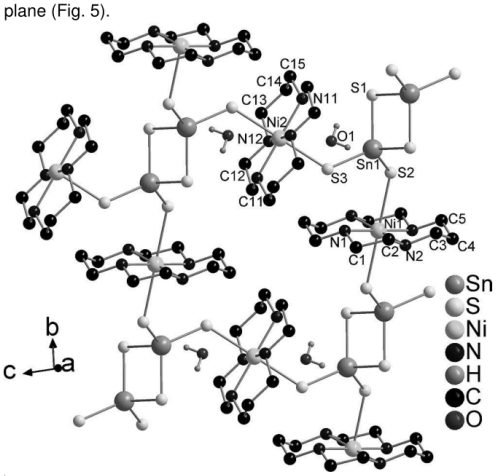

Figure 5. Direct linkage of the [Sn2S6]4- anions and [Ni(cyclam)]2+ complexes leading to layers in 4. Only H atoms of the crystal water molecules are shown and the remaining ones are omitted. Atoms of the asymmetric unit are labeled.

The octahedral environment of the Ni^{2+} cation is constructed by the four N atoms of the cyclam ligand (in the so called *trans* III orientation [40]) and two terminal S atoms of two [Sn_2S_6]$^{4-}$ units in *trans* position (Supporting Information, Fig.

S14). The crystal water molecules are located between the layers and interact via weak hydrogen bonding interactions with the terminal S atoms of the $[Sn_2S_6]^{4-}$ units leading to the formation of a three-dimensional network (Supporting Information, Tab. S10 and Fig. S15).

{[Mn(2,2'-bipy)$_2$]$_2$[Sn_2S_6]} (**5**) features the same connection mode of the $[Sn_2S_6]^{4-}$ unit with the $[TM(amine)_n]^{2+}$ complex as in compounds **1** and **2**. Two $[Mn(2,2'\text{-bipy})_2]^{2+}$ complexes are linked by one $[Sn_2S_6]^{4-}$ unit via all four terminal S atoms (Fig. 6).

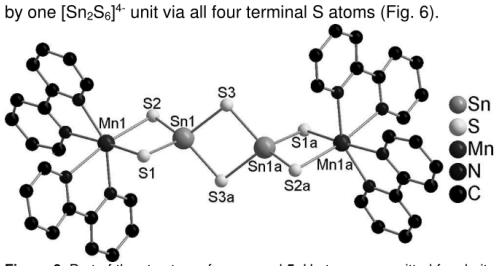

Figure 6. Part of the structure of compound **5**. H atoms are omitted for clarity. Only selected atoms are labeled. Symmetry transformations used to generate equivalent atoms: 1-x, -y, 1-z.

The structure of **5** is very similar to that of {[Mn(phen)$_2$]$_2$[Sn_2S_6]}.[6] The exchange of phen ligands by 2,2'-bipy results in a small change of the dihedral angles between the organic ligands (2,2'-bipy:|85.20(61)|-|89.90(36)|°(Supporting Information, Tab. S11); phen: |84.27(38)|-|94.75(46)|°[6]) and a slight distortion of the $[MnN_4S_2]$ octahedra (2,2'-bipy: 71.25(12) - 91.42(3)°, 153.4(2) - 170.54(16)°, phen: 70.68(13) - 92.44(11)°, 148.29(14) - 169.75(10)° [6]). In both compounds the deviation of the ideal octahedral geometry is caused by the rigid positions of the N donor atoms of the organic ligands. However, the 2,2'-bipy ligand causes a different arrangement of the molecules in the structure: in **5** the molecules are interleaved within the *bc* plane. Each molecule is surrounded by two other complexes along the *a* axis and further six molecules within the *bc* plane whereas the constituents are arranged in two orientations (A and B) in rows along the *c* axis (Supporting Information, Fig. S16). These two rows alternate continuously along the *b* axis. This arrangement seems to be impossible with the larger phen ligand. The structure of **5** is characterized by π–π interactions (off-center parallel stacking: 3.340 Å; perpendicular t-shaped: 3.936 Å; Supporting Information, Fig. S17), in a similar intermolecular range as in the phen containing compound (off-center parallel stacking: 3.448 - 3.683 Å [6]) and further literature data.[41]

Spectroscopic Properties

The absorptions in the IR spectra of the title compounds can be assigned to the respective amine ligands as well as the TM-N stretching vibrations around 410-450 cm^{-1}(Supporting Information, Tab. S1 - S3). Comparing compounds **1** and **2** the additional biphenyl molecule causes absorptions at 2980, 1482, 842 and 696 cm^{-1}. The signals of the NH_3^+ group of the additional protonated 1,2-dachH ligand in compound **3** are observed at 2506 and 1509 cm^{-1}. The absorption above 3500 cm^{-1} (compound **4**) can be assigned to the crystal water.

In the Raman spectra the Sn-S modes of the thiostannates are located in the region of 400 to 100 cm^{-1}. The assignment of the modes for **1**-**5** was done on the basis of literature data for the $[Sn_2S_6]^{4-}$ anion. [37] (Supporting Information, Tab. S4) The resonance of the Sn-S_{term} stretching mode is found at 391 cm^{-1} and 377 cm^{-1} in the discrete anion. In compounds **1**, **2** and **5** the TM-S binding mode cause slightly shorter Sn-S bonds and results in a shift of the signals towards higher wave numbers. This observation is not made for compound **3** and **4**, which exhibit a different TM-S binding mode. The signals for the Sn-S-Sn vibration are located at around 340 cm^{-1} with a slight shift toward higher wave numbers for the Fe and Mn containing compounds. The resonance for the Sn_2S_2 ring vibration is observed at 280 cm^{-1} in the free $[Sn_2S_6]^{4-}$ ion. For compounds **1**, **2** and **5** this signal is split into two signals which most probably is caused by the formation of a $TMSnS_2$ ring. In addition the bands overlap with NiS_2 or MnS_2 vibrations. [42] In the region below 200 cm^{-1} the deformation and lattice vibration of the $[Sn_2S_6]^{4-}$ anion as well as the resonances for different TMS_x modes are located. Therefore, a detailed assignment is not possible.

Applying the Kubelka-Munk method for the UV/Vis spectra of compounds **2** - **5** a bandgap (**2**: 2.64 eV **3**: 2.36 eV **4**: 2.85 eV **5**: 2.24 eV) according to the color of the compounds is estimated. (Supporting Information, Fig. S6) For compound **1** the color cannot be explained by the bandgap (4.42 eV), but in this spectrum three weak absorption bands can be observed below the absorption edge. (Supporting Information, Fig. S6) These bands can be assigned to the Ni^{2+} d-d transitions $^3A_{2g} \rightarrow {}^3T_{2g}$ (~1.2 eV), $^3A_{2g} \rightarrow {}^3T_{1g}(^3F)$ (~2.4 eV) and $^3A_{2g} \rightarrow {}^3T_{1g}(^3P)$ (~3.2 eV) [43] and are in the same range as for the related compounds with 2,2'-bipy and 4,4'-bipy.[8]

Conclusions

Following the solvothermal route and applying selected amines (1,2-dach, phen, 2,2'-bipy and cyclam) five new TM^{2+} containing tin-sulfur compounds could be synthesized and characterized. The assumption that aromatic or cyclic amine molecules increase the chance of bond formation between TM^{2+} centered complexes and thiostannate anions was successful: all title compounds feature covalent TM^{2+}-S bonds. The synthesis conditions for **2** ({[Ni(phen)$_2$]$_2$[Sn_2S_6]}·phen·H_2O) indicate that organic additives influence the product formation in a not well understood way. The successful preparation of **3** {[Fe(1,2-dach)$_2$][Sn_2S_6]}$_n$·2*n*1,2-dachH demonstrates that compounds with higher structural dimensionality can be synthesized even with bidentate amine molecules. For the syntheses of compounds **4** ({[Ni(cyclam)]$_2$[Sn_2S_6]}$_n$·2*n*H_2O) and **5** ({[Mn(2,2'-bipy)$_2$]$_2$[Sn_2S_6]) a new preparation method was developed applying $[TM(amine)_n]^{m+}$ complexes and $[SnS_4]^{4-}$ ions as educts. The crystallization of **5** requires a careful adjustment of the pH value for the successful product formation. In further syntheses the potential of $Na_4SnS_4 \cdot 14H_2O$ as starting material for formation of new thiostannate containing compounds will be explored.

Acknowledgements

Financial support by the State of Schleswig-Holstein is gratefully acknowledged.

Keywords: Crystal Structures, Solvothermal Syntheses, Spectroscopic Properties, Tin, Sulfur

[1] B. Seidlhofer, N. Pienack, W. Bensch, *Z. Naturforsch.* **2010**, *65b*, 937–975.

[2] a) A. K. Cheetham, G. Férey, T. Loiseau, *Angew. Chem.* **1999**, *111*, 3466–3492; b) S. Dehnen, M. Melullis, *Coord. Chem. Rev.* **2007**, *251*, 1259–1280; c) J. Zhou, J. Dai, G.-Q. Bian, C.-Y. Li, *Coord. Chem. Rev.* **2009**, *253*, 1221–1247; d) W. S. Sheldrick, M. Wachhold, *Coord. Chem. Rev.* **1998**, *176*, 211–322; e) W. S. Sheldrick, *J. Chem. Soc, Dalton Trans.* **2000**, 3041–3052;

[3] P. Feng, X. Bu, N. Zheng, *Acc. chem. res.* **2005**, *38*, 293–303.

[4] a) J. Zhou, X. Liu, L. An, F. Hu, W. Yan, Y. Zhang, *Inorg. Chem.* **2012**, *51*, 2283–2290; b) C. Tang, J. Lu, J. Han, Y. Liu, Y. Shen, D. Jia, *J. Solid State Chem.* **2015**, *230*, 118–125;

[5] C.-Y. Yue, X.-W. Lei, L. Yin, X.-R. Zhai, Z.-R. Ba, Y.-Q. Niu, Y.-P. Li, *CrystEngComm* **2015**, *17*, 814–823.

[6] J. Hilbert, C. Näther, W. Bensch, *Inorg. Chem.* **2014**, *53*, 5619–5630.

[7] J. Hilbert, C. Näther, W. Bensch, *Z. Anorg. Allg. Chem.* **2014**, *640*, 2858–2863.

[8] J. Hilbert, C. Näther, W. Bensch, *Dalton Trans.* **2015**, *44*, 11542–11550.

[9] J. Hilbert, C. Näther, R. Weihrich, W. Bensch, *Inorg. Chem.* **2016**, *55*, 7859–7865.

[10] C. Zeisler, C. Näther, W. Bensch, *CrystEngComm* **2013**, *15*, 8874–8876.

[11] N. Pienack, H. Lühmann, B. Seidlhofer, J. Ammermann, C. Zeisler, F. Danker, C. Näther, W. Bensch, *Solid State Sci.* **2014**, *33*, 67–72.

[12] a) T. Jiang, A. Lough, G. A. Ozin, *Adv. Mater.* **1998**, *10*, 42–46; b) X. Wang, T.-L. Sheng, S.-C. Xiang, S.-M. Hu, R.-B. Fu, X.-T. Wu, *Chinese J. Struct. Chem.* **2010**, *29*, 260–264;

[13] T. Jiang, A. Lough, G. A. Ozin, R. L. Bedard, R. Broach, *J. Mater. Chem.* **1998**, *8*, 721–732.

[14] Y. Ko, C. L. Cahill, J. B. Parise, *J. Chem. Soc, Chem. Commun.* **1994**, 69–70.

[15] Y. Ko, K. Tan, D. M. Nellis, S. Koch, J. B. Parise, *J. Solid State Chem.* **1995**, *114*, 506–511.

[16] P. Nørby, E. Eikeland, J. Overgaard, S. Johnsen, B. B. Iversen, *CrystEngComm* **2015**, *17*, 2413–2420.

[17] K. Tsamourtzi, J.-H. Song, T. Bakas, A. J. Freeman, P. N. Trikalitis, M. G. Kanatzidis, *Inorg. Chem.* **2008**, *47*, 11920–11929.

[18] X. Bu, N. Zheng, P. Feng, *Chem. Eur. J.* **2004**, *10*, 3356–3362.

[19] D.-X. Jia, Y. Zhang, J. Dai, Q.-Y. Zhu, X.-M. Gu, *Z. Anorg. Allg. Chem.* **2004**, *630*, 313–318.

[20] M.-L. Fu, G.-C. Guo, Liu, Bing, Wu, A-Qing, J.-S. Huang, *Chin. J. Inorg. Chem.* **2005**, *21*, 25–29.

[21] a) N. Pienack, D. Schinkel, A. Puls, M.-E. Ordolff, H. Lühmann, C. Näther, W. Bensch, *Z. Naturforsch.* **2012**, *67b*, 1098–1106; b) J. Zhou, G.-Q. Bian, J. Dai, Y. Zhang, A.-B. Tang, Q.-Y. Zhu, *Inorg. Chem.* **2007**, *46*, 1541–1543;

[22] N. Pienack, C. Näther, W. Bensch, *Z. Naturforsch.* **2008**, *63b*, 1243–1251.

[23] a) Z. Wang, G. Xu, Y. Bi, C. Wang, *CrystEngComm* **2010**, *12*, 3703–3707; b) N. Pienack, C. Näther, W. Bensch, *Eur. J. Inorg. Chem.* **2009**, 1575–1577; c) X.-M. Gu, J. Dai, D.-X. Jia, Y. Zhang, Q.-Y. Zhu, *Cryst. Growth Des.* **2005**, *5*, 1845–1848;

[24] G.-N. Liu, G.-C. Guo, F. Chen, S.-P. Guo, X.-M. Jiang, C. Yang, M.-S. Wang, M.-F. Wu, J.-S. Huang, *CrystEngComm* **2010**, *12*, 4035–4037.

[25] N. Pienack, S. Lehmann, H. Lühmann, M. El-Madani, C. Näther, W. Bensch, *Z. Anorg. Allg. Chem.* **2008**, *634*, 2323–2329.

[26] J. Zhou, X. Liu, G.-Q. Chen, F. Zhang, L.-R. Li, *Z. Naturforsch.* **2010**, *65b*, 1229–1234.

[27] M. Behrens, S. Scherb, C. Näther, W. Bensch, *Z. Anorg. Allg. Chem.* **2003**, *629*, 1367–1373.

[28] D.-X. Jia, J. Dai, Q.-Y. Zhu, Y. Zhang, X.-M. Gu, *Polyhedron* **2004**, *23*, 937–942.

[29] R. Kiebach, R. Warratz, C. Näther, W. Bensch, *Z. Anorg. Allg. Chem.* **2009**, *635*, 988–994.

[30] a) A. F. Holleman, E. Wiberg, N. Wiberg, *Lehrbuch der anorganischen Chemie,* de Gruyter, Berlin, New York, **2007**; b) M. Schaefer, D. Kurowski, A. Pfitzner, C. Näther, Z. Rejai, K. Möller, N. Ziegler, W. Bensch, *Inorg. Chem.* **2006**, *45*, 3726–3731; c) W. Bensch, M. Schur, *Eur. J. Solid State Inorg. Chem.* **1996**, *33*, 1149–1160; d) A. Puls, C. Näther, W. Bensch, *Z. Anorg. Allg. Chem.* **2006**, *632*, 1239–1243; e) N. Pienack, K. Möller, C. Näther, W. Bensch, *Solid State Sci.* **2007**, *9*, 1110–1114;

[31] a) C. Ruiz-Pérez, Lorenzo Luis, Pablo A, F. Lloret, M. Julve, *Inorg. Chim. Acta* **2002**, *336*, 131–136; b) E. K. Barefield, F. Wagner, A. W. Herlinger, A. R. Dahl, S. Holt, *Inorg. Syn.* **1976**, *16*, 220–225; c) Y. Oh, S. Bag, C. D. Malliakas, M. G. Kanatzidis, *Chem. Mater.* **2011**, *23*, 2447–2456;

[32] G. M. Sheldrick, SHELXS-97, **1997**.

[33] G. M. Sheldrick, SHELXL-97, **1997**.

[34] a) G. M. Sheldrick, SHELXL-2014, **2014**; b) G. M. Sheldrick, *Acta Cryst.* **2008**, *A64*, 112–122;

[35] a) A. Rabenau, *Angew. Chem.* **1985**, *97*, 1017–1032; b) W. S. Sheldrick, M. Wachhold, *Angew. Chem.* **1997**, *109*, 214–234; c) G. Demazeau, *J. Mater. Sci.* **2008**, *43*, 2104–2114; d) G. Demazeau, A. Largeteau, *Z. Anorg. Allg. Chem.* **2015**, *641*, 159–163; e) S. Santner, J. Heine, S. Dehnen, *Angew. Chem. Int. Ed. Engl.* **2016**, *55*, 876–893;

[36] T. Jiang, A. Lough, G. A. Ozin, R. L. Bedard, *J. Mater. Chem.* **1998**, *8*, 733–741.

[37] B. Krebs, S. Pohl, W. Schiwy, *Angew. Chem. Int. Ed. Engl.* **1970**, *9*, 897–898.

[38] G.-N. Liu, G.-C. Guo, M.-J. Zhang, J.-S. Guo, H.-Y. Zeng, J.-S. Huang, *Inorg. Chem.* **2011**, *50*, 9660–9669.

[39] a) C. Janiak, *J. Chem. Soc, Dalton Trans.* **2000**, 3885–3896; b) S. Grimme, *Angew. Chem. Int. Ed. Engl.* **2008**, *47*, 3430–3434;

[40] a) B. Bosnich, M. L. Tobe, G. A. Webb, *Inorg. Chem.* **1965**, *4*, 1109–1112; b) L. G. Warner, D. H. Busch, *J. Am. Chem. Soc.* **1969**, *91*, 4092–4101; c) M. Bakaj, M. Zimmer, *J. of Mol. Struct.* **1999**, *508*, 59–72;

[41] a) A. L. Ringer, M. O. Sinnokrot, R. P. Lively, C. D. Sherrill, *Chem. Eur. J.* **2006**, *12*, 3821–3828; b) C. R. Martinez, B. L. Iverson, *Chem. Sci.* **2012**, *3*, 2191–2201; c) Y.-H. Chi, J.-M. Shi, H.-N. Li, W. Wei, E. Cottrill, N. Pan, H. Chen, Y. Liang, L. Yu, Y.-Q. Zhang, C. Hou, *Dalton Trans.* **2013**, *42*, 15559–15569;

[42] a) D. W. Bishop, P. S. Thomas, A. S. Ray, *Mater. Res. Bull.* **1998**, *33*, 1303–1306; b) C. Avril, V. Malavergne, R. Caracas, B. Zanda, B. Reynard, E. Charon, E. Bobocioiu, F. Brunet, S. Borensztajn, S. Pont, M. Tarrida, F. Guyot, *Meteorit Planet Sci* **2013**, *48*, 1415–1426; c) J. R. L. Fernandez, M. de Souza-Parise, P. Morais, *Mater. Res. Express* **2015**, *2*, 1–5;

[43] S. P. Roe, J. O. Hill, R. J. Magee, *Monatsh. Chem.* **1991**, *122*, 467–478.

3.1.5 {[Ni(1,2-dach)(ma)]$_4$[$Sn_{10}S_{20}O_4$]}, Synthese der seltenen [$Sn_{10}S_{20}O_4$]$^{8-}$-Einheit mit direkter Verknüpfung zum ladungsausgleichenden Komplex. *(submitted 10.10.16)*

Zusammenfassung der Publikation „{[Ni(1,2-dach)$_2$(ma)]$_4$[$Sn_{10}S_{20}O_4$]} – An Example of the Rare Tin-Oxo-Sulfide Cluster with Uncommon Connection Mode Towards a Charge Compensating Ni(II) Complex“

Die Verbindung {[Ni(1,2-dach)$_2$(ma)]$_4$[$Sn_{10}S_{20}O_4$]} ($P\bar{4}2_1c$, Z=2) wurde unter solvothermalen Bedingungen unter Verwendung von $NiCl_2 \cdot 6H_2O$, Sn, S, phen, 1,2-dach (mmol: 1:1:3:1:2) in wässriger Methylaminlösung (pH ~12, 120°C, 7d) erhalten. Dies ist insofern bemerkenswert, da bisherige Ergebnisse davon ausgingen, dass dieser seltene [$Sn_{10}S_{20}O_4$]$^{8-}$-Cluster erst bei niedrigen pH Werten (~3) gebildet wird.[94,95]

Die [$Sn_{10}S_{20}O_4$]$^{8-}$-Einheit, bestehend aus zehn eckenverknüpften SnS_4-Tetraedern, gehört zur Gruppe der so genannten super-tetragonalen Cluster, welche aus MX_4 (M = Metallion, X= Chalkogenid) Tetraedern aufgebaut werden. In Anlehnung der allgemein akzeptierten Notation T_n (*n* = Anzahl der Grundbaueinheiten/Tetraeder entlang jeder Kante) ergibt sich für diesen Cluster die Bezeichnung T3. Der vorliegende Cluster ist außerdem als ein sogenannter „gefüllter“ Cluster anzusehen, da die Lücken eines formalen, ladungsneutralen [$Sn_{10}S_{20}$]-Clusters mit Sauerstoffatomen besetzt sind. Diese Sauerstoffatome sind tetraedrisch von Sn-Atomen umgeben, was zur Ausbildung eines [O_4Sn_{10}]$^{32+}$ anti T2-Clusters in dem [$Sn_{10}S_{20}O_4$]$^{8-}$-Anion führt. In der Titelverbindung ist dieser Cluster über die (μ_3-S)-Atome mit den ladungsausgleichenden Ni(II)-zentrierten Komplexen verknüpft. Dieser Verknüpfungsmodus wurde bei diesem Clustertyp bisher noch nicht beobachtet.

Journal Name, **Year,** *Volume* **1**

{[Ni(1,2-dach)$_2$(ma)]$_4$[Sn$_{10}$S$_{20}$O$_4$]} An Example of the Rare Tin-Oxo-Silfide Cluster with Uncommon Connection Mode Towards a Charge Compensating Ni(II) Complex

Jessica Hilbert[a], Wolfgang Bensch[a*], Christian Näther[a]

[a] *Institute of Inorganic Chemistry, Christian-Albrechts-University of Kiel, Max-Eyth-Str. 2*

Abstract: The title compound {[Ni(1,2-dach)$_2$(ma)]$_4$[Sn$_{10}$S$_{20}$O$_4$]} was obtained following the solvothermal approach. The Ni^{2+} centered complex contains two different amine molecules and is *in-situ* formed during the reaction. The tin-oxo-sulfide cluster self-assembled during the chemical reaction. The compound features the rare [Sn$_{10}$S$_{20}$O$_4$]$^{8-}$ anion which is constructed by corner-sharing of two unique SnO$_2$S$_2$ nearly flat distorted rectangles and one unique SnS$_4$ tetrahedron considering the shortest Sn-O and Sn-S bonds. Taking into account longer Sn-S and Sn-O bonds the SnO$_2$S$_2$ rectangles are expanded to SnO$_2$S$_4$ octahedra and the SnS$_4$ tetrahedron to a SnS$_4$O trigonal bipyramid. The unique [Ni(1,2-dach)$_2$(ma)]$^{2+}$ complex has a Ni-S bond to a μ_3-acting S atom of the anion leading to a NiN$_5$S octahedral environment. All O atoms of cluster anion act μ_4-briding and are in a tetrahedral environment of Sn atoms forming an anti-T2 cluster.

Keywords: Tin-Oxo-Sulfide Cluster, [Sn$_{10}$S$_{20}$O$_4$]$^{8-}$, Charge Compensating Ni(II) complex, Solvothermal Syntheses, Crystal Structure

1. INTRODUCTION

In the last decades chalogenidometalates of the heavier group 13-15 elements have been intensively investigated because of their promising applicability for catalysis, sensors, ion exchange or light driven hydrogen generation. [1–7] Among them, metal chalcogenide clusters constructed by tetrahedral building units (T_n, P_n, $T_{p,q}$) [8] are promising candidates for the formation of multifunctional porous materials. The notation for the different series of cluster types describes the construction of the respective cluster: T_n is a series of super-tetrahedral clusters built by corner-sharing of MX$_4$ tetrahedra (M = metal cation, X = chalcogenide), where *n* be regarded as the number of metal layers or as the number of tetrahedra along each edge. [8, 9] P_n is a series of penta-super-tetrahedral clusters, formally constructed by joining four T_n clusters on each face of an anti-T_n cluster (e.g. XM$_4$). [8] $T_{p,q}$ is the notation for a series of so called super-super-tetrahedral clusters, with a T_q super-tetrahedron of T_p super-tetrahedra, where *q* and *p* are the number of building units along each edge. [8, 10] However research has been focused on T_n clusters of group 13 (In, Ga) and 14 (Sn, Ge) metals. [11] The T_n clusters are super-tetrahedral arrangements of regular tetrahedral fragments of the cubic ZnS lattice type, with the compositions MX$_4$ (T1), M$_4$X$_{10}$ (T2), M$_{10}$X$_{20}$ (T3), M$_{20}$X$_{35}$ (T4) and M$_{35}$X$_{56}$ (T5). [8]

* Institute of Inorganic Chemistry, Christian-Albrechts-University of Kiel, Max-Eyth-Str. 2, 24118 Kiel, Germany, Tel/Fax: +49 -431-880-2419, +49-431-880-1520; E-mails: wbensch@ac.uni-kiel.de

The maximum cluster size for a specific metal ion (e.g. In^{3+} or Sn^{4+}) is limited by Pauling's electrostatic valance rule: the coordination number (c.n.) of the anion (e.g. S^{2-}) increases with larger cluster sizes. Starting with c.n = 2 for the T2 cluster, a successive increase to c.n =2-3 for T3 and to c.n = 2-4 for T4 clusters are observed.[8] This results in a limitation of the maximum cluster size for thioindates (In^{3+}) to T3 and for thiostannates (Sn^{4+}) to T2. [8] Generally, the latter group of compounds features mainly the [Sn$_2$S$_6$]$^{4-}$ ion, or the less common [SnS$_4$]$^{4-}$ anion. [5, 12–15] Larger clusters consisting of Sn and S are so called "stuffed clusters" like the [Sn$_{10}$S$_{20}$O$_4$]$^{8-}$ ion with additional O atoms for more charge balance within the cluster. [8] Until now only few examples are known for tin-oxo-sulfide cluster: [Sn$_4$S$_8$OCl$_4$]$^{2-}$ [16], [Sn$_8$S$_{12}$O$_4$(SPh)$_6$]$^{6-}$ [17], [Sn$_8$S$_{12}$O$_2$(OH)$_2$Cl$_6$] [18], [Sn$_{10}$O$_4$S$_{16}$Cl$_4$] [18] and [Sn$_{10}$S$_{20}$O$_4$]$^{8-}$ [11, 19–21]. During the solvothermal syntheses of new thiostannates we prepared the new compound {[Ni(1,2-dach)$_2$(ma)]$_4$[Sn$_{10}$S$_{20}$O$_4$]} featuring covalent Ni-S bonds between the Ni^{2+} centered complexes and the anion. Such an expansion of the [Sn$_{10}$S$_{20}$O$_4$]$^{8-}$ anion was never observed before. Here we report the synthesis and characterization of this unusual compound.

2. EXPERIMENTAL

2.1 Synthesis

General: The following chemicals were used as purchased without further purification: NiCl$_2$·6H$_2$O (pure, Merck); Sn (99.5%, Alfa Aesar); S (99.5% Alfa Aesar), 1,10-phenanthroline (phen, C$_{12}$H$_8$N$_2$, 99%, abcr); methylamine

solution (ma, in water 40%, abcr); *trans*-1,2-diaminocyclohexane (1,2-dach, $C_6H_{14}N_2$, 99% Aldrich).The reaction product was filtrated, washed with water and ethanol and dried over silica gel.

Synthesis of {[Ni(1,2-dach)$_2$(ma)]$_4$[Sn$_{10}$S$_{20}$O$_4$]}: 59.5 mg (0.25 mmol) $NiCl_2 \cdot 6H_2O$, 29.7 mg (0.25 mmol) Sn, 24.1 mg (0.75 mmol) S, 45.1 mg (0.25 mmol) phen were reacted with 60 µL 1,2-dach in 2 mL 30% ma in a glass tube (inner volume 11 mL) at 120°C for 7 days. The product consists of pale purple needles in relatively low yield and X-ray amorphous black and reddish powder. Elemental analysis, results in %: found: C 12.3, H 2.8, N 6.0, calculated: C 12.4, H 2.8, N 6.2.

2.2 Structure determination

The intensity data for the compound were collected using a STOE IPDS-1 (Imaging Plate Diffraction System) with Mo-Kα radiation at T = 200(2) K (Tab. 1). The structure was solved with direct methods using the program SHELXS-97 [22] and the refinements were done against F^2 with SHELXL-97 [23]. All non-hydrogen atoms were refined anisotropic. Most of the C-H and all N-H hydrogen atoms were positioned with idealized geometry and were refined isotropic with $U_{iso}(H) = 1.2\ U_{eq}(C, N)$ using a riding model. Three of the C atoms of one 1,2-dach ligand are disordered. For the three disordered C atoms the C-H hydrogen atoms were positioned with idealized geometry (methyl hydrogen atoms allowed to rotate but not to tip) and refined isotropic with $U_{iso}(H) = 1.5\ U_{eq}(C)$ using a riding model.

Selected structural data and refinement results are summarized in Tab. 1. Structural data have been deposited in the Cambridge Crystallographic Data Centre as publication no. CCDC 1504447. Copies of the data can be obtained, free of charge, on application to CCDC, 12 Union Road, Cambridge CB2 1 EZ, UK (mail: deposit@ccdc.ca.ac.uk).

2.3 Characterization methods

X-ray powder diffractometry The X-ray powder diffraction patterns were measured on a STOE Stadi-P powder diffractometer (Cu-Kα_1 radiation, λ = 1.540598 Å, Ge monochromator) in transmission geometry with a MYTHEN 1K detector (DECTRIS) (ESI, Fig. S1).

Infrared Spectroscopy MIR spectra (400-4000 cm^{-1}) were measured with a Bruker Alpha P spectrometer (ESI, Fig. S2 and Tab. S1).

Elemental Analysis CHN analyses were done with a EURO EA Elemental Analyzer, fabricated by EURO VECTOR Instruments and Software.

Energy Dispersive X-ray Spectroscopy Scanning electron microscopy investigations and EDX analyses were done using a Philips Environmental Scanning Electron Microscope ESEM XL30 equipped with an EDAX detector.

Table 1. Selected details of the data collection and structure refinement results.

	{[Ni(1,2-dach)$_2$(ma)]$_4$[Sn$_{10}$S$_{20}$O$_4$]}
crystal system	tetragonal
space group	$P\bar{4}2_1c$
M (g/ mol)	3144.56
a (Å)	20.9912(4)
b (Å)	20.9912(4)
c (Å)	11.2091(3)
α (°)	90
β (°)	90
γ (°)	90
V (Å^3)	4939.07(19)
temperature (K)	200(2)
Z	2
Dcalculated (g/ cm^3)	2.114
μ (mm^{-1})	3.693
scan range (deg)	2.06≤ θ ≤26.80
reflections collected	38556
independent reflections	5249
observed reflections	4983
goodness-of-fit on F^2	1.048
R values (I > 2σ(I))	R1 = 0.0373, wR2 = 0.0858
R values (all data)	R1 = 0.0401, wR2 = 0.0875
res. elec. dens. (e/Å^3)	0.739 and -0.671

3. RESULTS AND DISCUSSIONS:

3.1 Synthetic aspects

Recently we performed synthetic studies of the Ni/phen/Sn/S system and revealed that for the formation and crystallization of tin-sulfur-compounds with general formulae ({[Ni(phen)$_2$]$_2$[Sn$_2$S$_6$]}·amine) (phen = 1,10-phenanthroline, amine = 2,2'-bipyridine (2,2'-bipy), 4,4'-bipyridine (4,4'-bipy), biphenyl (biph)) equimolar amounts of aromatic molecule are necessary. [24, 25] It is assumed that these aromatic molecules ease formation and crystallization of the compounds without being integrated into the final products. The aromatic component may be an amine molecule but must show a weaker tendency to coordinate to the Ni^{2+} ion and therefore without competition with the coordination behavior of the phen ligand. Such aromatic molecules were identified as 2,2'-bipy, 4,4'-bipy and biph. [24, 25] Synthetic drawbacks of the syntheses with aromatic molecules are the low solubility in water and the resulting pH value not high enough to react with elemental sulfur. Therefore, methylamine was added which generates the basic reaction milieu and has only a slight tendency to coordinate to Ni^{2+} in the presence of bidentate or tridentate ligands. As mentioned above aromatic molecules play an important role for formation and crystallization of ({[Ni(phen)$_2$]$_2$[Sn$_2$S$_6$]}·amine) compounds. Now we extended the research to the bidentate aliphatic amine 1,2-dach (1,2-dach = 1,2-diaminocyclohexane) with the aim to examine whether the aromatic character of the additive

amine molecule is essential for the formation of a $\{[Ni(phen)_2]_2[Sn_2S_6]\}$·amine compound or if such materials can be also obtained applying aliphatic amines. In case that a compound with composition $\{[Ni(phen)_2]_2[Sn_2S_6]\}$·amine) is obtained with 1,2-dach, our hypothesis of the necessity of addition of an aromatic amine must be discarded.

We selected 1,2-dach which has a similar complex stability like 2,2'-bipy ($[Ni(2,2'\text{-bipy})_3]^{2+}$: log β_3: 20.1, ($[Ni(trans\text{-}1,2\text{-}dach)_3]^{2+}$: log β_3: 20.1 [26]) but a lower stability like phen ($[Ni(phen)_3]^{2+}$: log β_3: 24.3 [27]). Analogous synthesis conditions as for $\{[Ni(phen)_2]_2[Sn_2S_6]\}$·2,2'-bipy (0.25 mmol $NiCl_2{\cdot}6H_2O$, 0.25 mmol Sn, 0.75 mmol S, 0.25 mmol phen, 0.25 mmol 2,2'bipy, 2 mL 30% ma, 120°C, 7d) [25] were applied. Actually $\{[Ni(1,2\text{-}dach)_2(ma)]_4[Sn_{10}S_{20}O_4]\}$ was obtained and not a structure analogous to synthesis with 2,2'-bipy, confirming that an aromatic amine seems to be essential for the formation of $\{[Ni(phen)_2]_2[Sn_2S_6]\}$·amine compounds. Interestingly, the title compound feature the $[Sn_{10}S_{20}O_4]^{8-}$ unit, because previous observations showed a rise of the condensation grade with decreasing pH value [19, 20], and $\{[Ni(1,2\text{-}dach)_2(ma)]_4[Sn_{10}S_{20}O_4]\}$ was obtained in a reaction mixture with a pH of 12-13. It is worth mentioning that the amount of phen (0.25 mmol) in the reaction mixture is crucial for the formation, although it is not part of the crystal structure. Decrease (0.1 mmol) or increase (0.5 mmol) of the phen concentration results in an X-ray amorphous product. A distinct increase of the phen portion (2 mmol) leads to the formation of $\{[Ni(phen)_2]_2[Sn_2S_6]\}{\cdot}phen{\cdot}H_2O$. [24] Although the 1,2-dach ligand feature two different possible configurations (*cis* and t*rans*), the title compound only contains 1,2-dach ligands with the *trans* configuration, but the yield could not be significant improved by applying the pure *trans*-amine. Raising the amount of 1,2-dach finally leads to the formation of $[Ni(1,2\text{-}dach)_3]_2[Sn_2S_6]{\cdot}4H_2O$.[28] Analogous reactions with other TM were not successful: even with small amounts of phen (0.25 mmol) $\{[TM(phen)_2]_2[Sn_2S_6]\}$ and $\{[TM(phen)_2]_2[Sn_2S_6]\}{\cdot}phen{\cdot}H_2O$ (TM = Mn, Fe, Co) were formed.[29, 30]

3.2 Crystal structure

$\{[Ni(1,2\text{-}dach)_2(ma)]_4[Sn_{10}S_{20}O_4]\}$ crystallizes in the tetragonal space group $P\bar{4}2_1c$ (Z = 2) and feature the rare $[Sn_{10}S_{20}O_4]^{8-}$ unit (Fig. 1). Except the Sn1 atom all unique atoms are located on general positions. The anionic unit is covalently linked to the charge compensating $[Ni(1,2\text{-}dach)_2(ma)]^{2+}$ complexes by Ni-(μ_3-S)-Sn bonds. Only few compounds were reported containing the $[Sn_{10}S_{20}O_4]^{8-}$- anion: $[Cs_8(H_2O)_{13}][Sn_{10}O_4S_{20}]{\cdot}13H_2O$ [20], $[Li_8(H_2O)_{29}][Sn_{10}S_{20}O_4]{\cdot}2H_2O$ [19], $\{[Sn_{10}S_{18}O_4]\}_n{\cdot}4n[HN(CH_3)_3]$ [21] and $\{[Ga_{3.2}Sn_{0.8}S_{10}][Sn_{10}S_{20}O_4]\}_n{\cdot}14.4n[C_6H_{14}NO]$ [11]. The $[Sn_{10}S_{20}O_4]^{8-}$ anion is constructed by ten corner-sharing $[SnS_4]^{4-}$ tetrahedra leading to the formation of a T3-type super-tetrahedron, $[Sn_{10}S_{20}]$, which is formally charge neutral.[3, 8, 9, 31] The spaces between these corner linked $[SnS_4]$ tetrahedra are occupied by O atoms (Fig. 1).

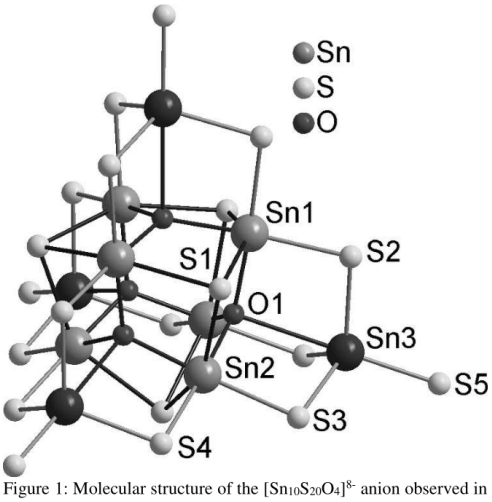

Figure 1: Molecular structure of the $[Sn_{10}S_{20}O_4]^{8-}$ anion observed in the title compound. Color code for the Sn atoms: inner Sn atoms: light grey, outer Sn atoms: dark grey. Atoms of the asymmetric unit are labeled.

Considering the shortest Sn-S and Sn-O distances, the six inner Sn atoms (Sn1 and Sn2, Fig.1, light grey spheres) are surrounded by two S and two O atoms forming slightly distorted rectangles with similar angles around the Sn centers (S-Sn1-O: 176.21(13)°, S-Sn2-O: 176.67(13) - 177.00(13)°, S-Sn1-S: 96.73(8)°, S-Sn2-S: 96.00(6)°, O-Sn1-O: 89.2(2)°; O-Sn2-O: 89.7(2)°) and comparable to hitherto known compounds.[11, 19] The Sn-O bond lengths (Sn1-O1: 2.075(4) Å, Sn2-O1: 2.072(4) Å) are significantly shorter than the Sn-S bonds (Sn1-S: 2.4458(18) Å, Sn2-S: 2.4650(17) - 2.4691(17) Å), but in the range of literature data (Sn-O: 2.0610(6) - 2.1030(6) Å; Sn-(μ-S): 2.4130(7) - 2.5060(7) Å) [19] (ESI: Tab. S2). The geometry of the external $[SnS_4]$ tetrahedron (Sn3, Fig. 1, dark grey spheres) exhibits only a slight distortion from ideal geometry (S-Sn-S: 106.10(7) - 113.13(6) Å) and the angles around the Sn3 atom is comparable to the free $[SnS_4]^{4-}$ anion [32] (S-Sn-S: 107.7 - 113.0 Å). The bonding pattern of a short Sn-Sterm bond (Sn3-S5: 2.3384(18) Å) and longer Sn-(μ_2-S) bonds (2.4213(18) - 2.4361(17) Å) is typical for thiostannates,[15] and the geometric parameters are comparable to literature data of similar compounds (Sn-Sterm: 2.3556(8) - 2.3715(7) Å; Sn-(μ-S): 2.4130(7) - 2.4386(7) Å). [19]

Taking into account the longer Sn-S bonds (Sn1/Sn2-S1: 2.6169(16) - 2.6474(16) Å) the SnO_2S_2 rectangles are expanded to distorted SnO_2S_4 octahedra ((μ_2-S)-Sn1/Sn2-(μ_2-S): 96.00(6) - 101.04(6)°, (μ_3-S)-Sn1/Sn2-(μ_3-S): 147.15(7) - 148.71(6)°, (μ_2/μ_3-S)-Sn1/Sn2-(μ_4-O): 78.18(12) - 87.31(13)°, (μ_4-O)-Sn-(μ_4-O): 89.2(2) - 89.7(2)°), and similar data were reported in literature. [11, 19] Considering the longer Sn-O bonds (2.7880(43) Å) the SnS_4 tetrahedron is expanded to a distorted SnS_4O trigonal bipyramid ((μ_4-O)-Sn-(μ_2-S): 73.35(9) - 73.97(9)°, (μ_2-S)-Sn3-(μ_2-S): 111.72(5) - 113.13(6)°, (μ_4-O)-Sn3-S5: 179.21(10)°). This Sn3-O bond is

longer than reported in literature compounds (Sn-O: 2.6037(78) Å [19], 2.511(8) Å [11]), but still shorter than the sum of the van der Waal's radii of these two atoms (3.68 Å) [33, 34] Considering the long Sn3-O bond the bond valence sum (BVS) [35–37] was calculated to be 3.90 for the Sn atom and 2.28 for the O atom, both values are close to the expected values of 4 (Sn^{4+}) and 2 (O^{2-}). Neglecting this bond the BVS values are 3.79 for Sn and 2.17 for O, which are also in the expected ranges.

All compounds reported in literature are isolated anionic clusters with inorganic counterions [19, 20] or the clusters are linked via terminal S atoms to form three-dimensional networks.[11, 21] In the title compound an expansion of the central cluster is observed via a Ni-(μ_3-S1) bond to the $[Ni(1,2\text{-dach})_2(ma)]^{2+}$ complexes. (Fig. 2) The dimensions of the neutral molecule are about 19 · 19 Å. The oxygen atoms are in a tetrahedral environment of Sn atoms (Fig. 3) to form an anti T2-cluster. [8]

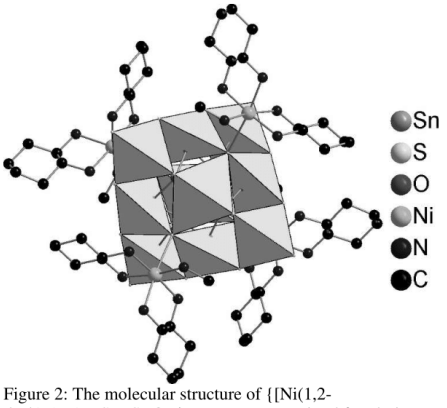

Figure 2: The molecular structure of $\{[Ni(1,2\text{-dach})_2(ma)]_4[Sn_{10}S_{20}O_4]\}$. H atoms are omitted for clarity.

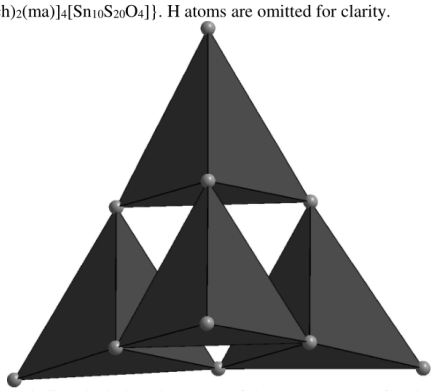

Figure 3: Tetrahedral environment of the oxygen atoms forming an anti-T2 Cluster.

Analogous $[In_{10}S_{20}]^{10-}$ or $[Mn_2Ga_4Sn_4S_{20}]^{8-}$ T3 clusters are either isolated anions like in $[Mn(dien)]_4[Mn_2Ga_4Sn_4S_{20}]$ [38] or expanded via the terminal S atoms as observed in $\{[Mn_2(en)_5]_2[Mn_2Ga_4Sn_4S_{20}]\}_n{\cdot}4nH_2O$ or e.g. $\{[In_{10}S_{18}][InS_3]\}_n{\cdot}7n$ deaH (dea = diethylamine).[11, 38–45] In $\{[Ni(1,2\text{-dach})_2(ma)]_4[Sn_{10}S_{20}O_4]\}$ the octahedral coordination sphere of the Ni^{2+} cation is formed by five N atoms (two 1,2-dach molecules and one ma ligand) and one (μ_3-S) atom of the anionic cluster. The Ni-N (2.067(6) - 2.119(6) Å) as well as the Ni-S (2.5561(18) Å) bonds are in the range of literature reported data. [25, 28, 46] (ESI, Fig. S4 and Tab. S3) Due to the different ligands the resulting octahedron is distorted as evidenced by the angles around the Ni^{2+} center (83.4(3) - 94.2(3)°; 170.4(3) - 175.6(3)°), but comparable to compounds with similar octahedra. [28, 46]

The arrangement of the $\{[Ni(1,2\text{-dach})_2(ma)]_4[Sn_{10}S_{20}O_4]\}$ moieties is symmetric: one cluster is positioned on each corner of the unit cell and one moiety is placed in the middle (Fig. 4) resembling the CsCl type structure.

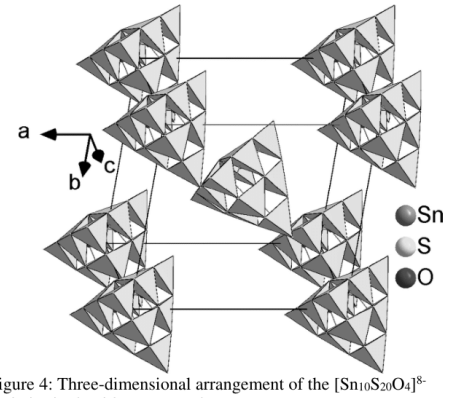

Figure 4: Three-dimensional arrangement of the $[Sn_{10}S_{20}O_4]^{8-}$ moieties in the title compound.

The $\{[Ni(1,2\text{-dach})_2(ma)]_4[Sn_{10}S_{20}O_4]\}$ units are stacked in a way that the $[Ni(1,2\text{-dach})_2(ma)]^{2+}$ complexes are arranged in parallel along the *c* axis. (Fig. 5)

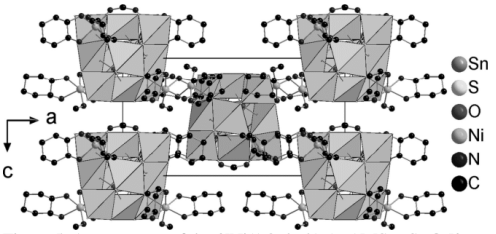

Figure 5: Arrangement of the $\{[Ni(1,2\text{-dach})_2(ma)]_4[Sn_{10}S_{20}O_4]\}$ moieties within the ac plane. Hydrogen atoms are not depicted for reasons of clarity.

Hydrogen bonding interactions between the S5 atoms and (NH_2) hydrogen atoms of 1,2-dach ligands of adjacent moieties as well as hydrogen bonding interactions between (μ_2-S) atoms and (NH_2) hydrogen atoms of 1,2-dach ligands of direct linked complexes stabilize the structure. (Fig. 6; ESI, Tab. S4)

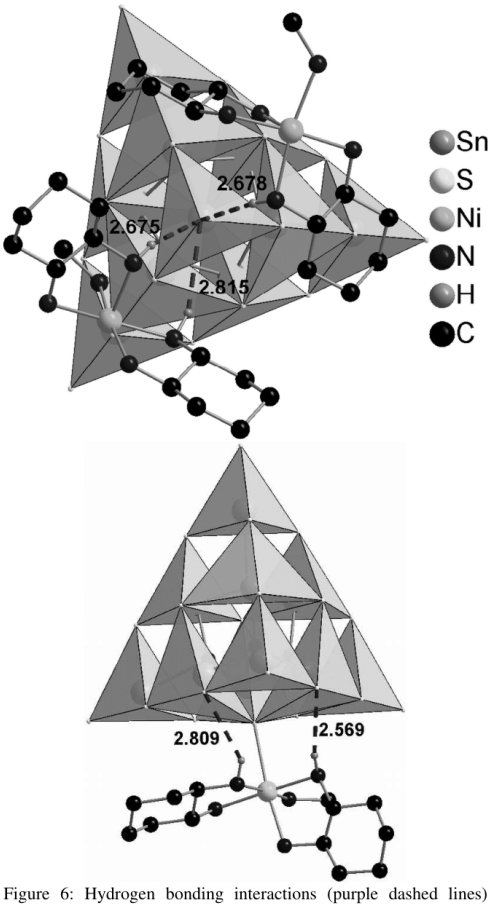

Figure 6: Hydrogen bonding interactions (purple dashed lines) between terminal S atoms and 1,2-dach ligands of adjacent moieties (top) and interactions between edge S atoms and amine ligands of covalent bond $[Ni(1,2\text{-dach})_2(ma)]^{2+}$ complexes (bottom). For reasons of clarity only part of the molecular structure is depicted.

Each corner of the $[Sn_{10}S_{20}O_4]^{8-}$ unit interacts via three contacts with two neighbored moieties (ESI, Fig. S6 & S7) leading to the formation of a three-dimensional network.

CONCLUSION

The title compound is an example that large anionic units like $[Sn_{10}S_{20}O_4]^{8-}$ can be prepared even at higher pH values, in contrast what was reported in literature. Moreover this compound exhibits a hitherto never observed connection mode of the (μ_3-S) atoms with the charge compensating Ni^{2+} centered complexes. The synthesis conditions indicate that organic additives like for example phen influence the product formation in a so far not well understood way leading to the formation of unexpected compounds with unusual structural motifs. Hence, further systematic studies are required which may shed light onto processes occurring under solvothermal reactions.

ACKNOWLEDGEMENTS

Financial support by the State of Schleswig-Holstein is gratefully acknowledged.

SUPPLEMENTARY MATERIAL

Experimental and simulated XRPD pattern of the title compound (Fig. S1); results of the IR measurements (Fig. S2 and Tab. S1); selected bond length and angles (Tab. S2 and Tab. S3); interatomic S···H distances (Tab. S4).

REFERENCES

[1] Parise, J.B.; Ko, Y.; Rijssenbeek, J.; Nellis, D.M.; Tan, K.; Koch, S. Novel layered sulfides of tin: synthesis, structural characterization and ion exchange properties of TMA-SnS-1, $Sn_3S_7{\cdot}(NMe_4)_2{\cdot}H_2O$. *J. Chem. Soc., Chem. Commun.*, **1994**, (4), 527.

[2] Sarma, D.; Malliakas, C.D.; Subrahmanyam, K.S.; Islam, S.M.; Kanatzidis, M. $K_{2x}Sn_{4-x}S_{8-x}$ (x=0.65-1): A New Metal Sulfide for Rapid and Selective Removal of Cs^+, Sr^{2+} and UO_2^{2+} ions. *Chem. Sci.*, **2016**, *7*(2), 1121–1132.

[3] Zheng, N.; Bu, X.; Vu, H.; Feng, P. Open-framework chalcogenides as visible-light photocatalysts for hydrogen generation from water. *Angew. Chem. Int. Ed. Engl.*, **2005**, *44*(33), 5299–5303.

[4] Enzel, P.; Henderson, G.S.; Ozin, G.A.; Bedard, R.L. Imaging the surfaces of nanoporous semiconductors by atomic force microscopy. *Adv. Mater.*, **1995**, *7*(1), 64–68.

[5] Sheldrick, W.S.; Wachhold, M. Chalcogenidometalates of the heavier Group 14 and 15 elements. *Coord. Chem. Rev.*, **1998**, *176*(1), 211–322.

[6] Jiang, T.; Lough, A.; Ozin, G.A. Very Soft Chemistry: Room Temperature Self-Assembly of $(DABCOH)_2Sn_3S_7$, a Microporous Layered Tin(IV) Sulfide. *Adv. Mater.*, **1998**, *10*(1), 42–46.

[7] Ahari, H.; Ozin, G.A.; Bedard, R.L.; Petrov, S.; Young, D. Synthesis and compositional tuning of the band properties of isostructural TMA-SnS_xSe_{1-x}-1 Nanoporous Materials. *Adv. Mater.*, **1995**, *7*(4), 370–374.

[8] Bu, X.; Zheng, N.; Feng, P. Tetrahedral chalcogenide clusters and open frameworks. *Chem. Eur. J.*, **2004**, *10*(14), 3356–3362.

[9] Li, H. Supertetrahedral Sulfide Crystals with Giant Cavities and Channels. *Science*, **1999**, *283*(5405), 1145–1147.

[10] Li, H.; Kim, J.; O'Keeffe, M.; Yaghi, O.M. $[Cd_{16}In_{64}S_{134}]^{44-}$: 31-A tetrahedron with a large cavity. *Angew. Chem. Int. Ed. Engl.*, **2003**, *42*(16), 1819–1821.

[11] Han, X.; Wang, Z.; Liu, D.; Xu, J.; Liu, Y.; Wang, C. Co-assembly of a three-dimensional open framework sulfide with a novel linkage between an oxygen-encapsulated T3

cluster and a supertetrahedral T2 cluster. *Chemical Commun.*, **2014**, *50*(7), 796–798.
[12]Zhou, J.; Dai, J.; Bian, G.-Q.; Li, C.-Y. Solvothermal synthesis of Group 13–15 chalcogenidometalates with chelating organic amines. *Coord. Chem. Rev.*, **2009**, *253*(9+10), 1221–1247.
[13]Seidlhofer, B.; Pienack, N.; Bensch, W. Review. Synthesis of Inorganic-Organic Hybrid Thiometallate Materials with a Special Focus on Thioantimonates and Thiostannates and in situ X-Ray Scattering Studies of their Formation. *Z. Naturforsch.*, **2010**, *65b*(8), 937–975.
[14]Dehnen, S.; Melullis, M. A coordination chemistry approach towards ternary M/14/16 anions. *Coord. Chem. Rev.*, **2007**, *251*(9+10), 1259–1280.
[15]Krebs, B. Thio- and Seleno-Compounds of Main Group Elements - Novel Inorganic Oligomers and Polymers. *Angew. Chem. Int. Ed. Engl.*, **1983**, *95*(2), 113–134.
[16]Bubenheim, W.; Müller, U. Reaktionen von Zinnchloriden mit Polysulfiden. Die Kristallstrukturen von $(PPh_4)_2[SnCl_2(S_6)_2]$, $(PPh_4)_2[Sn_4Cl_4S_5(S_3)O]$ und $(PPh_4)_2[SnCl_6]\cdot S_8\cdot 2CH_3CN$. *Z. Anorg. Allg. Chem.*, **1993**, *619*(4), 779–785.
[17]Wu, L.; Chen, L.; Dai, J.; Cui, C.; Fu, Z.; Wu, X. The first octanuclear tin(IV)–oxosulfide cluster. *Inorg. Chem. Commun.*, **2001**, *4*(10), 574–576.
[18]Zhang, J.-J.; Hu, S.-M.; Wu, X.-T.; Du, W.-X.; Fu, R.-B.; Wang, L.-S. A simple method for the preparation of octanuclear tin (IV) oxosulfide cluster and the conversion of it to decanuclear cluster. *Inorg. Chem. Commun.*, **2003**, *6*(6), 744–747.
[19]Kaib, T.; Kapitein, M.; Dehnen, S. Synthesis and Crystal Structure of $[Li_8(H_2O)_{29}]$-$[Sn_{10}O_4S_{20}]\cdot 2H_2O$. *Z. anorg. allg. Chem.*, **2011**, *637*(12), 1683–1686.
[20]Schiwy, W.; Krebs, B. $Sn_{10}O_4S_{20}^{8-}$: Ein neuer Typ eines Polyanions. *Angew. Chem.*, **1975**, *87*(12), 451–452.
[21]Parise, J.B.; Ko, Y. Material Consisting of Two Interwoven 4-Connected Networks: Hydrothermal Synthesis and Structure of $[Sn_5S_9O_2][HN(CH_3)_3]_2$. *Chem. Mater.*, **1994**, *6*, 718–720.
[22]Sheldrick, G.M. SHELXS-97: *Program for the Solution of Crystal Structures, University of Göttingen, Göttingen (Germany)*, **1997**.
[23]Sheldrick, G.M. SHELXL-97: *Program for the Refinement of Crystal Structures, University of Göttingen, Göttingen (Germany)*, **1997**.
[24]Hilbert, J.; Pienack, N.; Lühmann, H.; Näther, C.; Bensch, W. Transition Metal Complexes with Linkage to the Thiostannate Units Forced by Suitable Amine Molecules. *to be published*.
[25]Hilbert, J.; Näther, C.; Bensch, W. Utilization of mixtures of aromatic N-donor ligands of different coordination ability for the solvothermal synthesis of thiostannate containing molecules. *Dalton Trans.*, **2015**, *44*(25), 11542–11550.
[26]Schwarzenbach, G.; Baur, R. 86. Metallkomplexe mit Polyaminen XI: Mit *cis*- und *trans*-1,2-Diaminocyclohexan. *Helv. Chim. Acta*, **1956**, *86*, 722–728.
[27]Irving, H.; Mellor, J. 1002. The Stability of Metal Complexes of 1,10-Phenanthroline and its Analogues. Part I. 1,10-Phenathroline and 2,2'Bipyridyl. *J. Chem. Soc.*, **1962**, 5222–5237.
[28]Pienack, N.; Lühmann, H.; Seidlhofer, B.; Ammermann, J.; Zeisler, C.; Danker, F.; Näther, C.; Bensch, W. Six new tin–sulfur containing compounds obtained under solvothermal conditions. *Solid State Sci.*, **2014**, *33*, 67–72.
[29]Hilbert, J.; Näther, C.; Bensch, W. The [Sn2S6]4- Anion Acting as Tetradentate Linker: Solvothermal Synthesis and Selected Properties of $\{[TM(phen)_2]_2[Sn_2S_6]\}$ and $\{[TM(phen)_2]_2[Sn_2S_6]\cdot phen\cdot H_2O$ (TM = Fe, Co). *Z. Anorg. Allg. Chem.*, **2014**, *640*(14), 2858–2863.
[30]Hilbert, J.; Näther, C.; Bensch, W. Influence of the synthesis parameters onto nucleation and crystallization of five new tin-sulfur containing compounds. *Inorg. Chem.*, **2014**, *53*(11), 5619–5630.
[31]Cahill, C.L.; Parise, J.B. On the formation of framework indium sulfides. *J. Chem. Soc., Dalton Trans.*, **2000**, (9), 1475–1482.
[32]Schiwy, W.; Pohl, S.; Krebs, B. Darstellung und Struktur von $Na_4SnS_4\cdot 14H_2O$. *Z. Anorg. Allg. Chem.*, **1973**, *402*(1), 77–78.
[33]Mantina, M.; Chamberlin, A.C.; Valero, R.; Cramer, C.J.; Truhlar, D.G. Consistent van der Waals radii for the whole main group. *J. Phys. Chem. A*, **2009**, *113*(19), 5806–5812.
[34]Bondi, A. van der Waals Volumes and Radii. *J. Phys. Chem.*, **1964**, *68*(3), 441–451.
[35]Palenik, G.J. Bond Valance Sums in Coordination Chemistry Using Oxidation State Independent R_0 Values. *Inorg. Chem.*, **1997**, *36*, 122.
[36]O'Keeffe, M.; Brese, N.E. Atom Sizes and Bond Lengths in Molecules and Crystals. *J. Am. Chem. Soc.*, **1991**, *113*, 3226–3229.
[37]Brown, I.D.; Altermatt, D. Bond-Valance Parameters Obtained from a Systematic Analysis of the Inorganic Crystal Structure Database. *Acta Cryst. B*, **1985**, *41*, 244–247.
[38]Yue, C.-Y.; Lei, X.-W.; Feng, L.-J.; Wang, C.; Gong, Y.-P.; Liu, X.-Y. $[Mn_2Ga_4Sn_4S_{20}]^{(8-)}$ T3 supertetrahedral nanocluster directed by a series of transition metal complexes. *Dalton Trans.*, **2015**, *44*(5), 2416–2424.
[39]Wang, C.; Bu, X.; Zheng, N.; Feng, P. Nanocluster with One Missing Core Atom: A Three-Dimensional Hybrid Superlattice Built from Dual-Sized Supertetrahedral Clusters. *J. Am. Chem. Soc.*, **2002**, *124*(35), 10268–10269.
[40]Li, H.; Eddaoudi, M.; Laine, A.; O'Keeffe, M.; Yaghi, O.M. Noninterpenetrating Indium Sulfide Supertetrahedral Cristobalite Framework. *J. Am. Chem. Soc.*, **1999**, *121*(25), 6096–6097.
[41]Zhang, C.; Liu, J.; Ji, M.; An, Y. Hydrothermal syntheses and characterization of two tetramethylammonium templated indium sulfides. *Inorg. Chem. Commun.*, **2014**, *44*, 169–172.

[42]Su, Z.; Li, X.; Lan, Y.; Wen, J.; Jin, G.; Xie, J.; Zheng, C.; Jin, J.; Li, S. A new chalcogenide ion-exchanging material: Porous indium sulfide built from condensed $[In_{10}S_{18}]^{6-}$ T3 supertetrahedral clusters. *Mater Lett*, **2008**, *62*(17-18), 2802–2805.

[43]Pitzschke, D.; Näther, C.; Bensch, W. $(DEA\text{-}H)^{+}{}_{7}In_{11}S_{21}H_2$: a new layered open framework indium sulfide based on the interconnection of $[In_{10}S_{20}]^{10-}$ supertetrahedra. *Solid State Sci.*, **2002**, *4*(9), 1167–1171.

[44]Yang, C.-S.; Su, Y.-H.; Wang, Y.-J.; Cheng, J.-H.; Lin, X.-H. Synthesis of three dimensional photoluminescent $[In_{10}S_{20-x}Se_x]^{10-}$ supertetrahedral clusters: ($x < 0.3$). *Mater Lett*, **2008**, *62*(24), 4015–4017.

[45]Cahill, C.L.; Ko, Y.; Parise, J.B. A Novel 3-Dimensional Open Framework Sulfide Based upon the $[In_{10}S_{20}]^{10}$-Supertetrahedron: DMA-InS-SB1. *Chem. Mater.*, **1998**, *10*(1), 19–21.

[46]Pienack, N.; Lehmann, S.; Lühmann, H.; El-Madani, M.; Näther, C.; Bensch, W. Solvothermal Syntheses, Crystal Structures and Selected Optical Properties of $[M(C_8N_5H_{23})]_2Sn_2S_6$ (M = Co, Fe, Ni; $C_8N_5H_{23}$ = tetraethylenepentamine). *Z. Anorg. Allg. Chem.*, **2008**, *634*(12-13), 2323–2329.

3.2 Publikationen zur Synthese übergangsmetallhaltiger Thiostannate mit Precursoren bei Raumtemperatur (kumulativer Hauptteil, Teil 2)

Die Verbindung {[Ni(tren)]$_2$[Sn_2S_6]} wurde vor einiger Zeit synthetisiert und eine vorläufige Struktur publiziert.[50] Das [Sn_2S_6]$^{4-}$-Anion ist über zwei terminale S^{2-}-Anionen an den ladungsneutralisierenden [Ni(tren)]$^{2+}$-Komplex gebunden. Das Ni^{2+}-Kation ist oktaedrisch von vier N-Donoratomen und zwei S^{2-}-Ionen umgeben. Zwei NiN_4S_2-Oktaeder bilden über Kantenverknüpfung einen $Ni_2N_8S_4$-Bioktaeder, welcher über die [Sn_2S_6]$^{4-}$-Einheiten zu Ketten verknüpft ist. Eine aktuellere Strukturverfeinerung wies auf ein besonderes Merkmal dieser Struktur hin: Die Ni-S-Bindungen sind mit 2.434(2) Å und 2.745(2) Å außerordentlich unterschiedlich lang. Mit DFT-Berechnungen konnten unterschiedliche Ni-S-Bindungsstärken nachgewiesen werden (s. Kap. 3.2.1). Daher sollte bei einem Aminmolekülüberschuss die schwächere Bindung gebrochen werden können und die Ni-S- durch eine Ni-N-Bindung substituiert werden. Diese Annahme erwies sich als richtig und auf Basis dieser Vermutung konnten vier neue Verbindungen synthetisiert werden.

Die Struktur des Precursors sowie die Reaktionsprodukte bei Verwendung von en, 1,2-dach, 1,2-dap und ma werden in Abschnitt 3.2.1 diskutiert. Die Ergebnisse der Synthesen mit weiteren Aminen (tren und 2amp) werden in Abschnitt 3.2.2 vorgestellt.

3.2.1 Verwendung der Verbindung $\{[Ni(tren)]_2[Sn_2S_6]\}_n$ als Precursor zur Darstellung von Thiostannaten bei Raumtemperatur

Zusammenfassung der Veröffentlichung „Room-Temperature Synthesis of Thiostannates from $\{[Nitren)]_2[Sn_2S_6]\}_n$“.

Der Precursor $\{[Ni(tren)]_2[Sn_2S_6]\}_n$ (*C*2/*c*, Z=4) wurde unter solvothermalen Bedingungen mit $NiCl_2 \cdot 6H_2O$, Sn, S, tren (1:1:3:2) in wässriger Methylamin Lösung (120°C, 4d) dargestellt. Bei der Reaktion dieser Verbindung bei RT in 30% Methylamin- bzw. 1,2-Diaminopropanlösung wurden innerhalb einer Woche Kristalle von $[Ni(tren)(ma)(H_2O)]_2[Sn_2S_6] \cdot 4H_2O$ ($P2_1/n$, Z=2) bzw. $[Ni(tren)(1,2\text{-dap})]_2[Sn_2S_6] \cdot 2H_2O$ ($P2_1/n$, Z=2) erhalten.

Bei RT konnte die Umsetzung des Precursors zu weiteren Thiostannaten nicht nur in Anwesenheit von ma und 1,2-dap, sondern auch unter Verwendung von en und 1,2-dach realisiert werden. Bei Einsatz dieser Aminmoleküle wurde ein vollständiger Ligandenaustausch beobachtet und die bekannten Verbindungen $[Ni(en)_3]_2[Sn_2S_6]$[50] und $[Ni(1,2\text{-dach})_2]_2[Sn_2S_6] \cdot 4H_2O$[43] kristallisierten. Bei Verwendung von 1,3-dap fand keine Reaktion statt und der Precursor wurde erhalten. Eine weitere Synthesereihe unter solvothermalen Bedingungen führte zu ähnlichen Ergebnissen. Nur bei der Reaktion mit ma bildete sich $[Ni(tren)(ma)(H_2O)]_2[Sn_2S_6] \cdot 4H_2O$ erst beim Abkühlen der Reaktionslösung auf RT. Bei Abschrecken der Reaktionslösung von höheren Temperaturen wurde die Bildung des Precursor beobachtet.

Inorganic Chemistry

Article

pubs.acs.org/IC

Room-Temperature Synthesis of Thiostannates from $\{[Ni(tren)]_2[Sn_2S_6]\}_n$

Jessica Hilbert,[†] Christian Näther,[†] Richard Weihrich,[‡] and Wolfgang Bensch*[,†]

[†]Institute of Inorganic Chemistry, Christian-Albrechts-University of Kiel, Max-Eyth-Str. 2, 24118 Kiel, Germany

[‡]Institute of Inorganic Chemistry, University of Regensburg, Universitätsstraße 31, 93040 Regensburg, Germany

Supporting Information

ABSTRACT: The compound $\{[Ni(tren)]_2[Sn_2S_6]\}_n$ (**1**) (tren = tris(2-aminoethyl)amine, $C_6H_{18}N_4$) was successfully applied as source for the room-temperature synthesis of the new thiostannates $[Ni(tren)(ma)(H_2O)]_2[Sn_2S_6]\cdot 4H_2O$ (**2**) (ma = methylamine, CH_5N) and $[Ni(tren)(1,2\text{-dap})]_2[Sn_2S_6]\cdot 2H_2O$ (**3**) (1,2-dap = 1,2-diaminopropane, $C_3H_{10}N_2$). The Ni−S bonds in the $Ni_2S_2N_8$ bioctahedron in the structure of **1** are analyzed with density functional theory calculations demonstrating significantly differing Ni−S bond strengths. Because of this asymmetry they are easily broken in the presence of an excess of ma or 1,2-dap immediately followed by Ni−N bond formation to N donor atoms of the amine ligands thus generating $[Ni(tren)(amine)]^{2+}$ complexes. The chemical reactions are fast, and compounds **2** and **3** are formed within 1 h. The synthesis concept presented here opens hitherto unknown possibilities for preparation of new thiostannates.

■ INTRODUCTION

Thiometallates based on main group elements like In, Ge, Sn, or Sb exhibit a fascinating structural chemistry and often unusual physicochemical properties. For example, the thiostannate $K_{2x}Sn_{4-x}S_{8-x}$ ($x = 0.65-1$)[1] was used successfully for heavy metal cation removal, and the compound $Na_4In_7Cu_3S_{35}\cdot x H_2O$ shows promising properties for light-driven hydrogen generation.[2]

Thiometallate compounds are usually prepared by a solvothermal route, and in several review articles focusing on the synthetic approaches and aspects, the structural variability and flexibility of the anions have appeared.[3−12] Incorporation of transition metal (TM) cation amine complexes into the thiometallate frameworks is still an attractive synthetic approach for altering the structural, chemical, and physical properties. Because several first-row 3d cations and numerous amine ligands are available an enormous number of new compounds is possible. Analyzing carefully compositions and structural features of such inorganic−organic hybrid thiometallates, evidently, only Mn^{2+} cations seem to be easily integrated into the anionic framework, which was explained on the comparable affinity to both S and N donor atoms, independent from the denticity of the amine used in the reaction mixtures.[13−32] Other TMs like Fe^{2+}, Co^{2+}, Ni^{2+}, and Zn^{2+} prefer bonding to N donor atoms usually leading to the formation of discrete $[TM(amine)_x]^{2+}$ cations and thiometallate anions. Synthetic tricks like using multidentate amines,[17,18,33,34] leading to coordinately unsaturated TM^{2+} complexes or stabilization via aromatic amines[35,36] can force TM-S bond formation. Comparing the different TMs further, it is noticeable that thiometallate compounds obtained with $[Ni(amine)_x]^{2+}$ ions exhibit the largest variability with respect to the amine ligands.[17,18,33,37] This is not quite surprising keeping in mind that $[Ni(amine)_x]^{2+}$ complexes with common amines like ethylenediamine (en), diethylenetriamine (dien), tris(2-aminoethyl)amine (tren), triethylenetetramine (trien), tetraethylenepentamine (tepa), pentaethylenehexamine (peha), 1,4,8,11-tetraazacyclotetradecane (cyclam), or 1,2-diaminocyclohexane (1,2-dach) exhibit the highest complex stabilities among the late TM^{2+} cations.[38−44]

In the synthesis of thiometallates the formation of the Ni^{2+} amine complexes usually occurs in situ during the solvothermal reaction, where often elemental Ni[17,18] was used, but $NiCl_2\cdot 6H_2O$,[18,33,37] $Ni(NO_3)_2\cdot 6H_2O$,[45] $Ni(CH_3COO)_2\cdot 4H_2O$,[46,47] $NiSO_4\cdot 7H_2O$,[48,49] and NiS[50,51] were also applied. Usually the amines are added in large excess, serving not only as reactant but also as solvent. The usage of preformed $[Ni(amine)_x]^{2+}$ cations or in general $[TM(amine)_x]^{2+}$ complexes for the preparation of thiometallates is little-explored. To the best of our knowledge thiostannates have not been synthesized applying $[Ni(amine)]^{2+}$ complexes as educt, while for other thiometallates the use of $[TM(amine)_x]^{2+}$ complexes was successful demonstrating the large synthetic potential of this approach.[34,52−56] Thiostannates containing $[TM(amine1)_n(amine2)_m]^{2+}$ complexes (n and m depend on the denticity of

Received: March 11, 2016
Published: August 1, 2016

DOI: 10.1021/acs.inorgchem.6b00625
Inorg. Chem. 2016, 55, 7859−7865

the amine ligand and the coordination geometry) are not known, while for thioantimonates several examples were reported.[54,57−60]

The use of preformed thiostannates is also relatively little explored. Typically the thiostannates units are formed in situ from the elements, for example, Sn and S, or from starting materials like, for example, $SnCl_4{\cdot}5H_2O$,[37,61−63] $SnCl_4$,[64,65] SnS_2,[66−68] $SnCl_2{\cdot}2H_2O$[15,33] and $Cl_3SnCMe_2CH_2COMe$,[69,70] or $Na_2S{\cdot}9H_2O$[64,69,70] and $(NH_4)_2S$[67,68,71] during the synthesis. Among the thiogermanates, the compound $[(CH_3)\text{-}N]_4[Ge_4S_{10}]$[56,72−75] is a popular precursor for the synthesis of new compounds. However, very few experiments have been performed with Na_4SnS_4.[76] To the best of our knowledge the use of an inorganic−organic TM-containing tin sulfur compound as precursor at ambient temperature has not been examined.

In solvothermal syntheses using the tetradentate amine tren, which leaves Ni^{2+} coordinatively unsaturated, we crystallized $\{[Ni(tren)]_2[Sn_2S_6]\}_n$ (**1**). A preliminary structure of this compound has been published, but the single crystals were nonmerohedrally twinned preventing a good structure refinement.[17] The structure refinement performed in the present investigation revealed that the main building block, a $Ni_2S_2N_8$ bioctahedron, is characterized by two very different Ni−S bonds to the thiostannate anion, that is, one short and a long bond. Hence we performed density functional theory (DFT) calculations on this compound for evaluation of the bond strengths of the Ni−S bonds. The different bonds and the asymmetry in the Ni−S−Ni interconnection of two Ni clusters are characterized from the electronic charge density within the theory of atoms in molecules (AIM)[77,78] and the electron localization function (ELF).[79,80] The results suggest that this compound might be used as a precursor for the generation of new thiostannates due to the following consideration: The long Ni−S bond is weaker than a Ni−N bond, and offering an amine in excess may break the long Ni−S bond followed by formation of Ni^{2+}-centered complexes with two different amine ligands, while the $[Sn_2S_6]^{4-}$ anion is retained. Because of the large amine excess one may also envisage that both Ni−S bonds are broken thus leading to formation of separated Ni^{2+} amine complexes and the thiostannate anion. Here we report the room-temperature syntheses of the new compounds $[Ni(tren)(H_2O)ma]_2[Sn_2S_6]{\cdot}4H_2O$ (**2**) and $[Ni(1,2dap)(tren)]_2[Sn_2S_6]{\cdot}2H_2O$ (**3**) applying **1** as educt. Two further compounds, $[Ni(en)_3]_2[Sn_2S_6]$[17] and $[Ni(1,2\text{-dach})_3]_2[Sn_2S_6]{\cdot}4H_2O$,[18] were also obtained using **1** as starting material under ambient and solvothermal conditions.

■ EXPERIMENTAL SECTION

Syntheses. *General.* All chemicals were purchased and used without further purifications. The following chemicals were used: tris(2-aminoethyl)amine (tren, $C_6H_{18}N_4$, 96%, Aldrich); methylamine solution (ma, in water 40%, ABCR); $NiCl_2{\cdot}6H_2O$ (reinst. Merck); Sn (99.5% Alfa Aesar); S (99.5% Alfa Aesar), ethylenediamine (en, $C_2H_8N_2$, reinst. 99%, Grüssing); 1,2-diaminopropane (1,2-dap, $C_3H_{10}N_2$, 99% ABCR); trans-1,2-diaminocyclohexane (1,2-dach, $C_6H_{14}N_2$, 99% Aldrich), 1,3-diaminopropane (1,3-dap, $C_3H_{10}N_2$, 99% Aldrich).

All reaction products were filtered off, washed with water and ethanol, and then dried over silica gel. In the case of the static synthesis the crystalline products were separated manually, and the homogeneity was confirmed by X-ray powder diffraction (see Supporting Information, Figure S1 and Table S2).

Syntheses at room temperature with $\{[Ni(tren)]_2[Sn_2S_6]\}_n$ (**1**) as educt were done in glass tubes (inner volume 11 mL) with 0.25 mmol of compound **1** and 2 mL of a water−amine mixture stirring the slurries for at least 1 h (Table S3 and Figures S2−S4, Supporting Information). Solvothermal syntheses under static and stirring conditions (magnetic stirrer) were undertaken in glass tubes (inner volume: 11 mL) at T = 120 °C with the ratio Ni/Sn/S being fixed at 0.25:0.25:0.75 mmol and 2 mL of aqueous amine mixture as solvent. In the section Results and Discussion the influence of the amine mixtures onto product formation as well as the motivations for applying these mixtures are discussed. The Ni educts, amines, reaction times, and yields of the products are listed in Table S4 (Supporting Information). Special details of the static solvothermal syntheses (T = 120 °C), which differ from that mentioned above and resulted in single crystals for structure determination, are presented below together with the results of chemical analyses.

*Synthesis of $\{[Ni(tren)]_2[Sn_2S_6]\}_n$ (**1**).* $NiCl_2{\cdot}6H_2O$, Sn, S, and 74 μL (0.5 mmol) of tren were mixed with 1.5 mL of ma and 0.5 mL of H_2O and reacted at 120 °C for 4 d. The product contained small green crystals and few dark, X-ray amorphous crumbs (energy-dispersive X-ray (EDX): Ni, Sn, S). Elemental analysis of **1**: found: C 17.18, H 4.05, N 13.25, calculated: C 17.17, H 4.32, N 13.34%.

*Synthesis of $[Ni(tren)(ma)(H_2O)]_2[Sn_2S_6]{\cdot}4H_2O$ (**2**).* Green crystals of $\{[Ni(tren)]_2[Sn_2S_6]\}_n$ (**1**) (0.25 mmol) appeared at the bottom of the glass tube in a solution of 2 mL of ma (30%). The slurry was kept at room temperature for another week. The green crystals disappeared after 2 d, and purple crystals of **2** were formed as well as some X-ray amorphous black powder (EDX: Ni, Sn, S). Elemental analysis: found: C 16.60, H 5.82, N 13.67, calculated: C 16.65, H 5.79, N 13.87%.

*Synthesis of $[Ni(1,2\text{-}dap)(tren)]_2[Sn_2S_6]{\cdot}2H_2O$ (**3**).* Green crystals of **1** (0.25 mmol) were reacted with 2 mL of 1,2-dap (30%) at 120 °C yielding purple crystals of **3** and dark X-ray amorphous powder (EDX: Ni, Sn, S) within 7 d. Elemental analysis: found: C 21.08, H 5.72, N 16.24, calculated: C 21.11, H 5.91, N 16.41%.

Structure Determination. The intensity data for **1**−**3** were collected using a STOE IPDS-1 (Imaging Plate Diffraction System) with Mo Kα radiation at 200(2) or 293(2) K. The structures were solved with direct methods using the program SHELXS-97,[81] and the refinements were done against F^2 with SHELXL-97[82] and SHELXL-2014.[83] For all non-hydrogen atoms an anisotropic refinement was done. The hydrogen atoms in compound **1** were positioned with idealized geometry and refined isotropic using a riding model. The disordered carbon atoms C1, C3, and C5 were refined using a split model with the site occupation factors (sof) of C1/C1′ = 65:35; C3/C3′ = 60:40; and C5/C5′ = 55:45. In the structures of **2** and **3** the C−H and N−H hydrogen atoms were positioned with idealized geometry and were isotropically refined with $U_{iso}(H)$ = 1.2 $U_{eq}(C,N)$ using a riding model. The O−H H atoms for compounds **2** and **3** were located in the difference Fourier maps, their bond lengths were set to ideal values, and finally they were refined isotropic with $U_{iso}(H)$ = 1.5 $U_{eq}(O)$ using a riding model. In compound **3** two C atoms of the 1,2-diaminopropane ligand are disordered and were refined using a split model (sof: C11/C11′ = 62:38; C12/C12′ = 62:38). Selected refinement results are summarized in Table S1, and additional crystallographic information is available in the Supporting Information.

X-ray Powder Diffraction. The X-ray powder diffraction patterns were recorded on a STOE Stadi-P powder diffractometer (Cu Kα1 radiation, λ = 1.540 598 Å, Mythen) in transmission geometry (see Figure S1 and Table S2, Supporting Information).

Infrared Spectroscopy. MIR spectra (400−4000 cm^{-1}) were recorded with a Bruker Alpha P spectrometer (see Figure S7 and Table S5, Supporting Information).

Raman Spectroscopy. Raman spectra were collected with a Bruker IFS 66 Fourier transform Raman spectrometer (wavelength: 541.5 nm) in the region from 100 to 3500 cm^{-1} (see Figure S8 and Table S6 Supporting Information).

Ultraviolet−Visible Spectroscopy. UV/visible (UV/vis) spectroscopic investigations were performed at room temperature using a UV/vis/NIR two-channel spectrometer Cary 5 from Varian Techtron Pty, Darmstadt (200−3300 cm^{-1}). The optical properties of

DOI: 10.1021/acs.inorgchem.6b00625
Inorg. Chem. 2016, 55, 7859−7865

compounds **1**–**3** were investigated by evaluating the UV/vis reflectance spectra of the powdered samples (with $BaSO_4$ powder used as reference material). The absorption data were calculated applying the Kubelka–Munk relation for diffuse reflectance data (see Figure S9, Supporting Information, and Table 1).

Table 1. Bands[a] of the UV–Vis Diffuse Reflectance Spectra for Compounds 1–3 Compared to the [Ni(tren)(H_2O)Cl]Cl (Nitren) Complex

Nitren	1	2	3	assignment[b,c]
1.19	1.09	1.38	1.47	$^3A_{2g} \rightarrow {}^3T_{2g}$
2.09	2.00	2.27	2.31	$^3A_{2g} \rightarrow {}^3T_{1g}$ (^3F)
3.24		*d*	*d*	$^3A_{2g} \rightarrow {}^3T_{1g}$ (^3P)
	2.37	3.65	3.55	optical band gap

[a]Values given in electronvolts. [b]Reference 105. [c]Reference 107. [d]Overlapped.

Energy-Dispersive X-ray Experiments. Scanning electron microscopy investigations and EDX analyses were done with a Philips Environmental Scanning Electron Microscope ESEM XL30 equipped with an EDAX detector.

Elemental Analysis. CHN analyses were done using a EURO EA Elemental Analyzer, fabricated by EURO VECTOR Instruments and Software.

Ab Initio Calculations. Crystal and electronic structure calculations were performed with the CRYSTAL14 code.[84,85] GGA (PBE) and LDA as well as implemented hybrid (B3LYP, PBE0) functionals were applied. All electron basis sets for Sn, Ni, and S were taken from previous calculations on $Ni_3Sn_2S_2$-type compounds (see literature[86–89]); for N, C, and H the electron basis sets were taken from online resources [see Supporting Information]. For crystal structure predictions atomic positions were relaxed according to the implemented Schlegel-type algorithm. The electronic structures were converged to changes in energy of less than 1×10^{-8} H on $2 \times 2 \times 2$ and $4 \times 4 \times 4$ k-point grids. All direct space bonding analysis (AIM, ELF) was performed with TOPOND[90–92] that is implemented in CRYSTAL14.

■ RESULTS AND DISCUSSION

Crystal Structure of {[Ni(tren)]$_2$[Sn_2S_6]}$_n$. The compound {[Ni(tren)]$_2$[Sn_2S_6]}$_n$ (**1**) crystallizes in the monoclinic space group $C2/c$ ($Z = 4$). The unique Ni^{2+} ion is surrounded by four N atoms of tren and two S^{2-} anions of the $[Sn_2S_6]^{4-}$ anion in a distorted octahedral environment. Two symmetry-related NiN_4S_2 octahedra share a common edge to form a $Ni_2N_8S_2$ bioctahedron. Such bioctahedron is found in {[Ni(μ-SH)(cyclam)]$_2$}[SH]$_2$[93] or {[NiS(Me$_3$TPA)]$_2$}[ClO_4]$_2$·2CH$_2$Cl$_2$[94] (Me$_3$TPA = tris[(6-methylpyridin-2-yl)methyl]amine), with Ni–S bond lengths ranging from 2.328(9) to 2.470(2) Å.[93–96] In contrast, the Ni–S bonds in **1** are 2.434(2) and 2.745(2) Å with the former bond being in the normal range, while the latter is exceptionally elongated. Neighbored bioctahedra are interlinked by $[Sn_2S_6]^{4-}$ to form a neutral zigzag chain directed along the *c* axis (Figure 1).

The chains are arranged in parallel along the *a* as well as the *b* axis (Figure S10 and S11, see Supporting Information). The terminal S and the bridging S atoms are involved in hydrogen-bonding interactions within the chain and with adjacent chains (S···H: 2.568–2.838 Å, angles: 142.71–163.53°), stabilizing the zigzag mode and leading to the formation of a three-dimensional network.

Electronic Structure and Bonding in {[Ni(tren)]$_2$[Sn_2S_6]}$_n$ (1). Bonding in the title compound **1** was analyzed from structure optimizations as well as from electronic band structures, AIM, and ELF. From all crystal structure relaxations with different functionals asymmetric Ni–S–Ni bonding is obtained. In close relation to experimental data one shorter Ni–S distance of 2.46 Å and a longer of 2.77 Å is predicted from GGA calculations, as well as different Ni–N distances (see Table S7 in the supplement for all data). For comparison equal Ni–N and Ni–S distances were found from calculations on single $[Ni(NH_3)_4(SH)_2]$ and condensed $[Ni_2(NH_3)_8(SH)_4]$ model clusters. The observed distortion in **1** is thus related to the ligand and the crystal structure. The electronic structure calculations confirm Ni^{2+} with $3d^8$ configuration. Consequently, two electrons per Ni^{2+} ion are located in e_g-like states. According to the calculations on the model compounds an anti-ferromagnetic coupling of the spins of neighboring Ni^{2+} ions is preferred compared to parallel spin orientation. The calculated band gap is 1.9 eV (GGA).

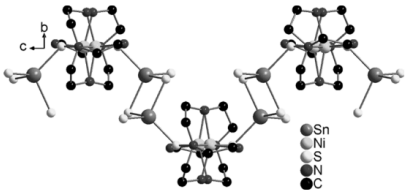

Figure 1. Zigzag chain in the structure of 1 with view along [110]. H atoms are not displayed.

Bonding in direct space is described by the topology of the charge density according to the AIM theory in Figure S12 (see Supporting Information). Thus, Ni and N as well as Ni and S atoms are interlinked by bond paths. The saddle points along the paths signal are the bond critical points (BCP) that are the necessary condition for interactions of neighboring atoms within AIM.[77,78] Whereas bond paths are found for the shorter and the longer Ni–S bonds, the latter can be classified weaker. Calculated values for the total charge density at this BCP (0.029 e/au^3) and for the ELF (0.20) are lower than for the BCP of the shorter Ni–S bond (ρ = 0.055 e/au^3 and ELF = 0.26). The related asymmetry of the Ni–S–Ni interactions is graphically represented by plots of the electronic charge density and ELF in Figure 2. The ELF sketch indicates ionic Ni–N and Ni–S bonding that is typical for TM clusters.[97] The observation made in the spin density suggests a possible relation of magnetism and asymmetry of the present bonding situation. It might deviate from a simple anti-ferromagnetic state found for the double-cluster model. The H bonds around S atoms are visualized in Figure S13 of the Supporting Information.

Usage of {[Ni(tren)]$_2$[Sn_2S_6]}$_n$ (1) as Educt for Preparation of New Thiostannates at Room Temperature. Using **1** as source the formation of $[Ni(amine2)_3]^{2+}$ complexes should depend on the excess of amine2 and/or on the complex stability constant compared to that of the tren complex. Therefore, {[Ni(tren)]$_2$[Sn_2S_6]}$_n$ (**1**) was reacted at room temperature for 1 h with methylamine, en, 1,2-dach, 1,2-dap, or 1,3-dap (Supporting Information, Table S3). The X-ray powder patterns of the reaction products (Supporting Information, Figure S2–S4) and data of the chemical analyses indicated that two recently reported compounds ($[Ni(en)_3]_2[Sn_2S_6]$[17] and $[Ni(1,2\text{-dach})_3]_2[Sn_2S_6]\cdot 4H_2O$[18]), as well as two new compounds, were formed (Figure 3) The poor quality of the crystallites of the two new compounds prevented crystal

DOI: 10.1021/acs.inorgchem.6b00625
Inorg. Chem. 2016, 55, 7859–7865

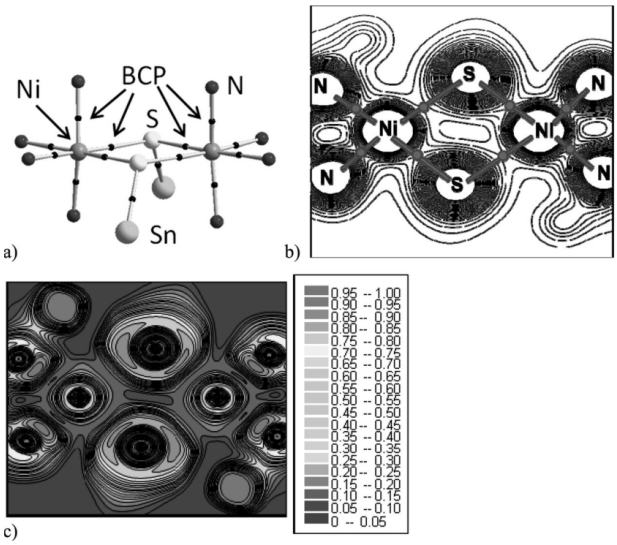

Figure 2. Results of direct space bonding analysis of the double cluster unit of **1** interlinked by S atoms (C and H atoms are not shown) with bond paths and bond critical points (a, black dots), electronic charge density map (b), and ELF (c).

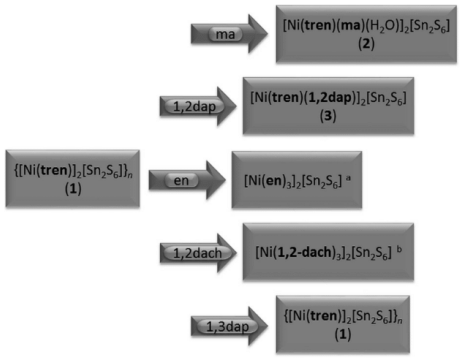

Figure 3. Overview of the results obtained at room temperature (blue arrows) applying compound **1** as starting material with different solvents under stirring conditions. Crystal water was omitted in the formulas for clarity.[17,18]

structure determinations. Hence, the reaction conditions were optimized resulting in crystals suitable for crystal structure analysis (see Experimental Section, Syntheses). During the reaction of **1** with ma a Ni−S bond breakage occurred, and ma, tren, and H_2O coordinate to Ni^{2+} generating the desired octahedral environment. Another mixed complex, $[Ni(tren)(1,2\text{-dap})]^{2+}$, was formed using 1,2-dap (compound **3**), while a full amine ligand exchange and Ni−S bond breakage occurred with en and 1,2-dach (Figure 3). Only for 1,3-dap no transformation of the starting material was observed, even if the reaction time was extended to 10 h.

The results demonstrate that even at room temperature the Ni−S bond is broken and that amine ligands bind to the free coordination sites of Ni^{2+}. The yields of the reactions were ~70% based on the amount of **1** used in the experiments, which is twice as much as those reported for $[Ni(en)_3]_2[Sn_2S_6]$ (~40%)[17] and $[Ni(1,2\text{-dach})_3]_2[Sn_2S_6]\cdot 4H_2O$ (~30%).[18]

Use of $\{[Ni(tren)]_2[Sn_2S_6]\}_n$ (1) as Educt for Preparation of New Thiostannates under Solvothermal Conditions with Stirring. In a second set of experiments the reactivity of $\{[Ni(tren)]_2[Sn_2S_6]\}_n$ (**1**) toward the amines was investigated under solvothermal conditions (Supporting Information, Table S4). Using en, 1,2-dach, 1,2-dap, and 1,3-dap the compounds $[Ni(en)_3]_2[Sn_2S_6]$,[17] $[Ni(1,2\text{-dach})_3]_2[Sn_2S_6]\cdot 4H_2O$,[18] and **3** were obtained at room temperature (Figure 4). But reactions with ma did not directly afford formation of **2** at T = 120 °C, and even after 10 h green crystals of **1** were observed. To verify that compound **1** is still present, some samples were quenched and examined via XRPD (Supporting Information, Figure S5). Only after the slurry was cooled to room temperature compound **1** was slowly converted, and purple crystals of **2** appeared (Supporting Information, Figure S5). The results demonstrate that the reactivity of **1** at T = 120 °C is not significantly different than that at room temperature.

Crystal Structures of Compounds 2 and 3. The compounds $[Ni(tren)(ma)(H_2O)]_2[Sn_2S_6]\cdot 4H_2O$ (**2**) and $[Ni(tren)(1,2\text{-dap})]_2[Sn_2S_6]\cdot 2H_2O$ (**3**) crystallize in the monoclinic space group $P2_1/n$ (Z = 2) (Table S1, Supporting Information). Both structures feature the $[Sn_2S_6]^{4-}$ anion and charge compensating Ni^{2+} centered complexes. The Ni^{2+} cations are surrounded by one tetradentate tren molecule leaving two binding sites free on Ni^{2+} that can act in the following fashion: In compound **2** the vacant coordination sites at Ni^{2+} are saturated by monodentate ligands (ma and H_2O; Figure S15, see Supporting Information), while in compound **3** the octahedron around Ni^{2+} is completed by the bidentate ligand 1,2-dap (Figure S16, see Supporting Information). Comparing the geometric parameters of the $[Sn_2S_6]^{4-}$ anion of the title compounds with that of $Na_4Sn_2S_6\cdot 14H_2O$,[98,99] the Sn−

DOI: 10.1021/acs.inorgchem.6b00625
Inorg. Chem. 2016, 55, 7859−7865

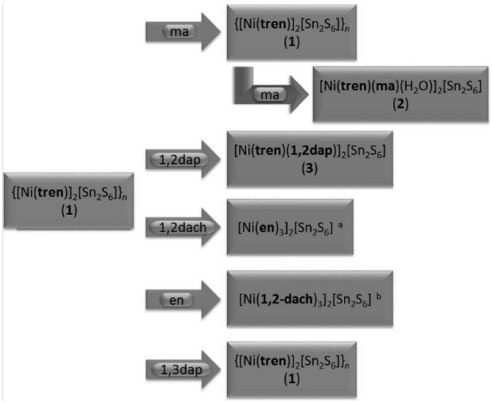

Figure 4. Overview of the results obtained under solvothermal conditions with stirring using compound **1** as starting material. Red arrows: Syntheses at 120 °C, blue arrow: cooling the reaction mixture to room temperature. Crystal water in the formulas was omitted for clarity.[17,18]

S bond lengths do not significantly differ (Table S9, see Supporting Information).[17,18,37,62,68,98−101] Compared to the salt-like compound[98,99] slight differences of the S−Sn−S angles are observed in **1**−**3**. This observation demonstrates that both direct bonds (**1**) as well as secondary interactions (**2**−**3**) influence the orientation of the angles, but the data are within the range recently published on the basis of a statistical analysis.[68] The Ni−N bond lengths (2.089(2)−2.138(2) Å) are typical for Ni^{2+} complexes containing the amine ligands used here.[17,18,37,62,101] Interestingly, these bonds do not significantly differ, either in terms of being in trans position to the Ni−S bonds (**1**) or being in trans position to N atoms of amines (**2**−**3**, Supporting Information Table S9). The angles around the Ni^{2+} ions scatter between 80.98(5) and 177.48(8)° indicating a severe distortion of the octahedra but comparable to data reported in literature (Table S10, see Supporting Information).[18] The structure of $[Ni(tren)(ma)(H_2O)]_2[Sn_2S_6]\cdot 4H_2O$ (**2**) features two unique $[Ni(tren)(ma)(H_2O)]^{2+}$ complexes, which are connected through S···H bonds to the $[Sn_2S_6]^{4-}$ units (Figure 5).

The two unique terminal S atoms are involved in N−H···S (2.624−2.824 Å, angles: 152.62−156.87°) and O−H···S (2.458−2.524 Å, angles: 167.00−169.25°) bonding interactions. The intermolecular H bonding generates a triple unit, which is arranged repetitively in all three crystallographic directions. The empty spaces host the water molecules, which

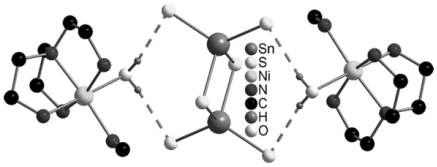

Figure 5. Part of the structure of **2** with hydrogen-bonding interactions between adjacent molecules (purple dashed lines); only selected hydrogen atoms are shown.

form tetramers via O−H···O bonds (O···H: 1.954−2.029 Å, angles: 164.68−167.16°) and are connected further to neighbored $[Sn_2S_6]^{4-}$ units by hydrogen bridges via the terminal S atoms (O−H···S: 2.365−2.518 Å, angles: 165.87−174.24°; Figure S17, see Supporting Information). All S atoms of the $[Sn_2S_6]^{4-}$ anions are involved in hydrogen-bonding interactions, and each $[Sn_2S_6]^{4-}$ interacts with six neighbored $[Ni(tren)(ma)(H_2O)]^{2+}$ complexes and two water molecules (Figure S18; see Supporting Information) forming a three-dimensional network.

In the structure of **3**, $[Ni(tren)(1,2\text{-dap})]_2[Sn_2S_6]\cdot 2H_2O$, the cations and anions are separately arranged in rods along [100]. The cations are oriented alternating with the 1,2-dap ligands pointing up and down, whereas the $[Sn_2S_6]^{4-}$ units alternate with the water molecules (Figure 6). Each $[Sn_2S_6]^{4-}$ unit is

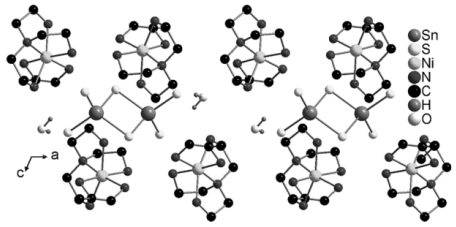

Figure 6. Arrangement of the molecules in **3** within the *ac* plane; hydrogen atoms of the amines are omitted for clarity.

involved in eight S···H bonds to cations (H···S: 2.552−3.028 Å; angles: 139.20−175.80°) and two water molecules (H···S: 2.348−2.665 Å; angles: 157.72−170.99°) generating a three-dimensional network (Figure S19, see Supporting Information).

Ultraviolet−Visible Spectroscopy. The optical band gaps for compounds **1**−**3** were determined from UV/vis diffuse reflectance spectra applying the Kubelka−Munk relation. The optical band gap of compound **1** is lower compared to compounds **2** and **3** (Table 1). This can be explained by the theory whereupon the band gap depends on the dimensionality of the structure of the respective compound. An increasing orbital overlap and reduction of the distances of the bands with decreasing dimensionality lead to a widening of the band gap of the compound. For instance, the compounds $Cs_2Hg_3Se_4$ (one-dimensional) and $Cs_2Hg_6Se_7$ (three-dimensional) exhibit the band gaps 1.61 and 1.17 eV. As with the compounds presented here, the compounds with the lower dimensionality (**2** and **3**, zero-dimensional) feature the major band gap. (Table 1).[102] Below the band edge two additional absorptions, observed in all spectra, are assigned to the Ni^{2+} d−d transitions $^3A_{2g}\rightarrow{}^3T_{2g}$ and $^3A_{2g}\rightarrow{}^3T_{1g}(^3F)$.[103−105] Comparing the values for these transitions with those reported for $[Ni(tren)(H_2O)Cl)]Cl$ (prepared by literature procedure),[106] the values for compound **1** are slightly shifted to smaller and for compounds **2**−**3** to larger values. These observations suggest that the additional amine ligands in **2** and **3** cause an increase in the ligand field splitting, whereas Ni−S bonds the $[Sn_2S_6]^{4-}$ has the opposite effect.

■ CONCLUSIONS

A new synthetic approach was developed allowing fast preparation of new thiostannates at room temperature. The

DOI: 10.1021/acs.inorgchem.6b00625
Inorg. Chem. 2016, 55, 7859−7865

approach bases on the weaker Ni−S bond compared to a Ni−N bond. Using an excess of amine molecules forces the reaction and after bond breakage the octahedral environment of Ni^{2+} cations is completed by bond formation to N donor atoms of the amine molecules. The observation that no new compound is formed if 1,3-dap is used indicates that the complex stability of the finally formed Ni^{2+} complex plays also a role. The results obtained during the experiments open new opportunities for the preparation of thiostannate compounds.

■ ASSOCIATED CONTENT

Supporting Information

The Supporting Information is available free of charge on the ACS Publications website at DOI: 10.1021/acs.inorgchem.6b00625. For the ab initio calculations, N, C, and H electron basis sets were taken from the online resource www.crystal.unito.it. Structural data were deposited in the Cambridge Crystallographic Data Centre as publication Nos. CCDC 1420440 (**1**), 1420437 (**2**) and 1420438 (**3**). Copies of the data can be obtained, free of charge, on application to CCDC, 12 Union Road, Cambridge CB2 1 EZ, U.K. (E-mail: deposit@ccdc.ca.ac.uk).

Experimental PXRD pattern of compounds **1**−**3** with their corresponding simulated single-crystal X-ray data, overview of the reaction conditions and resulting products at room temperature and solvothermal conditions with additional PXRD pattern, IR, Raman, and UV−vis spectra of compounds **1**−**3**, calculated atomic distances (*d*, Å), charge density plot, atomic site projected density of states of the electronic band structure from the spin polarized PBE-calculation, additional tables with selected bond length and angles of compounds **1**−**3**, additional figures. (PDF)

X-ray crystallographic information. (CIF)

X-ray crystallographic information. (CIF)

X-ray crystallographic information. (CIF)

■ AUTHOR INFORMATION

Corresponding Author

*E-mail: wbensch@ac.uni-kiel.de. Phone: +49 431 880-2419. Fax: +49 431 880-1520.

Notes

The authors declare no competing financial interest.

■ ACKNOWLEDGMENTS

We acknowledge gratefully the State of Schleswig-Holstein for the financial support and M.-E. Ordolff for the initial work on compound **1**.

■ REFERENCES

(1) Sarma, D.; Malliakas, C. D.; Subrahmanyam, K. S.; Islam, S. M.; Kanatzidis, M. *Chem. Sci.* **2016**, *7*, 1121−1132.

(2) Zheng, N.; Bu, X.; Vu, H.; Feng, P. *Angew. Chem., Int. Ed.* **2005**, *44*, 5299−5303.

(3) Rabenau, A. *Angew. Chem.* **1985**, *97*, 1017−1032.

(4) Sheldrick, W. S.; Wachhold, M. *Angew. Chem.* **1997**, *109*, 214−234.

(5) Sheldrick, W. S.; Wachhold, M. *Coord. Chem. Rev.* **1998**, *176*, 211−322.

(6) Dehnen, S.; Melullis, M. *Coord. Chem. Rev.* **2007**, *251*, 1259−1280.

(7) Demazeau, G. *J. Mater. Sci.* **2008**, *43*, 2104−2114.

(8) Sheldrick, W. S. *J. Chem. Soc., Dalton Trans.* **2000**, 3041−3052.

(9) Bu, X.; Zheng, N.; Feng, P. *Chem. - Eur. J.* **2004**, *10*, 3356−3362.

(10) Seidlhofer, B.; Pienack, N.; Bensch, W. *Z. Naturforsch., B: J. Chem. Sci.* **2010**, *65*, 937−975.

(11) Xiong, W.-W.; Zhang, G.; Zhang, Q. *Inorg. Chem. Front.* **2014**, *1*, 292−301.

(12) Santner, S.; Heine, J.; Dehnen, S. *Angew. Chem., Int. Ed.* **2016**, *55*, 876−893.

(13) Pienack, N.; Näther, C.; Bensch, W. *Z. Naturforsch., B: J. Chem. Sci.* **2008**, *63b*, 1243−1251.

(14) Wang, Z.; Xu, G.; Bi, Y.; Wang, C. *CrystEngComm* **2010**, *12*, 3703−3707.

(15) Zhou, J.; Bian, G.-Q.; Dai, J.; Zhang, Y.; Tang, A.-B.; Zhu, Q.-Y. *Inorg. Chem.* **2007**, *46*, 1541−1543.

(16) Pienack, N.; Näther, C.; Bensch, W. *Eur. J. Inorg. Chem.* **2009**, *2009*, 1575−1577.

(17) Behrens, M.; Scherb, S.; Näther, C.; Bensch, W. *Z. Anorg. Allg. Chem.* **2003**, *629*, 1367−1373.

(18) Pienack, N.; Lühmann, H.; Seidlhofer, B.; Ammermann, J.; Zeisler, C.; Danker, F.; Näther, C.; Bensch, W. *Solid State Sci.* **2014**, *33*, 67−72.

(19) Hilbert, J.; Näther, C.; Bensch, W. *Inorg. Chem.* **2014**, *53*, 5619−5630.

(20) Liu, G.-N.; Guo, G.-C.; Chen, F.; Guo, S.-P.; Jiang, X.-M.; Yang, C.; Wang, M.-S.; Wu, M.-F.; Huang, J.-S. *CrystEngComm* **2010**, *12*, 4035−4037.

(21) Bensch, W.; Schur, M. *Eur. J. Solid State Inorg. Chem.* **1996**, *33*, 1149−1160.

(22) Bensch, W.; Schur, M. *Z. Naturforsch., B: J. Chem. Sci.* **1997**, *52*, 405−409.

(23) Schur, M.; Näther, C.; Bensch, W. *Z. Naturforsch., B: J. Chem. Sci.* **2001**, *56*, 79−84.

(24) Puls, A.; Näther, C.; Bensch, W. *Z. Anorg. Allg. Chem.* **2006**, *632*, 1239−1243.

(25) Rejai, Z.; Lühmann, H.; Näther, C.; Kremer, R. K.; Bensch, W. *Inorg. Chem.* **2010**, *49*, 1651−1657.

(26) Näther, C.; Herzberg, N.; Bensch, W. *Z. Naturforsch., B: J. Chem. Sci.* **2013**, *68*, 605−610.

(27) Schur, M.; Bensch, W. *Z. Naturforsch., B: J. Chem. Sci.* **2002**, *57*, 1−7.

(28) Schaefer, M.; Näther, C.; Bensch, W. *Solid State Sci.* **2003**, *5*, 1135−1139.

(29) Engelke, L.; Stähler, R.; Schur, M.; Näther, C.; Bensch, W.; Pöttgen, R.; Möller, M. H. *Z. Naturforsch., B: J. Chem. Sci.* **2004**, *59b*, 869−876.

(30) Schaefer, M.; Kurowski, D.; Pfitzner, A.; Näther, C.; Rejai, Z.; Möller, K.; Ziegler, N.; Bensch, W. *Inorg. Chem.* **2006**, *45*, 3726−3731.

(31) Pienack, N.; Möller, K.; Näther, C.; Bensch, W. *Solid State Sci.* **2007**, *9*, 1110−1114.

(32) Seidlhofer, B.; Spetzler, V.; Näther, C.; Bensch, W. *J. Solid State Chem.* **2012**, *187*, 269−275.

(33) Pienack, N.; Lehmann, S.; Lühmann, H.; El-Madani, M.; Näther, C.; Bensch, W. *Z. Anorg. Allg. Chem.* **2008**, *634*, 2323−2329.

(34) Zeisler, C.; Näther, C.; Bensch, W. *CrystEngComm* **2013**, *15*, 8874−8876.

(35) Hilbert, J.; Näther, C.; Bensch, W. *Z. Anorg. Allg. Chem.* **2014**, *640*, 2858−2863.

(36) Hilbert, J.; Näther, C.; Bensch, W. *Dalton Trans.* **2015**, *44*, 11542−11550.

(37) Jia, D.-X.; Dai, J.; Zhu, Q.-Y.; Zhang, Y.; Gu, X.-M. *Polyhedron* **2004**, *23*, 937−942.

(38) Carlson, G. A.; McReynolds, J. P.; Verhoek, F. H. *J. Am. Chem. Soc.* **1945**, *67*, 1334−1339.

(39) Irving, H.; Williams, R. J. *J. Chem. Soc.* **1953**, 3192−3210.

(40) Schwarzenbach, G.; Baur, R. *Helv. Chim. Acta* **1956**, *39*, 722−728.

(41) Reilley, C. N.; Holloway, J. H. *J. Am. Chem. Soc.* **1958**, *80*, 2917−2919.

(42) Irving, H.; Mellor, J. *J. Chem. Soc.* **1962**, *0*, 5222−5237.

DOI: 10.1021/acs.inorgchem.6b00625
Inorg. Chem. 2016, 55, 7859−7865

(43) Evers, A.; Hancock, R. D. *Inorg. Chim. Acta* **1989**, *160*, 245−248.
(44) Cotton, F. A.; Harris, F. E. *J. Phys. Chem.* **1955**, *59*, 1203−1208.
(45) Schur, M.; Bensch, W. *Acta Crystallogr., Sect. C: Cryst. Struct. Commun.* **2000**, *56*, 1107−1108.
(46) Kiebach, R.; Studt, F.; Näther, C.; Bensch, W. *Eur. J. Inorg. Chem.* **2004**, *2004*, 2553−2556.
(47) Yue, C.-Y.; Lei, X.-W.; Ma, Y.-X.; Sheng, N.; Yang, Y.-D.; Liu, G.-D.; Zhai, X.-R. *Cryst. Growth Des.* **2014**, *14*, 101−109.
(48) Powell, A. V.; Lees, R. J.; Chippindale, A. M. *Inorg. Chem.* **2006**, *45*, 4261−4267.
(49) Seidlhofer, B.; Djamil, J.; Näther, C.; Bensch, W. *Cryst. Growth Des.* **2011**, *11*, 5554−5560.
(50) Lees, R. J.; Powell, A. V.; Chippindale, A. M. *J. Phys. Chem. Solids* **2007**, *68*, 1215−1219.
(51) Zhou, J.; Bian, G.-Q.; Zhang, Y.; Dai, J.; Cheng, N. *Z. Anorg. Allg. Chem.* **2007**, *633*, 2701−2705.
(52) Stähler, R.; Bensch, W. *Acta Crystallogr., Sect. C: Cryst. Struct. Commun.* **2002**, *58*, m537−m538.
(53) Stähler, R.; Näther, C.; Bensch, W. *J. Solid State Chem.* **2003**, *174*, 264−275.
(54) Seidlhofer, B.; Näther, C.; Bensch, W. *CrystEngComm* **2012**, *14*, 5441−5445.
(55) Anderer, C.; Delwa de Alarcón, N.; Näther, C.; Bensch, W. *Chem. - Eur. J.* **2014**, *20*, 16953−16959.
(56) Mu, W.-Q.; Zhu, Q.-Y.; You, L.-S.; Zhang, X.; Luo, W.; Bian, G.-Q.; Dai, J. *Inorg. Chem.* **2012**, *51*, 1330−1335.
(57) Engelke, L.; Näther, C.; Leisner, P.; Bensch, W. *Z. Anorg. Allg. Chem.* **2008**, *634*, 2959−2965.
(58) Lichte, J.; Lühmann, H.; Näther, C.; Bensch, W. *Z. Anorg. Allg. Chem.* **2009**, *635*, 2021−2026.
(59) Lühmann, H.; Näther, C.; Bensch, W. *Z. Anorg. Allg. Chem.* **2011**, *637*, 1007−1012.
(60) Lühmann, H.; Rejai, Z.; Möller, K.; Leisner, P.; Ordolff, M.-E.; Näther, C.; Bensch, W. *Z. Anorg. Allg. Chem.* **2008**, *634*, 1687−1695.
(61) Zhao, Q.; Jia, D.; Zhang, Y.; Song, L.; Dai, J. *Inorg. Chim. Acta* **2007**, *360*, 1895−1901.
(62) Jia, D.-X.; Zhang, Y.; Dai, J.; Zhu, Q.-Y.; Gu, X.-M. *Z. Anorg. Allg. Chem.* **2004**, *630*, 313−318.
(63) Gu, X.-M.; Dai, J.; Jia, D.-X.; Zhang, Y.; Zhu, Q.-Y. *Cryst. Growth Des.* **2005**, *5*, 1845−1848.
(64) Li, J.; Marler, B.; Kessler, H.; Soulard, M.; Kallus, S. *Inorg. Chem.* **1997**, *36*, 4697−4701.
(65) Jia, D.-X.; Zhu, A.-M.; Deng, J.; Suzhou, Y. Z. *Z. Anorg. Allg. Chem.* **2007**, *633*, 1246−1250.
(66) Ko, Y.; Tan, K.; Nellis, D. M.; Koch, S.; Parise, J. B. *J. Solid State Chem.* **1995**, *114*, 506−511.
(67) Nørby, P.; Overgaard, J.; Christensen, P. S.; Richter, B.; Song, X.; Dong, M.; Han, A.; Skibsted, J.; Iversen, B. B.; Johnsen, S. *Chem. Mater.* **2014**, *26*, 4494−4504.
(68) Nørby, P.; Eikeland, E.; Overgaard, J.; Johnsen, S.; Iversen, B. B. *CrystEngComm* **2015**, *17*, 2413−2420.
(69) HassanzadehFard, Z.; Müller, C.; Harmening, T.; Pöttgen, R.; Dehnen, S. *Angew. Chem.* **2009**, *121*, 4507−4511.
(70) Nayek, H. P.; Massa, W.; Dehnen, S. *Inorg. Chem.* **2008**, *47*, 9146−9148.
(71) Jiang, T.; Lough, A.; Ozin, G. A. *Adv. Mater.* **1998**, *10*, 42−46.
(72) Yaghi, O. M.; Sun, Z.; Richardson, D. A.; Groy, T. L. *J. Am. Chem. Soc.* **1994**, *116*, 807−808.
(73) Wang, M.-S.; Chen, W.-T.; Cai, L.-Z.; Zhou, G.-W.; Guo, G.-C.; Huang, J.-S. *J. Cluster Sci.* **2003**, *14*, 495−504.
(74) Liu, X.; Zhou, J.; He, J.; Huang, Z.-W. *Z. Naturforsch., B: J. Chem. Sci.* **2011**, *66*, 659−663.
(75) Sun, X.-L.; Zhu, Q.-Y.; Mu, W.-Q.; Qian, L.-W.; Yu, L.; Wu, J.; Bian, G.-Q.; Dai, J. *Dalton Trans.* **2014**, *43*, 12582−12589.
(76) Nie, L.; Zhang, Y.; Ye, K.; Han, J.; Wang, Y.; Rakesh, G.; Li, Y.; Xu, R.; Yan, Q.; Zhang, Q. *J. Mater. Chem. A* **2015**, *3*, 19410−19416.
(77) Bader, R. F. W. *Atoms in molecules: A quantum theory*, The International Series of Monographs on Chemistry; Clarendon Press: Oxford, U.K., 1990; Vol. *22*.
(78) Bader, R. F. W. *J. Phys. Chem. A* **1998**, *102*, 7314−7323.
(79) Becke, A. D.; Edgecombe, K. E. *J. Chem. Phys.* **1990**, *92*, 5397−5403.
(80) Savin, A.; Becke, A. D.; Flad, J.; Nesper, R.; Preuss, H.; von Schnering, H. G. *Angew. Chem., Int. Ed. Engl.* **1991**, *30*, 409−412.
(81) Sheldrick, G. M. *SHELXS-97: Program for the Solution of Crystal Structures*; University of Göttingen: Germany, 1997.
(82) Sheldrick, G. M. *SHELXL-97: Program for the Refinement of Crystal Structures*; University of Göttingen: Germany, 1997.
(83) Sheldrick, G. M. *SHELXL-2014: Program for the Refinement of Crystal Structures*; University of Göttingen: Germany, 2014.
(84) Dovesi, R.; Roetti, C.; Orlando, R.; Zicovich-Wilson, C. M.; Pascale, F.; Civalleri, B.; Doll, K.; Harrison, N. M.; Bush, I. J.; D'Arco, P.; Llunell, M.; Causà, M.; Noël, Y. *CRYSTALL14*: University of Torino: Italy, 2014.
(85) Dovesi, R.; Orlando, R.; Erba, A.; Zicovich-Wilson, C. M.; Civalleri, B.; Casassa, S.; Maschio, L.; Ferrabone, M.; De La Pierre, M.; D'Arco, P.; Noël, Y.; Causà, M.; Rérat, M.; Kirtman, B. *Int. J. Quantum Chem.* **2014**, *114*, 1287−1317.
(86) Weihrich, R.; Anusca, I.; Zabel, M. *Z. Anorg. Allg. Chem.* **2005**, *631*, 1463−1470.
(87) Rothballer, J.; Bachhuber, F.; Pielnhofer, F.; Schappacher, F. M.; Pöttgen, R.; Weihrich, R. *Eur. J. Inorg. Chem.* **2013**, *2013*, 248−255.
(88) Rothballer, J.; Bachhuber, F.; Rommel, S. M.; Söhnel, T.; Weihrich, R. *RSC Adv.* **2014**, *4*, 42183−42189.
(89) Rommel, S. M.; Weihrich, R. *Chem. - Eur. J.* **2015**, *21*, 9863−9867.
(90) Gatti, C.; Saunders, V. R.; Roetti, C. *J. Chem. Phys.* **1994**, *101*, 10686−10696.
(91) Gatti, C. *Z. Kristallogr. - Cryst. Mater.* **2005**, *220*, 339−457.
(92) Gatti, C.; Casassa, S. *TOPOND User's Manual*; CNR-ISTM of Milano: Italy, 2014.
(93) Pleus, R. J.; Waden, H.; Saak, W.; Haase, D.; Pohl, S. *J. Chem. Soc., Dalton Trans.* **1999**, 2601−2610.
(94) Inosako, M.; Kunishita, A.; Kubo, M.; Ogura, T.; Sugimoto, H.; Itoh, S. *Dalton Trans.* **2009**, 9410−9417.
(95) Higgs, T. C.; Ji, D.; Czernuszewicz, R. S.; Spartalian, K.; O'Connor, C. J.; Seip, C.; Carrano, C. J. *J. Chem. Soc., Dalton Trans.* **1999**, 807−814.
(96) Brines, L. M.; Shearer, J.; Fender, J. K.; Schweitzer, D.; Shoner, S. C.; Barnhart, D.; Kaminsky, W.; Lovell, S.; Kovacs, J. A. *Inorg. Chem.* **2007**, *46*, 9267−9277.
(97) Kohout, M.; Wagner, F. R.; Grin, Y. *Theor. Chem. Acc.* **2002**, *108*, 150−156.
(98) Krebs, B.; Pohl, S.; Schiwy, W. *Angew. Chem., Int. Ed. Engl.* **1970**, *9*, 897−898.
(99) Krebs, B.; Pohl, S.; Schiwy, W. *Z. Anorg. Allg. Chem.* **1972**, *393*, 241−252.
(100) Fu, M.-L.; Guo, G.-C.; Liu, B.; Wu, A.-Q.; Huang, J.-S.; et al. *Eur. J. Inorg. Chem.* **2005**, *2005*, 3104−3108.
(101) Zhou, J.; Liu, X.; Chen, G.-Q.; Zhang, F.; Li, L.-R. *Z. Naturforsch., B: J. Chem. Sci.* **2010**, *65*, 1229−1234.
(102) Axtell, E. A.; Park, Y.; Chondroudis, K.; Kanatzidis, M. G. *J. Am. Chem. Soc.* **1998**, *120*, 124−136.
(103) Holleman, A. F.; Wiberg, E.; Wiberg, N. *Lehrbuch der anorganischen Chemie*, 102nd ed.; de Gruyter: Berlin, Germany, 2007.
(104) Riedel, E. *Anorganische Chemie*, 4th ed.; de Gruyter: Berlin, Germany, 1999.
(105) Roe, S. P.; Hill, J. O.; Magee, R. J. *Monatsh. Chem.* **1991**, *122*, 467−478.
(106) Marzotto, A.; Clemente, D. A.; Valle, G. *Acta Crystallogr., Sect. C: Cryst. Struct. Commun.* **1993**, *49*, 1252−1255.
(107) González, E.; Rodrigue-Witchel, A.; Reber, C. *Coord. Chem. Rev.* **2007**, *251*, 351−363.

DOI: 10.1021/acs.inorgchem.6b00625
Inorg. Chem. 2016, 55, 7859−7865

3.2.2 Reaktion von $\{[Ni(tren)]_2[Sn_2S_6]\}_n$ mit tren und 2amp bei RT zu zwei weiteren Thiostannaten: Untersuchung der temperaturabhängigen Stabilität des Precursors und der Verbindungen $[Ni(tren)_2]_2[Sn_2S_6]\cdot 8H_2O$ und $[Ni(tren)(2amp)]_2[Sn_2S_6]$. *(submitted 03.11.16)*

Zusammenfassung der Publikation „Studies of the Reactivity of $\{[Ni(tren)]_2[Sn_2S_6]\}_n$: Synthesis and Crystal Structure of two New Thiostannates Prepared at Room Temperature“

Die Verbindungen $[Ni(tren)_2]_2[Sn_2S_6]\cdot 8H_2O$ ($P\bar{1}$, Z=1) und $[Ni(tren)(2amp)]_2[Sn_2S_6]$ ($P4_2/n$, Z=8) wurden analog zu den in Abschnitt 3.2.1 beschriebenen Synthesen durch Reaktion des Precursors $\{[Ni(tren)]_2[Sn_2S_6]\}_n$ bei RT in wässriger tren- bzw. 2amp-Lösungen erhalten.

In den Verbindungen $[Ni(tren)_2]_2[Sn_2S_6]\cdot 8H_2O$ und $[Ni(tren)(2amp)]_2[Sn_2S_6]$ liegen diskrete $[Ni(tren)(Amin)]^{2+}$-Kationen (Amin = tren, 2amp) und $[Sn_2S_6]^{4-}$-Anionen vor. Die Anordnung der Ionen wird durch zahlreiche Wasserstoffbrückenbindungen stabilisiert. Bemerkenswert in der Struktur von $[Ni(tren)_2]_2[Sn_2S_6]\cdot 8H_2O$ ist der Bindungsmodus der tren Liganden: Nur jeweils drei der möglichen vier N-Atome sind in Bindungen involviert. Die vierte Aminogruppe ragt in den freien Raum. Die Wassermoleküle bilden ein cyclisches Tetramer, welches durch vier zusätzliche Wassermoleküle an gegenüberliegenden Seiten zu einem Oktamer erweitert wird. Dieser Wassercluster, sowie ein tren Ligand können durch thermischen Abbau entfernt werden, sodass der Precursor erhalten wird.

Weitere Synthesen unter dynamischen Bedingungen zur Bildung der Verbindungen $[Ni(tren)_2]_2[Sn_2S_6]\cdot 8H_2O$ bzw. $[Ni(tren)(2amp)]_2[Sn_2S_6]$ mit dem Precursor in wässrigen tren bzw. 2amp Lösungen haben ergeben, dass die Umwandlung des Precursors zu den Verbindungen $[Ni(tren)_2]_2[Sn_2S_6]\cdot 8H_2O$ und $[Ni(tren)(2amp)]_2[Sn_2S_6]$ temperaturabhängig und reversibel ist: Bei niedrigen Temperaturen liegen $[Ni(tren)_2]_2[Sn_2S_6]\cdot 8H_2O$ bzw. $[Ni(tren)(2amp)]_2[Sn_2S_6]$ vor, beim Aufheizen bildet sich der Precursor, beim erneuten Abkühlen wird wieder $[Ni(tren)_2]_2[Sn_2S_6]\cdot 8H_2O$ bzw. $[Ni(tren)(2amp)]_2[Sn_2S_6]$ gebildet. Der Temperaturbereich, in dem die Verbindungen $[Ni(tren)_2]_2[Sn_2S_6]\cdot 8H_2O$ bzw. $[Ni(tren)(2amp)]_2[Sn_2S_6]$ gebildet werden und in dem diese stabil sind, ist unterschiedlich. Der Temperaturbereich, in dem die Verbindungen gebildet bzw. stabil sind, ist von der Konzentration der Aminlösung abhängig. $[Ni(tren)_2]_2[Sn_2S_6]\cdot 8H_2O$ wird erst ab einer tren Konzentration von 20% erhalten und bei dieser Konzentration kristallisiert die Verbindung in dem Temperaturbereich von RT - 50°C und ist zwischen RT und 70°C nachweisbar. Oberhalb dieser Temperatur findet keine Reaktion statt und der Precursor wird gebildet. Bei einer tren Konzentration von 30% ist die Verbindung sogar bis 85°C stabil, wird aber allerdings nur zwischen RT und 50°C gebildet. Ähnliches gilt für das Gleichgewicht zwischen dem Precursor und $[Ni(tren)(2amp)]_2[Sn_2S_6]$.

Studies of the Reactivity of $\{[Ni(tren)]_2[Sn_2S_6]\}_n$: Synthesis and Crystal Structures of two New Thiostannates Prepared at Room Temperature

Jessica Hilbert, Christian Näther and Wolfgang Bensch*

Institute of Inorganic Chemistry

Christian-Albrechts-University of Kiel

Max-Eyth-Str. 2

24118 Kiel

Germany

* Corresponding author, email: wbensch@ac.uni-kiel.de, phone: +49 431 880-2419, fax: +49 431 880-1520

Abstract

The reactions of $\{[Ni(tren)]_2[Sn_2S_6]\}_n$ (tren = tris(2-aminoethyl)amine, $C_6H_{18}N_4$) at room temperature in aqueous solutions of tren or 2amp (2amp = 2-(aminomethyl)pyridine, $C_6H_8N_2$) lead to crystallization of the new compounds $[Ni(tren)_2]_2[Sn_2S_6]\cdot 8H_2O$ (**1**) and $[Ni(tren)(2amp)]_2[Sn_2S_6]$ (**2**). For the formation of these compounds the two Ni-S bonds in $\{[Ni(tren)]_2[Sn_2S_6]\}_n$ are broken during the chemical reactions and the free coordination sites at Ni^{2+} are occupied by N-donor atoms of the amine molecules. Interestingly, in the structure of **1** the two tren ligands both coordinate tridentate while in the educt $\{[Ni(tren)]_2[Sn_2S_6]\}_n$ tren acts tetradentate. Hence, in this case not only the two Ni-S bonds are broken but also one Ni-N bond. The eight H_2O molecules form an octamer by strong O-H···O hydrogen bonds. In the structure of **2** the two free coordination sites at the Ni^{2+} after Ni-S bond breakage are occupied by the two N atoms of the 2amp ligand. The two compounds can be transferred reversible into the starting compound by heating the reaction slurry. The minimum conversion temperature depends on the amine concentration of the reaction mixture. Investigations of the thermal behavior of compound **1** verify that the water and amine molecules are removed step wise during the heating process leading to the formation of a water free thiostannate, and finally results in the formation of the precursor $\{[Ni(tren)]_2[Sn_2S_6]\}_n$.

Keywords: Tin-Sulfur Compounds, Thiostannate, Room Temperature Synthesis, Crystal Structure, Thermal Investigation

1. Introduction

Thiometallates and especially thiostannate compounds are mainly synthesized by the solvothermal route which was reviewed in several articles.[1–10] Under solvothermal conditions insoluble starting materials like, e.g. Sn or transition metals are at least partially dissolved by reaction with the solvent and/or with additives[1,2,4] or by generation of polysulfide species employing amine molecules as solvent.[3] As discussed in literature [2-11] solvothermal reactions are complex preventing any prediction of the crystalline products. The processes occurring during solvothermal conditions become more complex with increasing number of components applied. For example, the preparation of transition metal (TM) complex containing thiostannates requires the use of four to five ingredients: Sn, S, and TM sources and a ligand which often also acts as the solvent. The reactions could be significantly simplified if suitable water soluble precursors are available enabling the preparation of thiostannates under controlled conditions. Only few solvothermal approaches were reported in literature where for example transition metal (TM) complexes or soluble thiostannates were applied. The compound $[Co(dien)_2]_2[Sn_2S_6]$ [11] (dien = diethylene-triamine) was obtained using $[Co(NH_3)_6]Cl_3$ as reactant and $[Co_2(cyclam)_2Cl_2]Cl$ (cyclam = 1,4,8,11-tetraazacyclotetradecane) was applied for the preparation of $\{[Co(cyclam)]_2[Sn_2S_6]\}_n \cdot 2nH_2O$ [12]. An aqueous solution of $Na_4SnS_4 \cdot 14H_2O$ was used for the preparation of $(H_3O)_2(enH_2)Cu_8Sn_3S_{12}$ [13] (en = ethylenediamine), $(CP)_xM_ySn_2S_6$ [14] (CP = cetylpyridinium; M = Zn, Cd, Ga), was prepared using $Na_4Sn_2S_6 \cdot 14H_2O$ in formamide at 70°C, and $\{[(CMe_2CH_2COMe)Sn]_4S_6\}$ was used to crystallize $\{[(CMe_2CH_2COMe)Sn)_2(S)_2]_3[Sn_2S_6]\}$ [15]. The latter compound was prepared at room temperature, but the synthesis must be carried out in an inert and water free atmosphere. Regarding the synthesis of thiostannates at room temperature, very

long reactions times for the formation of crystalline products were required. For example, $(dda)_4[Sn_2S_6]\cdot 2H_2O$ (dda = dodecylamine) was obtained by using a mixture of $SnCl_4\cdot 5H_2O$, $Na_2S\cdot 9H_2O$ and dda in a H_2O/EtOH solution within 45 d.[16] The two compounds $[CH_3C(NH_2)_2]_8[Sn_2S_6]$ and $[(CH_3)_2NH_2(NH_4)]_n[SnS_3]_n$ were prepared dissolving freshly prepared SnS_2 in $(NH_4)_2S$ and adding acetonitrile or *N,N*-dimethylformamide for precipitation, but crystallization times of several months were necessary.[17] These examples already indicate some problems of room temperature syntheses of thiostannates: lowering the reaction temperature causes a decrease of the reaction rate. One way out of this situation is using more reactive (water) soluble sulfur containing educts: In this case undesired insoluble (by)products like binary sulfides may be formed fast, which do not participate in the product formation at room temperature. Using soluble reactants, the challenge is to reach supersaturation, because otherwise no solid product will be obtained within reasonable reaction times. If the supersaturation is reached too fast, too many nuclei and small crystallites will be formed immediately preventing further crystal growth.[18] Recently, we identified $\{[Ni(tren)]_2[Sn_2S_6]\}_n$[19] as source for the preparation of thiostannates at room temperature delivering crystals suitable for single crystal structure determination within 1 - 2 days. Now we extended the experiments with the new precursor and applied the amines tren and 2amp. Here we report the room temperature syntheses of the new compounds $[Ni(tren)_2]_2[Sn_2S_6]\cdot 8H_2O$ (**1**) and $[Ni(tren)(2amp)]_2[Sn_2S_6]$ (**2**) which were obtained applying $\{[Ni(tren)]_2[Sn_2S_6]\}_n$.

2. Experimental section

2.1 Synthesis

General: Tris-(2-aminoethyl)amine (tren, $C_6H_{18}N_4$, 96%, Aldrich) and 2-(aminomethyl)pyridine (2amp, $C_6H_8N_2$, 99%, ABCR) were purchased and applied

without further purifications. $\{[Ni(tren)]_2[Sn_2S_6]\}_{n[19]}$ were synthesised using literature procedures.

*Synthesis of $[Ni(tren)_2]_2[Sn_2S_6]\cdot 8H_2O$ (**1**):*

209.9 mg (0.25 mmol) $\{[Ni(tren)]_2[Sn_2S_6]\}_n$ were stirred in a glass tube (inner volume 11 mL) with 2 mL 30% tren for ½ hour at 120°C and t hen stored at RT for two days. The product mixture containing small pale purple crystals and few pale pink powder was filtered off, washed with water and ethanol and dried over silica gel (Yield: ~65% based on tin). Elemental analysis, results in %: found: C 22.3, H 6.5, N 17.6, calculated: C 22.6, H 6.9, N 17.6.

*Synthesis of $[Ni(2amp)(tren)]_2[Sn_2S_6]$ (**2**):*

209.9 mg (0.25 mmol) $\{[Ni(tren)]_2[Sn_2S_6]\}_n$ were stirred in a glass tube (inner volume 11 mL) with 2 mL 30% 2amp for ½ hour at 120°C and t hen stored at RT for two days. The product consisting of purple needles and few black powder was filtrated, washed with water and ethanol and dried over silica gel (Yield: ~70% based on tin). Elemental analysis, results in %: found: C 27.3, H 5.1, N 15.9, calculated: C 27.3, H 4.9, N 15.9.

2.2 Structure determination

The intensity data for the compounds were collected using a STOE IPDS-1 (Imaging Plate Diffraction System) with Mo-K_α radiation at 170(2) K. The structures were solved with direct methods using the program SHELXS-97 [20] and the refinements were done against F^2 with SHELXL-2014 [21]. All non-hydrogen atoms were refined anisotropic. For compound **1** the C-H and N-H H atoms of the coordinated amino groups were positioned with idealized geometry and refined isotropic with $U_{iso}(H)$ = 1.2 U_{eq} (C,N) using a riding model. The terminal N-H and water H atoms were first located in difference map, their bond lengths were set to ideal values and finally they were refined isotropic with $U_{iso}(H)$ = 1.5 U_{eq} (N,O) using a riding model refinement.

5

For compound **2** the C-H and N-H H atoms were positioned with idealized geometry and refined isotropic using a riding model. Some atoms of one of the 2amp ligands are disordered in two orientations and were refined using a split model. In this case artificial short C-C distances occur to a neighbored ligand generated by symmetry. If the structure is refined, e.g. in space group $P4_2$, where both of these ligands are located in general positions the disorder remain constant and there are also no hints for super structure reflections.

Selected refinement results are summarized in Table 1. Structural data have been deposited in the Cambridge Crystallographic Data Centre as publication no. CCDC 1512949 (**1**) and CCDC 1512950 (**2**). Copies of the data can be obtained, free of charge, on application to CCDC, 12 Union Road, Cambridge CB2 1 EZ, UK (mail: deposit@ccdc.ca.ac.uk).

Table 1: Selected details of the data collection and structure refinement results.

	$[Ni(tren)_2]_2[Sn_2S_6]\cdot 8H_2O$	$[Ni(tren)(2amp)]_2[Sn_2S_6]$
crystal system	triclinic	tetragonal
space group	$P\bar{1}$	$P4_2/n$
M (g/ mol)	1276.26	1055.93
a (Å)	10.2878(4)	26.1885(3)
b (Å)	11.1100(4)	26.1885(3)
c (Å)	11.4206(4)	11.11220(10)
α (°)	84.740(3)	90
β (°)	84.395(3)	90
γ (°)	79.093(3)	90
V (Å^3)	1272.05(8)	7621.16(19)
temperature (K)	170(2)	170(2)
Z	1	8
$D_{calculated}$ (g/ cm^3)	1.666	1.841
μ (mm^{-1})	2.001	2.634
scan range (deg)	1.797≤ θ ≤27.004	1.555≤ θ ≤26.005
reflections collected	18612	71138
independent reflections	5546	7498
observed reflections	4850	7197
goodness-of-fit on F^2	1.039	1.150
R values (I > 2σ(I))	R1 = 0.0272	R1 = 0.0389
	wR2 = 0.0625	wR2 = 0.0950
R values (all data)	R1 = 0.0339	R1 = 0.0411
	wR2 = 0.0641	wR2 = 0.0964
res. elec. dens. (e/Å^3)	0.655 and -0.549	0.836 and -0.568

6

2.3 Instrumentation

X-ray powder diffractometry

The X-ray powder diffraction patterns were recorded on a STOE Stadi-P powder diffractometer (Cu-$K_{\alpha 1}$ radiation, λ = 1.540598 Å, Ge monochromator) in transmission geometry with a MYTHEN 1K detector (DECTRIS). (Supporting Information, Figure S1)

EDX experiments

Scanning electron microscopy investigations and energy dispersive X-ray analyses (EDX) were done with a Philips Environmental Scanning Electron Microscope ESEM XL30 equipped with an EDAX detector.

Elemental Analysis

CHN analyses were done using a EURO EA Elemental Analyzer, fabricated by EURO VECTOR Instruments and Software.

Infrared spectroscopy

MIR spectra (400-4000 cm^{-1}) were recorded with a Bruker Alpha P spectrometer. (Supporting Information, Figure S2 and Table S1)

Raman spectroscopy

Raman spectra were recorded with a Bruker IFS 66 Fourier transform Raman spectrometer (wavelength: 541.5 nm) in the region from 100 to 3500 cm^{-1}. (Supporting Information, Figure S3 and Table S2)

UV/visible spectroscopy

UV/visible (UV/vis) spectroscopic investigations were carried out at room temperature using an UV/vis/NIR two-channel spectrometer Cary 5 from Varian Techtron Pty., Darmstadt (250-2000 nm). The optical properties of the compounds were investigated by analysing the UV/vis reflectance spectra of the powdered samples (with $BaSO_4$ powder used as reference material). The absorption data were

calculated applying the Kubelka-Munk relation for diffuse reflectance data (Supporting Information, Figure S4 and Table S3).

Thermal properties

DTA-TG measurements were performed using a Netzsch STA 409 CD. All compounds were heated with 4℃/min to 500℃ under a nitrogen flow of 75 mL min^{-1}. The instrument was calibrated using standard reference materials.

3. Results and Discussion

3.1 Considerations concerning syntheses with $\{[Ni(tren)]_2[Sn_2S_6]\}_n$ as precursor

Recently, we discovered that $\{[Ni(tren)]_2[Sn_2S_6]\}_n$ can be used as source for the preparation of new thiostannates in aqueous amine solutions at room temperature and under solvothermal conditions.[19] An important structural feature of this compound is a distorted $Ni_2S_2N_8$ bioctahedron with significantly different Ni-S bond strengths.[19] We demonstrated that an excess of ma or 1,2-dap (ma = methylamine; 1,2-dap = 1,2-diaminopropane) leads to the Ni-S bond breakage followed by the formation of $[Ni(tren)(amine)]^{2+}$ complexes and the crystallization of compounds with the general formula $[Ni(tren)(amine)]_2[Sn_2S_6]\cdot nH_2O$.[19] Using en or 1,2-dach (en = ethylenediamine; 1,2-dach = 1,2-diaminocyclohexane) the tren ligands in the starting material were fully exchanged and $[Ni(amine)_3]^{2+}$ complexes were formed. On the basis of these results we hypothesized that both the complex stability and the sterical demands of the amine molecules determine whether a $[Ni(amine)_3]^{2+}$ or a $[Ni(tren)(amine)]^{2+}$ complex is formed. We now extended the experimental work with this precursor and applied the amines tren and 2amp.

Three different chemical environments were reported for Ni^{2+} centered complexes with tren as ligand: a) $[Ni_2(tren)_2Cl_2]$ [22], b) $[Ni(tren)(H_2O)Cl]Cl$ [23] and c) $[Ni(tren)_2][ClO_4]_2$ [24]. In the precursor compound the coordination of Ni^{2+} is

comparable to that of a) and in the compound $[Ni(tren)(ma)(H_2O)]_2[Sn_2S_6]$ [19] the situation is similar to that of b). But no thiostannate is known with a Ni^{2+} centered complex showing the coordination geometry which was observed in c). Based on our observations presented above, we selected tren to probe whether this type of complex is formed if the Ni-S bond of the starting material is broken and N-donor atoms of the tren ligands occupy the free coordination sites at Ni^{2+}. According to our observations described above this would correspond to formation of a $[Ni(tren)(amine)]^{2+}$ complex with amine = tren.

The bidentate ligand 2amp was chosen due the comparable complex stability ($[Ni(2amp)_3]^{2+}$: log β_3: 18.9 [25]) with that of $[Ni(1,2\text{-dap})_3]^{2+}$ (log β_3: 18.0 [26]) for which formation of a $[Ni(tren)(1,2\text{-dap})]^{2+}$ complex was observed.[19] Due to the lower stability than $[Ni(1,2\text{-dach})_3]^{2+}$ (log β_3: 20.1 [27]) but exhibiting more sterical demands than en thus favoring formation of a $[Ni(tren)(2amp)]^{2+}$ complex rather than $[Ni(2amp)_3]^{2+}$.

3.2 Experiments with $\{[Ni(tren)]_2[Sn_2S_6]\}_n$

First experiments were done stirring a solution of $\{[Ni(tren)]_2[Sn_2S_6]\}_n$ with 30% tren or 2amp at 120°C and the new compounds $[Ni(tren)_2]_2[Sn_2S_6]\cdot 8H_2O$ (**1**) respectively $[Ni(tren)(2amp)]_2[Sn_2S_6]$ (**2**) crystallized after cooling the reaction mixture to room temperature. Quenching the hot reaction mixtures and analyzing the product by X-ray powder diffraction show only reflections of the precursor, i.e., cooling to room temperature is essential for crystallization of **1** and **2** (Supporting Information, Figure S5).

These intriguing observations prompted us to investigate the formation of **1** and **2** in more detail. In further experiments $\{[Ni(tren)_2[Sn_2S_6]\}_n$ was stirred at room temperature in an aqueous solution (20%) of tren or 2amp and surprisingly compounds **1** or **2** crystallized. Heating these slurries to 120°C the color turned from

pink-purple to bright green indicating the formation of the precursor. Cooling the slurries down, compounds **1** or **2** were formed again. This transformation could be performed for many times and is shown in a video (Supporting Information, *VIDEO: 20amp_120_final*).

Further experiments demonstrate that the concentration of the amine solution has a significant influence on these reversible processes and that the temperature for the experiments with 2amp has to be raised to 130℃ achieving a full transformation. (Figure 1 and 2)

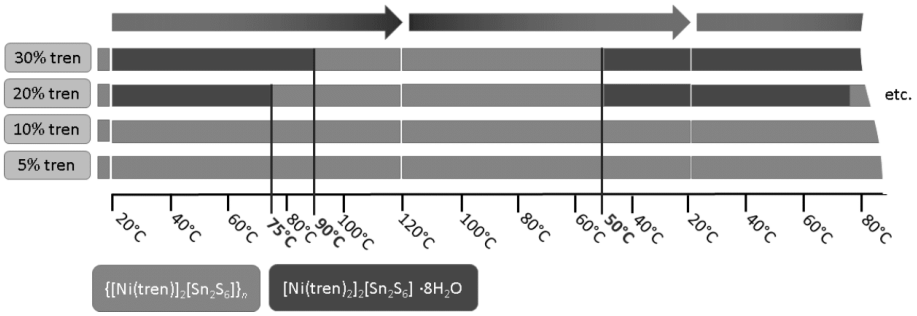

Figure 1: Temperatures of the conversion of $\{[Ni(tren)_2[Sn_2S_6]\}_n$ to compound **1** and vice versa depending on the concentration of the tren solution. Color code: green & purple: color of the reaction slurry indicating the presence of the precursor or **1**; the arrows indicate temperature increase and decrease coded as blue to red and vice versa. Vertical red lines: transformation temperatures during either heating or cooling processes.

The experiments with the precursor and with **1** as starting materials were performed in the following way: the slurries were heated stepwise (10℃ per step) up to 120 ℃ and each distinct temperature was held for ten hours. Afterwards the reaction mixture was quenched from a distinct temperature and the products were analyzed by X-ray powder diffraction. For mixtures of the precursor and an aqueous tren solution of 5% or 10% no conversion could be observed in the temperature range up to 120℃. This observation is surprising because the molar ratios precursor:tren is 1:2.7 (5% tren) and 1:5.4 (10% tren). Only if the tren concentration approaches 20%

$\{[Ni(tren)_2[Sn_2S_6]\}_n$ is transformed into compound **1.** Furthermore using concentrations 20% or 30% of tren a distinct influence on the conversion temperature could be observed. Starting with $\{[Ni(tren)_2[Sn_2S_6]\}_n$ in 20% aqueous tren solution (note that **1** is formed immediately) a conversion of **1** took place at 75 °C. Cooling a mixture from a higher temperature leads to crystallization of **1** at T = 50 °C. Increasing the tren concentration to 30 % the precursor was formed at T = 90 °C, while cooling from higher temperatures afforded crystallization of **1** at T = 50 °C.

As discussed above the conversion of **1** into the starting compound is reversible, depending on the reaction conditions (cooling or quenching). Syntheses performed with **1** as educt in a 20% tren solution the conversion into the precursor is observed within ten minutes but required at least a temperature of minimum 75°C. During cooling crystallization of **1** took than place at a temperature less or equal to 50°C. A similar observation was made for a 30% aqueous tren solution: compound **1** is converted to $\{[Ni(tren)_2[Sn_2S_6]\}_n$ at T≥ 90°C, during cooling **1** was regained at T ≤ 50°C.

An even more temperature depending behavior could be observed during the experiments with different concentrations of 2amp solutions (Figure 2).

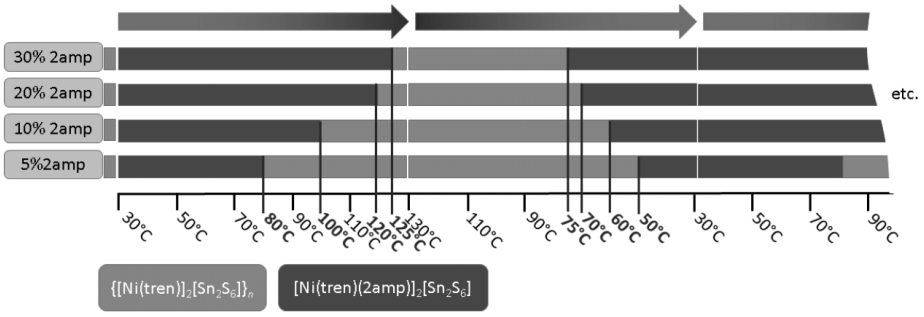

Figure 2: Temperatures of the conversions of $\{[Ni(tren)_2[Sn_2S_6]\}_n$ to compound **2** and vice versa depending on the concentration of the 2amp solution. Color code: green & purple: color of the reaction slurry indicating the presence of the precursor or **2**; blue arrow: reaction temperature was low enough for the formation of **2**; red arrow: temperature range for the formation of the precursor.

First a conversion from the precursor to compound **2** could be observed at all chosen concentrations (5/10/20/30% 2amp) within less than half an hour. With increasing concentration of 2amp the temperature necessary to obtain the precursor increased from 80℃ (5%) to 125℃ (30%). During the cooling e xperiments a concentration dependent formation of **2** was also observed: crystalline powders of **2** were obtained below T = 50℃ for 5% 2amp solution while crystals of **2** occurred T = 75℃ for 30% 2amp solution.

These observations suggest that the precursor is more stable at elevated temperatures and compounds **1** and **2** at lower temperatures. It is most likely that the precursor and **1** are in equilibrium and this equilibrium can be shifted to the product side for c_{tren} = 20% and 30% but not for c_{tren} = 5% or 10 %. The situation is different applying 2amp: even at low concentration of 5% compound **2** is formed within ten minutes. The temperature dependent equilibrium strongly depends on the amine concentration as can be seen in Fig. 1 and 2.

3.3 Crystal structures

The compound $[Ni(tren)_2]_2[Sn_2S_6]\cdot 8H_2O$ (**1**) crystallizes in the triclinic space group $P\bar{1}$ (Z = 1), whereas $[Ni(tren)(2amp)]_2[Sn_2S_6]$ (**2**) adopts the tetragonal space group $P4_2/n$ (Z = 8). Both structures contain discrete $[Sn_2S_6]^{4-}$ anions and charge compensating Ni^{2+} centered complexes. The $[Sn_2S_6]^{4-}$ units in the two compounds feature almost identical bond lengths and angles and the geometric data are comparable with those of $Na_4Sn_2S_6\cdot 14H_2O$ [28] (Supporting Information, Table S4). The charge compensating Ni^{2+} centered complexes are composed of two tren ligands acting only as a tridentate ligand in **1** (Supporting Information, Figure S6, left), and of one tetradentate tren and one 2amp ligand in **2**, (Supporting Information, Figure S6, right). Both of these complexes exhibit a weak (**1**) to pronounced (**2**) distortion of the ideal geometry (Supporting Information, Table S5). This distortion as well as the Ni-N

bond lengths (2.006 Å – 2.182 Å) correspond with literature data.[11,19,29–32] It should be noted that the tren molecule acts as tetradentate ligand in the precursor but coordinate tridentate in the structure of **1**. Hence, during the chemical reaction not only Ni-S bonds are broken but also at least one Ni-N bond allowing that two tren ligands coordinate in a tridentate fashion to the Ni^{2+} ion.

In compound **1** the $[Sn_2S_6]^{4-}$ units and the $[Ni(tren)_2]^{2+}$ complexes are arranged alternating along the *b* axis as well as along the *c* axis. The eight water molecules are located in the open space between the anions and cations (Figure 3).

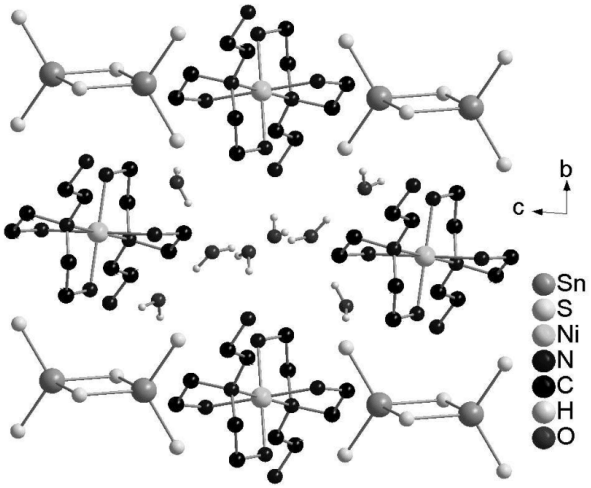

Figure 3: Arrangement of the building blocks in compound **1** viewed along the *a* axis. Only selected hydrogen atoms are depicted.

13

Hydrogen bonding interactions between the H_2O molecules form octamers (Supporting Information, Table S6). These octamers are composed of a central cyclic water tetramer with the notation R4 [33] with two additional water molecules at two opposing corners (Figure 4).

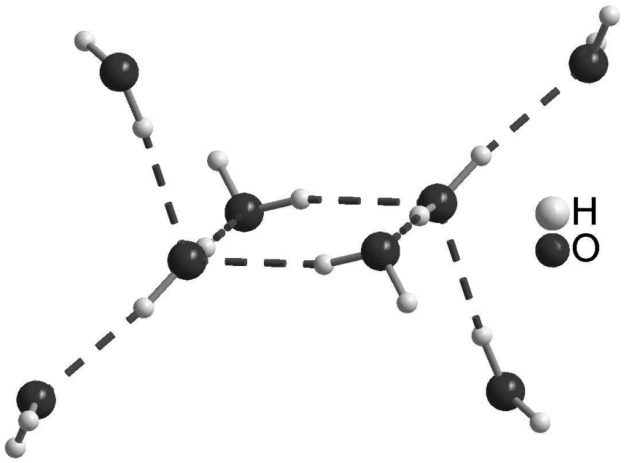

Figure 4: View of the water cluster in compound **1** with intermolecular O-H···O hydrogen bonding as purple lines.

This kind of water octamer has been observed in the voids of coordination polymers like ({[Zn(bipy)(aba)$_2$]·4H$_2$O}$_n$, aba = 4-dimethylamino benzoate).[34,35] Further hydrogen bonding interactions occur between these water clusters and adjacent $[Sn_2S_6]^{4-}$ anions and $[Ni(tren)_2]^{2+}$ cations (Supporting Information, Table S6). The extended H bonding generates a layer-like arrangement within the *bc* plane (Supporting Information, Figure S7). The $[Ni(tren)_2]^{2+}$ cations are located in the gaps within these layers and interact via the non-coordinated N atom of the tren ligand with the water clusters (Supporting Information, Figure S8). The layers are joined by further H bonding of $[Ni(tren)_2]^{2+}$ complexes leading the formation of a three dimensional network (Supporting Information, Figure S9). The entire structure

consists of two interwoven individuals of these networks (Supporting Information, Figure S10).

In compound **2** the $[Sn_2S_6]^{4-}$ anions are arranged in rods along the *a* as well as the *c* axis. The individual rods alternate in ···ABA··· fashion along *b* (Supporting Information, Figure S11). The $[Ni(tren)(2amp)]^{2+}$ (Figure 5, left) cations are grouped in pairs and are located between the anions (Figure 5, right).

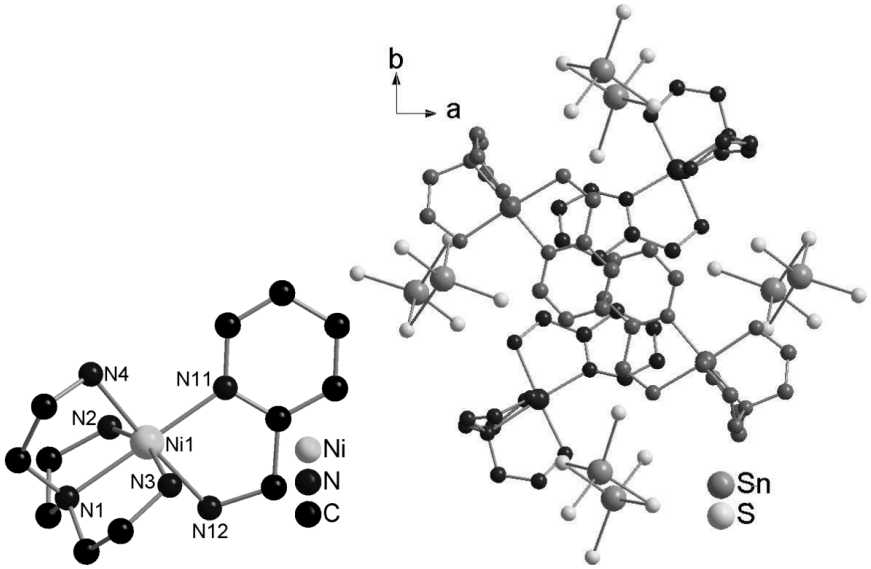

Figure 5: right: Arrangement of the $[Sn_2S_6]^{4-}$ anions and the $[Ni(tren)(2amp)]^{2+}$ complexes (left) viewed along the *c* axis. For reasons of clarity the $[Ni(tren)(2amp)]^{2+}$ units are colored pairwise and the H atoms are omitted.

The pair wise arrangement is caused by π-π interactions (off-centre parallel 3.343 - 3.580 Å) between the 2amp ligands of the complexes (Figure 6, and Supporting Information Figure S12).

15

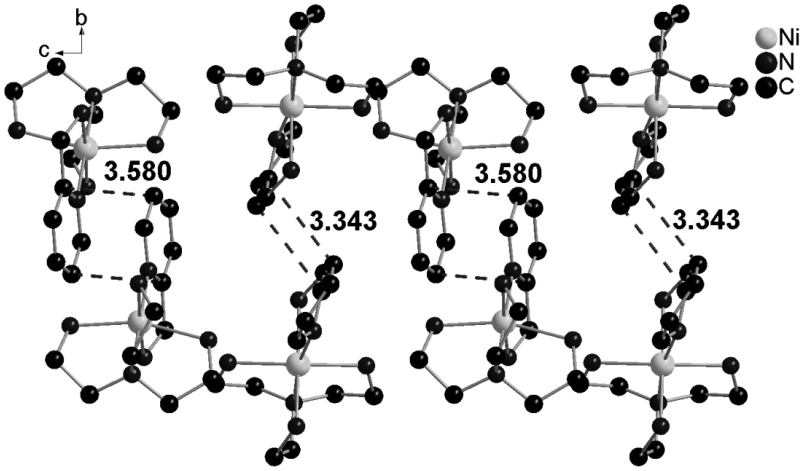

Figure 6: Shortest intermolecular distances between the pyridine rings in compound **2**, which indicates π-π-interactions.

Calculations of the interaction energies for a comparable type of stacking with similar distances of the aromatic moieties ({[Mn(phen)$_2$]$_2$[Sn$_2$S$_6$]}: 3.366 - 3.500 Å[36]) yielded values between about 10 and 13 kcal/ mol.

A three dimensional network is generated considering hydrogen bonding interactions between the Ni(II)complexes and $[Sn_2S_6]^{4-}$ units. Each thiostannate unit interacts with six adjacent Ni(II)complexes (Supporting Information, Figure S13 and Table S7).

3.4 Investigation of the thermal behavior

The thermal behavior of compounds **1** and **2** were investigated by simultaneous differential thermoanalysis and thermogravimetry (DTA-TG). The question was whether the water molecules and amine ligands can be stepwise removed leading to formation of {[Ni(tren)]$_2$[Sn$_2$S$_6$]}$_n$ [19].

While heating compound **1** four distinct mass steps could be observed, which are accompanied by endothermic events in the DTA curve (Figure 7). The first two mass losses (7% and 3%) are in good agreement with the calculated value for the removal

of all H_2O molecules (also confirmed by CHNS analyses). The next two mass changes (21% and 26%, endothermic DTA signals) match approximately with the loss of two tren ligands in each step (calculated value for two tren ligands: 23%).

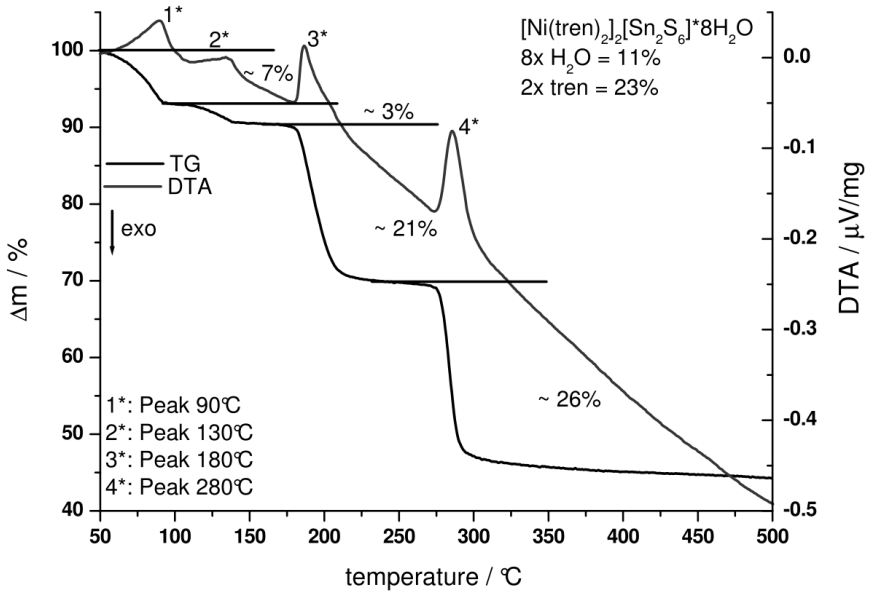

Figure 7: DTA and TG curves of compound **1** at 4 ℃/min measured in nitrogen atmosphere.

The CHN data of the sample obtained at 260℃ (Suppo rting Information, Tab. S8) are in a good agreement with the calculated values for $\{[Ni(tren)]_2[Sn_2S_6]\}_n$ [19] and interestingly the sample is light green as observed for this compound. However, the reflections in the powder pattern are too broad for a definite decision (Supporting Information, Figure S14). But reacting this decomposition product with 30% 2amp leads to the formation of $[Ni(tren)(2amp)]_2[Sn_2S_6]$ (**2**) (Supporting Information, Figure S15). The powder patterns of the two samples obtained after the first two mass losses (100℃ and 140℃) are significantly differen t from that of the starting compound (Supporting Information, Figure S14). The IR and Raman spectra of these products still show the typical vibrations of the amine ligands (Supporting Information, Figure S16) and of $[Sn_2S_6]^{4-}$ anion (Supporting Information, Figure S17, Table S9).

17

The IR spectra of the sample obtained at 260℃ exhibits also bands of the amine molecules, while the vibrations in the Raman spectrum are less pronounced compared to those measured for $\{[Ni(tren)]_2[Sn_2S_6]\}_n$. The water removal is not reversible as evidenced by storing the samples in a water atmosphere leading not to the formation of $[Ni(tren)_2]_2[Sn_2S_6]\cdot 8H_2O$.

The TG curve of compound **2** features two not well resolved mass steps, accompanied by two endothermic events in the DTA curve (Figure 8). Measurements with a lower heating rate (1 ℃/min) did not improve the resolution.

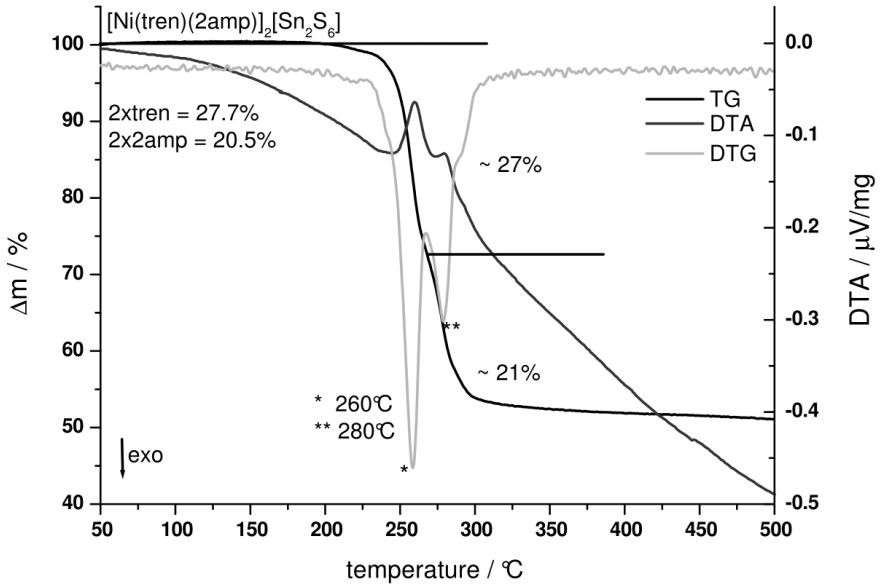

Figure 8: DTA, TG and DTG curves of compound **2** at 4 ℃/min measured in nitrogen atmosphere.

The mass losses can be approximately explained by the loss of two tren or 2amp ligands, respectively. Without accompanying mass spectrometry no unambiguous interpretation is possible. A sample obtained at 260 ℃ was analyzed with CHNS (Table 3) and IR spectroscopy (Supporting Information, Figure S18), but both characterizations deliver no helpful hints.

18

Table 2: Results of the elemental analysis of the residues obtained by thermal decomposition of compound **2** at 260℃ and of compounds that might form in the r eaction

compound	N %	C %	H %
$[Ni(2amp)]_2[Sn_2S_6]_{theo}$	7.34	18.88	2.11
$[Ni(tren)]_2[Sn_2S_6]_{theo}$	13.34	17.17	4.32
isolated at 260℃	8.6	11.7	2.2

The reflections in the powder pattern are not well resolved, but indicating the presence of at least two compounds (Supporting Information, Figure S19). However in the Raman spectrum no vibrations of the $[Sn_2S_6]^{4-}$ ion are present suggesting that the anion is at least partially decomposed at this temperature (Supporting Information, Figure S20).

4. Conclusion

We demonstrated that the compound $\{[Ni(tren)]_2[Sn_2S_6]\}_n$ is a versatile precursor for the fast preparation of new thiostannate compounds at room-temperature. During the reaction with tren and 2amp the two Ni-S bonds are broken and the amine molecules coordinate to the free binding sites of the Ni^{2+} cation. If **1** and **2** is heated in tren, respectively 2amp solution a transformation into the precursor is observed, in which the transition temperature depends on the actual amine concentration. This indicates that the precursor seems to be more stable at higher temperatures. Heating compound **1** up to 100℃ leads to removal of the crystal water, while leading the thiostannate unit and Ni(II)amine complex intact. Further heating resulted in removal of half of the organic ligands, which is also observed upon heating of compound **2**, leading to the formation of a compound of same composition as the precursor $\{[Ni(tren)]_2[Sn_2S_6]\}_n$. Currently, further experiments are under way to explore the potential of $\{[Ni(tren)]_2[Sn_2S_6]\}_n$ as synthon for the generation of new thiostannate compounds.

19

Acknowledgements

Financial support by the State of Schleswig-Holstein is gratefully acknowledged.

Appendix A. Supplementary data

Supplementary data associated with this article can be found, in the online version, at XXX.

References

[1] A. Rabenau, Angew. Chem. 97 (1985) 1017–1032.
[2] W.S. Sheldrick, M. Wachhold, Angew. Chem. 109 (1997) 214–234.
[3] G. Demazeau, J. Mater. Sci. 43 (2008) 2104–2114.
[4] G. Demazeau, A. Largeteau, Z. Anorg. Allg. Chem. 641 (2015) 159–163.
[5] W.S. Sheldrick, M. Wachhold, Coord. Chem. Rev. 176 (1998) 211–322.
[6] W.S. Sheldrick, J. Chem. Soc., Dalton Trans. (2000) 3041–3052.
[7] S. Dehnen, M. Melullis, Coord. Chem. Rev. 251 (2007) 1259–1280.
[8] J. Zhou, J. Dai, G.-Q. Bian, C.-Y. Li, Coord. Chem. Rev. 253 (2009) 1221–1247.
[9] B. Seidlhofer, N. Pienack, W. Bensch, Z. Naturforsch. 65b (2010) 937–975.
[10] W.-W. Xiong, G. Zhang, Q. Zhang, Inorg. Chem. Front. 1 (2014) 292–301.
[11] N. Pienack, H. Lühmann, B. Seidlhofer, J. Ammermann, C. Zeisler, F. Danker, C. Näther, W. Bensch, Solid State Sci. 33 (2014) 67–72.
[12] C. Zeisler, C. Näther, W. Bensch, CrystEngComm 15 (2013) 8874–8876.
[13] L. Nie, Y. Zhang, K. Ye, J. Han, Y. Wang, G. Rakesh, Y. Li, R. Xu, Q. Yan, Q. Zhang, J. Mater. Chem. A 3 (2015) 19410–19416.
[14] K.K. Rangan, P.N. Trikalitis, C. Canlas, T. Bakas, D.P. Weliky, M.G. Kanatzidis, Nano Lett. 2 (2002) 513–517.
[15] Z.H. Fard, C. Müller, T. Harmening, R. Pöttgen, S. Dehnen, Angew. Chem. 121 (2009) 4507–4511.
[16] J. Li, B. Marler, H. Kessler, M. Soulard, S. Kallus, Inorg. Chem. 36 (1997) 4697–4701.
[17] P. Nørby, E. Eikeland, J. Overgaard, S. Johnsen, B.B. Iversen, CrystEngComm 17 (2015) 2413–2420.
[18] J.W. Mullin, Crystallization, 4th ed., Butterworth-Heinemann, Oxford, Boston, 2001.
[19] J. Hilbert, C. Näther, R. Weihrich, W. Bensch, Inorg. Chem. 55 (2016) 7859–7865.
[20] G.M. Sheldrick, SHELXS-97: Program for the Solution of Crystal Structures, University of Göttingen, Göttingen (Germany), 1997.
[21] G.M. Sheldrick, SHELXL-2014: Program for the Refinement of Crystal Structures, University of Göttingen, Göttingen (Germany), 2014.
[22] J. Ellermeier, R. Stähler, W. Bensch, Acta Cryst. C58 (2002) m70-m73.
[23] A. Marzotto, D.A. Clemente, V. Giovanni, Acta Cryst. C49 (1993) 1252–1255.
[24] J.-E. Jee, C.-H. Kwak, Inorg. Chem. Commun. 33 (2013) 95–98.
[25] G. Anderegg, Helv. Chim. Acta 54 (1971) 509–512.
[26] G.A. Carlson, J.P. McReynolds, F.H. Verhoek, J. Am. Chem. Soc. 67 (1945) 1334–1339.
[27] G. Schwarzenbach, R. Baur, Helv. Chim. Acta 86 (1956) 722–728.
[28] B. Krebs, S. Pohl, W. Schiwy, Z. Anorg. Allg. Chem. 393 (1972) 241–252.
[29] M. Behrens, S. Scherb, C. Näther, W. Bensch, Z. Anorg. Allg. Chem. 629 (2003) 1367–1373.
[30] D.-X. Jia, J. Dai, Q.-Y. Zhu, Y. Zhang, X.-M. Gu, Polyhedron 23 (2004) 937–942.
[31] D.-X. Jia, Y. Zhang, J. Dai, Q.-Y. Zhu, X.-M. Gu, Z. Anorg. Allg. Chem. 630 (2004) 313–318.
[32] J. Zhou, X. Liu, G.-Q. Chen, F. Zhang, L.-R. Li, Z. Naturforsch. 65b (2010) 1229–1234.
[33] L. Infantes, S. Motherwell, CrystEngComm 4 (2002) 454.
[34] S. Das, P.K. Bharadwaj, Cryst. Growth Des. 6 (2006) 187–192.
[35] M.C. Das, S.B. Maity, P.K. Bharadwaj, Curr. Opin. Solid State Mater. Sci. 13 (2009) 76–90.
[36] J. Hilbert, C. Näther, W. Bensch, Inorg. Chem. 53 (2014) 5619–5630.

3.3 weitere Ergebnisse – Synthesen mit vorgefertigten Komplexen und Thiostannat-Einheiten

Ein weiteres Ziel der Doktorarbeit war die Entwicklung alternativer Synthesewege bei Raumtemperatur. Mit diesen Synthesen sollte die Komplexität der Reaktionen verringert werden. Als Edukte wurden (wasser)lösliche TM-Amin-Komplexe und $Na_4SnS_4 \cdot 14H_2O$ ausgewählt, welche ohne besonderen synthetischen Aufwand herstell- und handhabbar sind.

In ersten Versuchen wurden $[TM(phen)_3][ClO_4]_2$- bzw. $[TM(2,2'\text{-bipy})_3][ClO_4]_2$-Komplexe als Edukte gewählt. In einer weiteren Versuchsreihe wurden weitere $[Ni(Amin)_n]^{2+}$-Komplexe verwendet (s. Kap. 3.3.2). Aufgrund der großen Affinität von Ni^{2+} zu N-Donoratomen sind diese Komplexe im Vergleich zu anderen TM^{2+} stabiler und weisen zudem die größte Vielfalt an Aminmolekülen als Liganden auf (Tab. 1).

Tabelle 7: Komplexstabilitäten von Mn^{2+}-, Fe^{2+}-, Co^{2+}-, Ni^{2+}- und Cu^{2+}-Amin-Komplexen ausgewählter Aminmoleküle.

Ligand	Mn^{2+} [log β]	Fe^{2+} [log β]	Co^{2+} [log β]	Ni^{2+} [log β]	Cu^{2+} [log β]
NH_3	---	---	5.5 (β_4)[65]	8.7 (β_6)[65]	12.7 (β_4)[65]]
en	5.7[65]	9.5[65]	13.8[65]	18.1[65]	19.6 (β_2)[65]
1,2-dach	---	---	15.22[70]a	20.07[70]a	20.93 (β_2)[70]a
1,2-dap	---	---	---	18.00[69]	19.66 (β_2)[69]
1,3-dap	---	---	---	13.81[96]	16.94 (β_2)[97]
2amp	2.66[67]	---	13.98[67]	18.9[67]	17.2 (β_2)[67]
phen	10.5[66]	21.2[66]	19.9[66]	24.3[66]	20.8[66]
2,2'-bipy	6[66]	17.5[66]	16.1[66]	20.1[66]	17.0[66]
dien	---	---	14.1[65]	18.9[65]	21.3[65]
tren	5.8[65]	8.8[65]	12.8[65]	14.8[65]	18.8[65]
trien	4.9[65]	7.8[65]	12.8[65]	14.8[65]	18.8[65]
tepa	7.0[68]	11.4[98]	15.1[98]	17.8[68]	22.9[68]
peha	---	---	15.8[99]	19.3[99]	21.3[99]
cyclam	4.8[100]	---	12.7[101]	22.2[71]	26.5[71]

a: Werte bezogen auf das *trans* Isomer; --- = keine Literaturdaten gefunden

Um zu überprüfen, ob bei dieser Synthesestrategie (Komplex + Thiostannatsalz) die Zielverbindungen erhalten werden, wurden zunächst Synthesen unter solvothermalen Bedingungen (120°C) durchgeführt. Das System Mn/S/Sn/phen wurde zunächst gewählt, da in diesem bereits fünf Verbindungen bekannt sind (s. Kap. 3.1.1). Danach wurden die Synthesen auf weitere $[TM(phen)_3][ClO_4]_2$-Komplexe (TM = Co, Fe, Ni, Cu) ausgedehnt. Die Synthesen mit Mn-, Co- und Fe-haltigen Komplexen führten zur erfolgreichen Reproduktion der in Abschnitt 3.1.1 & 3.1.2 beschriebenen Verbindungen $\{[TM(phen)_2]_2[Sn_2S_6]\}$ und $\{[TM(phen)_2]_2[Sn_2S_6]\} \cdot phen \cdot H_2O$ (TM = Mn, Fe, Co). Bei Mn-haltigen Komplexe wurden diese Verbindungen auch bei T = 80°C gebildet, d.h. solvothermale Bedingungen waren nicht erforderlich. Unterhalb von 80°C wurde jedoch der eingesetzte Komplex teilweise nicht umgesetzt und verschieden röntgenamorphe Mn/Sn-S-Spezies wurden erhalten. Die Synthesen mit nickelhaltigen Komplexen führten zur Umkristallisation des eingesetzten Komplexes. Vermutlich sind höhere Temperaturen als 120°C erforderlich, um eine Reaktion mit dem Thiostannatsalz zu initiieren. Die Synthesen mit Cu^{2+}-zentrierten Komplexen resultierten in der Bildung von Cu_xS_y. Die Affinität von Cu^+ zu S^{2-} ist offensichtlich so stark

ausgeprägt, dass eine Reduktion der Cu^{2+} Spezies zu Cu^{+} erfolgt und eine Bildung von Thiostannaten verhindert wird.

Untersuchungen des Mn/Sn/S/phen-Systems hatten unter solvothermalen Bedingungen eine Abhängigkeit der Produktbildung vom pH-Wert gezeigt (s. Kap. 3.1.1). Daher wurde das chemische Verhalten von $Na_4SnS_4 \cdot 14H_2O$ bei unterschiedlichen pH-Werten untersucht (s. Kap. 3.3.1.1). Zusätzlich wurden Löslichkeitstests beider Edukte ($[Mn(phen)_3][ClO_4]_2$ und $Na_4SnS_4 \cdot 14H_2O$) durchgeführt, da der Mn-Komplex nur schlecht bei RT in Wasser löslich ist (s. Kap. 3.3.1.2). Die Edukte wurden in verschiedenen, schlecht/nicht mischbaren LM gelöst, um an der LM-Grenze eine Kristallisation zu ermöglichen. Die Ergebnisse dieser Synthesen sind in Abschnitt 3.3.1.3 zusammengefasst.

Bei Synthesen mit $[Ni(Amin)_3]^{2+}$ (Amin = en, 1,2-dach, 1,2-dap, 2amp) und $Na_4SnS_4 \cdot 14H_2O$ bei RT in Wasser trat folgendes Problem auf: bei Kontakt mit Wasser reagierte $Na_4SnS_4 \cdot 14H_2O$ zu H_2S und diversen Sn-Oxid-/-Hydroxid-Spezies.[102–105] Eine schnelle Reaktion dieser Zwischenprodukte bei pH ≥8 mit Ni^{2+} führte zur Bildung diverse Ni-Sulfide.[106] Durch Zugabe minimaler Mengen (0.5 mmol) tren vor der Wasserzugabe konnte diese Reaktionskaskade unterdrückt werden. Mit diesem synthetischen Vorgehen konnten insgesamt acht Verbindungen mit der allgemeinen Formel $[Ni(tren)(Amin)]_2[Sn_2S_6] \cdot xH_2O$ (Amin = en, 1,2-dach, 1,2-dap, 2amp, tren) synthetisiert und charakterisiert werden (s. Kap. 3.3.2).

Um zu überprüfen, ob diese Synthesemethode nur auf das $[Ni(Amin)_3]^{2+}$-tren-System beschränkt ist, wurden die Synthesen a) mit $[Ni(tren)(H_2O)Cl]Cl$ und b) in der Kombination jeder Komplex (Amin = en, 1,2-dach, 1,2-dap, 2amp, tren) mit jedem Amin (Amin = tren, en, 1,2-dach, 1,2-dap, 2amp) durchgeführt. Bei diesen Experimenten kristallisierte die Verbindung $[Ni(2amp)_3]_2[Sn_2S_6] \cdot 9.5H_2O$ (s Kap. 3.3.3.1).

Mit anderen TM^{2+}-Ionen (TM = Fe, Co, Mn) ist die Auswahl an geeigneten Komplexen auf z.B. solche mit phen oder 2,2‘-bipy als Liganden beschränkt. Daher wurden orientierende Synthesen mit $[Ni(phen)_3][ClO_4]_2$ bzw. $[Ni(2,2'\text{-bipy})_3][ClO_4]_2$ in wässrigen Aminlösungen durchgeführt. Diese Synthesen sollten aufzeigen, ob für die Bildung von Thiostannaten das entsprechende Amin im Komplex enthalten sein muss oder ob diese Komplexe als vergleichsweise stabile TM-Quelle agieren können (s. Kap. 3.3.3).

3.3.1 Systematische Untersuchungen der chemischen Reaktivität von $Na_4SnS_4 \cdot 14H_2O$ und $[Mn(phen)_3][ClO_4]_2$ und der Synthesen mit diesen Edukten

Experimente mit Mn/Sn/S/phen unter solvothermalen Bedingungen führten zur Kristallisation von fünf Verbindungen u.a. in Abhängigkeit des pH-Wertes (s. Kap. 3.1.1). Bei Synthesen mit $Na_4SnS_4 \cdot 14H_2O$ und $[Mn(phen)_3][ClO_4]_2$ waren bei $T \geq 80°C$ nur zwei Verbindungen erhalten worden. Daher wurden pH-Wert abhängige Synthesen durchgeführt und zunächst das Verhalten des Thiostannat-Salzes bei Erniedrigung des pH-Wertes untersucht (s. Kap. 3.3.1.1). Zusätzlich wurde ein LM gesucht, bei dem der Komplex bereits bei RT löslich ist, um eine Reaktion bei niedrigeren Temperaturen zu ermöglichen (s. Kap. 3.3.1.2). Die Ergebnisse dieser Untersuchungen erlaubte letztlich die Präparation aller fünf Mn-Phen-Verbindungen, welche in Abschnitt 3.1.1 vorgestellt wurden (s. Kap. 3.3.1.3).

3.3.1.1 Untersuchungen zum Verhalten von $Na_4SnS_4 \cdot 14H_2O$ in wässriger Lösung bei Zugabe von HCl

0.2 mmol $Na_4SnS_4 \cdot 14H_2O$ wurden in 1 mL dest. H_2O gelöst, schrittweise mit 100 µL 0.2 m HCl versetzt und nach jeder HCl-Zugabe der pH-Wert gemessen. Der pH-Wert der Anfangslösungen betrug 11.8. Bis zu einer Zugabe von 0.8 mL 0.2 m HCl nahm der pH-Wert der Lösung langsam aber stetig auf ca. 10.6 ab. Bei Zugabe 0.8 – 1 mL HCl wurde eine starke Abnahme des pH-Werts auf 8.4 gemessen. Daher wurde zwischen 0.8 und 1.0 mL HCl in 10 µL Schritten zugegeben. Ab einer Zugabe von 1 mL nahm der pH-Wert deutlich langsamer ab. Bei Zugabe von 1.1 mL 0.2 mL HCl wurde ein gelblicher Niederschlag von SnS_2 beobachtet. Da ab dieser Menge keine signifikanten Veränderungen des pH-Wertes zu beobachten waren, wurden die Messungen nach der Zugabe bei 1.5 mL 0.2 m HCl nicht weiter geführt (s. Abb. 2. und Tab. 8).

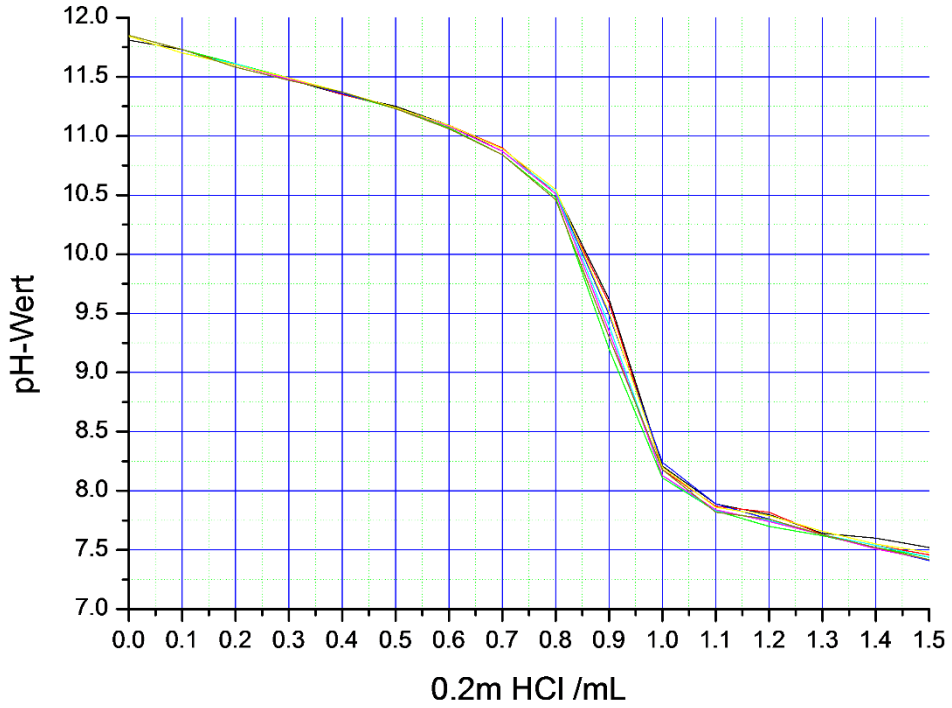

Abbildung 2: Veränderung des pH-Werts einer 0.2 m Na_4SnS_4 Lösung (1 mL) mit zunehmender Zugabe von 0.2 m HCl.

Tabelle 8: Tabellarische Auflistung der pH-Werte gemessen bei der schrittweisen Zugabe von 0.2 m HCl zu einer 0.2 m Na_4SnS_4 Lösung (1 mL). (1.-6.: 1. Messung - 6. Messung)

0.2 m HCl (mL)	pH (1.)	pH (2.)	pH (3.)	pH (4.)	pH (5.)	pH (6.)
0	11.82	11.84	11.84	11.84	11.85	11.86
0.1	11.75	11.73	11.74	11.74	11.74	11.74
0.2	11.64	11.61	11.61	11.61	11.63	11.63
0.3	11.53	11.52	11.52	11.51	11.50	11.51
0.4	11.40	11.39	11.39	11.38	11.38	11.37
0.5	11.27	11.27	11.27	11.27	11.26	11.26
0.6	11.12	11.11	11.11	11.11	11.10	11.10
0.7	10.93	10.91	10.91	10.90	10.90	10.90
0.8	10.62	10.61	10.62	10.60	10.61	10.63
0.82	10.51	10.49	10.50	10.51	10.50	10.48
0.84	10.39	10.34	10.38	10.39	10.40	10.36
0.86	10.26	10.19	10.25	10.25	10.26	10.22
0.88	9.95	9.99	10.03	9.96	10.01	9.94
0.9	9.65	9.58	9.74	9.63	9.74	9.62
0.92	9.34	9.26	9.48	9.39	9.52	9.34
0.94	8.98	8.88	9.20	9.06	9.26	9.08
0.96	8.71	8.64	8.78	8.64	8.84	8.75
0.98	8.51	8.43	8.59	8.50	8.65	8.64
1.0	8.40	8.36	8.48	8.40	8.49	8.42
1.05	8.15	8.14	8.20	8.21	8.22	8.24
1.1	8.02	8.01	8.04	8.01	8.02	8.03
1.2	7.82	7.81	7.86	7.84	7.80	7.79
1.3	7.70	7.67	7.66	7.65	7.64	7.65
1.4	7.58	7.55	7.54	7.54	7.53	7.54
1.5	7.46	7.45	7.47	7.47	7.46	7.45

3.3.1.2 Löslichkeitsversuche mit $[Mn(phen)_3][ClO_4]_2$ und $Na_4SnS_4 \cdot 14H_2O$

Die Löslichkeit von $[Mn(phen)_3][ClO_4]_2$ und $Na_4SnS_4 \cdot 14H_2O$ wurde in verschiedenen LM untersucht (s. Tab. 9).

Tabelle 9: Verwendete LM für $[Mn(phen)_3][ClO_4]_2$ und $Na_4SnS_4 \cdot 14H_2O$. Es wurden jeweils 0.25 mmol der Substanz mit 1 mL des LM versetzt.

LM	$[Mn(phen)_3][ClO_4]_2$	$Na_4SnS_4 \cdot 14H_2O$
dest. H_2O	---	X
MeOH	---	---
EtOH	---	---
2-Propanol	---	---
Acetonitril	X	---
Aceton	x	---
Chloroform	---	---
Cyclohexan	---	---
Dichlormethan	x	---
n-Hexan	---	---
Toluol	---	---

X = komplett gelöst, x = teilweise gelöst, --- = nicht gelöst

Bei weiteren Synthesen wurde Acetonitril verwendet, da hierin der Komplex sehr gut löslich ist, das Thiostannat-Salz aber nicht. Wasser und Acetonitril lassen sich zudem bei vorsichtiger Arbeitsweise überschichten, aber auch bei kräftigem Schütteln durchmischen.

3.3.1.3 Synthesen mit $[Mn(phen)_3][ClO_4]_2$ und $Na_4SnS_4 \cdot 14H_2O$

Jeweils 0.25 mmol des Komplexes bzw. des Thiostannat-Salzes wurden getrennt in Acetonitril bzw. dest. H_2O gelöst. Anschließend wurden diese Lösungen a) vorsichtig überschichtet oder b) gut durchmischt und bei 80°C getempert.

Die Ergebnisse in Tab. 4 belegen, dass das Lösungsmittel bzw. LM-Gemisch einen signifikanten Einfluss auf die Produktbildung hat: In Abhängigkeit vom Lösungsmittel wurden unterschiedliche Verbindungen erhalten (s. Tab. 10).

Tabelle 10: Abhängigkeit der Produktbildung von der Art des LM(-Gemisches) bei 80°C (Pulverdiffraktogramme: s. Abb. A1, Abschnitt 5.4, Anhang).

LM	Produkt
H_2O	$\{[Mn(phen)_2]_2[Sn_2S_6]\} \cdot phen \cdot H_2O$
Acetonitril & H_2O, geschichtet	$\{[Mn(phen)_2]_2[Sn_2S_6]\} \cdot phen$
Acetonitril & H_2O, gemischt	$\{[Mn(phen)_2]_2[Mn(phen)]_2[SnS_4]_2\}$

Da bisherige Untersuchungen eine Zunahme des Kondensationsgrades der $[SnS_4]^{4-}$-Tetraeder mit abnehmendem pH-Wert belegen, wurde überprüft, bis zu welchem pH-Wert noch $\{[Mn(phen)_2]_2[Mn(phen)]_2[SnS_4]_2\}$ gebildet wird. Daher wurde der pH-Wert der Thiostannatlösung in 0.5er Schritten auf einen Wert zwischen 7.5 und 12 eingestellt und anschließend mit der Komplex-Lösung gemischt. Die Ergebnisse belegen, dass $\{[Mn(phen)_2]_2[Mn(phen)]_2[SnS_4]_2\}$ nur bei pH ~12 gebildet wird und bei pH ~11.5 die Bildung

von {[Mn(phen)$_2$]$_2$[Sn$_2$S$_6$]}·phen·H$_2$O bzw. {[Mn(phen)$_2$]$_2$[Sn$_2$S$_6$]} bevorzugt ist. Bei pH ≤ 10 kristallisiert nur noch {[Mn(phen)$_2$]$_2$[Sn$_2$S$_6$]} (s. Tab. 11).

Tabelle 11: Abhängigkeit der Produktbildung vom pH-Wert bei Verwendung des LM-Gemisches bei 80°C (Pulverdiffraktogramme: s. Abb. A2, Abschnitt 5.4, Anhang).

pH-Wert	Produkt
7.5 – 10	{[Mn(phen)$_2$]$_2$[Sn$_2$S$_6$]}
10.5 – 11.5	{[Mn(phen)$_2$]$_2$[Sn$_2$S$_6$]}, {[Mn(phen)$_2$]$_2$[Sn$_2$S$_6$]}·phen·H$_2$O
12	{[Mn(phen)$_2$]$_2$[Mn(phen)]$_2$[SnS$_4$]$_2$}

Bei Synthesen bei RT konnten durch Überschichten oder direktes Mischen der Lösungen keine unterschiedlichen Produkte erhalten werden. Allerdings beeinflussen der pH-Wert und die Reaktionszeit die Produktbildung: Bei kurzen Reaktionszeiten (1 Tag) wurde bei pH = 7.5 - 9.5 nur ein rötliches, röntgenamorphes Pulver erhalten. Bei pH > 9.5 wurde eine unbekannte feinkristalline Verbindung (A) gebildet. Nach eine Woche konnte bei pH = 7.5 - 9.5 eine weitere unbekannte feinkristalline Verbindung (B) nachgewiesen werden. Bei pH = 10 - 11 konnten {[Mn(phen)$_3$]$_2$]Sn$_2$S$_6$]} bzw. „A“ nachgewiesen werden. Nach zwei Wochen Reaktionszeit lag bei pH ≤ 11 {[Mn(phen)$_3$]$_2$]Sn$_2$S$_6$]} vor, bei höheren pH-Werten weiterhin „A“ (s. Tab. 12)

Tabelle 12: Abhängigkeit der Produktbildung vom pH-Wert bei RT (Pulverdiffraktogramme: s. Abb. A3, Abschnitt 5.4, Anhang)

Reaktionszeit	pH-Wert	Produkt
1d	7.5 – 9.5	röntgenamorph
	10 - 12	A
1w	7.5-9.5	B
	10 -11	{[Mn(phen)$_2$]$_2$]Sn$_2$S$_6$]} & A
	11.5 - 12	A
2w	7.5 - 11	{[Mn(phen)$_2$]$_2$]Sn$_2$S$_6$]}
	11.5 - 12	A

Diese Untersuchungen belegen, dass a) die Synthese von Zinn-Schwefel-Verbindungen bei RT möglich ist und b) eine Variation des pH-Wertes zu unterschiedlichen Produkten führt. Allerdings wurden auch bei Reaktionen an der Phasengrenze keine größeren Kristalle erhalten, sondern nur feinkristallines Pulver. Diese Beobachtung legt den Schluss nahe, dass die Übersättigung zu schnell erreicht wird. Daher sind weitere Variationen notwendig, um ein langsameres Erreichen der Übersättigung zu erreichen und damit einhergehend ein langsameres Kristallwachstum.

3.3.2 Synthesen von Thiostannaten bei RT bei Verwendung von $[Ni(Amin)_3]^{2+}$-Komplexen und $Na_4SnS_4 \cdot 14H_2O$.

Bei Synthesen mit $[Ni(Amin)_3]^{2+}$-Komplexen (Amin = en, 1,2-dach, 1,2-dap, 2amp) und $Na_4SnS_4 \cdot 14H_2O$ bei RT konnten insgesamt sechs neue Verbindungen erhalten werden: $[Ni(tren)(en)]_2[Sn_2S_6] \cdot 2H_2O$ ($P2_1/n$, Z=2), $[Ni(tren)(en)]_2[Sn_2S_6] \cdot 6H_2O$ ($P2_1/c$, Z=2), $[Ni(tren)(1,2\text{-dach})]_2[Sn_2S_6] \cdot 3H_2O$ ($P\bar{1}$, Z=1), $[Ni(tren)(1,2\text{-dach})]_2[Sn_2S_6] \cdot 4H_2O$ ($P2_1/c$, Z=2), $[Ni(tren)(1,2\text{-dap})]_2[Sn_2S_6] \cdot 4H_2O$ ($C2/c$, Z=4) sowie $[Ni(tren)(2amp)]_2[Sn_2S_6] \cdot 10H_2O$ ($P2_1/n$, Z=4) (s. Kap 5.3.21 – 5.3.26, Anhang). Zusätzlich konnte die Bildung von $[Ni(tren)_2]_2[Sn_2S_6] \cdot 8H_2O$ und $[Ni(tren)(1,2\text{-dap})]_2[Sn_2S_6] \cdot 2H_2O$ beobachtet werden, welche vorher bei Reaktionen mit $\{[Ni(tren)]_2[Sn_2S_6]\}_n$ kristallisierten (s. Kap. 3.2.1).

Zuerst wurden jeweils 0.25 mmol des Komplexes und des Thiostannat-Salzes in ein 5 mL Schnappdeckelglas eingewogen und mit 0.5 mmol tren sowie 2 mL dest. Wasser versetzt. Anschließend wurde das verschlossene Gefäß eine Minute kräftig geschüttelt. Bei einigen Synthesen wurde bereits innerhalb dieser Zeit das Produkt (= Thiostannat) als feinkristallines Pulver gebildet. Das Pulver wurde abfiltriert und die Mutterlauge für die Züchtung von Einkristallen benutzt. Die klaren Reaktionslösungen bzw. Mutterlaugen wurden bei RT stehen gelassen. Bei nachfolgenden Versuchen wurde der Anteil an tren schrittweise auf 30% erhöht, um den Einfluss auf die Produktbildung zu untersuchen. Bei der Verwendung von $[Ni(en)_3]Cl_2$, $[Ni(1,2\text{-dach})_3]Cl_2$ und $[Ni(1,2\text{-dap})_3]Cl_2$ konnte beobachtet werden, dass bei niedrigen tren-Konzentrationen die wasserreichere Variante der Verbindung (z.B. $[Ni(tren)(en)]_2[Sn_2S_6] \cdot 6H_2O$) kristallisiert, bei Erhöhung der Amin-Konzentration zunächst die Bildung der wasserärmeren Verbindung (z.B. $[Ni(tren)(en)]_2[Sn_2S_6] \cdot 2H_2O$) bevorzugt ist. Bei Verlängerung der Reaktionszeit werden jedoch immer die wasserreichen Verbindungen gebildet (s. Abb. 3).

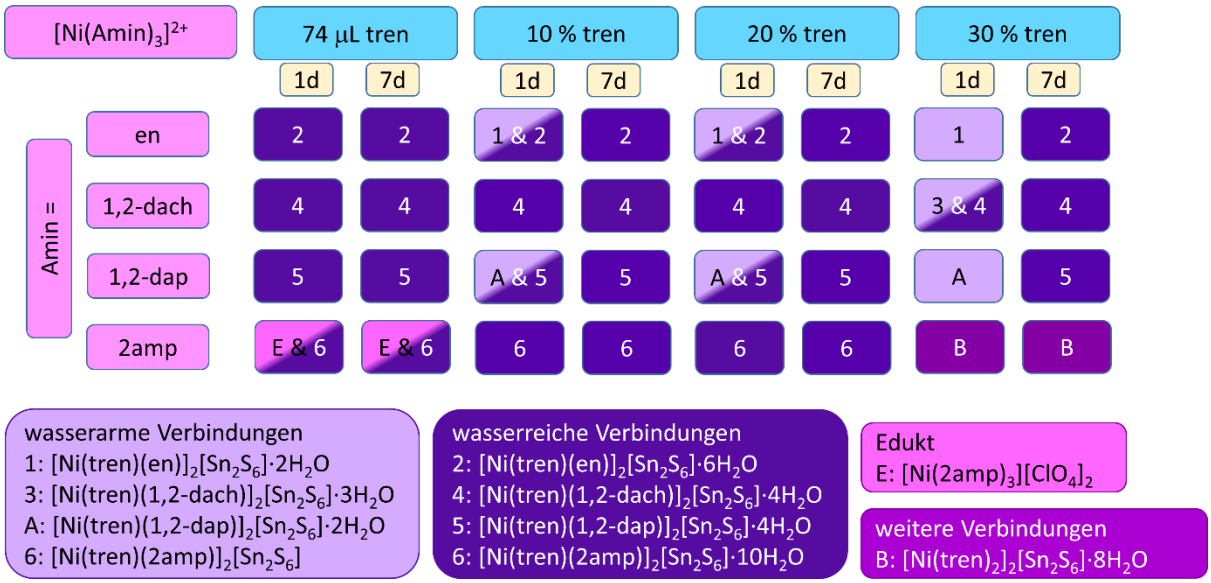

Abbildung 3: Übersicht der Produkte bei Synthesen mit $Na_4SnS_4 \cdot 14H_2O$ und $[Ni(Amin)_3]^{2+}$-Komplexen in wässrigen tren-Lösungen in Abhängigkeit von der tren-Konzentration und Reaktionszeit.

Mit $[Ni(2amp)_3][ClO_4]_2$ wurden andere Ergebnisse erhalten: Wurde eine weniger als 10% tren-Lösung verwendet, kristallisierte neben $[Ni(tren)(2amp)]_2[Sn_2S_6]\cdot 10H_2O$ auch der eingesetzte Komplex. Bei Konzentrationen von 10% und 20% tren wurde die Verbindung $[Ni(tren)(2amp)]_2[Sn_2S_6]\cdot 10H_2O$ allein erhalten. Wurde die Konzentration auf 30% erhöht, so kristallisierte $[Ni(tren)_2]_2[Sn_2S_6]\cdot 8H_2O$.

Alle Verbindungen weisen diskrete Ni^{2+} zentrierte Komplexe und $[Sn_2S_6]^{4-}$-Anionen auf, deren Anordnung durch zahlreiche Wasserstoffbrückenbindungen zwischen den terminalen S-Atomen der Thiostannat-Einheit und Wassermolekülen bzw. Aminogruppen der Amin-Liganden stabilisiert bzw. hervorgerufen wird. Die H_2O-Moleküle in den wasserreicheren Verbindungen bilden so genannte Wassercluster[107,108], welche in $[Ni(tren)(en)]_2[Sn_2S_6]\cdot 6H_2O$ und $[Ni(tren)(2amp)]_2[Sn_2S_6]\cdot 10H_2O$ besonders auffällig sind.

3.3.2.1 Die neuen Verbindungen $[Ni(tren)(en)]_2[Sn_2S_6]\cdot xH_2O$ (x =2 bzw. 6)

Der direkte Vergleich der Strukturen der beiden Verbindungen ergibt eine ähnliche Anordnung der Baueinheiten: In beiden Strukturen sind sowohl die $[Sn_2S_6]^{4-}$-Anionen als auch die $[Ni(tren)(en)]^{2+}$-Kationen in Reihen in der *ac*-Ebene angeordnet. Die Kationen weisen dabei eine alternierende Ausrichtung der en Liganden auf, während die Anionen mit den H_2O-Molekülen alternieren (Abb. 4, geometrische Parameter dieser Verbindungen befinden sich im Anhang, Abschnitt 5.3.21 und 5.3.22).

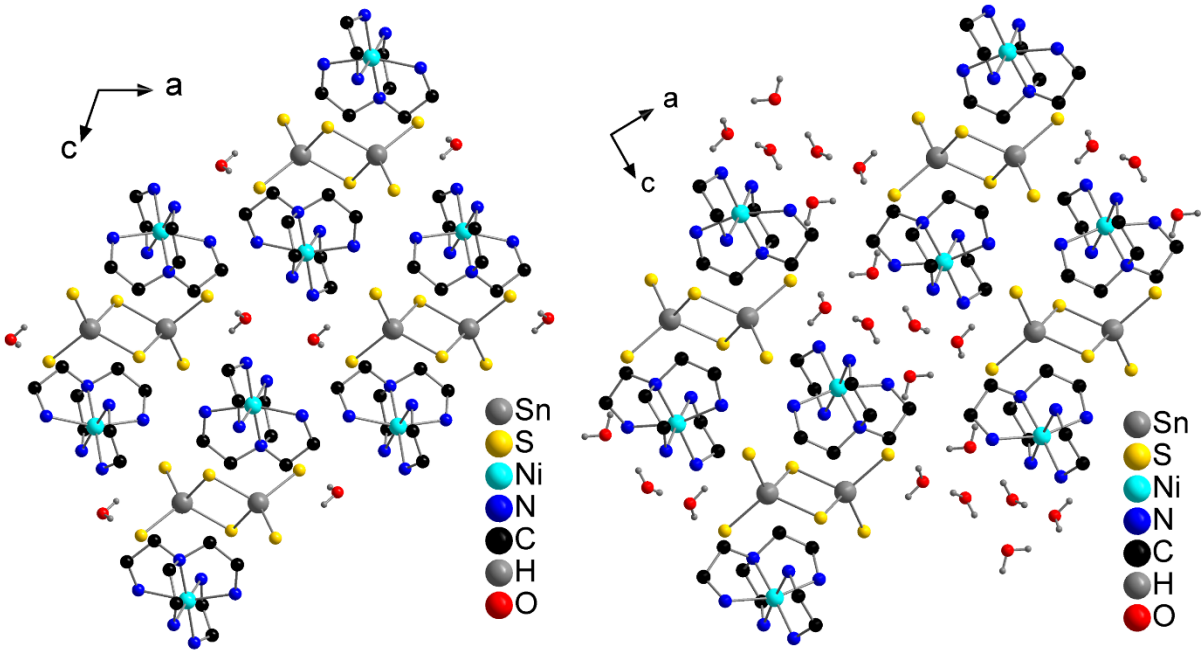

Abbildung 4: Ausschnitt aus den Strukturen der Verbindungen $[Ni(tren)(en)]_2[Sn_2S_6]\cdot xH_2O$ in der *ac*-Ebene.

In der wasserärmeren Verbindung liegen keine Wechselwirkungen zwischen benachbarten Wassermolekülen vor. Es werden aber Wasserstoffbrückenbindungen zu den terminalen S-Atomen der $[Sn_2S_6]^{4-}$-Einheit (H···S: 2.47 - 2.53 Å, Winkel: 146.1 – 170.5°) sowie mit H-Atomen benachbarter Amin-Liganden (H···O: 2.12 - 2.63 Å, Winkel: 138.9 - 163.9°) (Abb. 5, links)

beobachtet. Wasserstoffbrückenbindungen zwischen $[Sn_2S_6]^{4-}$-Anionen und Komplexen (H···S: 2.64 - 2.92 Å, Winkel: 142.3 - 174.9°) führen zu einem dreidimensionalen Netzwerk. In der Struktur von $[Ni(tren)(en)]_2[Sn_2S_6]\cdot 6H_2O$ bilden die Wassermoleküle Cluster, welche als D3-Cluster (Abb. 5, rechts) bezeichnet werden können[108] (O-H···O: 1.92 - 2.00 Å, Winkel: 161.4 - 175.5°). Die H_2O-Moleküle dieses Clusters weisen Wasserstoffbrückenbindungen zu den benachbarten Anionen (O-H···S: 2.35 - 2.60 Å, Winkel: 150.5 – 177.9°) und Kationen (N-H···O: 2.08 Å, Winkel: 177.6°; s. Abschnitt 5.3.21 & 5.3.22, Tab. 6, Anhang) auf (Abb. 5, rechts).

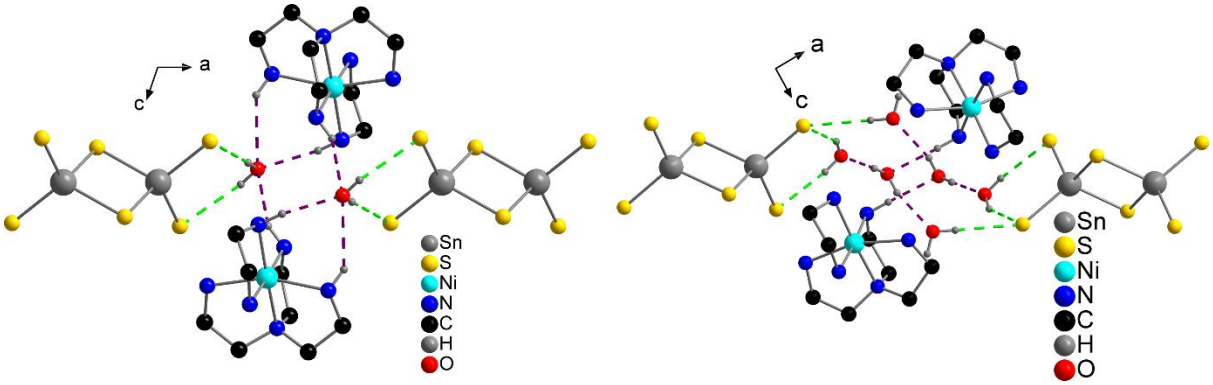

Abbildung 5: Wasserstoffbrückenbindungen (grün und violett gestrichelte Linien) in der Struktur von $[Ni(tren)(en)]_2[Sn_2S_6]\cdot 2H_2O$ (links) und $[Ni(tren)(en)]_2[Sn_2S_6]\cdot 6H_2O$ (rechts) zwischen H_2O-Molekülen, Anionen und Kationen.

Durch Wechselwirkungen zwischen H_2O und $[Sn_2S_6]^{4-}$-Anionen wird in der Struktur von $[Ni(tren)(en)]_2[Sn_2S_6]\cdot 6H_2O$ eine Schicht in der *bc*-Ebene gebildet, welche mit der Notation von Infantes als L4(4)16(6) beschrieben werden kann[108] (Abb. 6). Diese Beobachtung ist nicht ungewöhnlich und wurde beispielsweise für Cl^- (L8(6) [107]) und $[S_4O_6]^{2-}$ (L20(6) [109]) beobachtet.

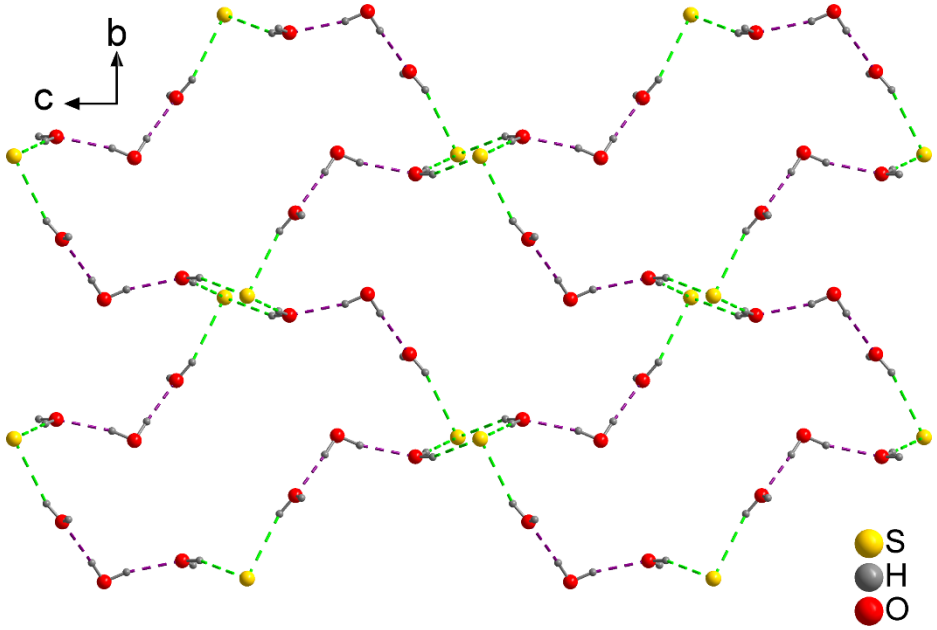

Abbildung 6: Anordnung der Wassermoleküle und S-Atome der $[Sn_2S_6]^{4-}$-Anionen mit Wasserstoffbrückenbindungen (grün und violett gestrichelte Linien) in der Struktur der Verbindung $[Ni(tren)(en)]_2[Sn_2S_6]\cdot 6H_2O$.

Eine Verknüpfung dieser Schichten über Ni(II)-Komplexe führt zur Ausbildung eines dreidimensionalen Netzwerkes.

3.3.2.2 Die neuen Verbindungen [Ni(tren)(1,2-dach)]$_2$[Sn$_2$S$_6$]·xH$_2$O (x =3 bzw. 4)

In beiden Verbindungen sind die Anionen und Kationen stabartig entlang der *a*-Achse ([Ni(tren)(1,2-dach)]$_2$[Sn$_2$S$_6$]·3H$_2$O) bzw. entlang der *c*-Achse ([Ni(tren)(1,2-dach)]$_2$[Sn$_2$S$_6$]·4H$_2$O) angeordnet (Abb. 7).

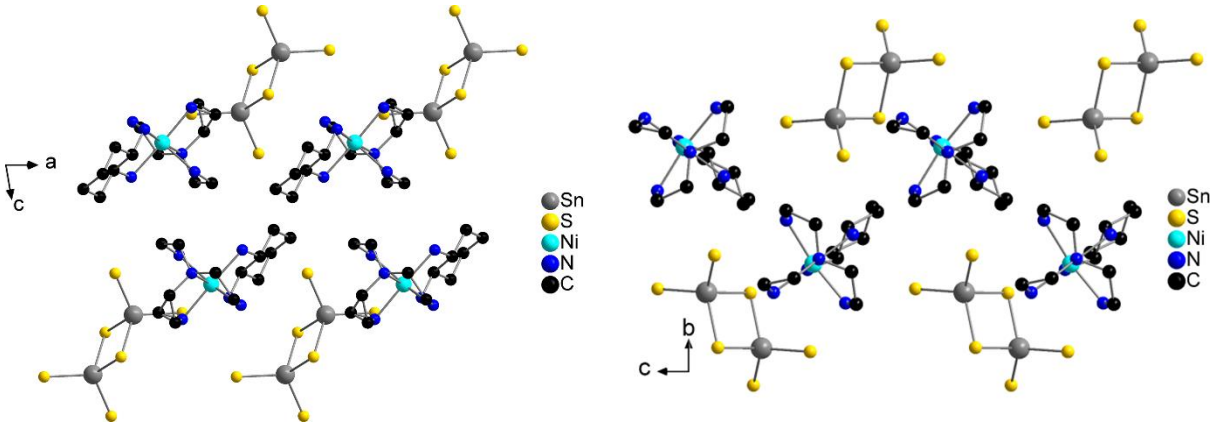

Abbildung 7: Anordnung der Anionen und Kationen der Verbindungen [Ni(tren)(1,2-dach)]$_2$[Sn$_2$S$_6$]·*x*H$_2$O (*x* = 3 (links) bzw. 4 (rechts)).

Der wesentliche Unterschied ist die Art der Stapelabfolge: In der Struktur von [Ni(tren)(1,2-dach)]$_2$[Sn$_2$S$_6$]·3H$_2$O liegt als Abfolge ABA'ABA' (A: [Ni(tren)(1,2-dach)]$^{2+}$, A': Kation mit inverser Orientierung, B: [Sn$_2$S$_6$]$^{4-}$) vor, während in der Struktur von [Ni(tren)(1,2-dach)]$_2$[Sn$_2$S$_6$]·4H$_2$O die [Sn$_2$S$_6$]$^{4-}$-Anionen eine alternierende Orientierung aufweisen, so dass die Abfolge ABA'AB'A' ist.

In den Strukturen beider Verbindungen befinden sich die [Sn$_2$S$_6$]$^{4-}$-Anionen zwischen zwei entgegengesetzt orientierten [Ni(tren)(1,2-dach)]$^{2+}$-Kationen. Zwischen Kationen, Anionen und Wassermolekülen werden Wasserstoffbrückenbindungen ausgebildet (Abb. 8, die geometrischen Parameter dieser Verbindungen befinden sich im Anhang, Abschnitt 5.3.23 und 5.3.24). In der Struktur von [Ni(tren)(1,2-dach)$_2$]$_2$[Sn$_2$S$_6$]·3H$_2$O konnten nicht alle H-Atome der Wassermoleküle lokalisiert werden, über Wechselwirkungen dieser Wassermoleküle kann daher keine fundierte Aussage getroffen werden.

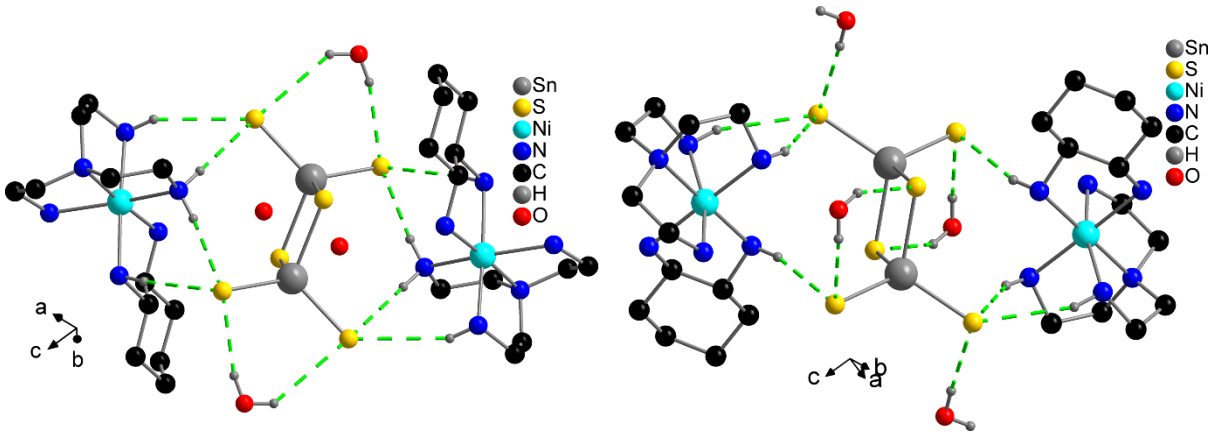

Abbildung 8: Wasserstoffbrücken (grün gestrichelte Linien) in den Strukturen von [Ni(tren)(1,2-dach)]$_2$[Sn$_2$S$_6$]·3H$_2$O (links) und [Ni(tren)(1,2-dach)]$_2$[Sn$_2$S$_6$]·4H$_2$O (rechts).

Ein wesentlicher struktureller Unterschied ist die Orientierung eines Wassermoleküls, welches mit den terminalen S-Atomen das Anions wechselwirkt: In der Struktur von $[Ni(tren)(1,2\text{-dach})]_2[Sn_2S_6]\cdot 3H_2O$ verbrückt ein Wassermolekül die beiden terminalen S-Atome, während in der Struktur von $[Ni(tren)(1,2\text{-dach})]_2[Sn_2S_6]\cdot 4H_2O$ ein Wassermolekül nur mit einem der terminalen S-Atome eine Wasserstoffbrückenbindung aufweist. Weitere Wechselwirkung dieses Wassermoleküls mit benachbarten Wassermolekülen führt zur Ausbildung von D2-Clustern[108], welche die $[Sn_2S_6]^{4-}$-Anionen zu Ketten entlang der *a* Achse verknüpfen (Abb. 9). Diese Ketten sind über die Ni(II) zentrierten Komplexe zu einem dreidimensionalen Netzwerk verbunden.

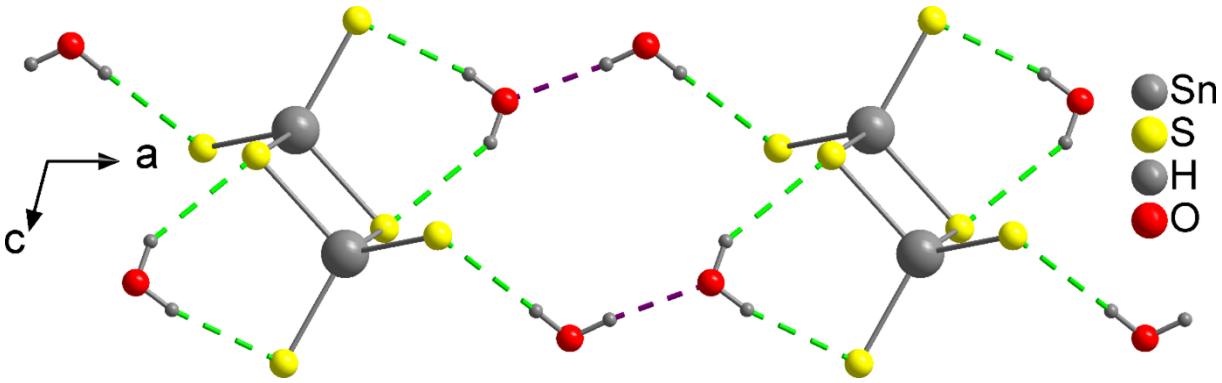

Abbildung 9: Verknüpfung der $[Sn_2S_6]^{4-}$-Anionen in der Struktur von $[Ni(tren)(1,2\text{-dach})]_2[Sn_2S_6]\cdot 4H_2O$ über Wasserstoffbrückenbindungen (grün und violett gestrichelte Linien) mit H_2O-Molekülen.

In $[Ni(tren)(1,2\text{-dach})]_2[Sn_2S_6]\cdot 3H_2O$ wird die Ausbildung von Schichten durch Verknüpfung der unterschiedlichen Baueinheiten über Wasserstoffbrückenbindungen beobachtet (Abb. 10).

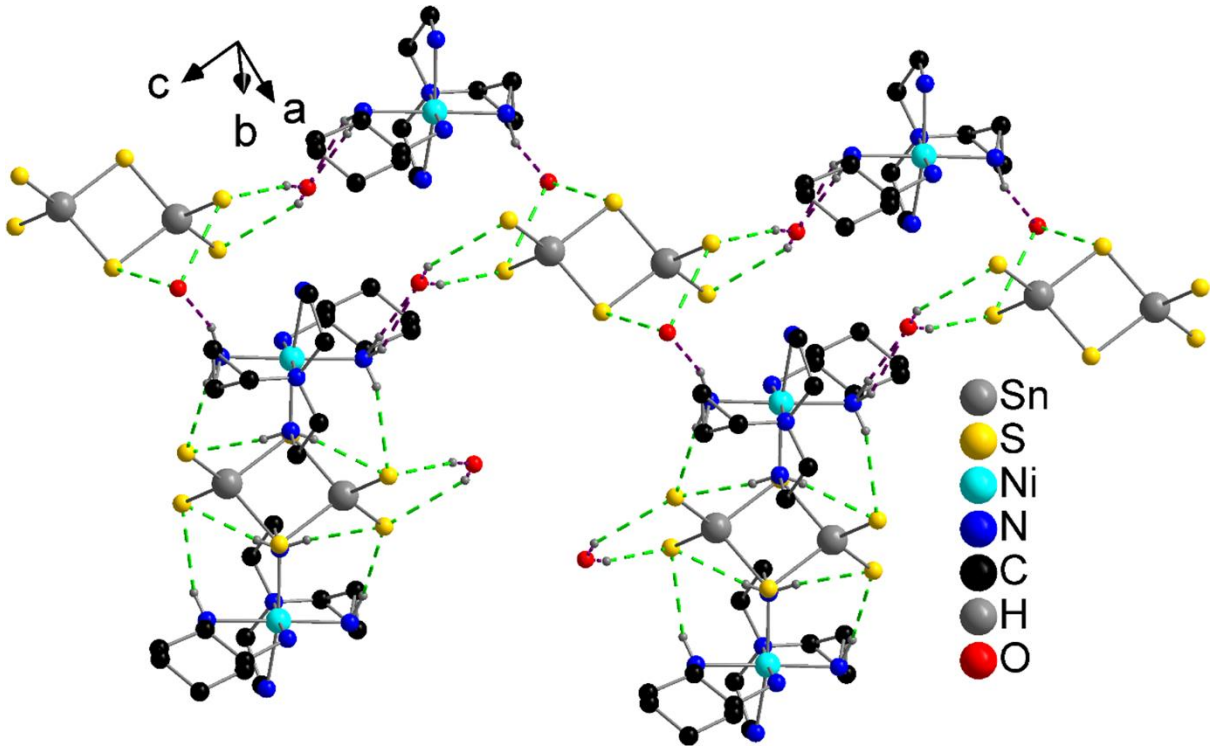

Abbildung 10: Schichtartige Anordnung der Anionen und Kationen in der Struktur von $[Ni(tren)(1,2\text{-dach})]_2[Sn_2S_6]\cdot 3H_2O$ generiert durch Wasserstoffbrückenbindungen (grün und violett gestrichelte Linien).

3.3.2.3 Die neue Verbindung [Ni(tren)(1,2-dap)]$_2$[Sn$_2$S$_6$]·4H$_2$O

Der strukturelle Vergleich der neuen Verbindung [Ni(tren)(1,2-dap)]$_2$[Sn$_2$S$_6$]·4H$_2$O (geometrische Parameter dieser Verbindung befinden sich im Anhang, Abschnitt 5.3.25) mit der wasserärmeren Verbindung [Ni(tren)(1,2-dap)]$_2$[Sn$_2$S$_6$]·2H$_2$O (s. Kap. 3.2.1) zeigt deutliche Unterschiede auf (Abb. 11). Die Struktur der wasserärmeren Verbindung ist analog zu der von [Ni(tren)(en)]$_2$[Sn$_2$S$_6$]·2H$_2$O aufgebaut: Alle Baueinheiten sind entlang der *a*-Achse in Stapeln angeordnet. Die [Sn$_2$S$_6$]$^{4-}$-Anionen alternieren mit H$_2$O-Molekülen, während die Ni(II)-zentrierten Komplexe mit entgegen gesetzter Orientierung alternieren. In der Struktur von [Ni(tren)(1,2-dap)]$_2$[Sn$_2$S$_6$]·4H$_2$O sind die Anionen und Kationen wellenförmig entlang der *c*-Achse angeordnet.

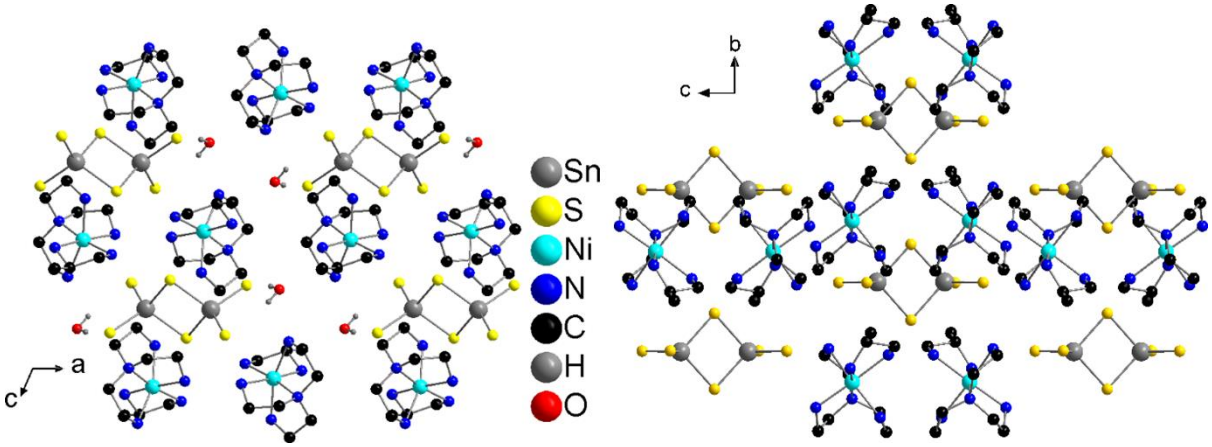

Abbildung 11: Anordnung der Anionen und Kationen in den Strukturen der Verbindungen [Ni(tren)(1,2-dap)]$_2$[Sn$_2$S$_6$]·*x*H$_2$O (*x* = 2(links) bzw. 4 (rechts)).

Die H$_2$O-Moleküle in [Ni(tren)(1,2-dap)]$_2$[Sn$_2$S$_6$]·4H$_2$O befinden sich zwischen den [Sn$_2$S$_6$]$^{4-}$-Anionen entlang der *b*-Achse. Wasserstoffbrückenbindungen zwischen Wassermolekülen und [Sn$_2$S$_6$]$^{4-}$-Anionen generieren Ketten entlang der *b*-Achse und Schichten in der *ab*-Ebene (Abb. 12, Abschnitt 5.3.25, Tab. 6, Anhang). Diese Schichten sind über Wasserstoffbrückenbindungen zu den N-Atomen der Komplexe zu einem dreidimensionalen Netzwerk verknüpft.

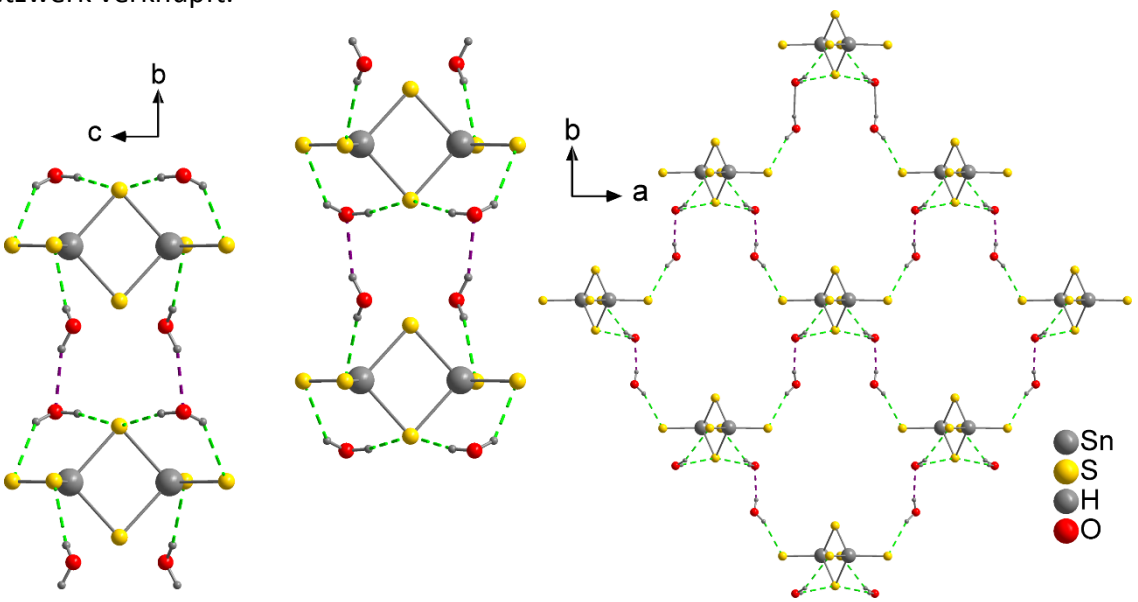

Abbildung 12: Schichten in der *ab*-Ebene erzeugt durch Wasserstoffbrückenbindungen Wechselwirkungen (grün und violett gestrichelte Linien) in der Struktur von [Ni(tren)1,2-dap)]$_2$[Sn$_2$S$_6$]·4H$_2$O.

3.3.2.4 Die neue Verbindung $[Ni(tren)(2amp)]_2[Sn_2S_6]\cdot 10H_2O$

In der Struktur sind die $[Sn_2S_6]^{4-}$-Anionen alternierend entlang [010] angeordnet (Abb. 13, geometrische Parameter dieser Verbindung befinden sich im Anhang, Abschnitt 5.3.26). Im Gegensatz zu $[Ni(tren)(2amp)]_2[Sn_2S_6]$ (s. Kap. 3.2.2) werden zwischen den 2amp-Molekülen keine π-π-Wechselwirkungen beobachtet.

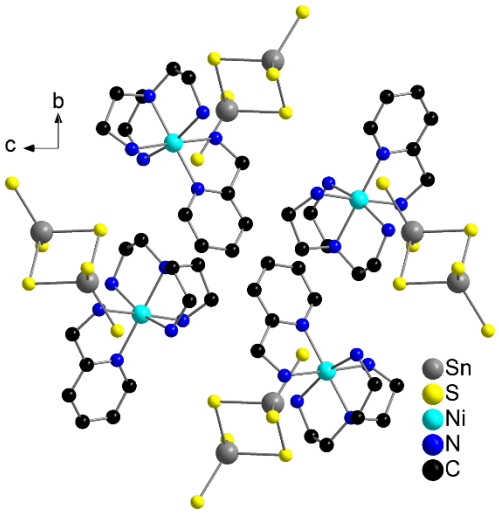

Abbildung 13: Räumlichen Anordnung der Anionen und Kationen in der Verbindung $[Ni(tren)(2amp)]_2[Sn_2S_6]\cdot 10H_2O$.

Die Wassermoleküle in der Struktur von $[Ni(tren)(2amp)]_2[Sn_2S_6]\cdot 10H_2O$ sind über O-H···O-Bindungen (Abstände: 1.92 – 2.54 Å, Winkel: 161.9 – 176.1°) zu Ketten entlang [001] verknüpft. O-H···S-Bindungen (Abstände: 2.42 – 2.48 Å, Winkel: 167.2 – 174.8°) zu terminalen S-Atomen der $[Sn_2S_6]^{4-}$-Anionen führen zur Ausbildung von Schichten (Notation: L6(4)8(8)12(8))[107,108,108] (Abb. 14, links). Diese Schichten sind wiederum über $[Sn_2S_6]^{4-}$-Anionen zu einem dreidimensionalen Netzwerk verknüpft, in dessen Poren sich die $[Ni(tren)(2amp)]^{2+}$-Komplexe befinden (Abb. 14, rechts).

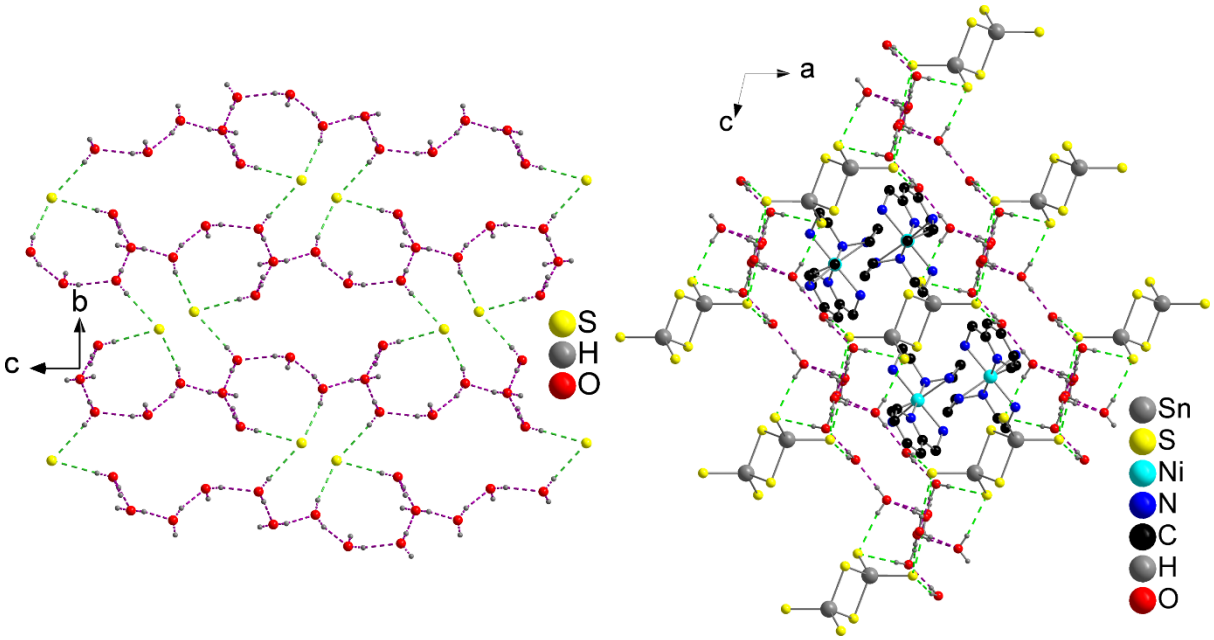

Abbildung 14: Verknüpfung der Wassermoleküle und $[Sn_2S_6]^{4-}$-Anionen über O-H···O- und O-H···S-Bindungen zu Schichten (links) und einem dreidimensionalen Netzwerk mit den Komplexen in den Poren (rechts), gestrichelte Linien: Wasserstoffbrückenbindungen.

3.3.2.5 Spektroskopische Untersuchungen der neuen Verbindungen

Die Raman-Spektren der in Kap. 3.3.2.1 – 3.3.2.4 vorgestellten Verbindungen weisen die für diese Verbindungsklasse typischen Sn-S-Schwingungen im Bereich von 400 bis 100 cm^{-1} auf und lassen sich auf Basis von Literaturdaten für die Verbindung $Na_4Sn_2S_6{\cdot}14H_2O$ zuordnen (Tab. 13).[88]

Tabelle 13: Resonanzen der Raman-Spektren und deren Zuordnung auf der Basis der Absorptionen von $Na_4Sn_2S_6{\cdot}14H_2O$.

$[Sn_2S_6]^{4-}$	**1**	**2**	**3**	**4**	**5**	**6**	**Zuordnung**
391	380	380	377	378	381	375	$\nu_{as}(SnS_2)$
377	368	369					$\nu_s(SnS_2)$
341	341	342	339	336	340	331	ν_{as}(Sn-S-Sn)
281	279	279	274	277	272	268	ν (Sn_2S_2)
190	191		192		191		
151			168	161	162		Deformations-
136	130	133	133	128	132		&
	117	118	117			123	Torsionsschwingungen
	85	84	85	85	84	84	

1: $[Ni(tren)(en)]_2[Sn_2S_6]{\cdot}2H_2O$ 4: $[Ni(tren)(1,2\text{-dach})]_2[Sn_2S_6]{\cdot}4H_2O$
2: $[Ni(tren)(en)]_2[Sn_2S_6]{\cdot}6H_2O$ 5: $[Ni(tren)(1,2\text{-dap})]_2[Sn_2S_6]{\cdot}4H_2O$
3: $[Ni(tren)(1,2\text{-dach})]_2[Sn_2S_6]{\cdot}3H_2O$ 6: $[Ni(tren)(2amp)]_2[Sn_2S_6]{\cdot}10H_2O$

Anhand dieser Daten lässt sich z.T. ein Einfluss des Ni(II)-Komplexes und der Kristallwassermoleküle auf die energetische Lage der Signale feststellen: In der Verbindung $Na_4Sn_2S_6{\cdot}14H_2O$ werden die Sn-S_{term} Streckschwingungen bei 391 und 377 cm^{-1} beobachtet. Diese Signale sind für die Verbindungen mit $[Ni(tren)(en)]^{2+}$-Komplexen zu kleineren Wellenzahlen verschoben, ein Einfluss des Wassergehalts kann nicht festgestellt werden. Bei den anderen Verbindungen ist nur eine Sn-S_{term} Streckschwingungen zu beobachten. Bei $[Ni(tren)(2amp)]_2[Sn_2S_6]{\cdot}$sind alle Signale zu kleineren Wellenzahlen verschoben.

Die Absorptionen in den IR-Spektren lassen sich denen von tren und den jeweiligen Aminmolekülen zuordnen.[110–114] Die Schwingungen von H_2O treten im Bereich 3420 – 3640 cm^{-1} (Streckschwingungen) sowie zwischen 1630 und 1660 cm^{-1} (Deformationsschwingungen) auf. Die Signale der Ni-N-Schwingung befinden sich in dem Bereich um 410 – 440 cm^{-1}. (s. Abb. A4 - A7 und Tab. A1 – A4, Abschnitt 5.5, Anhang).

In den UV/vis-Spektren mit der Kubelka-Munk-Methode sind neben der Bandlücke zwischen 3.2 – 3.4 eV jeweils zwei schwache Banden vor der Absorptionskante beobachten. Diese lassen sich den d-d Übergängen $^3A_{2g} \rightarrow {}^3T_{2g}$ (~1.4 – 1.5 eV) und $^3A_{2g} \rightarrow {}^3T_{1g}(^3F)$ (~2.3 – 2.4 eV) des Ni^{2+}-Zentrums der Komplexkationen zuordnen (Tab. 14).[115]

Tabelle 14: Bandlücken und elektronische Übergänge Banden in den UV/vis-Spektren der Verbindungen mit dem [Ni(tren)]-Komplex. Angaben in eV. .

1	**2**	**3**	**4**	**5**	**6**	**Zuordnung**
~1.38	~1.39	~1.48	~1.43	~1.40	~1.44	$^3A_{2g} \rightarrow {}^3T_{2g}$
~2.34	~3.34	~2.33	~2.33	~2.32	~2.33	$^3A_{2g} \rightarrow {}^3T_{1g}$ (^3F)
3.23	3.16	3.43	3.29	3.32	3.28	optical band gap

1: $[Ni(tren)(en)]_2[Sn_2S_6]\cdot 2H_2O$ 4: $[Ni(tren)(1,2\text{-dach})]_2[Sn_2S_6]\cdot 4H_2O$

2: $[Ni(tren)(en)]_2[Sn_2S_6]\cdot 6H_2O$ 5: $[Ni(tren)(1,2\text{-dap})]_2[Sn_2S_6]\cdot 4H_2O$

3: $[Ni(tren)(1,2\text{-dach})]_2[Sn_2S_6]\cdot 3H_2O$ 6: $[Ni(tren)(2amp)]_2[Sn_2S_6]\cdot 10H_2O$

3.3.3 Synthesen mit weiteren $[TM(Amin)_n]Cl_2$- bzw. $[TM(Amin)_n][ClO_4]_2$- Komplexen und Na_4SnS_4 $14H_2O$ bei RT

Zur Überprüfung des neuen Syntheseweges wurden weitere Synthesen mit $[Ni(tren)(H_2O)Cl]Cl$, $[Ni(en)_3]Cl_2$, $[Ni(1,2\text{-dach})_3]Cl_2$, $[Ni(1,2\text{-dap})_3]Cl_2$ und $[Ni(2amp)_3][ClO_4]_2$ durchgeführt.

Jeweils 0.25 mmol des Komplexes und 0.25 mmol des Thiostannatsalzes wurden mit 0.5 mmol Amin (= tren, en, 1,2-dach, 1,2-dap, 2amp) sowie 2 mL dest. H_2O versetzt, in einem 5 mL Schnappdeckelglas gut durchmischt und bei RT aufbewahrt. Bei der Verwendung von $[Ni(2amp)_3][ClO_4]_2$ wurden 10% Aminlösungen verwendet, damit nicht nur Komplex als Produkt erhalten wird (Tab. 15).

Tabelle 15: Ergebnisse der Synthesen mit $[Ni(Amin)_3]^{2+}$-Komplexen und $Na_4SnS_4{\cdot}14H_2O$ in wässrigen Aminlösungen

	$[Ni(tren)]^{2+}$	$[Ni(en)_3]^{2+}$	$Ni(1,2\text{-dach})_3]^{2+}$	$[Ni(1,2\text{-dap})_3]^{2+}$	$[Ni(2amp)_3]^{2+}$
tren	A	B	C	D	E
en	B	F	?	---	**G**
1,2-dach	C	?	H	H	?
1,2-dap	D	?	H	I	**G**
2amp	E	?	?	?	**G**

A = $[Ni(tren)_2[Sn_2S_6]{\cdot}8H_2O$	F = $[Ni(en)_3]_2[Sn_2S_6]$
B = $[Ni(tren)(en)]_2[Sn_2S_6]{\cdot}6H_2O$	**G = $[Ni(2amp)_3]_2[Sn_2S_6]{\cdot}9.5H_2O$**
C = $[Ni(tren)(1,2\text{-dach})]_2[Sn_2S_6]{\cdot}4H_2O$	H = $[Ni(1,2\text{-dach})_3]_2[Sn_2S_6]{\cdot}4H_2O$
D = $[Ni(tren)(1,2\text{-dap})]_2[Sn_2S_6]{\cdot}4H_2O$	I = $[Ni(1,2\text{-dap})_3]_2[Sn_2S_6]$
E = $[Ni(tren)(2amp)]_2[Sn_2S_6]{\cdot}10H_2O$	
? = unbekannte kristalline Verbindung	--- = röntgenamorphes Produkt

Wenn der Komplex das Aminmolekül enthält, welches auch zugesetzt wurde, so werden die entsprechenden Thiostannate mit der allgemeinen Formel $[Ni(Amin)_3]_2[Sn_2S_6]{\cdot}xH_2O$[43,50] erhalten. Neben den bereits bekannten Verbindungen wurde auf diesem Weg die neue Verbindung $[Ni(2amp)_3]Sn_2S_6]{\cdot}9.5H_2O$ ($P2_1/n$, Z=4) synthetisiert (s. Kap. 3.3.3.1). Bei den Synthesen mit $[Ni(tren)(H_2O)Cl]Cl$ wurden Verbindungen mit der allgemeinen Formel $[Ni(tren)(Amin)]_2[Sn_2S_6]{\cdot}xH_2O$ gebildet, analog zu den Synthesen mit $[Ni(Amin)_3]^{2+}$ in wässriger tren Lösung (s. Kap. 3.3.2). Bei den Synthesen mit $[Ni(1,2\text{-dap})_3]Cl_2$, $Na_4SnS_4{\cdot}14H_2O$ und 0.5 mmol 1,2-dach kristallisierte $[Ni(1,2\text{-dach})_3]_2[Sn_2S_6]{\cdot}4H_2O$[43]. D.h., 1,2-dach ersetzt den Liganden 1,2-dap. Der Ligand 2amp scheint stärkere eine N-Donorfähigkeit im Vergleich zu en und 1,2-dap zu haben, da bei Synthesen mit $[Ni(en)_3]^{2+}$ bzw. $[Ni(1,2\text{-dap})_3]^{2+}$ in wässriger 2amp Lösung jeweils $[Ni(2amp)_3]_2[Sn_2S_6]{\cdot}9.5H_2O$ gebildet wurde. Bei allen weiteren Kombinationen konnte bisher nur feinkristalline Pulver erhalten und keine weitere Verbindung identifiziert werden.

Diese orientierenden Versuche verdeutlichen, dass die Bildung von Thiostannaten nicht nur auf das Amin-tren-System beschränkt ist. Allerdings müssen die Synthesebedingungen weiter optimiert werden, um Einkristalle für die Strukturbestimmung zu erhalten.

Die Erweiterung dieser Syntheseroute auf weitere TM^{2+} (TM = Mn, Fe, Co) ist schwieriger, da diese $[TM(Amin)_3]^{2+}$-Komplexe nicht so einfach herstellbar sind wie die Ni^{2+}-zentrierten Komplexe. Ausnahmen sind $[TM(phen)_3][ClO_4]_2$ und $[TM(2,2'\text{-bipy})_3][ClO_4]_2$.
Von diesen beiden Komplexen wurden 0.25 mmol $[Ni(phen)_3][ClO_4]_2$ bzw. $[Ni(2,2'\text{-bipy})_3][ClO_4]_2$ mit 0.25 mmol des Thiostannat-Salzes in 2 mL 30% Aminlösungen auf analoge Weise eingesetzt. Niedrigere Aminkonzentrationen führten zur Kristallisation der eingesetzten Komplexe. Bei den Synthesen in wässriger tren-Lösung konnte die Verbindung $[Ni(tren)_2]_2[Sn_2S_6]\cdot 8H_2O$ und bei Versuchen mit wässriger 2amp-Lösung die Verbindung $[Ni(2amp)_3]_2[Sn_2S_6]\cdot 9.5H_2O$ erhalten werden. Bei Synthesen mit anderen Aminen konnten die Produkte noch nicht identifiziert werden. (Tab. 16).

Tabelle 16: Ergebnisse der Synthesen mit $[Ni(phen)_3]^{2+}$ bzw. $[Ni(2,2'\text{-bipy})_3]^{2+}$ und $Na_4SnS_4\cdot 14H_2O$ in 30% Aminlösungen

Komplex	tren	en	1,2-dach	1,2-dap	2amp
$[Ni(phen)_3][ClO_4]_2$	$[Ni(tren)_2]_2[Sn_2S_6]$	?	?	?	$[Ni(2amp)_3]_2[Sn_2S_6]$
$[Ni(2,2'\text{-bipy})_3][ClO_4]_2$	$[Ni(tren)_2]_2[Sn_2S_6]$	?	?	?	$[Ni(2amp)_3]_2[Sn_2S_6]$

? = Produkt konnte noch nicht identifiziert werden
Kristallwasser wurde aus Gründen der besseren Übersicht weggelassen

Diese Ergebnisse belegen, dass für die Synthese von nickelhaltigen Thiostannaten das entsprechende Amin nicht im Komplex enthalten sein muss. Da die anderen $[TM(phen)_3][ClO_4]_2$ bzw. $[TM(2,2'\text{-bipy})_3][ClO_4]$ ebenfalls leicht zugänglich sind, könnte mit diesen Precursoren überprüft werden, ob sich die neue Syntheseroute auf andere TM übertragen lässt.

3.3.3.1 Die neue Verbindung $[Ni(2amp)_3]_2[Sn_2S_6]\cdot 9.5H_2O$

Im Gegensatz zu anderen Verbindungen mit diskreten $[Sn_2S_6]^{4-}$-Anionen und Ni(II) Komplexkationen mit bidentaten Aminen (en, 1,2-dach, 1,2-dap) konnte die Verbindung $[Ni(2amp)_3]_2[Sn_2S_6]\cdot 9.5H_2O$ ($P2_1/n$, Z=4; geometrische Parameter dieser Verbindung befinden sich in Abschnitt 5.3.27, Anhang) nicht unter solvothermalen Bedingungen, sondern nur unter ambienten Bedingungen erhalten werden.

In der Verbindung sind die $[Sn_2S_6]^{4-}$-Anionen entlang der *a*- und *c*-Achse gestapelt. Die $[Ni(2amp)_3]^{2+}$-Komplexe sind paarweise in allen drei Raumrichtungen angeordnet. Diese Paare werden durch π-π–Wechselwirkungen (T-shaped: 3.906 - 4.216°Å)[82,116] gebildet (Abb. 15, links). Zwischen Anion und Kationen werden Wasserstoffbrückenbindungen beobachtet (N-H···S: Abstände: 2.42 – 2.81 Å, Winkel: 147.5 – 175.3°; Abb. 15, rechts).

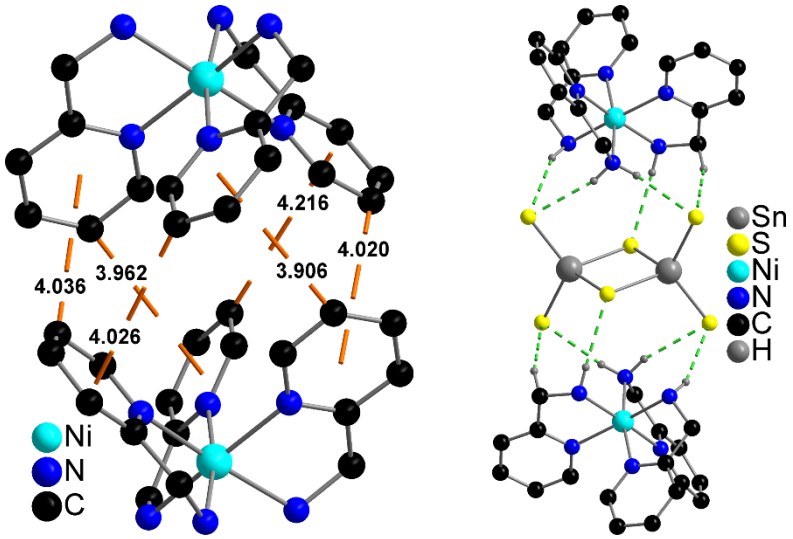

Abbildung 15: links: π-π–Wechselwirkungen (orange gestrichelte Linien) zwischen $[Ni(2amp)_3]^{2+}$-Komplexen. rechts: Wasserstoffbrückenbindungen (grüne gestrichelte Linien) zwischen den S-Atomen des $[Sn_2S_6]^{4-}$-Anions und Wasserstoffatomen der Liganden benachbarter $[Ni(2amp)_3]^{2+}$-Komplexe.

Das bemerkenswerte an dieser Struktur ist die Anordnung der Wassermoleküle, welche entlang [010] zu Wasserbändern angeordnet sind. Jeweils zwölf Wassermoleküle sind über O-H···O-Bindungen zu Ringen verbunden, welche über vier gemeinsame H_2O-Moleküle zu Bändern in der *bc*-Ebene kondensiert sind. Der resultierende Wassercluster kann nach der Notation von Infantes et al. [108] als T12(4) beschrieben werden (Abb. 16, links). Zwei weitere Wassermoleküle befinden sich außerhalb dieser Wasserbänder und sind an jeweils einen der 12er Ringe gebunden. Über ähnliche Wasserbänder mit kleineren Ringen, wie z.B. T5(2)[117] oder T8(3)[118] wurde bereits berichtet. Einer der kristallographisch unabhängigen $[Ni(2amp)_3]^{2+}$-Komplexe befindet sich jeweils ober- und unterhalb der 12er Ringe, während der zweite Komplex in der Peripherie des Wasserclusters lokalisiert ist und mit diesem über Wasserstoffbrückenbindungen verbunden ist. Die Wasserstoffbrückenbindungen generieren ein dreidimensionales Netzwerk (Abb. 16, rechts; s. Abschnitt 5.3.27, Tab. 6, Anhang).

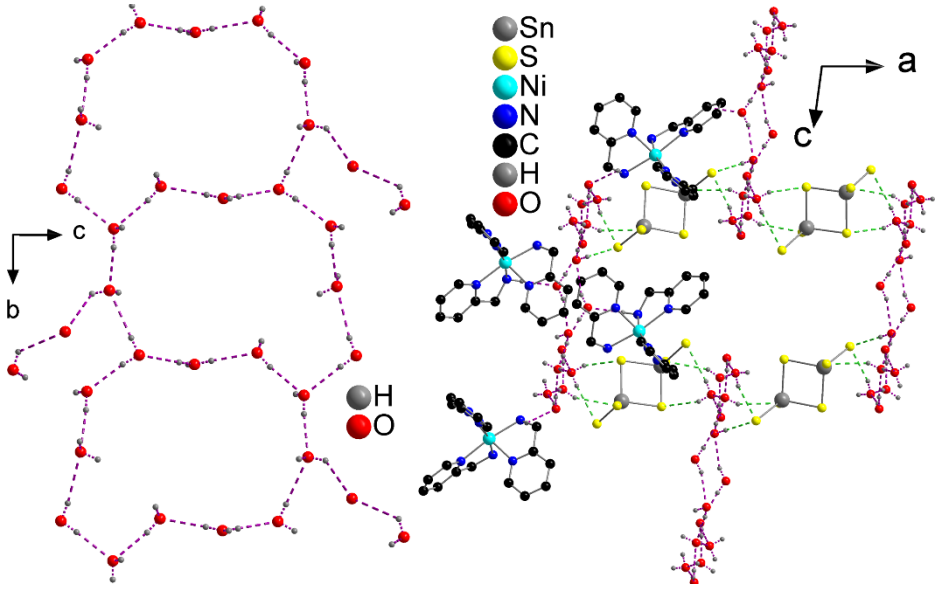

Abbildung 16: links: Wasserstoffbrückenbindungen (violett gestrichelte Linien) zwischen den Wassermolekülen in der *bc*-Ebene. rechts: Anordnung der Anionen, Kationen und H_2O-Moleküle in der Struktur von $[Ni(2amp)_3]_2[Sn_2S_6]\cdot 9.5H_2O$ (Wasserstoffbrückenbindungen: grün und violett gestrichelte Linien).

Spektroskopische Untersuchungen

Die Zuordnung der für $[Ni(2amp)_3]_2[Sn_2S_6]\cdot 9.5H_2O$ beobachteten Ramanresonanzen (s. Abb. A8, Abschnitt 5.6, Anhang) basiert auf Daten von $Na_4Sn_2S_6\cdot 14H_2O$ (s. Tab. A5, Abschnitt 5.6, Anhang).[88] Die Sn-S_{term}-Streckschwingung liegt bei 391 und 377 cm^{-1}. Die Resonanz bei 377 cm^{-1} sowie das Signal für die Sn-S-S Schwingungen bei 340 cm^{-1} sind aufgespalten. Dies wurde auch bei Verbindungen mit anderen aromatischen Liganden (phen und 2,2-bipy) beobachtet. Allerdings ist der Komplex in diesen Verbindungen kovalent über Ni-S an das Thiostannatanion gebunden.[45,55] Die Bande des Sn_2S_2-Ringes ist Vergleich zu anderen Verbindungen zu kleineren Wellenzahlen (273 cm^{-1}) verschoben. Die Aufspaltung von Resonanzen und diese Verschiebung könnten durch Wasserstoffrückenbindungen verursacht werden.[43,76] Die Signale unterhalb von 200 cm^{-1} werden von Deformations- und Torsionsschwingungen verursacht und lassen sich nicht genauer zuordnen. Die Absorptionen im IR-Spektrum der Verbindung $[Ni(2amp)_3]_2[Sn_2S_6]\cdot 9.5H_2O$ konnten dem Liganden 2amp[114,119] sowie Kristallwasser zugeordnet werden (s. Abb. A9 und Tab. A6, Abschnitt 5.6, Anhang).

Mit der Kubelka-Munk-Methode konnte für die Verbindung $[Ni(2amp)_3]_2[Sn_2S_6]\cdot 9.5H_2O$ eine optische Bandlücke von 3.1 eV aus dem UV/Vis Spektrum ermittelt werden. Die Bandlücke kann die Farbe dieser Verbindung (violett) nicht erklären, so dass d-d-Übergänge des Ni^{2+}-Ions dafür verantwortlich sind.[115,120] Diese Übergänge treten bei 1.4 eV ($^3A_{2g} \rightarrow {}^3T_{2g}$) und 2.3 eV ($^3A_{2g} \rightarrow {}^3T_{1g}(^3F)$) auf.

Thermische Untersuchungen

Beim Aufheizen in Stickstoffatmosphäre treten in der TG-Kurve drei Masseverluste (Δm = 12%, 30% und 15%) auf, welche von endothermen Ereignissen in der DTA-Kurve begleitet werden (Abb. 17). Die DTA-Kurve als auch die DTG-Kurve deuten darauf hin, dass der erste Massenverlust komplizierter ist. Die einzelnen Masseabgaben konnten jedoch auch mit einer Heizrate von 1 °C/Min nicht weiter aufgelöst werden. Der Masseverlust der ersten Stufe stimmt in guter Näherung mit dem Verlust aller Wassermoleküle überein. Die beiden weiteren Masseverluste können dem schrittweisen Verlust der aromatischen Liganden zugeordnet werden. Wichtig bei der Durchführung der Messungen war, auf das Evakuieren der Probenkammer vor der Messung zu verzichten. Normalerweise wird die Probekammer bei Stickstoffmessungen je dreimal evakuiert und mit Stickstoff gespült, um eventuell vorhandene Restmengen von Sauerstoff zu entfernen. Bei diesem Vorgehen konnte bei den Messungen die erste Masseabgabe in der TG-Kurve nicht mehr beobachtet werden und der Masseverlust begann erst bei ~160°C. Dies legt den Schluss nahe, dass bereits durch Evakuieren das Kristallwasser entfernt wird.

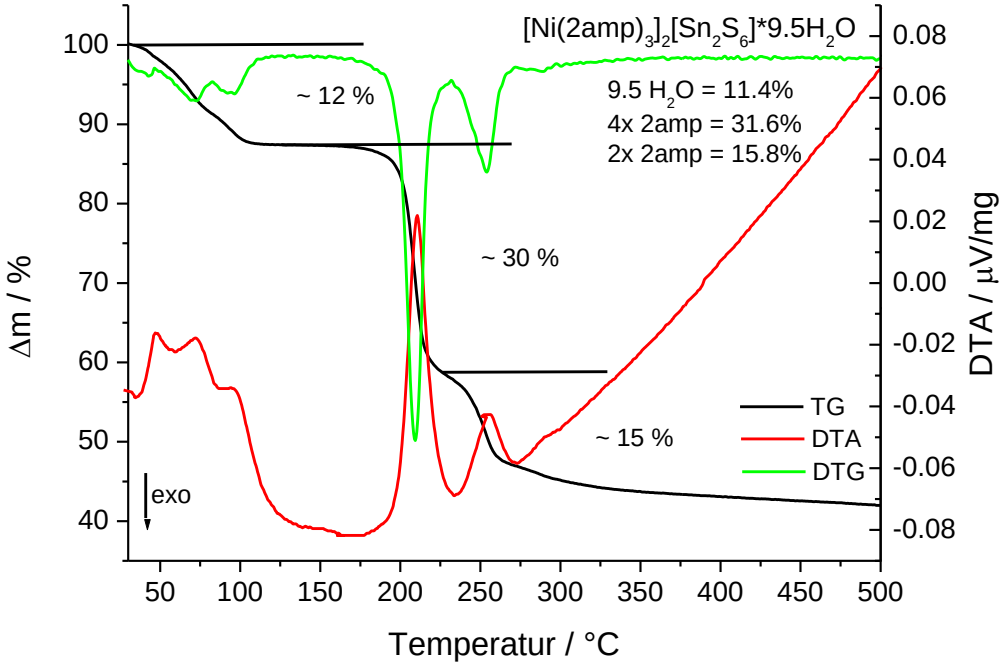

Abbildung 17: TG-, DTA- und DTG-Kurven des thermischen Abbaus der Verbindung $[Ni(2amp)_3]_2[Sn_2S_6]\cdot 9.5H_2O$ (Heizrate: 4 °C/Min, N_2-Atmosphäre).

Pulverdiffraktometrische Untersuchungen belegen, dass nach dem ersten Masseverlust eine neue kristalline Verbindung erhalten wird (Abb. 18).

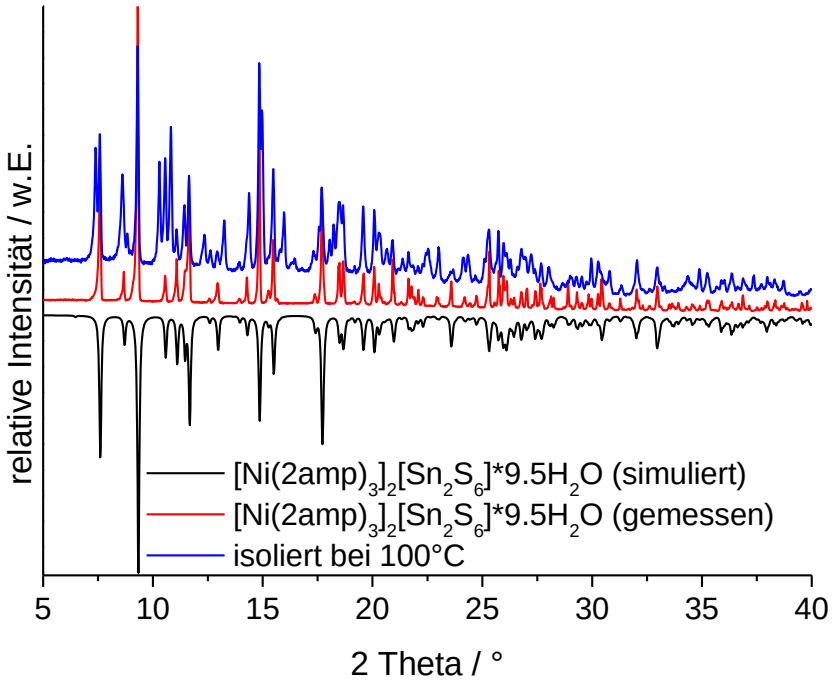

Abbildung 18: Pulverdiffraktogramm der bei 100°C isolierten Probe mit Vergleich der Ausgangsverbindung $[Ni(2amp)_3]_2[Sn_2S_6]\cdot 9.5H_2O$.

Interessanterweise liegen in dem Pulverdiffraktogramm bei längeren Messzeiten Reflexe der neuen und der Ausgangsverbindung vor. Das deutet darauf hin, dass die entwässerte Probe Wasser aus der Atmosphäre einlagert. Diese Annahme wurde bestätigt, indem eine bei 100°C isolierte Probe über einer Wasseratmosphäre gelagert wurde. Nach 24 h wurde wieder die Ausgangsverbindung $[Ni(2amp)_3]_2[Sn_2S_6]\cdot 9.5H_2O$ erhalten (s. Abb. A10, Abschnitt 5.6, Anhang). Es war auch unerheblich, ob die entwässerte Probe offen, verschlossen in einem Schnappdeckelglas oder präpariert zwischen zwei Schichten Scotch-Tape vorlag: immer wurde das Kristallwasser vollständig eingelagert. Auch Messungen in Kapillaren zeigten eine zeitliche Veränderung der Diffraktogramme. Optisch ließ sich dieser Prozess allerdings nicht verfolgen, da der Verlust bzw. die Einlagerung des Kristallwassers keine farbliche Änderung zur Folge hatte. Um die Struktur der entwässerten Probe zu bestimmen, müssen weitere Experimente durchgeführt werden.

4. Zusammenfassung und Ausblick

Verschiedene Ziele dieser Arbeit konnten erfolgreich realisiert werden:

Durch Verwendung aromatischer und cyclischer Aminmoleküle in Gegenwart eines „Hilfsamins“ konnten vierzehn neue Verbindungen synthetisiert werden, in deren Strukturen das Thiostannatanion kovalent an das Übergangsmetallkation gebunden ist. Die chemische Reaktivität verschiedener TM (TM = Mn, Fe, Co, Ni, Cu) sowie der aromatischen Liganden phen und 2,2‘-bipy wurden detailliert untersucht (s. Abschnitt 4.1).

Die Verbindung $\{[Ni(tren)]_2[Sn_2S_6]\}_n$ hat sich als neuer Precursor für die Synthese von Thiostannaten erwiesen. Mit diesem Synthon konnten vier neue Thiostannate synthetisiert und charakterisiert werden(s. Abschnitt 4.2).

Bei der Verwendung von $Na_4SnS_4 \cdot 14H_2O$ und $[Ni(Amin)_3]^{2+}$-Komplexen konnten bei Raumtemperatur sieben neue und fünf bereits bekannte Verbindungen synthetisiert und charakterisiert werden. Weitere Verbindungen konnten zwar präpariert aber noch nicht vollständig charakterisiert werden (s. Abschnitt 4.3).

4.1 Solvothermale Synthesen mit festen Aminen unter Verwendung von Hilfsaminen

Verbindungen mit der allgemeinen Formel $\{[TM(phen)_2]_2[Sn_2S_6]\}$ und $\{[TM(phen)_2]_2[Sn_2S_6]\} \cdot phen \cdot H_2O$ (TM = Mn, Fe, Co) kristallisierten bei Versuchen mit phen, TM, Sn und S in wässriger Methylaminlösung. In den Strukturen sind die Übergangsmetallkationen über TM-S-Bindungen an das Thiostannation gebunden. Die Ergebnisse belegen, dass a) Methylamin als „Hilfsamin“ geeignet ist die notwendigen Polysulfide für die Auflösung von Sn und TM zu generieren, selbst aber nicht an die TM^{2+}-Kationen koordiniert und b) phen ein geeigneter Ligand für die Stabilisierung von TM-S-Bindungen ist. Obwohl dieser bidentate Ligand durch Koordination von drei Molekülen in der Lage ist, die Koordinationssphäre am Metallzentrum vollständig zu sättigen, wurden Verbindungen mit zwei phen Liganden und zwei TM-S-Bindungen gebildet. Die Anordnung der phen-Moleküle führt zu π-π-Wechselwirkungen, welche eventuell wichtig für die Stabilisierung dieser Verbindungen sind.

Obwohl Verbindungen mit Mn^{2+}, Fe^{2+} und Co^{2+} isostrukturell sind, hat sich ein unterschiedliches Verhalten dieser Kationen bestätigt: Mit Mn^{2+}, welches vergleichsweise leicht in Thiometallatnetzwerke aufgrund der vergleichbaren Affinität zu Stickstoff und Schwefel integriert werden kann, konnten drei weitere Verbindungen erhalten werden. In einer Verbindung wird das deutlich seltenere $[SnS_4]^{4-}$-Anion gefunden, welches mit seinen vier S^{2-}-Anionen in Bindungen zu drei Mn^{2+} Zentren involviert ist. Während die Verbindungen mit Mn^{2+} auch unter dynamischen Synthesebedingungen synthetisiert werden konnten, wurden die Verbindungen mit Fe^{2+} und Co^{2+} nur unter statischen Bedingungen und in zum Teil deutlich schlechteren Ausbeuten erhalten. Dies lässt sich eventuell damit erklären, dass die bevorzugte Oxidationsstufe von Fe und Co in Komplexen sowie im basischen Milieu +III ist,[105] aber in den Verbindungen Fe(II) bzw. Co(II) vorliegt. Gerade in Bezug auf Fe werden

offensichtlich Aminmoleküle (z.B. phen) benötigt, welche Fe(II) stabilisieren,[105,121] was die geringe Anzahl eisenhaltiger Thiostannate bzw. Zinn-Schwefel-Verbindungen erklärt.[48,49]

Im Gegensatz dazu belegen Synthesen mit Ni, dass die Affinität von Ni^{2+} zu N-Donatoren so ausgeprägt ist, dass weitere organische Moleküle zur Bildung von Verbindungen mit Ni-S-Bindungen an das Thiostannation benötigt werden. Die bisherigen Untersuchungen legen nahe, dass es sich um ein aromatisches Molekül mit „passender Form und Größe“ (2,2‘-bipy, 4,4‘-bipy, biph) handeln muss, um optimale π-π-Wechselwirkungen mit dem phen Liganden zu ermöglichen. Auf der Basis der geringen Anzahl der mit diesem synthetischen Vorgehen hergestellten Verbindungen kann nicht entschieden werden, ob dies ein generelles synthetisches Konzept darstellt.

Versuche mit Cu führten nicht zur Bildung eines Thiostannates/einer Zinn-Schwefel-Verbindung: Selbst bei der Verwendung eines so starken Liganden wie phen war die Affinität zu Sulfidanionen so ausgeprägt, so dass nur verschiedene Kupfersulfide erhalten wurden.

Synthesen mit 2,2‘-bipy unter analogen Bedingungen wie Synthesen mit phen führten nicht zum Erfolg. Erst die Entwicklung eines alternativen Syntheseweges führte zur Kristallisation von $\{[Mn(2,2‘\text{-bipy})_2]_2[Sn_2S_6]\}$. Über die Gründe kann nur spekuliert werden: entweder ist 2,2‘-bipy aufgrund des weniger ausgedehnten π-Systems nicht wie phen in der Lage durch π-π–Wechselwirkungen Strukturen zu stabilisieren oder die Bildung der entsprechenden TM^{2+}-2,2‘-bipy-Komplexe findet bei den Synthesebedingungen nicht statt. Letztlich führte die Synthese mit vorgefertigtem $[Mn(2,2‘\text{-bipy})_3]^{2+}$-Komplex und $Na_4SnS_4{\cdot}14H_2O$ zum Erfolg. Dieser neue Syntheseweg der Reaktion eines vorgefertigten Komplexes und eines Thiostannat-Salzes konnte dann auf andere Komplexe erweitert werden: Synthesen mit $[TM(phen)_3][ClO_4]_2$ (TM = Mn, Fe, Co) und $[Ni(cyclam)][ClO_4]_2$ waren erfolgreich. Durch Verwendung weiterer Komplexe sollte diese Syntheseroute noch weitreichendes Potential für die Synthese neuer Verbindungen aufweisen. Voraussetzung für die erfolgreiche Bildung neuer Verbindungen sind Komplexe, welche für längere Zeit stabil sind, allerdings nicht so stabil, dass bei den gewählten Reaktionsbedingungen keine Reaktion stattfindet. Synthesen mit $[TM(2,2‘\text{-bipy}]_3][ClO_4]_2$ (TM = Fe, Co, Ni) oder $[TM(2amp)_3][ClO_4]_2$ bieten sich an, da diese Komplexe leicht darstellbar sind und die notwendige Stabilität aufweisen.

Die erfolgreiche Synthese mit cyclam, welche zur Bildung von $\{[Ni(cyclam)]_2[Sn_2S_6]\}_n{\cdot}nH_2O$ führte, deutet darauf hin, dass die Bildung zweidimensionaler Verbindungen mit cyclischen Aminmolekülen möglich sein sollte. Weitere Synthesen sollten mit Aminmolekülen mit vergleichbarem molekularem Aufbau durchgeführt werden, um diese Annahme zu bestätigen.

4.2 Synthesen mit dem Precursor {[Ni(tren)]$_2$[Sn$_2$S$_6$]}$_n$ bei Raumtemperatur

Mit {[Ni(tren)]$_2$[Sn$_2$S$_6$]}$_n$ konnten vier neue Verbindungen mit der allgemeinen Formel [Ni(tren)(Amin)]$_2$[Sn$_2$S$_6$]·*x*H$_2$O (Amin = 1,2-dap, ma, tren, 2amp) erhalten werden. Zusätzlich konnten zwei Verbindungen mit der allgemeinen Formel [Ni(Amin)$_3$[Sn$_2$S$_6$]·*x*H$_2$O (Amin = en, 1,2-dach)[43,50] synthetisiert werden. Ein wesentlicher Aspekt der neuen Syntheseroute ist, dass die Reaktion bei Raumtemperatur stattfindet und der synthetische Aufwand erheblich verringert werden kann. In zukünftigen Arbeiten muss die Tauglichkeit des Precursors z.B. durch Verwendung weiterer Amine überprüft werden. besonders attraktiv erscheint es, den Precursor mit anderen Übergangsmetallkomplexen reagieren zu lassen.

4.3 Synthesen mit [TM(Amin)$_n$]Cl$_2$ bzw. [TM(Amin)$_n$][ClO$_4$]$_2$ und Na$_4$SnS$_4$ 14H$_2$O bei Raumtemperatur

In einer ersten Versuchsreihe konnten bei Synthesen mit [Ni(Amin)$_3$]$^{2+}$-Komplexen (Amin = en, 1,2-dach, 1,2-dap, 2amp) und Na$_4$SnS$_4$·14H$_2$O in wässriger tren Lösung bei Raumtemperatur insgesamt sechs neue Verbindungen mit der allgemeinen Zusammensetzung [Ni(tren)(Amin)]$_2$[Sn$_2$S$_6$]·*x*H$_2$O (Amin = en, 1,2-dach, 1,2-dap, 2amp) dargestellt werden. Zusätzlich konnten die Verbindungen [Ni(tren)$_2$]$_2$[Sn$_2$S$_6$]·8H$_2$O und [Ni(1,2-dap)(tren)]$_2$[Sn$_2$S$_6$]·2H$_2$O synthetisiert werden, welche bereits bei Reaktion mit {[Ni(tren)]$_2$[Sn$_2$S$_6$]}$_n$ erhalten wurden.

Beim Einsatz von [Ni(Amin)$_3$]$^{2+}$ bzw. [Ni(tren)(H$_2$O)Cl]Cl und Na$_4$SnS$_4$·14H$_2$O in wässrigen Aminlösungen (Amin = tren, en, 1,2-dach, 1,2-dap, 2amp) wurden fünf Verbindungen mit der allgemeinen Formel [Ni(tren)(Amin)]$_2$[Sn$_2$S$_6$]·*x*H$_2$O (Amin = tren, en, 1,2-dach, 1,2-dap, 2amp) sowie vier Verbindungen der allgemeinen Zusammensetzung [Ni(Amin)$_3$]$_2$[Sn$_2$S$_6$]·*x*H$_2$O (Amin = en, 1,2-dach, 1,2-dap, 2amp) erhalten. Die Verbindung [Ni(2amp)$_3$]$_2$[Sn$_2$S$_6$]·9.5H$_2$O konnte auf diese Weise erstmalig dargestellt werden. Zusätzlich wurden neue Verbindungen erhalten, welche noch nicht identifiziert werden konnten. Die Optimierung der Synthesebedingungen (Variation der Einwaage, Amin-Konzentration, LM-Volumen) sollte letztlich zum Erfolg führen. Bisher wurden nur tren bzw. bidentate Aminmoleküle eingesetzt und es erscheint aussichtsreich, weitere multidentate Aminmoleküle (dien, trien, tepa, …) einzusetzen.

Bei orientierenden Versuchen mit [Ni(phen)$_3$][ClO$_4$]$_2$ bzw. [Ni(bipy)$_3$][ClO$_4$]$_2$ und Na$_4$SnS$_4$·14H$_2$O in 30% Aminlösungen (Amin = tren, en, 1,2-dach, 1,2-dap, 2amp) konnten [Ni(tren)$_2$]$_2$[Sn$_2$S$_6$]·8H$_2$O bzw. [Ni(2amp)$_3$]$_2$[Sn$_2$S$_6$]·9.5H$_2$O synthetisiert werden. Drei weitere Verbindungen konnten noch nicht identifiziert werden. Die Optimierung der Synthesebedingungen (Einwaage, Amin Konzentration, LM Volumen, etc.) sollte jedoch zum Erfolg führen. Analoge Reaktionen mit Mn^{2+}, Fe^{2+} und Co^{2+} sollten es erlauben, das synthetische Potential der Syntheseroute auszuloten.

5. Anhang

5.1 Publikationsliste

5.1.1 Publikationen

Influence of the Synthesis Parameters onto Nucleation and Crystallization of Five New Tin-Sulfur Containing Compounds,
J. Hilbert, C. Näther, W. Bensch;
Inorg. Chem. **2014**, *53*, 5619-5630.

The $[Sn_2S_6]^{4-}$ Anion Acting as Tetradentate Linker: Solvothermal Synthesis and Selected Properties of $\{[TM(phen)_2]_2Sn_2S_6\}$ and $\{[TM(phen)_2]_2Sn_2S_6\}\cdot phen\cdot H_2O$ (TM = Fe, Co),
J. Hilbert, C. Näther, W. Bensch;
Z. Anorg. Allg. Chem. **2014**, *640*, 2858-2863.

Utilization of Mixtures of Aromatic N-donor Ligands of Different Coordination Ability for the Solvothermal Synthesis of Thiostannate Containing Molecules,
J. Hilbert, C. Näther, W. Bensch
Dalton Trans. **2015***, 44*, 11542-11550.

Crystal structure of tris(N-methylsalicylaldiminato-κ^2N,O)vanadium(III),
J. Hilbert, S. Kabus, C. Näther, W. Bensch;
Acta Cryst. **2015**, *E71*, m225.

Crystal structure of tris(N-methylsalicylaldiminato-κ^2N,O)chromium(III),
J. Hilbert, S. Kabus, C. Näther, W. Bensch;
Acta Cryst. **2015**, *E71*, m247-m248.

Room temperature synthesis of thiostannates from $\{[Ni(tren)]_2[Sn_2S_6]\}_n$,
J. Hilbert, C. Näther, R. Weihrich, W. Bensch;
Inorg. Chem. **2016**, *55*, 7859-7865.

Transition Metal Complexes with Linkage to the Thiostannate Units Forced by Suitable Amine Molecules,
J. Hilbert, N. Pienack, H. Lühmann, C. Näther, W. Bensch;
Z. Anorg. Allg. Chem. **2016**, accepted 24.10.16

$\{[Ni(1,2\text{-}dach)_2(ma)]_4[Sn_{10}S_{20}O_4]\}$ – An Example of the Rare Tin-Oxo-Sulfide Cluster with Uncommon Connection Mode Towards a Charge Compensating Ni(II) Complex,
J. Hilbert, C. Näther, W. Bensch
Current Inorg. Chem. **2016**, submitted 10.10.16

Studies on the Formation of Thiostannates at Room Temperature with the Amine Ligands Tris(2-Aminoethyl)amine and 2-(Aminomethy)pyridin,
J. Hilbert, C. Näther, W. Bensch
Inorg. Chim. Acta **2016**, submitted 03.11.16

5.1.2 Posterbeiträge und Präsentationen

Einsatz stabilisierender aromatischer Amine bei der solvothermalen Synthese übergangsmetallhaltiger Thiostannate,
J. Hilbert, C. Näther, W. Bensch
15. NDDK, Krelingen, September **2012**

Untersuchung der Bildung 1,10-Phenanthrolinhaltiger Mangan-Thiostannate in Abhängigkeit der Syntheseparameter,
J. Hilbert, C. Näther, W. Bensch
GDCh-Wissenschaftsforum, Darmstadt, September **2013**

Solvothermal Synthesis to Modify Transition Element Containing Thiostannates, Thioantimonates and Polyoxoniobates,
J. Hilbert, C. Anderer, J. Dopta, W. Bensch
The DGK's Young Crystallographers - Lab Meeting @ STOE, Darmstadt, September **2015**

Ein alternativer Syntheseweg für die Herstellung von Thiostannaten
J. Hilbert, W. Bensch
AC-Kolloquium 2015/16, Kiel, Februar **2016**

5.2 Supporting Information (SI)

5.2.1 SI für die Publikation: "Influence of the Synthesis Parameters onto Nucleation and Crystallization of Five New Tin-Sulfur Containing Compounds"

Supplementary Information

Influence of Synthesis Parameters onto Nucleation and Crystallization of Five New Tin Sulfur Containing Compounds

Jessica Hilbert, Christian Näther, Wolfgang Bensch*

Institut für Anorganische Chemie, Christian-Albrechts-Universität Kiel, May-Eyth-Str. 2, D-24118 Kiel, Germany,

*correspondence address: Prof. Dr. Wolfgang Bensch, Fax: +49-431-880-1520, E-Mail: wbensch@ac.uni-kiel.de

Table S1 Overview of the reaction conditions of the syntheses performed under static conditions.

reaction vessel	Mn:Sn:S:phen mmolar ratios	solvent	time	compound
Teflon-lined steel autoclave (150°C)	2:1:4:1	ma (30%)	5d	**X*, 5**
			3-6 weeks	**X*, 5**
			7 weeks	**X*, 3, 5**
Teflon-lined steel autoclave (150°C)	1:1:3:2	ma (30%)	5d	**1**
			3 weeks	**1**
			4+5 weeks	**3, 4**
			6+7 weeks	**3**
Teflon-lined steel autoclave (120°C)	2:1:4:1	ma (30%)	5d	**1**
		ba (50%)	5d	**1**
Teflon-lined steel autoclave (120°C)	1:1:3:2	ma (30%)	5d	**4**
		ba (50%)	5d	**1**
Glass tube	1:1:3:2	ma (30%)	5d	**1**
			3 weeks	**1, 3**
			4 weeks	**3, 4**
			5-7 weeks	**4**
Glass tube	2:1:4:1	ma (30%)	5d /14d	**X***
		ea (50%)		**1**
		npa (100%)		**1**
		npa (50%)		**X***
		ba (100%)		**1**
		ba (50%)		**1**
Glass tube	1:1:3:2	ma + HCl (pH = 11)	5d	**2**
			21 d	**4**

X* = **{[Mn(phen)]$_2$(SnS$_4$)}$_n$·*n*H$_2$O[15];**
ma = methylamine; ea = ethylamine; ba = butylamine; npa = n-propylamine
Yields based on Sn: (1) ~40%; (2) ~30%, (3) ~30%, (4) 50%, (5) 5-10%

Due to the pore structure of Teflon containers several Teflon containers are used basically just for one amine, since small molecules remain in the pores and could affect the formation of the compounds in subsequent syntheses. Following this rule and a time-consuming cleaning procedure will assure the reproducibility of the experiments.
One advantage of glass as reaction vessels is the presence of OH groups which can be protonated and deprotonated.

Table S2 Overview of the solvent mixtures used in the dynamic synthesis and the resulting pH values (ma = methylamine).

mixture	pH
2 mL ma	14
1.5 mL ma, 0.5 mL H$_2$O	14
1.0 mL ma, 1.0 mL H$_2$O	14
0.5 mL ma, 1.5 mL H$_2$O	14
1.9 mL ma, 0.1 mL H$_2$O	13
1.5 mL ma, 0.5 mL H$_2$O	12
1.3 mL ma, 0.7 mL H$_2$O	11

The dynamic syntheses were all carried out using an IKA ® C-MAG HS7 magnetic stirrer with heating with an IKA ® ETS-D5 thermometer. In order to control the temperature of

several culture tubes, they were transferred to an aluminum block, which then was placed on the hot stirrer. The temperature of the aluminum block was checked / controlled by the thermometer. A detailed verification / read off the stirring speed were not possible in this construction.

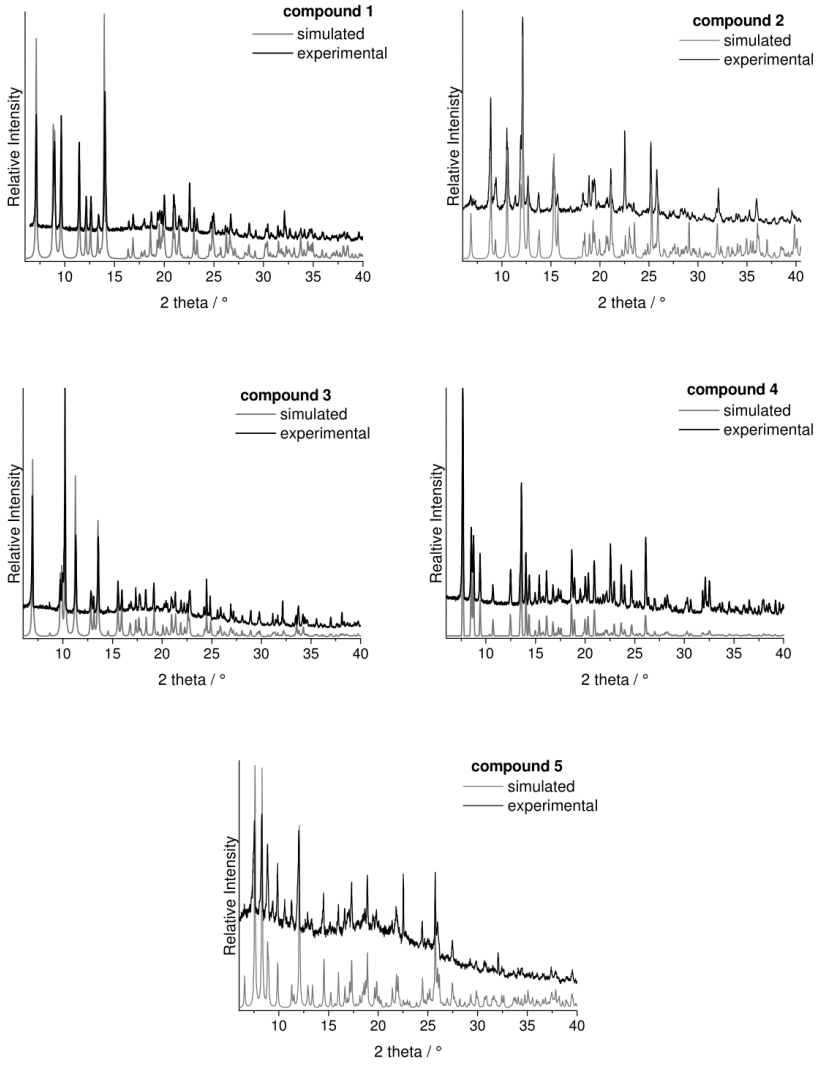

Fig. S1: Comparison of the experimental of **1–5** (black) PXRD patterns with their corresponding simulated from single-crystal X-ray data (red).

Spectroscopic Properties

UV/Vis spectroscopy

The optical band gap were estimated to 2.08 eV (**1**), 1.92 eV (**2**), 2.06 eV (**3**), 2.05 eV (**4**) and 2.11 eV (**5**) (see Figure S2). Further a maximum was observed at about 4.6 eV which can be assigned to 1,10-phenanthroline.

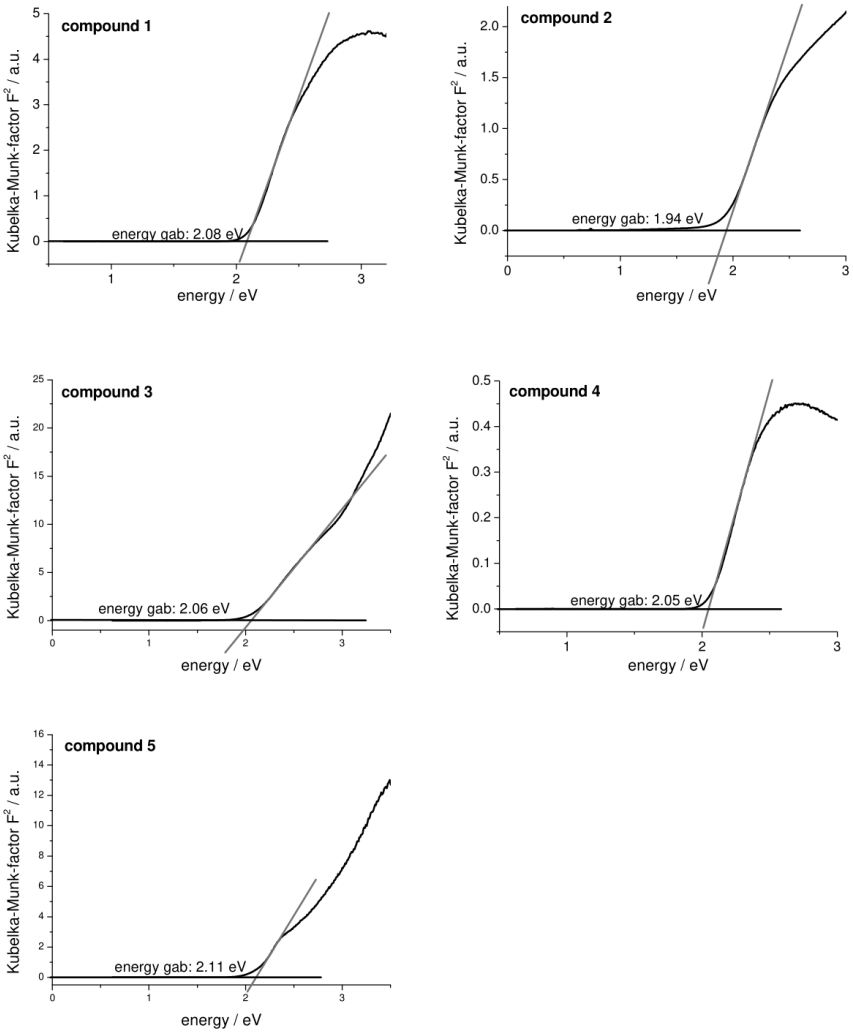

Fig. S2 Determination of the optical band gab of **1**-**5** from UV/Vis diffuse reflectance spectrum using the Kubelka-Munk method.

Infrared spectroscopy

The absorptions in the IR spectra for the compounds **1-5** can be assigned to 1,10-phenathroline as well as the Mn-N stretching vibration at $\tilde{\nu}$ ~ 420 cm^{-1} [49] (see Figure S3 and Table S3).The absorption at about 1030 cm^{-1} of compound **2** and **4** can be associate to the additional 1,10-phenantroline molecule in the structure. The weak absorption above 3000 cm^{-1} in compound **4** and **5** can be assigned to water (Table S3).

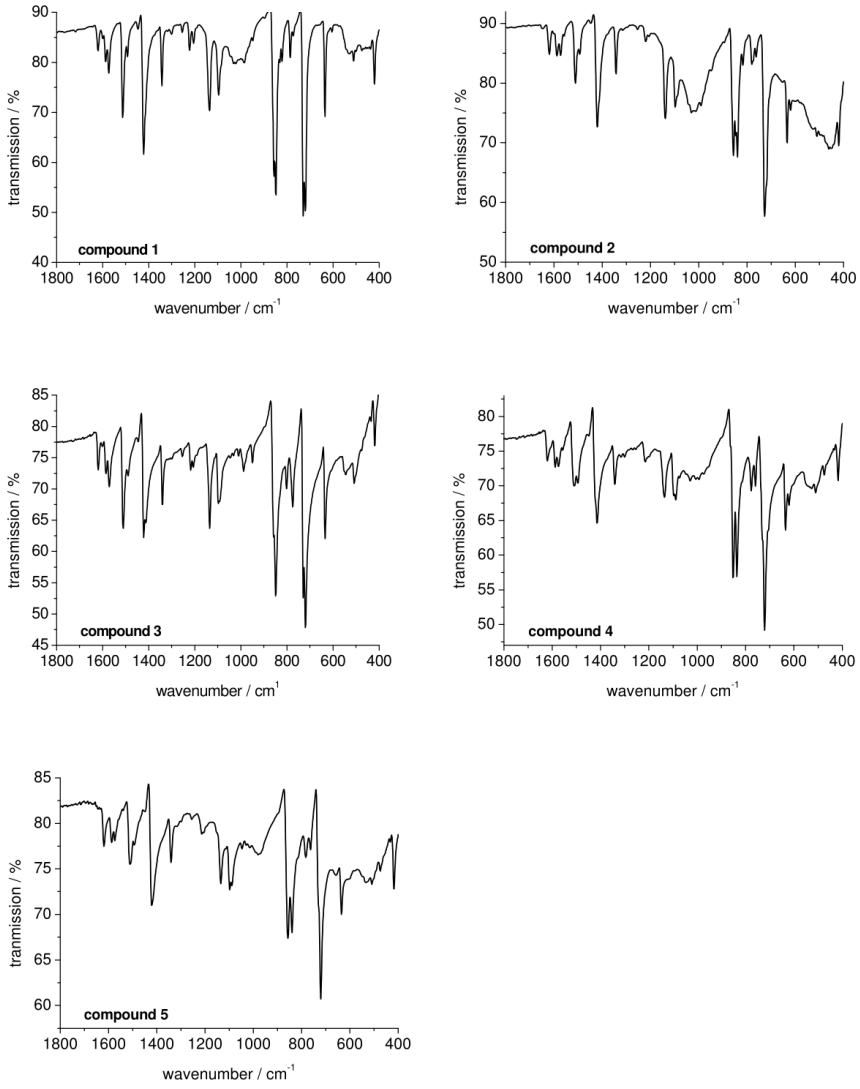

Fig. S3 IR spectra of **1-5**.

Table S3 Absorptions of the IR-spectra of 1,10-phenanthroline and compounds **1**-**5**.

phen	1	3	2	4	5	Assignment
---	---	---	---	~ 3330	~3300	ν (O-H)
3033	3038	3039	3033	3033	3028	ν (C-H)
1616	1620	1619	1619	1620	1619	ν (C=C)
1560	1573	1571	1588	1588	1587	ν (C=C)
1502	1513	1511	1510	1509	1510	ν (C=C)
1421	1421	1422	1419	1414	1421	combined
1344	1342	1340	1343	1341	1340	ν (C=C)
1216	1222	1218	1220	1214	1214	ν (C=C)
1137	1136	1135	1239	1135	1135	δ (C=C-H)
1035	1096	1097	1097	1088	1098	ν (C-N) bonded phen
	---	---	1030	1029	---	ν (C-N) free molecule
987	985	988	989	990	981	δ (C=C-H)
853	848	849	856	851	857	δ (C=C=C)
779	786	775	780	777	782	δ (C-H)
738	729	730	---	---	---	δ (C-H)
721	720	720	721	721	721	δ (C-H)
625	635	635	634	636	635	δ (C-H)
---	420	419	419	418	417	ν (Mn-N)

Raman spectroscopy

Raman spectra were recorded with a Bruker IFS 66 Fourier transform spectrometer (wavelength: 541.5 nm) in the range from 100 to 3500cm^{-1}. The Sn-S modes are between 100 and 400 cm^{-1} in the Raman spectrum[48-51]. The assignment of the modes was done based on these published data (**1**-**4**) (Table S4). A further signal at about 420 cm^{-1} in all compounds can be assigned to the vibration of the Mn-N bond.[31]

Table S4 Data of the signals in the Raman spectra of $Na_4Sn_2S_6 \cdot 14\ H_2O$ and compounds **1-4** (all wave numbers are given in cm^{-1}).

$Na_4Sn_2S_6 \cdot 14\ H_2O$	1	3	2	4
---	422	420	421	421
391	391	392	393	392
377	377	375	379	377
341	342	342	342	344
281	279	283	282	284
190	197	199	191	195
151	165	161	152	159
136	140	138	131	135

The resonances of the symmetric Sn-S_t stretching modes are located around 380 cm^{-1}. In compound **1-4** the Sn-S_t bond lengths vary between 2.3350(6) and 2.33568(12) Å and the signal observed in the spectra is slightly shifted to 379-375 cm^{-1}, similar to $Na_4Sn_2S_6 \cdot 14$

H_2O. The Sn-S_b vibrations are located at lower wave numbers at about 344 cm^{-1}(**1-4**). The mode around 280 cm^{-1} (**1-4**) is caused by a Sn_2S_2 ring vibration. The energetic differences between the resonances in **1-4** and to the data reported for $Na_4Sn_2S_6 \cdot 14\ H_2O$ are caused by slight differing bond lengths and angles. In compound **5**, the signal at 348 cm^{-1} can be assigned to the $[SnS_4]^{4-}$ unit.[52] The bands at 280, 218 and 195 cm^{-1} are caused by the Mn-S bonds.[53,54] Deformation vibrations occur below 200 cm^{-1}, but a detailed assignment is not unambiguous due to resonances for lattice vibrations. A further signal at about 420 cm^{-1} in all compounds can be assigned to the vibration of the Mn-N bond.[31]

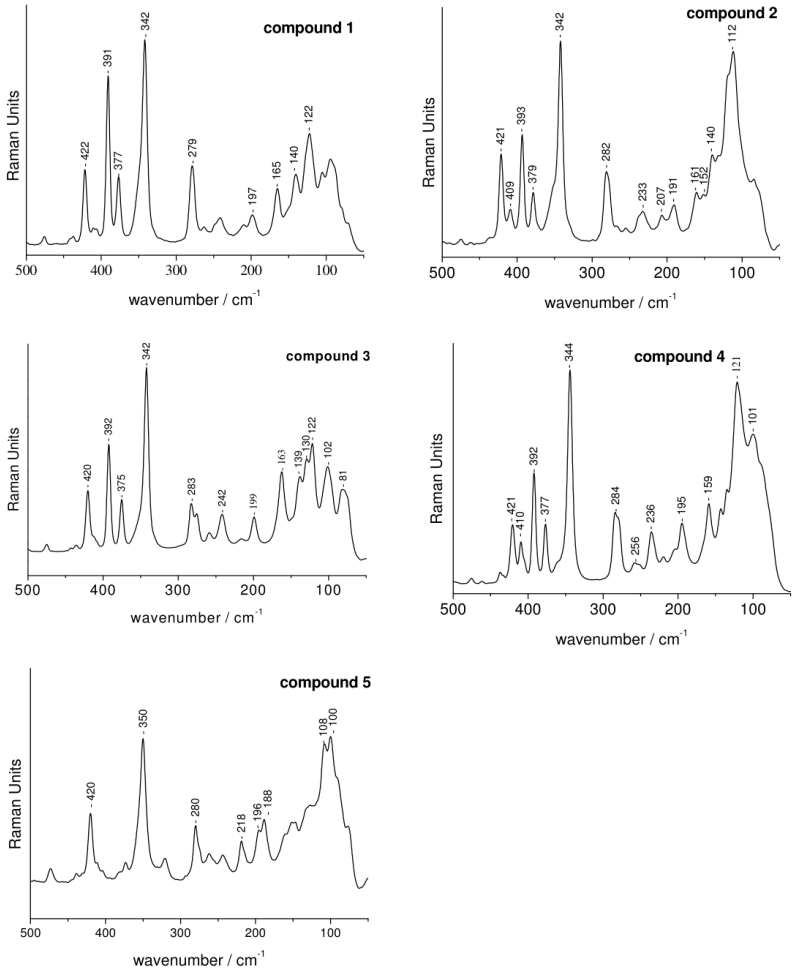

Fig. S4 Raman spectra of **1-5**.

Table S5 Selected Bond Lengths (Å) and Angles (°) in the structures of **1-5**.

1	Sn(1)-S(1)	2.3413(12)	N(4)-Mn(1)-N(3)	70.68(13)
	Sn(1)-S(2)	2.3568(12)	N(2)-Mn(1)-N(3)	86.20(14)
	Sn(1)-S(3)#1	2.4377(11)	N(1)-Mn(1)-S(2)	97.73(12)
	Sn(1)-S(3)	2.4501(11)	N(4)-Mn(1)-S(2)	101.65(11)
	Mn(1)-N(1)	2.288(4)	N(2)-Mn(1)-S(2)	169.75(10)
	Mn(1)-N(4)	2.297(4)	N(3)-Mn(1)-S(2)	92.06(10)
	Mn(1)-N(2)	2.303(4)	N(1)-Mn(1)-S(1)	107.38(11)
	Mn(1)-N(3)	2.378(4)	N(4)-Mn(1)-S(1)	97.06(10)
	Mn(1)-S(2)	2.5454(14)	N(2)-Mn(1)-S(1)	92.44(11)
	Mn(1)-S(1)	2.5685(13)	N(3)-Mn(1)-S(1)	167.70(10)
	S(3)-Sn(1)#1	2.4377(11)	S(2)-Mn(1)-S(1)	91.37(4)
			N(1)-Mn(1)-Sn(1)	106.96(11)
	S(1)-Sn(1)-Mn(1)	51.47(3)	N(4)-Mn(1)-Sn(1)	104.57(9)
	S(2)-Sn(1)-Mn(1)	50.86(3)	N(2)-Mn(1)-Sn(1)	136.80(11)
	S(3)#1-Sn(1)-Mn(1)	132.44(3)	N(3)-Mn(1)-Sn(1)	137.00(10)
	S(3)-Sn(1)-Mn(1)	134.90(3)	S(2)-Mn(1)-Sn(1)	45.90(3)
	N(1)-Mn(1)-N(4)	148.29(14)	S(1)-Mn(1)-Sn(1)	45.49(3)
	N(1)-Mn(1)-N(2)	72.04(15)	Sn(1)-S(1)-Mn(1)	83.04(4)
	N(4)-Mn(1)-N(2)	87.32(15)	Sn(1)-S(2)-Mn(1)	83.24(4)
	N(1)-Mn(1)-N(3)	83.85(14)	Sn(1)#1-S(3)-Sn(1)	87.43(4)
2	Sn(1)-S(1)	2.335(2)	N(1)-Mn(1)-N(2)	70.39(19)
	Sn(1)-S(2)	2.356(2)	N(21)-Mn(1)-N(2)	84.08(19)
	Sn(1)-S(3)	2.4422(18)	N(22)-Mn(1)-S(2)	165.60(16)
	Sn(1)-S(3A)	2.4512(18)	N(1)-Mn(1)-S(2)	98.19(16)
	Mn(1)-N(1)	2.301(5)	Sn(1)-S(1)-Mn(1)	82.23(7)
	Mn(1)-N(22)	2.251(6)	Sn(1)-S(2)-Mn(1)	82.39(7)
	Mn(1)-N(2)	2.378(6)	Sn(1)-S(3)-Sn(1A)	86.67(6)
	Mn(1)-N(21)	2.307(6)	N(21)-Mn(1)-S(2)	95.30(16)
	Mn(1)-S(2)	2.562(2)	N(2)-Mn(1)-S(2)	95.05(15)
	Mn(1)-S(1)	2.588(2)	N(22)-Mn(1)-S(1)	86.29(16)
	S(3)-Sn(1A)	2.4512(18)	N(1)-Mn(1)-S(1)	95.13(14)
			N(21)-Mn(1)-S(1)	109.00(14)
	S(1)-Sn(1)-Mn(1)	52.26(5)	N(2)-Mn(1)-S(1)	164.83(14)
	S(2)-Sn(1)-Mn(1)	51.55(5)	S(2)-Mn(1)-S(1)	91.41(7)
	S(3)-Sn(1)-Mn(1)	138.55(5)	N(22)-Mn(1)-Sn(1)	129.01(15)
	S(3A)-Sn(1)-Mn(1)	128.10(5)	N(1)-Mn(1)-Sn(1)	102.65(14)
	N(22)-Mn(1)-N(1)	96.2(2)	N(21)-Mn(1)-Sn(1)	104.40(14)
	N(22)-Mn(1)-N(21)	72.1(2)	N(2)-Mn(1)-Sn(1)	140.23(15)
	N(1)-Mn(1)-N(21)	151.98(19)	S(2)-Mn(1)-Sn(1)	46.06(5)
	N(22)-Mn(1)-N(2)	90.7(2)	S(1)-Mn(1)-Sn(1)	45.52(5)
3	Sn(1)-S(2)	2.3350(6)	N(2)-Mn(1)-N(21)	84.84(8)
	Sn(1)-S(1)	2.3561(6)	N(22)-Mn(1)-N(21)	70.88(8)
	Sn(1)-S(3)	2.4415(6)	N(1)-Mn(1)-N(21)	86.23(8)
	Sn(1)-S(3A)	2.4422(6)	N(2)-Mn(1)-S(1)	97.30(6)
	S(1)-Mn(1)	2.5387(7)	N(22)-Mn(1)-S(1)	102.96(6)
	S(2)-Mn(1)	2.5515(7)	N(1)-Mn(1)-S(1)	169.57(6)
	S(3)-Sn(1A)	2.4422(6)	N(21)-Mn(1)-S(1)	94.11(6)
	Mn(1)-N(2)	2.279(2)	N(2)-Mn(1)-S(2)	104.70(6)
	Mn(1)-N(22)	2.295(2)	N(22)-Mn(1)-S(2)	97.71(6)
	Mn(1)-N(1)	2.310(2)	N(1)-Mn(1)-S(2)	89.90(5)
	Mn(1)-N(21)	2.364(2)	N(21)-Mn(1)-S(2)	168.11(7)
			S(1)-Mn(1)-S(2)	91.73(2)
	S(2)-Sn(1)-Mn(1)	51.336(16)	N(2)-Mn(1)-Sn(1)	106.00(5)
	S(1)-Sn(1)-Mn(1)	50.958(16)	N(22)-Mn(1)-Sn(1)	104.79(5)
	S(3)-Sn(1)-Mn(1)	133.495(17)	N(1)-Mn(1)-Sn(1)	134.60(5)
	N(2)-Mn(1)-N(22)	149.18(8)	N(21)-Mn(1)-Sn(1)	139.17(6)
	N(2)-Mn(1)-N(1)	72.33(8)	S(1)-Mn(1)-Sn(1)	46.122(15)

	N(22)-Mn(1)-N(1)	87.01(8)	S(2)-Mn(1)-Sn(1)	45.607(14)
4	Sn(1)-S(1)	2.3358(8)	N(21)-Mn(1)-N(2)	86.99(8)
	Sn(1)-S(2)	2.3537(8)	N(1)-Mn(1)-N(2)	71.72(8)
	Sn(1)-S(3)	2.4362(7)	N(22)-Mn(1)-N(2)	86.14(8)
	Sn(1)-S(3A)	2.4437(7)	N(21)-Mn(1)-S(1)	102.39(7)
	S(1)-Mn(1)	2.5407(9)	N(1)-Mn(1)-S(1)	98.81(6)
	S(2)-Mn(1)	2.5818(8)	N(22)-Mn(1)-S(1)	94.83(7)
	S(3)-Sn(1A)	2.4437(7)	N(2)-Mn(1)-S(1)	170.42(6)
	Mn(1)-N(21)	2.257(2)	N(21)-Mn(1)-S(2)	97.57(7)
	Mn(1)-N(1)	2.274(2)	N(1)-Mn(1)-S(2)	101.93(6)
	Mn(1)-N(22)	2.333(2)	N(22)-Mn(1)-S(2)	168.45(7)
	Mn(1)-N(2)	2.342(2)	N(2)-Mn(1)-S(2)	88.68(6)
			S(1)-Mn(1)-S(2)	92.00(3)
	S(3A)-Sn(1)-Mn(1)	132.055(18)	N(21)-Mn(1)-Sn(1)	105.59(6)
	Sn(1)-S(1)-Mn(1)	82.80(3)	N(1)-Mn(1)-Sn(1)	103.85(6)
	Sn(1)-S(2)-Mn(1)	81.57(2)	N(22)-Mn(1)-Sn(1)	140.12(7)
	N(21)-Mn(1)-N(1)	150.53(9)	N(2)-Mn(1)-Sn(1)	133.74(5)
	N(21)-Mn(1)-N(22)	71.88(9)	S(1)-Mn(1)-Sn(1)	45.873(18)
	N(1)-Mn(1)-N(22)	86.22(9)	S(2)-Mn(1)-Sn(1)	46.151(17)
5	Sn(1)-S(1)	2.3670(11)	N(1)-Mn(1)-N(42)	151.70(13)
	Sn(1)-S(2)	2.3678(10)	N(1)-Mn(1)-N(41)	86.63(12)
	S(1)-Mn(1)	2.5521(12)	N(42)-Mn(1)-N(41)	71.72(12)
	S(2)-Mn(1)	2.5289(12)	N(1)-Mn(1)-N(2)	72.11(12)
	S(3)-Mn(2)#1	2.4555(11)	N(42)-Mn(1)-N(2)	87.28(12)
	S(3)-Mn(2)	2.6090(12)	N(41)-Mn(1)-N(2)	83.85(12)
	S(4)-Mn(2)	2.4775(13)	N(1)-Mn(1)-S(2)	100.48(10)
	Sn(1)-S(4)	2.3816(11)	N(42)-Mn(1)-S(2)	97.00(10)
	Sn(1)-S(3)	2.4471(10)	N(41)-Mn(1)-S(2)	88.43(9)
	Mn(1)-N(1)	2.234(3)	S(4)-Sn(1)-S(3)	97.55(4)
	Mn(1)-N(42)	2.251(3)	S(1)-Sn(1)-Mn(1)	51.38(3)
	Mn(1)-N(41)	2.368(3)	S(2)-Sn(1)-Mn(1)	50.81(3)
	Mn(1)-N(2)	2.370(4)	S(4)-Sn(1)-Mn(1)	131.47(3)
	N(22)-Mn(2)	2.246(4)	S(3)-Sn(1)-Mn(1)	130.31(3)
			N(2)-Mn(1)-S(2)	169.55(9)
	S(1)-Sn(1)-S(2)	102.17(4)	N(1)-Mn(1)-S(1)	100.59(9)
	S(1)-Sn(1)-S(4)	113.99(4)	N(42)-Mn(1)-S(1)	100.55(9)
	S(2)-Sn(1)-S(4)	116.12(4)	N(41)-Mn(1)-S(1)	172.26(9)
	S(1)-Sn(1)-S(3)	121.99(4)	N(2)-Mn(1)-S(1)	95.64(9)
	S(2)-Sn(1)-S(3)	105.60(4)	S(2)-Mn(1)-S(1)	92.95(4)
	Sn(1)-S(1)-Mn(1)	82.19(3)	N(1)-Mn(1)-Sn(1)	106.17(9)
	Sn(1)-S(2)-Mn(1)	82.67(3)	N(42)-Mn(1)-Sn(1)	102.01(9)
	Sn(1)-S(3)-Mn(2)#1	116.60(4)	N(41)-Mn(1)-Sn(1)	134.29(9)
	Sn(1)-S(3)-Mn(2)	82.44(3)	N(2)-Mn(1)-Sn(1)	141.83(8)
	Mn(2)#1-S(3)-Mn(2)	80.14(3)	S(2)-Mn(1)-Sn(1)	46.52(2)
	Sn(1)-S(4)-Mn(2)	86.62(4)	S(1)-Mn(1)-Sn(1)	46.44(3)

Table S6 Selected bond lengths (Å) and angles (°) of **1** and **3** compared to those in $Na_4Sn_2S_6 \cdot 14H_2O$.[36]

	$Na_4Sn_2S_6 \cdot 14H_2O$	**1**	**3**
Sn – S	2.325 -2.452	2.3413(12) - 2.4501(11)	2.3350(6) - 2.4422(6)
S1 – Sn – S2	119.8(2)	102.31(4)	102.29(2)
S1 – Sn – S3	108.2	117.64(4)	113.73(2)
S2 – Sn – S3	110.6	113.59(5)	117.32(2)
S1 – Sn – S3[a]	110.4	115.96(5)	115.67(2)
S2 – Sn – S3[a]	110.8	115.53(4)	115.45(2)
S3 – Sn – S3[a]	94.0	92.57(4)	93.15(2)
Sn – S3 – Sn[a]	86.0	87.43(4)	86.85(2)

Symmetry transformations used to generate equivalent atoms: a: -x+1,-y+1,-z

Table S7 Dihedral angles between the phenanthroline moieties for compounds **1**-**5**.

1	N(12)-Mn(1)-N(1)-C(1)	-94.27 (0.44)	N(12)-Mn(1)-N(2)-C(10)	94.75 (0.46)
	N(12)-Mn(1)-N(1)-C(12)	86.26 (0.34)	N(12)-Mn(1)-N(2)-C(11)	-84.27 (0.38)
2	N(22)-Mn(1)-N(1)-C(1)	89.88 (0.75)	N(22)-Mn(1)-N(2)-C(10)	-85.93 (0.71)
	N(22)-Mn(1)-N(1)-C(12)	-97.82 (0.59)	N(22)-Mn(1)-N(2)-C(11)	105.68 (0.47)
3	N(21)-Mn(1)-N(1)-C(1)	-99.26 (0.25)	N(21)-Mn(1)-N(2)-C(10)	93.96 (0.24)
	N(21)-Mn(1)-N(1)-C(12)	84.91 (0.18)	N(21)-Mn(1)-N(2)-C(11)	-85.99 (0.18)
4	N(22)-Mn(1)-N(1)-C(1)	-93.21 (0.24)	N(22)-Mn(1)-N(2)-C(10)	96.35 (0.23)
	N(22)-Mn(1)-N(1)-C(12)	83.10 (0.20)	N(22)-Mn(1)-N(2)-C(11)	-84.07 (0.18)
5	N(41)-Mn(1)-N(1)-C(1)	-92.51 (0.36)	N(41)-Mn(1)-N(2)-(10)	90.10 (0.36)
	N(41)-Mn(1)-N(1)-C(12)	87.05 (0.29)	N(41)-Mn(1)-N(2)-(11)	-91.58 (0.27)

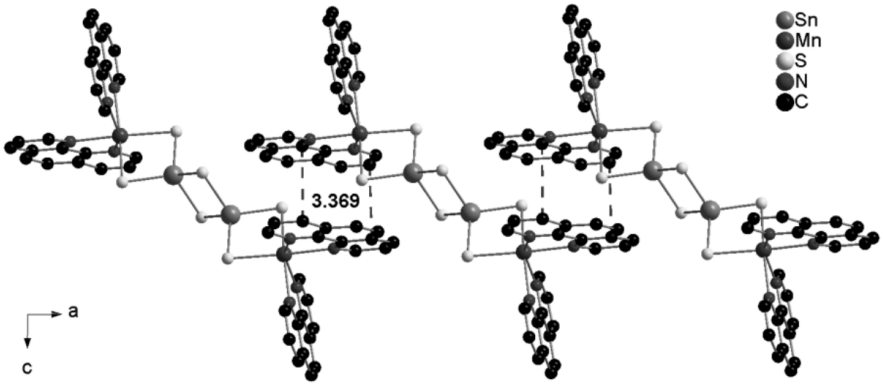

Fig. S5 Parallel arrangement of the molecules in 1 along a, assembled by hydrogen bonds and off-centre parallel stacking along c. Hydrogen atoms are omitted for clarity.

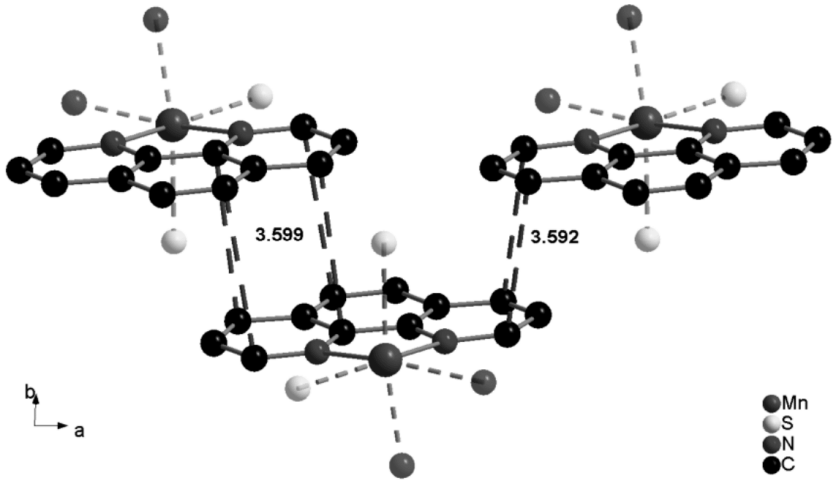

Fig. S6 Slightly staggered arrangement of the units along a and interaction via off-centre parallel stacking (blue dashed lines) along b in compound 2. Hydrogen atoms are omitted for clarity.

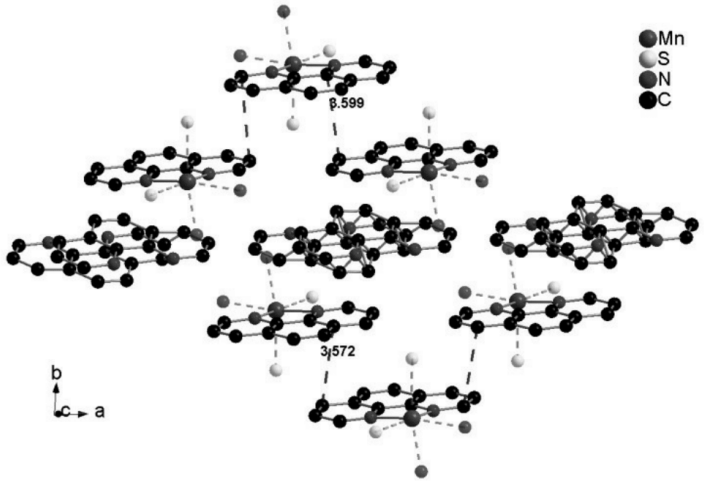

Fig. S7 Arrangement of the disordered phenanthroline in channels along a. Hydrogen atoms are omitted for clarity.

Table S8 Selected bond lengths (Å) and angles (°) of compound **5** compared to $Na_4SnS_4 \cdot 14\ H_2O$.[41]

	$Na_4SnS_4 \cdot 14H_2O$	**5**
Sn – S1	2.394(5)	2.3670(11)
Sn – S2	2.385	2.3678(10)
Sn – S3	2.394	2.4471(10)
Sn – S4	2.385	2.3816(11)
S1 – Sn – S2	107.9	102.17(4)
S1 – Sn – S3	112.9(2)	121.99(4)
S2 – Sn – S3	107.7	105.60(4)
S1 – Sn – S4	107.7	113.99(4)
S2 – Sn – S4	113.0	116.12(4)
S3 – Sn – S4	107.9	97.55(4)

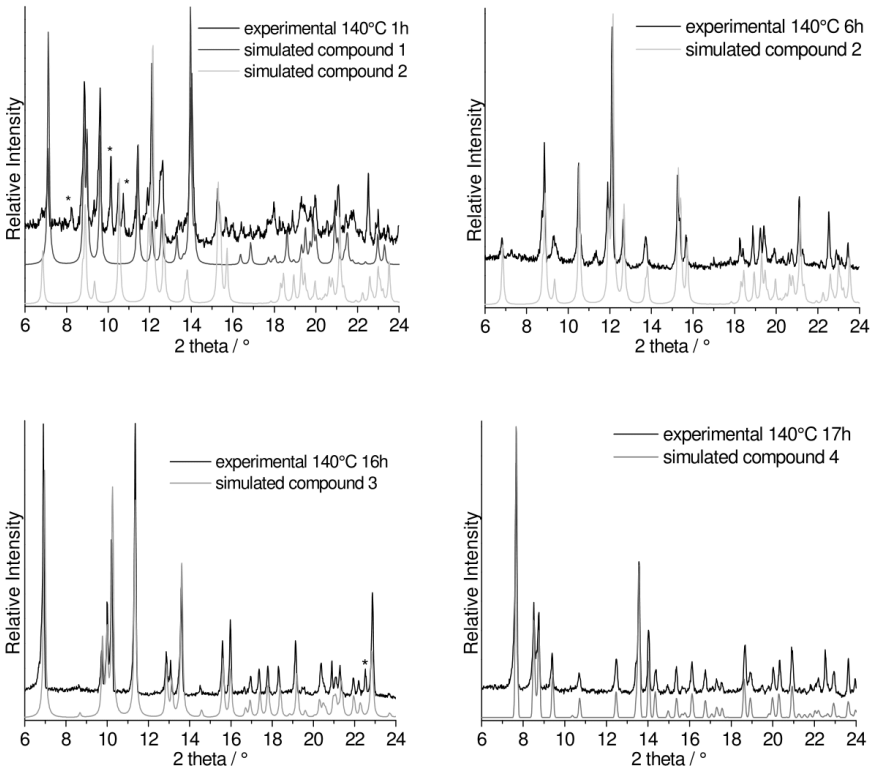

Fig. S8 Selected XRPD pattern for the series of time depended formation experiments at 140°C.

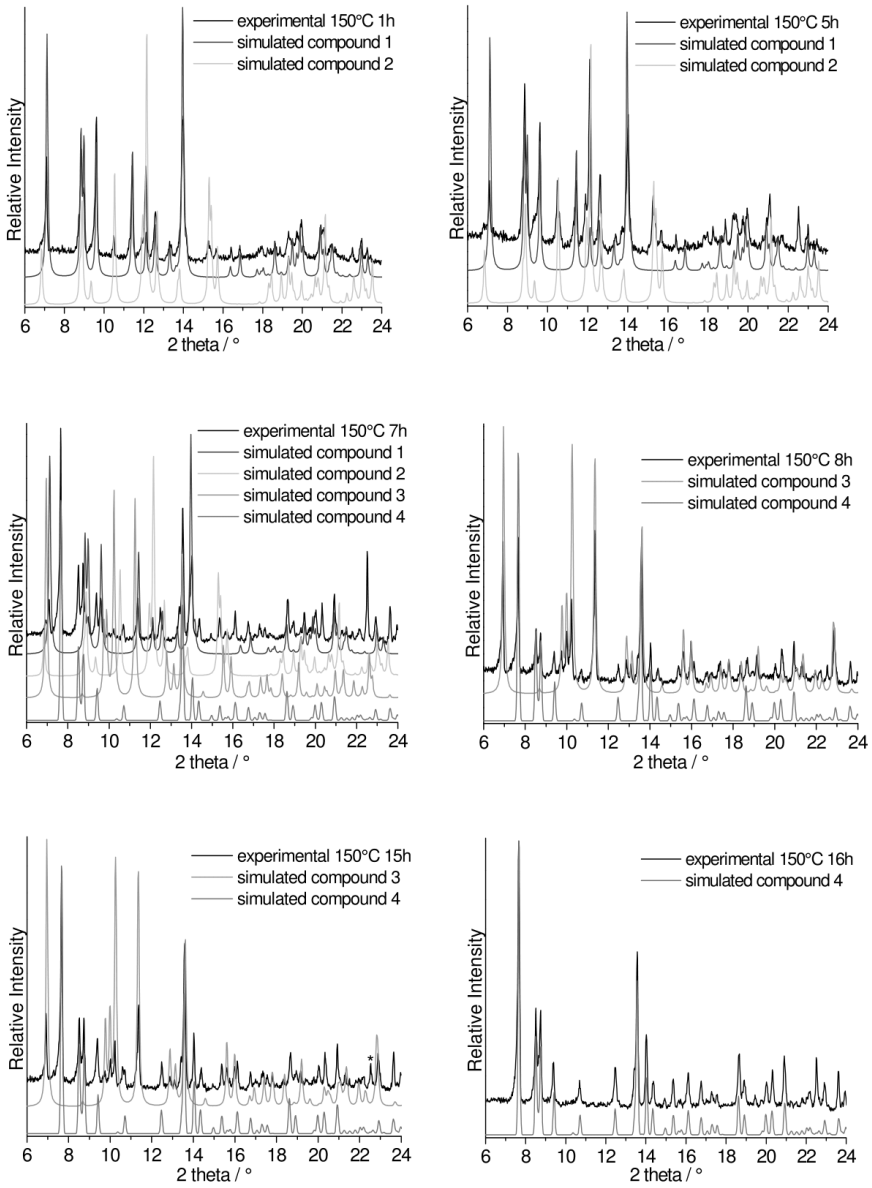

Fig. S9 Selected XRPD pattern for the series of time depended formation experiments at 150°C.

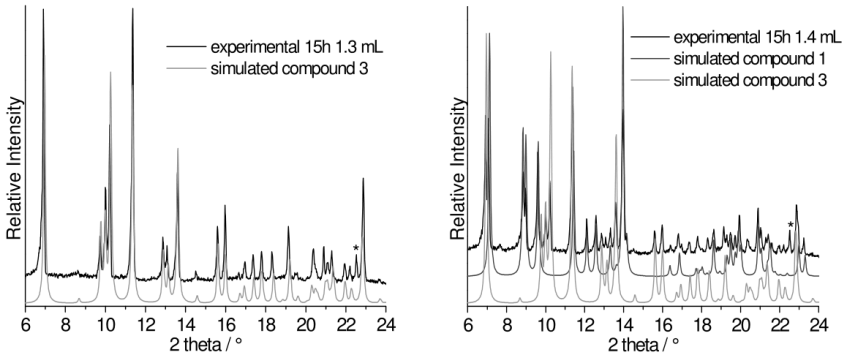

Fig. S10 Selected XRPD pattern for the series of solvent volume depended formation experiments after 15h.

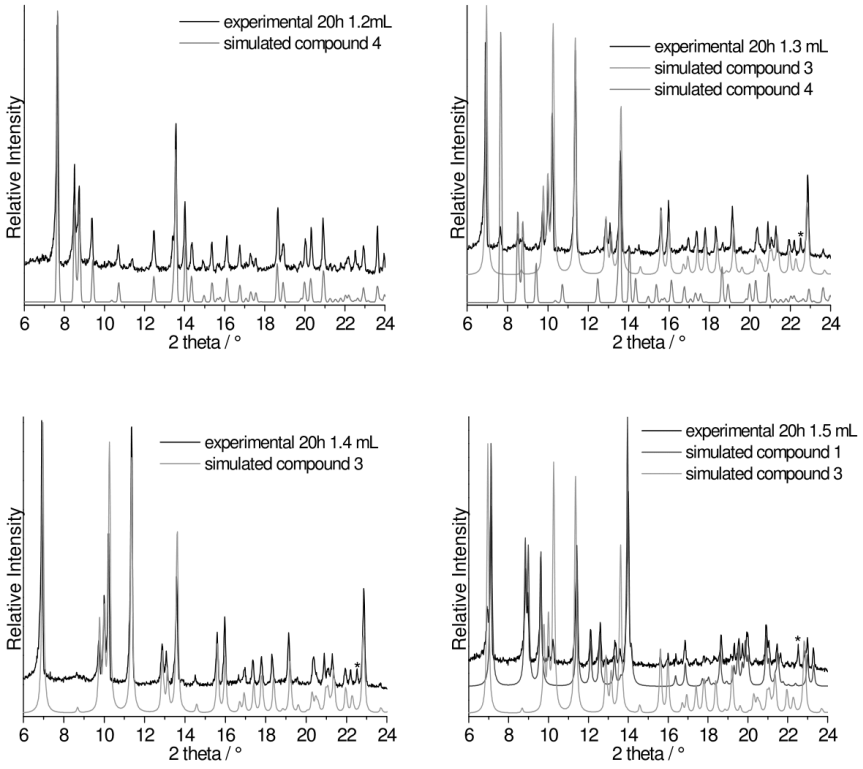

Fig. S11 Selected XRPD pattern for the series of solvent volume depended formation experiments after 20h.

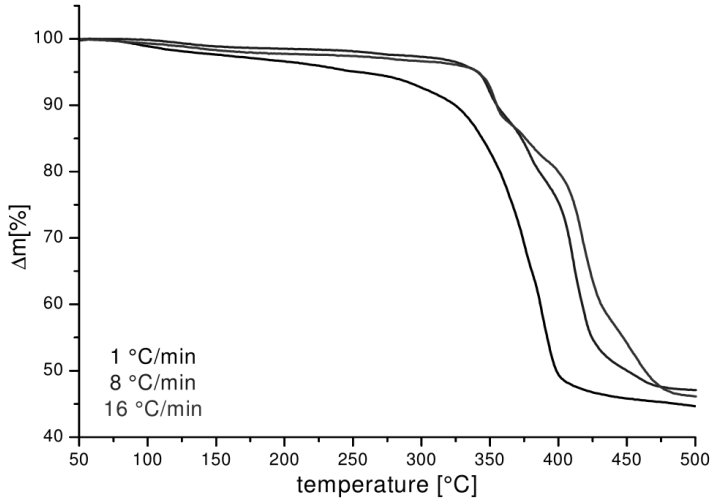

Fig. S12 Thermogravimetric curves of compound 4 measured at heating rates of 1 °C/min, 8 °C/min and 16 °C/Min.

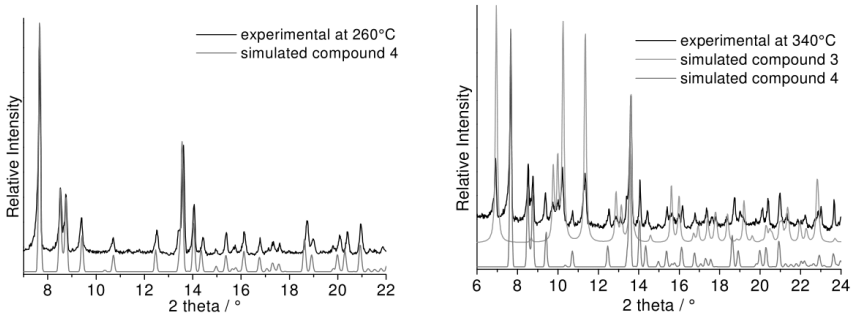

Fig. S13 The measured powder pattern of the decomposition of 4 at 260°C is in good agreement with the simulated powder pattern of compound 4 (left). The measured powder pattern of the decomposition of 4 at 340°C is in good agreement with the simulated powder pattern of compound 3 and 4 (right).

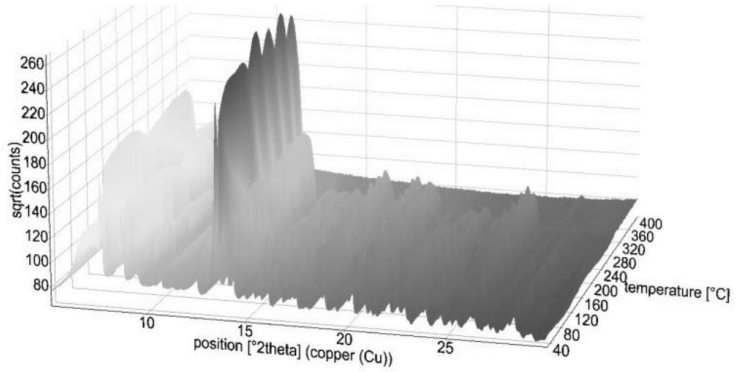

Fig. S14 Overview of the temperature dependent XRPD experiment. At about 315°C all reflections of compound **4** disappear and an amorphous phase is formed.

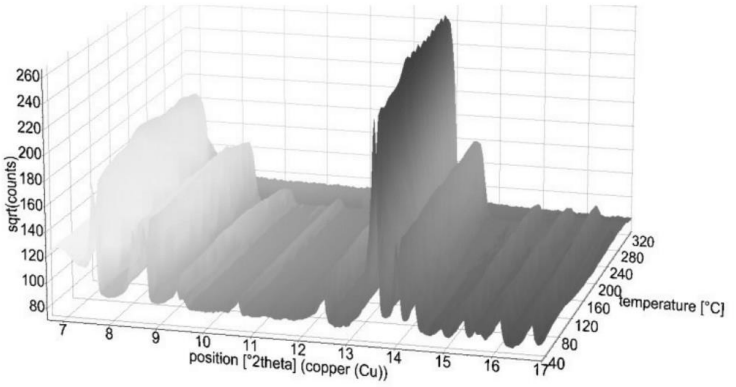

Fig. S15 The temperature dependent XRPD indicate an anisotropic behaviour of **4** concerning the thermal expansion.

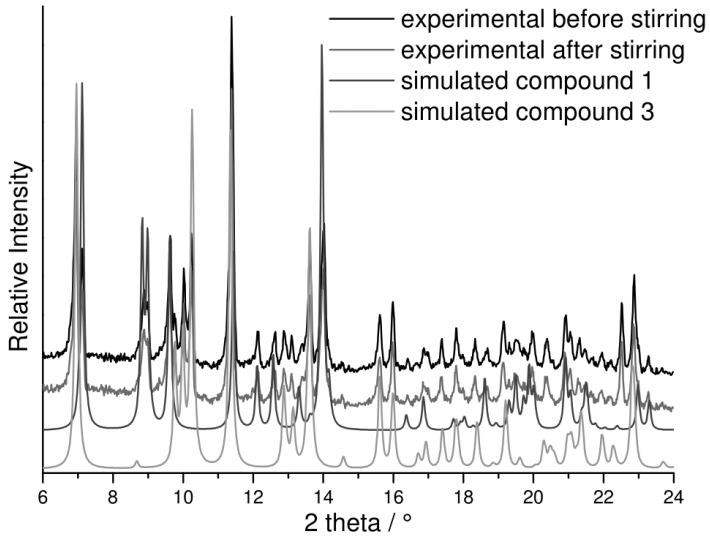

Fig. S16 The measured powder pattern before and after the solvent mediated conversion experiment of **1** and **3** is in both cases in good agreement with the simulated powder pattern of compound **1** and **3**.

Table S9 Results of the solubility measurement by AAS.

solvent	solubility of **1** [mg/L]	solubility of **3** [mg/L]
H_2O	4.94	2.31

5.2.2 SI für die Publikation: "Utilization of Mixtures of Aromatic N-donor Ligands of Different Coordination Ability for the Solvothermal Synthesis of Thiostannate Containing Molecules"

Electronic Supplementary Material (ESI) for Dalton Transactions.

Supplementary Information

Utilization of Mixtures of Aromatic N-Donor Ligands of Different Coordination Ability for the Solvothermal Synthesis of Thiostannate Containing Molecules

Jessica Hilbert, Christian Näther and Wolfgang Bensch

Content

Figure S1	Comparison of the experimental PXRD pattern of **I** and **II** with those simulated from single-crystal X-ray data.	2
Table S1	Selected angles (°) of the octahedral Ni^{2+} environment of **I** and **II**.	3
Table S2	Dihedral angles between the phen moieties for compounds **I** and **II**.	3
Figure S2	IR spectra of **I** (top) and **II** (bottom).	3
Figure S3	Raman spectra of **I** (top) and **II** (bottom).	4
Figure S4	UV/vis spectra of compound **I**.	4
Figure S5	UV/Vis spectra of compound **II**.	5
Figure S6	DTA, TG and DTG curves for compound **I**.	5
Figure S7	DTA, TG and DTG curves for compound **II**.	6
Figure S8	Temperature dependence of the magnetic susceptibility for compound **I** in field of 100 Oe.	6
Figure S9	Temperature dependence of the magnetic susceptibility for compound **II** in field of 100 Oe.	7

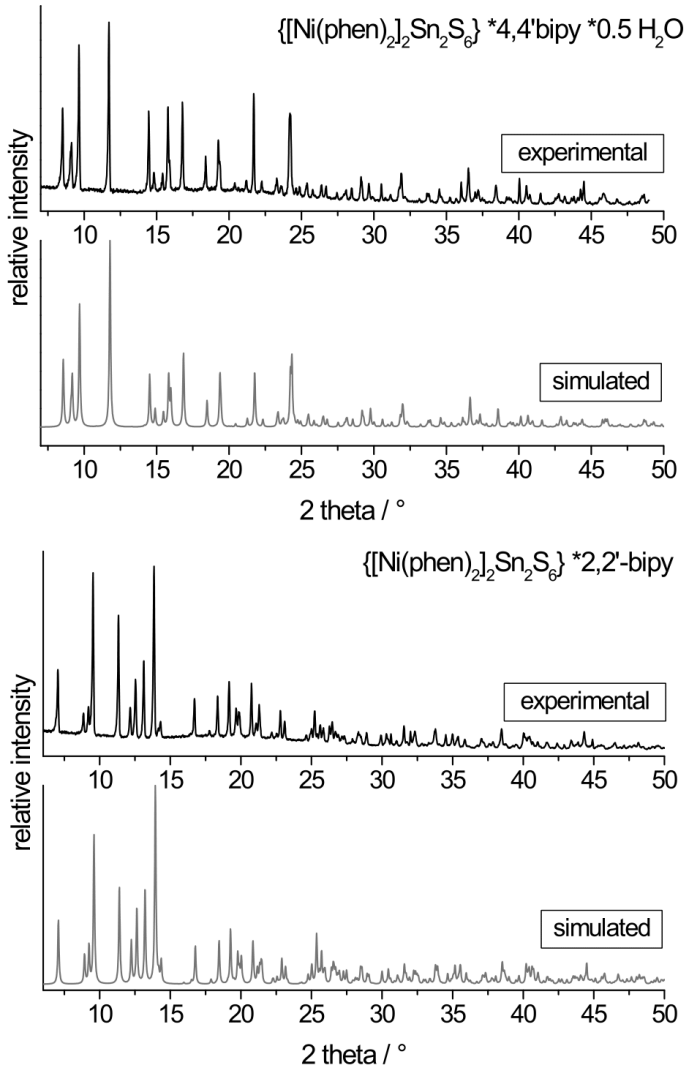

Fig. S1: Comparison of the experimental PXRD pattern of **I** (top) and **II** (bottom) with those simulated from single-crystal X-ray data.

Table S1: Selected angles (°) of the octahedral Ni^{2+} environment of **I** and **II**.

	I		II
N1[a] – Ni1 – N1	165.69(1)	N21 – Ni1 – N1	162.82(12)
N2 – Ni1 – S1[a]	173.19(9)	N22 – Ni1 – S2	172.28(9)
N2[a] – Ni1 – S1	173.19(9)	N2 – Ni1 – S3	172.36(8)
N1[a] – Ni1 – N2	91.54(13)	N22 – Ni1 – N1	92.95(12)
N1 – Ni1 – N2[a]	91.54(13)	N21 – Ni1 – N2	88.00(11)
N2 – Ni1 – N2[a]	93.84(18)	N22 – Ni1 – N2	91.35(11)
N1 – Ni1 – N2	78.64(13)	N1 – Ni1 – N2	77.38(11)
N1[a] – Ni1 – N2[a]	78.64(13)	N22 – Ni1 – N22	78.25(12)
N1[a] – Ni1 – S1[a]	95.27(9)	N21 – Ni1 – S2	94.11(9)
N1 – Ni1 – S1[a]	94.64(9)	N2 – Ni1 – S2	89.46(8)
N2 – Ni1 – S1[a]	87.36(9)	N1 – Ni1 – S2	94.72(8)
N1[a] – Ni1 – S1	94.64(9)	N21 – Ni1 – S3	99.34(8)
N1 – Ni1 – S1	95.27(9)	N22 – Ni1 – S3	88.13(9)
N2 – Ni1 – S1	87.36(9)	N1 – Ni1 – S3	95.04(8)
S1[a] – Ni1 – S1	92.23(5)	S2 – Ni1 – S3	92.08(3)

Table S2: Dihedral angles between the phen moieties for compounds **I** and **II**.

	I		II
N2[a] – Ni1 – N1 – C10	82.70(33)	N22 – Ni1 – N1 – C1	-88.73(33)
N2[a] – Ni1 – N1 – C11	-96.72(26)	N22 – Ni1 – N1 – C12	92.57(24)
N2[a] – Ni1 – N2 – C1	-90.95(33)	N22 – Ni1 – N2 – C10	88.26(32)
N2[a] – Ni1 – N2 – C12	95.23(26)	N22 – Ni1 – N2 – C11	-95.65(24)

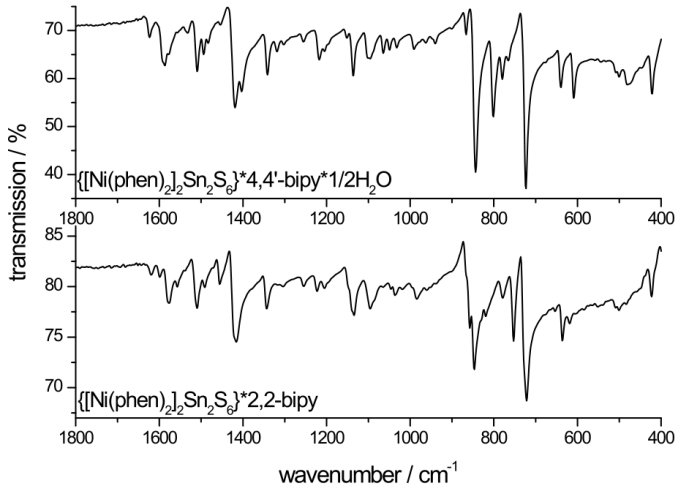

Fig. S2: IR spectra of **I** (top) and **II** (bottom).

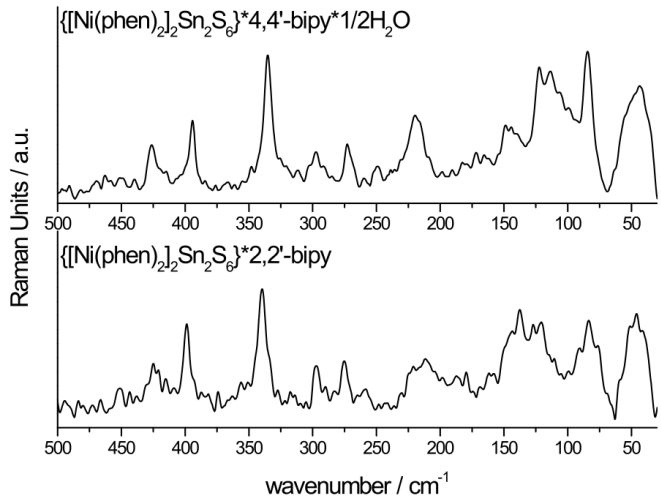

Fig. S3: Raman spectra of **I** (top) and **II** (bottom).

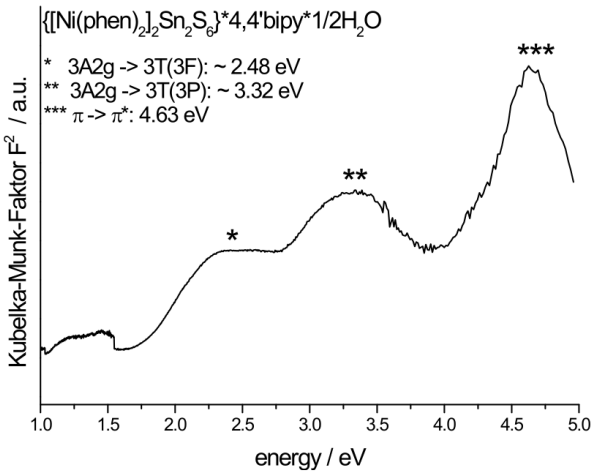

Fig. S4: UV/vis spectra of compound **I**.

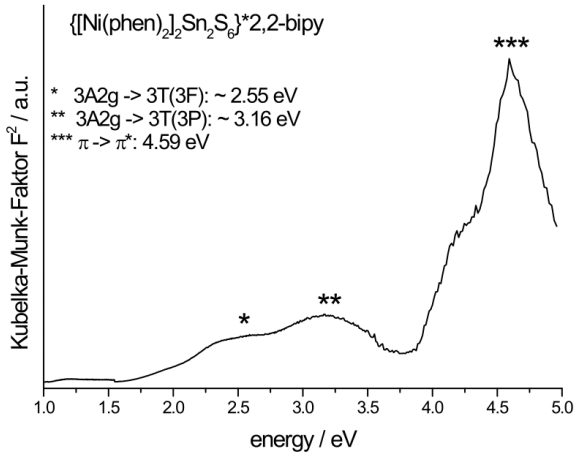

Fig. S5: UV/Vis spectra of compound **II**.

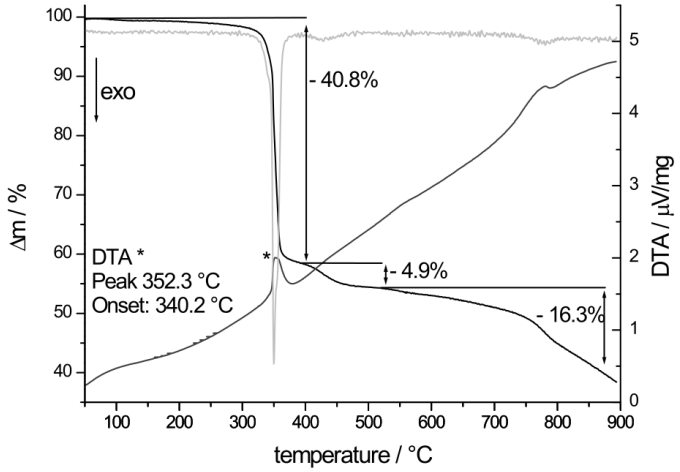

Fig. S6: DTA, TG and DTG curves for compound **I**.

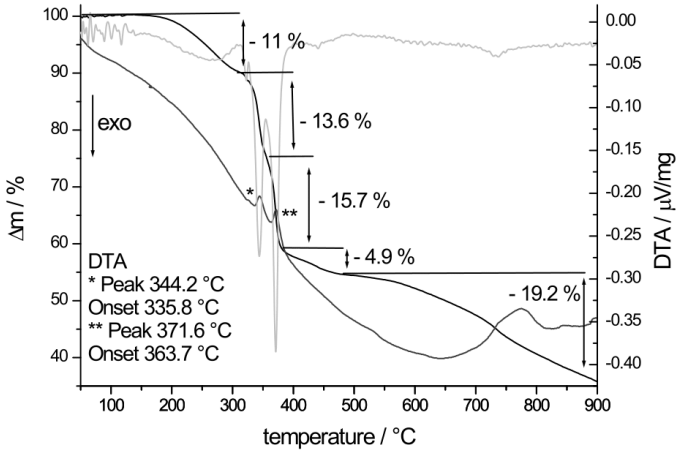

Fig. S7: DTA, TG and DTG curves for compound **II**.

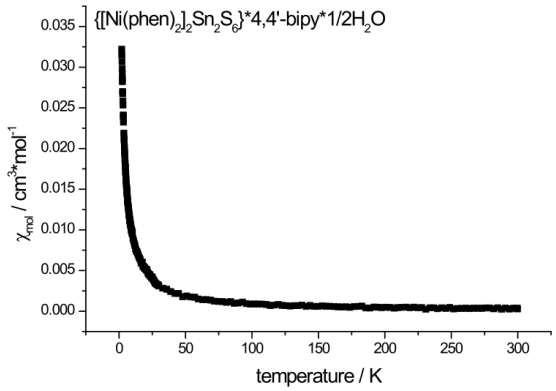

Fig. S8: Temperature dependence of the magnetic susceptibility for compound **I** in field of 100 Oe.

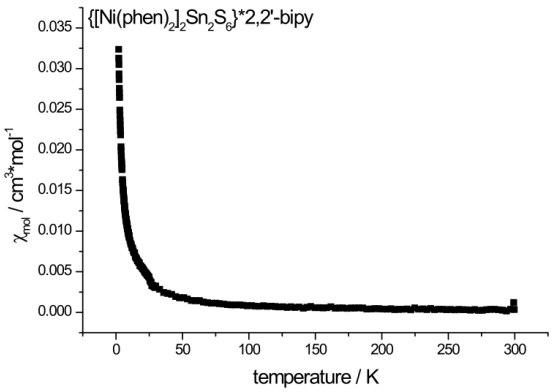

Fig. S9: Temperature dependence of the magnetic susceptibility for compound **II** in field of 100 Oe.

5.2.3 SI für die Publikation:“ Room temperature synthesis of thiostannates from $\{[Ni(tren)]_2[Sn_2S_6]\}_n$”

Supplementary Information

Room temperature synthesis of thiostannates from $\{[Ni(tren)]_2[Sn_2S_6]\}_n$

Jessica Hilbert, Christian Näther, Richard Weihrich, Wolfgang Bensch*

Content

Figure S1	Comparison of the experimental PXRD patterns of **1-3** (black) with their corresponding simulated from single-crystal X-ray data (red).	3-4
Table S1	Comparison of the lattice parameters for compound $[Ni(tren)(1,2\text{-dap})]_2[Sn_2S_6] \cdot 2H_2O$ at 200K and room temperature (RT).	4
Table S2	Overview of the reaction conditions and products of the syntheses at RT	5
Figure S2	PXRD pattern of compound **1** (left) which resulted in formation of compound **2** (right).	5
Figure S3	PXRD pattern of the obtained products when stirring compound **1** at room temperature with 1,2-dap (left) and en (right).	5
Figure S4	PXRD pattern of the obtained results when stirring compound **1** at room temperature with 1,2-dach (left) and 1,3-dap (regaining **1**, right).	6
Table S3	Overview of the resulting products under stirring conditions (120°C).	6
Figure S5	PXRD pattern of the products obtained from the reaction mixture of **1** in ma (30%) when filtering the hot reaction mixture (left) and synthesis mixture after several days (right).	7
Figure S6	PXRD pattern of the products obtained from the reaction mixture of **1** in 2 mL aqueous 1,2dap solution when applying < 0.2 mL (2.35 mmol) 1,2dap in the synthesis mixture (left) and > 0.6 mL 1,2dap (7.05 mmol) (RT) (right).	7
Figure S7	IR spectra of **1-3**.	8
Table S4	Absorption of the IR spectra of compounds **1-3** compared to tren	9
Figure S8	Raman spectra of **1-3**	10
Table S5	Data of the signals in the Raman spectra of compound **1-3** compared to $Na_4Sn_2S_6 \cdot 14 H_2O$	10
Figure S9	Determination of the optical band gap of **1-3** from UV/vis diffuse reflectance spectrum using the Kubelka-Munk method.	11

Figure S10	Parallel arrangement of the $\{[Ni(tren)]_2[Sn_2S_6]\}_n$- chains within the *ac* plane (top) and *bc* plane (bottom stabilized via hydrogen bridges (purple dashed lines).	12
Figure S11	Stabilizing of the structure in **1** via hydrogen bridges (purple dashed lines) within and between the chains.	12
Table S6	Calculated atomic distances (d/Å)	13
Figure S12	a) Charge density plot for density values from 0.01 to 0.3 e/au³. The charge density at the BCP of the longer Ni-S bond is lower (0.029 e/au³) than for the shorter	14
Table S7	BCP data for A-X bonds from the topological analysis of the charge density (PBE calculation) with calculated values at the BCPs for the charge density (ρ), its gradient, and its laplacian. ELF (Becke´s electron localisation function) values are calculated from α- (ELF) and ß-spin (ELFB) densities, and distances of the atoms to the BCP are given in Å.	14
Figure S13	Molgraph with all bonds and H-bonds at S atoms.	14
Figure S14	Atomic site projected density of states (DOS) of the electronic band structure from the spin polarized PBE-calculation.	15
Figure S15	Octahedral environment of the Ni^{2+} ion in compound **1** (left) and **2** (right).	15
Figure S16	Octahedral environment of the Ni^{2+} ion in compound **3**.	16
Table S8	Selected bond length (Å) and angles (°) of compounds **1**-**3** compared to $Na_4Sn_2S_6 \cdot 14H_2O$	16
Table S9	Selected angles (°) of the octahedral Ni^{2+} environment of **1**-**3**.	17
Figure S17	Hydrogen bridging interactions of the water molecules in **2** with each other and with adjacent $[Sn_2S_6]^{4-}$ units	17
Figure S18	Maximum hydrogen bridging interactions of the $[Sn_2S_6]^{4-}$ unit with adjacent molecules in **2**, only selected hydrogen atoms are shown.	18
Figure S19	Maximum hydrogen bridging interactions of the $[Sn_2S_6]^{4-}$ unit with adjacent molecules in **3**, only selected hydrogen atoms are depicted	18

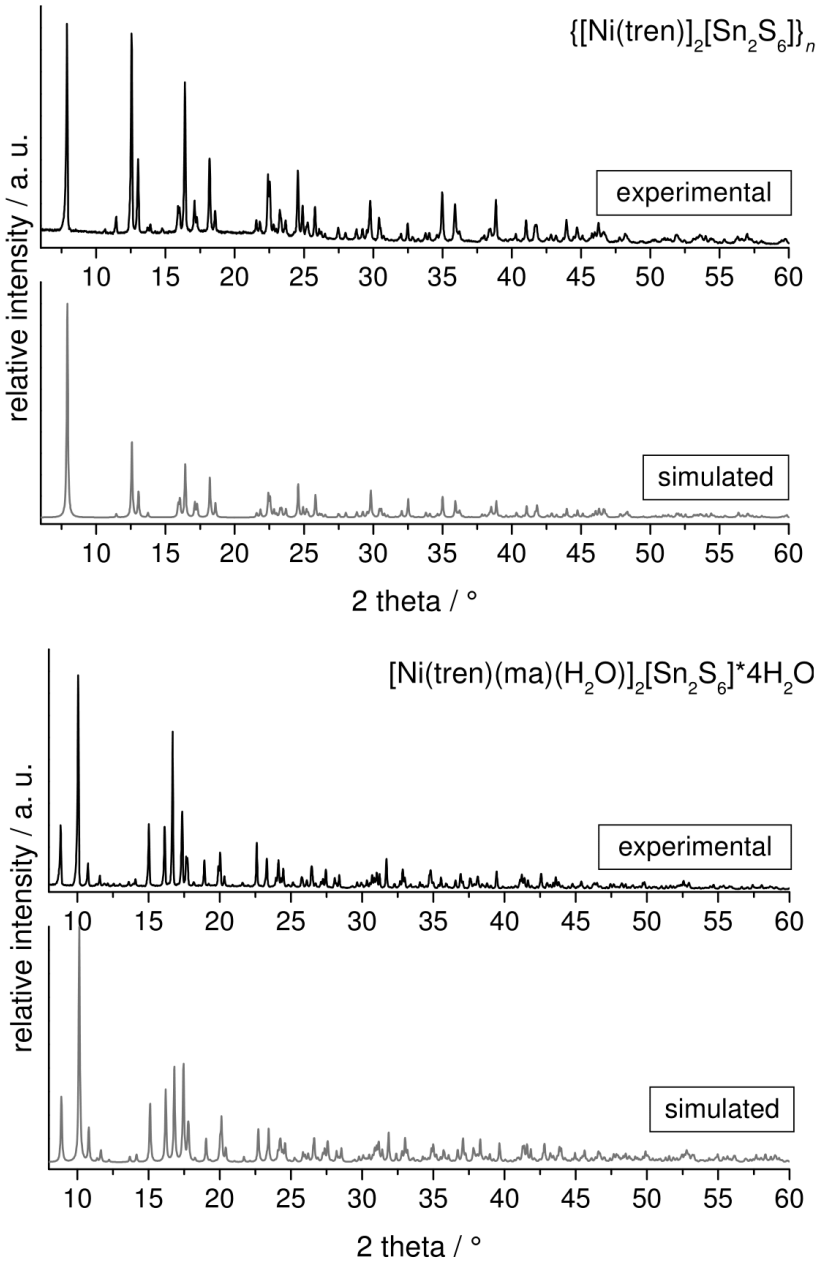
{[Ni(tren)]2[Sn2S6]}n
experimental
simulated
relative intensity / a. u.
2 theta / °
[Ni(tren)(ma)(H2O)]2[Sn2S6]*4H2O
experimental
simulated
relative intensity / a. u.
2 theta / °

S3

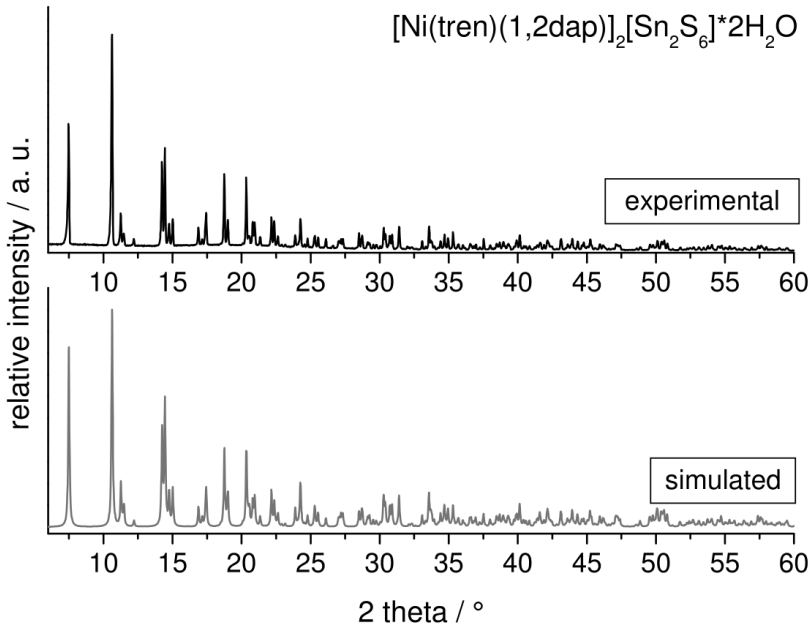

Fig. S1: Comparison of the experimental PXRD patterns of **1-3** (black) with their corresponding simulated from single-crystal X-ray data (red).

The lattice parameters for compound $[Ni(tren)(1,2\text{-dap})]_2[Sn_2S_6] \cdot 2H_2O$ at room temperature were determinate from the PXRD pattern (Table S1). For this compounds these lattice parameters were used for the simulated patterns. For the two other compounds, no major deviation could be observed.

Table S1: Comparison of the lattice parameters for compound $[Ni(tren)(1,2\text{-dap})]_2[Sn_2S_6] \cdot 2H_2O$ at 200K and room temperature (RT).

$[Ni(tren)(1,2\text{-dap})]_2[Sn_2S_6] \cdot 2H_2O$	
200K	RT
a: 12.9264(3) Å	a: 13.0486(9) Å
b: 10.1627(3) Å	b: 10.1623(2) Å
c: 15.6585(4) Å	c: 15.7482(1) Å

Syntheses at room temperature (stirring conditions)

Table S2: Overview of the reaction conditions and resulting products of the syntheses at room temperature (t = 1-10 h). Total volume of the solvent 2 mL.

Ni educt 0.5 mmol	solvent	amount amine	product	yield
$\{[Ni(tren)]_2[Sn_2S_6]\}_n$ (**1**)$_n$	ma[a]	1.5 mL (17.2 mmol)	$[Ni(tren)(ma)(H_2O)]_2[Sn_2S_6]\cdot 4H_2O$ (**2**)	60%
	1,2dap	64 µL (0.75 mmol) – 2 mL (23.5 mmol)	$[Ni(tren)(1,2dap)]_2[Sn_2S_6]\cdot 2H_2O$ (**3**)	70%
	en	50 µL (0.75 mmol) – 2 mL (29.9 mmol)	$[Ni(en)_3]_2[Sn_2S_6]$[b]	70%
	1,2dach	90 µL (0.75 mmol) – 2 mL (16.6 mmol)	$[Ni(1,2dach)_3]_2[Sn_2S_6]\cdot 4H_2O$[c]	70%
	1,3dap	63 µL (0.75 mmol) – 2 mL (23.7 mmol)	$\{[Ni(tren)]_2[Sn_2S_6]\}_n$ (**1**)	90%

a: aqueous solution 40%
b: Behrens, M.; Scherb, S.; Näther, C.; Bensch, W. *Z. Anorg. Allg. Chem.* **2003**, *629*, 1367–1373.
c: Pienack, N.; Lühmann, H.; Seidlhofer, B.; Ammermann, J.; Zeisler, C.; Danker, F.; Näther, C.; Bensch, W. *Solid State Sci.* **2014**, *33*, 67–72.

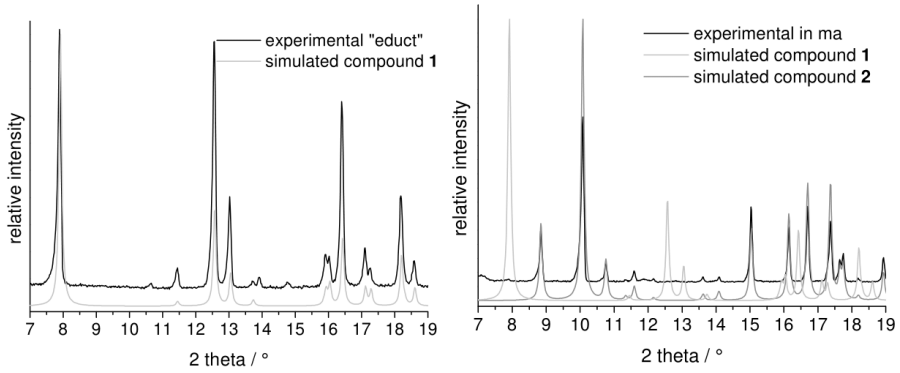

Fig. S2: PXRD pattern of compound **1** (left) which was then stirred with ma at room temperature resulting in formation of compound **2** (right).

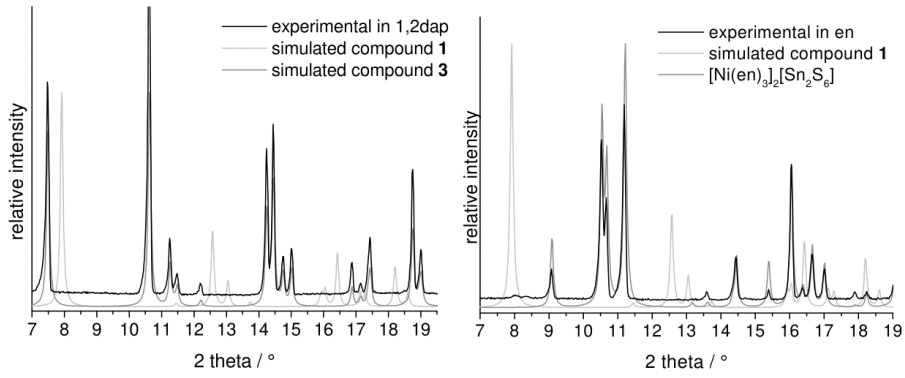

Fig. S3: PXRD pattern of the obtained products when stirring compound **1** at room temperature with 1,2-dap (resulting in **3**, left) and en (resulting in $[Ni(en)_3]_2[Sn_2S_6]$, right).

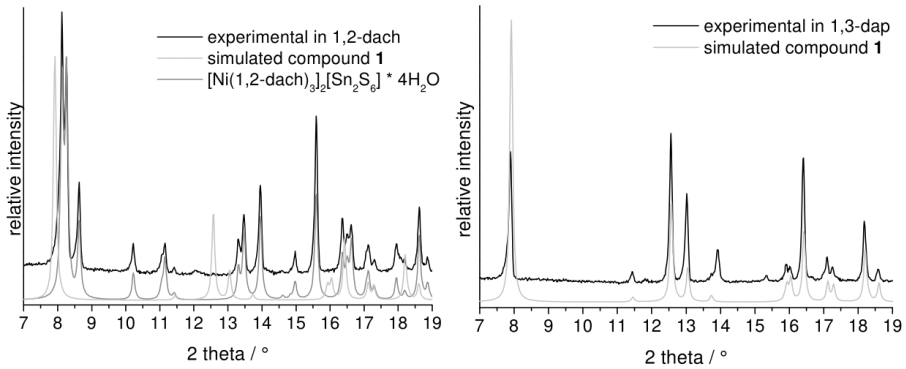

Fig. S4: PXRD pattern of the obtained results when stirring compound **1** at room temperature with 1,2-dach (resulting in $[Ni(1,2\text{-dach})_2]_2[Sn_2S_6] \cdot 4H_2O$, left) and 1,3-dap (regaining **1**, right).

Results obtained under stirring solvothermal conditions

Table S3: Overview of the resulting products under stirring conditions (T = 120°C; t = 1-10 h). Further educts: Sn (0.25 mmol) and S (0.75 mmol). Total volume of the solvent 2 mL.

Ni educts (0.25 mmol)	solvent	amount amine	product	yield
$\{[Ni(tren)]_2[Sn_2S_6]\}_n$ (**1**)	ma[a]	1.5 mL (17.2 mmol)	hot solution: $\{[Ni(tren)]_2[Sn_2S_6]\}_n$ (**1**)	90%
			RT: $[Ni(tren)(ma)(H_2O)]_2[Sn_2S_6]\cdot 4H_2O$ (**2**)	60%
	1,2dap	< 0.2 mL (2.35 mmol)	$\{[Ni(tren)]_2[Sn_2S_6]\}_n$ (**1**)	90%
		0.2 mL (2.35 mmol) – 0.6 mL (7.05 mmol)	*x-ray amorphous*	--
		> 0.6 mL (7.05 mmol) – 2 mL (23.5 mmol)	$[Ni(tren)(1,2dap)]_2[Sn_2S_6] \cdot 2H_2O$ (**3**)	70%
	en	50 µL (0.75 mmol) – 2 mL (29.9 mmol)	$[Ni(en)_3]_2[Sn_2S_6]$[b]	70%
	1,2dach	90 µL (0.75 mmol) – 2 mL (16.6 mmol)	$[Ni(1,2dach)_3]_2[Sn_2S_6] \cdot 4H_2O$[c]	70%
	1,3dap	63 µL (0.75 mmol) – 2 mL (23.7 mmol)	$\{[Ni(tren)]_2[Sn_2S_6]\}_n$ (**1**)	90%

a: aqueous solution 40%

b: Behrens, M.; Scherb, S.; Näther, C.; Bensch, W. *Z. Anorg. Allg. Chem.* **2003**, *629*, 1367–1373.

c: Pienack, N.; Lühmann, H.; Seidlhofer, B.; Ammermann, J.; Zeisler, C.; Danker, F.; Näther, C.; Bensch, W. *Solid State Sci.* **2014**, *33*, 67–72.

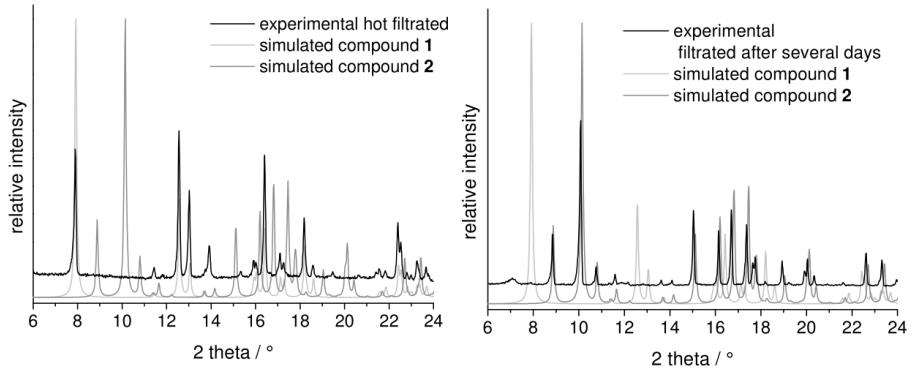

Fig. S5: PXRD pattern of the products obtained from the reaction mixture of **1** in ma (30%) when filtering the hot reaction mixture (left) and synthesis mixture after several days (right).

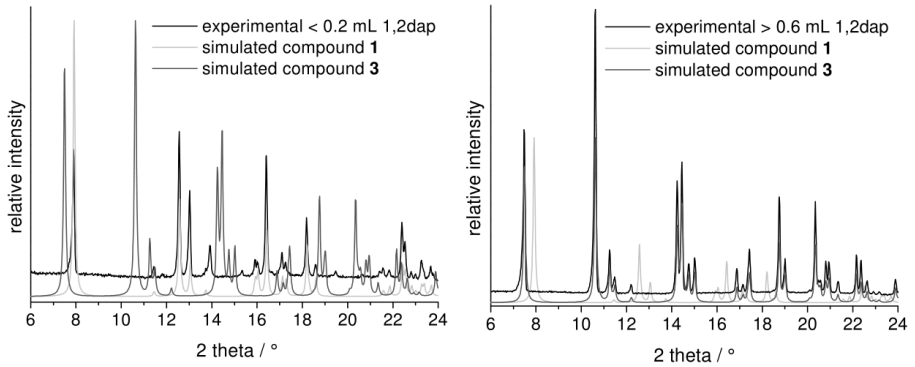

Fig. S6: PXRD pattern of the products obtained from the reaction mixture of **1** in an aqueous 1,2dap solution when applying < 0.2 mL (2.35 mmol) 1,2dap in the synthesis mixture (left) and > 0.6 mL 1,2dap (7.05 mmol) (RT) (right).

Spectroscopic Properties

Infrared spectroscopy

The observed absorptions in the IR spectra of compound **1**-**3** can be mostly assigned to tren [Marzotto, A; Ciccarese, A; Clemente, D. A.; Valle, G. *J. Chem. Soc. Dalton Trans.* **1995**, 1461-1468.] and the Ni-N-stretching vibration at below 420 cm^{-1}. The absorption of the other amines are mostly overlapping with the tren signals, but for example the absorption at 1206 and 828 cm^{-1} can be associate to a CH_3-group which is only present in compound **3** (Table S5).

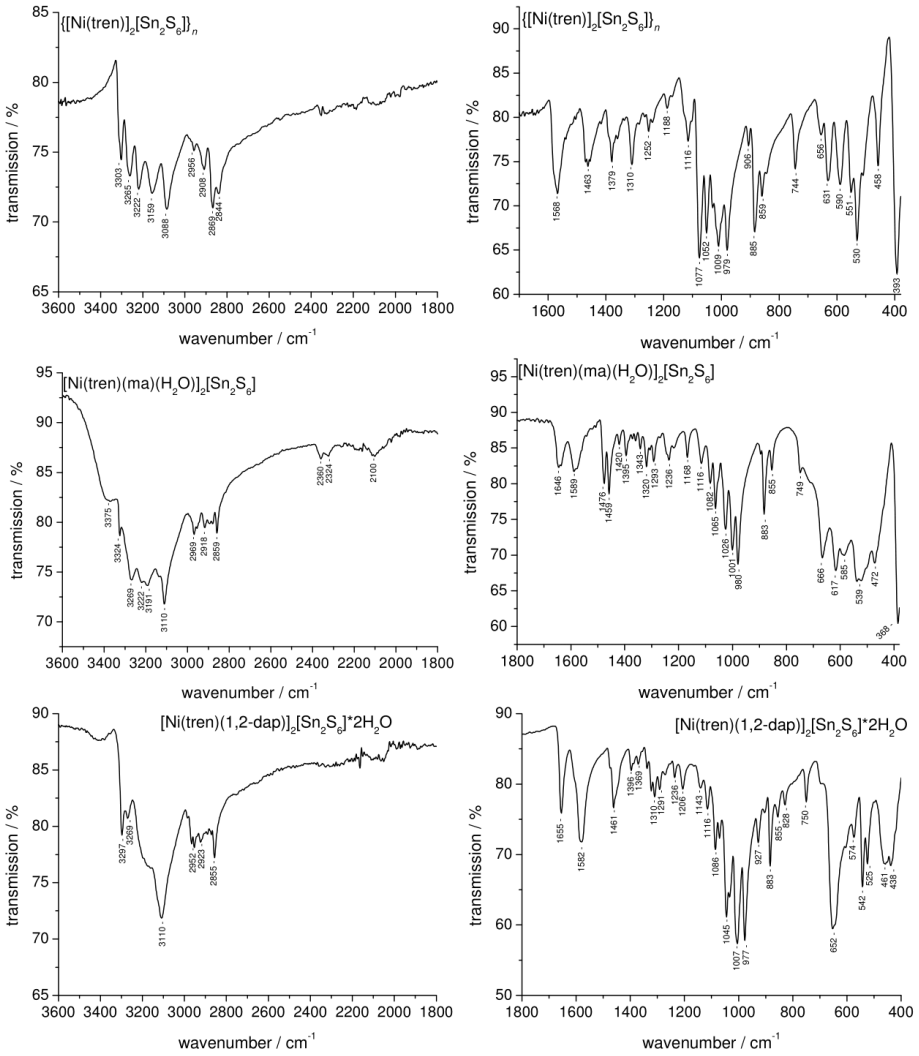

Fig. S7: IR spectra of **1-3**

Table S4: Absorption of the IR spectra of compounds **1-3** compared to tris(2-aminethyl)amine (tren).

tren[Marzotto et al.]	**1**	**2**	**3**	assignment
		~3375	~3409	ν (O-H)
3270s	3303m, 3265m	3324m, 3269m	3297m, 3269w	ν (NH_2)
3180m	3222m, 3159m	3222w, 3191w, 3110s	3110s	ν (NH)
	3088m			ν (NH_2)
2930s, 2855s, 2800s	2956vw, 2908w, 2869m, 2844w	2969m, 2918w, 2859m	2966w, 2952w, 2923w, 2855m	ν (CH_2)
		2360w, 2324w, 2100w		ν (NH)
		1646m	1655m	δ(HOH)
1590s, 1445m	1568s, 1463m	1589m, 1476m, 1459m	1582s, 1461m	δ (NH_2) + □ (CH_2)
1390w, 1365(sh)	1379m	1420w, 1395w, 1361w	1396w, 1369w	δ (CH_2)
		1343w		δ (NH_2)
1348m, 1304m	1310m	1320w	1338w, 1323w, 1310w	δ (CH_2)
1270m, 1230w	1252w	1293w, 1236w	1291w, 1271vw, 1236w	ν (C-NH_2)+ ν (C-N)
			1206m	δ (CH_3)
	1188w	1168w	1143w	ν (C-N)
1112vs	1116m	1116w	1116m	ν (C-NH_2)+ ν (C-N)
1090m, 1070m, 1035s, 1020(sh)	1077s, 1052s, 1009s	1082w, 1065m, 1026m, 1001s	1086m, 1070w, 1045s, 1007s	δ (NH_2) region
	979s	980s	977s	
				skeleton vib. (cyclohex.)
902s (br), 865s(br), 840(sh)	906w, 885s, 859m	883s, 855m	927m, 906vw, 883m, 855w	δ (NH_2)
			828w	δ (CH_3)
765(sh), 730w	744m, 656w	749w, 666m	750m, 652s	δ (NH_2)
	631m, 590m, 551w, 530s, 458m	617m, 585w, 539m, 522m, 472w	574w, 542s, 525m, 461w,	main skeleton vib. (tren chain)
			438w	
	393s	386s		ν (M-N_{tren})

Raman spectroscopy

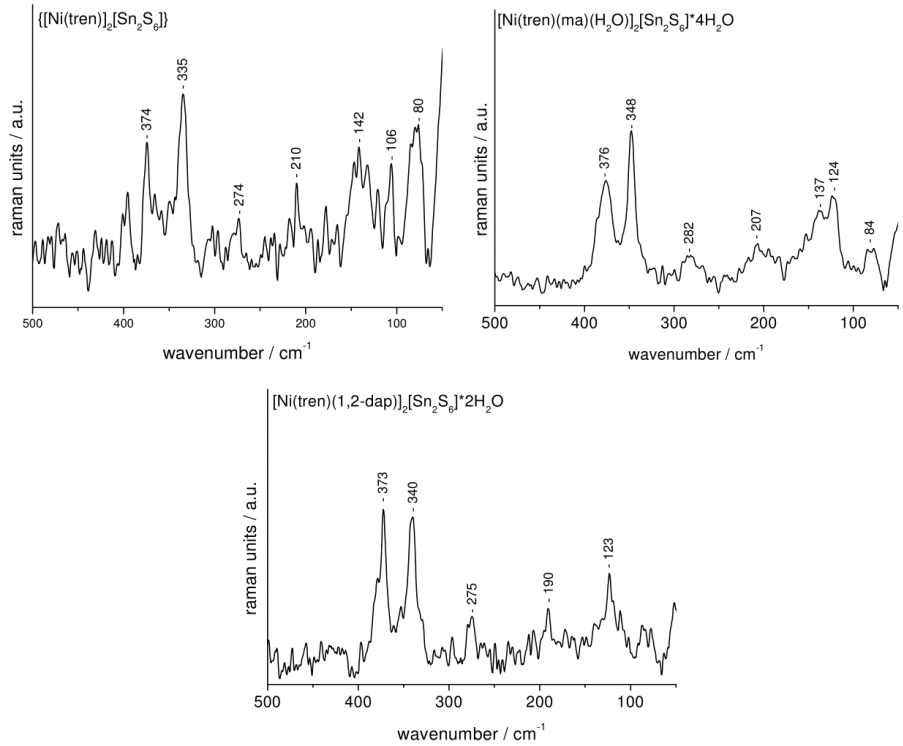

Fig. S8: Raman spectra of **1-3**.

Table S5: Data of the signals in the Raman spectra of $Na_4Sn_2S_6 \cdot 14\ H_2O$ [Krebs, B; Pohl, S.; Schiwy, W. *Angew. Chem. Int. Ed. Engl.* **1970**, *9*, 897-898] and compounds **1-3** (all wave numbers given in cm^{-1}).

$[Sn_2S_6]^{4-}$	**1**	**2**	**3**
391, 377	374	376	379, 373
341	335	348	340
281	274	282	275
190	210	207	190
151	178		
136	142	137	123
	106	124	
	80	84	

UV/vis spectroscopy

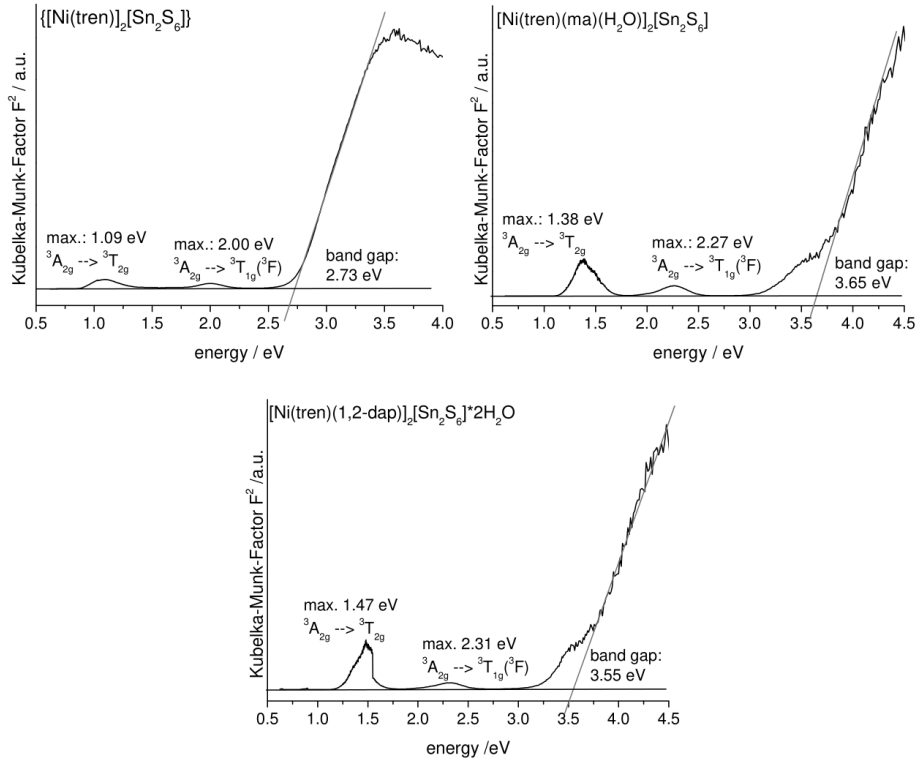

Fig. S9: Determination of the optical band gap of **1-3** from UV/vis diffuse reflectance spectrum using the Kubelka-Munk method.

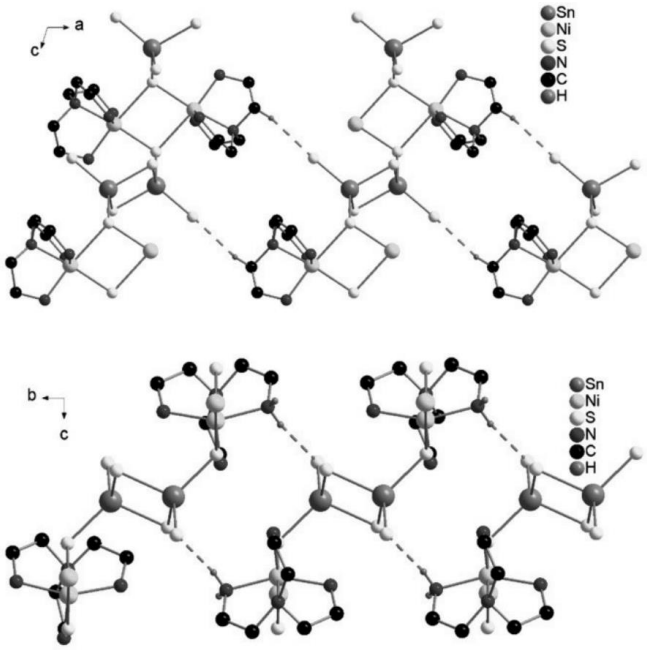

Fig. S10: Parallel arrangement of the $\{[Ni(tren)]_2[Sn_2S_6]\}_n$- chains within the *ac* plane (top) and bc-plane (bottom stabilized via hydrogen bridges (purple dashed lines).

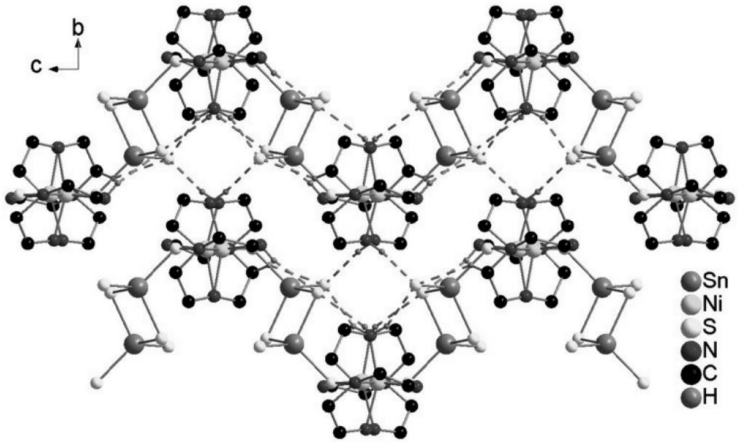

Fig. S11: Stabilizing of the structure in **1** via hydrogen bridges (purple dashed lines) within and between the chains.

Table S6: Calculated atomic distances (d/Å)

	Ni-N1	Ni-N2	Ni-N3	Ni-N4	Ni-S1	Ni-S2	N-H	S-Hc	Sn-S	Sn-S
XRD (exp)	2.088	2.102	2.115	2.130	2.434	2.745	1.036	-	2.311 2.363	2.452 2.467
Basis 1										
LDA	2.011	2.011	2.015	2.057	2.456	2.507	1.029 1.044		2.346 2.418	2.490 2.526
PBE	2.056	2.057	2.062	2.118	2.439	2.624	1.023 1.035		2.358 2.419	2.510 2.526
PBE0	2.055	2.056	2.058	2.100	2.462	2.694	1.011 1.020		2.333 2.385	2.478 2.490
Basis 2										
LDA	2.036	2.037	2.047	2.089	2.386	2.659	1.027 1.040		2.346 2.405	2.489 2.524
PBE	2.098	2.099	2.102	2.155	2.461	2.767	1.022 1.033		2.359 2.410	2.510 2.526
PBE0	2.095	2.104	2.104	2.140	2.481	2.825	1.013 1.023		2.334 2.381	2.478 2.490
Model 1										
LDA-BS1	2.035	2.035	2.045	2.045	2.373	2.374	1.031	1.366		
PBE-BS1	2.086	2.086	2.099	2.099	2.513	2.513	1.030	1.362		
B3LYP-BS1	2.072	2.072	2.089	2.089	2.452	2.452	1.018	1.346		
LDA-BS2	2.060	2.060	2.060	2.070	2.418	2.20	1.030	1.366		
PBE-BS2	2.125	2.125	2.125	2.135	2.590	2.591	1.027	1.362		
B3LYP-BS2	2.131	2.131	2.131	2.140	2.714	2.724	1.020	1.035		
Modell 2	BS1									
LDA-f	2.007	2.007	2.011	2.013	2.426	2.437	1.028	1.365		
LDA-BS1-af	2.008	2.008	2.020	2.011	2.407	2.424	1.029	1.373		
PBE-BS1-f	2.065	2.065	2.076	2.079	2.500	2.519	1.026	1.361		
PBE-BS1-af	2.069	2.069	2.069	2.077	2.493	2.495	1.026	1.365		
B3LYP-f	2.084	2.084	2.091	2.096	2.543	2.578	1.018	1.349		
B3LYP-af	2.086	2.092	2.095	2.095	2.544	2.551	1.018	1.350		
Mod2-BS2										
LDA-fm	2.031	2.031	2.037	2.040	2.464	2.476	1.028	1.365		
LDA-afm	2.034	2.034	2.036	2.036	2.443	2.464	1.028	1.372		
PBE-fm	2.101	2.101	2.116	2.120	2.540	2.567	1.026	1.361		
PBE-afm	2.103	2.103	2.115	2.118	2.537	2.545	1.025	1.365		
B3LYP-fm										
B3LYP-afm	2.126	2.126	2.134	2.140	2.584	2.617	1.018	1.351		

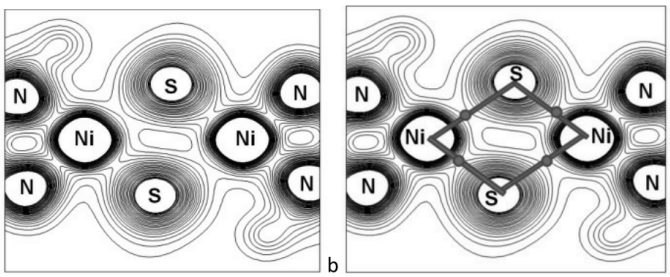

Fig. S12: a) Charge density plot for density values from 0.01 to 0.3 e/au³. The charge density at the BCP of the longer Ni-S bond is lower (0.029 e/au³) than for the shorter (0.051 e/au³, see also Tab. S8).

Table S7: BCP data for A-X bonds from the topological analysis of the charge density (PBE calculation) with calculated values at the BCPs for the charge density (ρ), its gradient, and its laplacian. ELF (Becke´s electron localisation function) values are calculated from α- (ELF) and ß-spin (ELFB) densities, and distances of the atoms to the BCP are given in Å.

BCP	Bond	ρ(e/au³)	Δρ	Δ²ρ	ELFA	ELFB	d(A-BCP)	d(BCP-X)
CP34	Sn-S	8.6625E-02	0	1.1815E-01	0.400	0.402	1.139	1.220
CP35	Sn-S	8.0602E-02	0	1.0433E-01	0.400	0.415	1.156	1.254
CP36	Sn-S	6.7958E-02	0	9.6166E-02	0.369	0.369	1.186	1.324
CP38	Sn-S	6.6023E-02	0	9.2107E-02	0.369	0.372	1.193	1.333
CP40	Ni-N	7.2764E-02	0	2.9572E-01	0.122	0.215	1.003	1.096
CP41	Ni-N	7.2711E-02	0	2.9330E-01	0.116	0.243	0.999	1.100
CP42	Ni-N	7.2313E-02	0	2.9049E-01	0.122	0.219	1.005	1.098
CP43	Ni-N	6.6176E-02	0	2.4589E-01	0.119	0.241	1.023	1.132
CP44	Ni-S	5.0957E-02	0	1.3404E-01	0.154	0.264	1.093	1.368
CP46	Ni-S	2.8845E-02	0	5.5496E-02	0.137	0.195	1.221	1.546
CP45	S-H	1.1371E-02	0	2.3027E-02	0.073	0.068	0.948	1.804
CP47	S-H	1.1647E-02	0	3.3221E-02	0.050	0.045	1.037	1.733
CP48	S-H	1.9349E-02	0	3.1873E-02	0.145	0.145	0.844	1.656
CP49	S-H	1.9205E-02	0	2.9482E-02	0.152	0.152	0.840	1.665
CP50	S-H	1.3211E-02	0	2.9092E-02	0.074	0.074	0.984	1.745
CP51	S-H	9.4996E-03	0	2.6443E-02	0.039	0.039	1.068	1.732

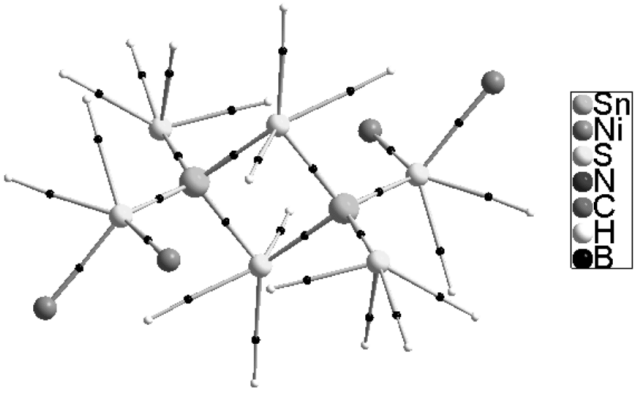

Fig. S13: Molgraph with all bonds and H-bonds at S atoms

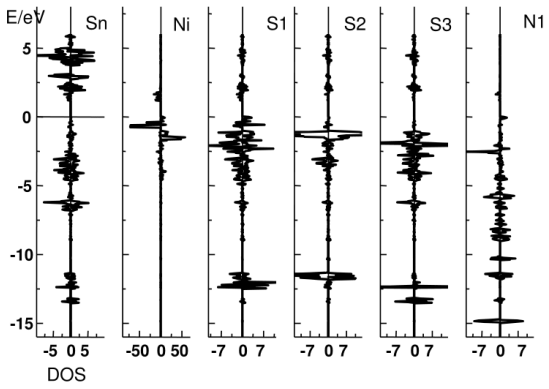

Fig. S14: Atomic site projected density of states (DOS) of the electronic band structure from the spin polarized PBE-calculation.

Octahedral coordination of the Ni^{2+} atom in compound **1**-**3** (Fig. S15, S16 and Table S9).

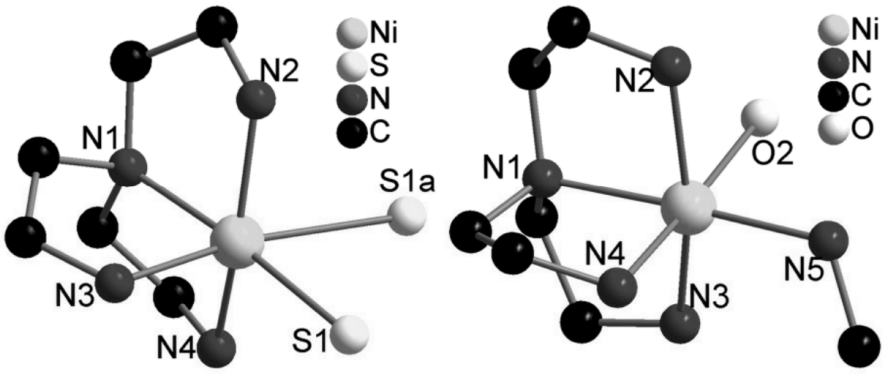

Fig .S15: Octahedral environment of the Ni^{2+} ion in compound **1** (top, left) and **2** (top, right).

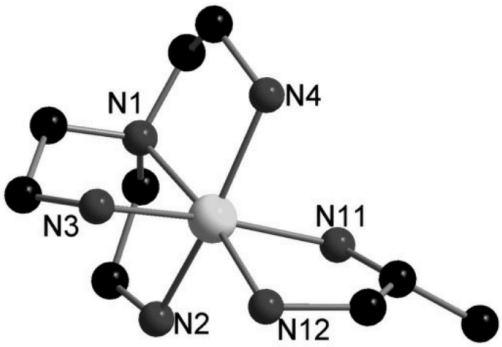

Fig. S16: Octahedral environment of the Ni^{2+} ion in compound **3**.

Table S8: Selected bond length (Å) and angles (°) of compounds **1** – **3** compared to $Na_4Sn_2S_6 \cdot 14H_2O$

	1[a]	**2**[b]	**3**[c]	$[Sn_2S_6]^{4-}$
Sn1 – S1	2.3634(3)	2.3412(7)	2.3343(7)	2.325
Sn1 – S2	2.3106(4)	2.3551(7)	2.3380(6)	2.338
Sn1 – S3	2.4523(3)	2.4433(6)	2.4512(6)	2.452
Sn1 – S3^x	2.4670(4)	2.4434(7)	2.4553(6)	2.448
S1 – Sn – S2	114.75(5)	120.61(3)	114.08(2)	119.8
S1 – Sn – S3	113.75(5)	111.11(3)	110.60(3)	108.2
S1 – Sn – S3^x	110.97(5)	110.37(2)	110.31(2)	110.4
S2 – Sn – S3	110.52(5)	108.11(2)	110.72(2)	110.6
S2 – Sn – S3^x	111.84(5)	109.45(2)	117.16(2)	110.8
S3 – Sn – S3^x	93.07(4)	93.92(2)	91.81(2)	94.0
Sn1 – S3 – Sn2/Sn1^x	86.93(4)	86.08(2)	88.18(5)	86.0
Ni1 – S1 – Ni2	80.98(5)	---	---	
S1 – Ni1 – S1^x	99.00(5)	---	---	
Ni1 – N1	2.130(4)	2.097(2)	2.120(4)	
Ni1 – N2	2.089(4)	2.138(2)	2.129(2)	
Ni1 – N3	2.102(5)	2.118(2)	2.115(2)	
Ni1 – N4	2.115(4)	2.090(2)	2.134(2)	
Ni1 – N5[2]/ N11[3]	---	2.089(2)	2.167(2)	
Ni1 – N12	---	---	2.091(2)	
Ni1 – S1	2.4343(4)	---	---	
Ni1 – S1^x	2.7449(5)	---	---	

Symmetry transformations used to generate equivalent atoms: x = a, b, c,
a: -x, y, ½-z; b: -x+2,-y+1,-z; c: -x,-y+1,-z+1

Table S9: Selected angles (°) of the octahedral Ni^{2+} environment of **1** and **2**.

1		**2**		**3**	
N(1)-Ni(1)-S(1)	174.27(13)	N(5)-Ni(1)-N(1)	174.82(9)	N(12)-Ni(1)-N(1)	171.43(9)
N(3)-Ni(1)-S(1)a	171.36(13)	N(4)-Ni(1)-O(2)	177.48(8)	N(3)-Ni(1)-N(11)	171.68(8)
N(2)-Ni(2)-N(4)	154.48(17)	N(3)-Ni(1)-N(2)	161.64(9)	N(2)-Ni(1)-N(4)	160.93(8)
N(3)-Ni(2)-S(1)	92.52(13)	N(5)-Ni(1)-N(4)	90.97(9)	N(12)-Ni(1)-N(3)	90.58(9)
N(3)-Ni(2)-N(1)	81.81(18)	N(4)-Ni(1)-N(1)	83.98(9)	N(3)-Ni(1)-N(1)	82.31(8)
N(4)-Ni(2)-S(1)	98.30(13)	N(5)-Ni(1)-N(3)	98.95(10)	N(12)-Ni(1)-N(2)	94.73(9)
N(4)-Ni(2)-N(1)	81.52(17)	N(1)-Ni(1)-N(3)	82.74(9)	N(1)-Ni(1)-N(2)	80.91(8)
N(3)- Ni(2)-N(4)	95.69(18)	N(4)-Ni(1)-N(3)	95.29(9)	N(3)-Ni(1)-N(2)	92.78(8)
S(1)-Ni(1)-S(1)a	80.98(5)	N(5)-Ni(1)-O(2)	90.34(9)	N(12)-Ni(1)-N(11)	81.11(8)
N(1)-Ni(1)-S(1)a	104.57(13)	N(1)-Ni(1)-O(2)	94.65(8)	N(1)-Ni(1)-N(11)	105.94(7)
N(4)-Ni(1)-S(1)a	79.75 (13)	N(3)-Ni(1)-O(2)	86.63(8)	N(2)-Ni(1)-N(11)	87.55(8)
N(2)-Ni(1)-S(1)	101.74(13)	N(5)-Ni(1)-N(2)	96.52(10)	N(12)-Ni(1)-N(4)	102.62(10)
N(2)-Ni(1)-N(1)	80.10(17)	N(1)-Ni(1)-N(2)	82.72(9)	N(1)-Ni(1)-N(4)	82.84(8)
N(2)-Ni(1)-S(1)a	87.91(13)	N(2)-Ni(1)-O(2)	86.63(8)	N(4)-Ni(1)-N(11)	87.38(8)
N(2)-Ni(1)-N(3)	99.04(18)	N(4)-Ni(1)-N(2)	94.26(9)		

Symmetry transformations used to generate equivalent atoms: a: -x, y, ½-z

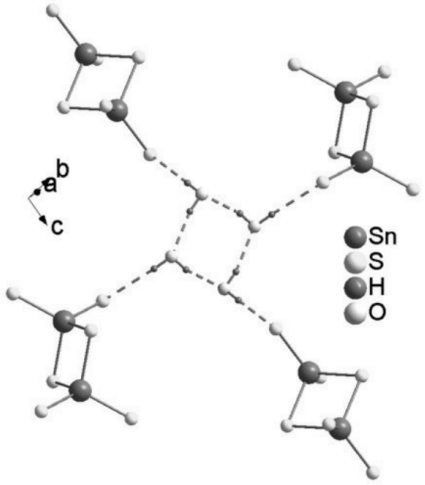

Fig. S17: Hydrogen bridging interactions of the water molecules in **2** with each other and with adjacent $[Sn_2S_6]^{4-}$ units.

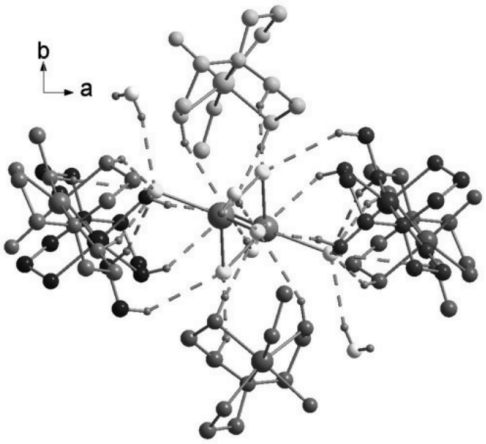

Fig. S18: Maximum hydrogen bridging interactions of the $[Sn_2S_6]^{4-}$ unit with adjacent molecules in **2**, only selected hydrogen atoms are shown.

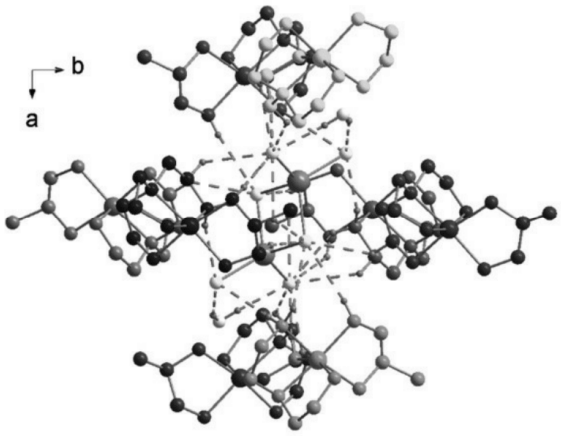

Fig. S19: Maximum hydrogen bridging interactions of the $[Sn_2S_6]^{4-}$ unit with adjacent molecules in **3**, only selected hydrogen atoms are depicted.

5.2.4 SI für die Publikation: “Transition Metal Complexes with Linkage to the Thiostannate Units Forced by Suitable Amine Molecules”

Supporting Information

Transition Metal Complexes with Linkage to the Thiostannate Units Forced by Suitable Amine Molecules

Jessica Hilbert, Nicole Pienack, Henning Lühmann, Christian Näther, Wolfgang Bensch*

Content

Figure S1	Comparison of the experimental PXRD patterns of **1**-**5** (black) with their corresponding simulated from single-crystal X-ray data (red).	p. 3-5
Figure S2	Infrared spectra of **1** and **2.**	p. 6
Table S1	Absorption of the IR spectra of compound **1** and **2** compared to phen and biph.	p. 7
Figure S3	Infrared spectra of **3**.	p. 8
Table S2	Absorption of the IR spectra of compound **3** compared to 1,2-dach.	p. 8
Figure S4	Infrared spectra of **4** and **5**.	p. 9
Table S3	Absorption of the IR spectra of compound **4** compared to cyclam and **5** compared to 2,2’-bipy.	p. 10
Figures S5	Raman spectra of compound **1** - **5**.	p. 11-13
Table S4	Data of the signals in the Raman spectra of $Na_4Sn_2S_6 \cdot 14\ H_2O$ compared to the signals of compound **1** - **5** (all wavenumbers given in cm^{-1}).	p. 13
Figure S6	UV/Vis spectra of compound **1**-**5**.	p. 14-16
Table S5	Bond length (Å) and angles (°) of the $[Sn_2S_6]^{4-}$ units in compound **1**-**5** compared to literature data of $Na_4Sn_2S_6 \cdot 14H_2O$.	p. 16
Table S6	Selected angles (°) of the octahedral TM^{2+} environment of **1** and **2**.	p. 17
Table S7	Selected bond length (Å) and angles (°) of the octahedral TM^{2+} environment of **5**.	p. 17
Table S8	Selected bond lengths (Å) and angles (°) of the octahedral TM^{2+} environment of **3** and **4**.	p. 17
Figure S7	Arrangement of the molecules in compound **1** within the *ac* plane.	p. 18
Figure S8	Disorder of the biph molecules along the *b* axis in compound **1**.	p. 18
Figure S9	Arrangement of the aromatic molecules in **1** with π-π interaction between adjacent molecules.	p. 19
Figure S10	Arrangement of the molecules within the *ab* plane in compound **2**.	p. 19
Figure S11	3D arrangement of the molecules in **2** showing the off-center parallel stacking (purple dashed lines).	p. 20
Figure S12	Arrangement of the molecules along the *b* axis in compound **3**.	p. 20
Table S9	Interatomic S···H distances (Å) and angles (°) in **3** indicating hydrogen bonding interactions.	p. 20

Figure S13	Packing of the chains of compound **3** within the *ab* plane. Purple dashed lines: Hydrogen bonding interactions between the 1,2-dach molecules and the chains.	p. 21
Figure S14	Octahedral environment of the Ni^{2+} ion in compound **4** with orientation of the cyclam ligand.	p. 21
Table S10	Interatomic S···H distances (Å) and angles (°) in **4** indicating weak hydrogen bonding interactions.	p. 21
Figure S15	Packing of the layers of compound **4** within the *ab* plane.	p. 22
Table S11	Dihedral angles between the 2,2'-bipyridine moieties for compound **5**.	p. 22
Figure S16	Arrangement of the molecules within the *bc* plane of compound **5**.	p. 22
Figure S17	Arrangement of the molecules in **5** with π-π interactions between the 2,2'-bipyridine moieties.	p. 23

p. 2

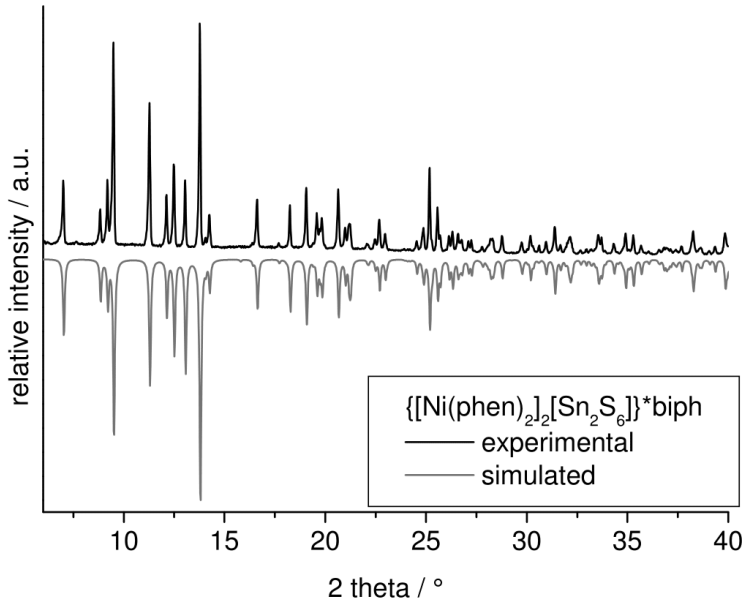
relative intensity / a.u.
{[Ni(phen)2]2[Sn2S6]}*biph
experimental
simulated
10
15
20
25
30
35
40
2 theta / °

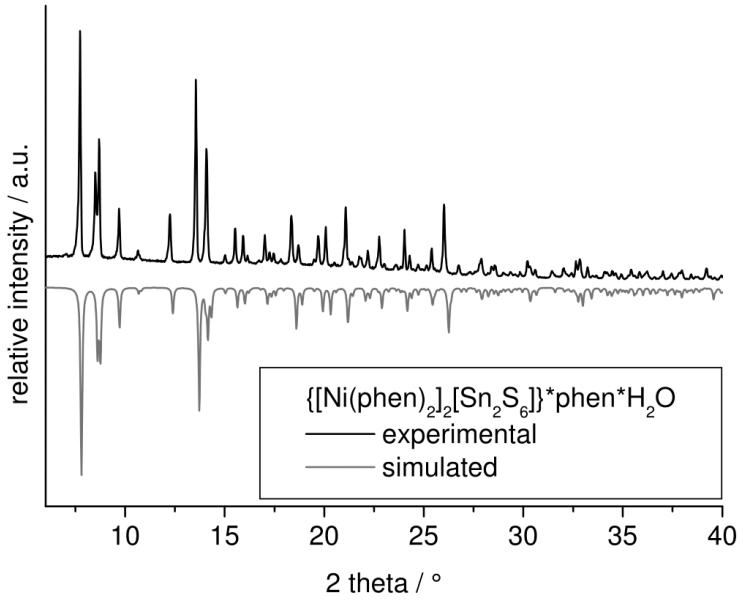
relative intensity / a.u.
{[Ni(phen)2]2[Sn2S6]}*phen*H2O
experimental
simulated
10
15
20
25
30
35
40
2 theta / °

p. 3

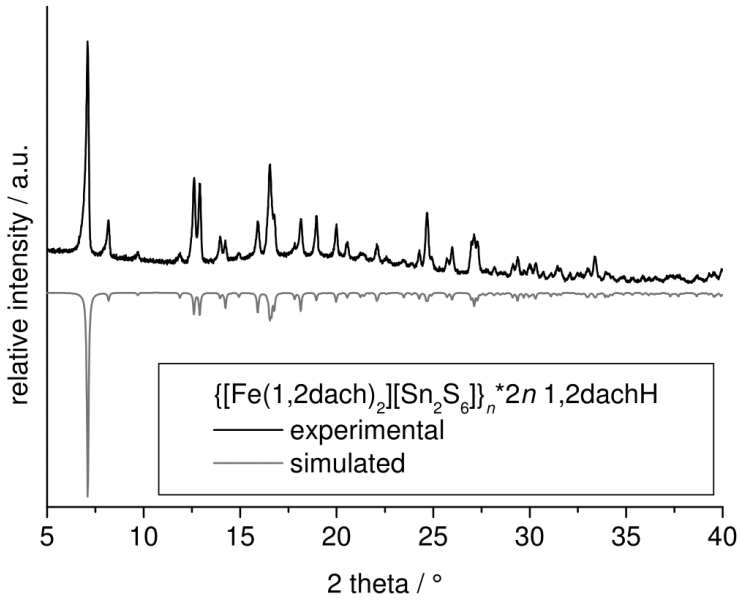
relative intensity / a.u.
{[Fe(1,2dach)2][Sn2S6]}n*2n 1,2dachH
experimental
simulated
5
10
15
20
25
30
35
40
2 theta / °

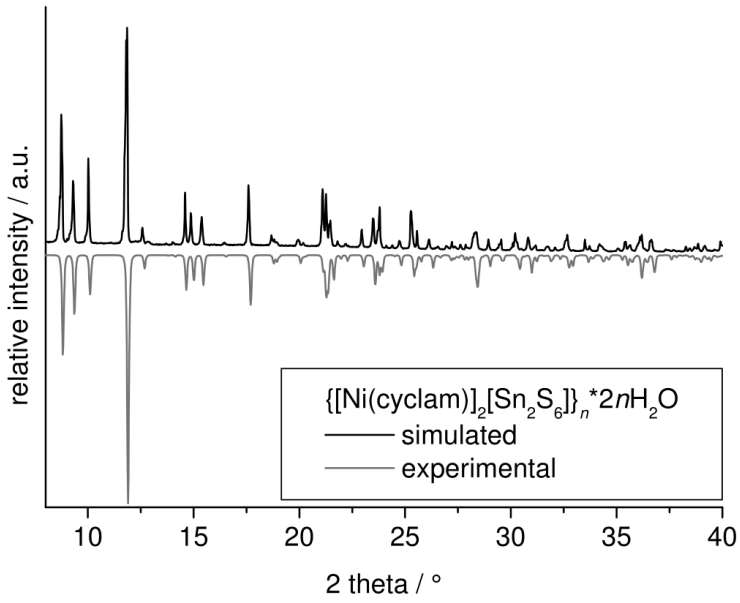
relative intensity / a.u.
{[Ni(cyclam)]2[Sn2S6]}n*2nH2O
simulated
experimental
10
15
20
25
30
35
40
2 theta / °

p. 4

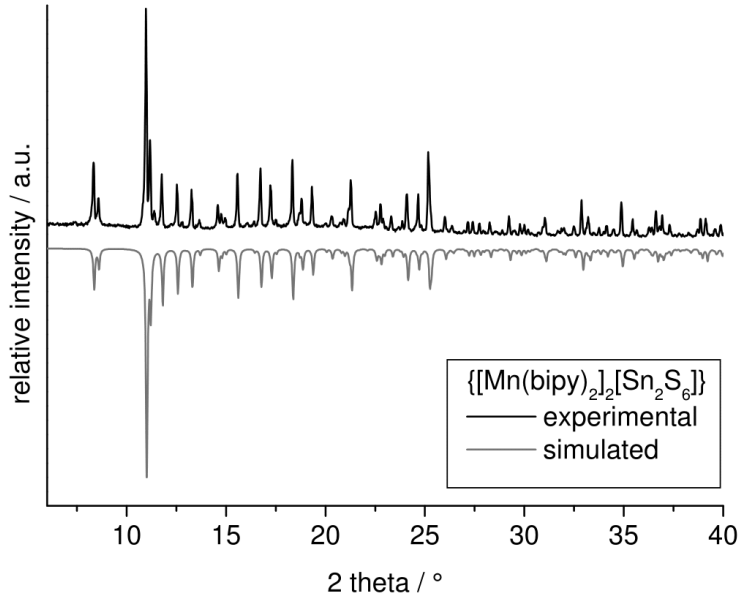

Figure S1: Comparison of the experimental PXRD patterns of **1**-**5** (black) with their corresponding simulated from single-crystal X-ray data (red).

Spectroscopic Properties

Infrared spectra

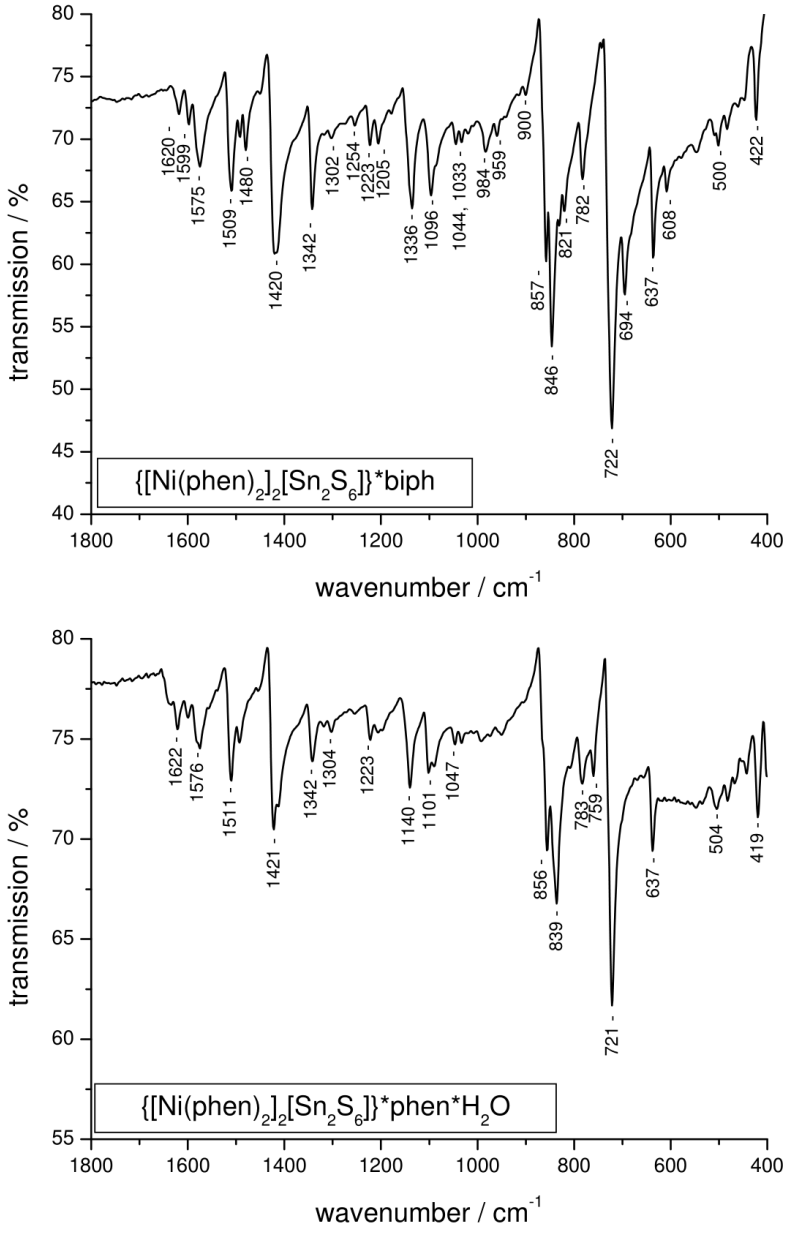

Figure S2: Infrared spectra of **1** and **2**.

Table S1: Absorption of the IR spectra of compound **1** and **2** compared to phen and biph.

phen[1,2]	biph[3,4]	**1**	**2**	Assignment
3032	3033	3036w	~ 3028vw	ν (C-H)
	2980	2985w		*ν* (C-H)
			~2972vw	ν (C-H)
1616	1612	1620w	1622w	ν (C=C)
1599	1597	1599w	1600vw	ν (C=C); ν(C-C) + ν(C-N)
	1570	1575m	1576w	--- / i.p. ring
1502	1507	1509m	1511m	ν (C=C); *ν*(C-H)
1493		1491vw	1494w	(--C=N-); ν (C=C)
	1482	1480w		ν (C-C)
1421		1420m	1421m-s	combination band
1344	1345	1342m	1342m	ν (C=C), δ (C=C-H)
1312			1319vw	ν (C=C)
	1309	1302vw	1304w	ν (C=C)
		1254vw	1255vw	ν (C=C)
1216		1223w	1223w	ν (C=C), δ (C=C-H)
1204		1205w	1205vw	δ (C=C-H)
1137		1136m	1140m	δ (C=C-H)
1092	1093	1096m	1101m 1090m	ν (C=C), δ (C=C-H)
1035	1043 1030	1044vw, 1033vw	1047w 1033w	ν (C=C), δ (C=C-H)
987		984w	992vw	δ (C=C-H)
955	965	959w	949vw	δ (C=C-H)
	903	900vw		δ (C=C=C)
854		857m shoulder	856m-s	δ (C=C=C)
	842	846s		δ (C=C=C)
			836s	δ (C=C=C)
		821 m		--- / (*)o.p. CH
779		782m	783w	δ (C-H)
			759w	δ (C-H)
721	730	722s	721	δ (C-H)
	696	694m		δ (C-H)
		637m	637m	δ (C=C=C)
606	608	608w		δ (C=C=C)
		544 w		δ (C=C=C)
497		500w	504w	δ (C=C=C)
		483w	482w	δ (C=C=C)
---		422m	419m	ν (Ni-N)

[1] M. S. Atanasoova, G. D. Dimitrov, *Spectrochim. Acta A* **2003**, *59*, 1655-1662.
[2] M. Reiher, G. Brehm, S. Schneider, *J. Phys. Chem. A* **2004**, *108*, 734-742.
[3] G. Zerbi, S. Sandroni, *Spectrochim. Acta A* **1968**, *24*, 511-528.
[4] A. Bree, M. Edelson, R. A. Kydd, *Spectrochim. Acta A* **1975**, *31,* 1569-1576.

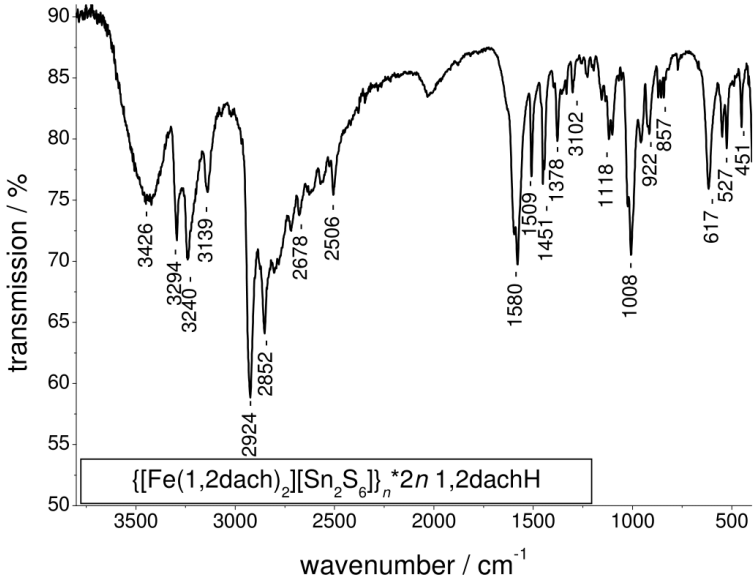

Figure S3: Infrared spectra of **3**.

Table S2: Absorption of the IR spectra of compound **3** compared to 1,2-dach.

1,2-dach[5]	**3**	Assignment
3285	3294s	ν (N-H_2)
3240	3240s	ν (N-H_2)
3144	3139m	ν (N-H_2)
2925	2924s	ν (C-H)
2868	2852s	ν (N-H_2)
2665	2678w	ν (N-H_2)
---	2506m	ν (N-H_3^+)
1592	1580s	δ (N-H_2)
---	1509s	δ (N-H_3^+)
1467	1451s	δ (C-H_2)
1370	1378m	δ (C-C-H), δ (N-H_2)
1305	1302w	δ (C-C-H), δ (N-H_2)
1129	1118s	δ (C-C-H), ν (C-N)
1011	1008s	ν (C-N)
921	922w	δ (C-C-C), ν (C-N)
867	857w	δ (C-C-C)
619	617s	δ (C-C-C)
545	549m	δ (C-C-C)
527	527m	δ (C-C-C)
---	451m	ν (Fe-N)

[5] G. Borch, P. Klaeboe, P.H. Nielsen, *Acta Chem. Scan. A* **1979**, *33*, 19-29.

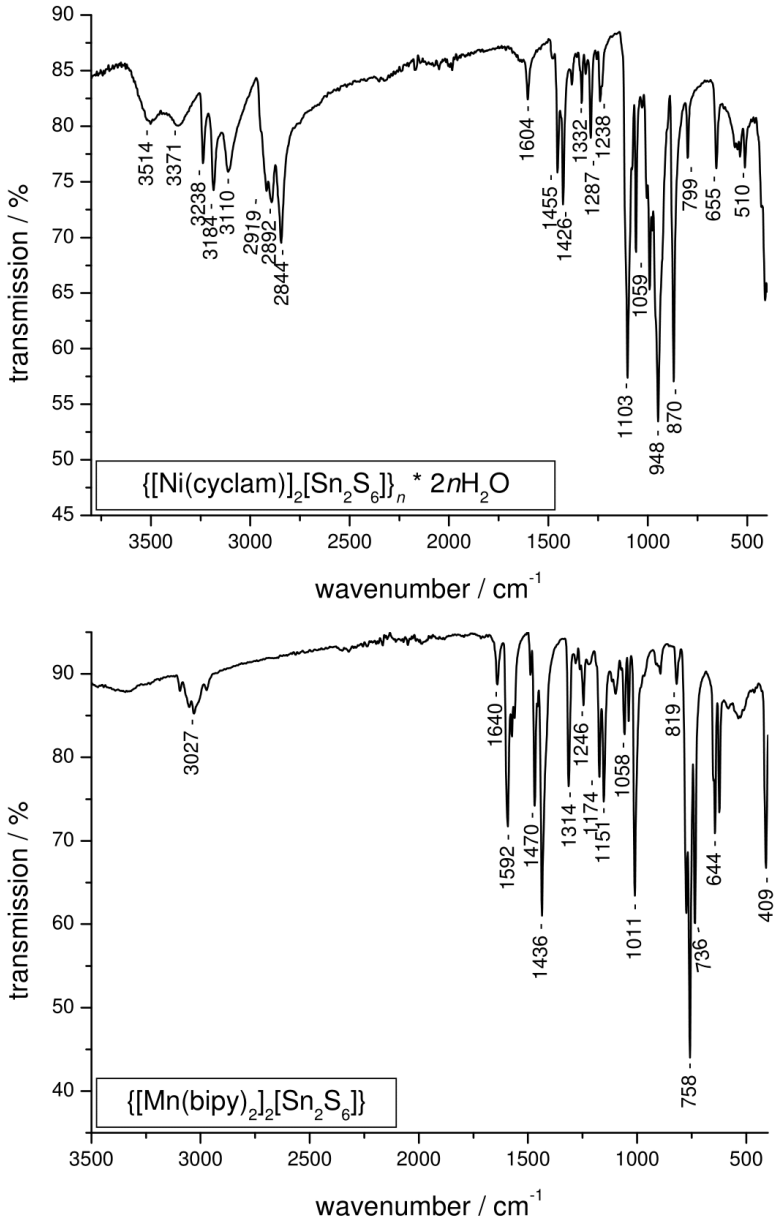

Figure S4: Infrared spectra of compound **4** and **5**.

p. 9

Table S3: Absorption of the IR spectra of compound **4** compared to cyclam and **5** compared to 2,2'-bipy.

cyclam[6]	**4**	assignment		2,2'bipy[7,8]	**5**	assignment
---	3514 b	ν (O-H) H_2O		3053	3051 vw	ν (C-H)
3268	3371 b	ν (N-H)		3030	3027 vw	ν (C-H)
3236	3238 m	ν (N-H)			1640 w	ν (C-C) + ν (C-N
3187	3184 m	ν (N-H)		1591	1592 m	ν (C-C) + ν (C-N)
---	3110 m	ν (C-H)		1571	1574 m	ν (C-C) + ν (C-N)
2917	2919 m	ν (C-H)		1479	1470 m	δ (C-H)
2873	2892 m	ν (C-H)		1440	1436 s	δ (C-H)
---	2844 m	ν (C-H)		1311	1314 m	δ (C-H)
---	1604 m	ν (C-C) + ν (C-N)		1255	1246 w	ν (C-C-H)
1467	1455 m	ν (C-C) + ν (C-N)		1174	1174 m	ν (C-C-H)
1434	1426 m	ν (C-C) + ν (C-N)		1147	1151 m	δ (C-H)
1377	1383 vw	ν (C-C) + ν (C-N)		1094	1099 vw	ν (C-C) + ν (C-N)
1335	1332 w	ν (C-C) + ν (C-N)		1056	1058 m	ν (C-C) inter ring
1286	1287 m	ν (C-C) + ν (C-N)		1042	1038 m	ν (C-C) inter ring
1237	1238 w	ν (C-N) + δ (C-H)		1011	1011 s	δ (C-H)
1110	1103 s	ν (C-N) + δ (C-H)		818	819 w	δ (C-H)
1068	1059 m	ν (C-N) + δ (C-H)		758	758 s	δ (C-H)
997	990 m	δ (N-H)		737	736 m	δ (C-H)
941	948 s	δ (N-H)		650	644 m	δ (C-H)
894	870 s	*ρ* (C-H)		616	622 m	δ (C-H)
794	799 m	macrocycl. def.		410	409 m	δ (C-C) inter ring; ν (Mn-N)
644	655 m	macrocycl. def.				
522	537 w	macrocycl. def.				
---	510 w	ν Ni-N				

[6] G. F. Diaz, R.E. C. Clavijo, M. M. Campos-Vallette, M. S. Saavedra, S. Diez, R. Munoz, *Vibrational Spectroscopy* **1997**, *15*, 201-209.
[7] M. L. Niven, G. C. Percy, *Transition Met. Chem.* **1978**, *3*, 267-271.
[8] E. Casellucci, L. Angeloni, *Chem. Phys.* **1979**, *43*, 365-373.

Raman spectra

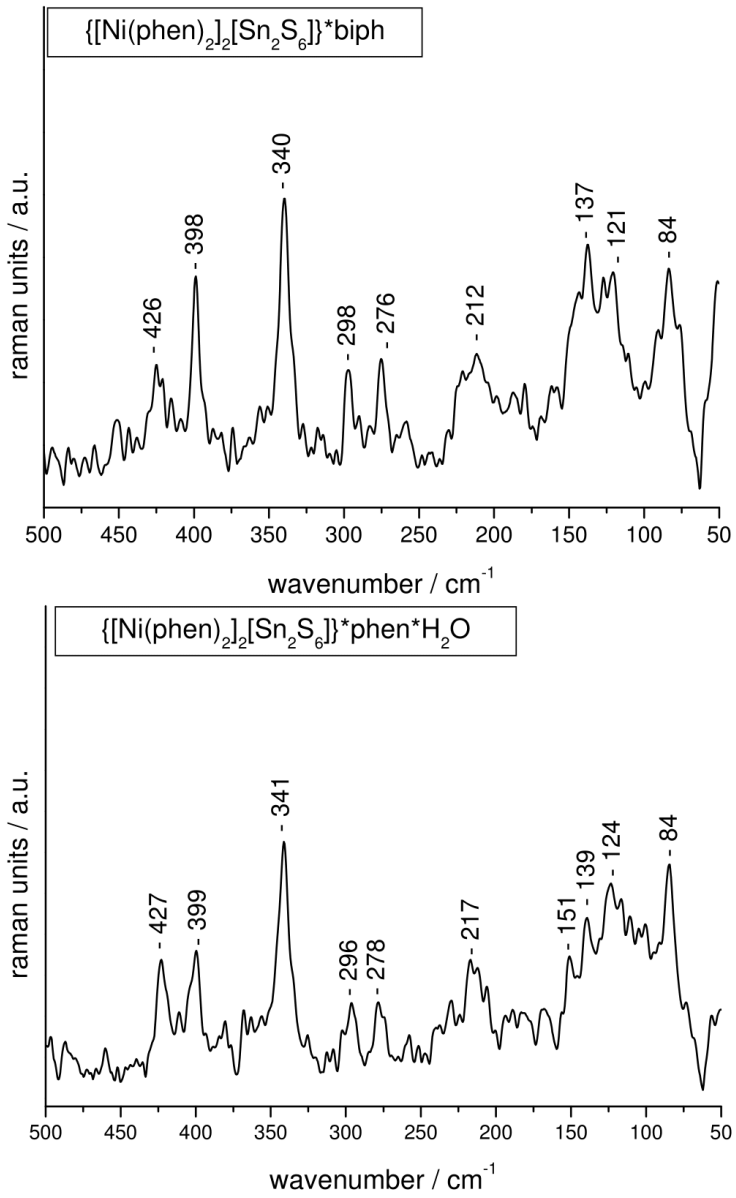

p. 11

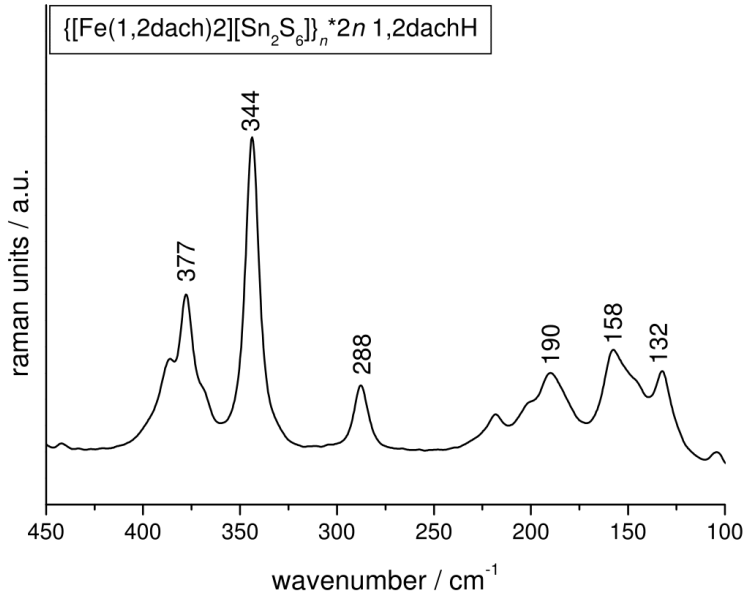
{[Fe(1,2dach)2][Sn2S6]}n*2n 1,2dachH
raman units / a.u.
377
344
288
190
158
132
450
400
350
300
250
200
150
100
wavenumber / cm-1

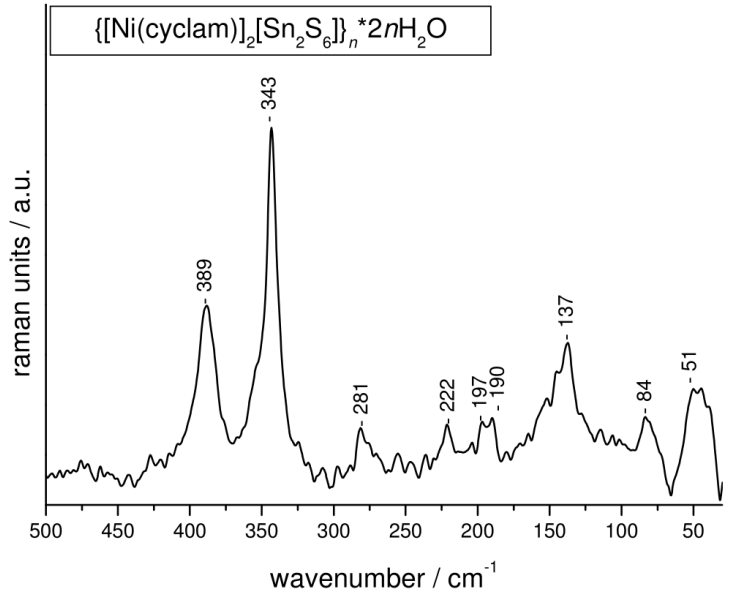
{[Ni(cyclam)]2[Sn2S6]}n*2nH2O
raman units / a.u.
389
343
281
222
197
190
137
84
51
500
450
400
350
300
250
200
150
100
50
wavenumber / cm-1

p. 12

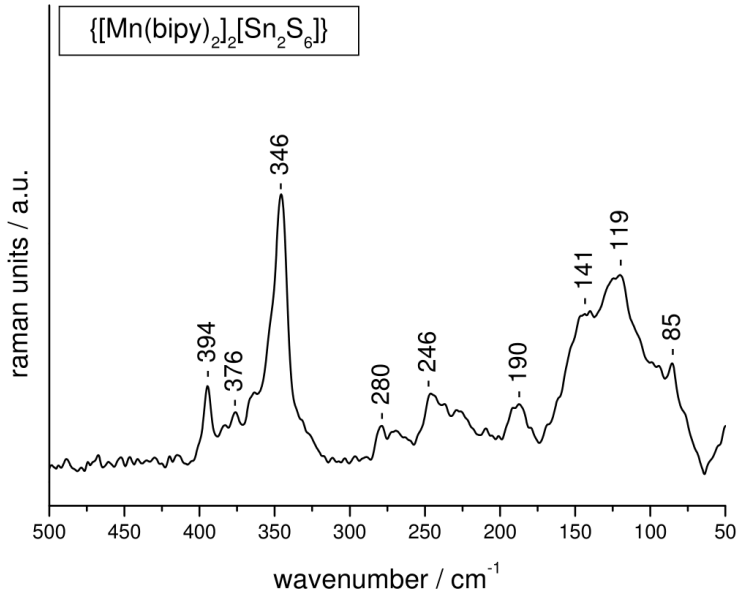

Figure S5: Raman spectra of compound **1** - **5**.

Table S4: Data of the signals in the Raman spectra of $Na_4Sn_2S_6 \cdot 14\ H_2O$[9] compared to the signals of compound **1 - 5** (all wave numbers given in cm^{-1}).

$[Sn_2S_6]^{4-}$[9]	1	2	3	4	5	assignment
	426	427				Ni-S
391	398	399		389	394	$\nu_{as}(SnS_2)$
377			377		376	$\nu_{s}(SnS_2)$
341	340	341	344	343	346	ν_{as}(Sn-S-Sn)
281	298	296	288	281	280	$\nu\ (Sn_2S_2)$
	276	278			246	
190	212	217	190	197 190	190	
151		151	158		141	deformation & torsional vibration
136	137	139	132	137		
	121	124			119	
	84	84		84	85	

[9] Krebs, B; Pohl, S.; Schiwy, W. *Angew. Chem. Int. Ed. Engl.* **1970**, *9*, 897-898.

UV/vis spectra

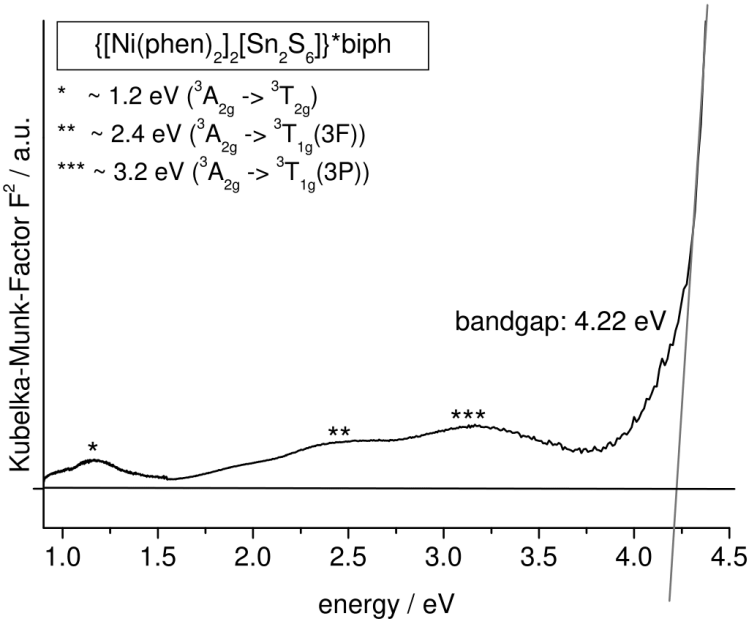

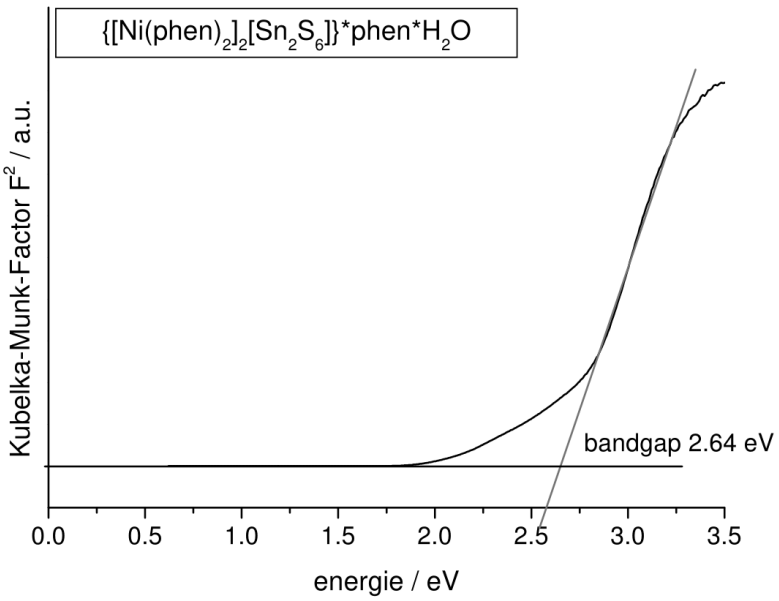

p. 14

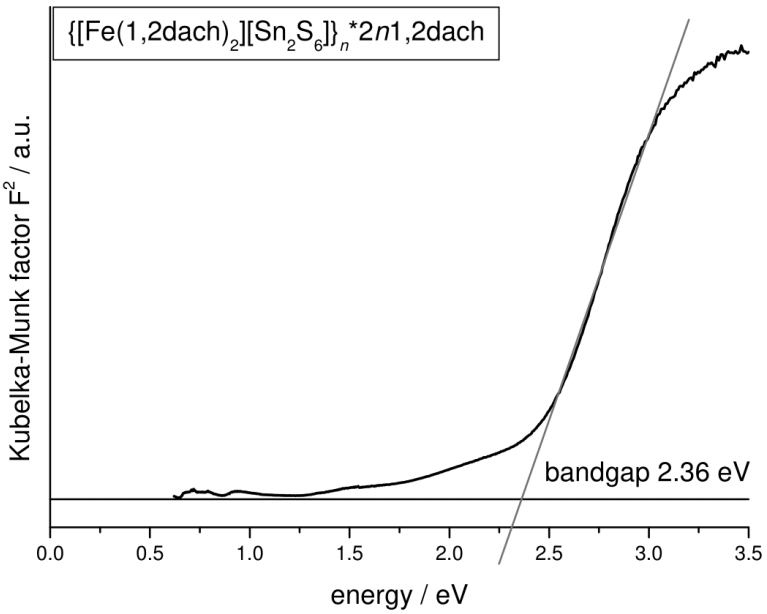
{[Fe(1,2dach)2][Sn2S6]}n*2n1,2dach
Kubelka-Munk factor F2 / a.u.
bandgap 2.36 eV
0.0
0.5
1.0
1.5
2.0
2.5
3.0
3.5
energy / eV

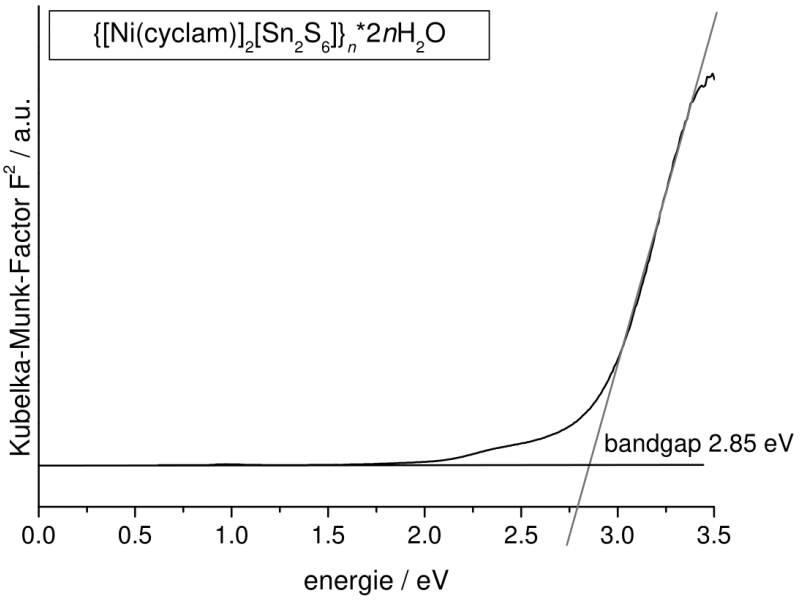
{[Ni(cyclam)]2[Sn2S6]}n*2nH2O
Kubelka-Munk-Factor F2 / a.u.
bandgap 2.85 eV
0.0
0.5
1.0
1.5
2.0
2.5
3.0
3.5
energie / eV

p. 15

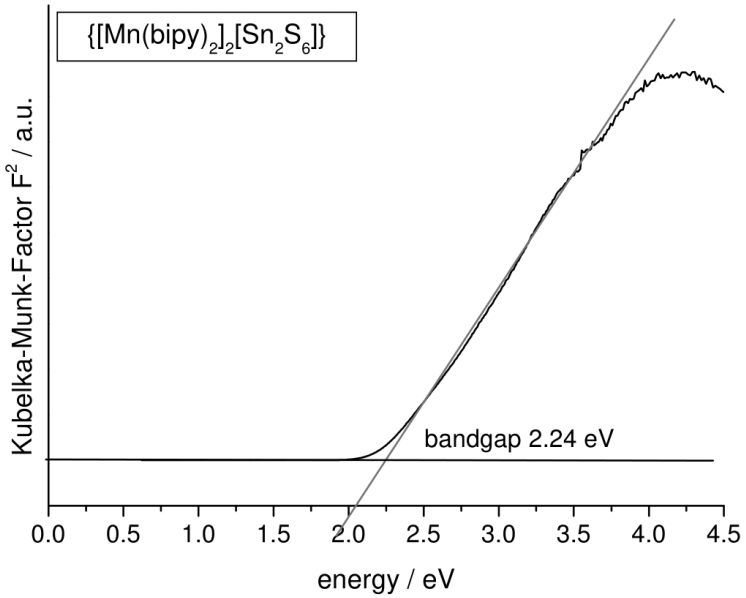

Figure S6: UV/Vis spectra of compound **1**-**5**.

Table S5: Bond length (Å) and angles (°) of the $[Sn_2S_6]^{4-}$ units in compound **1-5** compared to literature data of $Na_4Sn_2S_6{\cdot}14H_2O$.[9]

	1	**2**	**3**	**4**	**5**	**$[Sn_2S_6]^{4-}$**
Sn1 – S1	2.3292(9)	2.3304(10)	2.3355(7)	3.3406(8)	2.3396(9)	2.325
Sn1 – S2	2.3485(9)	2.3495(10)	2.3316(6)	2.3433(8)	2.3461(9)	2.338
Sn1 – S3	2.4520(9)	2.4434(10)	2.4377(7)	2.4382(8)	2.4369(9)	2.452
Sn1 – S3[a]	2.4463(9)	2.4536(10)	2.4395(7)	2.4543(8)	2.4409(9)	2.448
S1 – Sn – S2	100.25(3)	100.70(4)	117.28(2)	114.03(3)	103.69(9)	119.8
S1 – Sn – S3	120.43(3)	118.26(4)	112.63(3)	113.44(3)	114.97(4)	108.2
S1 – Sn – S3[a]	113.53(3)	116.71(4)	111.85(3)	111.09(3)	114.47(4)	110.4
S2 – Sn – S3	113.31(3)	113.81(4)	110.54(3)	110.96(3)	117.62(3)	110.6
S2 – Sn – S3[a]	118.50(3)	115.55(4)	111.85(3)	112.55(3)	113.66(4)	110.8
S3 – Sn – S3[a]	92.15(3)	92.84(3)	93.83(2)	93.17(3)	92.89(3)	94.0
Sn1 – S3 – Sn1[a]/Sn2	87.85(3)	87.16(3)	86.17(2)	86.86(3)	87.10(3)	86.0

Symmetry transformations used to generate equivalent atoms: a -x,-y+1,-z

[9] B. Krebs, S. Pohl, W. Schiwy, *Angew. Chem.* **1970**, *82*, 884.

Table S6: Selected bond length (Å) and angles (°) of the octahedral TM^{2+} environment of **1** and **2**.

	1	**2**		**1**	**2**
TM – N1	2.108(3)	2.103(3)	N1 – TM – N2	77.50(11)	78.55(13)
TM – N2	2.156(3)	2.130(3)	N1 – TM – N21	162.09(12)	163.29(12)
TM – N21	2.108(3)	2.089(3)	N1 – TM – N22	92.77(13)	89.50(13)
TM – N22	2.113(3)	2.136(3)	N1 – TM – S1	94.83(9)	96.79(10)
TM – S1	2.4940(10)	2.4737(11)	N1 – TM – S2	95.23(8)	95.13(9)
TM – S2	2.5016(10)	2.5070(10)	S1 – TM – S2	91.88(3)	92.68(3)
			N2 – TM – S1	172.55(8)	175.30(9)
			N22 – TM – S2	172.36(10)	173.95(10)

Table S7: Selected bond length (Å) and angles (°) of the octahedral TM^{2+} environment of **5**.

	5		**5**
TM – N1	2.335(3)	N1 – TM – N2	71.25(12)
TM – N2	2.280(3)	N1 – TM – N11	90.13(19)
TM – N11	2.202(6)	N1 – TM – N12	82.51(17)
TM – N12	2.351(6)	N1 – TM – S1	89.73(9)
TM – S1	2.6120(11)	N1 – TM – S2	169.17(9)
TM – S2	2.5348(10)	S1 – TM – S2	91.42(3)
		N2 – TM – N11	153.4(2)
		N12 – TM – S2	170.54(16)

Table S8: Selected bond length (Å) and angles (°) of the octahedral TM^{2+} environment of **3** and **4**.

	3[a]	**4**[b]		**3**[a]	**4**[b]
TM – N1	2.201(2)	2.055(3)	N1 – TM – N2	80.21(8)	85.40(12)
TM – N2	2.183(2)	2.067(3)	N1 – TM – N1[a/b]	180.00(11)	180.00(17)
TM – N1[a/b]	2.201(2)	2.055(3)	N1 – TM – N2[a/b]	99.79(8)	94.60(12)
TM – N2[a/b]	2.183(2)	2.067(3)	N1 – TM – S1	95.09(6)	92.86(8)
TM – S1	2.6138(7)	2.6188(7)	N1 – TM – S1 [a/b]	84.91(6)	87.14(8)
TM – S1 [a/b]	2.6138(7)	2.6022(8)	S1 – TM – S1 [a/b]	180.0	180.00(3)
			N2 – TM – N2[a/b]	180.0	180.0

Symmetry transformations used to generate equivalent atoms:
a: -x+1,-y,-z; b:

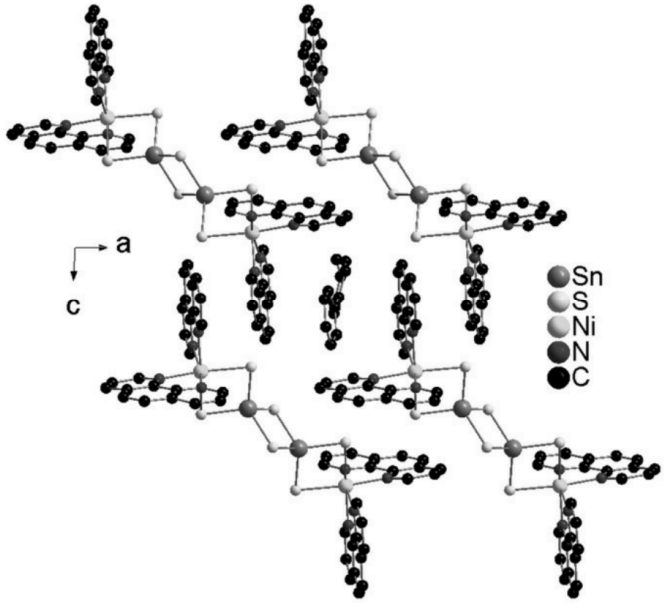

Figure S7: Arrangement of the molecules in compound **1** within the *ac* plane.

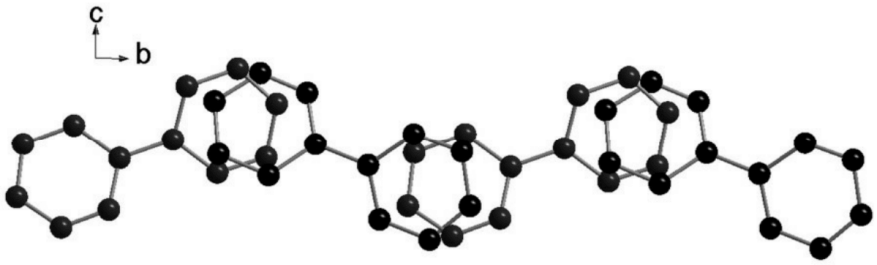

Figure S8: Disorder of the biph molecules along the *b* axis in compound **1**. Hydrogen atoms are omitted.

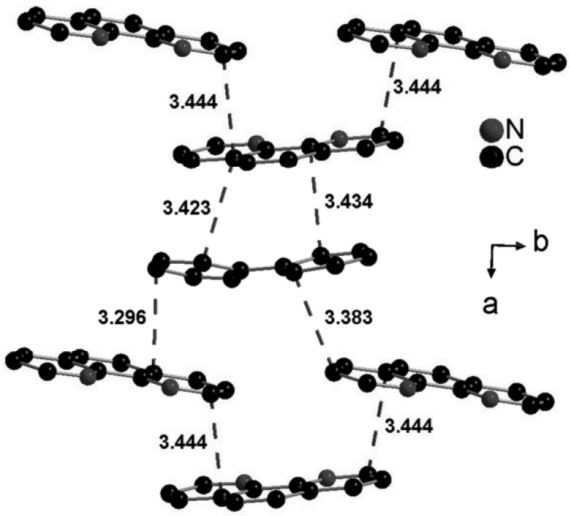

Figure S9: Arrangement of the aromatic molecules in **1** with π-π interaction between adjacent molecules. The shortest distances are shown (purple dashed lines. For reasons of clarity only one arrangement of the biph molecule is shown. Hydrogen atoms are omitted.

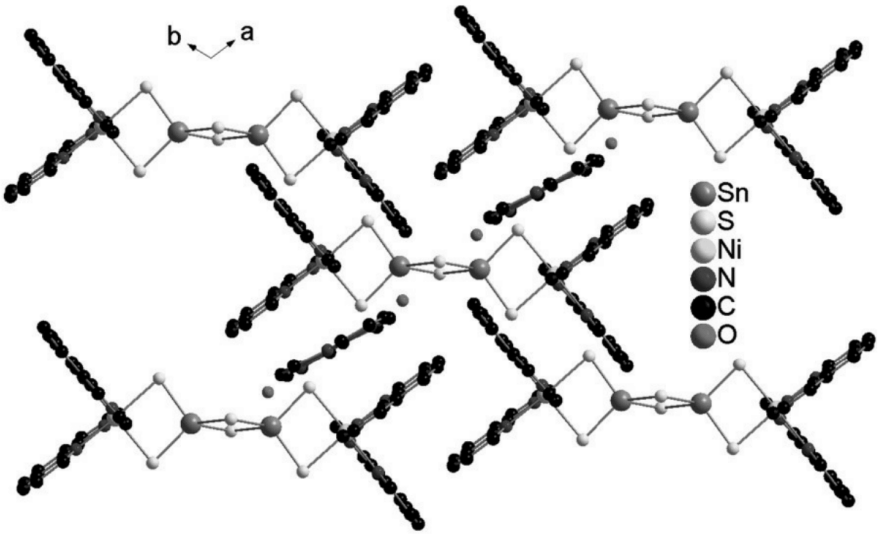

Figure S10: Arrangement of the molecules within the *ab* plane in compound **2**.

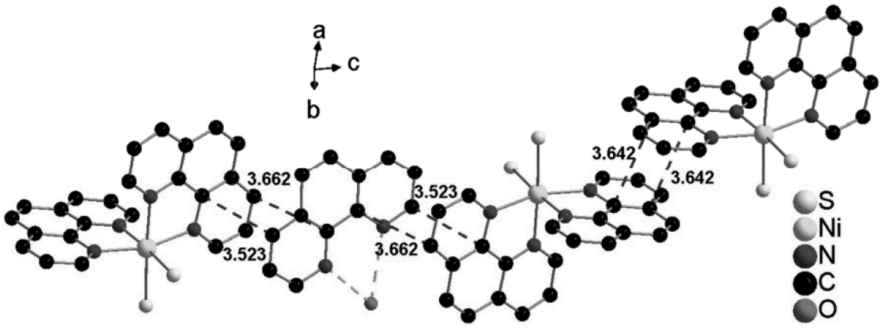

Figure S11: 3D arrangement of the molecules in **2** showing the off-center parallel stacking (purple dashed lines). Hydrogen atoms are omitted for clarity. Only part of the {[Ni(phen)$_2$]$_2$[Sn$_2$S$_6$]} moieties are depicted. The dashed lines between O and

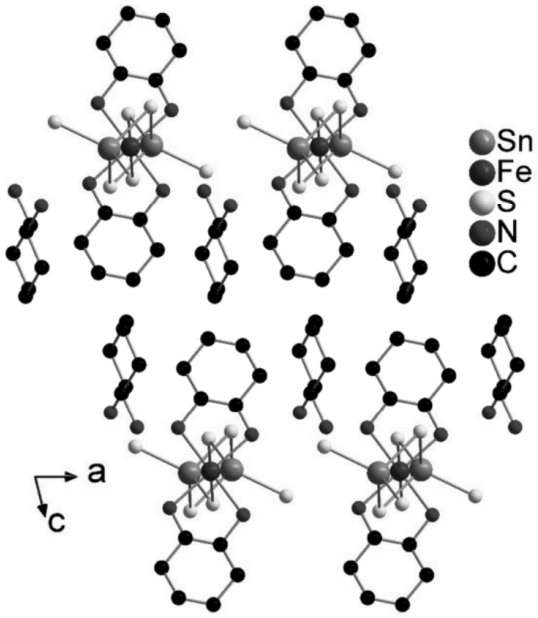

Figure S12: Arrangement of the molecules along the *b* axis in compound **3**.

Table S9: Interatomic S···H distances (Å) and angles (°) in **3** indicating hydrogen bonding interactions.

distances	**3**	angles	**3**
S1 ··· H-N3	2.510	S1-H-N3	147.91
S1·····H-N4	2.849	S1-H-N4	146.14
S2 ··· H-N1	2.659 (intramolecular)	S2-H-N1	173.59
S2 ··· H-N3	2.411	S2-H-N3	165.84
S2·····H-N3	2.434	S2-H-N3	168.99
S2·····H-N4	2.810	S2-H-N4	144.53

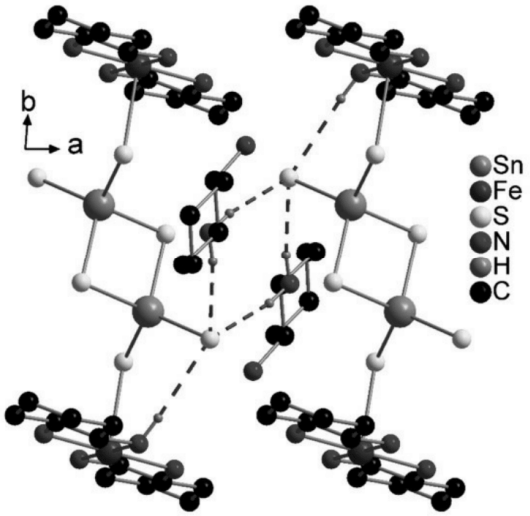

Figure S13: Packing of the chains of compound **3** within the *ab* plane. Purple dashed lines: Hydrogen bonding interactions between the 1,2dach molecules and the chains. Only selected H atoms are shown.

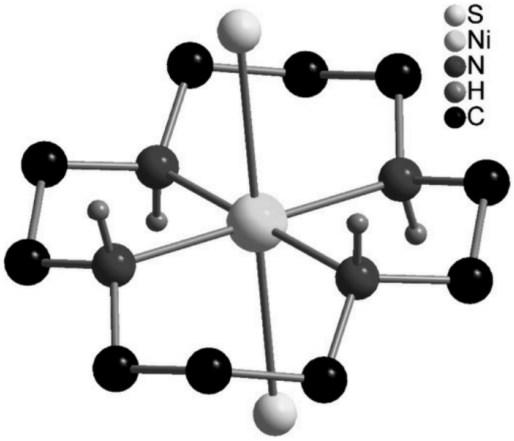

Figure S14: Octahedral environment of the Ni^{2+} ion in compound **4** with orientation of the cyclam ligand. Only selected H atoms are depicted.

Table S10*:* Interatomic S···H distances (Å) and angles (°) in **4** indicating weak hydrogen bonding interactions.

distances	**4**	angles	**4**
S2 ··· H1-O	3.327	S2-H-O	170.90
S2·····H2-O	3.696	S2-H-O	177.12

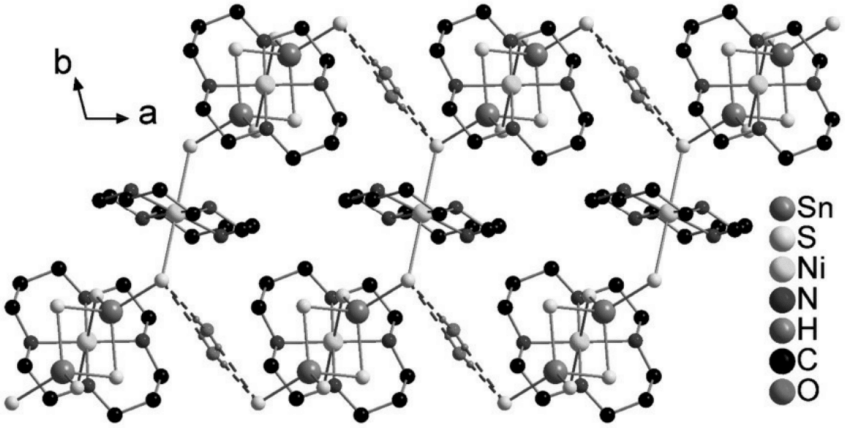

Figure S15: Packing of the layers of compound **4** within the *ab* plane. Purple dashed lines: Hydrogen bonding interactions between the water molecules and the layers. Only the H atoms of the water molecules are shown.

Table S11: Dihedral angles between the 2,2'-bipyridine moieties for compound **5**.

N12-Mn1-N1-C6	-88.92 (0.31)	N1-Mn1-N12-C16	86.82 (0.46)
N12-Mn1-N1-C10	89.90 (0.36)	N1-Mn1-N12-C20	-85.20 (0.61)

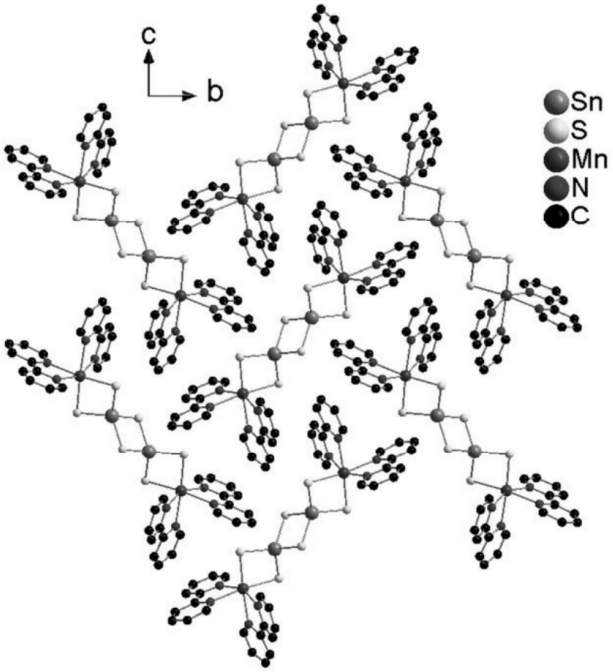

Figure S16: Arrangement of the molecules within the *bc* plane of compound **5**.

p. 22

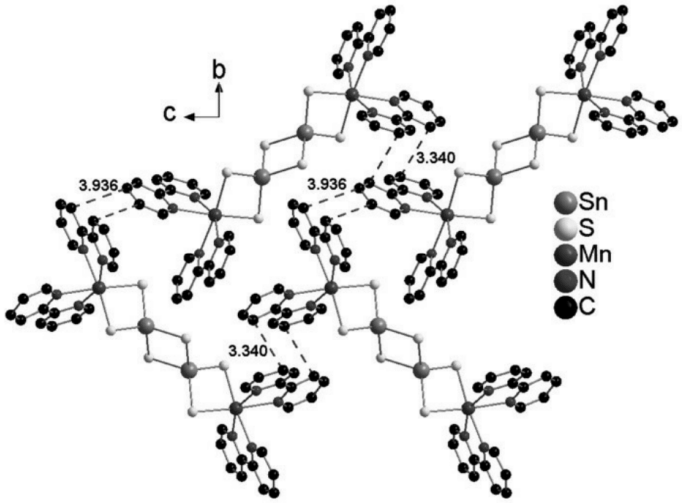

Figure S17: Arrangement of the molecules in **5** with π-π interactions (purple dashed lines) between the 2,2'-bipyridine moieties. H atoms are not shown.

p. 23

5.2.5 SI für die Publikation: "{[Ni(1,2-dach)$_2$(ma)]$_4$[Sn$_{10}$S$_{20}$O$_4$]} – An Example of the Rare Tin-Oxo-Sulfide Cluster with Uncommon Connection Mode Towards a Charge Compensating Ni(II) Complex"

Supporting Information

{[Ni(1,2-dach)$_2$(ma)]$_4$[Sn$_{10}$S$_{20}$O$_4$]}
An Example of the Rare Tin-Oxo-Sulfide Unit with Uncommon Bonding Mode Towards the Charge Compensating Ni(II) Complex

Jessica Hilbert, Christian Näther, Wolfgang Bensch*

Content

Figure S1	Comparison of the experimental PXRD pattern of the title compound with the corresponding simulated from single-crystal X-ray data.	p. 2
Figure S2	Infrared spectra of {[Ni(1,2-dach)$_2$(ma)]$_4$[Sn$_{10}$S$_{20}$O$_4$]}.	p. 2
Table S1	Absorption of the IR spectra of {[Ni(1,2-dach)$_2$(ma)]$_4$[Sn$_{10}$S$_{20}$O$_4$]} compared to 1,2dach.	p. 3
Figure S3	The [Sn$_{10}$S$_{20}$O$_4$]$^{8-}$ anion. Only selected atoms are labelled.	p. 3
Table S2	Bond length (Å) of the [Sn$_{10}$S$_{20}$O$_4$]$^{4-}$ unit in {[Ni(1,2-dach)$_2$(ma)]$_4$[Sn$_{10}$S$_{20}$O$_4$]} compared to literature data of [Li$_8$(H$_2$O)$_{29}$][Sn$_{10}$S$_{20}$O$_4$]·2H$_2$O	p. 4
Figure S4	Octahedral environment of the Ni^{2+} ion in the title compound.	p. 4
Table S3	Selected bond length (Å) and angles (°) of the octahedral TM^{2+} environment in {[Ni(1,2-dach)$_2$(ma)]$_4$[Sn$_{10}$S$_{20}$O$_4$]}.	p. 4
Figure S5	Packing of the molecule cluster within the *ab* plane.	p. 5
Table S4	Interatomic S···H distances (Å) and angles (°) indicating hydrogen bonding interactions.	p. 5
Figure S6	Hydrogen bonding interactions (purple dashed lines) between the terminal S atoms of the [Sn$_{10}$S$_{20}$O$_4$]$^{8-}$ units and [Ni(1,2-dach)(ma)]$^{2+}$ moieties of neighboured clusters. Only selected hydrogen atoms are depicted.	p. 6
Figure S7	Arrangement of the molecules with hydrogen bonding interactions (purple dashed lines) between adjacent moieties.	

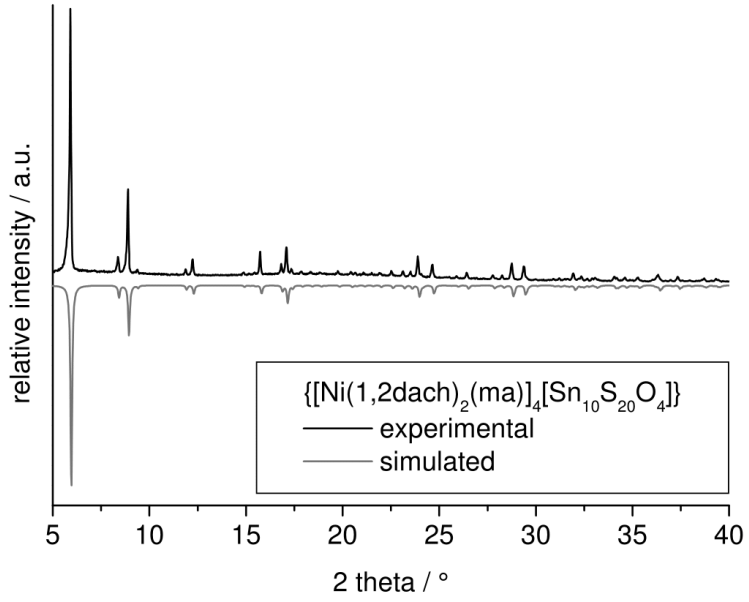

Figure S1: Comparison of the experimental PXRD pattern of {[Ni(1,2-dach)$_2$(ma)]$_4$[Sn$_{10}$S$_{20}$O$_4$]} (black) with the corresponding simulated from single-crystal X-ray data (red).

Spectroscopic Properties

Infrared spectra

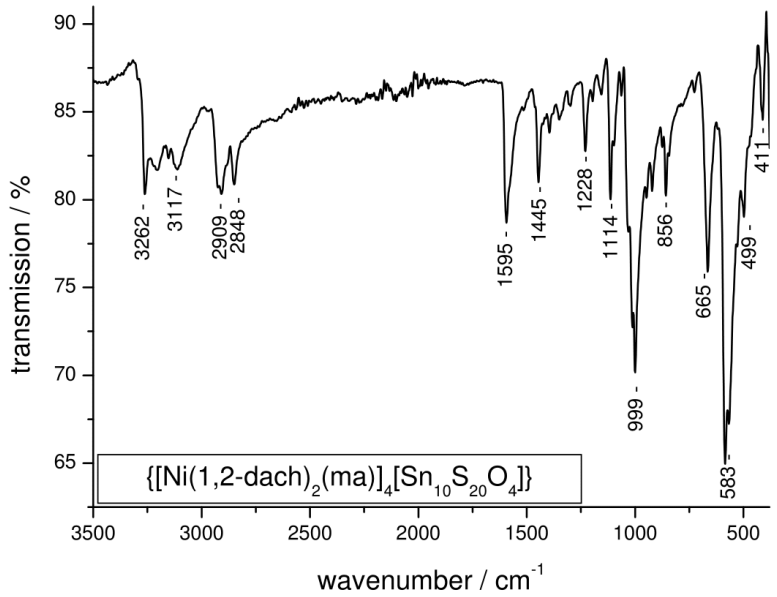

Figure S2: Infrared spectra of {[Ni(1,2-dach)$_2$(ma)]$_4$[Sn$_{10}$S$_{20}$O$_4$]}.

Table S1: Absorption of the IR spectra of {[Ni(1,2-dach)$_2$(ma)]$_4$[Sn$_{10}$S$_{20}$O$_4$]} compared to 1,2-dach.

1,2-dach[1]	{[Ni(1,2-dach)$_2$(ma)]$_4$[Sn$_{10}$S$_{20}$O$_4$]}	Assignment
3255	3262 m	ν (N-H$_2$)
3210	3210 w	ν (N-H$_2$)
3160	3156 w	ν (N-H$_2$)
3120	3117 w	ν (N-H$_2$)
2908	2909 m	ν (C-H)
2858	2848 m	ν (N-H$_2$)
1591	1595 s	δ (N-H$_2$)
1449	1445 m	δ (C-H$_2$)
1390	1394 w	δ (C-C-H), δ (N-H$_2$)
1345	1348 w	δ (C-C-H), δ (N-H$_2$)
1300	1299 w	δ (C-C-H), δ (N-H$_2$)
1227	1228 m	δ (C-C-H)
---	1195 vw	
1157	1157 w	δ (C-C-H)
1112	1114 s	δ (C-C-H), ν (C-N)
1062	1065 w	ν (C-N)
---	999 vs	
921	920 w	δ (C-C-C), ν (C-N)
855	856 m	δ (C-C-C)
---	724 vw	
650	665 s	δ (C-C-C)
580	583 vs	δ (C-C-C)
502	499 w	
---	411 m	ν (Ni-N)

[1] G. Borch, P. Klaeboe, P.H. Nielsen, *Acta Chem. Scan. A* **1979**, *33*, 19-29.

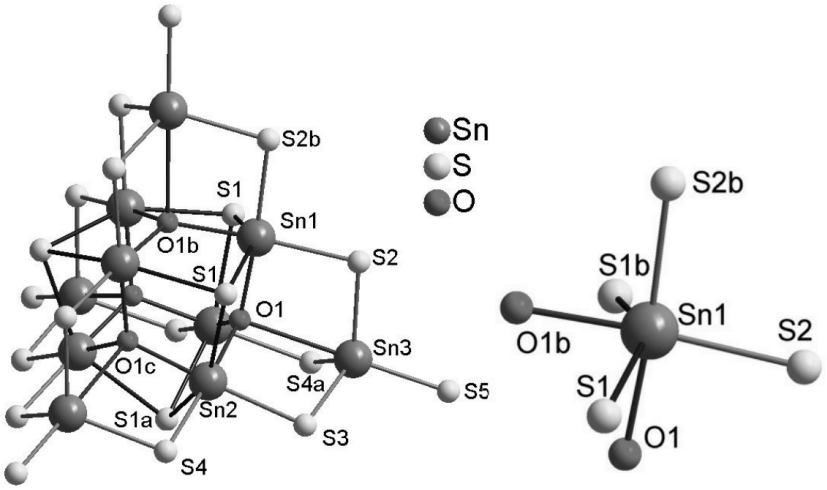

Figure S3: The [Sn$_{10}$S$_{20}$O$_4$]$^{8-}$ anion left) and the [SnS$_4$O$_2$] octahedron (right). Only selected atoms are labelled.

Table S2: Bond length (Å) of the $[Sn_{10}S_{20}O_4]^{4-}$ unit in $\{[Ni(1,2\text{-dach})_2(ma)]_4[Sn_{10}S_{20}O_4]\}$ compared to literature data of $[Li_8(H_2O)_{29}][Sn_{10}S_{20}O_4]\cdot 2H_2O$.[11]

	$\{[Ni(1,2\text{-dach})_2(ma)]_4[Sn_{10}S_{20}O_4]\}$	$[Sn_{10}S_{20}O_4]^{8-}$
Sn1 – S1	2.6474(16)	2.5878(8) – 2.6541(8)
Sn2 – S1	2.6169(16)	
Sn1 – S2	2.4458(18)	2.4394(9) – 2.5060(7)
Sn2 – S3	2.4650(17)	
Sn2 – S4	2.4691(17)	
Sn3 – S2	2.4213(18)	2.4130(7) – 2.4386(7)
Sn3 – S3	2.4351(18)	
Sn3 – S4a	2.4361(17)	
Sn3 – S5	2.3384(18)	2.3556(8) – 2.3715(7)
Sn1 – O1	2.075(4)	2.0610(6) – 2.1030(6)
Sn2 – O1	2.072(4)	
Sn3 – O1	2.7880(43)	2.6037(7)

[11] T. Kaib, M. Kapitein, S. Dehnen, *Z. Anorg. Allg. Chem.* **2011**, *637*, 1683-1686.

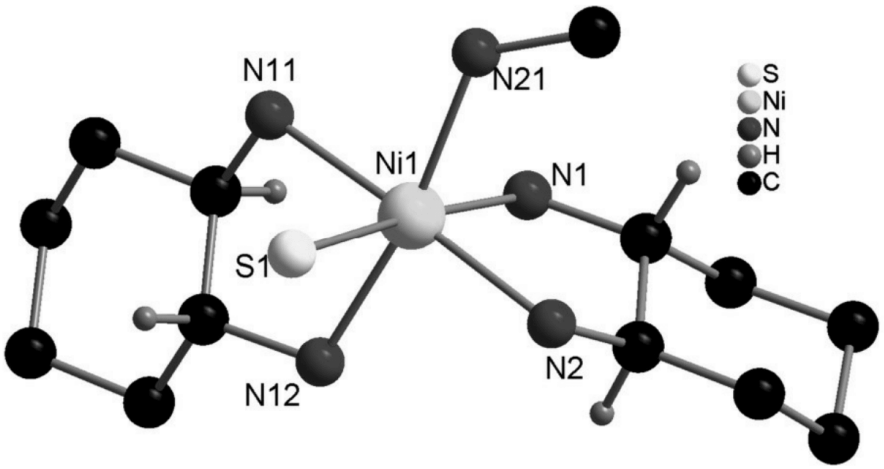

Figure S4: Octahedral environment of the Ni^{2+} ion in the title compound. Only selected atoms are labelled and selected hydrogen atoms are depicted.

Table S3: Selected bond length (Å) and angles (°) of the octahedral TM^{2+} environment.

	bond length		angles
TM – N1	2.119(6)	N1 – TM – N2	83.4(3)
TM – N2	2.067(6)	N1 – TM – N11	94.2(3)
TM – N11	2.089(6)	N1 – TM – N12	91.1(3)
TM – N12	2.114(6)	N1 – TM – N21	91.9(3)
TM – N21	2.116(6)	N1 – TM – S1	173.5(2)
TM – S1	2.5561(18)	N2 – TM – N11	175.6(3)
		N12 – TM – N21	170.4(3)

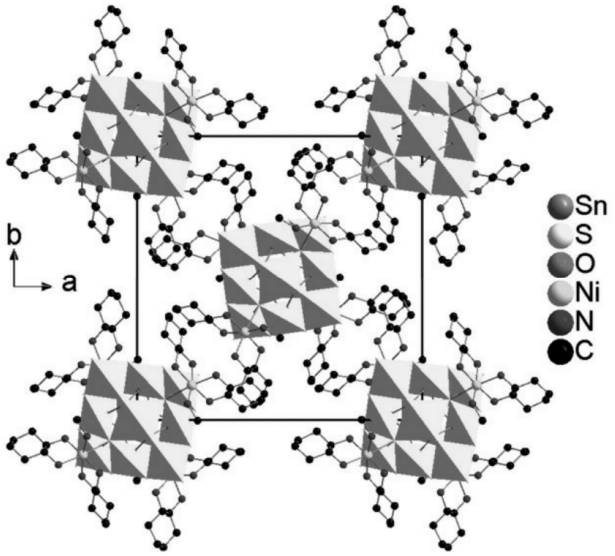

Figure S5: Packing of the molecule cluster within the *ab* plane.

Table S4: Interatomic S···H distances (Å) and angles (°) indicating hydrogen bonding interactions.

distances		angles	
S5 ··· H-N1	2.676	S5 H-N1	159.63
S3 ··· H-N2	2.569	S3-H-N2	160.06
S5·····H-N11	2.816	S5-H-N11	155.94
S4·····H-N12	2.808	S4-H-N12	141.82
S5·····H-N12	2.677	S5-H-N12	168.98

p. 5

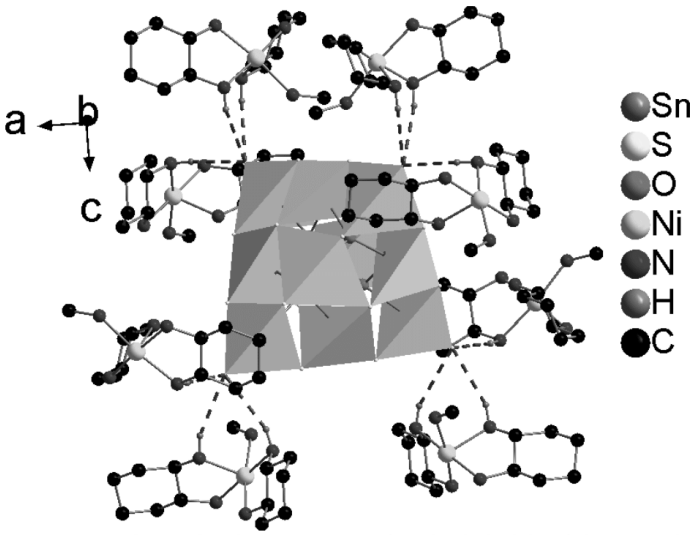

Figure S6: Hydrogen bonding interactions (purple dashed lines) between the terminal S atoms of the $[Sn_{10}S_{20}O_4]^{8-}$ units and $[Ni(1,2\text{-dach})(ma)]^{2+}$ moieties of neighboured clusters. Only selected hydrogen atoms are depicted.

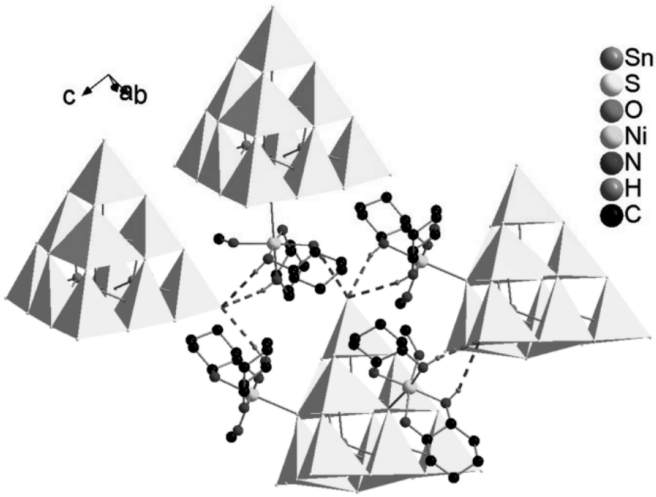

Figure S7: Arrangement of the molecules with hydrogen bonding interactions (purple dashed lines) between adjacent moieties.

5.2.6 SI für die Publikation: "Studies of the Reactivity of $\{[Ni(tren)]_2[Sn_2S_6]\}_n$: Synthesis and Crystal Structure of two New Thiostannates at Room Temperature"

Supplementary Information

Studies of the Reactivity of $\{[Ni(tren)]_2[Sn_2S_6]\}_n$: Synthesis and Crystal Structures of two New Thiostannates Prepared at Room Temperature

Jessica Hilbert, Christian Näther, Wolfgang Bensch*

Contents

Figure S1	Experimental and simulated XRPD pattern of compound $[Ni(tren)_2]_2[Sn_2S_6]\cdot 8H_2O$ and $[Ni(tren)(2amp)]_2[Sn_2S_6]$.	p. 3
Figure S2	IR spectra of compound $[Ni(tren)_2]_2[Sn_2S_6]\cdot 8H_2O$ and $[Ni(tren)(2amp)]_2[Sn_2S_6]$.	p. 4
Table S1	Absorptions in the IR spectra of $[Ni(tren)_2]_2[Sn_2S_6]\cdot 8H_2O$ and $[Ni(tren)(2amp)]_2[Sn_2S_6]$ compared to literature data of tris(2-aminethyl)amine (tren) and 2-(aminomethyl)pyridine (2amp).	p. 5
Figure S3	Raman spectra of $[Ni(tren)_2]_2[Sn_2S_6]\cdot 8H_2O$ and $[Ni(tren)(2amp)]_2[Sn_2S_6]$.	p. 6
Table S2	Assignment of the bands observed in the Raman spectra of $[Ni(tren)_2]_2[Sn_2S_6]\cdot 8H_2O$ (**1**) and $[Ni(tren)(2amp)]_2[Sn_2S_6]$ (**2**) compared to literature data of $Na_4Sn_2S_6\cdot 14\ H_2O$	p. 7
Figure S4	UV/vis spectrum of compound $[Ni(tren)_2]_2[Sn_2S_6]\cdot 8H_2O$ and $[Ni(tren)(2amp)]_2[Sn_2S_6]$. Showing the determination of the optical band gab using the Kubelka-Munk method	p. 8
Table S3	Assignment of the bands of the UV/Vis diffuse reflectance spectra of $[Ni(tren)_2]_2[Sn_2S_6]\cdot 8H_2O$ and $[Ni(tren)(2amp)]_2[Sn_2S_6]$.	p. 9
Figure S5	Experimental XRPD pattern of the residue isolated from a suspension of $\{[Ni(tren)]_2[Sn_2S_6]\}_n$ in an aqueous tren solution (20%) at 120°C (green) and after cooling this suspension to room-temperature (violet) together with simulated XRPD pattern for $\{[Ni(tren)]_2[Sn_2S_6]\}_n$	p. 9
Table S4	Selected bond length (Å) and angles (°) of compound $[Ni(tren)_2]_2[Sn_2S_6]\cdot 8H_2O$ (**1**) and $[Ni(tren)(2amp)]_2[Sn_2S_6]$ (**2**) compared to literature data of $Na_4Sn_2S_6\cdot 14H_2O$	p. 10
Figure S6	Octahedral environment of the Ni^{2+} ion in the compounds $[Ni(tren)_2]_2[Sn_2S_6]\cdot 8H_2O$ (**1**) and $[Ni(tren)(2amp)]_2[Sn_2S_6]$ (**2**).	p. 10
Table S5	Selected angles (°) of the octahedral Ni^{2+} environment of $[Ni(tren)_2]_2[Sn_2S_6]\cdot 8H_2O$ (**1**) and $[Ni(tren)(2amp)]_2[Sn_2S_6]$ (**2**).	p. 11
Table S6	Hydrogen bonds in $[Ni(tren)_2]_2[Sn_2S_6]\cdot 8H_2O$.	p. 11
Figure S7	View of the layers formed by the $[Sn_2S_6]^{4-}$ units and the crystal water molecules in compound **1** along the *a* axis (green and violet dashed lines: hydrogen bonding interactions).	p. 12
Figure S8	Crystal structure of compound **1** with view along the *a* axis. Purple dashed lines: hydrogen bonding interactions between the water molecules	p. 12

Figure S9	Crystal structure of compound **1** with view along the *b* axis. Hydrogen bonding interactions resulting in the formation of a three dimensional network.	p. 13
Figure S10	Crystal structure of compound **1** with view along the *b* axis. Hydrogen bonding interactions resulting in the formation of a three dimensional network. Two individuals of this network (bottom, green and violet) are interwoven.	p. 14
Figure S11	Arrangement of the $[Sn_2S_6]^{4-}$ units within the *ab* plane.	p. 15
Figure S12	View of the pairwise arrangement of the Ni(II) complexes in compound **2**.	p. 15
Figure S13	Arrangement of the thiostannate unit in compound **2** with hydrogen bonding.	p. 16
Table S7	Hydrogen bonds in $[Ni(tren)(2amp)]_2[Sn_2S_6]$	p. 16
Table S8	Results of the elemental analysis of the residues obtained by thermal decomposition of compound **1** at different temperatures and of compounds that might form in the reaction.	p. 17
Figure S14	Powder diffraction pattern of the thermal decomposition products of compound **1** isolated at different temperatures compared to that calculated for $[Ni(tren)_2]_2[Sn_2S_6]\cdot 8H_2O$ (**1**) and the precursor $\{[Ni(tren)]_2[Sn_2S_6]\}_n$.	p. 17
Figure S15	Experimental XRPD pattern of the product reacting the decomposition product of **1** with an aqueous 2amp solution (30%) at RT.	p. 18
Figure S16	IR spectra of the thermal decomposition products of compound **1** isolated at 100°C, 140°C and 260°C compared to the IR spectrum of compound **1**.	p. 18
Figure S17	Raman spectra of the thermal decomposition products of compound **1** obtained at 100°C, 140°C and 260°C compared to the Raman spectra of compound **1**.	p. 19
Table S9	Assignment of the bands in the Raman spectra of compound **1** and the thermal decomposition products of compound **1** isolated at 100°C and 140°C compared to literature data of $Na_4Sn_2S_6\cdot 14H_2O$	p. 19
Figure S18	Experimental XRPD pattern of the thermal decomposition product of compound **1** isolated at 260°C compared to that simulated for compound **2** and the precursor $\{[Ni(tren)]_2]Sn_2S_6]\}_n$.	p. 20
Figure S19	IR spectrum of the thermal decomposition product of compound **2** obtained at 260°C compared to IR spectrum for compound **2**.	p. 20
Figure S20	Raman spectra of the thermal decomposition product of compound **2** isolated at 260°C compared to the Raman spectra of compound **2**.	p. 21

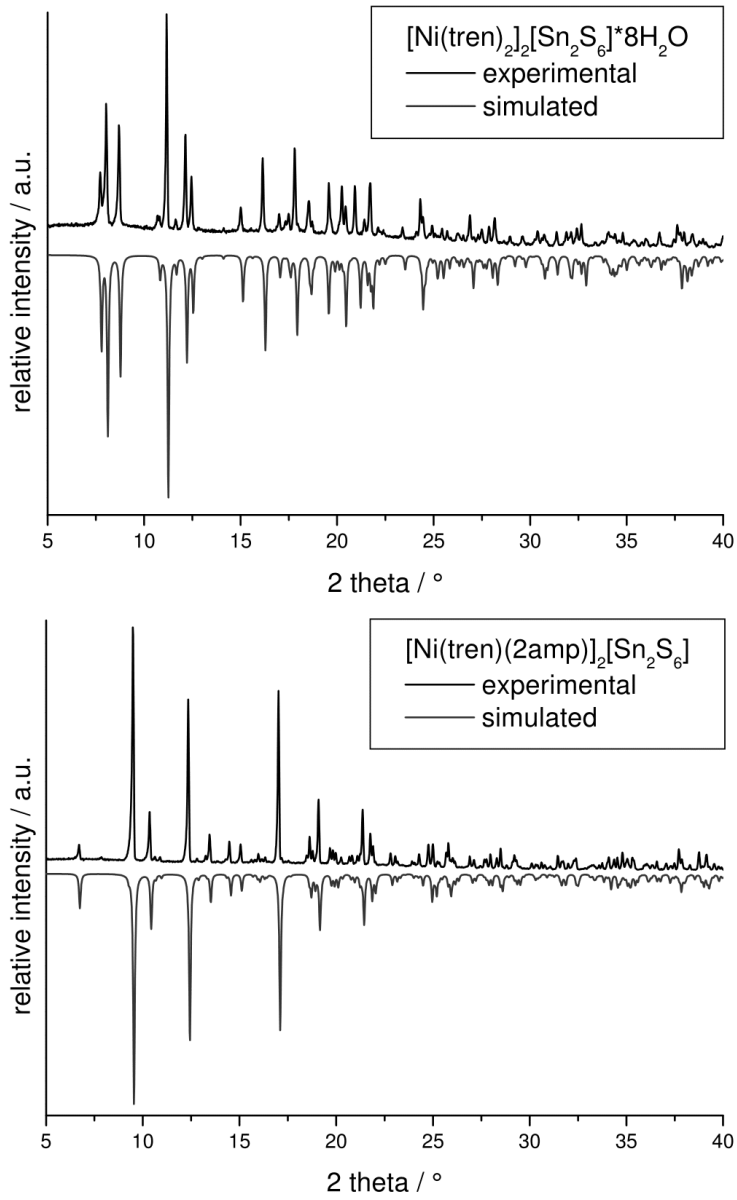

Fig. S1: Experimental (black) and simulated (red) XRPD pattern of compound $[Ni(tren)_2]_2[Sn_2S_6]\cdot 8H_2O$ (**1**, top) and $[Ni(tren)(2amp)]_2[Sn_2S_6]$ (**2**, bottom).

Spectroscopic Properties

Infrared spectroscopy

The observed absorptions in the IR spectra of the compounds can be mostly assigned to tren [Marzotto, A; Ciccarese, A; Clemente, D. A.; Valle, G. *J. Chem. Soc. Dalton Trans.* **1995**, 1461-1468.] and the Ni-N-stretching vibration at below 420 cm^{-1}. (Table S1). In compound **2** further absorptions can be assigned to 2-(aminomethyl)pyridine [S. Bruda, M. M. Turnbull, C. P. Landee, Q. Xu, *Inorg. Chim. Acta* **2006**, *359*, 298-308.].

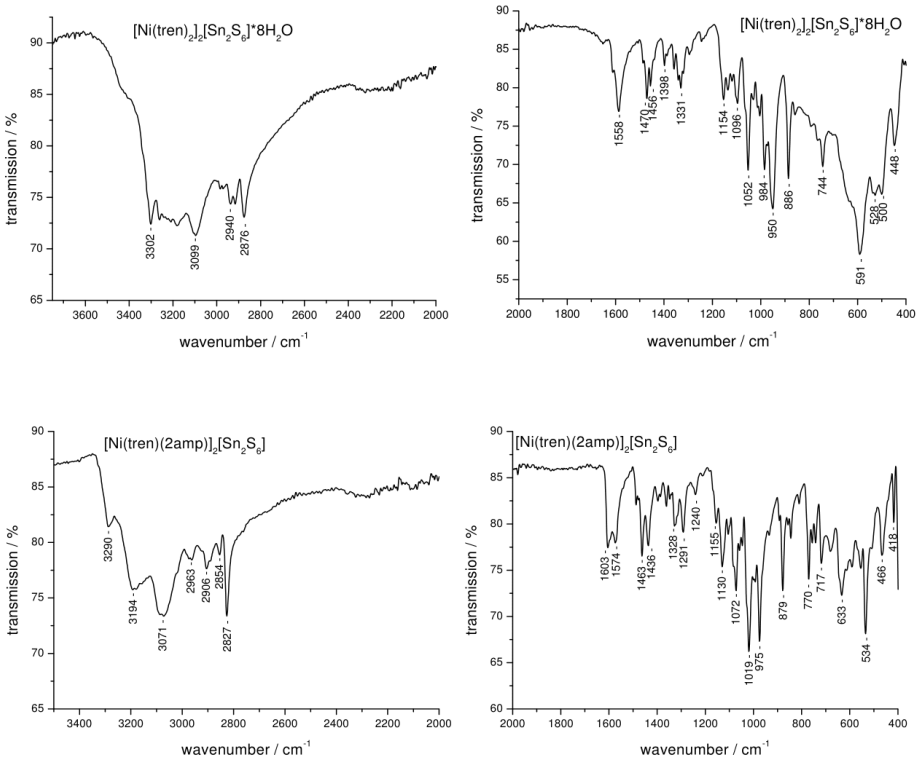

Fig. S2: IR spectra of compound $[Ni(tren)_2]_2[Sn_2S_6]\cdot 8H_2O$ (**1**, top) and $[Ni(tren)(2amp)]_2[Sn_2S_6]$ (**2**, bottom).

Table S1: Absorptions in the IR spectra of $[Ni(tren)_2]_2[Sn_2S_6]\cdot 8H_2O$ (**1**) and $[Ni(tren)(2amp)]_2[Sn_2S_6]$ (**2**) compared to literature data[a-e] of tris(2-aminethyl)amine (tren) and 2-(aminomethyl)pyridine (2amp).

tren[a, b]	2-amp[c-d]	1	2	Assignment
3298	3291	3302 w	3290 w	ν (NH_2)
3270	3258	3262 vw		ν (NH_2)
3180	3171	3184 vw	3194 m	ν (NH_2)
---	3079		3071m	ν $(NH)_{arom}$
2983	---	2940 vw	2963 w	ν (CH_2)
2910	2909	2916 vw	2906 w	ν (CH_2), ν $(NH)_{arom}$
2885	---	2876 w		ν (CH_2)
2858	2856		2854 w	ν (CH_2)
2827	---		2827 m	ν (CH_2)
1609	1604		1603 m	δ(NH_2)
1599	---	1588 m		δ(NH_2)
---	---		1574 w	unassigned band
---	---		1487 w	unassigned band
1473	1466	1470 m	1463 m	δ(NH_2) + δ(CH_2)
1456	---	1456 m		δ(NH_2) + δ(CH_2)
1437	---		1436 m	δ(CH_2)
1396	1405	1398 w	1398 w	δ(CH_2)
1359	1351	1358 w	1362 w	δ(CH_2)
1348	---	1341 w		δ(CH_2)
1336	1325	1331 w	1328 m	δ(CH_2)
1293	1291	1290 vw	1291 m	ν (C-NH_2)+ ν (C-N)
1248	1253	1246 vw	1240 w	ν (C-NH_2)+ ν (C-N)
1165	1161	1154 w	1155 w	ν (C-NH_2)+ ν (C-N)
1134	---	1137 w	1130 m	δ(CH_2)
1110	1115		1106 w	ρ(NH_2) region, δ(CH_2), ν(C-C)$_{amp}$
1091	1086	1096 m		δ(CH_2), δ$(CH)_{in\text{-}plane}$
1082	---		1072 m	ρ(NH_2) region
1055	1057	1052 s		ρ(NH_2) region, δ$(CH)_{in\text{-}plane}$
1038	1032	1030 vw		ρ(NH_2) region, , δ$(CH)_{in\text{-}plane}$
1020	1020		1019 s	ρ(NH_2) region, ν(C-N)$_{amp}$
1000	---	1003 w	994 w	ν (C-N)
979	---	984 m	975 s	δ(NH_2)
950	---	950 s		ν (C-C), CH_2 rock
883	---	886 s	879 s	NH_2 rock, CH_2 rock, ν (C-C)
848	---		845 w	ν (C-C)
812	818		809 vw	CH_2 rock
792	---	792 vw		δ(NH_2)
765	767	766 vw	770 m	δ(NH_2), γ(C-H)
743	746	744 m	743 w	δ(NH_2)
---	725		717 m	δ(C- CH_2)
---	666		680 w	NH_2 rock
625	---		633 m	δ(tren chelate ring)
578	590	591 s	589 w	δ(tren chelate ring), NH_2 rock
538, 532	---	538; 528	534 s	δ(tren chelate ring)
508	---	500		δ(tren chelate ring)
470	---	448	466 m	δ(tren chelate ring)
	445*			ν (M-NH_2)$_{amp}$
---	415		418 m	δ(py)
362*	381	381 s	390 s	ν (M-NH_2)

[a] A. Marzotto, A. Ciccarese, D. A. Clemente, G. Valle, *J. Chem. Soc. Dalton Trans.* **1995**, *9*, 1461-1468
[b] J. Yin, C. Li, X. Chen, Q. Luo, *Spectrochim. Acta. A* **1997**, *53*, 2209-2218.
[c] M. L. Niven, G. C. Percy, *Transition Met. Chem.* **1978**, *3*, 267-271.
[d] M. L. Niven, G. C. Percy, D. A. Thornton, *J. Mol. Struct.* **1980**, *68*, 73-80.
[e] S. Bruda, M. M. Turnbull, C. P. Landee, Q. Xu, *Inorg. Chim. Acta* **2006**, *359*, 298-308.

Raman spectroscopy

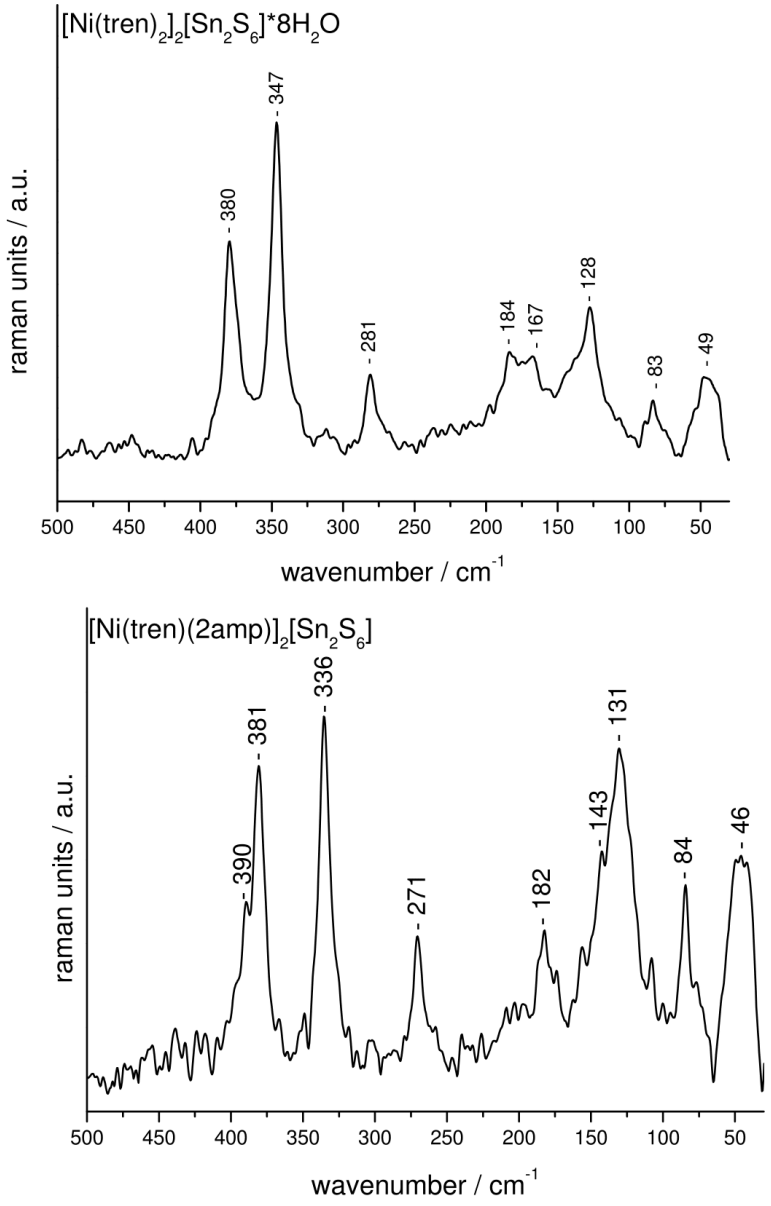

Fig. S3: Raman spectra of $[Ni(tren)_2]_2[Sn_2S_6]\cdot 8H_2O$ (**1**, top) and $[Ni(tren)(2amp)]_2[Sn_2S_6]$ (**2**, bottom).

p. 6

Table S2: Assignment of the bands observed in the Raman spectra of $[Ni(tren)_2]_2[Sn_2S_6]\cdot 8H_2O$ (**1**) and $[Ni(tren)(2amp)]_2[Sn_2S_6]$ (**2**) compared to literature data of $Na_4Sn_2S_6\cdot 14\ H_2O$[f] (all wave numbers are given in cm^{-1}).

$[Sn_2S_6]^{4-}$	**1**	**2**	**assingment**[f]
391	380	390	$\nu_{as}(SnS_2)$
377		381	$\nu_s(SnS_2)$
341	347	336	ν_{as}(Sn-S-Sn)
281	281	271	ν (Sn_2S_2)
190	184	182	
	167		
151			
		143	deformation &
136		131	torsional
	128		vibration
118			
	83	84	
	49	46	

[f] Krebs, B; Pohl, S.; Schiwy, W. *Angew. Chem. Int. Ed. Engl.* **1970**, *9*, 897-898.

UV/vis spectroscopy

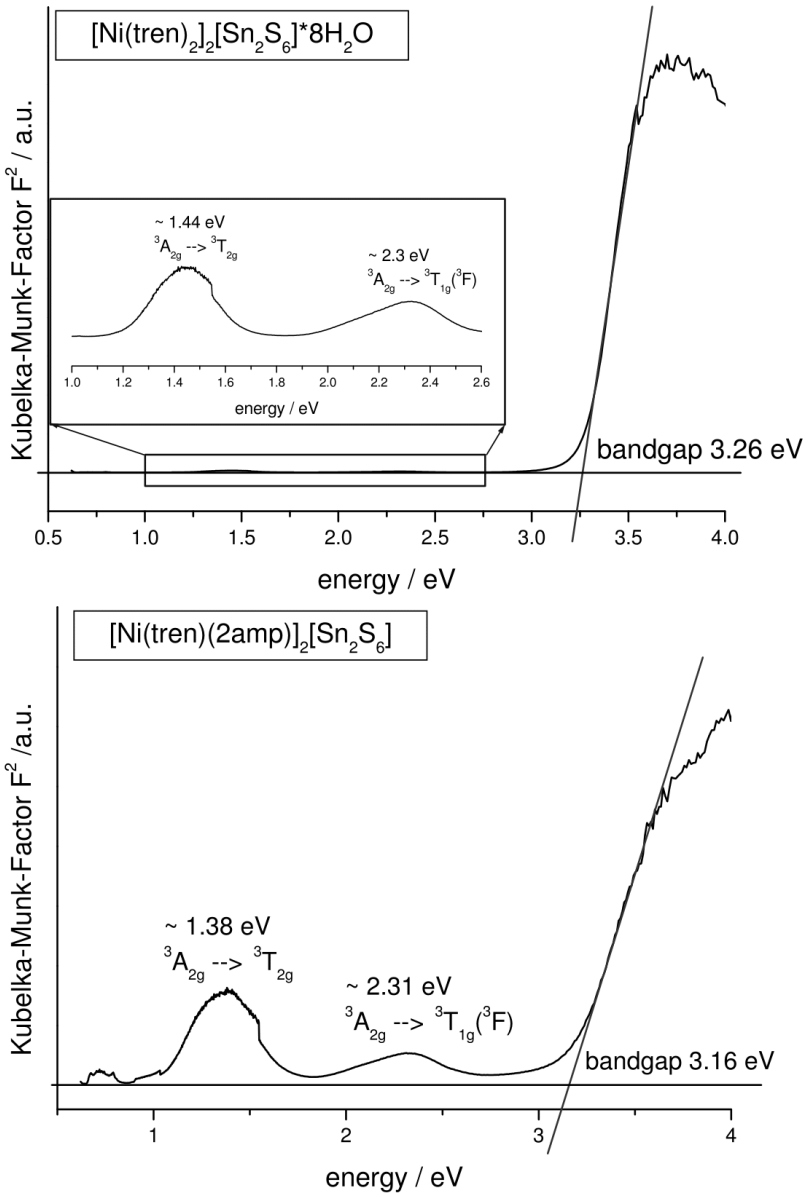

Fig. S4: UV/vis spectrum of compound $[Ni(tren)_2]_2[Sn_2S_6]\cdot 8H_2O$ (**1**, top) and $[Ni(tren)(2amp)]_2[Sn_2S_6]$ (**2**, bottom). Showing the determination of the optical band gab using the Kubelka-Munk method.

p. 8

Table S3: Assignment of the bands of the UV/Vis diffuse reflectance spectra of $[Ni(tren)_2]_2[Sn_2S_6]\cdot 8H_2O$ (**1**, top) and $[Ni(tren)(2amp)]_2[Sn_2S_6]$ (**2**, bottom).

1	**2**	assignment[g,h]
~1.44	~1.38	$^3A_{2g} \rightarrow {}^3T_{2g}$
~2.30	~2.31	$^3A_{2g} \rightarrow {}^3T_{1g}$ (^3F)
3.26	3.16	optical band gap

[g]: Roe, S. P.; Hill, J. O.; Magee, R. J. *Monatsh. Chem.* **1991**, *122*, 467–478.
[h]: González, E.; Rodrigue-Witchel, A.; Reber, C. *Coord. Chem. Rev.* **2007**, *251*, 351–363.

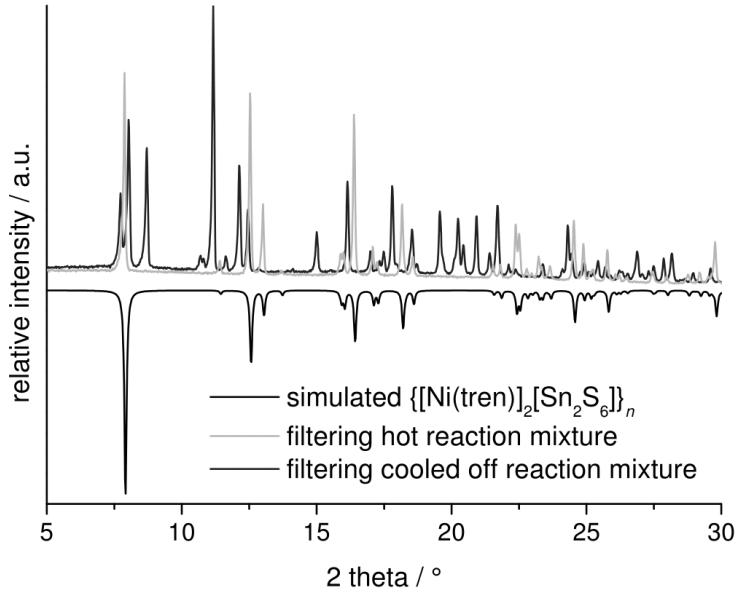

Fig. S5: Experimental XRPD pattern of the residue isolated from a suspension of $\{[Ni(tren)]_2[Sn_2S_6]\}_n$ in an aqueous tren solution (20%) at 120°C (green) and after cooling this suspension to room-temperature (violet) together with simulated XRPD pattern for $\{[Ni(tren)]_2[Sn_2S_6]\}_n$ (black).

Table S4: Selected bond length (Å) and angles (°) of compound $[Ni(tren)_2]_2[Sn_2S_6]\cdot 8H_2O$ (**1**) and $[Ni(tren)(2amp)]_2[Sn_2S_6]$ (**2**) compared to $Na_4Sn_2S_6\cdot 14H_2O$[f]

	1[a]	**2**	$[Sn_2S_6]^{4-}$
Sn1 – S1	2.3317(6)	2.3345(11)	2.325
Sn1 – S2	2.3422(6)	2.3221(11)	2.338
Sn1 – S3	2.4487(6)	2.4569(11)	2.452
Sn1 – S3^n/S4	2.4511(7)	2.4569(11)	2.448
S1 – Sn1 – S2	115.24(2)	114.76(4)	119.8
S1 – Sn1 – S3	113.56(2)	111.46(4)	108.2
S1 – Sn1 – S3^n/S4	110.18(2)	111.74(4)	110.4
S2 – Sn1 – S3	110.57(2)	112.98(4)	110.6
S2 – Sn1 – S3^n/S4	113.51(2)	111.12(4)	110.8
S3 – Sn1 – S3^n/S4	91.48(2)	92.67(4)	94.0
Sn1 – S3 – Sn1^n/Sn2	88.52(2)	87.36(4)	86.0
Ni1 – N1	2.154(2)	2.116(4)	
Ni1 – N2	2.102(2)	2.127(4)	
Ni1 – N3/N11	2.144(2)	2.182(4)	
Ni1 – N1a^b/N4/N12	2.154(2)	2.099(4)	
Ni1 – N2a^b/N11/N21	2.102(2)	2.066(4)	
Ni1 – N3a^b/N12/N22	2.144(2)	2.126(3)	

Symmetry transformations used to generate equivalent atoms: n =a,c,d
a: -x+1,-y,-z; b: -x,-y,-z+1; c:-x,-y+1,-z+2; d: -x+1,-y+1,-z+2

[f] Krebs, B; Pohl, S.; Schiwy, W. *Angew. Chem. Int. Ed. Engl.* **1970**, *9*, 897-898.

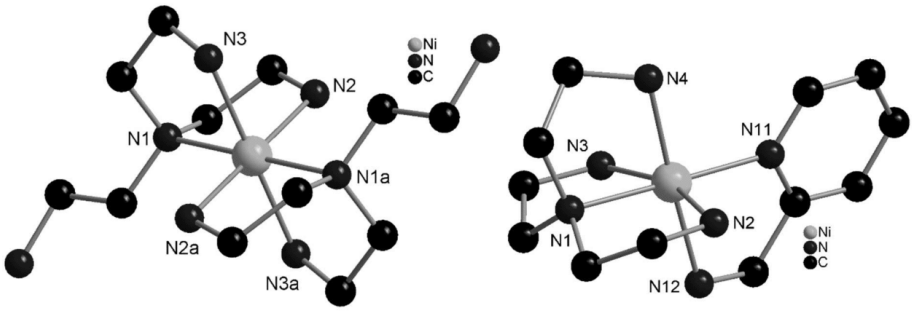

Fig. S6: Octahedral environment of the Ni^{2+} ion in the compounds $[Ni(tren)_2]_2[Sn_2S_6]\cdot 8H_2O$ (**1**, left) and $[Ni(tren)(2amp)]_2[Sn_2S_6]$ (**2**, right). Hydrogen atoms are omitted for clarity.

Table S5: Selected angles (°) of the octahedral Ni^{2+} environment of $[Ni(tren)_2]_2[Sn_2S_6]\cdot 8H_2O$ (**1**) and $[Ni(tren)(2amp)]_2[Sn_2S_6]$ (**2**).

1		**2**	
N3-Ni1-N1	82.74(9)	N1-Ni1-N2	83.02(16)
N3-Ni1-N2	90.59(10)	N1-Ni1-N3	80.94(15)
N3-Ni1-N1[a]	97.26(9)	N1-Ni1-N4	82.93(14)
N3-Ni1-N2[a]	89.41(10)	N1-Ni1-N12	100.58(14)
N1-Ni1-N2	82.71(8)	N4-Ni1-N2	93.21(15)
N1-Ni1-N2[a]	97.29(8)	N4-Ni1-N3	93.39(15)
N1-Ni1-N3[a]	97.26(9)	N4-Ni1-N11	96.56(15)
N2-Ni1-N1[a]	97.29(8)	N2-Ni1-N11	97.97(16)
N1-Ni1-N1[a]	180.0	N1-Ni1-N11	178.91(16)
N2-Ni1-N2[a]	180.0	N2-Ni1-N3	161.75(16)
N3-Ni1-N3[a]	180.0	N4-Ni1-N12	175.98(15)

a: -x,-y,-z+1

Table S6: Hydrogen bonds [Å and °] ($[Ni(tren)_2]_2[Sn_2S_6]\cdot 8H_2O$ (**1**)).

hydrogen bonding interactions between:	D-H...A	d(D-H)	d(H...A)	d(D...A)	<(DHA)
water molecules forming octamers	O(1)-H(1O1)...O(2)	0.84	1.85	2.685(3)	173.1
	O(1)-H(2O1)...O(4)	0.84	1.90	2.734(3)	177.1
	O(3)-H(2O3)...O(1)	0.84	1.96	2.796(4)	175.5
	O(4)-H(2O4)...O(1)#9	0.84	1.96	2.780(3)	166.5
water clusters and $[Sn_2S_6]^{4-}$ units	O(2)-H(2O2)...S(2)#6	0.84	2.38	3.151(2)	152.6
	O(3)-H(1O3)...S(1)	0.84	2.43	3.270(2)	175.8
	O(4)-H(1O4)...N(4)	0.84	2.00	2.843(4)	175.7
	O(2)-H(1O2)...N(14)#8	0.84	1.95	2.741(3)	155.9
water clusters and $[Ni(tren)_2]^{2+}$ cations	N(2)-H(2N)...O(3)#2	0.91	2.29	3.097(3)	148.4
	C(11)-H(11B)...O(4)#7	0.99	2.59	3.516(4)	154.8
	N(12)-H(11N)...O(2)	0.91	2.47	3.336(3)	160.0
	C(13)-H(13B)...O(2)#3	0.99	2.61	3.457(4)	143.5
	N(14)-H(16N)...O(3)#3	0.91	2.35	3.247(4)	169.5
$[Sn_2S_6]^{4-}$ units and $[Ni(tren)_2]^{2+}$ cations	C(1)-H(1B)...S(3)#4	0.99	2.73	3.689(3)	162.9
	N(2)-H(1N)...S(2)#2	0.91	2.55	3.459(3)	173.1
	N(3)-H(4N)...S(2)	0.91	2.81	3.626(3)	150.4
	C(5)-H(5B)...S(1)	0.99	2.80	3.711(3)	153.2
	N(4)-H(5N)...S(2)#5	0.91	2.86	3.643(2)	145.4
	N(4)-H(6N)...S(1)	0.91	2.75	3.599(2)	156.2
	C(11)-H(11A)...S(2)#6	0.99	2.89	3.752(3)	145.4
	N(12)-H(12N)...S(1)	0.91	2.73	3.514(2)	145.0
	N(13)-H(13N)...S(1)	0.91	2.56	3.392(2)	153.1
	N(13)-H(14N)...S(2)#1	0.91	2.64	3.540(2)	170.3
	C(15)-H(15A)...S(3)#3	0.99	3.02	3.848(3)	142.1
	N(14)-H(15N)...S(3)#3	0.91	2.57	3.449(3)	161.3

Symmetry transformations used to generate equivalent atoms: #1 -x+1,-y,-z; #2 -x,-y,-z+1;#3 -x+1,-y+1,-z; #4 x,y,z+1; #5 -x+1,-y,-z+1; #6 x,y+1,z; #7 -x+1,-y+1,-z+1; #8 x-1,y,z; #9 -x,-y+1,-z+1

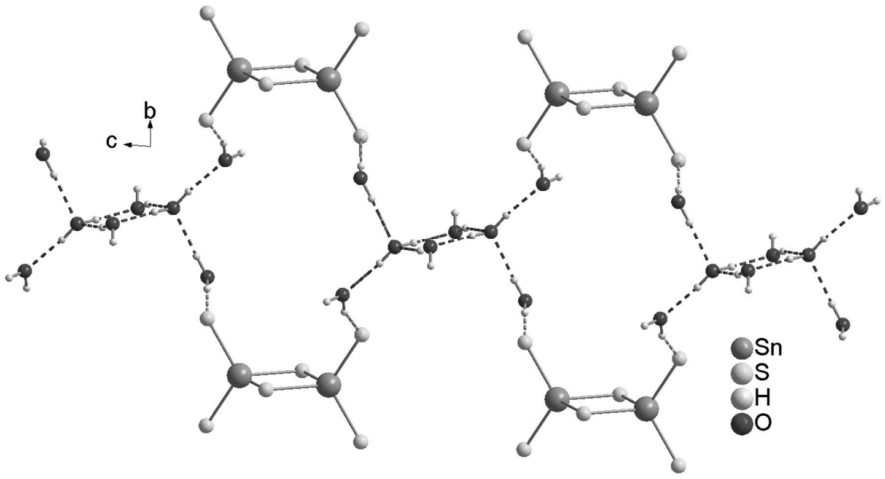

Fig. S7: View of the layers formed by the $[Sn_2S_6]^{4-}$ units and the crystal water molecules in compound **1** along the *a* axis (green and violet dashed lines: hydrogen bonding interactions).

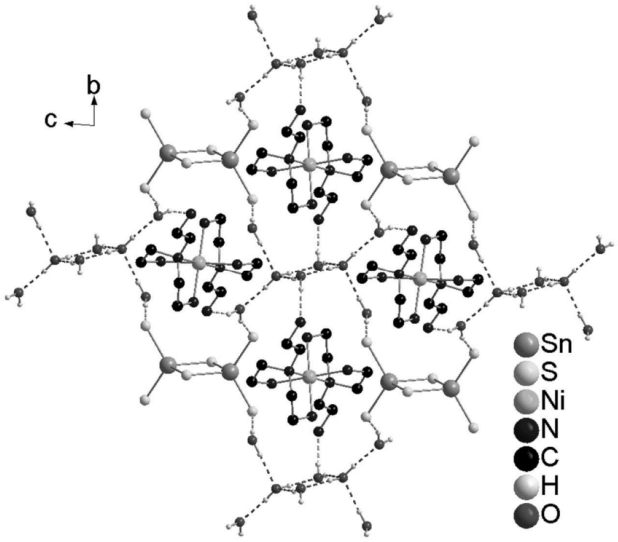

Fig. S8: Crystal structure of compound **1** with view along the *a* axis. Purple dashed lines: hydrogen bonding interactions between the water molecules. Green dashed lines: hydrogen bonding interactions between the water cluster and adjacent units. For reasons of clarity only selected hydrogen atoms are displaced.

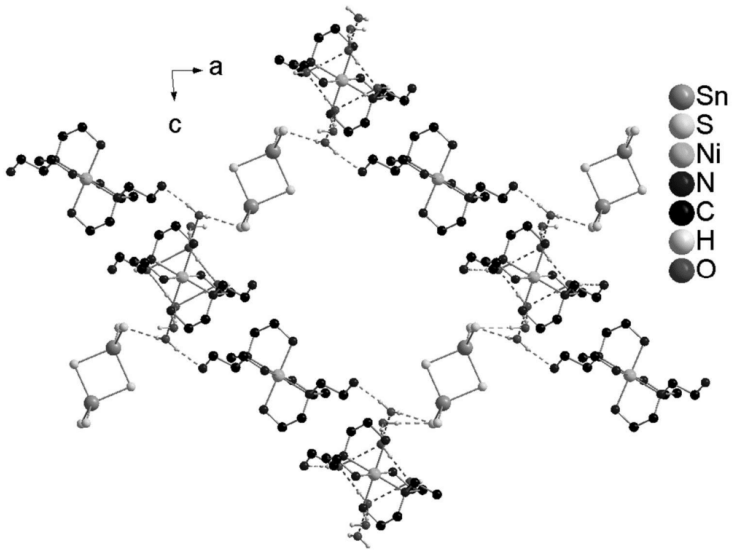

Fig. S9: Crystal structure of compound **1** with view along the *b* axis. Hydrogen bonding interactions resulting in the formation of a three dimensional network. Purple dashed lines: hydrogen bonding interactions between the water molecules. Green dashed lines: hydrogen bonding interactions between the water cluster and adjacent units. For reasons of clarity only selected hydrogen atoms are displaced.

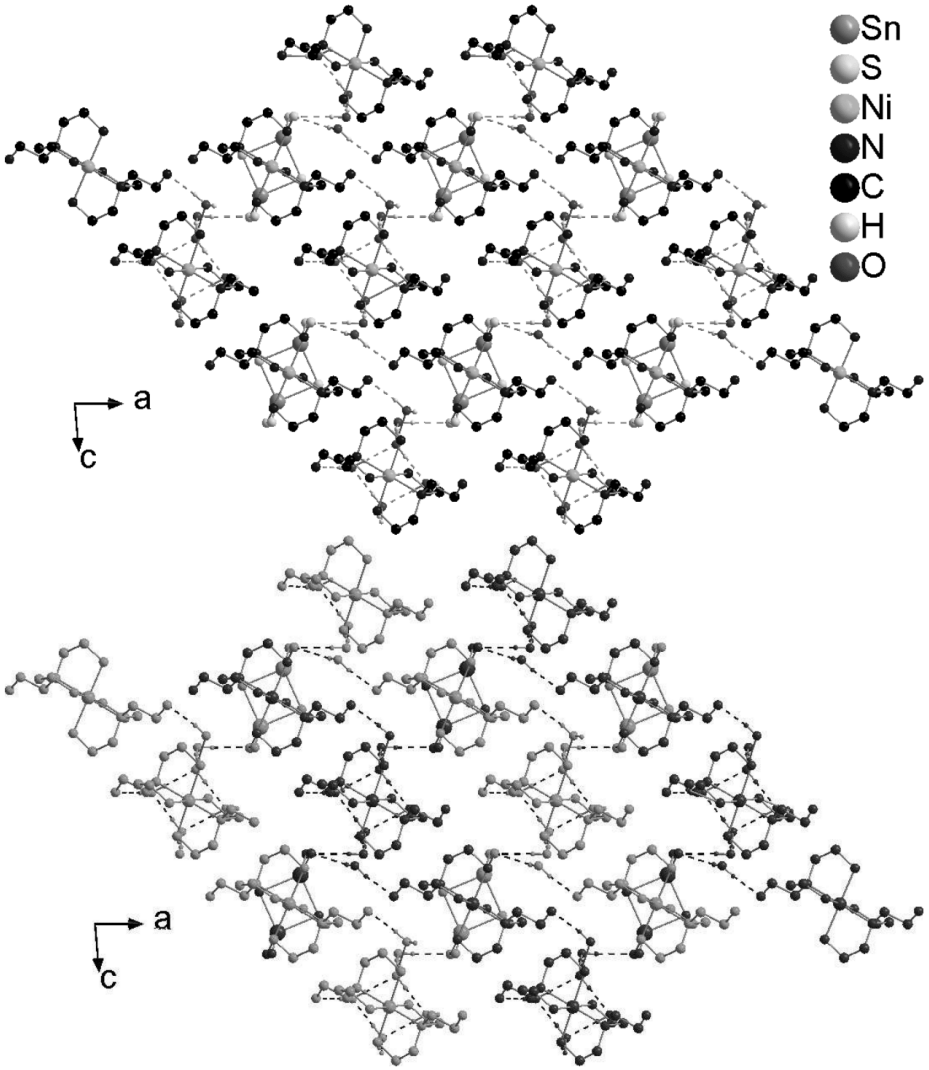

Fig. S10: Crystal structure of compound **1** with view along the *b* axis. Hydrogen bonding interactions (dashed lines) resulting in the formation of a three dimensional network. Two individuals of this network (bottom, green and violet) are interwoven.

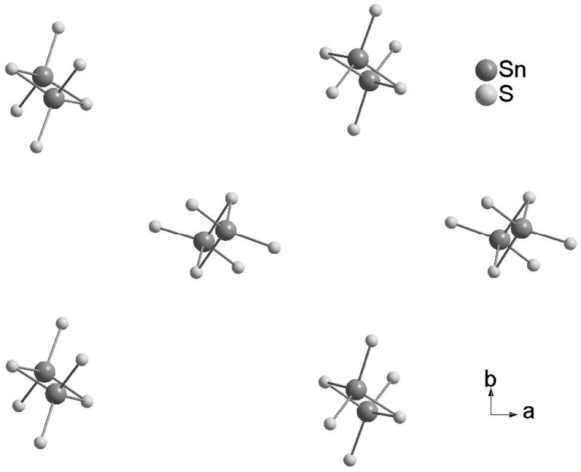

Fig. S11: Arrangement of the $[Sn_2S_6]^{4-}$ units within the *ab* plane (compound **2**).

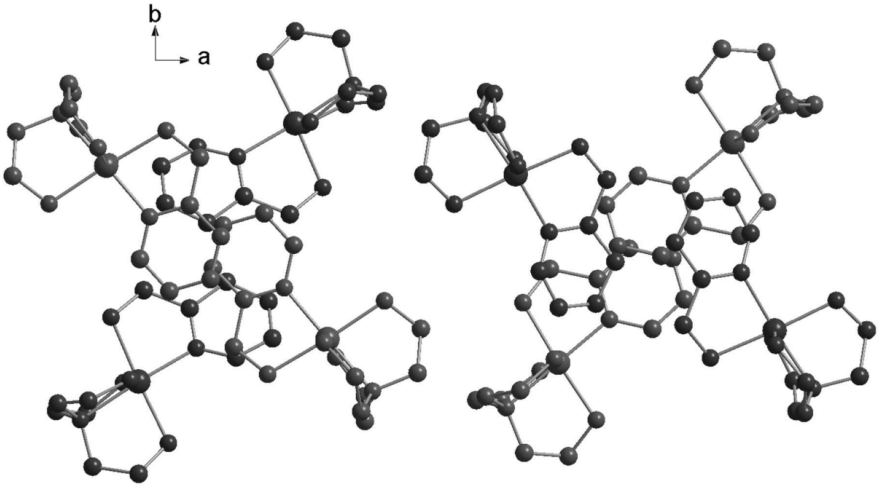

Fig. S12: View of the pairwise arrangement of the Ni(II) complexes in compound **2**.

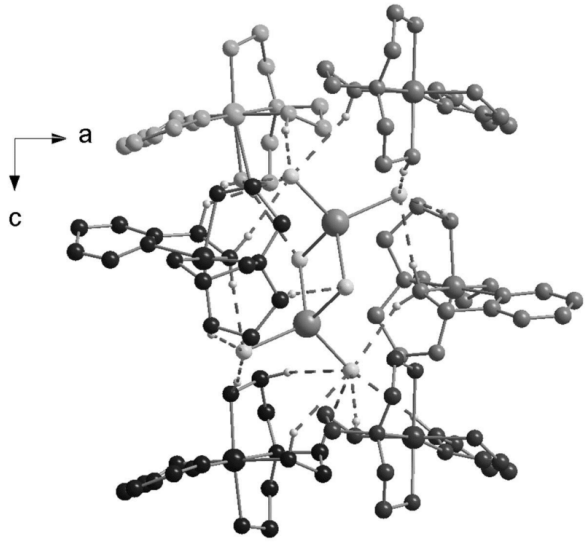

Fig. S13: Arrangement of the thiostannate unit in compound **2** with hydrogen bonding shown as dashed lines.

Table S7: Hydrogen bonds [Å and °] ([Ni(tren)(2amp)]$_2$[Sn_2S_6] (**2**)).

D-H...A	d(D-H)	d(H...A)	d(D...A)	<(DHA)
C(2)-H(2B)...S(6)#1	0.99	2.94	3.868(5)	156.9
N(2)-H(1N)...S(5)#1	0.91	2.72	3.618(4)	170.6
N(2)-H(2N)...S(2)	0.91	2.57	3.443(4)	159.9
N(3)-H(4N)...S(3)#2	0.91	2.76	3.582(4)	150.6
N(4)-H(5N)...S(1)#2	0.91	2.61	3.507(4)	170.0
N(4)-H(6N)...S(6)#1	0.91	2.72	3.486(4)	143.0
C(12)-H(12)...S(5)#3	0.95	2.78	3.679(6)	157.9
N(12)-H(7N)...S(6)	0.91	2.58	3.405(4)	151.9
N(12)-H(8N)...S(2)	0.91	2.47	3.376(4)	174.2
C(21)-H(21A)...S(4)	0.99	2.77	3.724(5)	163.2
N(22)-H(9N)...S(5)	0.91	2.76	3.614(4)	156.9
N(22)-H(10N)...S(4)#4	0.91	2.94	3.665(4)	137.4
N(23)-H(11N)...S(2)#5	0.91	2.62	3.481(4)	158.8
N(23)-H(12N)...S(1)	0.91	2.80	3.576(4)	143.5
N(24)-H(13N)...S(6)#4	0.91	2.57	3.464(4)	167.8
N(24)-H(14N)...S(1)#5	0.91	2.61	3.452(4)	153.7
C(35)-H(35)...S(6)#4	0.95	2.60	3.529(8)	167.2
N(32)-H(15N)...S(5)	0.91	2.46	3.360(4)	172.6
N(32)-H(18N)...S(1)	0.91	2.44	3.335(4)	169.4
N(32)-H(15N)...S(5)	0.91	2.46	3.360(4)	172.6
N(32)-H(18N)...S(1)	0.91	2.44	3.335(4)	169.4

Symmetry transformations used to generate equivalent atoms: #1 y+1/2,-x+1,z+1/2; #2 y+1/2,-x+1,z-1/2; #3 -y+3/2,x,-z+1/2; #4 y,-x+3/2,-z+1/2; #5 y,-x+3/2,-z+3/2

Table S8: Results of the elemental analysis of the residues obtained by thermal decomposition of compound **1** at different temperatures and of compounds that might form in the reaction.

Compound	N %	C %	H %
$[Ni(tren)_2]_2[Sn_2S_6]\cdot 8H_2O$ theo	17.56	22.59	6.95
$[Ni(tren)_2]_2[Sn_2S_6]\cdot 5H_2O$ theo	18.34	23.59	6.76
$[Ni(tren)_2]_2[Sn_2S_6]\cdot 4H_2O$ theo	18.61	23.94	6.70
$[Ni(tren)_2]_2[Sn_2S_6]\cdot 3H_2O$ theo	18.89	24.30	6.63
$[Ni(tren)_2]_2[Sn_2S_6]$ theo	19.80	25.46	6.41
$[Ni(tren)]_2[Sn_2S_6]$ theo	13.34	17.17	4.32
isolated at 100°C	18.4	24.0	6.4
isolated at 140°C	18.8	22.6	6.1
isolated at 195°C	13.4	17.4	4.4

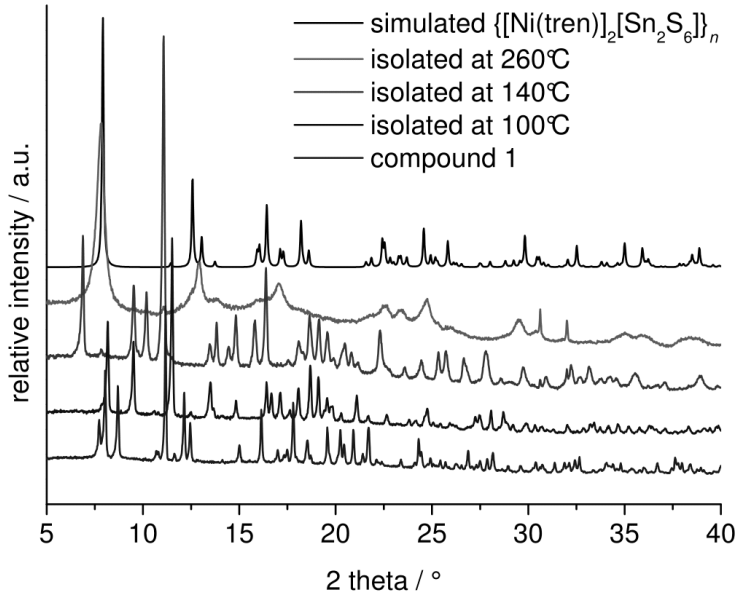

Fig. S14: Powder diffraction pattern of the thermal decomposition products of compound **1** isolated at different temperatures compared to that calculated for $[Ni(tren)_2]_2[Sn_2S_6]\cdot 8H_2O$ (**1**) and the precursor $\{[Ni(tren)]_2[Sn_2S_6]\}_n$.

p. 17

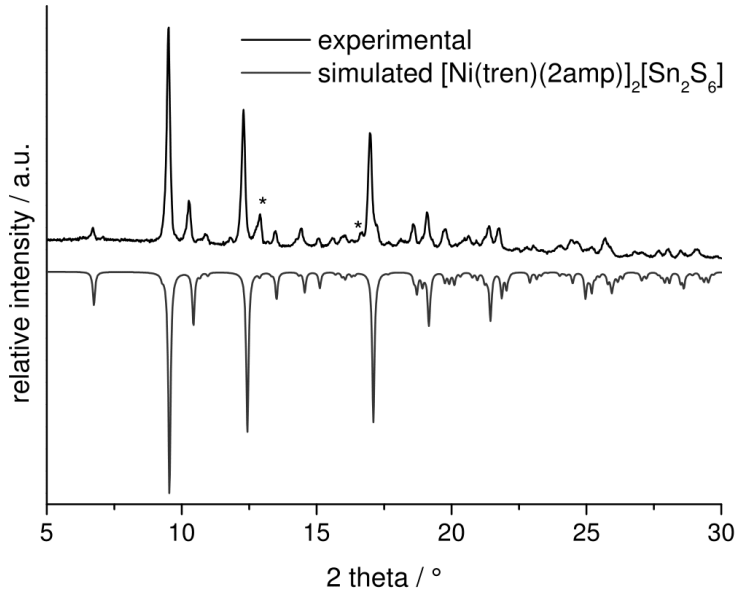

Fig. 15: Experimental XRPD pattern of the product reacting the decomposition product of **1** with an aqueous 2amp solution (30%) at RT, unidentified peaks are marked with an asterisk.

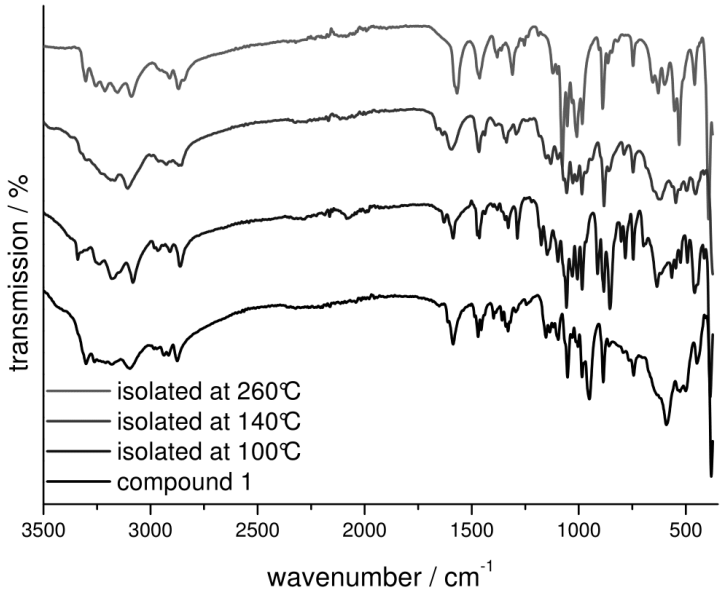

Fig. S16: IR spectra of the thermal decomposition products of compound **1** isolated at 100°C, 140°C and 260°C compared to the IR spectrum of compound **1**.

p. 18

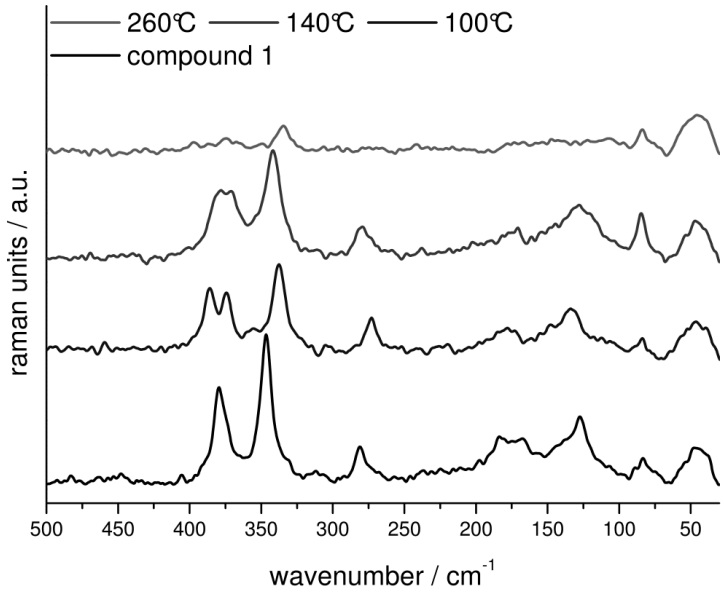

Fig. S17: Raman spectra of the thermal decomposition products of compound **1** obtained at 100°C, 140°C and 260°C compared to the Raman spectra of compound **1**.

Table S9: Assignment of the bands in the Raman spectra of compound **1** and the thermal decomposition products of compound **1** isolated at 100°C and 140°C compared to literature data of $Na_4Sn_2S_6{\cdot}14H_2O$[f].

$[Sn_2S_6]^{4-}$	**1**	**100°C**	**140°C**	**assingment**[a]
391	380	386	379	$\nu_{as}(SnS_2)$
377		375	371	$\nu_s(SnS_2)$
341	347	338	342	ν_{as}(Sn-S-Sn)
281	281	273	280	ν (Sn_2S_2)
190	184	178		
	167		170	
151				
136		134		deformation & torsional vibration
	128		128	
118				
	83	84	84	
	49	47	47	

[f] Krebs, B; Pohl, S.; Schiwy, W. *Angew. Chem. Int. Ed. Engl.* **1970**, *9*, 897-898.

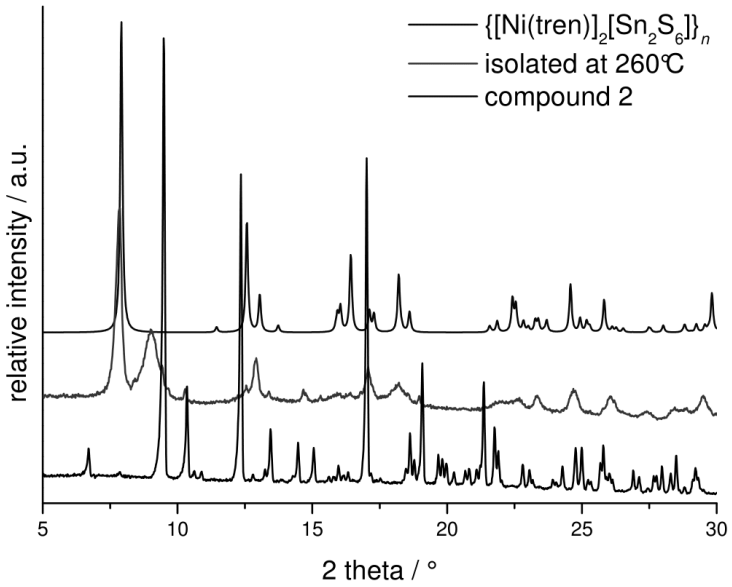

Fig. S18: Experimental XRPD pattern of the thermal decomposition product of compound **1** isolated at 260°C compared to that simulated for compound **2** and the precursor $\{[Ni(tren)]_2]Sn_2S_6]\}_n$.

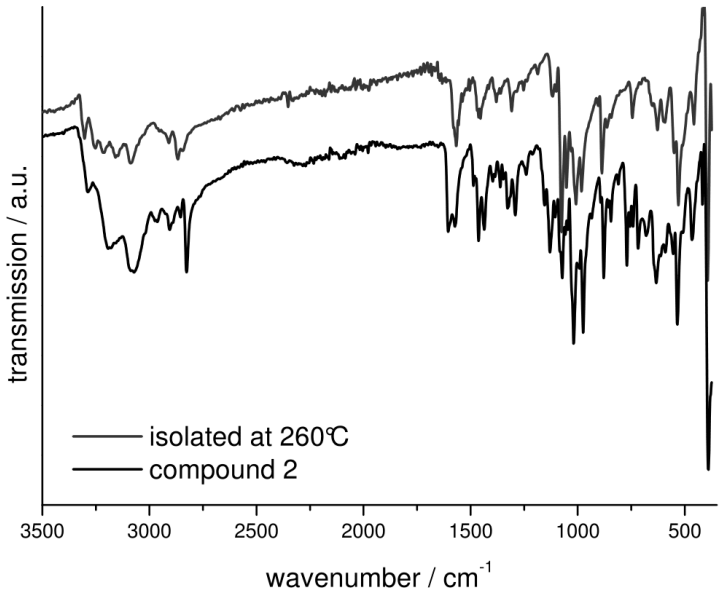

Fig. S19: IR spectrum of the thermal decomposition product of compound **2** obtained at 260°C compared to IR spectrum for compound **2**.

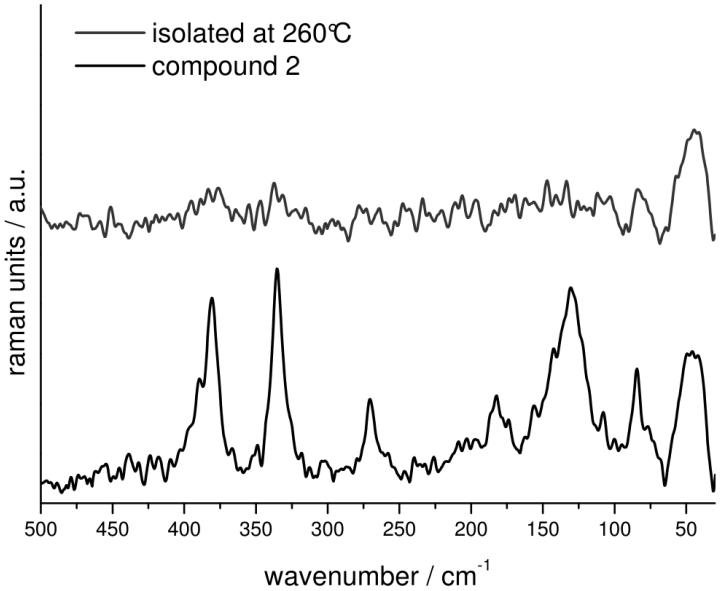

Fig. S20: Raman spectra of the thermal decomposition product of compound **2** isolated at 260°C compared to the Raman spectra of compound **2**.

p. 21

5.3 Strukturdaten / Messprotokolle

5.3.1 Messprotokoll der Verbindung {[Mn(phen)$_2$]$_2$[Sn$_2$S$_6$]}

Table 1. Crystal data and structure refinement for {[Mn($C_{12}H_8N_2$)$_2$]$_2$[Sn$_2$S$_6$]} ($C_{12}H_8N_2$; phen = 1,10-Phenanthrolin)

Identification code	jh231	
Empirical formula	{[Mn($C_{12}H_8N_2$)$_2$]$_2$[Sn$_2$S$_6$]}	
Crystal color, - habitus	red blocks	
Formula weight	1260.53	
Temperature	293(2) K	
Wavelength	0.71073 Å	
Crystal system	monoclinic	
Space group	$P2_1/n$	
Unit cell dimensions	a = 10.8230(4) Å	α = 90°.
	b = 9.8940(2) Å	β = 91.356(3)°.
	c = 24.8107(10) Å	γ = 90°.
Volume	2656.05(15) Å^3	
Z	2	
Density (calculated)	1.576 g / cm^3	
Absorption coefficient	1.670 mm^{-1}	
F(000)	1244	
Crystal size	0.2190 x 0.1150 x 0.0321 mm^3	
Theta range for data collection	1.64 to 24.62°.	
Index ranges	-11≤ h ≤ 12, -11≤ k ≤ 11, -28 ≤ l ≤ 29	
Reflections collected	28044	
Independent reflections	4454 [R(int) = 0.1025]	
Completeness to theta = 24.62°	99.4 %	
Absorption correction	Numerical	
Max. and min. transmission	0.8877 and 0.6059	
Refinement method	Full-matrix least-squares on F^2	
Data / restraints / parameters	4454 / 0 / 299	
Goodness-of-fit on F^2	1.373	
Final R indices [I>2sigma(I)]	R1 = 0.0428, wR2 = 0.1045	
R indices (all data)	R1 = 0.0517, wR2 = 0.1078	
Extinction coefficient	0.0059(5)	
Largest diff. peak and hole	0.566 and -0.681 e.Å^{-3}	

Comments:
All non–hydrogen atoms were refined using anisotropic displacement parameters. The C–H hydrogen atoms were positioned with idealised geometry and refined isotropic using a riding model.

Table 2. Atomic coordinates ($\cdot 10^4$) and equivalent isotropic displacement parameters ($Å^2 \cdot 10^3$). U(eq) is defined as one third of the trace of the orthogonalized U_{ij} tensor.

	x	y	z	U(eq)
Sn(1)	1206(1)	9378(1)	366(1)	42(1)
Mn(1)	3456(1)	8071(1)	1090(1)	45(1)
S(1)	3338(1)	9571(1)	245(1)	48(1)
S(2)	1113(1)	8063(1)	1157(1)	54(1)
S(3)	-1(1)	11469(1)	405(1)	53(1)
N(1)	3689(4)	5886(4)	806(2)	56(1)
N(2)	5536(4)	7674(4)	992(2)	52(1)
C(1)	2776(7)	5032(6)	690(2)	76(2)
C(2)	3028(9)	3668(6)	521(3)	88(2)
C(3)	4218(9)	3248(6)	491(3)	85(2)
C(4)	5177(7)	4105(5)	620(2)	73(2)
C(5)	6460(8)	3733(7)	596(3)	84(2)
C(6)	7362(7)	4608(7)	695(3)	88(2)
C(7)	7104(6)	5988(6)	830(2)	69(2)
C(8)	8007(6)	6988(7)	891(3)	79(2)
C(9)	7682(6)	8275(7)	992(3)	80(2)
C(10)	6431(5)	8588(5)	1038(3)	63(1)
C(11)	5849(5)	6387(5)	874(2)	53(1)
C(12)	4881(5)	5449(4)	776(2)	54(1)
N(3)	3716(4)	7113(3)	1964(2)	51(1)
N(4)	4005(4)	9740(4)	1693(2)	50(1)
C(13)	3531(5)	5847(5)	2113(2)	59(1)
C(14)	3730(6)	5373(5)	2633(3)	70(2)
C(15)	4123(6)	6225(6)	3027(2)	74(2)
C(16)	4305(6)	7610(5)	2894(2)	67(1)
C(17)	4671(8)	8585(6)	3285(3)	89(2)
C(18)	4808(8)	9900(6)	3146(2)	90(2)
C(19)	4586(6)	10338(5)	2611(2)	67(2)
C(20)	4721(8)	11682(5)	2440(3)	87(2)
C(21)	4456(8)	12020(5)	1924(3)	89(2)
C(22)	4106(6)	11026(5)	1548(2)	71(2)
C(23)	4239(5)	9387(4)	2204(2)	52(1)
C(24)	4085(5)	7998(4)	2363(2)	50(1)

Table 3. Bond lengths [Å] and angles [°].

Sn(1)-S(1)	2.3413(12)		
Sn(1)-S(2)	2.3568(12)	S(1)-Sn(1)-S(2)	102.31(4)
Sn(1)-S(3)#1	2.4377(11)	S(1)-Sn(1)-S(3)#1	115.96(5)
Sn(1)-S(3)	2.4501(11)	S(2)-Sn(1)-S(3)#1	115.53(4)
Sn(1)-Mn(1)	3.2589(7)	S(1)-Sn(1)-S(3)	117.64(4)
Mn(1)-N(1)	2.288(4)	S(2)-Sn(1)-S(3)	113.59(5)
Mn(1)-N(4)	2.297(4)	S(3)#1-Sn(1)-S(3)	92.57(4)
Mn(1)-N(2)	2.303(4)	S(1)-Sn(1)-Mn(1)	51.47(3)
Mn(1)-N(3)	2.378(4)	S(2)-Sn(1)-Mn(1)	50.86(3)
Mn(1)-S(2)	2.5454(14)	S(3)#1-Sn(1)-Mn(1)	132.44(3)
Mn(1)-S(1)	2.5685(13)	S(3)-Sn(1)-Mn(1)	134.90(3)
S(3)-Sn(1)#1	2.4377(11)	N(1)-Mn(1)-N(4)	148.29(14)
N(1)-C(1)	1.327(7)	N(1)-Mn(1)-N(2)	72.04(15)
N(1)-C(12)	1.364(7)	N(4)-Mn(1)-N(2)	87.32(15)
N(2)-C(10)	1.328(6)	N(1)-Mn(1)-N(3)	83.85(14)
N(2)-C(11)	1.351(6)	N(4)-Mn(1)-N(3)	70.68(13)
C(1)-C(2)	1.440(10)	N(2)-Mn(1)-N(3)	86.20(14)
C(2)-C(3)	1.357(11)	N(1)-Mn(1)-S(2)	97.73(12)
C(3)-C(4)	1.373(10)	N(4)-Mn(1)-S(2)	101.65(11)
C(4)-C(12)	1.423(7)	N(2)-Mn(1)-S(2)	169.75(10)
C(4)-C(5)	1.439(10)	N(3)-Mn(1)-S(2)	92.06(10)
C(5)-C(6)	1.324(10)	N(1)-Mn(1)-S(1)	107.38(11)
C(6)-C(7)	1.435(8)	N(4)-Mn(1)-S(1)	97.06(10)
C(7)-C(8)	1.396(9)	N(2)-Mn(1)-S(1)	92.44(11)
C(7)-C(11)	1.421(8)	N(3)-Mn(1)-S(1)	167.70(10)
C(8)-C(9)	1.346(9)	S(2)-Mn(1)-S(1)	91.37(4)
C(9)-C(10)	1.397(8)	N(1)-Mn(1)-Sn(1)	106.96(11)
C(11)-C(12)	1.417(7)	N(4)-Mn(1)-Sn(1)	104.57(9)
N(3)-C(13)	1.323(6)	N(2)-Mn(1)-Sn(1)	136.80(11)
N(3)-C(24)	1.373(6)	N(3)-Mn(1)-Sn(1)	137.00(10)
N(4)-C(22)	1.327(6)	S(2)-Mn(1)-Sn(1)	45.90(3)
N(4)-C(23)	1.335(6)	S(1)-Mn(1)-Sn(1)	45.49(3)
C(13)-C(14)	1.386(8)	Sn(1)-S(1)-Mn(1)	83.04(4)
C(14)-C(15)	1.352(8)	Sn(1)-S(2)-Mn(1)	83.24(4)
C(15)-C(16)	1.424(7)	Sn(1)#1-S(3)-Sn(1)	87.43(4)
C(16)-C(24)	1.389(7)	C(1)-N(1)-C(12)	119.1(5)
C(16)-C(17)	1.418(8)	C(1)-N(1)-Mn(1)	125.6(4)
C(17)-C(18)	1.355(9)	C(12)-N(1)-Mn(1)	115.3(3)
C(18)-C(19)	1.412(8)	C(10)-N(2)-C(11)	118.4(4)
C(19)-C(20)	1.404(8)	C(10)-N(2)-Mn(1)	125.9(3)
C(19)-C(23)	1.422(7)	C(11)-N(2)-Mn(1)	115.7(3)
C(20)-C(21)	1.346(9)	N(1)-C(1)-C(2)	121.0(7)
C(21)-C(22)	1.402(8)	C(3)-C(2)-C(1)	119.3(6)
C(23)-C(24)	1.440(6)	C(2)-C(3)-C(4)	120.7(6)

C(3)-C(4)-C(12)	117.8(7)	C(23)-N(4)-Mn(1)	118.2(3)
C(3)-C(4)-C(5)	123.9(6)	N(3)-C(13)-C(14)	124.0(5)
C(12)-C(4)-C(5)	118.3(6)	C(15)-C(14)-C(13)	120.2(5)
C(6)-C(5)-C(4)	122.2(6)	C(14)-C(15)-C(16)	118.4(5)
C(5)-C(6)-C(7)	121.2(7)	C(24)-C(16)-C(17)	120.0(5)
C(8)-C(7)-C(11)	117.6(5)	C(24)-C(16)-C(15)	117.7(5)
C(8)-C(7)-C(6)	124.0(6)	C(17)-C(16)-C(15)	122.3(5)
C(11)-C(7)-C(6)	118.3(6)	C(18)-C(17)-C(16)	120.6(6)
C(9)-C(8)-C(7)	120.3(6)	C(17)-C(18)-C(19)	121.2(5)
C(8)-C(9)-C(10)	118.9(6)	C(20)-C(19)-C(18)	123.9(5)
N(2)-C(10)-C(9)	123.2(5)	C(20)-C(19)-C(23)	116.1(5)
N(2)-C(11)-C(12)	117.8(4)	C(18)-C(19)-C(23)	119.9(5)
N(2)-C(11)-C(7)	121.5(5)	C(21)-C(20)-C(19)	120.0(5)
C(12)-C(11)-C(7)	120.6(5)	C(20)-C(21)-C(22)	120.4(5)
N(1)-C(12)-C(11)	118.6(4)	N(4)-C(22)-C(21)	121.1(5)
N(1)-C(12)-C(4)	122.1(5)	N(4)-C(23)-C(19)	122.8(4)
C(11)-C(12)-C(4)	119.2(5)	N(4)-C(23)-C(24)	119.2(4)
C(13)-N(3)-C(24)	116.5(4)	C(19)-C(23)-C(24)	117.9(5)
C(13)-N(3)-Mn(1)	128.0(3)	N(3)-C(24)-C(16)	123.2(4)
C(24)-N(3)-Mn(1)	115.4(3)	N(3)-C(24)-C(23)	116.4(4)
C(22)-N(4)-C(23)	119.5(4)	C(16)-C(24)-C(23)	120.3(4)
C(22)-N(4)-Mn(1)	122.4(3)		

Symmetry transformations used to generate equivalent atoms:

#1 -x+1,-y+1,-z

Table 4. Anisotropic displacement parameters ($Å^2 \cdot 10^3$). The anisotropic displacement factor exponent takes the form: $-2\pi^2[h^2 a^{*2} U_{11} + ... + 2 h k a^* b^* U_{12}]$

	U_{11}	U_{22}	U_{33}	U_{23}	U_{13}	U_{12}
Sn(1)	42(1)	43(1)	41(1)	0(1)	-8(1)	0(1)
Mn(1)	47(1)	41(1)	47(1)	2(1)	-9(1)	-1(1)
S(1)	45(1)	48(1)	50(1)	5(1)	-4(1)	-2(1)
S(2)	50(1)	64(1)	48(1)	14(1)	-3(1)	-4(1)
S(3)	58(1)	46(1)	53(1)	-13(1)	-17(1)	7(1)
N(1)	73(3)	43(2)	50(3)	0(2)	-8(2)	-13(2)
N(2)	48(2)	49(2)	59(3)	6(2)	-4(2)	0(2)
C(1)	103(5)	64(3)	61(4)	-1(3)	-13(3)	-33(3)
C(2)	140(7)	65(4)	58(4)	6(3)	-9(4)	-48(4)
C(3)	151(7)	50(3)	53(4)	0(3)	1(4)	-12(4)
C(4)	121(5)	48(3)	48(3)	3(2)	8(3)	3(3)
C(5)	123(6)	65(3)	65(4)	2(3)	16(4)	39(4)
C(6)	96(5)	84(4)	84(5)	4(4)	11(4)	37(4)
C(7)	75(4)	76(3)	57(3)	11(3)	5(3)	23(3)
C(8)	53(3)	102(5)	83(5)	16(4)	1(3)	8(3)
C(9)	54(3)	95(4)	90(5)	13(4)	-1(3)	-10(3)
C(10)	52(3)	59(3)	79(4)	5(3)	-5(3)	-11(2)
C(11)	58(3)	55(3)	45(3)	9(2)	2(2)	10(2)
C(12)	78(3)	42(2)	41(3)	2(2)	2(2)	7(2)
N(3)	53(2)	46(2)	52(2)	5(2)	-8(2)	-1(2)
N(4)	64(2)	42(2)	44(2)	1(2)	-6(2)	3(2)
C(13)	72(3)	49(2)	55(3)	8(2)	-6(3)	-5(2)
C(14)	87(4)	54(3)	69(4)	15(3)	3(3)	-2(3)
C(15)	106(5)	64(3)	52(3)	14(3)	-5(3)	7(3)
C(16)	87(4)	61(3)	53(3)	4(2)	-5(3)	8(3)
C(17)	147(7)	76(4)	41(3)	1(3)	-19(4)	7(4)
C(18)	147(7)	75(4)	45(3)	-14(3)	-22(4)	13(4)
C(19)	101(4)	50(3)	50(3)	-5(2)	-14(3)	6(3)
C(20)	139(6)	54(3)	65(4)	-17(3)	-19(4)	0(3)
C(21)	149(7)	43(3)	74(4)	2(3)	-13(4)	-6(3)
C(22)	111(5)	40(2)	62(4)	5(2)	-5(3)	-1(3)
C(23)	62(3)	47(2)	45(3)	-5(2)	-7(2)	6(2)
C(24)	58(3)	49(2)	44(3)	3(2)	-3(2)	4(2)

Table 5. Hydrogen coordinates ($\cdot 10^4$) and isotropic displacement parameters ($Å^2 \cdot 10^3$)

	x	y	z	U(eq)
H(1)	1962	5317	719	92
H(2)	2382	3082	434	106
H(3)	4385	2369	381	102
H(5)	6662	2848	507	101
H(6)	8179	4323	677	105
H(8)	8837	6763	862	95
H(9)	8281	8944	1031	96
H(10)	6213	9481	1105	76
H(13)	3251	5237	1852	71
H(14)	3592	4467	2712	84
H(15)	4271	5914	3377	89
H(17)	4819	8320	3640	106
H(18)	5051	10525	3407	108
H(20)	4992	12339	2683	104
H(21)	4507	12918	1817	107
H(22)	3941	11271	1192	85

5.3.2 Messprotokoll der Verbindung {[Mn(phen)$_2$]$_2$[Sn$_2$S$_6$]}

Table 1. Crystal data and structure refinement for {[Mn($C_{12}H_8N_2$)$_2$]$_2$[Sn$_2$S$_6$]} ($C_{12}H_8N_2$; phen = 1,10-Phenanthrolin)

Identification code	jh333	
Empirical formula	{[Mn($C_{12}H_8N_2$)$_2$]$_2$[Sn$_2$S$_6$]}	
Crystal color, - habitus	red blocks	
Formula weight	630.22 g/mol	
Temperature	293(2) K	
Wavelength	0.71073 Å	
Crystal system	monoclinic	
Space group	*C*2/*c*	
Unit cell dimensions	a = 25.6736(7) Å	α= 90°.
	b = 11.1006(4) Å	β= 98.164(2)°.
	c = 18.0647(5) Å	γ = 90°.
Volume	5096.1(3) Å^3	
Z	8	
Density (calculated)	1.643 Mg/m^3	
Absorption coefficient	1.741 mm^{-1}	
F(000)	2488	
Crystal size	0.14 x 0.10 x 0.08 mm^3	
Theta range for data collection	2.00 to 27.00°.	
Index ranges	-32<=h<=32, -14<=k<=14, -17<=l<=23	
Reflections collected	22159	
Independent reflections	5496 [R(int) = 0.0241]	
Completeness to theta = 27.00°	98.8 %	
Refinement method	Full-matrix least-squares on F^2	
Data / restraints / parameters	5496 / 0 / 298	
Goodness-of-fit on F^2	1.095	
Final R indices [I>2sigma(I)]	R1 = 0.0264, wR2 = 0.0574	
R indices (all data)	R1 = 0.0322, wR2 = 0.0593	
Largest diff. peak and hole	0.301 and -0.326 e.Å^{-3}	

Comments:

All non-hydrogen atoms were refined anisotropic. The C-H H atoms were positioned with idealized geometry and refined isotropic with $U_{iso}(H) = 1.2 \cdot U_{eq}(C)$ using a riding model. A numerical absorption correction was performed ($T_{min/max}$: 0.6934/0.8184). After structure

refinement there were two very small residual electron density maxima of 0.61 and 0.33 e/Å^3, which are located in small cavities of the structure indicating for a very small amount of disordered solvent. Therefore, the data were corrected for disordered solvent using the SQUEEZE option in Platon. The void volume was calculated to 585.9 Å^3 and the total electron count per cell amount to 12.

Table 2. Atomic coordinates ($\cdot 10^4$) and equivalent isotropic displacement parameters (Å$^2 \cdot 10^3$). U(eq) is defined as one third of the trace of the orthogonalized U_{ij} tensor.

	x	y	z	U(eq)
Sn(1)	5383(1)	8860(1)	5364(1)	37(1)
S(1)	6144(1)	8982(1)	6258(1)	49(1)
S(2)	5313(1)	6791(1)	5137(1)	43(1)
S(3)	4620(1)	9876(1)	5743(1)	49(1)
Mn(1)	6145(1)	6711(1)	6093(1)	41(1)
N(1)	6076(1)	4639(2)	6140(1)	48(1)
N(2)	5857(1)	6225(2)	7192(1)	49(1)
C(1)	6148(1)	3871(3)	5606(2)	65(1)
C(2)	6072(2)	2626(3)	5664(2)	80(1)
C(3)	5922(2)	2182(3)	6301(3)	80(1)
C(4)	5839(1)	2958(2)	6883(2)	62(1)
C(5)	5673(1)	2564(3)	7567(2)	79(1)
C(6)	5574(1)	3334(4)	8089(2)	76(1)
C(7)	5631(1)	4605(3)	7991(2)	59(1)
C(8)	5512(1)	5459(4)	8509(2)	73(1)
C(9)	5565(1)	6639(4)	8364(2)	75(1)
C(10)	5738(1)	6998(3)	7700(2)	62(1)
C(11)	5805(1)	5035(2)	7331(2)	48(1)
C(12)	5915(1)	4199(2)	6770(2)	48(1)
N(21)	6995(1)	6461(2)	6773(1)	57(1)
N(22)	6738(1)	6427(2)	5270(1)	47(1)
C(21)	7132(1)	6553(4)	7505(2)	78(1)
C(22)	7636(2)	6268(4)	7866(2)	97(1)
C(23)	8003(2)	5861(4)	7459(3)	94(1)
C(24)	7885(1)	5777(3)	6680(2)	70(1)
C(25)	8254(1)	5426(4)	6200(3)	87(1)
C(26)	8131(1)	5451(3)	5457(3)	83(1)
C(27)	7617(1)	5803(3)	5104(2)	61(1)
C(28)	7476(1)	5889(3)	4333(2)	71(1)
C(29)	6979(1)	6219(3)	4046(2)	69(1)
C(30)	6621(1)	6483(3)	4535(2)	57(1)
C(31)	7233(1)	6099(2)	5559(2)	50(1)
C(32)	7369(1)	6104(2)	6358(2)	53(1)

Table 3. Bond lengths [Å] and angles [°].

Sn(1)-S(2)	2.3350(6)	Sn(1)-S(3)	2.4415(6)
Sn(1)-S(1)	2.3561(6)	Sn(1)-S(3A)	2.4422(6)
Sn(1)-Mn(1)	3.2437(4)	S(2)-Mn(1)	2.5515(7)
S(1)-Mn(1)	2.5387(7)	S(3)-Sn(1A)	2.4422(6)
Mn(1)-N(2)	2.279(2)	Mn(1)-N(1)	2.310(2)
Mn(1)-N(22)	2.295(2)	Mn(1)-N(21)	2.364(2)
S(2)-Sn(1)-S(1)	102.29(2)	S(3)-Sn(1)-S(3A)	93.15(2)
S(2)-Sn(1)-S(3)	117.32(2)	S(2)-Sn(1)-Mn(1)	51.336(16)
S(1)-Sn(1)-S(3)	113.73(2)	S(1)-Sn(1)-Mn(1)	50.958(16)
S(2)-Sn(1)-S(3A)	115.45(2)	S(3)-Sn(1)-Mn(1)	133.495(17)
S(1)-Sn(1)-S(3A)	115.67(2)	S(3A)-Sn(1)-Mn(1)	133.312(16)
Sn(1)-S(1)-Mn(1)	82.92(2)	Sn(1)-S(3)-Sn(1A)	86.85(2)
Sn(1)-S(2)-Mn(1)	83.06(2)	N(2)-Mn(1)-S(2)	104.70(6)
N(2)-Mn(1)-N(22)	149.18(8)	N(22)-Mn(1)-S(2)	97.71(6)
N(2)-Mn(1)-N(1)	72.33(8)	N(1)-Mn(1)-S(2)	89.90(5)
N(22)-Mn(1)-N(1)	87.01(8)	N(21)-Mn(1)-S(2)	168.11(7)
N(2)-Mn(1)-N(21)	84.84(8)	S(1)-Mn(1)-S(2)	91.73(2)
N(22)-Mn(1)-N(21)	70.88(8)	N(2)-Mn(1)-Sn(1)	106.00(5)
N(1)-Mn(1)-N(21)	86.23(8)	N(22)-Mn(1)-Sn(1)	104.79(5)
N(2)-Mn(1)-S(1)	97.30(6)	N(1)-Mn(1)-Sn(1)	134.60(5)
N(22)-Mn(1)-S(1)	102.96(6)	N(21)-Mn(1)-Sn(1)	139.17(6)
N(1)-Mn(1)-S(1)	169.57(6)	S(1)-Mn(1)-Sn(1)	46.122(15)
N(21)-Mn(1)-S(1)	94.11(6)	S(2)-Mn(1)-Sn(1)	45.607(14)
N(1)-C(1)	1.320(4)	N(21)-C(21)	1.322(4)
N(1)-C(12)	1.357(4)	N(21)-C(32)	1.357(4)
N(2)-C(10)	1.323(3)	N(22)-C(30)	1.320(4)
N(2)-C(11)	1.356(3)	N(22)-C(31)	1.354(3)
C(1)-C(2)	1.401(4)	C(21)-C(22)	1.399(5)
C(2)-C(3)	1.357(6)	C(22)-C(23)	1.354(7)
C(3)-C(4)	1.398(5)	C(23)-C(24)	1.400(6)
C(4)-C(12)	1.410(3)	C(24)-C(32)	1.416(4)
C(4)-C(5)	1.431(5)	C(24)-C(25)	1.425(5)
C(5)-C(6)	1.324(6)	C(25)-C(26)	1.335(6)
C(6)-C(7)	1.433(5)	C(26)-C(27)	1.436(5)
C(7)-C(8)	1.396(5)	C(27)-C(28)	1.391(5)
C(7)-C(11)	1.413(4)	C(27)-C(31)	1.411(4)
C(8)-C(9)	1.347(5)	C(28)-C(29)	1.357(5)
C(9)-C(10)	1.394(5)	C(29)-C(30)	1.393(4)
C(11)-C(12)	1.431(4)	C(31)-C(32)	1.435(4)
C(1)-N(1)-C(12)	118.1(2)	C(21)-N(21)-C(32)	117.8(3)
C(10)-N(2)-C(11)	117.7(3)	C(30)-N(22)-C(31)	117.8(2)
N(1)-C(1)-C(2)	123.2(3)	N(21)-C(21)-C(22)	123.1(4)
C(3)-C(2)-C(1)	118.7(3)	C(23)-C(22)-C(21)	119.4(4)
C(2)-C(3)-C(4)	120.4(3)	C(22)-C(23)-C(24)	120.0(3)

C(3)-C(4)-C(12)	117.0(3)	C(23)-C(24)-C(32)	116.9(3)
C(3)-C(4)-C(5)	123.8(3)	C(23)-C(24)-C(25)	124.1(3)
C(12)-C(4)-C(5)	119.1(3)	C(32)-C(24)-C(25)	119.0(3)
C(6)-C(5)-C(4)	121.9(3)	C(26)-C(25)-C(24)	121.6(3)
C(5)-C(6)-C(7)	120.9(3)	C(25)-C(26)-C(27)	121.5(3)
C(8)-C(7)-C(11)	117.5(3)	C(28)-C(27)-C(31)	117.5(3)
C(8)-C(7)-C(6)	123.3(3)	C(28)-C(27)-C(26)	123.8(3)
C(11)-C(7)-C(6)	119.2(3)	C(31)-C(27)-C(26)	118.6(3)
C(9)-C(8)-C(7)	119.5(3)	C(29)-C(28)-C(27)	119.9(3)
C(8)-C(9)-C(10)	119.9(3)	C(28)-C(29)-C(30)	118.9(3)
N(2)-C(10)-C(9)	123.0(3)	N(22)-C(30)-C(29)	123.5(3)
N(2)-C(11)-C(7)	122.5(3)	N(22)-C(31)-C(27)	122.3(3)
N(2)-C(11)-C(12)	117.8(2)	N(22)-C(31)-C(32)	117.9(2)
C(7)-C(11)-C(12)	119.7(3)	C(27)-C(31)-C(32)	119.8(2)
N(1)-C(12)-C(4)	122.5(3)	N(21)-C(32)-C(24)	122.7(3)
N(1)-C(12)-C(11)	118.3(2)	N(21)-C(32)-C(31)	117.8(2)
C(4)-C(12)-C(11)	119.1(3)	C(24)-C(32)-C(31)	119.4(3)

Symmetry transformations used to generate equivalent atoms: A: -x+1,-y+2,-z+1

Table 4. Anisotropic displacement parameters ($Å^2 \cdot 10^3$). The anisotropic displacement factor exponent takes the form: $-2\pi^2[h^2 a^{*2} U_{11} + ... + 2 h k a^* b^* U_{12}]$

	U_{11}	U_{22}	U_{33}	U_{23}	U_{13}	U_{12}
Sn(1)	32(1)	33(1)	46(1)	1(1)	2(1)	5(1)
S(1)	44(1)	37(1)	62(1)	-5(1)	-11(1)	2(1)
S(2)	40(1)	36(1)	52(1)	-5(1)	-1(1)	2(1)
S(3)	45(1)	50(1)	54(1)	10(1)	16(1)	14(1)
Mn(1)	39(1)	38(1)	45(1)	1(1)	2(1)	7(1)
N(1)	52(1)	37(1)	53(1)	-4(1)	-2(1)	7(1)
N(2)	48(1)	49(1)	48(1)	0(1)	5(1)	6(1)
C(1)	72(2)	53(2)	67(2)	-13(1)	-2(2)	11(1)
C(2)	84(2)	49(2)	96(3)	-26(2)	-21(2)	13(2)
C(3)	80(2)	40(1)	108(3)	3(2)	-28(2)	-1(1)
C(4)	54(2)	42(1)	82(2)	10(1)	-21(1)	-3(1)
C(5)	65(2)	63(2)	99(3)	36(2)	-20(2)	-18(2)
C(6)	58(2)	89(2)	75(2)	37(2)	-12(2)	-17(2)
C(7)	38(1)	80(2)	56(2)	18(1)	-6(1)	-4(1)
C(8)	53(2)	113(3)	54(2)	16(2)	8(1)	5(2)
C(9)	68(2)	104(3)	56(2)	-6(2)	17(2)	19(2)
C(10)	65(2)	64(2)	59(2)	-6(1)	13(1)	13(1)
C(11)	35(1)	54(1)	50(1)	9(1)	-5(1)	1(1)
C(12)	40(1)	42(1)	59(2)	8(1)	-10(1)	1(1)
N(21)	47(1)	63(1)	56(1)	9(1)	-4(1)	2(1)
N(22)	38(1)	49(1)	53(1)	0(1)	3(1)	4(1)
C(21)	64(2)	109(3)	56(2)	13(2)	-7(2)	-7(2)

C(22)	74(2)	141(4)	68(2)	35(2)	-22(2)	-19(2)
C(23)	52(2)	116(3)	104(3)	52(3)	-23(2)	-7(2)
C(24)	41(2)	68(2)	96(2)	28(2)	-10(2)	3(1)
C(25)	36(2)	93(3)	130(4)	27(2)	5(2)	17(2)
C(26)	42(2)	78(2)	133(4)	7(2)	24(2)	12(2)
C(27)	43(1)	51(1)	93(2)	-1(1)	18(1)	2(1)
C(28)	62(2)	70(2)	87(2)	-18(2)	32(2)	-8(2)
C(29)	68(2)	79(2)	63(2)	-11(2)	19(2)	-13(2)
C(30)	48(2)	65(2)	56(2)	-4(1)	5(1)	-1(1)
C(31)	36(1)	41(1)	72(2)	4(1)	7(1)	4(1)
C(32)	36(1)	48(1)	73(2)	16(1)	-3(1)	3(1)

Table 5. Hydrogen coordinates ($\cdot 10^4$) and isotropic displacement parameters ($Å^2 \cdot 10^3$).

	x	y	z	U(eq)
H(1)	6254	4170	5170	78
H(2)	6124	2114	5273	96
H(3)	5873	1358	6350	96
H(5)	5633	1743	7646	94
H(6)	5465	3046	8525	91
H(8)	5397	5214	8950	88
H(9)	5486	7214	8705	90
H(10)	5771	7817	7611	75
H(21)	6882	6821	7792	93
H(22)	7717	6356	8382	117
H(23)	8334	5638	7696	113
H(25)	8587	5174	6410	104
H(26)	8385	5234	5161	100
H(28)	7721	5720	4015	85
H(29)	6879	6269	3531	83
H(30)	6282	6710	4333	68

5.3.3 Messprotokoll der Verbindung $\{[Mn(phen)_2]_2[Sn_2S_6]\}\cdot phen$

Table 1. Crystal data and structure refinement for $\{[Mn(C_{12}H_8N_2)_2]_2[Sn_2S_6]\}\cdot C_{12}H_8N_2$. ($C_{12}H_8N_2$; phen = 1,10-Phenanthrolin)

Identification code	jh607b	
Empirical formula	$\{[Mn(C_{12}H_8N_2)_2]_2[Sn_2S_6]\}\cdot C_{12}H_8N_2$.	
Crystal color, habitus	red, blocks	
Formula weight	1440.64	
Temperature	200(2) K	
Wavelength	0.71073 Å	
Crystal system	triclinic	
Space group	$P\bar{1}$	
Unit cell dimensions	a = 10.0642(9) Å	α = 71.700(7)°.
	b = 10.6249(9) Å	β = 81.458(7)°.
	c = 13.6927(12) Å	γ = 84.346(7)°.
Volume	1372.6(2) $Å^3$	
Z	1	
Density (calculated)	1.743 Mg/m^3	
Absorption coefficient	1.629 mm^{-1}	
F(000)	716	
Crystal size	0.07 x 0.10 x 0.12 mm^3	
Theta range for data collection	1.58 to 22.78°.	
Index ranges	$-10 \le h \le 10$, $-11 \le k \le 11$, $-14 \le l \le 14$	
Reflections collected	11651	
Independent reflections	11661 [R(int) = 5.87 (calculated after removal of the overlapping reflections]	
Completeness to theta = 22.78°	95.7 %	
Refinement method	Full-matrix least-squares on F^2	
Data / restraints / parameters	11661 / 42 / 355	
Goodness-of-fit on F^2	1.027	
Final R indices [I>2sigma(I)]	R1 = 0.0634, wR2 = 0.1115	
R indices (all data)	R1 = 0.1046, wR2 = 0.1242	
Largest diff. peak and hole	0.971 and -0.876 $e.Å^{-3}$	

Comments:
All non-hydrogen atoms of the $[Mn(1,10\text{-phenanthroline})_2]_2[Sn_2S_6]$-unit were refined anisotropic, whereas the C and N atoms of the disordered uncoordinated phenanthroline molecule were refined only isotropic. The C-H H atoms were positioned with idealized geometry and refined isotropic with $U_{iso}(H) = 1.2\ U_{eq}(C)$ using a riding model. A numerical absorption correction was performed ($T_{min/max}$: 0.7221, 0.8224).
All crystals investigated where non-merohedral twinned. This twinning unfortunately leads to reflections along the c-axis, which cannot be resolved. In the beginning a data set up to 2-Theta = 56° was measured for which both individuals can be separately be indexed. In this case refinement using the HKLF 5 option leads to very poor reliability factors. Therefore, a second data set up to 2-Theta = 45° was measured and in this case the reflections along the c-axis can be resolved and refinement using the HKLF-5 option leads to reasonable reliability factors. Unfortunately, using this procedure the equivalent reflections cannot be merged and therefore, the number of independent reflections is artificially too large. If the overlapping reflections are omitted the completeness is less than 60% which is inacceptable. The structure can easily be solved in space group P1 and P-1. In space group P1 the displacement factors of several atoms are non-positive defined and the Flack-x-parameter is always about 0.5. Large correlations of the parameters are observed indicating the absence of a centre of symmetry. Even if the uncoordinated phenanthroline ligand seems to be ordered in P1, Platon immediately suggest space group P-1 in which this ligand is disordered around a centre of inversion. However, in this case reasonable displacement parameters are observed except for some C atoms of one coordinating phenanthroline ligand, which are too large. Therefore space group P-1 was selected for the final refinements.

Table 2. Atomic coordinates ($\cdot 10^4$) and equivalent isotropic displacement parameters ($Å^2 \cdot 10^3$). U(eq) is defined as one third of the trace of the orthogonalized U_{ij} tensor.

	x	y	z	U(eq)
Sn(1)	5722(1)	9167(1)	9182(1)	26(1)
Mn(1)	7375(1)	7534(1)	7703(1)	31(1)
S(1)	5555(2)	6947(2)	9298(2)	34(1)
S(2)	7219(2)	9973(2)	7659(2)	34(1)
S(3)	3607(2)	10491(2)	9275(1)	36(1)
N(1)	5924(5)	7711(6)	6511(4)	36(1)
N(2)	8608(5)	7914(6)	6024(4)	32(2)
C(1)	4604(7)	7585(11)	6739(6)	66(3)
C(2)	3734(8)	7900(17)	6011(7)	137(7)
C(3)	4217(10)	8360(20)	4989(8)	168(10)
C(4)	5615(9)	8443(14)	4707(7)	93(4)
C(5)	6200(9)	8851(16)	3656(7)	116(6)
C(6)	7515(9)	8983(11)	3401(7)	74(3)
C(7)	8399(7)	8647(7)	4184(5)	37(2)
C(8)	9802(7)	8743(7)	3952(5)	39(2)
C(9)	10556(7)	8459(9)	4725(5)	55(2)
C(10)	9920(7)	8061(9)	5742(6)	55(2)
C(11)	7856(6)	8232(6)	5231(5)	28(2)
C(12)	6430(6)	8120(9)	5489(5)	44(2)
N(21)	9474(5)	7059(6)	8260(4)	34(1)
N(22)	7839(6)	5332(6)	8056(4)	38(2)
C(21)	10261(7)	7942(9)	8377(6)	49(2)
C(22)	11525(8)	7564(11)	8715(6)	58(2)
C(23)	11977(8)	6239(11)	8955(6)	61(3)
C(24)	11173(8)	5241(9)	8857(5)	43(2)
C(25)	11530(8)	3921(11)	9127(6)	62(3)
C(26)	10697(9)	3040(10)	9042(7)	58(2)
C(27)	9422(8)	3463(8)	8691(6)	48(2)
C(28)	8478(10)	2613(9)	8626(7)	60(2)
C(29)	7280(10)	3080(9)	8311(7)	62(2)
C(30)	6977(8)	4418(9)	8053(6)	51(2)
C(31)	9047(7)	4831(8)	8389(5)	40(2)
C(32)	9916(7)	5744(9)	8495(5)	41(2)
N(41)	5164(13)	5637(15)	3513(9)	61(4)
N(42)	2555(10)	5464(13)	4277(9)	47(3)
C(41)	6476(16)	5760(20)	3155(14)	70(6)
C(42)	7480(20)	5240(20)	3732(14)	91(7)
C(43)	7212(16)	4590(20)	4747(13)	79(6)
C(44)	5845(14)	4431(19)	5200(11)	65(5)
C(45)	5465(18)	3690(20)	6234(13)	87(7)
C(46)	4189(17)	3660(20)	6626(15)	83(7)
C(47)	3115(14)	4250(20)	6014(11)	69(5)
C(48)	1717(17)	4280(30)	6362(15)	102(8)
C(49)	815(17)	4799(19)	5728(12)	75(6)
C(50)	1247(15)	5369(19)	4663(12)	70(5)
C(51)	3450(12)	4888(15)	4931(9)	40(4)
C(52)	4865(12)	4982(16)	4546(10)	49(4)

Table 3. Bond lengths [Å] and angles [°].

Sn(1)-S(1)	2.335(2)	Sn(1)-S(3A)	2.4512(18)
Sn(1)-S(2)	2.356(2)	Sn(1)-Mn(1)	3.2431(15)
Sn(1)-S(3)	2.4422(18)	S(3)-Sn(1A)	2.4512(18)
Mn(1)-N(22)	2.251(6)	Mn(1)-N(2)	2.378(6)
Mn(1)-N(1)	2.301(5)	Mn(1)-S(2)	2.562(2)
Mn(1)-N(21)	2.307(6)	Mn(1)-S(1)	2.588(2)
S(1)-Sn(1)-S(2)	103.60(7)	S(3)-Sn(1)-S(3A)	93.33(6)
S(1)-Sn(1)-S(3)	116.52(7)	S(1)-Sn(1)-Mn(1)	52.26(5)
S(2)-Sn(1)-S(3)	115.05(7)	S(2)-Sn(1)-Mn(1)	51.55(5)
S(1)-Sn(1)-S(3A)	114.57(7)	S(3)-Sn(1)-Mn(1)	138.55(5)
S(2)-Sn(1)-S(3A)	114.27(7)	S(3A)-Sn(1)-Mn(1)	128.10(5)
N(22)-Mn(1)-N(1)	96.2(2)	N(2)-Mn(1)-S(2)	95.05(15)
N(22)-Mn(1)-N(21)	72.1(2)	N(22)-Mn(1)-S(1)	86.29(16)
N(1)-Mn(1)-N(21)	151.98(19)	N(1)-Mn(1)-S(1)	95.13(14)
N(22)-Mn(1)-N(2)	90.7(2)	N(21)-Mn(1)-S(1)	109.00(14)
N(1)-Mn(1)-N(2)	70.39(19)	N(2)-Mn(1)-S(1)	164.83(14)
N(21)-Mn(1)-N(2)	84.08(19)	S(2)-Mn(1)-S(1)	91.41(7)
N(22)-Mn(1)-S(2)	165.60(16)	N(22)-Mn(1)-Sn(1)	129.01(15)
N(1)-Mn(1)-S(2)	98.19(16)	N(1)-Mn(1)-Sn(1)	102.65(14)
Sn(1)-S(1)-Mn(1)	82.23(7)	N(21)-Mn(1)-Sn(1)	104.40(14)
Sn(1)-S(2)-Mn(1)	82.39(7)	N(2)-Mn(1)-Sn(1)	140.23(15)
Sn(1)-S(3)-Sn(1A)	86.67(6)	S(2)-Mn(1)-Sn(1)	46.06(5)
N(21)-Mn(1)-S(2)	95.30(16)	S(1)-Mn(1)-Sn(1)	45.52(5)
C(1)-N(1)-Mn(1)	124.7(5)	C(21)-N(21)-Mn(1)	125.8(5)
C(12)-N(1)-Mn(1)	117.4(4)	C(32)-N(21)-Mn(1)	115.1(4)
C(10)-N(2)-Mn(1)	128.7(5)	C(31)-N(22)-Mn(1)	117.9(5)
C(11)-N(2)-Mn(1)	115.4(4)	C(30)-N(22)-Mn(1)	126.2(5)
N(1)-C(1)	1.329(9)	C(12)-C(4)-C(3)	118.1(8)
N(1)-C(12)	1.362(8)	C(12)-C(4)-C(5)	119.7(7)
N(2)-C(10)	1.330(9)	C(3)-C(4)-C(5)	122.1(8)
N(2)-C(11)	1.353(8)	C(6)-C(5)-C(4)	121.5(7)
C(1)-C(2)	1.365(11)	C(5)-C(6)-C(7)	120.7(8)
C(2)-C(3)	1.360(13)	C(11)-C(7)-C(8)	117.8(6)
C(3)-C(4)	1.407(13)	C(11)-C(7)-C(6)	119.3(6)
C(4)-C(12)	1.383(10)	C(8)-C(7)-C(6)	122.8(7)
C(4)-C(5)	1.418(11)	C(9)-C(8)-C(7)	119.4(6)
C(5)-C(6)	1.327(12)	C(8)-C(9)-C(10)	118.5(7)
C(6)-C(7)	1.431(10)	N(2)-C(10)-C(9)	125.8(7)
C(7)-C(11)	1.402(9)	N(2)-C(11)-C(7)	123.6(6)
C(7)-C(8)	1.407(9)	N(2)-C(11)-C(12)	117.4(6)
C(8)-C(9)	1.334(9)	C(7)-C(11)-C(12)	119.0(6)
C(9)-C(10)	1.395(10)	N(1)-C(12)-C(4)	122.2(6)
C(11)-C(12)	1.433(9)	N(1)-C(12)-C(11)	118.1(6)
C(1)-N(1)-C(12)	117.5(6)	C(4)-C(12)-C(11)	119.7(7)
C(10)-N(2)-C(11)	114.9(6)	N(41)-C(41)	1.343(16)
N(1)-C(1)-C(2)	123.6(7)	N(41)-C(52)	1.368(14)
C(3)-C(2)-C(1)	119.6(8)	N(42)-C(51)	1.333(13)
C(2)-C(3)-C(4)	118.8(9)	N(42)-C(50)	1.344(15)

C(41)-C(42)	1.345(17)	C(25)-C(24)-C(32)	121.5(8)
C(42)-C(43)	1.343(18)	C(25)-C(24)-C(23)	124.3(8)
C(43)-C(44)	1.425(18)	C(32)-C(24)-C(23)	114.2(8)
C(44)-C(52)	1.392(15)	C(26)-C(25)-C(24)	120.7(8)
C(41)-N(41)-C(52)	116.2(13)	C(25)-C(26)-C(27)	121.3(8)
C(51)-N(42)-C(50)	117.0(12)	C(28)-C(27)-C(31)	116.4(7)
N(41)-C(41)-C(42)	124.4(16)	C(28)-C(27)-C(26)	124.9(8)
C(43)-C(42)-C(41)	120.2(18)	C(31)-C(27)-C(26)	118.8(8)
C(42)-C(43)-C(44)	119.3(16)	C(29)-C(28)-C(27)	121.6(8)
C(52)-C(44)-C(45)	119.8(13)	C(28)-C(29)-C(30)	118.6(8)
C(52)-C(44)-C(43)	116.8(13)	N(22)-C(30)-C(29)	124.4(8)
C(45)-C(44)-C(43)	123.3(14)	N(22)-C(31)-C(27)	123.2(7)
C(46)-C(45)-C(44)	120.3(17)	N(22)-C(31)-C(32)	117.1(7)
C(45)-C(46)-C(47)	123.0(17)	C(27)-C(31)-C(32)	119.5(7)
C(48)-C(47)-C(51)	114.2(13)	N(21)-C(32)-C(24)	124.1(7)
N(21)-C(21)	1.346(9)	N(21)-C(32)-C(31)	117.7(6)
N(21)-C(32)	1.376(10)	C(24)-C(32)-C(31)	118.2(8)
N(22)-C(31)	1.362(9)	C(44)-C(45)	1.403(17)
N(22)-C(30)	1.366(10)	C(45)-C(46)	1.316(18)
C(21)-C(22)	1.397(11)	C(46)-C(47)	1.437(17)
C(22)-C(23)	1.388(13)	C(47)-C(48)	1.418(17)
C(23)-C(24)	1.444(12)	C(47)-C(51)	1.428(15)
C(24)-C(25)	1.360(12)	C(48)-C(49)	1.310(17)
C(24)-C(32)	1.420(10)	C(49)-C(50)	1.411(16)
C(25)-C(26)	1.358(13)	C(51)-C(52)	1.444(15)
C(26)-C(27)	1.419(11)	C(48)-C(47)-C(46)	127.3(14)
C(27)-C(28)	1.404(12)	C(51)-C(47)-C(46)	118.4(13)
C(27)-C(31)	1.410(10)	C(49)-C(48)-C(47)	122.3(17)
C(28)-C(29)	1.337(12)	C(48)-C(49)-C(50)	119.1(16)
C(29)-C(30)	1.367(12)	N(42)-C(50)-C(49)	122.6(14)
C(31)-C(32)	1.422(10)	N(42)-C(51)-C(47)	124.5(11)
C(21)-N(21)-C(32)	119.1(6)	N(42)-C(51)-C(52)	118.5(11)
C(31)-N(22)-C(30)	115.7(7)	C(47)-C(51)-C(52)	116.8(11)
N(21)-C(21)-C(22)	121.9(8)	N(41)-C(52)-C(44)	123.0(12)
C(23)-C(22)-C(21)	119.3(9)	N(41)-C(52)-C(51)	115.9(11)
C(22)-C(23)-C(24)	121.5(8)	C(44)-C(52)-C(51)	121.1(11)

Symmetry transformations used to generate equivalent atoms:
A : #1 -x+1,-y+2,-z+2

Table 4. Anisotropic displacement parameters ($Å^2 \cdot 10^3$). The anisotropic displacement factor exponent takes the form: $-2\pi^2[h^2 a^{*2} U_{11} + ... + 2 h k a^* b^* U_{12}]$

	U_{11}	U_{22}	U_{33}	U_{23}	U_{13}	U_{12}
Sn(1)	25(1)	30(1)	26(1)	-11(1)	-3(1)	0(1)
Mn(1)	26(1)	36(1)	31(1)	-13(1)	-5(1)	-1(1)
S(1)	32(1)	32(1)	37(1)	-12(1)	2(1)	-3(1)
S(2)	36(1)	28(1)	36(1)	-11(1)	3(1)	-6(1)
S(3)	29(1)	46(1)	35(1)	-17(1)	-10(1)	8(1)
N(1)	27(3)	44(4)	38(4)	-14(3)	-1(3)	1(3)
N(2)	27(3)	29(4)	40(4)	-13(3)	-2(3)	0(3)
C(1)	29(5)	118(9)	42(5)	-8(5)	-1(4)	-15(5)
C(2)	24(5)	330(20)	38(5)	-14(8)	-5(4)	-42(8)
C(3)	46(7)	400(30)	34(6)	-13(10)	-17(5)	-34(11)
C(4)	49(6)	182(13)	35(5)	-8(7)	-8(4)	-19(7)
C(5)	36(6)	256(18)	33(6)	3(7)	-21(4)	-30(8)
C(6)	49(6)	127(10)	34(5)	-7(6)	-3(4)	-5(6)
C(7)	38(4)	39(5)	31(4)	-7(3)	-3(3)	-4(3)
C(8)	34(4)	42(5)	40(4)	-16(4)	9(3)	-3(3)
C(9)	31(4)	89(7)	40(5)	-17(5)	3(4)	-8(4)
C(10)	37(5)	86(7)	42(5)	-20(5)	-4(4)	-8(5)
C(11)	36(4)	16(4)	33(4)	-8(3)	-11(3)	5(3)
C(12)	23(4)	74(6)	36(4)	-16(4)	-4(3)	-8(4)
N(21)	32(3)	39(4)	30(3)	-14(3)	6(2)	-7(3)
N(22)	31(3)	45(4)	34(3)	-7(3)	-3(3)	3(3)
C(21)	41(5)	65(6)	44(5)	-18(4)	-13(4)	-2(4)
C(22)	36(5)	94(8)	42(5)	-16(5)	-5(4)	-16(5)
C(23)	33(4)	114(9)	30(5)	-13(5)	-2(3)	-8(5)
C(24)	34(4)	69(7)	23(4)	-10(4)	1(3)	-2(4)
C(25)	44(5)	91(8)	33(4)	2(5)	-15(4)	28(5)
C(26)	59(6)	61(6)	48(5)	-18(5)	-9(5)	36(5)
C(27)	62(5)	25(5)	44(5)	1(4)	-8(4)	25(4)
C(28)	87(7)	41(5)	57(5)	-25(4)	-11(5)	10(5)
C(29)	72(6)	47(6)	77(6)	-28(5)	-26(5)	3(5)
C(30)	49(5)	52(6)	57(5)	-23(5)	-6(4)	-6(4)
C(31)	39(4)	57(6)	17(3)	-4(4)	-1(3)	3(4)
C(32)	24(4)	61(6)	33(4)	-3(4)	-3(3)	-9(4)

Table 5. Hydrogen coordinates ($\cdot 10^4$) and isotropic displacement parameters ($Å^2 \cdot 10^3$).

	x	y	z	U(eq)
H(1)	4246	7257	7448	80
H(2)	2797	7796	6217	165
H(3)	3620	8630	4475	201
H(5)	5638	9035	3123	139
H(6)	7874	9303	2692	89
H(8)	10208	9009	3252	47
H(9)	11504	8525	4586	65
H(10)	10473	7879	6281	66
H(21)	9947	8847	8227	58
H(22)	12070	8208	8779	69
H(23)	12834	5981	9189	73
H(25)	12371	3611	9377	75
H(26)	10974	2124	9220	70
H(28)	8694	1684	8811	72
H(29)	6652	2495	8266	74
H(30)	6108	4733	7859	61
H(41)	6709	6236	2446	84
H(42)	8392	5343	3421	109
H(43)	7922	4247	5159	94
H(45)	6131	3214	6654	105
H(46)	3967	3238	7347	100
H(48)	1423	3916	7081	123
H(49)	-116	4791	5981	90
H(50)	589	5698	4201	84

5.3.4 Messprotokoll der Verbindung $\{[Mn(phen)_2]_2[Sn_2S_6]\}\cdot phen\cdot H_2O$

Table 1. Crystal data and structure refinement for $\{[Mn(C_{12}H_8N_2)_2]_2[Sn_2S_6]\}\cdot C_{12}H_8N_2\cdot H_2O$. ($C_{12}H_8N_2$; phen = 1,10-Phenanthrolin)

Identification code	jh337	
Empirical formula	$\{[Mn(C_{12}H_8N_2)_2]_2[Sn_2S_6]\}\cdot C_{12}H_8N_2\cdot H_2O$	
Crystal color, habitus	red blocks	
Formula weight	1458.66	
Temperature	293(2) K	
Wavelength	0.71073 Å	
Crystal system	triclinic	
Space group	$P\bar{1}$	
Unit cell dimensions	a = 11.3203(7) Å	α= 113.200(4)°.
	b = 12.1436(7) Å	β= 90.908(5)°.
	c = 12.7586(7) Å	γ = 110.974(4)°.
Volume	1479.92(15) $Å^3$	
Z	1	
Density (calculated)	1.637 Mg/m^3	
Absorption coefficient	1.513 mm^{-1}	
F(000)	726	
Crystal size	0.06 x 0.1 x 0.15 mm^3	
Theta range for data collection	1.77 to 27.00°.	
Index ranges	-14<=h<=14, -15<=k<=15, -16<=l<=16	
Reflections collected	13856	
Independent reflections	6406 [R(int) = 0.0304]	
Completeness to theta = 27.00°	99.0 %	
Refinement method	Full-matrix least-squares on F^2	
Data / restraints / parameters	6406 / 0 / 379	
Goodness-of-fit on F^2	0.938	
Final R indices [I>2sigma(I)]	R1 = 0.0284, wR2 = 0.0696	
R indices (all data)	R1 = 0.0432, wR2 = 0.0731	
Largest diff. peak and hole	0.653 and -0.660 e.$Å^{-3}$	

Comments:
All non-hydrogen atoms were refined anisotropic. The C-H H atoms were positioned with idealized geometry and refined isotropic with $U_{iso}(H) = 1.2 \cdot U_{eq}(C)$ using a riding model. The water H atoms were not located but considered in the formula. A numerical absorption correction was performed ($T_{min/max}$: 0.5192/0.7856). One phenanthroline ligand is disordered around a centre of inversion, in which also one water molecule is involved. Both of them were refined with half occupancy. The disorder remain constant if the structure refinement is performed in space group P1, where all atoms are located in general positions.

Table 2. Atomic coordinates ($\cdot 10^4$) and equivalent isotropic displacement parameters ($Å^2 \cdot 10^3$). U(eq) is defined as one third of the trace of the orthogonalized U_{ij} tensor.

	x	y	z	U(eq)
Sn(1)	5763(1)	3986(1)	4562(1)	32(1)
S(1)	7900(1)	4403(1)	4335(1)	44(1)
S(2)	4844(1)	1724(1)	4018(1)	38(1)
S(3)	5386(1)	5251(1)	6451(1)	41(1)
Mn(1)	7136(1)	1951(1)	3642(1)	33(1)
N(1)	6893(2)	1349(2)	1698(2)	36(1)
N(2)	6365(2)	-328(2)	2694(2)	33(1)
C(1)	7145(3)	2168(3)	1207(3)	45(1)
C(2)	7054(4)	1769(3)	11(3)	54(1)
C(3)	6689(3)	485(3)	-695(3)	53(1)
C(4)	6416(3)	-422(3)	-217(2)	42(1)
C(5)	6011(4)	-1790(3)	-905(3)	54(1)
C(6)	5716(4)	-2625(3)	-414(3)	56(1)
C(7)	5801(3)	-2178(3)	814(3)	45(1)
C(8)	5474(4)	-3010(3)	1369(3)	58(1)
C(9)	5593(4)	-2496(3)	2553(3)	54(1)
C(10)	6046(3)	-1152(3)	3173(3)	42(1)
C(11)	6234(3)	-831(3)	1523(2)	33(1)
C(12)	6530(3)	62(3)	991(2)	34(1)
N(21)	7824(2)	1791(2)	5226(2)	42(1)
N(22)	9186(2)	1936(3)	3537(2)	45(1)
C(21)	7142(4)	1726(3)	6053(3)	54(1)
C(22)	7609(5)	1632(4)	7022(3)	71(1)
C(23)	8787(5)	1597(4)	7123(3)	77(1)
C(24)	9530(4)	1666(4)	6274(3)	62(1)
C(25)	10793(5)	1657(5)	6317(5)	90(2)
C(26)	11474(5)	1739(5)	5472(5)	85(1)
C(27)	10966(3)	1832(4)	4500(4)	62(1)
C(28)	11637(4)	1919(4)	3608(5)	80(1)
C(29)	11104(4)	2033(5)	2730(5)	79(1)
C(30)	9881(3)	2041(4)	2732(4)	62(1)

C(31)	9729(3)	1842(3)	4422(3)	45(1)
C(32)	9007(3)	1761(3)	5328(3)	46(1)
N(41)	1429(4)	4851(4)	502(3)	75(1)
C(44')	1429(4)	4851(4)	502(3)	75(1)
C(41)	1957(5)	4823(5)	1461(5)	92(1)
C(42)	1365(5)	4921(5)	2393(4)	84(1)
C(43)	226(5)	5071(4)	2380(3)	76(1)
C(44)	-344(4)	5092(3)	1426(3)	65(1)
N(41')	-344(4)	5092(3)	1426(3)	65(1)
C(45)	282(4)	4985(4)	504(3)	57(1)
C(46)	-1573(9)	5362(7)	1451(7)	68(2)
C(47)	-2093(8)	5393(8)	551(9)	76(2)
O(1)	-2945(7)	5198(8)	1425(9)	133(3)

Table 3. Bond lengths [Å] and angles [°].

Sn(1)-S(1)	2.3358(8)	Sn(1)-S(3)	2.4362(7)
Sn(1)-S(2)	2.3537(8)	Sn(1)-S(3A)	2.4437(7)
Sn(1)-Mn(1)	3.2285(5)	S(2)-Mn(1)	2.5818(8)
S(1)-Mn(1)	2.5407(9)	S(3)-Sn(1A)	2.4437(7)
S(1)-Sn(1)-S(2)	103.59(3)	S(3)-Sn(1)-S(3A)	93.24(2)
S(1)-Sn(1)-S(3)	117.25(3)	S(1)-Sn(1)-Mn(1)	51.33(2)
S(2)-Sn(1)-S(3)	112.90(3)	S(2)-Sn(1)-Mn(1)	52.284(19)
S(1)-Sn(1)-S(3A)	115.56(3)	S(3)-Sn(1)-Mn(1)	134.66(2)
S(2)-Sn(1)-S(3A)	114.80(3)	Mn(1)-N(22)	2.333(2)
Mn(1)-N(21)	2.257(2)	Mn(1)-N(2)	2.342(2)
Mn(1)-N(1)	2.274(2)	N(22)-Mn(1)-S(1)	94.83(7)
S(3A)-Sn(1)-Mn(1)	132.055(18)	N(2)-Mn(1)-S(1)	170.42(6)
Sn(1)-S(1)-Mn(1)	82.80(3)	N(21)-Mn(1)-S(2)	97.57(7)
Sn(1)-S(2)-Mn(1)	81.57(2)	N(1)-Mn(1)-S(2)	101.93(6)
Sn(1)-S(3)-Sn(1A)	86.76(2)	N(22)-Mn(1)-S(2)	168.45(7)
N(21)-Mn(1)-N(1)	150.53(9)	N(2)-Mn(1)-S(2)	88.68(6)
N(21)-Mn(1)-N(22)	71.88(9)	S(1)-Mn(1)-S(2)	92.00(3)
N(1)-Mn(1)-N(22)	86.22(9)	N(21)-Mn(1)-Sn(1)	105.59(6)
N(21)-Mn(1)-N(2)	86.99(8)	N(1)-Mn(1)-Sn(1)	103.85(6)
N(1)-Mn(1)-N(2)	71.72(8)	N(22)-Mn(1)-Sn(1)	140.12(7)
N(22)-Mn(1)-N(2)	86.14(8)	N(2)-Mn(1)-Sn(1)	133.74(5)
N(21)-Mn(1)-S(1)	102.39(7)	S(1)-Mn(1)-Sn(1)	45.873(18)
N(1)-Mn(1)-S(1)	98.81(6)	S(2)-Mn(1)-Sn(1)	46.151(17)
N(1)-C(1)	1.325(4)	N(21)-C(21)	1.327(4)
N(1)-C(12)	1.357(3)	N(21)-C(32)	1.358(4)
N(2)-C(10)	1.317(3)	N(22)-C(30)	1.322(4)
N(2)-C(11)	1.355(3)	N(22)-C(31)	1.340(4)
C(1)-C(2)	1.397(4)	C(21)-C(22)	1.398(5)
C(2)-C(3)	1.354(5)	C(22)-C(23)	1.355(6)
C(3)-C(4)	1.404(4)	C(23)-C(24)	1.392(6)

C(4)-C(12)	1.402(4)	C(24)-C(32)	1.398(4)
C(4)-C(5)	1.426(4)	C(24)-C(25)	1.435(6)
C(5)-C(6)	1.340(5)	C(25)-C(26)	1.350(7)
C(6)-C(7)	1.431(4)	C(26)-C(27)	1.420(6)
C(7)-C(8)	1.402(4)	C(27)-C(28)	1.395(6)
C(7)-C(11)	1.407(4)	C(27)-C(31)	1.408(4)
C(8)-C(9)	1.372(5)	C(28)-C(29)	1.341(7)
C(9)-C(10)	1.386(5)	C(29)-C(30)	1.389(5)
C(11)-C(12)	1.441(4)	C(31)-C(32)	1.441(4)
C(1)-N(1)-C(12)	117.7(2)	C(21)-N(21)-C(32)	118.7(3)
C(10)-N(2)-C(11)	117.7(2)	C(30)-N(22)-C(31)	116.7(3)
N(1)-C(1)-C(2)	123.2(3)	N(21)-C(21)-C(22)	121.9(4)
C(3)-C(2)-C(1)	119.2(3)	C(23)-C(22)-C(21)	119.4(4)
C(2)-C(3)-C(4)	119.7(3)	C(22)-C(23)-C(24)	120.2(3)
C(12)-C(4)-C(3)	117.3(3)	C(23)-C(24)-C(32)	117.5(4)
C(12)-C(4)-C(5)	119.7(3)	C(23)-C(24)-C(25)	124.1(4)
C(3)-C(4)-C(5)	123.0(3)	C(32)-C(24)-C(25)	118.4(4)
C(6)-C(5)-C(4)	120.9(3)	C(26)-C(25)-C(24)	121.5(4)
C(5)-C(6)-C(7)	121.3(3)	C(25)-C(26)-C(27)	121.3(4)
C(8)-C(7)-C(11)	117.0(3)	C(28)-C(27)-C(31)	117.8(4)
C(8)-C(7)-C(6)	123.7(3)	C(28)-C(27)-C(26)	123.1(4)
C(11)-C(7)-C(6)	119.3(3)	C(31)-C(27)-C(26)	119.1(4)
C(9)-C(8)-C(7)	119.8(3)	C(29)-C(28)-C(27)	119.7(3)
C(8)-C(9)-C(10)	118.6(3)	C(28)-C(29)-C(30)	118.4(4)
N(2)-C(10)-C(9)	124.0(3)	N(22)-C(30)-C(29)	124.8(4)
N(2)-C(11)-C(7)	122.9(2)	N(22)-C(31)-C(27)	122.6(3)
N(2)-C(11)-C(12)	117.9(2)	N(22)-C(31)-C(32)	117.9(3)
C(7)-C(11)-C(12)	119.2(2)	C(27)-C(31)-C(32)	119.5(3)
N(1)-C(12)-C(4)	122.9(3)	N(21)-C(32)-C(24)	122.3(3)
N(1)-C(12)-C(11)	117.6(2)	N(21)-C(32)-C(31)	117.5(3)
C(4)-C(12)-C(11)	119.5(2)	C(24)-C(32)-C(31)	120.2(3)
N(41)-C(45)	1.364(5)	C(44)-C(45)	1.370(4)
N(41)-C(41)	1.370(6)	C(44)-C(46)	1.538(10)
N(41)-C(47A)	1.529(9)	C(45)-C(45A)	1.445(7)
C(41)-C(42)	1.360(6)	C(46)-C(47)	1.301(13)
C(42)-C(43)	1.366(7)	C(45)-C(44)-C(46)	121.1(4)
C(43)-C(44)	1.382(6)	C(47)-N(41A)	1.529(9)
C(45)-N(41)-C(41)	118.2(4)	C(43)-C(44)-C(46)	120.7(4)
C(45)-N(41)-C(47A)	123.4(5)	N(41)-C(45)-C(44)	122.1(3)
C(41)-N(41)-C(47A)	118.2(5)	N(41)-C(45)-C(45A)	118.6(4)
C(42)-C(41)-N(41)	121.6(5)	C(44)-C(45)-C(45A)	119.3(4)
C(41)-C(42)-C(43)	119.1(4)	C(47)-C(46)-C(44)	120.1(6)
C(42)-C(43)-C(44)	121.0(4)	C(46)-C(47)-N(41A)	117.0(7)
C(45)-C(44)-C(43)	117.9(4)		

Symmetry transformations used to generate equivalent atoms: A: -x+1,-y+1,-z+1 B: -x,-y+1,-z

Table 4. Anisotropic displacement parameters ($Å^2 \cdot 10^3$). The anisotropic displacement factor exponent takes the form: $-2\pi^2[h^2 a^{*2} U_{11} + ... + 2 h k a^* b^* U_{12}]$

	U_{11}	U_{22}	U_{33}	U_{23}	U_{13}	U_{12}
Sn(1)	40(1)	29(1)	31(1)	12(1)	10(1)	19(1)
S(1)	40(1)	35(1)	54(1)	15(1)	16(1)	15(1)
S(2)	38(1)	31(1)	46(1)	15(1)	11(1)	16(1)
S(3)	64(1)	43(1)	27(1)	15(1)	12(1)	33(1)
Mn(1)	39(1)	35(1)	30(1)	13(1)	9(1)	20(1)
N(1)	45(1)	33(1)	33(1)	15(1)	9(1)	18(1)
N(2)	39(1)	35(1)	32(1)	17(1)	11(1)	19(1)
C(1)	59(2)	40(2)	41(2)	22(1)	10(1)	19(2)
C(2)	73(2)	51(2)	44(2)	30(2)	13(2)	20(2)
C(3)	68(2)	60(2)	32(2)	23(2)	14(2)	23(2)
C(4)	49(2)	41(2)	32(1)	13(1)	8(1)	18(1)
C(5)	72(2)	47(2)	30(1)	5(1)	8(1)	23(2)
C(6)	77(2)	35(2)	43(2)	5(1)	7(2)	23(2)
C(7)	57(2)	33(2)	46(2)	14(1)	10(1)	21(1)
C(8)	80(3)	30(2)	60(2)	18(2)	14(2)	19(2)
C(9)	71(2)	43(2)	57(2)	31(2)	15(2)	23(2)
C(10)	49(2)	44(2)	39(2)	21(1)	10(1)	21(1)
C(11)	35(1)	32(1)	34(1)	13(1)	8(1)	18(1)
C(12)	36(1)	34(2)	32(1)	13(1)	8(1)	17(1)
N(21)	48(1)	41(1)	36(1)	17(1)	5(1)	17(1)
N(22)	39(1)	45(2)	57(2)	25(1)	14(1)	21(1)
C(21)	65(2)	56(2)	41(2)	25(2)	11(2)	20(2)
C(22)	100(3)	66(3)	45(2)	32(2)	8(2)	21(2)
C(23)	107(4)	66(3)	54(2)	31(2)	-18(2)	25(3)
C(24)	76(3)	51(2)	57(2)	21(2)	-15(2)	25(2)
C(25)	91(3)	81(3)	92(3)	28(3)	-36(3)	40(3)
C(26)	63(3)	75(3)	112(4)	30(3)	-19(3)	34(2)
C(27)	43(2)	46(2)	93(3)	22(2)	-6(2)	21(2)
C(28)	41(2)	74(3)	137(4)	49(3)	26(2)	31(2)
C(29)	52(2)	92(3)	116(4)	57(3)	41(2)	38(2)
C(30)	50(2)	76(3)	81(3)	47(2)	28(2)	33(2)
C(31)	39(2)	34(2)	61(2)	17(1)	-1(1)	15(1)
C(32)	49(2)	34(2)	51(2)	15(1)	-5(1)	17(1)
N(41)	61(2)	84(3)	68(2)	35(2)	7(2)	14(2)
C(44')	61(2)	84(3)	68(2)	35(2)	7(2)	14(2)
C(41)	79(3)	90(4)	89(3)	37(3)	-2(3)	17(3)
C(42)	87(3)	77(3)	72(3)	40(3)	-12(2)	7(3)
C(43)	93(3)	57(3)	56(2)	29(2)	9(2)	1(2)
C(44)	67(2)	58(2)	51(2)	25(2)	10(2)	4(2)
N(41')	67(2)	58(2)	51(2)	25(2)	10(2)	4(2)
C(45)	55(2)	53(2)	50(2)	24(2)	9(2)	6(2)
C(46)	89(6)	47(4)	61(5)	20(4)	36(4)	21(4)
C(47)	59(5)	62(5)	105(7)	33(5)	29(5)	26(4)
O(1)	79(5)	95(6)	207(9)	38(6)	49(6)	45(4)

Table 5. Hydrogen coordinates ($\cdot 10^4$) and isotropic displacement parameters ($Å^2 \cdot 10^3$).

	x	y	z	U(eq)
H(1)	7395	3052	1683	54
H(2)	7241	2378	-296	65
H(3)	6620	205	-1493	64
H(5)	5950	-2107	-1705	65
H(6)	5451	-3513	-882	67
H(8)	5176	-3909	935	70
H(9)	5375	-3036	2933	65
H(10)	6129	-812	3976	51
H(21)	6331	1744	5985	64
H(22)	7115	1594	7592	85
H(23)	9100	1527	7762	92
H(25)	11151	1594	6941	108
H(26)	12293	1735	5527	102
H(28)	12450	1897	3623	96
H(29)	11543	2105	2135	95
H(30)	9524	2127	2121	74
H(41)	2740	4736	1474	110
H(42)	1731	4887	3031	101
H(43)	-172	5160	3023	91
H(46)	-1946	5504	2111	82
H(47)	-2835	5557	549	91

5.3.5 Messprotokoll der Verbindung {[Mn(phen)$_2$]$_2$[SnS$_4$]$_2$[Mn(phen)$_2$}·H$_2$O

Table 1. Crystal data and structure refinement for {[Mn($C_{12}H_8N_2$)$_2$]$_2$[Mn($C_{12}H_8N_2$)]$_2$[SnS$_4$]$_2$}·H$_2$O. ($C_{12}H_8N_2$; phen = 1,10-Phenanthrolin)

Identification code	jh336	
Empirical formula	{[Mn($C_{12}H_8N_2$)$_2$]$_2$ [Mn($C_{12}H_8N_2$)]$_2$[SnS$_4$]$_2$}·H$_2$O.	
Crystal color, habitus	red needles	
Formula weight	1812.86	
Temperature	293(2) K	
Wavelength	0.71073 Å	
Crystal system	triclinic	
Space group	$P\bar{1}$	
Unit cell dimensions	a = 10.8703(5) Å	α= 103.381(3)°.
	b = 12.5183(6) Å	β= 108.390(3)°.
	c = 14.9644(6) Å	γ = 101.636(4)°.
Volume	1794.71(14) Å^3	
Z	1	
Density (calculated)	1.677 Mg/m^3	
Absorption coefficient	1.654 mm^{-1}	
F(000)	902	
Crystal size	0.07 x 0.11 x 0.16 mm^3	
Theta range for data collection	1.51 to 27.00°.	
Index ranges	-13<=h<=13, -15<=k<=15, -19<=l<=19	
Reflections collected	18641	
Independent reflections	7768 [R(int) = 0.0592]	
Completeness to theta = 27.00°	99.4 %	
Refinement method	Full-matrix least-squares on F^2	
Data / restraints / parameters	7768 / 0 / 451	
Goodness-of-fit on F^2	1.079	
Final R indices [I>2sigma(I)]	R1 = 0.0412, wR2 = 0.1039	
R indices (all data)	R1 = 0.0534, wR2 = 0.1084	
Largest diff. peak and hole	0.972 and -0.720 e.Å^{-3}	

Comments:
All non-hydrogen atoms were refined anisotropic. The C-H H atoms were positioned with idealized geometry and refined isotropic with $U_{iso}(H) = 1.2 \cdot U_{eq}(C)$ using a riding model. A numerical absorption correction was performed ($T_{min/max}$: 0.7010/0.8413). After structure refinement there was one remaining small electron density maximum to which a half occupied water molecule was assigned. Additional residual electron density peaks were located, that can be assigned to the water H atoms. The O-H H distances were set to ideal values and finally the H atoms were refined using a riding model.

Table 2. Atomic coordinates ($\cdot 10^4$) and equivalent isotropic displacement parameters ($Å^2$ 10^3). U(eq) is defined as one third of the trace of the orthogonalized U_{ij} tensor.

	x	y	z	U(eq)
Sn(1)	3905(1)	3422(1)	7563(1)	31(1)
S(1)	1578(1)	2515(1)	6556(1)	38(1)
S(2)	4875(1)	3580(1)	6370(1)	38(1)
S(3)	4710(1)	5352(1)	8768(1)	35(1)
S(4)	4851(1)	2457(1)	8682(1)	41(1)
Mn(1)	2450(1)	2572(1)	5166(1)	32(1)
N(1)	1840(3)	4053(3)	4766(3)	36(1)
N(2)	279(3)	1830(3)	3860(3)	35(1)
C(1)	2628(5)	5126(4)	5183(3)	43(1)
C(2)	2236(5)	6046(4)	4931(4)	52(1)
C(3)	981(5)	5838(4)	4232(4)	50(1)
C(4)	111(4)	4715(4)	3774(3)	39(1)
C(5)	-1227(5)	4423(4)	3033(4)	48(1)
C(6)	-2010(5)	3333(5)	2600(4)	50(1)
C(7)	-1536(4)	2407(4)	2844(3)	41(1)
C(8)	-2300(5)	1243(4)	2388(4)	51(1)
C(9)	-1775(5)	412(4)	2657(4)	50(1)
C(10)	-476(5)	749(4)	3402(3)	42(1)
C(11)	-243(4)	2665(3)	3580(3)	35(1)
C(12)	600(4)	3833(3)	4055(3)	33(1)
N(21)	7994(4)	3709(4)	10388(3)	51(1)
N(22)	8046(4)	5905(4)	10554(3)	51(1)
C(21)	7961(6)	2631(5)	10303(4)	61(1)
C(22)	9115(7)	2297(7)	10694(5)	77(2)
C(23)	10342(6)	3113(7)	11180(5)	77(2)
C(24)	10435(5)	4261(6)	11284(4)	65(2)
C(25)	11670(6)	5163(8)	11773(5)	80(2)
C(26)	11695(6)	6254(8)	11864(5)	83(2)
C(27)	10484(5)	6570(6)	11476(4)	68(2)
C(28)	10453(6)	7693(6)	11548(5)	80(2)
C(29)	9259(7)	7914(6)	11160(5)	79(2)
C(30)	8045(6)	6980(5)	10640(5)	63(1)

C(31)	9236(5)	5685(5)	10967(3)	54(1)
C(32)	9219(5)	4532(5)	10882(3)	52(1)
Mn(2)	6164(1)	4393(1)	9896(1)	35(1)
N(41)	3249(3)	2362(3)	3855(3)	35(1)
N(42)	2664(4)	792(3)	4752(3)	37(1)
C(41)	3559(5)	3135(4)	3426(4)	45(1)
C(42)	4103(6)	2960(5)	2703(4)	57(1)
C(43)	4372(6)	1945(5)	2425(5)	66(2)
C(44)	4102(5)	1095(4)	2872(4)	47(1)
C(45)	4397(6)	29(5)	2664(4)	59(1)
C(46)	4160(5)	-727(4)	3140(4)	53(1)
C(47)	3560(4)	-511(4)	3860(3)	40(1)
C(48)	3254(5)	-1281(4)	4351(4)	52(1)
C(49)	2650(6)	-1018(4)	5011(4)	59(1)
C(50)	2394(6)	40(4)	5198(4)	50(1)
C(51)	3236(4)	534(3)	4080(3)	34(1)
C(52)	3533(4)	1359(3)	3595(3)	36(1)
O(1)	4383(15)	880(13)	87(8)	140(5)

Table 3. Bond lengths [Å] and angles [°].

Sn(1)-S(1)	2.3670(11)	S(4)-Mn(2)	2.4775(13)
Sn(1)-S(2)	2.3678(10)	Sn(1)-S(4)	2.3816(11)
Sn(1)-Mn(1)	3.2363(7)	Sn(1)-S(3)	2.4471(10)
S(1)-Mn(1)	2.5521(12)	Mn(1)-N(1)	2.234(3)
S(2)-Mn(1)	2.5289(12)	Mn(1)-N(42)	2.251(3)
S(3)-Mn(2)#1	2.4555(11)	Mn(1)-N(41)	2.368(3)
S(3)-Mn(2)	2.6090(12)	Mn(1)-N(2)	2.370(4)
N(21)-Mn(2)	2.299(4)	N(22)-Mn(2)	2.246(4)
Mn(2)-S(3)#1	2.4555(11)	N(42)-Mn(1)-S(2)	97.00(10)
S(1)-Sn(1)-S(2)	102.17(4)	N(41)-Mn(1)-S(2)	88.43(9)
S(1)-Sn(1)-S(4)	113.99(4)	S(4)-Sn(1)-S(3)	97.55(4)
S(2)-Sn(1)-S(4)	116.12(4)	S(1)-Sn(1)-Mn(1)	51.38(3)
S(1)-Sn(1)-S(3)	121.99(4)	S(2)-Sn(1)-Mn(1)	50.81(3)
S(2)-Sn(1)-S(3)	105.60(4)	S(4)-Sn(1)-Mn(1)	131.47(3)
Sn(1)-S(1)-Mn(1)	82.19(3)	S(3)-Sn(1)-Mn(1)	130.31(3)
Sn(1)-S(2)-Mn(1)	82.67(3)	N(2)-Mn(1)-S(2)	169.55(9)
Sn(1)-S(3)-Mn(2)#1	116.60(4)	N(1)-Mn(1)-S(1)	100.59(9)
Sn(1)-S(3)-Mn(2)	82.44(3)	N(42)-Mn(1)-S(1)	100.55(9)
Mn(2)#1-S(3)-Mn(2)	80.14(3)	N(41)-Mn(1)-S(1)	172.26(9)
Sn(1)-S(4)-Mn(2)	86.62(4)	N(2)-Mn(1)-S(1)	95.64(9)
N(1)-Mn(1)-N(42)	151.70(13)	S(2)-Mn(1)-S(1)	92.95(4)
N(1)-Mn(1)-N(41)	86.63(12)	N(1)-Mn(1)-Sn(1)	106.17(9)
N(42)-Mn(1)-N(41)	71.72(12)	N(42)-Mn(1)-Sn(1)	102.01(9)
N(1)-Mn(1)-N(2)	72.11(12)	N(41)-Mn(1)-Sn(1)	134.29(9)
N(42)-Mn(1)-N(2)	87.28(12)	N(2)-Mn(1)-Sn(1)	141.83(8)
N(41)-Mn(1)-N(2)	83.85(12)	S(2)-Mn(1)-Sn(1)	46.52(2)

N(1)-Mn(1)-S(2)	100.48(10)	S(1)-Mn(1)-Sn(1)	46.44(3)
N(22)-Mn(2)-N(21)	72.54(16)	S(3)#1-Mn(2)-S(4)	107.31(4)
N(22)-Mn(2)-S(3)#1	101.30(10)	N(22)-Mn(2)-S(3)	94.60(12)
N(21)-Mn(2)-S(3)#1	107.27(11)	N(21)-Mn(2)-S(3)	151.69(11)
N(22)-Mn(2)-S(4)	149.38(10)	S(3)#1-Mn(2)-S(3)	99.86(3)
N(21)-Mn(2)-S(4)	88.53(12)	S(4)-Mn(2)-S(3)	91.09(4)
N(1)-C(1)	1.319(5)	N(21)-C(21)	1.319(7)
N(1)-C(12)	1.354(5)	N(21)-C(32)	1.361(7)
N(2)-C(10)	1.321(6)	N(22)-C(30)	1.322(7)
N(2)-C(11)	1.371(5)	N(22)-C(31)	1.360(6)
C(1)-C(2)	1.396(6)	C(21)-C(22)	1.397(7)
C(2)-C(3)	1.362(7)	C(22)-C(23)	1.359(10)
C(3)-C(4)	1.397(7)	C(23)-C(24)	1.388(10)
C(4)-C(12)	1.410(5)	C(24)-C(32)	1.413(7)
C(4)-C(5)	1.435(7)	C(24)-C(25)	1.414(10)
C(5)-C(6)	1.335(7)	C(25)-C(26)	1.335(11)
C(6)-C(7)	1.435(6)	C(26)-C(27)	1.435(9)
C(7)-C(11)	1.403(6)	C(27)-C(28)	1.393(10)
C(7)-C(8)	1.405(7)	C(27)-C(31)	1.414(7)
C(8)-C(9)	1.363(7)	C(28)-C(29)	1.357(10)
C(9)-C(10)	1.401(7)	C(29)-C(30)	1.422(8)
C(11)-C(12)	1.432(6)	C(31)-C(32)	1.416(8)
C(1)-N(1)-C(12)	118.5(3)	C(21)-N(21)-C(32)	117.8(4)
C(10)-N(2)-C(11)	117.6(4)	C(30)-N(22)-C(31)	119.3(5)
N(1)-C(1)-C(2)	122.9(4)	N(21)-C(21)-C(22)	123.3(6)
C(3)-C(2)-C(1)	119.1(4)	C(23)-C(22)-C(21)	119.1(7)
C(2)-C(3)-C(4)	119.9(4)	C(22)-C(23)-C(24)	120.0(5)
C(3)-C(4)-C(12)	117.3(4)	C(23)-C(24)-C(32)	117.6(6)
C(3)-C(4)-C(5)	123.3(4)	C(23)-C(24)-C(25)	123.6(6)
C(12)-C(4)-C(5)	119.3(4)	C(32)-C(24)-C(25)	118.8(7)
C(6)-C(5)-C(4)	121.2(4)	C(26)-C(25)-C(24)	121.0(6)
C(5)-C(6)-C(7)	121.3(4)	C(25)-C(26)-C(27)	122.1(6)
C(11)-C(7)-C(8)	117.5(4)	C(28)-C(27)-C(31)	117.3(6)
C(11)-C(7)-C(6)	118.9(4)	C(28)-C(27)-C(26)	124.5(6)
C(8)-C(7)-C(6)	123.6(4)	C(31)-C(27)-C(26)	118.3(7)
C(9)-C(8)-C(7)	120.1(4)	C(29)-C(28)-C(27)	120.5(6)
C(8)-C(9)-C(10)	118.6(4)	C(28)-C(29)-C(30)	119.2(7)
N(2)-C(10)-C(9)	123.7(4)	N(22)-C(30)-C(29)	121.6(6)
N(2)-C(11)-C(7)	122.5(4)	N(22)-C(31)-C(27)	122.1(6)
N(2)-C(11)-C(12)	117.4(4)	N(22)-C(31)-C(32)	118.7(4)
C(7)-C(11)-C(12)	120.1(4)	C(27)-C(31)-C(32)	119.2(5)
N(1)-C(12)-C(4)	122.3(4)	N(21)-C(32)-C(24)	122.2(6)
N(1)-C(12)-C(11)	118.6(3)	N(21)-C(32)-C(31)	117.1(4)
C(4)-C(12)-C(11)	119.1(4)	C(24)-C(32)-C(31)	120.6(5)
N(41)-C(41)	1.324(5)	C(44)-C(45)	1.423(7)
N(41)-C(52)	1.353(5)	C(45)-C(46)	1.341(8)

N(42)-C(50)	1.310(5)	C(46)-C(47)	1.428(6)
N(42)-C(51)	1.352(5)	C(47)-C(48)	1.390(7)
C(41)-C(42)	1.383(7)	C(47)-C(51)	1.415(5)
C(42)-C(43)	1.362(8)	C(48)-C(49)	1.363(7)
C(43)-C(44)	1.412(7)	C(49)-C(50)	1.392(6)
C(44)-C(52)	1.415(6)	C(51)-C(52)	1.434(6)
C(41)-N(41)-C(52)	117.7(4)	C(48)-C(47)-C(46)	123.6(4)
C(50)-N(42)-C(51)	118.5(3)	C(51)-C(47)-C(46)	118.6(4)
N(41)-C(41)-C(42)	124.1(4)	C(49)-C(48)-C(47)	119.7(4)
C(43)-C(42)-C(41)	118.7(5)	C(48)-C(49)-C(50)	118.7(5)
C(42)-C(43)-C(44)	120.2(5)	N(42)-C(50)-C(49)	123.6(4)
C(43)-C(44)-C(52)	116.4(4)	N(42)-C(51)-C(47)	121.6(4)
C(43)-C(44)-C(45)	124.6(4)	N(42)-C(51)-C(52)	118.3(3)
C(52)-C(44)-C(45)	119.0(4)	C(47)-C(51)-C(52)	120.0(4)
C(46)-C(45)-C(44)	121.8(4)	N(41)-C(52)-C(44)	122.9(4)
C(45)-C(46)-C(47)	121.3(4)	N(41)-C(52)-C(51)	117.9(3)
C(48)-C(47)-C(51)	117.8(4)	C(44)-C(52)-C(51)	119.2(4)

Symmetry transformations used to generate equivalent atoms: A: -x+1,-y+1,-z+2

Table 4. Anisotropic displacement parameters ($Å^2 \cdot 10^3$). The anisotropic displacement factor exponent takes the form: $-2\pi^2[h^2 a^{*2} U_{11} + ... + 2 h k a^* b^* U_{12}]$

	U_{11}	U_{22}	U_{33}	U_{23}	U_{13}	U_{12}
Sn(1)	32(1)	35(1)	27(1)	9(1)	11(1)	14(1)
S(1)	32(1)	45(1)	37(1)	13(1)	13(1)	13(1)
S(2)	34(1)	48(1)	34(1)	12(1)	15(1)	14(1)
S(3)	43(1)	35(1)	31(1)	12(1)	17(1)	15(1)
S(4)	49(1)	37(1)	34(1)	11(1)	9(1)	19(1)
Mn(1)	38(1)	29(1)	30(1)	11(1)	12(1)	15(1)
N(1)	40(2)	31(2)	39(2)	15(1)	13(2)	15(1)
N(2)	39(2)	34(2)	37(2)	14(1)	16(2)	13(1)
C(1)	47(2)	32(2)	44(2)	13(2)	9(2)	11(2)
C(2)	61(3)	29(2)	66(3)	17(2)	22(3)	13(2)
C(3)	63(3)	38(2)	64(3)	28(2)	27(3)	25(2)
C(4)	47(2)	42(2)	43(2)	21(2)	24(2)	25(2)
C(5)	53(3)	58(3)	46(3)	27(2)	20(2)	33(2)
C(6)	39(2)	69(3)	50(3)	29(2)	14(2)	27(2)
C(7)	35(2)	52(2)	39(2)	18(2)	15(2)	15(2)
C(8)	40(2)	58(3)	45(3)	14(2)	9(2)	8(2)
C(9)	46(3)	44(2)	50(3)	10(2)	16(2)	4(2)
C(10)	48(2)	38(2)	44(2)	16(2)	19(2)	13(2)
C(11)	39(2)	39(2)	33(2)	16(2)	16(2)	16(2)
C(12)	37(2)	36(2)	31(2)	14(2)	16(2)	17(2)
N(21)	39(2)	73(3)	45(2)	19(2)	15(2)	25(2)
N(22)	36(2)	60(3)	49(2)	6(2)	20(2)	7(2)
C(21)	53(3)	82(4)	61(3)	31(3)	24(3)	37(3)
C(22)	70(4)	103(5)	78(4)	39(4)	31(3)	52(4)

C(23)	56(3)	125(6)	69(4)	45(4)	22(3)	53(4)
C(24)	44(3)	115(5)	42(3)	29(3)	17(2)	31(3)
C(25)	39(3)	139(7)	60(4)	31(4)	15(3)	30(4)
C(26)	32(3)	133(7)	53(3)	13(4)	4(2)	-1(3)
C(27)	39(3)	98(5)	50(3)	10(3)	19(2)	0(3)
C(28)	52(3)	89(5)	69(4)	3(4)	22(3)	-15(3)
C(29)	71(4)	64(4)	79(4)	-3(3)	34(4)	-5(3)
C(30)	52(3)	64(3)	71(4)	12(3)	35(3)	8(2)
C(31)	31(2)	85(4)	35(2)	9(2)	15(2)	6(2)
C(32)	35(2)	86(4)	34(2)	18(2)	14(2)	17(2)
Mn(2)	30(1)	43(1)	33(1)	10(1)	13(1)	13(1)
N(41)	39(2)	34(2)	38(2)	13(1)	18(2)	15(1)
N(42)	52(2)	31(2)	40(2)	17(2)	23(2)	19(2)
C(41)	51(3)	44(2)	46(2)	23(2)	22(2)	14(2)
C(42)	62(3)	61(3)	61(3)	31(3)	34(3)	15(3)
C(43)	72(4)	72(4)	73(4)	27(3)	53(3)	18(3)
C(44)	48(2)	47(2)	53(3)	13(2)	31(2)	12(2)
C(45)	60(3)	54(3)	71(4)	7(3)	42(3)	17(2)
C(46)	48(3)	42(2)	71(3)	4(2)	33(2)	16(2)
C(47)	39(2)	34(2)	47(2)	8(2)	16(2)	17(2)
C(48)	65(3)	34(2)	60(3)	15(2)	24(2)	22(2)
C(49)	90(4)	38(2)	66(3)	27(2)	39(3)	30(3)
C(50)	75(3)	39(2)	52(3)	24(2)	34(3)	24(2)
C(51)	33(2)	31(2)	37(2)	9(2)	13(2)	11(2)
C(52)	36(2)	34(2)	35(2)	7(2)	14(2)	8(2)
O(1)	157(12)	192(14)	63(7)	52(8)	53(7)	4(10)

Table 5. Hydrogen coordinates ($\cdot 10^4$) and isotropic displacement parameters ($Å^2 \cdot 10^3$).

	x	y	z	U(eq)
H(1)	3484	5277	5666	52
H(2)	2824	6791	5237	63
H(3)	703	6443	4059	61
H(5)	-1555	5004	2851	57
H(6)	-2880	3169	2131	60
H(8)	-3166	1038	1902	61
H(9)	-2268	-361	2352	60
H(10)	-126	178	3584	51
H(21)	7128	2064	9965	73
H(22)	9044	1526	10624	92
H(23)	11119	2903	11443	92
H(25)	12477	4993	12035	96
H(26)	12523	6828	12189	100
H(28)	11256	8296	11865	96
H(29)	9235	8666	11232	95
H(30)	7231	7129	10354	75
H(41)	3402	3839	3623	54
H(42)	4281	3524	2413	68
H(43)	4734	1811	1938	79
H(45)	4764	-148	2185	71
H(46)	4392	-1405	2999	63
H(48)	3460	-1973	4230	62
H(49)	2415	-1535	5329	70
H(50)	2010	225	5665	60
H(1O1)	4476	1489	489	210
H(2O1)	3551	662	-144	210
H(3O1)	4461	1523	29	210
H(4O1)	5145	822	337	210

5.3.6 Messprotokoll der Verbindung {[Fe(phen)$_2$]$_2$[Sn$_2$S$_6$]}

Table 1. Crystal data and structure refinement for {[Fe($C_{12}H_8N_2$)$_2$]$_2$[Sn$_2$S$_6$]} ($C_{12}H_8N_2$; phen = 1,10-Phenanthrolin)

Identification code	jh409	
Empirical formula	{[Fe($C_{12}H_8N_2$)$_2$]$_2$[Sn$_2$S$_6$]}	
Crystal color, habitus	black blocks	
Formula weight	1262.26	
Temperature	293(2) K	
Wavelength	0.71073 Å	
Crystal system	monoclinic	
Space group	$P2_1/n$	
Unit cell dimensions	a = 10.7112(3) Å	α = 90°.
	b = 9.9266(4) Å	β = 93.194(3)°.
	c = 25.3421(8) Å	γ = 90°.
Volume	2690.33(16) Å^3	
Z	2	
Density (calculated)	1.558 Mg/m^3	
Absorption coefficient	1.719 mm^{-1}	
F(000)	1248	
Crystal size	0.11 x 0.09 x 0.08 mm^3	
Theta range for data collection	2.03 to 24.62°.	
Index ranges	-10 ≤ h ≤ 12, -11 ≤ k ≤ 11, -23 ≤ l ≤ 29	
Reflections collected	18892	
Independent reflections	4463 [R(int) = 0.0381]	
Completeness to theta = 24.62°	98.2 %	
Refinement method	Full-matrix least-squares on F^2	
Data / restraints / parameters	4463 / 0 / 299	
Goodness-of-fit on F^2	1.218	
Final R indices [I>2sigma(I)]	R1 = 0.0648, wR2 = 0.1629	
R indices (all data)	R1 = 0.0732, wR2 = 0.1661	
Extinction coefficient	0.0024(4)	
Largest diff. peak and hole	0.624 and -0.653 e.Å^{-3}	

Comments:
All non-hydrogen atoms were refined anisotropic. All H atoms were located in difference map but were positioned with idealized geometry and refined isotropic using a riding model. A numerical absorption correction was performed ($T_{min/max}$: 0.7230, 0.7902). The structure contains cavities, in which a small amount of disordered solvent is included, for which no reasonable structure model was found. Therefore, the data were corrected for disordered solvent using the SQUEEZE option in Platon, which leads to a void volume of 247.3 $Å^3$ and a total electron count per cell of 26.5

Table 2. Atomic coordinates ($\cdot 10^4$) and equivalent isotropic displacement parameters ($Å^2 \cdot 10^3$). U(eq) is defined as one third of the trace of the orthogonalized U_{ij} tensor.

	x	y	z	U(eq)
Sn(1)	1204(1)	4366(1)	384(1)	41(1)
S(1)	3367(2)	4470(2)	293(1)	45(1)
S(2)	1155(2)	3095(3)	1169(1)	49(1)
S(3)	-17(2)	6460(2)	401(1)	49(1)
Fe(1)	3476(1)	3034(1)	1116(1)	41(1)
N(1)	3761(7)	2076(8)	1942(3)	46(2)
N(2)	3989(7)	4679(7)	1668(3)	43(2)
C(1)	3602(10)	805(10)	2084(4)	53(2)
C(2)	3746(11)	346(11)	2600(4)	61(3)
C(3)	4030(11)	1233(11)	2992(4)	58(3)
C(4)	4187(10)	2600(10)	2875(4)	52(2)
C(5)	4495(11)	3612(11)	3268(4)	61(3)
C(6)	4612(10)	4918(12)	3120(4)	56(3)
C(7)	4421(9)	5333(10)	2585(4)	48(2)
C(8)	4495(11)	6658(11)	2422(5)	61(3)
C(9)	4297(12)	6987(12)	1912(5)	72(3)
C(10)	4038(11)	5950(11)	1529(5)	64(3)
C(11)	4160(9)	4355(10)	2193(4)	44(2)
C(12)	4044(9)	2982(10)	2336(4)	47(2)
N(11)	3583(8)	950(8)	833(3)	46(2)
N(12)	5472(8)	2676(8)	968(3)	51(2)
C(21)	2602(11)	96(11)	745(4)	58(3)
C(22)	2807(16)	-1224(13)	578(5)	79(4)
C(23)	3980(17)	-1694(12)	501(5)	80(4)
C(24)	5012(12)	-844(11)	596(4)	62(3)
C(25)	6264(16)	-1242(14)	512(5)	83(4)
C(26)	7167(15)	-374(18)	595(5)	94(5)
C(27)	6960(10)	1012(12)	741(4)	56(3)
C(28)	7933(11)	2009(15)	793(5)	71(3)
C(29)	7616(13)	3249(17)	889(6)	88(4)
C(30)	6376(9)	3563(12)	975(6)	69(3)
C(31)	5788(10)	1419(11)	840(4)	51(2)
C(32)	4749(10)	455(10)	759(4)	49(2)

Table 3. Bond lengths [Å] and angles [°].

Sn(1)-S(1)	2.344(2)	Sn(1)-S(3)#1	2.443(2)
Sn(1)-S(2)	2.359(2)	Sn(1)-S(3)	2.457(3)
S(1)-Fe(1)	2.523(3)	S(3)-Sn(1)#1	2.443(2)
S(2)-Fe(1)	2.498(3)	Fe(1)-N(12)	2.219(8)
Fe(1)-N(11)	2.194(8)	Fe(1)-N(1)	2.305(8)
Fe(1)-N(2)	2.202(8)	N(11)-Fe(1)-N(1)	84.3(3)
S(1)-Sn(1)-S(2)	100.10(9)	N(2)-Fe(1)-N(1)	73.3(3)
S(1)-Sn(1)-S(3)#1	114.00(9)	N(12)-Fe(1)-N(1)	90.4(3)
S(2)-Sn(1)-S(3)#1	118.22(9)	N(11)-Fe(1)-S(2)	96.4(2)
S(1)-Sn(1)-S(3)	119.62(9)	N(2)-Fe(1)-S(2)	99.3(2)
S(2)-Sn(1)-S(3)	113.64(9)	N(12)-Fe(1)-S(2)	169.8(2)
S(3)#1-Sn(1)-S(3)	92.56(8)	N(1)-Fe(1)-S(2)	92.4(2)
Sn(1)-S(1)-Fe(1)	83.91(8)	N(11)-Fe(1)-S(1)	105.3(2)
Sn(1)-S(2)-Fe(1)	84.16(8)	N(2)-Fe(1)-S(1)	96.0(2)
Sn(1)#1-S(3)-Sn(1)	87.44(8)	N(12)-Fe(1)-S(1)	87.3(2)
N(11)-Fe(1)-N(2)	153.0(3)	N(1)-Fe(1)-S(1)	169.0(2)
N(11)-Fe(1)-N(12)	74.1(3)	S(2)-Fe(1)-S(1)	91.77(9)
N(2)-Fe(1)-N(12)	90.9(3)		
N(1)-C(1)	1.326(12)	C(8)-C(7)-C(11)	117.3(9)
N(1)-C(12)	1.365(12)	C(8)-C(7)-C(6)	123.5(9)
N(2)-C(10)	1.312(13)	C(11)-C(7)-C(6)	119.1(9)
N(2)-C(11)	1.370(12)	C(9)-C(8)-C(7)	120.7(10)
C(1)-C(2)	1.385(15)	C(8)-C(9)-C(10)	119.6(11)
C(2)-C(3)	1.350(15)	N(2)-C(10)-C(9)	121.1(11)
C(3)-C(4)	1.402(14)	N(2)-C(11)-C(7)	122.3(9)
C(4)-C(12)	1.418(14)	N(2)-C(11)-C(12)	117.7(8)
C(4)-C(5)	1.440(15)	C(7)-C(11)-C(12)	120.0(9)
C(5)-C(6)	1.357(15)	N(1)-C(12)-C(11)	117.8(8)
C(6)-C(7)	1.421(14)	N(1)-C(12)-C(4)	122.5(9)
C(7)-C(8)	1.382(14)	C(11)-C(12)-C(4)	119.7(9)
C(7)-C(11)	1.406(13)	N(11)-C(21)	1.359(12)
C(8)-C(9)	1.338(16)	N(11)-C(32)	1.365(13)
C(9)-C(10)	1.433(16)	N(12)-C(30)	1.308(13)
C(11)-C(12)	1.418(13)	N(12)-C(31)	1.339(13)
C(1)-N(1)-C(12)	117.1(8)	C(21)-C(22)	1.397(17)
C(10)-N(2)-C(11)	118.8(9)	C(22)-C(23)	1.36(2)
N(1)-C(1)-C(2)	124.0(10)	C(23)-C(24)	1.402(19)
C(3)-C(2)-C(1)	119.3(10)	C(24)-C(32)	1.388(14)
C(2)-C(3)-C(4)	120.0(10)	C(24)-C(25)	1.425(19)
C(3)-C(4)-C(12)	117.0(9)	C(25)-C(26)	1.30(2)
C(3)-C(4)-C(5)	123.7(9)	C(26)-C(27)	1.445(19)
C(12)-C(4)-C(5)	119.3(9)	C(27)-C(31)	1.355(14)
C(6)-C(5)-C(4)	119.7(10)	C(27)-C(28)	1.438(17)
C(5)-C(6)-C(7)	122.0(9)	C(28)-C(29)	1.304(19)

C(29)-C(30)	1.394(17)	C(31)-C(27)-C(28)	116.9(11)
C(31)-C(32)	1.473(14)	C(31)-C(27)-C(26)	119.2(12)
C(21)-N(11)-C(32)	117.3(9)	C(28)-C(27)-C(26)	123.9(12)
C(30)-N(12)-C(31)	115.7(9)	C(29)-C(28)-C(27)	118.1(12)
N(11)-C(21)-C(22)	120.1(12)	C(28)-C(29)-C(30)	120.1(13)
C(23)-C(22)-C(21)	121.7(12)	N(12)-C(30)-C(29)	124.0(12)
C(22)-C(23)-C(24)	119.6(11)	N(12)-C(31)-C(27)	124.9(10)
C(32)-C(24)-C(23)	116.1(12)	N(12)-C(31)-C(32)	116.1(9)
C(32)-C(24)-C(25)	120.7(11)	C(27)-C(31)-C(32)	118.8(10)
C(23)-C(24)-C(25)	123.2(12)	N(11)-C(32)-C(24)	125.3(10)
C(26)-C(25)-C(24)	119.2(12)	N(11)-C(32)-C(31)	115.9(9)
C(25)-C(26)-C(27)	123.2(13)	C(24)-C(32)-C(31)	118.7(10)

Symmetry transformations used to generate equivalent atoms: #1 -x,-y+1,-z

Table 4. Anisotropic displacement parameters ($Å^2 \cdot 10^3$). The anisotropic displacement factor exponent takes the form: $-2\pi^2 [h^2 a^{*2} U_{11} + ... + 2 h k a^* b^* U_{12}]$

	U_{11}	U_{22}	U_{33}	U_{23}	U_{13}	U_{12}
Sn(1)	41(1)	41(1)	38(1)	2(1)	-2(1)	-1(1)
S(1)	44(1)	48(1)	44(1)	5(1)	4(1)	0(1)
S(2)	47(1)	55(1)	45(1)	13(1)	3(1)	1(1)
S(3)	52(1)	43(1)	51(1)	-10(1)	-11(1)	3(1)
Fe(1)	44(1)	38(1)	42(1)	1(1)	-3(1)	0(1)
N(1)	44(4)	39(4)	52(5)	1(4)	-7(4)	-2(3)
N(2)	52(5)	36(4)	39(4)	3(3)	-2(3)	-6(3)
C(1)	58(6)	45(6)	55(6)	3(5)	0(5)	-9(5)
C(2)	76(8)	52(6)	55(6)	10(5)	9(6)	-6(5)
C(3)	76(7)	58(6)	38(5)	8(5)	-2(5)	1(6)
C(4)	58(6)	51(6)	47(6)	4(5)	0(5)	5(5)
C(5)	84(8)	62(7)	37(5)	0(5)	10(5)	6(6)
C(6)	62(7)	67(7)	39(5)	-19(5)	4(5)	4(5)
C(7)	47(5)	46(6)	51(6)	-13(4)	-2(4)	2(4)
C(8)	73(7)	47(6)	60(7)	-9(5)	-14(6)	8(5)
C(9)	94(9)	45(6)	77(8)	-10(6)	1(7)	-25(6)
C(10)	82(8)	50(6)	58(7)	5(5)	-1(6)	1(6)
C(11)	46(5)	46(5)	39(5)	-8(4)	0(4)	1(4)
C(12)	55(6)	45(5)	41(5)	0(4)	8(4)	10(4)
N(11)	51(5)	40(4)	47(4)	-6(3)	-2(4)	0(4)
N(12)	53(5)	42(5)	58(5)	0(4)	4(4)	2(4)
C(21)	74(7)	56(6)	43(6)	-6(5)	3(5)	-26(6)
C(22)	117(12)	64(8)	56(7)	-4(6)	2(7)	-44(8)
C(23)	147(14)	42(6)	51(7)	-1(5)	2(8)	2(8)
C(24)	88(8)	45(6)	51(6)	-8(5)	-4(6)	6(6)

C(25)	117(12)	59(8)	72(9)	-23(7)	1(8)	21(8)
C(26)	86(10)	133(14)	64(8)	-9(9)	6(7)	54(10)
C(27)	57(6)	75(7)	36(5)	-5(5)	4(5)	15(6)
C(28)	51(7)	96(10)	64(7)	6(7)	3(5)	8(7)
C(29)	63(8)	99(11)	103(11)	31(9)	7(7)	-5(8)
C(30)	32(5)	61(7)	114(10)	6(7)	8(6)	-6(5)
C(31)	57(6)	62(7)	34(5)	1(5)	4(4)	-3(5)
C(32)	72(7)	44(5)	31(5)	-3(4)	0(4)	-6(5)

Table 5. Hydrogen coordinates ($\cdot 10^4$) and isotropic displacement parameters ($Å^2 \cdot 10^3$).

	x	y	z	U(eq)
H(1)	3380	183	1821	63
H(2)	3649	-564	2675	73
H(3)	4122	936	3340	69
H(5)	4612	3372	3622	73
H(6)	4824	5561	3376	68
H(8)	4683	7329	2670	73
H(9)	4327	7884	1808	87
H(10)	3902	6182	1175	76
H(21)	1793	390	796	69
H(22)	2126	-1796	518	95
H(23)	4093	-2573	386	96
H(25)	6435	-2111	400	99
H(26)	7985	-660	558	113
H(28)	8765	1776	758	85
H(29)	8218	3925	901	106
H(30)	6179	4458	1042	83

5.3.7 Messprotokoll der Verbindung $\{[Fe(phen)_2]_2[Sn_2S_6]\}\cdot phen\cdot H_2O$

Table 1. Crystal data and structure refinement for $\{[Fe(C_{12}H_8N_2)_2]_2[Sn_2S_6]\}\cdot C_{12}H_8N_2\cdot H_2O$ ($C_{12}H_8N_2$; phen = 1,10-Phenanthrolin)

Identification code	jh360a	
Empirical formula	$\{[Fe(C_{12}H_8N_2)_2]_2[Sn_2S_6]\}\cdot C_{12}H_8N_2\cdot H_2O$	
Crystal color, habitus	black blocks	
Formula weight	1460.48 g / mol	
Temperature	293(2) K	
Wavelength	0.71073 Å	
Crystal system	triclinic	
Space group	$P\bar{1}$	
Unit cell dimensions	a = 11.2219(5) Å	α= 113.956(4)°.
	b = 12.1407(6) Å	β= 89.821(4)°.
	c = 12.7130(6) Å	γ = 110.318(4)°.
Volume	1465.02(12) $Å^3$	
Z	1	
Density (calculated)	1.655 Mg/m^3	
Absorption coefficient	1.593 mm^{-1}	
F(000)	728	
Crystal size	0.13 x 0.09 x 0.07 mm^3	
Theta range for data collection	1.78 to 27.00°.	
Index ranges	-14<=h<=14, -15<=k<=15, -16<=l<=16	
Reflections collected	15811	
Independent reflections	6390 [R(int) = 0.0500]	
Completeness to theta = 27.00°	99.5 %	
Absorption correction	Numerical	
Refinement method	Full-matrix least-squares on F^2	
Data / restraints / parameters	6390 / 0 / 379	
Goodness-of-fit on F^2	1.128	
Final R indices [I>2sigma(I)]	R1 = 0.0404, wR2 = 0.0832	
R indices (all data)	R1 = 0.0597, wR2 = 0.0886	
Largest diff. peak and hole	0.846 and -0.618 $e.Å^{-3}$	

Comments:
All non-hydrogen atoms were refined anisotropic. The C-H H atoms were positioned with idealized geometry and refined isotropic with $U_{iso}(H) = 1.2 \cdot U_{eq}(C)$ using a riding model. The water H atoms were not located but considered in the formula. A numerical absorption correction was performed ($T_{min/max}$: 0.7005/0.8289). One phenanthroline ligand is disordered around a centre of inversion, in which also one water molecule is involved. Both of them were refined with half occupancy. The disorder remain constant if the structure refinement is performed in space group *P*1, where all atoms are located in general positions.

Table 2. Atomic coordinates ($\cdot 10^4$) and equivalent isotropic displacement parameters ($Å^2 \cdot 10^3$). U(eq) is defined as one third of the trace of the orthogonalized U_{ij} tensor.

	x	y	z	U(eq)
Sn(1)	5771(1)	3966(1)	4560(1)	32(1)
S(1)	7921(1)	4305(1)	4352(1)	42(1)
S(2)	4880(1)	1702(1)	3962(1)	37(1)
S(3)	5318(1)	5224(1)	6458(1)	41(1)
Fe(1)	7154(1)	1905(1)	3618(1)	32(1)
N(1)	6931(3)	1392(3)	1748(3)	35(1)
N(2)	6428(3)	-281(3)	2730(3)	32(1)
C(1)	7175(4)	2212(4)	1272(4)	45(1)
C(2)	7066(5)	1815(5)	59(4)	53(1)
C(3)	6707(5)	526(5)	-670(4)	50(1)
C(4)	6438(4)	-374(4)	-195(3)	41(1)
C(5)	6027(5)	-1749(5)	-892(4)	53(1)
C(6)	5728(5)	-2590(4)	-408(4)	55(1)
C(7)	5836(4)	-2137(4)	829(4)	45(1)
C(8)	5520(5)	-2966(4)	1387(4)	54(1)
C(9)	5666(5)	-2448(4)	2578(4)	52(1)
C(10)	6119(4)	-1108(4)	3211(3)	41(1)
C(11)	6273(3)	-793(3)	1548(3)	32(1)
C(12)	6564(4)	102(4)	1023(3)	33(1)
N(21)	7763(3)	1787(3)	5183(3)	39(1)
N(22)	9165(3)	1943(3)	3503(3)	42(1)
C(21)	7071(5)	1730(5)	6019(4)	50(1)
C(22)	7507(6)	1652(5)	6995(4)	63(1)
C(23)	8692(6)	1603(6)	7102(4)	72(2)
C(24)	9461(5)	1665(5)	6242(4)	59(1)
C(25)	10748(7)	1661(6)	6283(6)	85(2)
C(26)	11447(6)	1740(6)	5438(6)	79(2)
C(27)	10961(5)	1852(5)	4476(5)	60(1)
C(28)	11656(5)	1957(6)	3591(6)	74(2)
C(29)	11131(5)	2078(6)	2707(6)	77(2)
C(30)	9880(5)	2071(5)	2706(5)	59(1)
C(31)	9706(4)	1850(4)	4391(4)	43(1)

C(32)	8958(4)	1764(4)	5292(4)	43(1)
N(41)	1463(5)	4861(6)	483(5)	77(2)
C(44')	1463(5)	4861(6)	483(5)	77(2)
C(41)	1995(7)	4844(7)	1434(7)	92(2)
C(42)	1412(7)	4948(6)	2382(6)	88(2)
C(43)	254(7)	5099(5)	2395(5)	77(2)
C(44)	-334(5)	5100(5)	1443(4)	65(1)
N(41')	-334(5)	5100(5)	1443(4)	65(1)
C(45)	294(5)	4989(5)	499(4)	56(1)
C(46)	-1589(13)	5373(10)	1502(10)	74(3)
C(47)	-2123(12)	5383(11)	574(12)	74(3)
O(1)	-3009(10)	5163(10)	1433(12)	121(4)

Table 3. Bond lengths [Å] and angles [°].

Sn(1)-S(1)	2.3351(10)	Sn(1)-S(3)	2.4401(9)
Sn(1)-S(2)	2.3531(10)	Sn(1)-S(3A)	2.4508(10)
S(1)-Fe(1)	2.4814(11)	S(2)-Fe(1)	2.5313(11)
S(1)-Sn(1)-S(2)	101.22(3)	S(1)-Sn(1)-S(3A)	116.32(4)
S(1)-Sn(1)-S(3)	117.87(4)	S(2)-Sn(1)-S(3A)	115.23(4)
S(2)-Sn(1)-S(3)	113.82(4)	S(3)-Sn(1)-S(3A)	93.32(3)
Fe(1)-N(21)	2.181(3)	Fe(1)-N(22)	2.247(3)
Fe(1)-N(1)	2.191(3)	Fe(1)-N(2)	2.248(3)
Sn(1)-S(1)-Fe(1)	83.79(3)	Sn(1)-S(3)-Sn(1A)	86.68(3)
Sn(1)-S(2)-Fe(1)	82.34(3)	N(1)-Fe(1)-S(1)	98.11(8)
N(21)-Fe(1)-N(1)	154.72(11)	N(22)-Fe(1)-S(1)	92.03(9)
N(21)-Fe(1)-N(22)	74.42(13)	N(2)-Fe(1)-S(1)	172.83(8)
N(1)-Fe(1)-N(22)	87.25(12)	N(21)-Fe(1)-S(2)	97.26(9)
N(21)-Fe(1)-N(2)	87.23(11)	N(1)-Fe(1)-S(2)	99.66(9)
N(1)-Fe(1)-N(2)	74.75(11)	N(22)-Fe(1)-S(2)	171.08(9)
N(22)-Fe(1)-N(2)	88.27(12)	N(2)-Fe(1)-S(2)	88.12(8)
N(21)-Fe(1)-S(1)	99.75(9)	S(1)-Fe(1)-S(2)	92.57(3)
N(1)-C(1)	1.316(5)	N(21)-C(21)	1.324(5)
N(1)-C(12)	1.361(5)	N(21)-C(32)	1.359(5)
N(2)-C(10)	1.327(5)	N(22)-C(30)	1.316(5)
N(2)-C(11)	1.358(4)	N(22)-C(31)	1.345(5)
C(1)-C(2)	1.407(6)	C(21)-C(22)	1.386(6)
C(2)-C(3)	1.362(6)	C(22)-C(23)	1.362(8)
C(3)-C(4)	1.398(6)	C(23)-C(24)	1.400(8)
C(4)-C(12)	1.404(5)	C(24)-C(32)	1.399(6)
C(4)-C(5)	1.432(6)	C(24)-C(25)	1.447(8)
C(5)-C(6)	1.344(7)	C(25)-C(26)	1.344(9)
C(6)-C(7)	1.429(6)	C(26)-C(27)	1.415(8)
C(7)-C(8)	1.404(6)	C(27)-C(28)	1.389(8)
C(7)-C(11)	1.404(5)	C(27)-C(31)	1.412(6)
C(8)-C(9)	1.368(6)	C(28)-C(29)	1.352(9)

C(9)-C(10)	1.385(6)	C(29)-C(30)	1.401(7)
C(11)-C(12)	1.440(5)	C(31)-C(32)	1.435(6)
C(1)-N(1)-C(12)	117.8(3)	C(21)-N(21)-C(32)	118.1(4)
C(10)-N(2)-C(11)	117.3(3)	C(30)-N(22)-C(31)	116.6(4)
N(1)-C(1)-C(2)	123.1(4)	N(21)-C(21)-C(22)	123.2(5)
C(3)-C(2)-C(1)	119.4(4)	C(23)-C(22)-C(21)	119.1(5)
C(2)-C(3)-C(4)	119.2(4)	C(22)-C(23)-C(24)	119.7(4)
C(3)-C(4)-C(12)	117.9(4)	C(32)-C(24)-C(23)	117.7(5)
C(3)-C(4)-C(5)	123.1(4)	C(32)-C(24)-C(25)	117.9(5)
C(12)-C(4)-C(5)	118.9(4)	C(23)-C(24)-C(25)	124.4(5)
C(6)-C(5)-C(4)	121.5(4)	C(26)-C(25)-C(24)	121.7(5)
C(5)-C(6)-C(7)	120.9(4)	C(25)-C(26)-C(27)	121.2(5)
C(8)-C(7)-C(11)	116.9(4)	C(28)-C(27)-C(31)	117.5(5)
C(8)-C(7)-C(6)	123.6(4)	C(28)-C(27)-C(26)	123.3(5)
C(11)-C(7)-C(6)	119.5(4)	C(31)-C(27)-C(26)	119.2(5)
C(9)-C(8)-C(7)	119.8(4)	C(29)-C(28)-C(27)	119.8(5)
C(8)-C(9)-C(10)	119.0(4)	C(28)-C(29)-C(30)	118.3(5)
N(2)-C(10)-C(9)	123.7(4)	N(22)-C(30)-C(29)	124.6(5)
N(2)-C(11)-C(7)	123.3(3)	N(22)-C(31)-C(27)	123.2(4)
N(2)-C(11)-C(12)	117.4(3)	N(22)-C(31)-C(32)	117.3(3)
C(7)-C(11)-C(12)	119.4(3)	C(27)-C(31)-C(32)	119.5(4)
N(1)-C(12)-C(4)	122.7(3)	N(21)-C(32)-C(24)	122.2(4)
N(1)-C(12)-C(11)	117.6(3)	N(21)-C(32)-C(31)	117.4(4)
C(4)-C(12)-C(11)	119.7(3)	C(24)-C(32)-C(31)	120.4(4)
N(41)-C(41)	1.362(9)	C(44)-C(45)	1.373(6)
N(41)-C(45)	1.372(7)	C(44)-C(46)	1.551(14)
N(41)-C(47A)	1.505(12)	C(45)-C(45A)	1.447(10)
C(41)-C(42)	1.351(10)	C(46)-C(47)	1.331(18)
C(42)-C(43)	1.373(9)	C(47)-N(41A)	1.505(12)
C(43)-C(44)	1.380(8)		
C(41)-N(41)-C(45)	118.2(6)	C(45)-C(44)-C(46)	121.2(6)
C(41)-N(41)-C(47A)	118.4(8)	C(43)-C(44)-C(46)	120.4(6)
C(45)-N(41)-C(47A)	123.1(7)	N(41)-C(45)-C(44)	121.7(5)
C(42)-C(41)-N(41)	122.3(7)	N(41)-C(45)-C(45A)	119.5(5)
C(41)-C(42)-C(43)	118.8(6)	C(44)-C(45)-C(45A)	118.9(6)
C(42)-C(43)-C(44)	121.0(6)	C(47)-C(46)-C(44)	118.9(8)
C(45)-C(44)-C(43)	118.0(5)	C(46)-C(47)-N(41A)	117.9(10)

Symmetry transformations used to generate equivalent atoms: #1 -x+1,-y+1,-z+1 #2 -x,-y+1,-z

Table 4. Anisotropic displacement parameters ($Å^2 \cdot 10^3$). The anisotropic displacement factor exponent takes the form: $-2\pi^2[h^2 a^{*2} U_{11} + ... + 2 h k a^* b^* U_{12}]$

	U_{11}	U_{22}	U_{33}	U_{23}	U_{13}	U_{12}
Sn(1)	39(1)	29(1)	30(1)	11(1)	8(1)	18(1)
S(1)	38(1)	35(1)	49(1)	14(1)	12(1)	13(1)
S(2)	38(1)	30(1)	44(1)	15(1)	9(1)	16(1)
S(3)	62(1)	42(1)	27(1)	14(1)	10(1)	31(1)
Fe(1)	38(1)	35(1)	30(1)	14(1)	8(1)	19(1)
N(1)	41(2)	34(2)	31(1)	15(1)	6(1)	17(1)
N(2)	35(2)	32(2)	31(1)	15(1)	6(1)	15(1)
C(1)	55(2)	40(2)	42(2)	21(2)	6(2)	18(2)
C(2)	70(3)	54(3)	43(2)	31(2)	12(2)	21(2)
C(3)	65(3)	58(3)	32(2)	23(2)	12(2)	24(2)
C(4)	48(2)	45(2)	31(2)	15(2)	8(2)	20(2)
C(5)	71(3)	49(2)	32(2)	10(2)	7(2)	23(2)
C(6)	74(3)	36(2)	42(2)	3(2)	5(2)	22(2)
C(7)	57(3)	34(2)	40(2)	11(2)	6(2)	19(2)
C(8)	73(3)	33(2)	55(3)	17(2)	8(2)	19(2)
C(9)	69(3)	39(2)	54(3)	27(2)	10(2)	20(2)
C(10)	47(2)	42(2)	39(2)	21(2)	8(2)	20(2)
C(11)	33(2)	33(2)	32(2)	13(1)	7(1)	17(1)
C(12)	36(2)	37(2)	30(2)	14(2)	6(1)	17(2)
N(21)	44(2)	35(2)	36(2)	15(1)	4(1)	14(1)
N(22)	36(2)	43(2)	53(2)	24(2)	12(2)	18(1)
C(21)	58(3)	57(3)	40(2)	25(2)	11(2)	22(2)
C(22)	84(4)	63(3)	42(2)	29(2)	7(2)	19(3)
C(23)	95(4)	72(4)	50(3)	34(3)	-16(3)	22(3)
C(24)	68(3)	53(3)	55(3)	22(2)	-12(2)	23(2)
C(25)	83(4)	84(4)	85(4)	29(4)	-33(4)	38(4)
C(26)	56(3)	83(4)	102(5)	34(4)	-7(3)	36(3)
C(27)	44(2)	44(2)	87(4)	22(2)	-2(2)	19(2)
C(28)	39(3)	74(4)	116(5)	43(4)	19(3)	27(2)
C(29)	48(3)	103(5)	108(5)	62(4)	39(3)	40(3)
C(30)	48(3)	74(3)	74(3)	44(3)	23(2)	31(2)
C(31)	39(2)	31(2)	53(2)	13(2)	0(2)	14(2)
C(32)	45(2)	35(2)	44(2)	13(2)	-5(2)	14(2)
N(41)	66(3)	82(4)	72(3)	38(3)	1(3)	9(3)
C(44')	66(3)	82(4)	72(3)	38(3)	1(3)	9(3)
C(41)	85(5)	88(5)	90(5)	39(4)	-6(4)	16(4)
C(42)	96(5)	73(4)	78(4)	40(3)	-17(4)	5(4)
C(43)	100(5)	58(3)	52(3)	28(3)	6(3)	0(3)
C(44)	70(3)	60(3)	50(2)	27(2)	10(2)	4(2)
N(41')	70(3)	60(3)	50(2)	27(2)	10(2)	4(2)
C(45)	52(3)	54(3)	47(2)	24(2)	4(2)	2(2)
C(46)	95(9)	54(6)	61(6)	20(5)	39(6)	21(6)
C(47)	61(7)	58(6)	94(9)	26(6)	30(6)	22(5)
O(1)	76(6)	80(6)	199(12)	48(7)	50(7)	34(5)

Table 5. Hydrogen coordinates ($\cdot 10^4$) and isotropic displacement parameters ($Å^2 \cdot 10^3$).

	x	y	z	U(eq)
H(1)	7433	3096	1760	54
H(2)	7236	2426	-242	63
H(3)	6642	249	-1472	60
H(5)	5965	-2067	-1699	64
H(6)	5446	-3479	-884	66
H(8)	5213	-3864	949	65
H(9)	5464	-2988	2957	62
H(10)	6213	-769	4020	49
H(21)	6253	1743	5946	60
H(22)	6996	1634	7570	76
H(23)	8990	1530	7743	87
H(25)	11100	1603	6911	102
H(26)	12266	1721	5486	95
H(28)	12479	1943	3607	89
H(29)	11590	2164	2116	92
H(30)	9531	2164	2099	70
H(41)	2787	4758	1431	111
H(42)	1789	4918	3016	105
H(43)	-140	5203	3054	93
H(46)	-1963	5528	2175	88
H(47)	-2880	5536	579	89

5.3.8 Messprotokoll der Verbindung $\{[Co(phen)_2]_2[Sn_2S_6]\}$

Table 1. Crystal data and structure refinement for $\{[Co(C_{12}H_8N_2)_2]_2[Sn_2S_6]\}$ ($C_{12}H_8N_2$; phen = 1,10-Phenanthrolin)

Identification code	jh347	
Empirical formula	$\{[Co(C_{12}H_8N_2)_2]_2[Sn_2S_6]\}$	
Crytstal color, habitus	dark red blocks	
Formula weight	1268.42	
Temperature	293(2) K	
Wavelength	0.71073 Å	
Crystal system	monoclinic	
Space group	$P2_1/n$	
Unit cell dimensions	a = 10.7234(4) Å	α= 90°.
	b = 9.8026(2) Å	β= 94.046(3)°.
	c = 24.8913(10) Å	γ = 90°.
Volume	2609.98(15) $Å^3$	
Z	2	
Density (calculated)	1.614 Mg/m^3	
Absorption coefficient	1.851 m^{-1}	
F(000)	1252	
Crystal size	0.14 x 0.10 x 0.04 mm^3	
Theta range for data collection	1.64 to 24.60°.	
Index ranges	$-12 \le h \le 12$, $-11 \le k \le 11$, $-29 \le l \le 29$	
Reflections collected	23024	
Independent reflections	4378 [R(int) = 0.0306]	
Completeness to theta = 24.60°	99.4 %	
Refinement method	Full-matrix least-squares on F^2	
Data / restraints / parameters	4378 / 0 / 299	
Goodness-of-fit on F^2	1.187	
Final R indices [I>2sigma(I)]	R1 = 0.0405, wR2 = 0.1061	
R indices (all data)	R1 = 0.0498, wR2 = 0.1098	
Extinction coefficient	0.0012(2)	
Largest diff. peak and hole	0.572 and -0.356 $e.Å^{-3}$	

Comments:
All non-hydrogen atoms were refined anisotropic. All H atoms were located in difference map but were positioned with idealized geometry and refined isotropic using a riding model. A numerical absorption correction was performed ($T_{min/max}$: 0.6857/0.8625). The structure contains cavities, in which only very small residual electron density are found. Therefore, it might be that some small amount of additional solvent is included.

Table 2. Atomic coordinates ($\cdot 10^4$) and equivalent isotropic displacement parameters ($Å^2 \cdot 10^3$). U(eq) is defined as one third of the trace of the orthogonalized U_{ij} tensor.

	x	y	z	U(eq)
Sn(1)	1244(1)	4369(1)	376(1)	52(1)
S(1)	3392(1)	4453(2)	273(1)	59(1)
S(2)	1255(1)	3113(2)	1181(1)	62(1)
S(3)	61(1)	6508(2)	391(1)	62(1)
Co(1)	3541(1)	3069(1)	1114(1)	53(1)
N(1)	3747(4)	2111(4)	1938(2)	56(1)
N(2)	4030(4)	4723(4)	1665(2)	56(1)
C(1)	3542(6)	832(6)	2080(2)	66(1)
C(2)	3684(6)	360(7)	2609(3)	74(2)
C(3)	4042(7)	1241(7)	3009(3)	80(2)
C(4)	4251(6)	2618(6)	2884(2)	69(2)
C(5)	4600(8)	3639(8)	3281(3)	91(2)
C(6)	4734(7)	4939(8)	3138(3)	85(2)
C(7)	4553(6)	5363(6)	2596(3)	71(2)
C(8)	4677(8)	6713(7)	2429(3)	88(2)
C(9)	4470(8)	7038(7)	1900(3)	98(2)
C(10)	4127(7)	6005(6)	1525(3)	75(2)
C(11)	4231(5)	4384(6)	2190(2)	58(1)
C(12)	4091(5)	2996(5)	2338(2)	56(1)
N(11)	3678(5)	1014(4)	820(2)	60(1)
N(12)	5552(4)	2792(5)	1021(2)	59(1)
C(21)	2740(7)	164(7)	695(2)	75(2)
C(22)	2965(9)	-1189(8)	521(3)	92(2)
C(23)	4155(10)	-1628(7)	493(3)	92(2)
C(24)	5156(8)	-785(6)	624(2)	79(2)
C(25)	6426(9)	-1179(8)	592(3)	92(2)
C(26)	7352(9)	-283(9)	697(3)	101(3)
C(27)	7112(6)	1112(7)	836(3)	77(2)
C(28)	8021(6)	2123(9)	902(3)	86(2)
C(29)	7700(6)	3414(9)	1011(3)	92(2)
C(30)	6441(5)	3710(7)	1065(3)	73(2)
C(31)	5875(5)	1509(6)	894(2)	61(1)
C(32)	4876(6)	550(6)	783(2)	61(1)

Table 3. Bond lengths [Å] and angles [°].

Sn(1)-S(1)	2.3366(14)	Sn(1)-S(3A)	2.4414(13)
Sn(1)-S(2)	2.3528(14)	Sn(1)-S(3)	2.4522(15)
S(1)-Co(1)	2.4907(16)	S(3)-Sn(1A)	2.4414(13)
S(2)-Co(1)	2.4699(15)	Co(1)-N(12)	2.201(4)
Co(1)-N(11)	2.152(5)	Co(1)-N(1)	2.250(4)
Co(1)-N(2)	2.164(4)	S(2)-Sn(1)-S(3)	113.93(5)
S(1)-Sn(1)-S(2)	99.57(5)	S(3A)-Sn(1)-S(3)	92.53(5)
S(1)-Sn(1)-S(3A)	116.25(5)	Sn(1)-S(1)-Co(1)	83.93(5)
S(2)-Sn(1)-S(3A)	116.73(5)	Sn(1)-S(2)-Co(1)	84.06(5)
S(1)-Sn(1)-S(3)	119.13(5)	Sn(1A)-S(3)-Sn(1)	87.47(5)
N(11)-Co(1)-N(2)	153.89(17)	N(12)-Co(1)-S(2)	173.50(13)
N(11)-Co(1)-N(12)	75.98(18)	N(1)-Co(1)-S(2)	88.83(12)
N(2)-Co(1)-N(12)	87.96(17)	N(11)-Co(1)-S(1)	103.03(13)
N(11)-Co(1)-N(1)	85.12(17)	N(2)-Co(1)-S(1)	97.05(12)
N(2)-Co(1)-N(1)	74.45(16)	N(12)-Co(1)-S(1)	89.08(12)
N(12)-Co(1)-N(1)	90.62(16)	N(1)-Co(1)-S(1)	171.51(12)
N(11)-Co(1)-S(2)	97.52(14)	S(2)-Co(1)-S(1)	92.42(5)
N(2)-Co(1)-S(2)	98.13(12)		
		C(5)-C(6)-C(7)	121.8(6)
N(1)-C(1)	1.326(7)	C(8)-C(7)-C(6)	123.7(6)
N(1)-C(12)	1.353(7)	C(8)-C(7)-C(11)	116.9(6)
N(2)-C(10)	1.311(7)	C(6)-C(7)-C(11)	119.4(6)
N(2)-C(11)	1.352(7)	C(9)-C(8)-C(7)	119.9(6)
C(1)-C(2)	1.395(8)	C(8)-C(9)-C(10)	119.5(6)
C(2)-C(3)	1.352(9)	N(2)-C(10)-C(9)	122.3(6)
C(3)-C(4)	1.407(9)	N(2)-C(11)-C(7)	122.5(5)
C(4)-C(12)	1.407(8)	N(2)-C(11)-C(12)	118.2(5)
C(4)-C(5)	1.438(9)	C(7)-C(11)-C(12)	119.3(5)
C(5)-C(6)	1.334(10)	N(1)-C(12)-C(4)	123.4(5)
C(6)-C(7)	1.412(9)	N(1)-C(12)-C(11)	116.9(5)
C(7)-C(8)	1.397(9)	C(4)-C(12)-C(11)	119.6(5)
C(7)-C(11)	1.417(8)	N(11)-C(21)	1.325(7)
C(8)-C(9)	1.357(10)	N(11)-C(32)	1.372(8)
C(9)-C(10)	1.408(9)	N(12)-C(30)	1.310(7)
C(11)-C(12)	1.420(8)	N(12)-C(31)	1.348(7)
C(1)-N(1)-C(12)	116.8(5)	C(21)-C(22)	1.422(10)
C(10)-N(2)-C(11)	118.9(5)	C(22)-C(23)	1.353(11)
N(1)-C(1)-C(2)	123.8(6)	C(23)-C(24)	1.375(11)
C(3)-C(2)-C(1)	119.3(6)	C(24)-C(32)	1.407(8)
C(2)-C(3)-C(4)	119.5(6)	C(24)-C(25)	1.423(11)
C(3)-C(4)-C(12)	117.1(6)	C(25)-C(26)	1.338(12)
C(3)-C(4)-C(5)	123.6(6)	C(26)-C(27)	1.437(10)
C(12)-C(4)-C(5)	119.3(6)	C(27)-C(28)	1.392(10)
C(6)-C(5)-C(4)	120.6(6)	C(27)-C(31)	1.400(9)

C(28)-C(29)	1.344(11)	C(28)-C(27)-C(31)	116.8(6)
C(29)-C(30)	1.397(9)	C(28)-C(27)-C(26)	124.8(7)
C(31)-C(32)	1.437(8)	C(31)-C(27)-C(26)	118.4(7)
C(21)-N(11)-C(32)	118.3(5)	C(29)-C(28)-C(27)	120.5(6)
C(30)-N(12)-C(31)	117.6(5)	C(28)-C(29)-C(30)	118.5(7)
N(11)-C(21)-C(22)	121.1(7)	N(12)-C(30)-C(29)	123.6(7)
C(23)-C(22)-C(21)	119.5(7)	N(12)-C(31)-C(27)	123.0(6)
C(22)-C(23)-C(24)	121.3(7)	N(12)-C(31)-C(32)	117.0(5)
C(23)-C(24)-C(32)	116.5(7)	C(27)-C(31)-C(32)	119.9(6)
C(23)-C(24)-C(25)	123.9(7)	N(11)-C(32)-C(24)	123.2(6)
C(32)-C(24)-C(25)	119.5(7)	N(11)-C(32)-C(31)	117.4(5)
C(26)-C(25)-C(24)	120.7(7)	C(24)-C(32)-C(31)	119.4(6)
C(25)-C(26)-C(27)	121.9(8)		

Symmetry transformations used to generate equivalent atoms:
#1 -x+1,-y+1,-z

Table 4. Anisotropic displacement parameters ($Å^2 \cdot 10^3$). The anisotropic displacement factor exponent takes the form: $-2\pi^2[h^2 a^{*2} U_{11} + ... + 2 h k a^* b^* U_{12}]$

	U_{11}	U_{22}	U_{33}	U_{23}	U_{13}	U_{12}
Sn(1)	50(1)	55(1)	50(1)	1(1)	-4(1)	-2(1)
S(1)	54(1)	62(1)	60(1)	5(1)	1(1)	-2(1)
S(2)	56(1)	71(1)	58(1)	12(1)	2(1)	-1(1)
S(3)	64(1)	56(1)	62(1)	-12(1)	-13(1)	1(1)
Co(1)	53(1)	49(1)	55(1)	0(1)	-3(1)	-2(1)
N(1)	57(2)	52(3)	59(3)	4(2)	-2(2)	1(2)
N(2)	61(3)	51(3)	53(3)	0(2)	-5(2)	3(2)
C(1)	76(4)	57(3)	63(3)	2(3)	-3(3)	-6(3)
C(2)	86(4)	65(4)	72(4)	15(3)	4(3)	1(3)
C(3)	102(5)	74(4)	63(4)	13(3)	-1(3)	7(4)
C(4)	87(4)	63(4)	57(3)	5(3)	-2(3)	8(3)
C(5)	138(7)	82(5)	50(3)	-2(3)	-4(4)	10(5)
C(6)	120(6)	80(5)	53(4)	-12(3)	-8(3)	3(4)
C(7)	86(4)	56(4)	68(4)	-11(3)	-6(3)	4(3)
C(8)	128(6)	58(4)	75(4)	-16(3)	-11(4)	7(4)
C(9)	156(7)	52(4)	82(5)	-3(3)	-12(5)	-10(4)
C(10)	103(5)	50(3)	69(4)	3(3)	-5(3)	0(3)
C(11)	57(3)	59(3)	59(3)	-4(3)	-2(2)	3(3)
C(12)	59(3)	53(3)	54(3)	0(2)	1(2)	7(2)
N(11)	76(3)	48(2)	56(3)	0(2)	0(2)	-7(2)
N(12)	56(2)	58(3)	63(3)	4(2)	-1(2)	2(2)
C(21)	92(4)	66(4)	65(4)	-1(3)	-1(3)	-30(3)
C(22)	137(7)	74(5)	65(4)	3(3)	-1(4)	-46(5)
C(23)	163(8)	54(4)	58(4)	3(3)	7(4)	-8(5)

C(24)	130(6)	54(4)	53(3)	2(3)	5(3)	7(4)
C(25)	129(7)	70(4)	77(5)	9(4)	26(4)	34(5)
C(26)	112(6)	102(6)	89(5)	7(5)	21(5)	47(5)
C(27)	82(4)	86(5)	63(4)	12(3)	2(3)	23(4)
C(28)	57(4)	110(6)	91(5)	14(4)	3(3)	6(4)
C(29)	59(4)	111(6)	105(6)	9(5)	5(4)	-14(4)
C(30)	54(3)	75(4)	88(4)	3(3)	-2(3)	-8(3)
C(31)	69(3)	62(4)	53(3)	5(3)	4(3)	7(3)
C(32)	85(4)	51(3)	48(3)	4(2)	7(3)	3(3)

Table 5. Hydrogen coordinates ($\cdot 10^4$) and isotropic displacement parameters ($Å^2 x\ 10^3$).

	x	y	z	U(eq)
H(1)	3288	213	1811	79
H(2)	3534	-551	2687	89
H(3)	4149	939	3363	96
H(5)	4732	3391	3641	109
H(6)	4952	5583	3402	102
H(8)	4900	7389	2679	106
H(9)	4555	7935	1786	117
H(10)	3965	6242	1165	90
H(21)	1923	459	722	90
H(22)	2298	-1770	428	111
H(23)	4299	-2517	382	110
H(25)	6614	-2070	497	110
H(26)	8175	-570	681	121
H(28)	8856	1904	871	103
H(29)	8303	4096	1049	110
H(30)	6221	4606	1135	87

5.3.9 Messprotokoll der Verbindung $\{[Co(phen)_2]_2[Sn_2S_6]\}\cdot phen\cdot H_2O$

Table 1. Crystal data and structure refinement for $\{[Co(C_{12}H_8N_2)_2]_2[Sn_2S_6]\}\cdot C_{12}H_8N_2\cdot H_2O$ ($C_{12}H_8N_2$; phen = 1,10-Phenanthrolin)

Identification code	jh500	
Empirical formula	$\{[Co(C_{12}H_8N_2)_2]_2[Sn_2S_6]\}\cdot C_{12}H_8N_2\cdot H_2O$	
Crystal color, habitus	dark red blocks	
Formula weight	1466.64	
Temperature	200(2) K	
Wavelength	0.71073 Å	
Crystal system	triclinic	
Space group	$P\bar{1}$	
Unit cell dimensions	a = 11.1548(11) Å	α = 114.481(10)°.
	b = 12.1375(11) Å	β = 88.981(11)°.
	c = 12.6701(11) Å	γ = 110.404(10)°.
Volume	1447.0(2) $Å^3$	
Z	1	
Density (calculated)	1.683 Mg/m^3	
Absorption coefficient	1.685 mm^{-1}	
F(000)	730	
Crystal size	0.17 x 0.10 x 0.05 mm^3	
Theta range for data collection	2.21 to 27.00°.	
Index ranges	$-14 \le h \le 14$, $-15 \le k \le 15$, $-16 \le l \le 16$	
Reflections collected	20374	
Independent reflections	6188 [R(int) = 0.0498]	
Completeness to theta = 27.00°	97.7 %	
Refinement method	Full-matrix least-squares on F^2	
Data / restraints / parameters	6188 / 0 / 380	
Goodness-of-fit on F^2	1.022	
Final R indices [I>2sigma(I)]	R1 = 0.0370, wR2 = 0.0952	
R indices (all data)	R1 = 0.0455, wR2 = 0.0989	
Extinction coefficient	0.0139(9)	
Largest diff. peak and hole	1.291 and -1.378 $e.Å^{-3}$	

Comments:
All non-hydrogen atoms were refined anisotropic. The C-H H atoms were positioned with idealized geometry and refined isotropic with $U_{iso}(H) = 1.2 \cdot U_{eq}(C)$ using a riding model. The water H atoms were not located but conisdered in the formula. A numerical absorption correction was performed ($T_{min/max}$: 0.6713/0.8220). One phenanthroline ligand is disordered arount a center of inversion, in which also one water molecule is involved. Both of them were refined with half occupancy. The disorder remain constant if the structure refinement is performed in space group P1, where all atoms are located in general positions.

Table 2. Atomic coordinates ($\cdot 10^4$) and equivalent isotropic displacement parameters ($Å^2 \cdot 10^3$). U(eq) is defined as one third of the trace of the orthogonalized U_{ij} tensor.

	x	y	z	U(eq)
Sn(1)	5784(1)	3962(1)	4565(1)	12(1)
S(1)	7964(1)	4304(1)	4401(1)	19(1)
S(2)	4895(1)	1687(1)	3940(1)	15(1)
S(3)	5250(1)	5205(1)	6463(1)	18(1)
Co(1)	7193(1)	1908(1)	3623(1)	12(1)
N(1)	6958(2)	1419(2)	1775(2)	14(1)
N(2)	6449(2)	-261(2)	2753(2)	12(1)
C(1)	7202(3)	2253(3)	1305(3)	20(1)
C(2)	7109(3)	1867(3)	90(3)	26(1)
C(3)	6719(3)	563(3)	-656(3)	25(1)
C(4)	6440(3)	-351(3)	-189(2)	18(1)
C(5)	6007(3)	-1731(3)	-907(3)	25(1)
C(6)	5705(4)	-2578(3)	-418(3)	30(1)
C(7)	5821(3)	-2126(3)	832(3)	21(1)
C(8)	5515(4)	-2957(3)	1391(3)	31(1)
C(9)	5664(4)	-2440(3)	2588(3)	26(1)
C(10)	6145(3)	-1082(3)	3234(3)	17(1)
C(11)	6280(3)	-774(3)	1559(2)	13(1)
C(12)	6576(3)	128(3)	1042(2)	13(1)
N(21)	7765(2)	1801(2)	5164(2)	17(1)
N(22)	9190(2)	1969(3)	3471(2)	19(1)
C(21)	7054(3)	1750(3)	6006(3)	23(1)
C(22)	7493(4)	1662(4)	6985(3)	33(1)
C(23)	8690(4)	1619(4)	7095(3)	40(1)
C(24)	9476(4)	1681(4)	6229(3)	31(1)
C(25)	10764(4)	1675(5)	6256(4)	46(1)
C(26)	11474(4)	1750(4)	5406(4)	43(1)
C(27)	10983(3)	1856(3)	4425(3)	31(1)
C(28)	11695(4)	1957(4)	3520(4)	40(1)
C(29)	11159(4)	2082(5)	2643(4)	43(1)
C(30)	9909(3)	2081(4)	2650(3)	31(1)
C(31)	9730(3)	1869(3)	4366(3)	21(1)

C(32)	8971(3)	1781(3)	5267(3)	20(1)
N(41)	1471(4)	4854(4)	429(3)	49(1)
C(44')	1471(4)	4854(4)	429(3)	49(1)
C(41)	2054(5)	4823(5)	1383(4)	59(1)
C(42)	1456(5)	4948(4)	2361(4)	54(1)
C(43)	283(5)	5084(4)	2392(3)	45(1)
C(44)	-305(4)	5101(4)	1465(3)	41(1)
N(41')	-305(4)	5101(4)	1465(3)	41(1)
C(45)	310(4)	4987(4)	499(3)	33(1)
C(46)	-1636(8)	5364(7)	1551(7)	38(2)
C(47)	-2183(8)	5391(8)	644(8)	42(2)
O(1)	-2999(6)	5181(7)	1456(7)	63(2)

Table 3. Bond lengths [Å] and angles [°].

Sn(1)-S(1)	2.3404(8)	Sn(1)-S(3)	2.4459(8)
Sn(1)-S(2)	2.3533(8)	Sn(1)-S(3A)	2.4514(8)
S(1)-Co(1)	2.4647(9)	S(3)-Sn(1A)	2.4514(8)
S(2)-Co(1)	2.5256(9)	Co(1)-N(22)	2.211(3)
Co(1)-N(21)	2.134(2)	Co(1)-N(2)	2.222(2)
Co(1)-N(1)	2.159(2)	S(1)-Sn(1)-S(3A)	116.34(3)
S(1)-Sn(1)-S(2)	100.90(3)	S(2)-Sn(1)-S(3A)	115.63(3)
S(1)-Sn(1)-S(3)	118.05(3)	S(3)-Sn(1)-S(3A)	93.16(2)
S(2)-Sn(1)-S(3)	113.76(3)	Sn(1)-S(3)-Sn(1A)	86.84(2)
Sn(1)-S(1)-Co(1)	83.79(3)	N(1)-Co(1)-S(1)	98.60(7)
Sn(1)-S(2)-Co(1)	82.20(3)	N(22)-Co(1)-S(1)	91.08(7)
N(21)-Co(1)-N(1)	156.43(10)	N(2)-Co(1)-S(1)	174.45(6)
N(21)-Co(1)-N(22)	76.16(10)	N(21)-Co(1)-S(2)	97.65(7)
N(1)-Co(1)-N(22)	87.33(9)	N(1)-Co(1)-S(2)	97.63(7)
N(21)-Co(1)-N(2)	87.11(9)	N(22)-Co(1)-S(2)	173.05(7)
N(1)-Co(1)-N(2)	75.96(9)	N(2)-Co(1)-S(2)	86.73(6)
N(22)-Co(1)-N(2)	89.77(9)	S(1)-Co(1)-S(2)	92.97(3)
N(21)-Co(1)-S(1)	98.42(7)		
N(1)-C(1)	1.326(4)	C(7)-C(11)	1.407(4)
N(1)-C(12)	1.357(4)	C(8)-C(9)	1.368(5)
N(2)-C(10)	1.320(4)	C(9)-C(10)	1.398(5)
N(2)-C(11)	1.364(3)	C(11)-C(12)	1.439(4)
C(1)-C(2)	1.405(4)	C(1)-N(1)-C(12)	118.1(2)
C(2)-C(3)	1.372(5)	C(10)-N(2)-C(11)	117.7(2)
C(3)-C(4)	1.405(5)	N(1)-C(1)-C(2)	123.2(3)
C(4)-C(12)	1.410(4)	C(3)-C(2)-C(1)	119.0(3)
C(4)-C(5)	1.433(4)	C(2)-C(3)-C(4)	119.4(3)
C(5)-C(6)	1.354(5)	C(3)-C(4)-C(12)	117.6(3)
C(6)-C(7)	1.437(4)	C(3)-C(4)-C(5)	122.9(3)
C(7)-C(8)	1.407(5)	C(12)-C(4)-C(5)	119.4(3)

C(6)-C(5)-C(4)	120.8(3)	C(27)-C(31)	1.408(4)
C(5)-C(6)-C(7)	121.3(3)	C(28)-C(29)	1.357(6)
C(8)-C(7)-C(11)	117.0(3)	C(29)-C(30)	1.393(5)
C(8)-C(7)-C(6)	123.9(3)	C(31)-C(32)	1.427(5)
C(11)-C(7)-C(6)	119.1(3)	C(21)-N(21)-C(32)	118.6(3)
C(9)-C(8)-C(7)	119.9(3)	C(30)-N(22)-C(31)	117.0(3)
C(8)-C(9)-C(10)	118.8(3)	N(21)-C(21)-C(22)	122.3(3)
N(2)-C(10)-C(9)	123.6(3)	C(23)-C(22)-C(21)	120.0(3)
N(2)-C(11)-C(7)	122.9(3)	C(22)-C(23)-C(24)	119.5(3)
N(2)-C(11)-C(12)	117.3(2)	C(23)-C(24)-C(32)	117.4(3)
C(7)-C(11)-C(12)	119.8(2)	C(23)-C(24)-C(25)	124.8(3)
N(1)-C(12)-C(4)	122.7(3)	C(32)-C(24)-C(25)	117.8(4)
N(1)-C(12)-C(11)	117.7(2)	C(26)-C(25)-C(24)	122.0(3)
C(4)-C(12)-C(11)	119.6(3)	C(25)-C(26)-C(27)	121.1(4)
N(21)-C(21)	1.327(4)	C(28)-C(27)-C(31)	117.9(3)
N(21)-C(32)	1.363(4)	C(28)-C(27)-C(26)	123.4(3)
N(22)-C(30)	1.325(4)	C(31)-C(27)-C(26)	118.7(4)
N(22)-C(31)	1.361(4)	C(29)-C(28)-C(27)	119.1(3)
C(21)-C(22)	1.399(4)	C(28)-C(29)-C(30)	119.2(4)
C(22)-C(23)	1.366(6)	N(22)-C(30)-C(29)	124.2(3)
C(23)-C(24)	1.403(6)	N(22)-C(31)-C(27)	122.6(3)
C(24)-C(32)	1.418(4)	N(22)-C(31)-C(32)	117.2(3)
C(24)-C(25)	1.440(5)	C(27)-C(31)-C(32)	120.2(3)
C(25)-C(26)	1.341(6)	N(21)-C(32)-C(24)	122.3(3)
C(26)-C(27)	1.437(5)	N(21)-C(32)-C(31)	117.6(3)
C(27)-C(28)	1.406(6)	C(24)-C(32)-C(31)	120.1(3)
N(41)-C(45)	1.357(6)	C(44)-C(45)	1.372(5)
N(41)-C(41)	1.403(6)	C(44)-C(46)	1.617(10)
N(41)-C(47B)	1.536(9)	C(45)-C(45B)	1.469(7)
C(41)-C(42)	1.374(7)	C(46)-C(47)	1.328(12)
C(42)-C(43)	1.373(7)	C(47)-N(41B)	1.536(9)
C(43)-C(44)	1.366(5)	C(43)-C(44)-C(46)	120.4(4)
C(45)-N(41)-C(41)	118.2(4)	C(45)-C(44)-C(46)	121.0(4)
C(45)-N(41)-C(47B)	126.6(5)	N(41)-C(45)-C(44)	122.7(4)
C(41)-N(41)-C(47B)	115.0(5)	N(41)-C(45)-C(45B)	118.5(4)
C(42)-C(41)-N(41)	119.8(5)	C(44)-C(45)-C(45B)	118.8(5)
C(43)-C(42)-C(41)	119.8(4)	C(47)-C(46)-C(44)	119.4(6)
C(44)-C(43)-C(42)	121.1(4)	C(46)-C(47)-N(41B)	115.3(7)
C(43)-C(44)-C(45)	118.4(4)		

Symmetry transformations used to generate equivalent atoms:
#1 -x+1,-y+1,-z+1 #2 -x,-y+1,-z

Table 4. Anisotropic displacement parameters ($Å^2 \cdot 10^3$). The anisotropic displacement factor exponent takes the form: $-2\pi^2[h^2 a^{*2} U_{11} + ... + 2 h k a^* b^* U_{12}]$

	U_{11}	U_{22}	U_{33}	U_{23}	U_{13}	U_{12}
Sn(1)	19(1)	9(1)	9(1)	3(1)	4(1)	7(1)
S(1)	18(1)	14(1)	21(1)	5(1)	5(1)	5(1)
S(2)	17(1)	10(1)	17(1)	5(1)	2(1)	6(1)
S(3)	34(1)	17(1)	8(1)	6(1)	5(1)	16(1)
Co(1)	17(1)	12(1)	8(1)	5(1)	3(1)	7(1)
N(1)	21(1)	12(1)	9(1)	5(1)	2(1)	7(1)
N(2)	14(1)	13(1)	12(1)	7(1)	2(1)	7(1)
C(1)	31(2)	16(2)	16(1)	9(1)	5(1)	9(1)
C(2)	40(2)	26(2)	20(2)	18(1)	6(1)	12(2)
C(3)	31(2)	31(2)	13(1)	13(1)	4(1)	8(2)
C(4)	20(2)	21(2)	9(1)	5(1)	2(1)	7(1)
C(5)	34(2)	23(2)	10(1)	1(1)	2(1)	9(2)
C(6)	44(2)	16(2)	16(2)	-3(1)	1(1)	8(2)
C(7)	28(2)	14(2)	19(1)	5(1)	3(1)	7(1)
C(8)	46(2)	10(2)	30(2)	6(1)	7(2)	8(2)
C(9)	38(2)	18(2)	25(2)	15(1)	6(1)	9(2)
C(10)	22(2)	19(2)	17(1)	11(1)	5(1)	10(1)
C(11)	17(1)	13(1)	9(1)	4(1)	2(1)	8(1)
C(12)	14(1)	15(2)	12(1)	6(1)	4(1)	8(1)
N(21)	22(1)	16(1)	12(1)	6(1)	-1(1)	5(1)
N(22)	17(1)	20(1)	23(1)	11(1)	4(1)	9(1)
C(21)	27(2)	25(2)	16(1)	12(1)	1(1)	5(1)
C(22)	44(2)	35(2)	20(2)	17(2)	1(2)	8(2)
C(23)	49(2)	42(2)	25(2)	19(2)	-11(2)	9(2)
C(24)	33(2)	32(2)	28(2)	15(2)	-10(1)	10(2)
C(25)	40(2)	55(3)	47(2)	22(2)	-18(2)	21(2)
C(26)	26(2)	50(3)	54(2)	22(2)	-11(2)	18(2)
C(27)	20(2)	23(2)	47(2)	13(2)	-4(2)	8(1)
C(28)	20(2)	39(2)	63(3)	23(2)	8(2)	14(2)
C(29)	30(2)	56(3)	58(3)	36(2)	22(2)	21(2)
C(30)	27(2)	39(2)	37(2)	25(2)	13(2)	16(2)
C(31)	17(2)	14(2)	26(2)	5(1)	-4(1)	4(1)
C(32)	22(2)	16(2)	19(1)	5(1)	-7(1)	6(1)
N(41)	47(2)	48(3)	34(2)	20(2)	-3(2)	-6(2)
C(44')	47(2)	48(3)	34(2)	20(2)	-3(2)	-6(2)
C(41)	56(3)	51(3)	52(3)	22(2)	-3(2)	0(2)
C(42)	63(3)	40(3)	39(2)	23(2)	-18(2)	-11(2)
C(43)	58(3)	33(2)	30(2)	20(2)	-5(2)	-9(2)
C(44)	49(2)	32(2)	21(2)	14(1)	-2(2)	-12(2)
N(41')	49(2)	32(2)	21(2)	14(1)	-2(2)	-12(2)
C(45)	32(2)	29(2)	20(2)	12(1)	-2(1)	-9(2)
C(46)	51(5)	20(4)	32(4)	8(3)	18(3)	6(3)
C(47)	33(4)	26(4)	62(5)	13(4)	22(4)	13(3)
O(1)	47(4)	44(4)	99(6)	27(4)	34(4)	25(3)

Table 5. Hydrogen coordinates ($\cdot 10^4$) and isotropic displacement parameters ($Å^2 \cdot 10^3$).

	x	y	z	U(eq)
H(1)	7452	3156	1814	25
H(2)	7314	2499	-210	32
H(3)	6637	280	-1481	30
H(5)	5932	-2055	-1736	30
H(6)	5410	-3489	-911	36
H(8)	5205	-3877	937	37
H(9)	5445	-2993	2974	31
H(10)	6260	-732	4066	21
H(21)	6217	1774	5942	28
H(22)	6958	1631	7573	39
H(23)	8988	1549	7753	47
H(25)	11121	1615	6896	55
H(26)	12316	1733	5452	51
H(28)	12539	1939	3522	47
H(29)	11630	2169	2032	51
H(30)	9550	2165	2026	37
H(41)	2860	4717	1354	71
H(42)	1852	4939	3013	65
H(43)	-127	5169	3070	54
H(46)	-2024	5498	2245	45
H(47)	-2960	5550	658	51

5.3.10 Messprotokoll der Verbindung {[Ni(phen)$_2$]$_2$[Sn$_2$S$_6$]}·2,2'-bipy

Table 1. Crystal data and structure refinement for {[Ni($C_{12}H_8N_2$)$_2$]$_2$[Sn$_2$S$_6$]}·$C_{10}H_8N_2$ ($C_{12}H_8N_2$; phen = 1,10-Phenanthrolin; $C_{10}H_8N_2$; 2,2'-bipy = 2,2'-Bipyridin)

Identification code	jh1262	
Empirical formula	{[Ni($C_{12}H_8N_2$)$_2$]$_2$[Sn$_2$S$_6$]}·$C_{10}H_8N_2$	
Crystal color, habitus	red violet blocks	
Formula weight	1424.16	
Temperature	200(2) K	
Wavelength	0.71073 Å	
Crystal system	monoclinic	
Space group	$P2_1/n$	
Unit cell dimensions	a = 10.5715(2) Å	α= 90°.
	b = 9.9086(2) Å	β= 92.8000(10)°.
	c = 24.9960(4) Å	γ = 90°.
Volume	2615.17(8) Å^3	
Z	2	
Density (calculated)	1.809 Mg/m^3	
Absorption coefficient	1.946 mm^{-1}	
F(000)	1420	
Crystal size	0.09 x 0.14 x 0.18 mm^3	
Theta range for data collection	1.63 to 27.93°.	
Index ranges	-13<=h<=13, -13<=k<=13, -32<=l<=32	
Reflections collected	44107	
Independent reflections	6238 [R(int) = 0.0444]	
Completeness to theta = 27.93°	99.7 %	
Refinement method	Full-matrix least-squares on F^2	
Data / restraints / parameters	6238 / 15 / 407	
Goodness-of-fit on F^2	1.059	
Final R indices [I>2sigma(I)]	R1 = 0.0480, wR2 = 0.1274	
R indices (all data)	R1 = 0.0520, wR2 = 0.1307	
Extinction coefficient	0.0126(8)	
Largest diff. peak and hole	1.024 and -0.770 e.Å^{-3}	

Comments

All non H atoms were refined anisotropic. A numerical absorption correction was performed ($T_{min/max}$: 0.6253, 0.8131). The C-H H atoms were positioned with idealized geometry and were refined isotropic with $U_{iso}(H) = 1.2\ U_{eq}(C)$ using a riding model. The asymmetric unit consists of one $[Sn_2S_6]$ anions and one 2,2'-bipyridine ligand that are located on centers of inversion as well as one Ni cation and one phenanthroline ligand in general positions. The 2,2'-bipyridine ligand is disordered and was refined with half occupation and restraints for bond lengths and bond angles.

Table 2. Atomic coordinates ($\cdot 10^4$) and equivalent isotropic displacement parameters ($Å^2 \cdot 10^3$). U(eq) is defined as one third of the trace of the orthogonalized U_{ij} tensor.

	x	y	z	U(eq)
Sn(1)	1243(1)	5556(1)	394(1)	38(1)
S(1)	0(1)	3466(1)	363(1)	45(1)
S(2)	1218(1)	6656(1)	1225(1)	43(1)
S(3)	3412(1)	5521(1)	267(1)	42(1)
Ni(1)	3544(1)	6857(1)	1116(1)	38(1)
N(1)	4024(3)	5186(3)	1615(1)	40(1)
N(2)	3751(3)	7768(3)	1900(1)	41(1)
C(1)	4162(4)	3928(4)	1465(2)	49(1)
C(2)	4456(4)	2874(4)	1835(2)	54(1)
C(3)	4598(4)	3171(4)	2366(2)	50(1)
C(4)	4457(4)	4500(4)	2538(2)	45(1)
C(5)	4569(4)	4905(4)	3090(2)	53(1)
C(6)	4400(4)	6190(4)	3236(2)	54(1)
C(7)	4113(4)	7223(4)	2844(1)	45(1)
C(8)	3953(4)	8586(4)	2974(2)	51(1)
C(9)	3693(4)	9496(4)	2571(2)	49(1)
C(10)	3599(3)	9048(4)	2043(2)	44(1)
C(11)	4009(3)	6862(3)	2300(1)	40(1)
C(12)	4174(3)	5482(3)	2142(1)	40(1)
N(21)	3417(3)	8817(3)	792(1)	45(1)
N(22)	5454(3)	7270(3)	967(1)	44(1)
C(21)	2388(5)	9543(4)	684(2)	54(1)
C(22)	2438(6)	10902(5)	522(2)	70(1)
C(23)	3587(6)	11505(4)	477(2)	70(2)
C(24)	4701(5)	10768(4)	593(2)	59(1)
C(25)	5968(7)	11298(5)	551(2)	76(2)
C(26)	6993(6)	10508(6)	646(2)	75(2)
C(27)	6884(5)	9110(5)	779(2)	60(1)
C(28)	7898(4)	8191(6)	827(2)	67(1)
C(29)	7669(4)	6869(6)	913(2)	67(1)
C(30)	6426(4)	6445(5)	985(2)	55(1)
C(31)	5661(4)	8584(4)	842(1)	47(1)
C(32)	4569(4)	9409(4)	749(2)	48(1)

N(41)	7787(15)	2597(14)	2687(5)	75(3)
C(41)	7577(10)	1533(12)	2367(4)	74(3)
C(42)	7471(12)	1696(14)	1820(4)	77(3)
C(43)	7715(17)	2920(20)	1658(7)	95(5)
C(44)	7973(16)	4055(18)	1978(6)	91(5)
C(45)	7967(16)	3875(16)	2518(6)	89(4)
N(51)	7391(11)	-61(12)	3081(3)	81(3)
C(51)	7349(10)	149(13)	2555(4)	77(3)
C(52)	7191(15)	-910(20)	2201(5)	95(5)
C(53)	7080(40)	-2100(30)	2413(11)	190(20)
C(54)	7166(12)	-2407(15)	2968(7)	87(4)
C(55)	7245(17)	-1300(15)	3284(7)	76(4)

Table 3. Bond lengths [Å] and angles [°].

Sn(1)-S(3)	2.3296(9)	Sn(1)-S(1)	2.4524(9)
Sn(1)-S(2)	2.3475(9)	S(1)-Sn(1)#1	2.4488(9)
Sn(1)-S(1)#1	2.4488(9)	S(3)-Sn(1)-S(1)	120.84(3)
S(3)-Sn(1)-S(2)	100.43(3)	S(2)-Sn(1)-S(1)	113.00(3)
S(3)-Sn(1)-S(1)#1	113.30(3)	S(1)#1-Sn(1)-S(1)	92.46(3)
S(2)-Sn(1)-S(1)#1	118.10(3)	Sn(1)#1-S(1)-Sn(1)	87.54(3)
Sn(1)-S(2)-Ni(1)	83.47(3)	Sn(1)-S(3)-Ni(1)	83.75(3)
S(2)-Ni(1)	2.4946(10)	S(3)-Ni(1)	2.4984(10)
Ni(1)-N(21)	2.106(3)	Ni(1)-N(1)	2.120(3)
Ni(1)-N(22)	2.112(3)	Ni(1)-N(2)	2.161(3)
N(21)-Ni(1)-N(1)	162.82(12)	N(2)-Ni(1)-S(2)	89.46(8)
N(22)-Ni(1)-N(1)	92.95(12)	N(21)-Ni(1)-S(3)	99.34(8)
N(21)-Ni(1)-N(2)	88.00(11)	N(22)-Ni(1)-S(3)	88.13(9)
N(22)-Ni(1)-N(2)	91.35(11)	N(1)-Ni(1)-S(3)	95.04(8)
N(1)-Ni(1)-N(2)	77.38(11)	N(2)-Ni(1)-S(3)	172.36(8)
N(21)-Ni(1)-S(2)	94.11(9)	S(2)-Ni(1)-S(3)	92.08(3)
N(22)-Ni(1)-S(2)	172.28(9)	N(21)-Ni(1)-N(22)	78.25(12)
N(1)-Ni(1)-S(2)	94.72(8)		
N(1)-C(1)	1.312(5)	N(21)-C(21)	1.322(5)
N(1)-C(12)	1.353(5)	N(21)-C(32)	1.360(5)
N(2)-C(10)	1.330(4)	N(22)-C(30)	1.312(5)
N(2)-C(11)	1.361(4)	N(22)-C(31)	1.359(5)
C(1)-C(2)	1.420(6)	C(21)-C(22)	1.408(6)
C(2)-C(3)	1.360(6)	C(22)-C(23)	1.363(8)
C(3)-C(4)	1.396(5)	C(23)-C(24)	1.404(8)
C(4)-C(12)	1.409(5)	C(24)-C(32)	1.411(5)
C(4)-C(5)	1.436(6)	C(24)-C(25)	1.447(8)
C(5)-C(6)	1.339(6)	C(25)-C(26)	1.348(9)
C(6)-C(7)	1.440(6)	C(26)-C(27)	1.431(7)
C(7)-C(8)	1.401(5)	C(27)-C(28)	1.407(8)

C(7)-C(11)	1.404(5)	C(27)-C(31)	1.410(6)
C(8)-C(9)	1.369(6)	C(28)-C(29)	1.350(8)
C(9)-C(10)	1.391(5)	C(29)-C(30)	1.401(6)
C(11)-C(12)	1.436(5)	C(31)-C(32)	1.424(6)
C(1)-N(1)-C(12)	118.3(3)	C(21)-N(21)-C(32)	118.7(3)
C(10)-N(2)-C(11)	117.1(3)	C(30)-N(22)-C(31)	118.1(4)
N(1)-C(1)-C(2)	122.5(4)	N(21)-C(21)-C(22)	122.5(5)
C(3)-C(2)-C(1)	119.1(4)	C(23)-C(22)-C(21)	119.3(5)
C(2)-C(3)-C(4)	119.8(4)	C(22)-C(23)-C(24)	119.8(4)
C(3)-C(4)-C(12)	117.2(4)	C(23)-C(24)-C(32)	117.4(5)
C(3)-C(4)-C(5)	123.7(4)	C(23)-C(24)-C(25)	124.5(4)
C(12)-C(4)-C(5)	119.1(3)	C(32)-C(24)-C(25)	118.1(5)
C(6)-C(5)-C(4)	121.4(4)	C(26)-C(25)-C(24)	121.0(4)
C(5)-C(6)-C(7)	121.1(4)	C(25)-C(26)-C(27)	122.0(5)
C(8)-C(7)-C(11)	117.7(3)	C(28)-C(27)-C(31)	116.8(5)
C(8)-C(7)-C(6)	123.4(4)	C(28)-C(27)-C(26)	125.2(5)
C(11)-C(7)-C(6)	118.8(3)	C(31)-C(27)-C(26)	117.9(5)
C(9)-C(8)-C(7)	119.1(4)	C(29)-C(28)-C(27)	120.0(4)
C(8)-C(9)-C(10)	119.3(3)	C(28)-C(29)-C(30)	119.2(5)
N(2)-C(10)-C(9)	123.7(3)	N(22)-C(30)-C(29)	123.1(5)
N(2)-C(11)-C(7)	123.1(3)	N(22)-C(31)-C(27)	122.5(4)
N(2)-C(11)-C(12)	116.7(3)	N(22)-C(31)-C(32)	116.7(3)
C(7)-C(11)-C(12)	120.2(3)	C(27)-C(31)-C(32)	120.7(4)
N(1)-C(12)-C(4)	123.0(3)	N(21)-C(32)-C(24)	122.3(4)
N(1)-C(12)-C(11)	117.7(3)	N(21)-C(32)-C(31)	117.5(3)
C(4)-C(12)-C(11)	119.3(3)	C(24)-C(32)-C(31)	120.2(4)
N(41)-C(41)	1.335(14)	N(51)-C(51)	1.329(12)
N(41)-C(45)	1.351(18)	N(51)-C(55)	1.340(18)
C(41)-C(42)	1.375(13)	C(51)-C(52)	1.374(15)
C(41)-C(51)	1.474(19)	C(52)-C(53)	1.31(3)
C(42)-C(43)	1.30(2)	C(53)-C(54)	1.42(3)
C(44)-C(45)	1.362(18)	C(54)-C(55)	1.352(17)
C(41)-N(41)-C(45)	125.0(13)	C(51)-N(51)-C(55)	121.3(12)
N(41)-C(41)-C(42)	120.4(12)	N(51)-C(51)-C(52)	121.0(13)
N(41)-C(41)-C(51)	124.6(10)	N(51)-C(51)-C(41)	117.6(10)
C(42)-C(41)-C(51)	114.8(10)	C(52)-C(51)-C(41)	121.2(11)
C(43)-C(42)-C(41)	114.2(14)	C(53)-C(52)-C(51)	116.1(16)
C(42)-C(43)-C(44)	127.1(16)	C(52)-C(53)-C(54)	125.8(19)
C(45)-C(44)-C(43)	116.8(14)	C(55)-C(54)-C(53)	113.5(15)
N(41)-C(45)-C(44)	116.1(16)	N(51)-C(55)-C(54)	121.8(16)

Table 4. Anisotropic displacement parameters ($Å^2 \cdot 10^3$). The anisotropic displacement factor exponent takes the form: $-2\pi^2[h^2 a^{*2} U_{11} + ... + 2 h k a^* b^* U_{12}]$

	U_{11}	U_{22}	U_{33}	U_{23}	U_{13}	U_{12}
Sn(1)	38(1)	39(1)	36(1)	-1(1)	0(1)	1(1)
S(1)	48(1)	38(1)	47(1)	6(1)	-5(1)	-1(1)
S(2)	42(1)	48(1)	39(1)	-5(1)	2(1)	0(1)
S(3)	40(1)	46(1)	41(1)	-3(1)	3(1)	1(1)
Ni(1)	39(1)	36(1)	38(1)	0(1)	1(1)	1(1)
N(1)	42(1)	37(1)	41(1)	-1(1)	1(1)	0(1)
N(2)	40(1)	40(1)	41(1)	-1(1)	2(1)	1(1)
C(1)	59(2)	41(2)	48(2)	-3(2)	-2(2)	1(2)
C(2)	65(2)	39(2)	59(2)	0(2)	-2(2)	4(2)
C(3)	54(2)	44(2)	52(2)	10(2)	0(2)	-1(2)
C(4)	43(2)	44(2)	48(2)	6(1)	1(1)	-4(1)
C(5)	60(2)	56(2)	43(2)	9(2)	1(2)	-6(2)
C(6)	66(2)	61(2)	37(2)	2(2)	5(2)	-9(2)
C(7)	47(2)	49(2)	40(2)	-2(1)	3(1)	-4(2)
C(8)	54(2)	55(2)	44(2)	-9(2)	9(2)	-4(2)
C(9)	50(2)	43(2)	54(2)	-9(2)	6(2)	-1(1)
C(10)	47(2)	38(2)	48(2)	-3(1)	3(1)	-1(1)
C(11)	39(2)	42(2)	38(2)	0(1)	4(1)	-3(1)
C(12)	38(2)	42(2)	39(2)	2(1)	0(1)	-2(1)
N(21)	54(2)	42(2)	38(1)	2(1)	5(1)	5(1)
N(22)	40(1)	49(2)	43(2)	-3(1)	2(1)	-2(1)
C(21)	67(3)	52(2)	42(2)	4(2)	7(2)	19(2)
C(22)	107(4)	55(2)	47(2)	5(2)	11(2)	32(3)
C(23)	132(5)	41(2)	38(2)	1(2)	9(2)	8(2)
C(24)	98(3)	42(2)	37(2)	-1(1)	8(2)	-10(2)
C(25)	126(5)	57(3)	47(2)	-1(2)	11(3)	-34(3)
C(26)	90(4)	84(4)	50(3)	-3(2)	8(2)	-43(3)
C(27)	62(2)	81(3)	38(2)	-2(2)	4(2)	-27(2)
C(28)	46(2)	108(4)	47(2)	-3(2)	2(2)	-20(2)
C(29)	43(2)	97(4)	61(3)	-2(2)	5(2)	2(2)
C(30)	43(2)	66(2)	55(2)	-3(2)	4(2)	5(2)
C(31)	54(2)	53(2)	35(2)	-3(1)	3(1)	-11(2)
C(32)	65(2)	43(2)	36(2)	-1(1)	7(2)	-6(2)
N(41)	64(6)	94(8)	66(5)	-9(6)	-10(5)	18(6)
C(41)	54(5)	110(9)	58(5)	-4(6)	1(4)	25(5)
C(42)	78(7)	101(9)	49(5)	-2(6)	-6(5)	17(6)
C(43)	78(8)	123(14)	85(10)	21(12)	4(7)	18(11)
C(44)	93(10)	98(11)	81(10)	27(9)	-12(8)	28(9)
C(45)	86(9)	85(9)	97(12)	18(9)	1(9)	20(7)
N(51)	89(7)	102(7)	53(5)	-14(5)	6(4)	7(6)
C(51)	52(5)	123(10)	55(5)	-14(6)	-2(4)	18(6)
C(52)	65(7)	152(16)	66(8)	-49(10)	0(7)	-8(8)
C(53)	108(19)	190(30)	260(40)	-140(30)	20(20)	-20(20)
C(54)	69(7)	104(10)	89(9)	-35(9)	11(7)	-24(7)
C(55)	76(8)	85(10)	67(9)	-16(8)	-8(7)	-6(8)

Table 5. Hydrogen coordinates ($\cdot 10^4$) and isotropic displacement parameters ($Å^2 \cdot 10^3$).

	x	y	z	U(eq)
H(1)	4062	3714	1095	59
H(2)	4552	1973	1714	65
H(3)	4792	2476	2619	60
H(5)	4767	4246	3358	63
H(6)	4471	6424	3605	65
H(8)	4023	8874	3336	61
H(9)	3578	10424	2651	59
H(10)	3416	9694	1769	53
H(21)	1583	9132	716	64
H(22)	1680	11394	445	84
H(23)	3634	12421	368	84
H(25)	6080	12217	456	92
H(26)	7812	10891	624	90
H(28)	8743	8499	798	80
H(29)	8344	6235	924	80
H(30)	6278	5515	1051	66
H(42A)	7255	972	1584	92
H(43A)	7703	3034	1280	114
H(44A)	8136	4900	1816	109
H(45A)	8088	4613	2758	107
H(52A)	7174	-760	1826	113
H(53A)	6863	-2808	2167	222
H(54A)	7180	-3319	3086	105
H(55A)	7227	-1429	3660	92

5.3.11 Messprotokoll der Verbindung $\{[Ni(phen)_2]_2[Sn_2S_6]\}\cdot 4,4'bipy\cdot ½H_2O$

Table 1. Crystal data and structure refinement for for $\{[Ni(C_{12}H_8N_2)_2]_2[Sn_2S_6]\}\cdot C_{10}H_8N_2\cdot ½H_2O$ ($C_{12}H_8N_2$; phen = 1,10-Phenanthrolin; $C_{10}H_8N_2$; 4,4'-bipy = 4,4'-Bipyridin)

Identification code	jh483	
Empirical formula	$\{[Ni(C_{12}H_8N_2)_2]_2[Sn_2S_6]\}\cdot C_{10}H_8N_2\cdot ½H_2O$	
Crystal color, habitus	red violet blocks	
Formula weight	1442.18	
Temperature	200(2) K	
Wavelength	0.71073 Å	
Crystal system	monoclinic	
Space group	*C*2/*c*	
Unit cell dimensions	a = 18.3431(6) Å	α = 90°.
	b = 19.4475(6) Å	β = 95.556(2)°.
	c = 15.0835(5) Å	γ = 90°.
Volume	5355.4(3) $Å^3$	
Z	4	
Density (calculated)	1.789 Mg/m^3	
Absorption coefficient	1.903 mm^{-1}	
F(000)	2880	
Crystal size	0.07 x 0.11 x 0.14 mm^3	
Theta range for data collection	1.53 to 28.00°.	
Index ranges	$-24 \le h \le 23$, $-25 \le k \le 25$, $-19 \le l \le 19$	
Reflections collected	31723	
Independent reflections	6419 [R(int) = 0.0486]	
Completeness to theta = 28.00°	99.1 %	
Refinement method	Full-matrix least-squares on F^2	
Data / restraints / parameters	6419 / 0 / 364	
Goodness-of-fit on F^2	1.084	
Final R indices [I>2sigma(I)]	R1 = 0.0466, wR2 = 0.1038	
R indices (all data)	R1 = 0.0641, wR2 = 0.1113	
Extinction coefficient	0.00052(6)	
Largest diff. peak and hole	0.706 and -0.801 $e.Å^{-3}$	

Comments:
All non-hydrogen atoms were refined anisotropic. All C-H H atoms were positioned with idealized geometry and refined isotropic using a riding model. The O-H H atoms were located in difference map, their bond lengths set to ideal values and afterwards they were refined using a riding model. The water molecule is disordered over two positions, each half occupied and was refined using a split model. A numerical absorption correction was performed ($T_{min/max}$: 0.6810/0.7993). The structure contains additional 4,4'-bipyridine as solvent molecules.

Table 2. Atomic coordinates ($\cdot 10^4$) and equivalent isotropic displacement parameters ($Å^2 \cdot 10^3$). U(eq) is defined as one third of the trace of the orthogonalized U_{ij} tensor.

	x	y	z	U(eq)
Sn(1)	5000	1575(1)	2500	30(1)
Sn(2)	5000	3323(1)	2500	31(1)
S(1)	4419(1)	807(1)	1468(1)	35(1)
S(2)	4196(1)	2445(1)	3069(1)	35(1)
S(3)	4477(1)	4084(1)	1421(1)	36(1)
Ni(1)	5000	-82(1)	2500	30(1)
Ni(2)	5000	4976(1)	2500	31(1)
N(1)	4082(2)	-217(2)	3216(2)	34(1)
N(2)	4395(2)	-828(2)	1708(2)	34(1)
C(1)	4550(2)	-1113(2)	951(3)	40(1)
C(2)	4061(3)	-1550(2)	438(3)	46(1)
C(3)	3400(3)	-1688(2)	737(4)	49(1)
C(4)	3213(2)	-1405(2)	1543(3)	43(1)
C(5)	2535(3)	-1538(2)	1915(4)	51(1)
C(6)	2390(2)	-1253(2)	2696(4)	50(1)
C(7)	2910(2)	-806(2)	3175(3)	42(1)
C(8)	2797(2)	-504(2)	3993(3)	47(1)
C(9)	3317(3)	-76(2)	4399(3)	48(1)
C(10)	3952(2)	64(2)	3986(3)	40(1)
C(11)	3572(2)	-657(2)	2819(3)	34(1)
C(12)	3734(2)	-971(2)	2004(3)	35(1)
N(21)	5990(2)	5105(2)	1951(2)	34(1)
N(22)	5517(2)	5724(2)	3373(2)	35(1)
C(21)	6197(2)	4823(2)	1219(3)	42(1)
C(22)	6883(2)	4956(2)	915(3)	48(1)
C(23)	7367(2)	5381(2)	1391(3)	45(1)
C(24)	7165(2)	5687(2)	2175(3)	40(1)
C(25)	7627(2)	6138(2)	2717(3)	47(1)
C(26)	7405(3)	6430(2)	3461(3)	50(1)
C(27)	6685(2)	6300(2)	3720(3)	41(1)
C(28)	6403(3)	6592(2)	4473(3)	47(1)
C(29)	5701(3)	6458(2)	4645(3)	44(1)
C(30)	5272(2)	6021(2)	4074(3)	39(1)
C(31)	6214(2)	5860(2)	3195(3)	34(1)
C(32)	6462(2)	5540(2)	2423(3)	34(1)
C(41)	2148(2)	2504(2)	209(3)	43(1)

C(42)	1496(3)	2667(4)	-261(4)	83(2)
C(43)	860(3)	2668(4)	166(4)	87(2)
N(41)	831(3)	2532(2)	1018(3)	63(1)
C(44)	1459(3)	2374(3)	1465(4)	63(1)
C(45)	2121(3)	2350(3)	1099(3)	55(1)
O(1)	262(6)	2339(6)	2718(8)	121(5)

Table 3. Bond lengths [Å] and angles [°].

Sn(1)-S(1)	2.3382(10)	Sn(2)-S(3)#1	2.3366(10)
Sn(1)-S(1)#1	2.3382(10)	Sn(2)-S(3)	2.3366(10)
Sn(1)-S(2)#1	2.4532(9)	Sn(2)-S(2)	2.4630(9)
Sn(1)-S(2)	2.4532(9)	Sn(2)-S(2)#1	2.4630(9)
S(1)-Sn(1)-S(1)#1	100.59(5)	S(3)#1-Sn(2)-S(3)	101.36(5)
S(1)-Sn(1)-S(2)#1	117.27(4)	S(3)#1-Sn(2)-S(2)	114.57(3)
S(1)#1-Sn(1)-S(2)#1	115.02(3)	S(3)-Sn(2)-S(2)	117.52(3)
S(1)-Sn(1)-S(2)	115.02(3)	S(3)#1-Sn(2)-S(2)#1	117.53(3)
S(1)#1-Sn(1)-S(2)	117.28(4)	S(3)-Sn(2)-S(2)#1	114.57(3)
S(2)#1-Sn(1)-S(2)	92.78(4)	S(2)-Sn(2)-S(2)#1	92.30(4)
S(1)-Ni(1)	2.4960(11)	Sn(2)-S(3)-Ni(2)	83.13(4)
Sn(1)-S(1)-Ni(1)	83.59(4)	S(3)-Ni(2)	2.5047(11)
Sn(1)-S(2)-Sn(2)	87.46(3)	Ni(2)-N(21)#1	2.083(3)
Ni(1)-N(1)#1	2.103(3)	Ni(2)-N(21)	2.083(3)
Ni(1)-N(1)	2.103(3)	Ni(2)-N(22)	2.124(3)
Ni(1)-N(2)	2.122(3)	Ni(2)-N(22)#1	2.124(3)
Ni(1)-N(2)#1	2.122(3)	Ni(2)-S(3)#1	2.5047(11)
Ni(1)-S(1)#1	2.4960(11)	N(21)#1-Ni(2)-N(21)	166.14(17)
N(1)#1-Ni(1)-N(1)	165.69(17)	N(21)#1-Ni(2)-N(22)	91.43(13)
N(1)#1-Ni(1)-N(2)	91.54(13)	N(21)-Ni(2)-N(22)	79.03(13)
N(1)-Ni(1)-N(2)	78.64(13)	N(21)#1-Ni(2)-N(22)#1	79.03(13)
N(1)#1-Ni(1)-N(2)#1	78.64(13)	N(21)-Ni(2)-N(22)#1	91.43(13)
N(1)-Ni(1)-N(2)#1	91.54(13)	N(22)-Ni(2)-N(22)#1	93.47(18)
N(2)-Ni(1)-N(2)#1	93.84(18)	N(21)#1-Ni(2)-S(3)	92.71(10)
N(1)#1-Ni(1)-S(1)#1	95.27(9)	N(21)-Ni(2)-S(3)	96.87(10)
N(1)-Ni(1)-S(1)#1	94.64(9)	N(22)-Ni(2)-S(3)	175.86(9)
N(2)-Ni(1)-S(1)#1	173.19(9)	N(22)#1-Ni(2)-S(3)	87.22(9)
N(2)#1-Ni(1)-S(1)#1	87.36(9)	N(21)#1-Ni(2)-S(3)#1	96.87(10)
N(1)#1-Ni(1)-S(1)	94.64(9)	N(21)-Ni(2)-S(3)#1	92.71(9)
N(1)-Ni(1)-S(1)	95.27(9)	N(22)-Ni(2)-S(3)#1	87.22(9)
N(2)-Ni(1)-S(1)	87.36(9)	N(22)#1-Ni(2)-S(3)#1	175.86(9)
N(2)#1-Ni(1)-S(1)	173.19(9)	S(3)-Ni(2)-S(3)#1	92.39(5)
S(1)#1-Ni(1)-S(1)	92.23(5)		
N(1)-C(10)	1.326(5)	C(1)-C(2)	1.411(6)
N(1)-C(11)	1.363(5)	C(2)-C(3)	1.360(7)
N(2)-C(1)	1.324(5)	C(3)-C(4)	1.407(7)
N(2)-C(12)	1.361(5)	C(4)-C(12)	1.408(6)

C(4)-C(5)	1.436(6)	C(28)-C(29)	1.363(7)
C(5)-C(6)	1.351(7)	C(29)-C(30)	1.397(6)
C(6)-C(7)	1.433(6)	C(31)-C(32)	1.434(6)
C(7)-C(8)	1.400(7)	C(21)-N(21)-C(32)	118.3(3)
C(7)-C(11)	1.404(5)	C(30)-N(22)-C(31)	118.2(4)
C(8)-C(9)	1.367(7)	N(21)-C(21)-C(22)	122.4(4)
C(9)-C(10)	1.400(6)	C(23)-C(22)-C(21)	119.9(4)
C(11)-C(12)	1.430(6)	C(22)-C(23)-C(24)	119.2(4)
C(10)-N(1)-C(11)	118.0(3)	C(23)-C(24)-C(32)	117.4(4)
C(1)-N(2)-C(12)	118.0(3)	C(23)-C(24)-C(25)	123.7(4)
N(2)-C(1)-C(2)	123.1(4)	C(32)-C(24)-C(25)	118.9(4)
C(3)-C(2)-C(1)	118.5(4)	C(26)-C(25)-C(24)	121.7(4)
C(2)-C(3)-C(4)	120.6(4)	C(25)-C(26)-C(27)	120.6(4)
C(3)-C(4)-C(12)	116.7(4)	C(31)-C(27)-C(28)	116.4(4)
C(3)-C(4)-C(5)	124.1(4)	C(31)-C(27)-C(26)	119.1(4)
C(12)-C(4)-C(5)	119.2(4)	C(28)-C(27)-C(26)	124.4(4)
C(6)-C(5)-C(4)	121.1(4)	C(29)-C(28)-C(27)	120.1(4)
C(5)-C(6)-C(7)	120.8(4)	C(28)-C(29)-C(30)	119.0(4)
C(8)-C(7)-C(11)	117.2(4)	N(22)-C(30)-C(29)	123.0(4)
C(8)-C(7)-C(6)	123.4(4)	N(22)-C(31)-C(27)	123.2(4)
C(11)-C(7)-C(6)	119.3(4)	N(22)-C(31)-C(32)	117.1(3)
C(9)-C(8)-C(7)	119.6(4)	C(27)-C(31)-C(32)	119.7(4)
C(8)-C(9)-C(10)	119.6(4)	N(21)-C(32)-C(24)	122.8(4)
N(1)-C(10)-C(9)	122.5(4)	N(21)-C(32)-C(31)	117.3(3)
N(1)-C(11)-C(7)	123.0(4)	C(24)-C(32)-C(31)	119.9(4)
N(1)-C(11)-C(12)	117.0(3)		
C(7)-C(11)-C(12)	120.0(4)	C(41)-C(42)	1.368(7)
N(2)-C(12)-C(4)	123.0(4)	C(41)-C(45)	1.380(7)
N(2)-C(12)-C(11)	117.5(3)	C(41)-C(41)#2	1.490(9)
C(4)-C(12)-C(11)	119.5(4)	C(42)-C(43)	1.386(8)
N(21)-C(21)	1.321(5)	C(42)-C(41)-C(45)	116.2(4)
N(21)-C(32)	1.360(5)	C(42)-C(41)-C(41)#2	122.3(5)
N(22)-C(30)	1.321(5)	C(45)-C(41)-C(41)#2	121.5(5)
N(22)-C(31)	1.358(5)	C(41)-C(42)-C(43)	119.6(5)
C(21)-C(22)	1.404(6)	C(43)-N(41)	1.317(8)
C(22)-C(23)	1.365(7)	N(41)-C(44)	1.313(7)
C(23)-C(24)	1.406(6)	C(44)-C(45)	1.383(7)
C(24)-C(32)	1.406(5)	O(1)-O(1)#3	1.11(2)
C(24)-C(25)	1.422(6)	N(41)-C(43)-C(42)	124.6(6)
C(25)-C(26)	1.355(7)	C(44)-N(41)-C(43)	115.6(5)
C(26)-C(27)	1.436(6)	N(41)-C(44)-C(45)	124.3(5)
C(27)-C(31)	1.404(6)	C(41)-C(45)-C(44)	119.8(5)
C(27)-C(28)	1.413(6)		

Symmetry transformations used to generate equivalent atoms: #1 -x+1,y,-z+1/2 #2 -x+1/2,-y+1/2,-z #3 -x,y,-z+1/2

Table 4. Anisotropic displacement parameters ($Å^2 \cdot 10^3$). The anisotropic displacement factor exponent takes the form: $-2\pi^2[h^2 a^{*2} U_{11} + ... + 2 h k a^* b^* U_{12}]$

	U_{11}	U_{22}	U_{33}	U_{23}	U_{13}	U_{12}
Sn(1)	26(1)	28(1)	35(1)	0	5(1)	0
Sn(2)	29(1)	28(1)	38(1)	0	10(1)	0
S(1)	31(1)	34(1)	38(1)	-3(1)	2(1)	-1(1)
S(2)	31(1)	33(1)	45(1)	1(1)	14(1)	0(1)
S(3)	34(1)	35(1)	39(1)	2(1)	6(1)	1(1)
Ni(1)	26(1)	30(1)	35(1)	0	9(1)	0
Ni(2)	28(1)	31(1)	38(1)	0	11(1)	0
N(1)	30(2)	36(2)	38(2)	-1(1)	11(1)	2(1)
N(2)	31(2)	33(1)	38(2)	-3(1)	7(1)	-2(1)
C(1)	41(2)	35(2)	45(2)	-3(2)	10(2)	-1(2)
C(2)	50(3)	44(2)	43(3)	-8(2)	7(2)	-1(2)
C(3)	44(3)	46(2)	55(3)	-8(2)	1(2)	-9(2)
C(4)	37(2)	41(2)	50(3)	1(2)	1(2)	-5(2)
C(5)	36(2)	52(2)	64(3)	2(2)	2(2)	-14(2)
C(6)	29(2)	57(2)	66(3)	3(2)	13(2)	-9(2)
C(7)	32(2)	40(2)	54(3)	4(2)	10(2)	-3(2)
C(8)	38(2)	49(2)	57(3)	3(2)	25(2)	1(2)
C(9)	49(3)	49(2)	49(3)	-4(2)	24(2)	2(2)
C(10)	38(2)	42(2)	42(2)	-5(2)	17(2)	-2(2)
C(11)	25(2)	35(2)	41(2)	3(2)	7(2)	1(1)
C(12)	31(2)	33(2)	39(2)	2(2)	5(2)	-4(1)
N(21)	27(2)	36(2)	40(2)	0(1)	12(1)	1(1)
N(22)	33(2)	35(2)	38(2)	0(1)	11(1)	-2(1)
C(21)	38(2)	42(2)	48(3)	-5(2)	17(2)	-3(2)
C(22)	40(2)	51(2)	55(3)	-5(2)	22(2)	-2(2)
C(23)	31(2)	50(2)	56(3)	-2(2)	19(2)	0(2)
C(24)	31(2)	39(2)	50(3)	4(2)	9(2)	-1(2)
C(25)	31(2)	57(2)	54(3)	6(2)	6(2)	-9(2)
C(26)	39(2)	56(2)	53(3)	0(2)	0(2)	-17(2)
C(27)	40(2)	40(2)	43(2)	3(2)	2(2)	-6(2)
C(28)	55(3)	45(2)	42(3)	-3(2)	7(2)	-12(2)
C(29)	56(3)	40(2)	39(2)	-4(2)	13(2)	-6(2)
C(30)	40(2)	37(2)	41(2)	-2(2)	11(2)	-2(2)
C(31)	33(2)	33(2)	35(2)	2(1)	4(2)	-2(1)
C(32)	28(2)	33(2)	42(2)	6(2)	8(2)	-1(1)
C(41)	39(2)	43(2)	47(2)	3(2)	5(2)	2(2)
C(42)	46(3)	156(6)	49(3)	23(4)	6(2)	27(4)
C(43)	49(3)	150(6)	62(4)	23(4)	9(3)	24(4)
N(41)	47(2)	83(3)	62(3)	7(2)	16(2)	6(2)
C(44)	51(3)	87(4)	52(3)	11(3)	14(2)	2(3)
C(45)	44(2)	75(3)	47(3)	17(2)	5(2)	7(2)
O(1)	111(11)	175(9)	82(9)	54(8)	45(7)	78(8)

Table 5. Hydrogen coordinates ($\cdot 10^4$) and isotropic displacement parameters ($Å^2 \cdot 10^3$).

	x	y	z	U(eq)
H(1)	5013	-1020	745	48
H(2)	4190	-1743	-104	55
H(3)	3062	-1978	399	58
H(5)	2182	-1831	1606	61
H(6)	1939	-1350	2930	60
H(8)	2361	-597	4265	56
H(9)	3248	127	4958	57
H(10)	4304	371	4269	47
H(21)	5870	4520	886	50
H(22)	7010	4751	380	57
H(23)	7835	5469	1194	54
H(25)	8103	6238	2553	57
H(26)	7729	6724	3815	60
H(28)	6703	6883	4861	57
H(29)	5506	6659	5145	53
H(30)	4782	5933	4196	47
H(42)	1478	2779	-875	100
H(43)	413	2773	-180	104
H(44)	1458	2269	2080	75
H(45)	2556	2228	1458	66
H(2O1)	265	2424	3292	181
H(1O1)	119	2722	2442	181

5.3.12 Messprotokoll der Verbindung $[Ni(tren)(ma)(H_2O)]_2[Sn_2S_6]\cdot 4H_2O$

Table 1. Crystal data and structure refinement for $[Ni(C_6H_{18}N_4)(CH_5N)(H_2O)]_2[Sn_2S_6]\cdot 4H_2O$. ($C_6H_{18}N_4$, tren = Tris(2-aminoethyl)amin; CH_5N, ma) Methylamin)

Identification code	jh1331	
Empirical formula	$[Ni(C_6H_{18}N_4)(CH_5N)(H_2O)]_2[Sn_2S_6]\cdot 4H_2O$	
Crystal color, habitus	violet bars	
Formula weight	1009.86	
Temperature	200(2) K	
Wavelength	0.71073 Å	
Crystal system	monoclinic	
Space group	$P2_1/n$	
Unit cell dimensions	a = 11.1715(3) Å	α= 90°.
	b = 10.5384(3) Å	β= 101.833(2)°.
	c = 15.8594(5) Å	γ = 90°.
Volume	1827.45(9) $Å^3$	
Z	2	
Density (calculated)	1.835 Mg/m^3	
Absorption coefficient	2.751 mm^{-1}	
F(000)	1024	
Crystal size	0.07 x 0.10 x 0.13 mm^3	
Theta range for data collection	2.05 to 27.93°.	
Index ranges	-14<=h<=14, -13<=k<=13, -20<=l<=20	
Reflections collected	28097	
Independent reflections	4371 [R(int) = 0.0449]	
Completeness to theta = 27.93°	99.9 %	
Refinement method	Full-matrix least-squares on F^2	
Data / restraints / parameters	4371 / 0 / 183	
Goodness-of-fit on F^2	1.022	
Final R indices [I>2sigma(I)]	R1 = 0.0261, wR2 = 0.0637	
R indices (all data)	R1 = 0.0339, wR2 = 0.0656	
Extinction coefficient	0.0025(2)	
Largest diff. peak and hole	0.788 and -0.560 $e.Å^{-3}$	

Remarks:
All non H atoms were refined anisotropic. The C-H and N-H H atoms were positioned with idealized geometry and refined with $U_{iso}(H) = 1.2\ U_{eq}(C,N)$ using a riding model. The O-H H atoms were located in difference map, their bond lengths set to ideal values and finally they were refined isotropic with $U_{iso}(H) = 1.5\ U_{eq}(O)$ using a riding model. A numerical absorption correction was performed ($T_{min/max}$: 0.5922/0.7169).

Table 2. Atomic coordinates ($\cdot 10^4$) and equivalent isotropic displacement parameters ($Å^2 \cdot 10^3$). U(eq) is defined as one third of the trace of the orthogonalized U_{ij} tensor.

	x	y	z	U(eq)
Sn(1)	9330(1)	5205(1)	838(1)	20(1)
S(1)	7332(1)	5990(1)	654(1)	29(1)
S(2)	10445(1)	4701(1)	2209(1)	27(1)
S(3)	10595(1)	6576(1)	136(1)	25(1)
Ni(1)	5587(1)	4396(1)	-1931(1)	21(1)
N(1)	5144(2)	5107(2)	-3191(2)	24(1)
C(1)	4784(3)	6447(3)	-3118(2)	31(1)
C(2)	3921(3)	6580(3)	-2504(2)	34(1)
N(2)	4421(2)	5901(2)	-1687(2)	29(1)
C(3)	6269(3)	4987(3)	-3543(2)	30(1)
C(4)	6814(3)	3667(3)	-3351(2)	31(1)
N(3)	6902(2)	3352(2)	-2433(2)	28(1)
C(5)	4131(2)	4329(3)	-3702(2)	29(1)
C(6)	3358(2)	3668(3)	-3149(2)	31(1)
N(4)	4147(2)	3138(2)	-2368(2)	26(1)
N(5)	5878(2)	3598(2)	-700(2)	32(1)
C(7)	6263(3)	2268(3)	-604(2)	40(1)
O(2)	7041(2)	5783(2)	-1488(1)	29(1)
O(3)	9743(2)	5890(2)	3902(2)	46(1)
O(4)	6609(2)	9054(3)	355(2)	56(1)

Table 3. Bond lengths [Å] and angles [°].

Sn(1)-S(2)	2.3351(7)	Sn(1)-S(3)	2.4433(6)
Sn(1)-S(1)	2.3412(7)	Sn(1)-S(3)#1	2.4434(7)
S(3)-Sn(1)#1	2.4434(7)	S(2)-Sn(1)-S(3)#1	109.45(2)
S(2)-Sn(1)-S(1)	120.61(3)	S(1)-Sn(1)-S(3)#1	110.37(2)
S(2)-Sn(1)-S(3)	108.11(2)	S(3)-Sn(1)-S(3)#1	93.92(2)
S(1)-Sn(1)-S(3)	111.11(3)	Sn(1)-S(3)-Sn(1)#1	86.08(2)
Ni(1)-N(5)	2.089(2)	Ni(1)-N(3)	2.118(2)
Ni(1)-N(4)	2.090(2)	Ni(1)-N(2)	2.138(2)
Ni(1)-N(1)	2.097(2)	Ni(1)-O(2)	2.1914(18)
N(5)-Ni(1)-N(4)	90.97(9)	N(1)-Ni(1)-N(2)	82.72(9)
N(5)-Ni(1)-N(1)	174.82(9)	N(3)-Ni(1)-N(2)	161.64(9)
N(4)-Ni(1)-N(1)	83.98(9)	N(5)-Ni(1)-O(2)	90.34(9)
N(5)-Ni(1)-N(3)	98.95(10)	N(4)-Ni(1)-O(2)	177.48(8)
N(4)-Ni(1)-N(3)	95.29(9)	N(1)-Ni(1)-O(2)	94.65(8)
N(1)-Ni(1)-N(3)	82.74(9)	N(3)-Ni(1)-O(2)	86.63(8)
N(5)-Ni(1)-N(2)	96.52(10)	N(2)-Ni(1)-O(2)	83.45(8)
N(4)-Ni(1)-N(2)	94.26(9)		
N(1)-C(1)	1.479(3)	C(3)-C(4)	1.523(4)
N(1)-C(3)	1.482(4)	C(4)-N(3)	1.477(4)
N(1)-C(5)	1.494(3)	C(5)-C(6)	1.520(4)
C(1)-C(2)	1.510(4)	C(6)-N(4)	1.474(3)
C(2)-N(2)	1.485(4)	N(2)-C(2)-C(1)	110.0(2)
C(1)-N(1)-C(3)	112.1(2)	N(1)-C(3)-C(4)	109.7(2)
C(1)-N(1)-C(5)	112.3(2)	N(3)-C(4)-C(3)	110.2(2)
C(3)-N(1)-C(5)	110.8(2)	N(1)-C(5)-C(6)	113.3(2)
N(1)-C(1)-C(2)	111.0(2)	N(4)-C(6)-C(5)	110.2(2)
N(5)-C(7)	1.465(4)		

Symmetry transformations used to generate equivalent atoms: A: -x+2,-y+1,-z

Table 4. Anisotropic displacement parameters ($Å^2 \cdot 10^3$). The anisotropic displacement factor exponent takes the form: $-2\pi^2 [h^2 a^{*2} U_{11} + ... + 2 h k a^* b^* U_{12}]$

	U_{11}	U_{22}	U_{33}	U_{23}	U_{13}	U_{12}
Sn(1)	20(1)	22(1)	19(1)	0(1)	5(1)	-1(1)
S(1)	22(1)	34(1)	32(1)	-6(1)	7(1)	1(1)
S(2)	29(1)	31(1)	20(1)	2(1)	3(1)	0(1)
S(3)	31(1)	22(1)	25(1)	-2(1)	10(1)	-5(1)
Ni(1)	21(1)	21(1)	20(1)	0(1)	4(1)	-1(1)
N(1)	26(1)	23(1)	23(1)	1(1)	6(1)	2(1)
C(1)	41(2)	22(1)	32(2)	5(1)	8(1)	5(1)
C(2)	35(2)	24(1)	42(2)	-2(1)	9(1)	8(1)
N(2)	30(1)	28(1)	31(1)	-5(1)	11(1)	-1(1)
C(3)	30(1)	32(1)	27(1)	-1(1)	9(1)	-2(1)
C(4)	29(1)	35(1)	33(2)	-6(1)	12(1)	2(1)
N(3)	26(1)	24(1)	33(1)	-1(1)	6(1)	1(1)
C(5)	28(1)	34(1)	24(1)	-2(1)	0(1)	-1(1)
C(6)	22(1)	35(1)	33(2)	-3(1)	-2(1)	-3(1)
N(4)	24(1)	25(1)	29(1)	-2(1)	5(1)	-4(1)
N(5)	35(1)	34(1)	25(1)	3(1)	3(1)	-6(1)
C(7)	45(2)	36(2)	37(2)	10(1)	2(1)	-7(1)
O(2)	26(1)	32(1)	28(1)	-3(1)	4(1)	-5(1)
O(3)	52(1)	55(1)	32(1)	-4(1)	9(1)	12(1)
O(4)	48(1)	50(1)	63(2)	-9(1)	-4(1)	4(1)

Table 5. Hydrogen coordinates ($\cdot 10^4$) and isotropic displacement parameters ($Å^2 \cdot 10^3$).

	x	y	z	U(eq)
H(1A)	4383	6768	-3693	38
H(1B)	5524	6967	-2908	38
H(2A)	3809	7489	-2383	40
H(2B)	3112	6222	-2771	40
H(1N2)	3790	5576	-1461	35
H(2N2)	4857	6457	-1293	35
H(3A)	6872	5636	-3279	35
H(3B)	6072	5129	-4173	35
H(4A)	6292	3034	-3715	38
H(4B)	7637	3638	-3490	38
H(1N3)	7674	3542	-2127	33
H(2N3)	6772	2497	-2376	33
H(5A)	4486	3681	-4031	35
H(5B)	3598	4885	-4122	35
H(6A)	2776	4282	-2982	37
H(6B)	2879	2978	-3483	37
H(1N4)	4451	2364	-2492	31
H(2N4)	3700	3020	-1947	31
H(1N5)	6461	4077	-344	38
H(2N5)	5165	3676	-500	38
H(7A)	5687	1743	-1008	60
H(7B)	6275	1988	-13	60
H(7C)	7083	2183	-728	60
H(1O2)	7169	5930	-956	43
H(2O2)	7700	5551	-1618	43
H(1O3)	9881	5604	3436	69
H(2O3)	9346	5281	4050	69
H(1O4)	6131	8984	-126	84
H(2O4)	6914	8322	406	84

Table 6. Hydrogen bonds with H..A < r(A) + 2.000 Angstroms and <DHA > 110 deg.

D-H	d(D-H)	d(H..A)	<DHA	d(D..A)	A
N2-H1N2	0.920	2.567	157.68	3.436	S1 [-x+1, -y+1, -z]
N2-H2N2	0.920				
N3-H1N3	0.920	2.824	138.09	3.562	S2 [-x+2, -y+1, -z]
N3-H2N3	0.920	2.756	152.62	3.598	S2 [x-1/2, -y+1/2, z-1/2]
N4-H1N4	0.920	2.532	175.75	3.450	S2 [x-1/2, -y+1/2, z-1/2]
N4-H2N4	0.920	2.756	149.41	3.578	S1 [-x+1, -y+1, -z]
N5-H1N5	0.920	2.624	156.87	3.489	S1
N5-H2N5	0.920	2.772	155.26	3.628	S1 [-x+1, -y+1, -z]
O2-H1O2	0.840	2.524	169.25	3.353	S1
O2-H2O2	0.840	2.458	167.00	3.282	S2 [-x+2, -y+1, -z]
O3-H1O3	0.840	2.365	174.24	3.202	S2
O3-H2O3	0.840	2.029	167.16	2.855	O4 [-x+3/2, y-1/2, -z+1/2]
O4-H1O4	0.840	1.954	164.68	2.773	O3 [x-1/2, -y+3/2, z-1/2]
O4-H2O4	0.840	2.518	165.87	3.338	S1

5.3.13 Messprotokoll der Verbindung $[Ni(1,2dap)(tren)]_2[Sn_2S_6]\cdot 2H_2O$

Table 1. Crystal data and structure refinement for $[Ni(C_6H_{18}N_4)(C_3H_{10}N_2)]_2[Sn_2S_6]\cdot 2H_2O$. ($C_6H_{18}N_4$, tren = Tris(2-aminoethyl)amin); $C_3H_{10}N_2$, 1,2-dap = 1,2-Diaminopropane)

Identification code	jh1538	
Empirical formula	$[Ni(C_6H_{18}N_4)(C_3H_{10}N_2)]_2[Sn_2S_6]\cdot 2H_2O$	
Crystal color, habitus	violet blocks	
Formula weight	1023.94	
Temperature	200(2) K	
Wavelength	0.71073 Å	
Crystal system	monoclinic	
Space group	$P2_1/n$	
Unit cell dimensions	a = 12.9264(3) Å	α= 90°.
	b = 10.1627(3) Å	β= 113.263(2)°
	c = 15.6585(4) Å	γ = 90°.
Volume	1889.78(9) $Å^3$	
Z	2	
Density (calculated)	1.799 Mg/m^3	
Absorption coefficient	2.656 mm^{-1}	
F(000)	1040	
Crystal size	0.07 x 0.15 x 0.22 mm^2	
Theta range for data collection	1.740 to 27.005°	
Index ranges	-16<=h<=16, -12<=k<=12, -19<=l<=19	
Reflections collected	26578	
Independent reflections	4120 [R(int) = 0.0345]	
Completeness to theta = 25.242°	100.0 %	
Refinement method	Full-matrix least-squares on F^2	
Data / restraints / parameters	4120 / 0 / 209	
Goodness-of-fit on F^2	1.067	
Final R indices [I>2sigma(I)]	R1 = 0.0239, wR2 = 0.0575	
R indices (all data)	R1 = 0.0288, wR2 = 0.0590	
Extinction coefficient	0.0011(2)	
Largest diff. peak and hole	0.511 and -0.780 $e.Å^{-3}$	

Comments:
All non-hydrogen atoms were refined anisotropic. The C-H and N-H H atoms were positioned with idealized geometry and refined using a riding model. The O-H H atoms were located in difference map, their bind lengths were set to ideal values and finally they were refined using a riding model. A numerical absorption correction was performed ($T_{min/max}$: 0.4488/0.7825). Two C atoms of the 1,2-diaminopropane ligand are disordered and were refined using a split model.

Table 2. Atomic coordinates ($\cdot 10^4$) and equivalent isotropic displacement parameters ($Å^2 \cdot 10^3$). U(eq) is defined as one third of the trace of the orthogonalized U_{ij} tensor.

	x	y	z	U(eq)
Sn(1)	1223(1)	5653(1)	5013(1)	23(1)
S(1)	2162(1)	4632(1)	4190(1)	39(1)
S(2)	2174(1)	7467(1)	5891(1)	31(1)
S(3)	777(1)	4054(1)	5990(1)	30(1)
Ni(1)	4687(1)	3515(1)	7356(1)	23(1)
N(1)	5890(2)	5011(2)	7991(1)	26(1)
C(1)	6777(2)	4356(3)	8784(2)	33(1)
C(2)	6252(2)	3645(3)	9365(2)	36(1)
N(2)	5277(2)	2862(2)	8760(1)	30(1)
C(3)	5351(2)	6103(3)	8298(2)	33(1)
C(4)	4260(2)	5683(3)	8376(2)	35(1)
N(3)	3580(2)	4906(2)	7548(2)	32(1)
C(5)	6289(2)	5474(3)	7281(2)	35(1)
C(6)	5291(2)	5638(3)	6358(2)	38(1)
N(4)	4659(2)	4388(2)	6108(2)	33(1)
N(11)	5615(2)	1895(2)	7097(1)	29(1)
C(11)	4728(4)	1015(4)	6409(4)	32(1)
C(12)	3795(4)	844(5)	6756(4)	35(1)
C(11')	4929(6)	668(6)	6939(6)	30(1)
C(12')	3767(7)	1091(9)	6310(7)	35(2)
N(12)	3383(2)	2136(2)	6859(2)	39(1)
C(13)	5272(3)	-356(3)	6385(3)	58(1)
O(1)	6542(2)	2665(2)	5670(2)	51(1)

Table 3. Bond lengths [Å] and angles [°].

Sn(1)-S(1)	2.3343(7)	Sn(1)-S(3)	2.4512(6)
Sn(1)-S(2)	2.3380(6)	Sn(1)-S(3A)	2.4553(6)
S(3)-Sn(1A)	2.4553(6)	S(1)-Sn(1)-S(3A)	110.31(2)
S(1)-Sn(1)-S(2)	114.08(2)	S(2)-Sn(1)-S(3A)	117.16(2)
S(1)-Sn(1)-S(3)	110.60(3)	S(3)-Sn(1)-S(3A)	91.81(2)
S(2)-Sn(1)-S(3)	110.72(2)	Sn(1)-S(3)-Sn(1A)	88.185(19)
Ni(1)-N(12)	2.091(2)		
Ni(1)-N(3)	2.115(2)	Ni(1)-N(2)	2.129(2)
Ni(1)-N(1)	2.1204(19)	Ni(1)-N(4)	2.134(2)
N(12)-Ni(1)-N(3)	90.58(9)	Ni(1)-N(11)	2.167(2)
N(12)-Ni(1)-N(1)	171.43(9)	N(1)-Ni(1)-N(4)	82.84(8)
N(3)-Ni(1)-N(1)	82.31(8)	N(2)-Ni(1)-N(4)	160.93(8)
N(12)-Ni(1)-N(2)	94.73(9)	N(12)-Ni(1)-N(11)	81.11(8)
N(3)-Ni(1)-N(2)	92.78(8)	N(3)-Ni(1)-N(11)	171.68(8)
N(1)-Ni(1)-N(2)	80.91(8)	N(1)-Ni(1)-N(11)	105.94(7)
N(12)-Ni(1)-N(4)	102.62(10)	N(2)-Ni(1)-N(11)	87.55(8)
N(3)-Ni(1)-N(4)	94.87(9)	N(4)-Ni(1)-N(11)	87.38(8)
N(1)-C(5)	1.475(3)	C(3)-C(4)	1.524(4)
N(1)-C(1)	1.475(3)	C(4)-N(3)	1.475(3)
N(1)-C(3)	1.488(3)	C(5)-C(6)	1.519(4)
C(1)-C(2)	1.515(4)	C(6)-N(4)	1.477(4)
C(2)-N(2)	1.475(3)	N(2)-C(2)-C(1)	110.1(2)
C(5)-N(1)-C(1)	113.0(2)	N(1)-C(3)-C(4)	112.5(2)
C(5)-N(1)-C(3)	110.7(2)	N(3)-C(4)-C(3)	109.2(2)
C(1)-N(1)-C(3)	111.8(2)	N(1)-C(5)-C(6)	109.5(2)
N(1)-C(1)-C(2)	109.7(2)	N(4)-C(6)-C(5)	109.3(2)
N(11)-C(11')	1.493(7)	C(12)-N(12)	1.449(6)
N(11)-C(11)	1.516(5)	C(11')-C(12')	1.497(11)
C(11)-C(12)	1.517(7)	C(11')-C(13)	1.528(8)
C(11)-C(13)	1.567(5)	C(12')-N(12)	1.566(9)
N(11)-C(11)-C(12)	107.3(4)	N(11)-C(11')-C(13)	112.1(5)
N(11)-C(11)-C(13)	108.8(3)	C(12')-C(11')-C(13)	105.2(6)
C(12)-C(11)-C(13)	109.5(4)	C(11')-C(12')-N(12)	106.6(6)
N(12)-C(12)-C(11)	108.4(4)	C(12)-N(12)-Ni(1)	111.8(2)
N(11)-C(11')-C(12')	104.2(6)	C(12')-N(12)-Ni(1)	106.0(3)

Symmetry transformations used to generate equivalent atoms: A: #1 -x,-y+1,-z+1

Table 4. Anisotropic displacement parameters ($Å^2$ x 10^3). The anisotropic displacement factor exponent takes the form: $-2\pi^2[h^2 a^{*2}U_{11} + ... + 2 h k a^* b^* U_{12}]$

	U_{11}	U_{22}	U_{33}	U_{23}	U_{13}	U_{12}
Sn(1)	22(1)	24(1)	23(1)	-2(1)	10(1)	-2(1)
S(1)	31(1)	50(1)	43(1)	-22(1)	23(1)	-11(1)
S(2)	30(1)	28(1)	35(1)	-7(1)	14(1)	-6(1)
S(3)	24(1)	32(1)	29(1)	9(1)	7(1)	-1(1)
Ni(1)	22(1)	25(1)	21(1)	-1(1)	9(1)	0(1)
N(1)	26(1)	26(1)	26(1)	-2(1)	13(1)	-1(1)
C(1)	29(1)	37(1)	28(1)	-4(1)	5(1)	-3(1)
C(2)	40(1)	41(2)	22(1)	1(1)	6(1)	-1(1)
N(2)	34(1)	31(1)	26(1)	4(1)	16(1)	0(1)
C(3)	36(1)	26(1)	39(1)	-7(1)	17(1)	-1(1)
C(4)	37(1)	34(1)	42(1)	-9(1)	23(1)	1(1)
N(3)	28(1)	32(1)	40(1)	-4(1)	16(1)	2(1)
C(5)	33(1)	39(1)	37(1)	4(1)	20(1)	-4(1)
C(6)	45(2)	42(2)	33(1)	12(1)	22(1)	3(1)
N(4)	37(1)	40(1)	24(1)	5(1)	13(1)	8(1)
N(11)	26(1)	29(1)	32(1)	-3(1)	13(1)	-1(1)
C(11)	36(2)	29(2)	32(2)	-7(2)	15(2)	-3(2)
C(12)	32(2)	31(3)	44(3)	-6(2)	18(3)	-8(2)
C(11')	34(3)	22(3)	31(4)	-1(3)	12(3)	-3(3)
C(12')	27(4)	31(4)	40(5)	-11(4)	8(4)	-5(3)
N(12)	26(1)	36(1)	52(1)	-10(1)	13(1)	-4(1)
C(13)	50(2)	43(2)	86(3)	-26(2)	31(2)	-3(1)
O(1)	58(1)	55(1)	53(1)	-2(1)	38(1)	-14(1)

Table 5. Hydrogen coordinates ($\cdot 10^4$) and isotropic displacement parameters ($Å^2 \cdot 10^3$).

	x	y	z	U(eq)
H(1A)	7324	5017	9170	40
H(1B)	7186	3719	8553	40
H(2A)	6818	3058	9816	44
H(2B)	6007	4293	9718	44
H(1N)	4713	2931	8967	35
H(2N)	5478	1999	8790	35
H(3A)	5190	6839	7850	40
H(3B)	5883	6428	8911	40
H(4A)	4431	5147	8944	42
H(4B)	3832	6469	8421	42
H(3N)	3282	5437	7041	38
H(4N)	3008	4491	7638	38
H(5A)	6825	4829	7213	42
H(5B)	6684	6325	7476	42
H(6A)	4793	6347	6408	46
H(6B)	5559	5885	5868	46
H(5N)	4984	3838	5827	40
H(6N)	3937	4542	5707	40
H(7N)	6104	2193	6853	34
H(8N)	6009	1452	7632	34
H(9N)	5766	2073	6588	34
H(10N)	6281	1787	7593	34
H(11)	4427	1423	5776	38
H(12A)	3176	314	6308	42
H(12B)	4086	381	7362	42
H(11')	4945	297	7536	35
H(12C)	3248	329	6141	42
H(12D)	3774	1482	5732	42
H(11N)	3032	2085	7261	46
H(12N)	2868	2409	6299	46
H(13N)	3270	1749	7340	46
H(14N)	2731	2529	6479	46
H(13A)	4706	-934	5942	88
H(13B)	5901	-239	6193	88
H(13C)	5548	-752	7006	88
H(13D)	4803	-1143	6298	88
H(13E)	5167	10	5778	88
H(13F)	6065	-591	6726	88
H(1O1)	6911	3369	5774	76
H(2O1)	6746	2424	5247	76

Table 6. Hydrogen bonds with H..A < r(A) + 2.000 Angstroms and <DHA > 110 deg.

D-H	d(D-H)	d(H..A)	<DHA	d(D..A)	A
C2-H2A	0.990	2.996	118.61	3.578	S1 [x+1/2, -y+1/2, z+1/2]
N2-H1N	0.910	2.578	159.18	3.444	S2 [-x+1/2, y-1/2, -z+3/2]
N2-H2N	0.910	2.608	144.96	3.394	S1 [x+1/2, -y+1/2, z+1/2]
C4-H4A	0.990	2.630	110.08	3.112	N2
C4-H4B	0.990	2.764	139.24	3.573	S3 [-x+1/2, y+1/2, -z+3/2]
N3-H3N	0.910	2.741	161.92	3.617	S2
C5-H5A	0.990	3.018	118.78	3.600	S1 [-x+1, -y+1, -z+1]
C6-H6B	0.990	3.029	128.39	3.725	S1 [-x+1, -y+1, -z+1]
N4-H5N	0.910	2.434	155.16	3.282	O1
N4-H6N	0.910	2.571	160.32	3.441	S1
N11-H7N_a	0.910	2.193	151.78	3.026	O1
N11-H8N_a	0.910	2.552	175.90	3.460	S1 [x+1/2, -y+1/2, z+1/2]
N11-H9N_b	0.910	2.139	164.55	3.026	O1
N11-H10N_b	0.910	2.716	139.60	3.460	S1 [x+1/2, -y+1/2, z+1/2]
C12_a-H12B_a	0.990	2.855	162.68	3.812	S3 [-x+1/2, y-1/2, -z+3/2]
C11'_b-H11'_b	1.000	3.011	117.11	3.579	S1 [x+1/2, -y+1/2, z+1/2]
N12-H14N_b	0.910	2.800	157.58	3.658	S3
O1-H1O1	0.840	2.347	171.04	3.180	S1 [-x+1, -y+1, -z+1]
O1-H2O1	0.840	2.666	157.68	3.458	S2 [-x+1, -y+1, -z+1]

5.3.14 Messprotokoll der Verbindung $\{[Ni(phen)_2]_2[Sn_2S_6]\}\cdot biph$

Table 1. Crystal data and structure refinement for $\{[Ni(C_{12}H_8N_2)_2]_2[Sn_2S_6]\}\cdot C_{12}H_{10}$ ($C_{12}H_8N_2$, phen = 1,10-Phenanthrolin; $C_{12}H_{10}$, biph = Biphenyl)

Identification code	jh1769a	
Empirical formula	$\{[Ni(C_{12}H_8N_2)_2]_2[Sn_2S_6]\}\cdot C_{12}H_{10}$	
Crystal color, habitus	red-violet blocks	
Formula weight	1422.17	
Temperature	170(2) K	
Wavelength	0.71073 Å	
Crystal system	monoclinic	
Space group	$P2_1/n$	
Unit cell dimensions	a = 10.5704(3) Å	α= 90°.
	b = 9.9312(2) Å	β= 93.041(3)°.
	c = 25.1118(8) Å	γ = 90°.
Volume	2632.44(12) $Å^3$	
Z	2	
Density (calculated)	1.794 Mg/m^3	
Absorption coefficient	1.932 mm^{-1}	
F(000)	1420	
Crystal size	0.06 x 0.11 x 0.14 mm^3	
Theta range for data collection	1.624 to 27.004°.	
Index ranges	-13<=h<=12, -12<=k<=12, -32<=l<=32	
Reflections collected	18437	
Independent reflections	5764 [R(int) = 0.0273]	
Completeness to theta = 25.242°	99.9 %	
Refinement method	Full-matrix least-squares on F^2	
Data / restraints / parameters	5764 / 0 / 407	
Goodness-of-fit on F^2	1.030	
Final R indices [I>2sigma(I)]	R1 = 0.0381, wR2 = 0.0947	
R indices (all data)	R1 = 0.0496, wR2 = 0.0997	
Extinction coefficient	0.0024(3)	
Largest diff. peak and hole	0.746 and -0.807 $e.Å^{-3}$	

Comments: All non H atoms were refined anisotropic. A numerical absorption correction was performed ($T_{min/max}$: 0.6742/ 0.8050). The C-H H atoms were positioned with idealized geometry and were refined isotropic with $U_{iso}(H)$ = 1.2 $U_{eq}(C)$ using a riding model. The asymmetric unit consists of one $[Sn_2S_6]$ anions and one biphenyl molecule that are located on centers of inversion as well as one Ni cation and one phenanthroline ligand in general positions. The biphenyl molecule is disordered and was refined with half occupation and restraints for bond lengths and bond angles.

Table 2. Atomic coordinates ($\cdot 10^4$) and equivalent isotropic displacement parameters ($Å^2 \cdot 10^3$). U(eq) is defined as one third of the trace of the orthogonalized U_{ij} tensor.

	x	y	z	U(eq)
Sn(1)	1231(1)	5597(1)	394(1)	31(1)
S(1)	15(1)	3493(1)	372(1)	37(1)
S(2)	1191(1)	6733(1)	1213(1)	35(1)
S(3)	3402(1)	5571(1)	278(1)	36(1)
Ni(1)	3525(1)	6904(1)	1125(1)	31(1)
N(1)	3969(3)	5245(3)	1624(1)	35(1)
N(2)	3742(3)	7824(3)	1902(1)	34(1)
C(1)	4075(4)	3973(4)	1475(2)	42(1)
C(2)	4357(4)	2925(4)	1848(2)	49(1)
C(3)	4531(4)	3224(4)	2375(2)	44(1)
C(4)	4418(4)	4564(4)	2543(2)	38(1)
C(5)	4544(4)	4965(4)	3093(2)	45(1)
C(6)	4409(4)	6261(4)	3235(2)	45(1)
C(7)	4128(3)	7286(4)	2841(1)	39(1)
C(8)	3980(4)	8654(4)	2970(2)	43(1)
C(9)	3723(4)	9550(4)	2572(2)	41(1)
C(10)	3605(3)	9099(4)	2043(2)	38(1)
C(11)	4000(3)	6925(4)	2301(1)	33(1)
C(12)	4144(3)	5539(3)	2150(1)	34(1)
N(21)	3454(3)	8867(3)	805(1)	37(1)
N(22)	5446(3)	7252(3)	974(1)	40(1)
C(21)	2451(4)	9641(4)	708(2)	47(1)
C(22)	2545(6)	10993(5)	550(2)	57(1)
C(23)	3716(6)	11537(4)	491(2)	58(1)
C(24)	4804(5)	10757(4)	599(2)	50(1)
C(25)	6085(6)	11228(5)	538(2)	65(2)
C(26)	7072(5)	10399(6)	622(2)	65(1)
C(27)	6922(4)	9015(5)	762(2)	50(1)
C(28)	7908(4)	8061(6)	800(2)	60(1)
C(29)	7645(5)	6755(6)	895(2)	70(1)
C(30)	6391(4)	6386(5)	989(2)	58(1)
C(31)	5686(4)	8547(4)	841(1)	39(1)
C(32)	4623(4)	9412(4)	755(1)	40(1)
C(41)	7426(9)	1229(14)	2392(4)	65(3)
C(42)	7284(13)	1549(16)	1846(5)	75(3)
C(43)	7527(18)	2840(20)	1655(7)	76(5)
C(44)	7801(13)	3857(19)	2002(5)	70(3)
C(45)	7940(16)	3620(20)	2552(7)	75(4)
C(46)	7782(17)	2380(30)	2718(7)	73(5)
C(51)	7273(9)	-128(12)	2594(4)	63(2)
C(52)	7458(16)	-1310(30)	2268(7)	81(5)
C(53)	7460(20)	-2600(30)	2470(9)	82(6)
C(54)	7242(11)	-2735(16)	3010(6)	73(3)
C(55)	7041(16)	-1580(20)	3305(10)	70(5)
C(56)	7028(11)	-371(15)	3116(5)	63(3)

Table 3. Bond lengths [Å] and angles [°].

Sn(1)-S(3)	2.3292(9)	Sn(1)-S(1)#1	2.4463(9)
Sn(1)-S(2)	2.3485(9)	Sn(1)-S(1)	2.4520(9)
S(1)-Sn(1)#1	2.4462(9)	S(3)-Sn(1)-S(1)	120.43(3)
S(3)-Sn(1)-S(2)	100.25(3)	S(2)-Sn(1)-S(1)	113.31(3)
S(3)-Sn(1)-S(1)#1	113.53(3)	S(1)#1-Sn(1)-S(1)	92.15(3)
S(2)-Sn(1)-S(1)#1	118.50(3)	Sn(1)#1-S(1)-Sn(1)	87.85(3)
Sn(1)-S(2)-Ni(1)	83.75(3)	Sn(1)-S(3)-Ni(1)	83.98(3)
S(2)-Ni(1)	2.4940(10)	S(3)-Ni(1)	2.5016(10)
Ni(1)-N(1)	2.108(3)	Ni(1)-N(22)	2.113(3)
Ni(1)-N(21)	2.108(3)	Ni(1)-N(2)	2.156(3)
N(1)-Ni(1)-N(21)	162.09(12)	N(22)-Ni(1)-S(2)	172.36(10)
N(1)-Ni(1)-N(22)	92.77(13)	N(2)-Ni(1)-S(2)	90.39(8)
N(21)-Ni(1)-N(22)	78.19(13)	N(1)-Ni(1)-S(3)	95.23(8)
N(1)-Ni(1)-N(2)	77.50(11)	N(21)-Ni(1)-S(3)	99.59(8)
N(21)-Ni(1)-N(2)	87.29(11)	N(22)-Ni(1)-S(3)	86.65(9)
N(22)-Ni(1)-N(2)	92.01(12)	N(2)-Ni(1)-S(3)	172.55(8)
N(1)-Ni(1)-S(2)	94.83(9)	S(2)-Ni(1)-S(3)	91.88(3)
N(21)-Ni(1)-S(2)	94.68(9)		
		N(21)-C(21)	1.322(5)
N(1)-C(1)	1.324(5)	N(21)-C(32)	1.361(5)
N(1)-C(12)	1.357(4)	N(22)-C(30)	1.317(5)
N(2)-C(10)	1.325(5)	N(22)-C(31)	1.356(5)
N(2)-C(11)	1.360(4)	C(21)-C(22)	1.405(6)
C(1)-C(2)	1.421(6)	C(22)-C(23)	1.366(8)
C(2)-C(3)	1.361(6)	C(23)-C(24)	1.401(7)
C(3)-C(4)	1.403(5)	C(24)-C(32)	1.407(5)
C(4)-C(12)	1.401(5)	C(24)-C(25)	1.449(7)
C(4)-C(5)	1.437(5)	C(25)-C(26)	1.337(9)
C(5)-C(6)	1.346(6)	C(26)-C(27)	1.429(7)
C(6)-C(7)	1.438(6)	C(27)-C(28)	1.409(7)
C(7)-C(11)	1.402(5)	C(27)-C(31)	1.411(6)
C(7)-C(8)	1.407(5)	C(28)-C(29)	1.350(8)
C(8)-C(9)	1.355(6)	C(29)-C(30)	1.407(7)
C(9)-C(10)	1.402(5)	C(31)-C(32) 1.422(6)	
C(11)-C(12)	1.438(5)	C(21)-N(21)-C(32)	118.3(4)
		C(30)-N(22)-C(31)	118.3(4)
C(1)-N(1)-C(12)	118.1(3)	N(21)-C(21)-C(22)	122.7(5)
C(10)-N(2)-C(11)	116.9(3)	C(23)-C(22)-C(21)	119.1(4)
N(1)-C(1)-C(2)	122.0(4)	C(22)-C(23)-C(24)	119.9(4)
C(3)-C(2)-C(1)	119.7(4)	C(23)-C(24)-C(32)	117.2(4)
C(2)-C(3)-C(4)	119.3(4)	C(23)-C(24)-C(25)	124.2(4)
C(12)-C(4)-C(3)	117.5(3)	C(32)-C(24)-C(25)	118.5(5)
C(12)-C(4)-C(5)	119.4(3)	C(26)-C(25)-C(24)	120.7(4)
C(3)-C(4)-C(5)	123.1(4)	C(25)-C(26)-C(27)	122.3(5)
C(6)-C(5)-C(4)	120.9(4)	C(28)-C(27)-C(31)	117.1(4)
C(5)-C(6)-C(7)	121.1(4)	C(28)-C(27)-C(26)	124.9(5)
C(11)-C(7)-C(8)	117.6(4)	C(31)-C(27)-C(26)	117.9(5)
C(11)-C(7)-C(6)	119.3(4)	C(29)-C(28)-C(27)	119.9(4)
C(8)-C(7)-C(6)	123.1(3)	C(28)-C(29)-C(30)	119.0(5)
C(9)-C(8)-C(7)	119.0(3)	N(22)-C(30)-C(29)	123.0(5)

C(8)-C(9)-C(10)	119.6(4)	N(22)-C(31)-C(27)	122.3(4)
N(2)-C(10)-C(9)	123.5(4)	N(22)-C(31)-C(32)	117.0(3)
N(2)-C(11)-C(7)	123.4(3)	C(27)-C(31)-C(32)	120.6(4)
N(2)-C(11)-C(12)	117.0(3)	N(21)-C(32)-C(24)	122.7(4)
C(7)-C(11)-C(12)	119.6(3)	N(21)-C(32)-C(31)	117.4(3)
N(1)-C(12)-C(4)	123.3(3)	C(24)-C(32)-C(31)	119.8(4)
N(1)-C(12)-C(11)	116.9(3)	C(51)-C(56)	1.371(16)
C(4)-C(12)-C(11)	119.8(3)	C(51)-C(52)	1.45(2)
C(41)-C(42)	1.408(15)	C(52)-C(53)	1.38(4)
C(41)-C(46)	1.45(3)	C(53)-C(54)	1.39(3)
C(41)-C(51)	1.453(17)	C(54)-C(55)	1.38(3)
C(42)-C(43)	1.39(2)	C(55)-C(56)	1.29(2)
C(43)-C(44)	1.36(3)		
C(44)-C(45)	1.40(2)	C(56)-C(51)-C(41)	121.9(11)
C(45)-C(46)	1.31(4)	C(56)-C(51)-C(52)	115.7(14)
C(42)-C(41)-C(46)	112.6(15)	C(41)-C(51)-C(52)	122.2(12)
C(42)-C(41)-C(51)	122.9(12)	C(53)-C(52)-C(51)	123.0(17)
C(46)-C(41)-C(51)	124.5(12)	C(52)-C(53)-C(54)	117(2)
C(43)-C(42)-C(41)	122.1(16)	C(55)-C(54)-C(53)	118.7(18)
C(44)-C(43)-C(42)	119.9(14)	C(56)-C(55)-C(54)	125(2)
C(43)-C(44)-C(45)	120.9(17)	C(55)-C(56)-C(51)	121.0(17)
C(46)-C(45)-C(44)	118(2)		
C(45)-C(46)-C(41)	126.5(18)		

Symmetry transformations used to generate equivalent atoms: #1 -x,-y+1,-z

Table 4. Anisotropic displacement parameters ($Å^2 \cdot 10^3$). The anisotropic displacement factor exponent takes the form: $-2\pi^2[h^2 a^{*2} U_{11} + ... + 2 h k a^* b^* U_{12}]$

	U_{11}	U_{22}	U_{33}	U_{23}	U_{13}	U_{12}
Sn(1)	29(1)	31(1)	33(1)	-2(1)	3(1)	1(1)
S(1)	38(1)	31(1)	41(1)	4(1)	-2(1)	-1(1)
S(2)	32(1)	39(1)	35(1)	-6(1)	5(1)	0(1)
S(3)	30(1)	38(1)	40(1)	-5(1)	6(1)	1(1)
Ni(1)	30(1)	29(1)	36(1)	-2(1)	3(1)	1(1)
N(1)	36(2)	30(1)	39(2)	-2(1)	2(1)	-1(1)
N(2)	31(1)	32(2)	38(1)	-4(1)	4(1)	2(1)
C(1)	50(2)	32(2)	44(2)	-3(2)	-2(2)	1(2)
C(2)	59(2)	30(2)	58(2)	-2(2)	-1(2)	3(2)
C(3)	43(2)	36(2)	51(2)	7(2)	1(2)	-3(2)
C(4)	35(2)	36(2)	44(2)	4(2)	2(1)	-4(2)
C(5)	52(2)	45(2)	38(2)	9(2)	4(2)	-4(2)
C(6)	51(2)	50(2)	35(2)	1(2)	5(2)	-7(2)
C(7)	36(2)	42(2)	40(2)	-4(2)	6(1)	-4(2)
C(8)	45(2)	45(2)	40(2)	-8(2)	6(2)	-4(2)
C(9)	40(2)	36(2)	47(2)	-8(2)	6(2)	-1(2)
C(10)	35(2)	32(2)	45(2)	-2(1)	3(1)	0(1)
C(11)	32(2)	34(2)	34(2)	0(1)	5(1)	-2(1)
C(12)	33(2)	32(2)	37(2)	0(1)	3(1)	-3(1)
N(21)	45(2)	35(2)	32(1)	0(1)	10(1)	6(1)
N(22)	32(2)	40(2)	49(2)	-10(1)	7(1)	-3(1)
C(21)	57(2)	43(2)	40(2)	7(2)	11(2)	14(2)
C(22)	89(4)	43(2)	42(2)	4(2)	14(2)	26(2)
C(23)	112(4)	33(2)	30(2)	1(2)	10(2)	0(2)
C(24)	81(3)	38(2)	32(2)	1(2)	6(2)	-11(2)
C(25)	99(4)	56(3)	40(2)	6(2)	1(2)	-39(3)
C(26)	66(3)	77(3)	52(3)	12(2)	-2(2)	-35(3)
C(27)	50(2)	67(3)	34(2)	-3(2)	4(2)	-21(2)
C(28)	38(2)	93(4)	51(2)	-14(2)	10(2)	-14(2)
C(29)	36(2)	80(4)	93(4)	-23(3)	5(2)	1(2)
C(30)	30(2)	54(3)	90(3)	-19(2)	8(2)	4(2)
C(31)	41(2)	44(2)	33(2)	-6(1)	6(1)	-12(2)
C(32)	52(2)	38(2)	30(2)	-2(1)	7(2)	-9(2)
C(41)	44(5)	107(9)	45(5)	-2(5)	4(4)	26(5)
C(42)	75(8)	99(10)	51(6)	3(6)	2(5)	29(7)
C(43)	92(13)	95(14)	41(6)	11(8)	6(8)	46(10)
C(44)	71(8)	86(10)	53(7)	13(7)	16(6)	32(7)
C(45)	57(9)	88(10)	81(12)	24(9)	2(7)	6(8)
C(46)	39(8)	114(13)	64(9)	-16(10)	-10(6)	10(8)
C(51)	45(5)	82(7)	61(6)	-7(5)	-4(4)	7(5)
C(52)	57(10)	127(15)	57(9)	-26(9)	-10(6)	12(10)
C(53)	51(8)	79(10)	111(18)	16(12)	-33(9)	-1(7)
C(54)	52(6)	85(9)	82(10)	18(8)	2(6)	-8(6)
C(55)	55(8)	84(13)	71(10)	-14(9)	6(7)	-12(7)
C(56)	48(5)	86(8)	55(6)	-18(6)	5(4)	-5(6)

Table 5. Hydrogen coordinates ($\cdot 10^4$) and isotropic displacement parameters ($Å^2 \cdot 10^3$).

	x	y	z	U(eq)
H(1)	3958	3754	1107	50
H(2)	4425	2021	1729	59
H(3)	4727	2532	2628	52
H(5)	4726	4305	3360	54
H(6)	4500	6504	3601	54
H(8)	4060	8945	3331	52
H(9)	3624	10478	2651	49
H(10)	3415	9743	1770	45
H(21)	1633	9268	746	56
H(22)	1804	11521	485	69
H(23)	3793	12444	377	70
H(25)	6225	12136	438	78
H(26)	7903	10741	586	78
H(28)	8758	8335	758	72
H(29)	8296	6096	899	84
H(30)	6218	5470	1067	69
H(42A)	7067	825	1610	90
H(43A)	7515	2954	1277	91
H(44A)	7964	4702	1840	84
H(45A)	8062	4355	2791	90
H(46A)	7994	2237	3090	87
H(52A)	7440	-1168	1892	97
H(53A)	7244	-3306	2223	98
H(54A)	7256	-3647	3127	88
H(55A)	7023	-1713	3681	84
H(56A)	6826	371	3342	76

5.3.15 Messprotokoll der Verbindung $\{[Ni(phen)_2]_2[Sn_2S_6]\}\cdot phen\cdot H_2O$

Table 1. Crystal data and structure refinement for $\{[Ni(C_{12}H_8N_2)_2]_2[Sn_2S_6]\}\cdot C_{12}H_8N_2\cdot H_2O$ ($C_{12}H_8N_2$, phen = 1,10-Phenathrolin)

Identification code	jh1890	
Empirical formula	$\{[Ni(C_{12}H_8N_2)_2]_2[Sn_2S_6]\}\cdot C_{12}H_8N_2\cdot H_2O$	
Crystal color, habitus	red violet blocks	
Formula weight	1466.19	
Temperature	293(2) K	
Wavelength	0.71073 Å	
Crystal system	triclinic	
Space group	$P\bar{1}$	
Unit cell dimensions	a = 11.0469(4) Å	α= 115.055(3)°.
	b = 12.0833(5) Å	β= 88.190(3)°.
	c = 12.6141(5) Å	γ = 110.349(3)°.
Volume	1416.81(10) $Å^3$	
Z	1	
Density (calculated)	1.718 Mg/m^3	
Absorption coefficient	1.800 mm^{-1}	
F(000)	732	
Crystal size	0.12 x 0.09 x 0.06 mm^3	
Theta range for data collection	1.799 to 27.004°.	
Index ranges	-14<=h<=14, -15<=k<=15, -15<=l<=16	
Reflections collected	12598	
Independent reflections	6107 [R(int) = 0.0313]	
Completeness to theta = 25.242°	98.9 %	
Refinement method	Full-matrix least-squares on F^2	
Data / restraints / parameters	6107 / 0 / 380	
Goodness-of-fit on F^2	0.988	
Final R indices [I>2sigma(I)]	R1 = 0.0409, wR2 = 0.1005	
R indices (all data)	R1 = 0.0567, wR2 = 0.1074	
Extinction coefficient	0.0083(8)	
Largest diff. peak and hole	0.847 and -0.933 e.$Å^{-3}$	

All non-hydrogen atoms were refined anisotropic. The C-H H atoms were positioned with idealized geometry and refined isotropic with $U_{iso}(H) = 1.2 \cdot U_{eq}(C)$ using a riding model. The water H atoms were not located but considered in the formula. A numerical absorption correction was performed ($T_{min/max}$: 0.7303/0.8108). One phenanthroline ligand is disordered around a centre of inversion, in which also one water molecule is involved. Both of them were refined with half occupancy. The disorder remain constant if the structure refinement is

performed in space group *P*1, where all atoms are located in general positions.

Table 2. Atomic coordinates ($\cdot 10^4$) and equivalent isotropic displacement parameters ($Å^2 \cdot 10^3$). U(eq) is defined as one third of the trace of the orthogonalized U_{ij} tensor.

	x	y	z	U(eq)
Sn(1)	5802(1)	3953(1)	4569(1)	31(1)
S(1)	7998(1)	4286(1)	4431(1)	36(1)
S(2)	4908(1)	1666(1)	3920(1)	33(1)
S(3)	5206(1)	5198(1)	6467(1)	36(1)
Ni(1)	7212(1)	1862(1)	3606(1)	31(1)
N(1)	6956(3)	1470(3)	1820(3)	33(1)
N(2)	6501(3)	-231(3)	2759(3)	31(1)
C(1)	7198(4)	2315(4)	1359(4)	38(1)
C(2)	7105(4)	1935(5)	140(4)	43(1)
C(3)	6732(4)	636(5)	-623(4)	40(1)
C(4)	6453(4)	-294(4)	-171(4)	36(1)
C(5)	6023(4)	-1683(4)	-904(4)	40(1)
C(6)	5726(5)	-2539(5)	-433(4)	45(1)
C(7)	5857(4)	-2090(4)	826(4)	39(1)
C(8)	5550(5)	-2938(5)	1377(4)	46(1)
C(9)	5728(4)	-2419(4)	2578(4)	41(1)
C(10)	6209(4)	-1056(4)	3240(4)	36(1)
C(11)	6312(4)	-740(4)	1565(3)	31(1)
C(12)	6586(4)	171(4)	1057(3)	32(1)
N(21)	7727(3)	1852(3)	5181(3)	34(1)
N(22)	9163(3)	1923(4)	3451(3)	37(1)
C(21)	7010(4)	1832(4)	6038(4)	38(1)
C(22)	7427(5)	1744(5)	7021(4)	48(1)
C(23)	8630(5)	1682(5)	7120(5)	52(1)
C(24)	9424(5)	1711(5)	6240(4)	48(1)
C(25)	10720(5)	1688(6)	6262(5)	59(1)
C(26)	11440(5)	1751(6)	5403(5)	58(1)
C(27)	10960(4)	1848(5)	4420(5)	45(1)
C(28)	11668(5)	1903(6)	3492(5)	54(1)
C(29)	11137(5)	2004(6)	2601(5)	58(1)
C(30)	9869(4)	2004(5)	2604(5)	47(1)
C(31)	9695(4)	1859(4)	4357(4)	38(1)
C(32)	8927(4)	1802(4)	5282(4)	37(1)
N(41)	1475(5)	4803(5)	364(4)	58(1)
C(44')	1475(5)	4803(5)	364(4)	58(1)
C(41)	2058(6)	4757(6)	1296(6)	68(2)
C(42)	1490(6)	4876(6)	2302(5)	62(1)
C(43)	317(6)	5036(6)	2373(5)	58(1)
C(44)	-290(4)	5074(5)	1469(4)	54(1)
N(41')	-290(4)	5074(5)	1469(4)	54(1)
C(45)	313(5)	4975(5)	485(4)	48(1)
C(46)	-1574(10)	5386(9)	1623(8)	46(2)
C(47)	-2157(9)	5405(10)	724(10)	54(2)
O(1)	-3058(7)	5160(8)	1452(8)	67(2)

Table 3. Bond lengths [Å] and angles [°].

Sn(1)-S(1)	2.3304(10)	Sn(1)-S(3)	2.4434(10)
Sn(1)-S(2)	2.3495(10)	Sn(1)-S(3)#1	2.4536(10)
S(1)-Ni(1)	2.4737(11)	S(3)-Sn(1)#1	2.4536(10)
S(2)-Ni(1)	2.5070(10)	S(2)-Sn(1)-S(3)#1	115.55(4)
S(1)-Sn(1)-S(2)	100.70(4)	S(3)-Sn(1)-S(3)#1	92.84(3)
S(1)-Sn(1)-S(3)	118.26(4)	Sn(1)-S(1)-Ni(1)	83.77(4)
S(2)-Sn(1)-S(3)	113.81(4)	Sn(1)-S(2)-Ni(1)	82.66(3)
S(1)-Sn(1)-S(3)#1	116.71(4)	Sn(1)-S(3)-Sn(1)#1	87.16(3)
Ni(1)-N(21)	2.089(3)	Ni(1)-N(2)	2.130(3)
Ni(1)-N(1)	2.103(3)	Ni(1)-N(22)	2.136(3)
N(21)-Ni(1)-N(1)	163.29(12)	N(2)-Ni(1)-S(1)	175.30(9)
N(21)-Ni(1)-N(2)	89.86(13)	N(22)-Ni(1)-S(1)	90.63(10)
N(1)-Ni(1)-N(2)	78.55(13)	N(21)-Ni(1)-S(2)	96.29(9)
N(21)-Ni(1)-N(22)	78.37(13)	N(1)-Ni(1)-S(2)	95.13(9)
N(1)-Ni(1)-N(22)	89.50(13)	N(2)-Ni(1)-S(2)	87.16(8)
N(2)-Ni(1)-N(22)	89.96(13)	N(22)-Ni(1)-S(2)	173.95(10)
N(21)-Ni(1)-S(1)	94.82(10)	S(1)-Ni(1)-S(2)	92.68(3)
N(1)-Ni(1)-S(1)	96.79(10)		
N(1)-C(1)	1.325(5)	N(21)-C(21)	1.323(5)
N(1)-C(12)	1.362(5)	N(21)-C(32)	1.360(5)
N(2)-C(10)	1.320(5)	N(22)-C(30)	1.319(6)
N(2)-C(11)	1.354(5)	N(22)-C(31)	1.344(6)
C(1)-C(2)	1.402(6)	C(21)-C(22)	1.394(6)
C(2)-C(3)	1.362(7)	C(22)-C(23)	1.370(7)
C(3)-C(4)	1.405(6)	C(23)-C(24)	1.399(7)
C(4)-C(12)	1.400(6)	C(24)-C(32)	1.404(6)
C(4)-C(5)	1.434(6)	C(24)-C(25)	1.442(6)
C(5)-C(6)	1.344(7)	C(25)-C(26)	1.336(8)
C(6)-C(7)	1.437(6)	C(26)-C(27)	1.428(7)
C(7)-C(11)	1.398(6)	C(27)-C(28)	1.401(7)
C(7)-C(8)	1.413(6)	C(27)-C(31)	1.407(5)
C(8)-C(9)	1.362(7)	C(28)-C(29)	1.353(8)
C(9)-C(10)	1.395(6)	C(29)-C(30)	1.401(6)
C(11)-C(12)	1.437(6)	C(31)-C(32)	1.432(6)
C(1)-N(1)-C(12)	117.5(3)	C(21)-N(21)-C(32)	118.0(4)
C(10)-N(2)-C(11)	118.0(3)	C(30)-N(22)-C(31)	118.3(3)
N(1)-C(1)-C(2)	123.2(4)	N(21)-C(21)-C(22)	122.8(4)
C(3)-C(2)-C(1)	119.3(4)	C(23)-C(22)-C(21)	119.4(4)
C(2)-C(3)-C(4)	119.3(4)	C(22)-C(23)-C(24)	119.8(4)
C(12)-C(4)-C(3)	117.7(4)	C(23)-C(24)-C(32)	117.1(4)
C(12)-C(4)-C(5)	119.0(4)	C(23)-C(24)-C(25)	124.8(4)
C(3)-C(4)-C(5)	123.3(4)	C(32)-C(24)-C(25)	118.1(4)
C(6)-C(5)-C(4)	121.2(4)	C(26)-C(25)-C(24)	121.7(5)
C(5)-C(6)-C(7)	121.0(4)	C(25)-C(26)-C(27)	121.4(4)
C(11)-C(7)-C(8)	117.0(4)	C(28)-C(27)-C(31)	117.5(4)
C(11)-C(7)-C(6)	119.2(4)	C(28)-C(27)-C(26)	123.7(4)
C(8)-C(7)-C(6)	123.8(4)	C(31)-C(27)-C(26)	118.8(4)
C(9)-C(8)-C(7)	119.5(4)	C(29)-C(28)-C(27)	119.5(4)
C(8)-C(9)-C(10)	119.2(4)	C(28)-C(29)-C(30)	119.2(5)

N(2)-C(10)-C(9)	123.1(4)	N(22)-C(30)-C(29)	122.9(5)
N(2)-C(11)-C(7)	123.1(4)	N(22)-C(31)-C(27)	122.5(4)
N(2)-C(11)-C(12)	117.3(3)	N(22)-C(31)-C(32)	117.7(3)
C(7)-C(11)-C(12)	119.6(4)	C(27)-C(31)-C(32)	119.8(4)
N(1)-C(12)-C(4)	123.0(4)	N(21)-C(32)-C(24)	123.0(4)
N(1)-C(12)-C(11)	117.1(3)	N(21)-C(32)-C(31)	116.8(4)
C(4)-C(12)-C(11)	120.0(4)	C(24)-C(32)-C(31)	120.2(4)
N(41)-C(45)	1.364(7)	C(44)-C(45)	1.370(6)
N(41)-C(41)	1.388(8)	C(44)-C(46)	1.576(11)
N(41)-C(47)#2	1.514(11)	C(45)-C(45)#2	1.457(10)
C(41)-C(42)	1.373(9)	C(46)-C(47)	1.333(15)
C(42)-C(43)	1.370(8)	C(47)-N(41)#2	1.514(11)
C(43)-C(44)	1.366(7)		
C(45)-N(41)-C(41)	117.5(5)	C(43)-C(44)-C(46)	120.2(5)
C(45)-N(41)-C(47)#2	125.5(6)	C(45)-C(44)-C(46)	120.9(5)
C(41)-N(41)-C(47)#2	116.9(6)	N(41)-C(45)-C(44)	122.3(5)
C(42)-C(41)-N(41)	121.5(6)	N(41)-C(45)-C(45)#2	118.2(5)
C(43)-C(42)-C(41)	118.5(5)	C(44)-C(45)-C(45)#2	119.4(6)
C(44)-C(43)-C(42)	121.5(5)	C(47)-C(46)-C(44)	119.2(7)
C(43)-C(44)-C(45)	118.5(5)	C(46)-C(47)-N(41)#2	116.4(8)

Symmetry transformations used to generate equivalent atoms: #1 -x+1,-y+1,-z+1 #2 -x,-y+1,-z

Table 4. Anisotropic displacement parameters ($Å^2 \cdot 10^3$). The anisotropic displacement factor exponent takes the form: $-2\pi^2[h^2 a^{*2} U_{11} + ... + 2 h k a^* b^* U_{12}]$

	U_{11}	U_{22}	U_{33}	U_{23}	U_{13}	U_{12}
Sn(1)	36(1)	29(1)	30(1)	12(1)	7(1)	17(1)
S(1)	36(1)	34(1)	40(1)	14(1)	9(1)	15(1)
S(2)	36(1)	29(1)	36(1)	14(1)	6(1)	16(1)
S(3)	50(1)	35(1)	29(1)	14(1)	9(1)	24(1)
Ni(1)	36(1)	32(1)	29(1)	14(1)	7(1)	18(1)
N(1)	40(2)	34(2)	30(2)	14(1)	9(1)	21(1)
N(2)	34(2)	29(2)	32(2)	15(1)	7(1)	15(1)
C(1)	46(2)	36(2)	37(2)	18(2)	6(2)	19(2)
C(2)	55(2)	42(2)	40(2)	24(2)	11(2)	22(2)
C(3)	46(2)	46(2)	31(2)	19(2)	8(2)	19(2)
C(4)	39(2)	39(2)	31(2)	13(2)	6(2)	19(2)
C(5)	45(2)	43(2)	28(2)	12(2)	6(2)	17(2)
C(6)	55(2)	34(2)	35(2)	7(2)	3(2)	15(2)
C(7)	43(2)	37(2)	38(2)	15(2)	6(2)	17(2)
C(8)	60(3)	33(2)	45(2)	16(2)	9(2)	17(2)
C(9)	52(2)	36(2)	44(2)	22(2)	10(2)	20(2)
C(10)	40(2)	37(2)	36(2)	18(2)	7(2)	20(2)
C(11)	34(2)	31(2)	31(2)	11(2)	5(2)	17(2)
C(12)	34(2)	34(2)	33(2)	15(2)	7(2)	17(2)
N(21)	39(2)	32(2)	30(2)	13(1)	4(1)	14(1)
N(22)	35(2)	40(2)	44(2)	22(2)	9(1)	18(2)
C(21)	46(2)	38(2)	32(2)	17(2)	6(2)	16(2)
C(22)	60(3)	46(3)	43(2)	25(2)	10(2)	18(2)
C(23)	60(3)	56(3)	46(3)	27(2)	-1(2)	21(2)
C(24)	49(2)	50(3)	49(3)	22(2)	-1(2)	21(2)
C(25)	56(3)	72(4)	58(3)	31(3)	-8(2)	29(3)
C(26)	45(2)	69(4)	69(3)	33(3)	0(2)	30(2)
C(27)	39(2)	41(2)	60(3)	22(2)	4(2)	19(2)
C(28)	40(2)	58(3)	72(3)	31(3)	14(2)	26(2)
C(29)	48(3)	74(4)	72(4)	41(3)	27(3)	34(3)
C(30)	43(2)	58(3)	52(3)	31(2)	16(2)	26(2)
C(31)	35(2)	35(2)	42(2)	15(2)	4(2)	16(2)
C(32)	40(2)	35(2)	39(2)	15(2)	1(2)	18(2)
N(41)	56(3)	57(3)	50(3)	24(2)	5(2)	9(2)
C(44')	56(3)	57(3)	50(3)	24(2)	5(2)	9(2)
C(41)	64(3)	63(4)	66(4)	28(3)	3(3)	11(3)
C(42)	68(3)	55(3)	55(3)	28(3)	-8(3)	6(3)
C(43)	69(3)	50(3)	50(3)	29(2)	1(2)	6(2)
C(44)	55(2)	49(3)	45(2)	22(2)	3(2)	3(2)
N(41')	55(2)	49(3)	45(2)	22(2)	3(2)	3(2)
C(45)	48(2)	48(3)	39(2)	20(2)	4(2)	7(2)
C(46)	62(5)	33(4)	38(5)	11(4)	17(4)	17(4)
C(47)	44(5)	46(5)	68(7)	19(5)	18(5)	21(4)
O(1)	58(4)	57(5)	101(6)	42(5)	35(4)	32(4)

Table 5. Hydrogen coordinates ($\cdot 10^4$) and isotropic displacement parameters ($Å^2 \cdot 10^3$).

	x	y	z	U(eq)
H(1)	7442	3204	1870	45
H(2)	7296	2563	-145	51
H(3)	6663	368	-1434	48
H(5)	5948	-1997	-1721	48
H(6)	5431	-3436	-928	54
H(8)	5228	-3845	923	56
H(9)	5532	-2966	2952	49
H(10)	6328	-712	4059	43
H(21)	6193	1879	5982	46
H(22)	6893	1727	7604	58
H(23)	8917	1620	7771	63
H(25)	11063	1628	6891	71
H(26)	12270	1732	5446	69
H(28)	12498	1872	3488	64
H(29)	11608	2072	1992	70
H(30)	9509	2063	1983	56
H(41)	2852	4644	1237	82
H(42)	1892	4848	2922	75
H(43)	-75	5121	3052	70
H(46)	-1921	5554	2331	56
H(47)	-2940	5539	764	64

5.3.16 Messprotokoll der Verbindung $\{[Ni(cyclam)]_2[Sn_2S_6]\}_n \cdot 2nH_2O$

Table 1. Crystal data and structure refinement for $\{[Ni(C_{10}H_{24}N_4)]_2[Sn_2S_6]\}_n \cdot 2nH_2O$. ($C_{10}H_{24}N_4$, cyclam = 1,4,8,11-Tetraazacyclotetradecan)

Identification code	jh1266	
Empirical formula	$\{[Ni(C_{10}H_{24}N_4)]_2[Sn_2S_6]\}_n \cdot 2nH_2O$	
Crystal color, habitus	pale orange needles	
Formula weight	983.86	
Temperature	200(2) K	
Wavelength	0.71073 Å	
Crystal system	triclinic	
Space group	$P\bar{1}$	
Unit cell dimensions	a = 9.0689(4) Å	α= 97.227(3)°.
	b = 9.8368(4) Å	β= 94.227(3)°.
	c = 10.1537(4) Å	γ = 104.107(3)°.
Volume	866.36(6) Å^3	
Z	1	
Density (calculated)	1.886 Mg/m^3	
Absorption coefficient	2.890 mm^{-1}	
F(000)	496	
Crystal size	0.06 x 0.09 x 0.12 mm^3	
Theta range for data collection	2.03 to 27.92°.	
Index ranges	-11<=h<=11, -12<=k<=12, -13<=l<=13	
Reflections collected	13721	
Independent reflections	4135 [R(int) = 0.0376]	
Completeness to theta = 27.92°	99.8 %	
Refinement method	Full-matrix least-squares on F^2	
Data / restraints / parameters	4135 / 0 / 185	
Goodness-of-fit on F^2	1.047	
Final R indices [I>2sigma(I)]	R1 = 0.0337, wR2 = 0.0844	
R indices (all data)	R1 = 0.0380, wR2 = 0.0859	
Extinction coefficient	0.0113(11)	
Largest diff. peak and hole	0.912 and -0.988 e.Å^{-3}	

Comments: All non H atoms were refined anisotropic. A numerical absorption correction was performed ($T_{min/max}$: 0.5026/ 0.7412). The C-H H atoms were positioned with idealized geometry and were refined isotropic with $U_{iso}(H) = 1.2\ U_{eq}(C)$ using a riding model. The water H atoms were located in difference map, their bond lengths were set to ideal values and finally they were refined isotropic with $U_{iso}(H) = 1.5\ U_{eq}(O)$ using a riding model. The asymmetric unit consists of one $[Sn_2S_6]^{4-}$ anion, two Ni^{2+} cations and two cyclam (1,4,8,11-tetraazacyclotetradecane) ligands all of them located on centers of inversion.

Table 2. Atomic coordinates ($\cdot 10^4$) and equivalent isotropic displacement parameters ($Å^2 \cdot 10^3$). U(eq) is defined as one third of the trace of the orthogonalized U_{ij} tensor.

	x	y	z	U(eq)
Sn(1)	3703(1)	3835(1)	675(1)	23(1)
S(1)	4185(1)	6380(1)	649(1)	27(1)
S(2)	1307(1)	2624(1)	-458(1)	28(1)
S(3)	4121(1)	3219(1)	2799(1)	29(1)
Ni(1)	0	0	0	26(1)
N(1)	1419(3)	219(3)	1729(3)	31(1)
C(1)	2501(4)	-655(4)	1440(4)	37(1)
C(2)	2955(4)	-511(4)	44(4)	37(1)
N(2)	1572(3)	-896(3)	-914(3)	30(1)
C(3)	1872(4)	-547(4)	-2255(4)	39(1)
C(4)	399(5)	-918(4)	-3214(4)	43(1)
C(5)	-681(4)	32(4)	-2939(3)	36(1)
Ni(2)	5000	5000	5000	25(1)
N(11)	4585(3)	3302(3)	6026(3)	29(1)
C(11)	2903(4)	2801(4)	5998(4)	35(1)
C(12)	2230(4)	4068(4)	6154(4)	36(1)
N(12)	2720(3)	4959(3)	5121(3)	30(1)
C(13)	2352(4)	6337(4)	5336(4)	37(1)
C(14)	2925(5)	7254(4)	4275(4)	43(1)
C(15)	4646(5)	7836(3)	4345(4)	36(1)
O(1)	-4(5)	4544(5)	1896(4)	78(1)

Table 3. Bond lengths [Å] and angles [°].

Sn(1)-S(3)	2.3406(8)	Sn(1)-S(1)#1	2.4543(8)
Sn(1)-S(2)	2.3433(8)	S(1)-Sn(1)#1	2.4543(8)
Sn(1)-S(1)	2.4382(8)		
S(3)-Sn(1)-S(2)	113.44(3)	S(3)-Sn(1)-S(1)#1	110.96(3)
S(3)-Sn(1)-S(1)	114.03(3)	S(2)-Sn(1)-S(1)#1	112.55(3)
S(2)-Sn(1)-S(1)	111.09(3)	S(1)-Sn(1)-S(1)#1	93.17(3)
Sn(1)-S(1)-Sn(1)#1	86.83(3)	Sn(1)-S(3)-Ni(2)	125.34(3)
Sn(1)-S(2)-Ni(1)	119.30(3)		
S(2)-Ni(1)	2.6788(7)	S(3)-Ni(2)	2.6022(8)
Ni(1)-N(1)#2	2.055(3)	Ni(2)-N(11)	2.051(3)
Ni(1)-N(1)	2.055(3)	Ni(2)-N(11)#3	2.051(3)
Ni(1)-N(2)#2	2.067(3)	Ni(2)-N(12)	2.071(3)
Ni(1)-N(2)	2.067(3)	Ni(2)-N(12)#3	2.071(3)
Ni(1)-S(2)#2	2.6788(7)	Ni(2)-S(3)#3	2.6022(8)
N(1)#2-Ni(1)-N(1)	180.00(17)	N(11)-Ni(2)-N(11)#3	180.000(1)
N(1)#2-Ni(1)-N(2)#2	85.40(12)	N(11)-Ni(2)-N(12)	85.66(11)
N(1)-Ni(1)-N(2)#2	94.60(12)	N(11)#3-Ni(2)-N(12)	94.34(11)
N(1)#2-Ni(1)-N(2)	94.60(12)	N(11)-Ni(2)-N(12)#3	94.34(11)
N(1)-Ni(1)-N(2)	85.40(12)	N(11)#3-Ni(2)-N(12)#3	85.66(11)
N(2)#2-Ni(1)-N(2)	180.0	N(12)-Ni(2)-N(12)#3	180.00(16)
N(1)#2-Ni(1)-S(2)	87.14(8)	N(11)-Ni(2)-S(3)#3	91.85(8)
N(1)-Ni(1)-S(2)	92.86(8)	N(11)#3-Ni(2)-S(3)#3	88.15(8)
N(2)#2-Ni(1)-S(2)	85.69(7)	N(12)-Ni(2)-S(3)#3	92.52(8)
N(2)-Ni(1)-S(2)	94.31(7)	N(12)#3-Ni(2)-S(3)#3	87.48(8)
N(1)#2-Ni(1)-S(2)#2	92.86(8)	N(11)-Ni(2)-S(3)	88.15(8)
N(1)-Ni(1)-S(2)#2	87.14(8)	N(11)#3-Ni(2)-S(3)	91.85(8)
N(2)#2-Ni(1)-S(2)#2	94.31(7)	N(12)-Ni(2)-S(3)	87.48(8)
N(2)-Ni(1)-S(2)#2	85.69(7)	N(12)#3-Ni(2)-S(3)	92.52(8)
S(2)-Ni(1)-S(2)#2	180.00(3)	S(3)#3-Ni(2)-S(3)	180.0
N(1)-C(5)#2	1.461(4)	N(11)-C(15)#3	1.481(4)
N(1)-C(1)	1.476(5)	N(11)-C(11)	1.481(4)
C(1)-C(2)	1.519(5)	C(11)-C(12)	1.512(5)
C(2)-N(2)	1.469(5)	C(12)-N(12)	1.475(4)
N(2)-C(3)	1.474(5)	N(12)-C(13)	1.468(4)
C(3)-C(4)	1.531(6)	C(13)-C(14)	1.531(6)
C(4)-C(5)	1.527(6)	C(14)-C(15)	1.519(6)
C(5)-N(1)#2	1.461(4)	C(15)-N(11)#3	1.481(4)
C(5)#2-N(1)-C(1)	113.7(3)	C(15)#3-N(11)-C(11)	114.3(3)
N(1)-C(1)-C(2)	108.6(3)	N(11)-C(11)-C(12)	109.1(3)
N(2)-C(2)-C(1)	109.3(3)	N(12)-C(12)-C(11)	109.5(3)
C(2)-N(2)-C(3)	113.2(3)	C(13)-N(12)-C(12)	113.3(3)
N(2)-C(3)-C(4)	111.8(3)	N(12)-C(13)-C(14)	112.0(3)
C(5)-C(4)-C(3)	115.2(3)	C(15)-C(14)-C(13)	116.2(3)
N(1)#2-C(5)-C(4)	111.8(3)	N(11)#3-C(15)-C(14)	111.5(3)

Symmetry transformations used to generate equivalent atoms:
#1 -x+1,-y+1,-z #2 -x,-y,-z #3 -x+1,-y+1,-z+1

Table 4. Anisotropic displacement parameters ($Å^2 \cdot 10^3$). The anisotropic displacement factor exponent takes the form: $-2\pi^2[h^2 a^{*2} U_{11} + ... + 2 h k a^* b^* U_{12}]$

	U_{11}	U_{22}	U_{33}	U_{23}	U_{13}	U_{12}
Sn(1)	23(1)	22(1)	21(1)	5(1)	2(1)	1(1)
S(1)	30(1)	24(1)	30(1)	6(1)	8(1)	8(1)
S(2)	25(1)	27(1)	29(1)	6(1)	-1(1)	0(1)
S(3)	37(1)	25(1)	22(1)	5(1)	-1(1)	0(1)
Ni(1)	21(1)	34(1)	23(1)	7(1)	2(1)	8(1)
N(1)	33(2)	28(1)	27(1)	8(1)	-4(1)	1(1)
C(1)	29(2)	31(2)	49(2)	17(2)	-8(1)	5(1)
C(2)	21(2)	34(2)	58(2)	17(2)	7(1)	8(1)
N(2)	30(1)	26(1)	36(2)	9(1)	9(1)	6(1)
C(3)	44(2)	32(2)	44(2)	10(2)	24(2)	10(1)
C(4)	63(3)	38(2)	28(2)	6(2)	13(2)	6(2)
C(5)	47(2)	28(2)	28(2)	7(1)	-3(1)	-1(1)
Ni(2)	25(1)	23(1)	27(1)	7(1)	4(1)	4(1)
N(11)	33(1)	25(1)	28(1)	7(1)	1(1)	4(1)
C(11)	34(2)	32(2)	34(2)	10(1)	7(1)	-5(1)
C(12)	27(2)	45(2)	34(2)	8(2)	6(1)	2(1)
N(12)	27(1)	32(1)	30(1)	4(1)	3(1)	7(1)
C(13)	33(2)	44(2)	39(2)	6(2)	3(1)	20(2)
C(14)	52(2)	43(2)	41(2)	10(2)	1(2)	26(2)
C(15)	52(2)	25(2)	33(2)	8(1)	3(2)	12(1)
O(1)	87(3)	101(3)	66(2)	17(2)	31(2)	51(2)

Table 5. Hydrogen coordinates ($\cdot 10^4$) and isotropic displacement parameters ($Å^2 \cdot 10^3$).

	x	y	z	U(eq)
H(1N)	1996	1157	1882	37
H(1A)	2015	-1659	1497	44
H(1B)	3420	-332	2102	44
H(2A)	3529	477	13	44
H(2B)	3625	-1142	-194	44
H(2N)	1193	-1874	-1002	36
H(3A)	2588	-1075	-2619	46
H(3B)	2365	478	-2186	46
H(4A)	679	-872	-4134	52
H(4B)	-159	-1909	-3174	52
H(5A)	-98	1037	-2842	44
H(5B)	-1475	-149	-3709	44
H(11N)	4950	3668	6912	35
H(11A)	2648	2242	6733	42
H(11B)	2468	2184	5142	42
H(12A)	1100	3744	6064	43
H(12B)	2579	4627	7052	43
H(12N)	2184	4476	4313	36
H(13A)	2824	6844	6230	44
H(13B)	1230	6184	5317	44
H(14A)	2556	6685	3385	51
H(14B)	2451	8063	4346	51
H(15A)	4877	8550	3734	44
H(15B)	5051	8314	5263	44
H(1O1)	319	4133	1244	117
H(2O1)	-278	5211	1592	117

Table 6. Hydrogen bonds with H..A < r(A) + 2.000 Angstroms and <DHA > 110 deg.

D-H	d(D-H)	d(H..A)	<DHA	d(D..A)	A
N1-H1N	0.930	2.460	158.32	3.342	S3
N2-H2N	0.930	2.600	165.13	3.507	O1 [-x, -y, -z]
2-H2N	0.930	2.799	111.57	3.258	S2 [-x, -y, -z]
N11-H11N	0.930	2.552	157.10	3.428	S1 [-x+1, -y+1, -z+1]
O1-H1O1	0.840	2.495	170.90	3.327	S2
O1-H2O1	0.840	2.856	177.12	3.696	S2 [-x, -y+1, -z]

5.3.17 Messprotokoll der Verbindung {[Mn(bipy)$_2$]$_2$[Sn$_2$S$_6$]}

Table 1. Crystal data and structure refinement for {[Mn($C_{10}H_8N_2$)$_2$]$_2$[Sn$_2$S$_6$]} ($C_{10}H_8N_2$, 2,2'-bipy = 2,2'-Bipyridin)

Identification code	jh1582	
Empirical formula	{[Mn($C_{10}H_8N_2$)$_2$]$_2$[Sn$_2$S$_6$]}	
Crystal color, habitus	red blocks	
Formula weight	1164.35	
Temperature	300(2) K	
Wavelength	0.71073 Å	
Crystal system	monoclinic	
Space group	$P2_1/n$	
Unit cell dimensions	a = 8.7695(3) Å	α= 90°.
	b = 20.5296(6) Å	β= 95.791(3)°.
	c = 12.3761(4) Å	γ = 90°.
Volume	2216.75(12) Å^3	
Z	2	
Density (calculated)	1.744 Mg/m^3	
Absorption coefficient	1.993 mm^{-1}	
F(000)	1148	
Crystal size	0.08 x 0.10 x 0.12 mm^3	
Theta range for data collection	1.929 to 26.798°.	
Index ranges	-11<=h<=11, -26<=k<=22, -15<=l<=15	
Reflections collected	18518	
Independent reflections	4691 [R(int) = 0.0238]	
Completeness to theta = 25.242°	98.9 %	
Refinement method	Full-matrix least-squares on F^2	
Data / restraints / parameters	4691 / 30 / 252	
Goodness-of-fit on F^2	1.048	
Final R indices [I>2sigma(I)]	R1 = 0.0348, wR2 = 0.0910	
R indices (all data)	R1 = 0.0408, wR2 = 0.0944	
Extinction coefficient	0.0113(10)	
Largest diff. peak and hole	0.426 and -0.373 e.Å^{-3}	

Comments: All non-hydrogen atoms were refined anisotropic. The C-H H atoms were positioned with idealized geometry and refined isotropic with U_{iso}(H) = 1.2 U_{eq}(C) using a riding model. A numerical absorption correction was performed ($T_{min/max}$: 0.6939/0.7741). The asymmetric unit consists of one dimer, which is located on a center of inversion. One of the 2,2'-bipyridine ligands is disordered in two orientations and was refined using restraints for the geometry (SAME) and for the anisotropic displacement parameters (SIMU/DELU).

Table 2. Atomic coordinates (·10^4) and equivalent isotropic displacement parameters (Å^2·10^3).

U(eq) is defined as one third of the trace of the orthogonalized U_{ij} tensor.

	x	y	z	U(eq)
Sn(1)	4423(1)	570(1)	4072(1)	51(1)
S(1)	2611(1)	452(1)	2563(1)	64(1)
S(2)	5312(1)	1640(1)	3919(1)	62(1)
S(3)	3542(1)	246(1)	5799(1)	62(1)
Mn(1)	3856(1)	1550(1)	2049(1)	54(1)
N(1)	2942(4)	1381(2)	232(2)	66(1)
N(2)	5758(4)	1092(2)	1175(3)	64(1)
C(1)	1542(5)	1523(3)	-200(3)	82(1)
C(2)	916(6)	1270(3)	-1206(4)	98(2)
C(3)	1792(8)	858(3)	-1740(4)	96(2)
C(4)	3266(7)	723(2)	-1313(4)	85(1)
C(5)	3827(5)	1004(2)	-332(3)	66(1)
C(6)	5423(5)	902(2)	135(3)	66(1)
C(7)	6551(7)	640(2)	-451(4)	86(1)
C(8)	8005(7)	567(2)	25(6)	97(2)
C(9)	8346(6)	754(2)	1076(6)	93(2)
C(10)	7183(5)	1014(2)	1630(4)	78(1)
N(11)	2018(8)	2264(3)	2209(6)	58(2)
N(12)	4624(9)	2555(3)	1371(5)	56(2)
C(11)	753(9)	2091(5)	2644(7)	68(2)
C(12)	-548(10)	2469(5)	2697(8)	77(2)
C(13)	-416(11)	3082(5)	2267(8)	76(2)
C(14)	890(10)	3296(4)	1804(7)	73(2)
C(15)	2141(9)	2868(3)	1796(6)	51(2)
C(16)	3549(9)	3026(3)	1325(5)	51(2)
C(17)	3745(10)	3633(4)	854(7)	69(2)
C(18)	5112(11)	3723(4)	409(7)	76(2)
C(19)	6219(11)	3254(4)	436(7)	79(2)
C(20)	5906(10)	2673(4)	933(6)	67(2)
N(11')	1706(9)	2138(4)	2346(7)	55(2)
N(12')	4151(10)	2602(3)	1475(6)	55(2)
C(11')	582(10)	1886(6)	2828(8)	65(2)
C(12')	-710(11)	2224(5)	3038(9)	75(3)
C(13')	-765(12)	2852(6)	2635(9)	77(3)
C(14')	370(12)	3166(5)	2141(8)	66(2)
C(15')	1655(10)	2768(4)	2025(7)	48(2)
C(16')	2983(11)	3023(3)	1569(6)	46(2)
C(17')	3139(12)	3658(4)	1214(8)	71(2)
C(18')	4467(13)	3843(5)	735(9)	78(3)
C(19')	5619(14)	3423(5)	618(9)	78(3)
C(20')	5379(13)	2803(5)	1037(8)	70(3)

Table 3. Bond lengths [Å] and angles [°].

Sn(1)-S(1)	2.3396(9)	Sn(1)-S(3)#1	2.4409(9)
Sn(1)-S(2)	2.3461(9)	Sn(1)-Mn(1)	3.2126(5)
Sn(1)-S(3)	2.4369(9)	S(3)-Sn(1)#1	2.4409(9)
S(1)-Sn(1)-S(2)	103.69(3)	S(3)-Sn(1)-S(3)#1	92.89(3)
S(1)-Sn(1)-S(3)	114.97(4)	S(1)-Sn(1)-Mn(1)	53.35(3)
S(2)-Sn(1)-S(3)	117.62(3)	S(2)-Sn(1)-Mn(1)	51.42(2)
S(1)-Sn(1)-S(3)#1	114.47(4)	S(3)-Sn(1)-Mn(1)	144.73(2)
S(2)-Sn(1)-S(3)#1	113.66(4)	S(3)#1-Sn(1)-Mn(1)	122.37(2)
Sn(1)-S(1)-Mn(1)	80.70(3)	Sn(1)-S(3)-Sn(1)#1	87.10(3)
Sn(1)-S(2)-Mn(1)	82.23(3)		
S(1)-Mn(1)	2.6120(11)	S(2)-Mn(1)	2.5348(10)
Mn(1)-N(11)	2.202(6)	Mn(1)-N(11')	2.299(8)
Mn(1)-N(2)	2.280(3)	Mn(1)-N(1)	2.335(3)
Mn(1)-N(12')	2.295(7)	Mn(1)-N(12)	2.351(6)
N(11)-Mn(1)-N(2)	153.4(2)	N(12)-Mn(1)-S(2)	97.21(15)
N(2)-Mn(1)-N(12')	97.5(2)	N(11)-Mn(1)-S(1)	103.0(2)
N(2)-Mn(1)-N(11')	160.6(2)	N(2)-Mn(1)-S(1)	95.95(9)
N(12')-Mn(1)-N(11')	71.1(3)	N(12')-Mn(1)-S(1)	161.9(2)
N(11)-Mn(1)-N(1)	90.13(19)	N(11')-Mn(1)-S(1)	92.6(2)
N(2)-Mn(1)-N(1)	71.25(12)	N(1)-Mn(1)-S(1)	89.73(9)
N(12')-Mn(1)-N(1)	83.1(2)	N(12)-Mn(1)-S(1)	170.54(16)
N(11')-Mn(1)-N(1)	91.4(2)	S(2)-Mn(1)-S(1)	91.42(3)
N(11)-Mn(1)-N(12)	71.8(3)	N(11)-Mn(1)-Sn(1)	113.84(19)
N(2)-Mn(1)-N(12)	86.7(2)	N(2)-Mn(1)-Sn(1)	92.78(9)
N(1)-Mn(1)-N(12)	82.51(17)	N(12')-Mn(1)-Sn(1)	144.80(18)
N(11)-Mn(1)-S(2)	100.10(17)	N(11')-Mn(1)-Sn(1)	105.6(2)
N(2)-Mn(1)-S(2)	97.92(9)	N(1)-Mn(1)-Sn(1)	131.96(9)
N(12')-Mn(1)-S(2)	98.73(18)	N(12)-Mn(1)-Sn(1)	143.18(15)
N(11')-Mn(1)-S(2)	99.29(19)	S(2)-Mn(1)-Sn(1)	46.35(2)
N(1)-Mn(1)-S(2)	169.17(9)	S(1)-Mn(1)-Sn(1)	45.95(2)
N(1)-C(1)	1.321(5)	C(4)-C(5)	1.389(6)
N(1)-C(5)	1.341(5)	C(5)-C(6)	1.474(6)
N(2)-C(10)	1.328(5)	C(6)-C(7)	1.392(6)
N(2)-C(6)	1.348(5)	C(7)-C(8)	1.358(8)
C(1)-C(2)	1.408(7)	C(8)-C(9)	1.361(9)
C(2)-C(3)	1.358(9)	C(9)-C(10)	1.392(7)
C(3)-C(4)	1.374(8)		
C(1)-N(1)-C(5)	118.6(4)	C(4)-C(5)-C(6)	121.5(4)
C(10)-N(2)-C(6)	118.4(4)	N(2)-C(6)-C(7)	120.7(4)
N(1)-C(1)-C(2)	122.7(5)	N(2)-C(6)-C(5)	116.1(3)
C(3)-C(2)-C(1)	118.1(5)	C(7)-C(6)-C(5)	123.1(4)
C(2)-C(3)-C(4)	119.6(5)	C(8)-C(7)-C(6)	120.2(5)
C(3)-C(4)-C(5)	119.3(5)	C(7)-C(8)-C(9)	119.3(5)
N(1)-C(5)-C(4)	121.5(4)	C(8)-C(9)-C(10)	118.5(5)
N(1)-C(5)-C(6)	117.0(3)	N(2)-C(10)-C(9)	122.9(5)
N(11)-C(11)	1.330(10)	N(11')-C(11')	1.310(12)
N(11)-C(15)	1.350(9)	N(11')-C(15')	1.352(10)
N(12)-C(20)	1.319(10)	N(12')-C(20')	1.320(11)

N(12)-C(16)	1.347(9)	N(12')-C(16')	1.354(10)
C(11)-C(12)	1.387(10)	C(11')-C(12')	1.376(11)
C(12)-C(13)	1.376(13)	C(12')-C(13')	1.381(14)
C(13)-C(14)	1.402(12)	C(13')-C(14')	1.380(14)
C(14)-C(15)	1.406(9)	C(14')-C(15')	1.411(11)
C(15)-C(16)	1.454(9)	C(15')-C(16')	1.442(10)
C(16)-C(17)	1.395(9)	C(16')-C(17')	1.388(10)
C(17)-C(18)	1.381(12)	C(17')-C(18')	1.412(14)
C(18)-C(19)	1.365(12)	C(18')-C(19')	1.347(14)
C(19)-C(20)	1.383(10)	C(19')-C(20')	1.399(12)
C(11)-N(11)-C(15)	120.1(7)	C(11')-N(11')-C(15')	120.6(8)
C(20)-N(12)-C(16)	118.2(7)	C(20')-N(12')-C(16')	119.4(8)
N(11)-C(11)-C(12)	126.4(9)	N(11')-C(11')-C(12')	123.9(11)
C(13)-C(12)-C(11)	113.1(9)	C(11')-C(12')-C(13')	113.7(11)
C(12)-C(13)-C(14)	123.2(8)	C(14')-C(13')-C(12')	126.6(10)
C(13)-C(14)-C(15)	118.6(8)	C(13')-C(14')-C(15')	113.1(9)
N(11)-C(15)-C(14)	118.6(8)	N(11')-C(15')-C(14')	121.8(9)
N(11)-C(15)-C(16)	117.4(6)	N(11')-C(15')-C(16')	117.2(7)
C(14)-C(15)-C(16)	124.0(7)	C(14')-C(15')-C(16')	121.0(8)
N(12)-C(16)-C(17)	123.0(8)	N(12')-C(16')-C(17')	118.3(9)
N(12)-C(16)-C(15)	116.3(6)	N(12')-C(16')-C(15')	116.8(6)
C(17)-C(16)-C(15)	120.8(7)	C(17')-C(16')-C(15')	125.0(8)
C(18)-C(17)-C(16)	115.8(8)	C(16')-C(17')-C(18')	119.8(10)
C(19)-C(18)-C(17)	122.7(8)	C(19')-C(18')-C(17')	122.2(10)
C(18)-C(19)-C(20)	116.6(9)	C(18')-C(19')-C(20')	113.6(11)
N(12)-C(20)-C(19)	123.8(9)	N(12')-C(20')-C(19')	126.7(11)

Symmetry transformations used to generate equivalent atoms: A: -x+1,-y,-z+1

Table 4. Anisotropic displacement parameters ($Å^2 \cdot 10^3$). The anisotropic displacement factor exponent takes the form: $-2\pi^2[h^2 a^{*2} U_{11} + ... + 2 h k a^* b^* U_{12}]$

	U_{11}	U_{22}	U_{33}	U_{23}	U_{13}	U_{12}
Sn(1)	60(1)	44(1)	47(1)	2(1)	2(1)	6(1)
S(1)	68(1)	62(1)	59(1)	2(1)	-7(1)	-7(1)
S(2)	76(1)	48(1)	59(1)	1(1)	-8(1)	-4(1)
S(3)	72(1)	59(1)	57(1)	6(1)	18(1)	19(1)
Mn(1)	59(1)	52(1)	50(1)	4(1)	4(1)	6(1)
N(1)	71(2)	76(2)	51(2)	2(1)	3(1)	-8(2)
N(2)	66(2)	57(2)	71(2)	-7(1)	15(2)	-3(1)
C(1)	77(3)	107(4)	59(2)	6(2)	1(2)	-10(2)
C(2)	90(3)	138(5)	62(3)	24(3)	-12(2)	-32(3)
C(3)	136(5)	98(4)	52(2)	4(2)	1(3)	-37(3)
C(4)	127(4)	73(3)	56(2)	-3(2)	13(2)	-26(3)
C(5)	97(3)	54(2)	49(2)	2(1)	17(2)	-16(2)
C(6)	84(2)	52(2)	65(2)	-1(2)	24(2)	-8(2)
C(7)	119(4)	65(3)	84(3)	-2(2)	49(3)	-2(2)
C(8)	92(4)	78(3)	128(5)	1(3)	50(3)	3(3)
C(9)	69(3)	69(3)	146(5)	-5(3)	30(3)	-1(2)
C(10)	60(2)	70(2)	103(3)	-9(2)	12(2)	-2(2)

Table 5. Hydrogen coordinates ($x\ 10^4$) and isotropic displacement parameters ($Å^2 \times 10^3$).

	x	y	z	U(eq)
H(1)	946	1801	175	98
H(2)	-70	1381	-1495	118
H(3)	1397	668	-2392	116
H(4)	3881	447	-1678	102
H(7)	6308	515	-1170	104
H(8)	8760	390	-364	116
H(9)	9335	708	1417	112
H(10)	7414	1138	2351	93
H(11)	739	1675	2941	82
H(12)	-1420	2323	2993	92
H(13)	-1233	3369	2285	92
H(14)	927	3711	1507	88
H(17)	3002	3957	840	82
H(18)	5285	4119	78	91
H(19)	7136	3322	136	95
H(20)	6643	2346	961	81
H(11')	662	1452	3041	79
H(12')	-1475	2046	3415	90
H(13')	-1658	3086	2702	92
H(14')	296	3597	1910	80
H(17')	2370	3961	1293	86
H(18')	4550	4269	491	93
H(19')	6492	3535	291	94
H(20')	6165	2502	1004	84

5.3.18 Messprotokoll der Verbindung {[Ni(1,2dach)$_2$(ma)]$_4$[Sn$_{10}$S$_{20}$O$_4$]}

Table 1. Crystal data and structure refinement for {[Ni($C_6H_{14}N_2$)$_2$(CH_5N)]$_4$[$Sn_{10}S_{20}O_4$]}. ($C_6H_{14}N_2$, 1,2-dach = 1,2-Diaminocyclohexan; CH_5N, ma = Methylamin)

Identification code	jh1337	
Empirical formula	{[Ni($C_6H_{14}N_2$)$_2$(CH_5N)]$_4$[$Sn_{10}S_{20}O_4$]}.	
Crystal color, habitus	pale violet needles	
Formula weight	3144.56	
Temperature	200(2) K	
Wavelength	0.71073 Å	
Crystal system	tetragonal	
Space group	$P\bar{4}2_1c$	
Unit cell dimensions	a = 20.9912(4) Å	α= 90°.
	b = 20.9912(4) Å	β= 90°.
	c = 11.2091(3) Å	γ = 90°.
Volume	4939.07(19) Å^3	
Z	2	
Density (calculated)	2.114 Mg/m^3	
Absorption coefficient	3.693 mm^{-1}	
F(000)	3056	
Crystal size	0.07 x 0.10 x 0.12 mm^3	
Theta range for data collection	2.06 to 26.80°.	
Index ranges	-26<=h<=25, -21<=k<=26, -14<=l<=14	
Reflections collected	38556	
Independent reflections	5249 [R(int) = 0.0425]	
Completeness to theta = 26.80°	99.4 %	
Refinement method	Full-matrix least-squares on F^2	
Data / restraints / parameters	5249 / 3 / 247	
Goodness-of-fit on F^2	1.048	
Final R indices [I>2sigma(I)]	R1 = 0.0373, wR2 = 0.0858	
R indices (all data)	R1 = 0.0401, wR2 = 0.0875	
Absolute structure parameter	0.04(3)	
Extinction coefficient	0.00106(10)	
Largest diff. peak and hole	0.739 and -0.671 e.Å^{-3}	

Comments: All non-hydrogen atoms except three disordered C atoms were refined anisotropic. The C-H and N-H H atoms were positioned with idealized geometry (methyl H atoms allowed to rotate but not to tip) and refined isotropic with $U_{iso(}$H) = 1.2 U_{eq}(C,N) (1.5 for methyl H atoms) using a riding model. A numerical absorption correction was performed ($T_{min/max}$: 0.5291/0.6100). The absolute structure was determined and is in agreement with the selected setting (Flack x-parameter: 0.04 (3)).

Table 2. Atomic coordinates ($\cdot 10^4$) and equivalent isotropic displacement parameters ($Å^2 \cdot 10^3$). U(eq) is defined as one third of the trace of the orthogonalized U_{ij} tensor.

	x	y	z	U(eq)
Sn(1)	0	10000	7751(1)	29(1)
Sn(2)	1179(1)	9823(1)	9998(1)	29(1)
Sn(3)	1427(1)	11061(1)	7634(1)	30(1)
S(1)	720(1)	9028(1)	8419(1)	30(1)
S(2)	702(1)	10515(1)	6301(2)	36(1)
S(3)	2045(1)	10322(1)	8844(2)	34(1)
S(4)	1868(1)	9094(1)	11147(2)	32(1)
S(5)	2157(1)	11595(1)	6414(2)	40(1)
O(1)	560(2)	10410(2)	9070(4)	25(1)
Ni(1)	1227(1)	8082(1)	7340(1)	34(1)
N(1)	1568(3)	7233(3)	6542(6)	46(2)
N(2)	653(3)	7463(3)	8288(6)	39(1)
C(1)	1123(5)	6736(4)	6848(10)	65(3)
C(2)	882(5)	6801(4)	8085(10)	62(2)
C(3)	395(6)	6309(5)	8445(16)	94(5)
C(4)	710(11)	5649(11)	8440(20)	68(5)
C(5)	916(10)	5539(10)	7157(19)	67(5)
C(6)	1381(9)	6048(9)	6843(19)	54(4)
C(4')	540(13)	5647(14)	7770(20)	92(8)
C(5')	747(13)	5642(13)	6480(20)	88(7)
C(6')	1301(10)	6088(10)	6350(20)	60(5)
N(11)	1867(3)	8670(3)	6431(6)	46(2)
N(12)	1967(3)	8060(3)	8617(6)	41(1)
C(11)	2509(4)	8553(4)	6956(8)	50(2)
C(12)	2460(4)	8521(5)	8285(8)	51(2)
C(13)	3094(4)	8403(5)	8883(8)	54(2)
C(14)	3583(6)	8882(6)	8492(12)	75(3)
C(15)	3638(4)	8895(5)	7144(10)	64(2)
C(16)	3009(4)	9039(5)	6576(9)	56(2)
N(21)	570(3)	8234(3)	5937(5)	42(1)
C(21)	-17(5)	7882(6)	5710(9)	68(3)

Table 3. Bond lengths [Å] and angles [°].

Sn(1)-O(1)	2.075(4)	Sn(1)-S(2)	2.4458(18)
Sn(1)-O(1)#1	2.075(4)	Sn(1)-S(1)#1	2.6474(16)
Sn(1)-S(2)#1	2.4458(18)	Sn(1)-S(1)	2.6474(16)
Sn(2)-O(1)	2.072(4)	Sn(2)-S(4)	2.4691(17)
Sn(2)-O(1)#2	2.084(4)	Sn(2)-S(1)	2.6169(16)
Sn(2)-S(3)	2.4650(17)	Sn(2)-S(1)#3	2.6234(16)
Sn(3)-S(5)	2.3384(18)	Sn(3)-S(3)	2.4351(18)
Sn(3)-S(2)	2.4213(18)	Sn(3)-S(4)#3	2.4361(17)
S(4)-Sn(3)#2	2.4361(17		
O(1)-Sn(1)-O(1)#1	89.2(2)	S(2)#1-Sn(1)-S(1)#1	100.62(6)
O(1)-Sn(1)-S(2)#1	176.21(13)	S(2)-Sn(1)-S(1)#1	101.04(6)
O(1)#1-Sn(1)-S(2)#1	87.06(13)	O(1)-Sn(1)-S(1)	78.18(12)
O(1)-Sn(1)-S(2)	87.06(13)	O(1)#1-Sn(1)-S(1)	78.58(12)
O(1)#1-Sn(1)-S(2)	176.21(13)	S(2)#1-Sn(1)-S(1)	101.04(6)
S(2)#1-Sn(1)-S(2)	96.73(8)	S(2)-Sn(1)-S(1)	100.62(6)
O(1)-Sn(1)-S(1)#1	78.58(12)	S(1)#1-Sn(1)-S(1)	147.15(7)
O(1)#1-Sn(1)-S(1)#1	78.18(12)	O(1)-Sn(2)#3	2.084(4)
S(1)-Sn(2)#2	2.6234(16)	S(3)-Sn(2)-S(1)	100.78(6)
O(1)-Sn(2)-O(1)#2	89.7(2)	S(4)-Sn(2)-S(1)	99.95(6)
O(1)-Sn(2)-S(3)	86.96(13)	O(1)-Sn(2)-S(1)#3	79.00(12)
O(1)#2-Sn(2)-S(3)	176.67(13)	O(1)#2-Sn(2)-S(1)#3	79.01(12)
O(1)-Sn(2)-S(4)	177.00(13)	S(3)-Sn(2)-S(1)#3	99.94(6)
O(1)#2-Sn(2)-S(4)	87.31(13)	S(4)-Sn(2)-S(1)#3	100.92(6)
S(3)-Sn(2)-S(4)	96.00(6)	S(1)-Sn(2)-S(1)#3	148.71(6)
O(1)-Sn(2)-S(1)	78.96(12)	O(1)#2-Sn(2)-S(1)	78.95(12)
S(5)-Sn(3)-S(2)	106.10(7)	S(5)-Sn(3)-S(4)#3	106.79(7)
S(5)-Sn(3)-S(3)	106.40(7)	S(2)-Sn(3)-S(4)#3	113.13(6)
S(2)-Sn(3)-S(3)	112.14(6)	S(3)-Sn(3)-S(4)#3	111.73(6)
Ni(1)-S(1)-Sn(2)	131.49(7)	Sn(3)-S(2)-Sn(1)	100.27(6)
Ni(1)-S(1)-Sn(2)#2	119.34(6)	Sn(3)-S(3)-Sn(2)	99.77(6)
Sn(2)-S(1)-Sn(2)#2	84.96(5)	Sn(3)#2-S(4)-Sn(2)	99.41(6)
Ni(1)-S(1)-Sn(1)	134.60(7)	Sn(2)-O(1)-Sn(1)	117.8(2)
Sn(2)-S(1)-Sn(1)	84.82(5)	Sn(2)-O(1)-Sn(2)#3	116.78(19)
Sn(2)#2-S(1)-Sn(1)	84.78(5)	Sn(1)-O(1)-Sn(2)#3	117.41(19)
S(1)-Ni(1)	2.5561(18)	Ni(1)-N(12)	2.114(6)
Ni(1)-N(2)	2.067(6)	Ni(1)-N(21)	2.116(6)
Ni(1)-N(11)	2.089(6)	Ni(1)-N(1)	2.119(6)
N(2)-Ni(1)-N(11)	175.6(3)	N(12)-Ni(1)-N(1)	91.1(3)
N(2)-Ni(1)-N(12)	93.8(3)	N(21)-Ni(1)-N(1)	91.9(3)
N(11)-Ni(1)-N(12)	82.5(3)	N(2)-Ni(1)-S(1)	90.18(17)
N(2)-Ni(1)-N(21)	95.6(3)	N(11)-Ni(1)-S(1)	92.3(2)
N(11)-Ni(1)-N(21)	88.2(3)	N(12)-Ni(1)-S(1)	90.14(18)
N(12)-Ni(1)-N(21)	170.4(3)	N(21)-Ni(1)-S(1)	87.93(19)
N(2)-Ni(1)-N(1)	83.4(3)	N(1)-Ni(1)-S(1)	173.5(2)
N(11)-Ni(1)-N(1)	94.2(3)		
N(1)-C(1)	1.443(12)	C(3)-C(4)	1.54(3)
N(2)-C(2)	1.488(11)	C(3)-C(4')	1.61(3)
C(1)-C(2)	1.482(14)	C(4)-C(5)	1.52(2)
C(1)-C(6')	1.52(2)	C(5)-C(6)	1.49(2)

C(1)-C(6)	1.54(2)	C(4')-C(5')	1.52(3)
C(2)-C(3)	1.508(14)	C(5')-C(6')	1.50(2)
N(1)-C(1)-C(2)	112.1(8)	C(2)-C(3)-C(4)	108.9(12)
N(1)-C(1)-C(6')	113.6(10)	C(2)-C(3)-C(4')	109.7(13)
C(2)-C(1)-C(6')	120.7(12)	C(4)-C(3)-C(4')	30.3(11)
N(1)-C(1)-C(6)	116.6(10)	C(5)-C(4)-C(3)	105.4(17)
C(2)-C(1)-C(6)	102.1(11)	C(6)-C(5)-C(4)	107.5(17)
C(6')-C(1)-C(6)	22.0(9)	C(5)-C(6)-C(1)	116.1(16)
C(1)-C(2)-N(2)	109.8(8)	C(5')-C(4')-C(3)	121(2)
C(1)-C(2)-C(3)	114.8(10)	C(6')-C(5')-C(4')	108(2)
N(2)-C(2)-C(3)	112.2(8)	C(5')-C(6')-C(1)	109.6(17)
N(11)-C(11)	1.491(11)	C(12)-C(13)	1.511(12)
N(12)-C(12)	1.464(11)	C(13)-C(14)	1.502(14)
C(11)-C(12)	1.495(11)	C(14)-C(15)	1.516(16)
C(11)-C(16)	1.523(12)	C(15)-C(16)	1.497(14)
N(11)-C(11)-C(12)	109.8(7)	C(11)-C(12)-C(13)	112.9(8)
N(11)-C(11)-C(16)	113.8(8)	C(14)-C(13)-C(12)	111.3(9)
C(12)-C(11)-C(16)	110.9(7)	C(13)-C(14)-C(15)	110.8(9)
N(12)-C(12)-C(11)	109.4(7)	C(16)-C(15)-C(14)	111.1(9)
N(12)-C(12)-C(13)	113.7(8)	C(15)-C(16)-C(11)	110.8(8)
N(21)-C(21)	1.459(12)		

Symmetry transformations used to generate equivalent atoms:
#1 -x,-y+2,z #2 y-1,-x+1,-z+2 #3 -y+1,x+1,-z+2

Table 4. Anisotropic displacement parameters ($Å^2 \cdot 10^3$). The anisotropic displacement factor exponent takes the form: $-2\pi^2[h^2 a^{*2} U_{11} + ... + 2 h k a^* b^* U_{12}]$

	U_{11}	U_{22}	U_{33}	U_{23}	U_{13}	U_{12}
Sn(1)	27(1)	29(1)	31(1)	0	0	-3(1)
Sn(2)	25(1)	28(1)	34(1)	3(1)	1(1)	0(1)
Sn(3)	29(1)	29(1)	33(1)	1(1)	2(1)	-2(1)
S(1)	28(1)	29(1)	33(1)	-1(1)	0(1)	-1(1)
S(2)	35(1)	40(1)	33(1)	0(1)	1(1)	-9(1)
S(3)	26(1)	35(1)	42(1)	6(1)	3(1)	0(1)
S(4)	26(1)	35(1)	36(1)	3(1)	1(1)	2(1)
S(5)	40(1)	40(1)	41(1)	3(1)	6(1)	-12(1)
O(1)	21(2)	20(2)	33(2)	-5(2)	0(2)	2(2)
Ni(1)	35(1)	32(1)	36(1)	0(1)	0(1)	2(1)
N(1)	48(4)	39(4)	51(4)	-12(3)	1(3)	3(3)
N(2)	42(3)	26(3)	49(3)	0(2)	1(3)	6(2)
C(1)	56(6)	44(5)	95(7)	-18(5)	4(5)	-6(4)
C(2)	57(6)	38(5)	92(7)	4(4)	17(5)	0(4)
C(3)	59(7)	48(6)	176(14)	-4(7)	29(8)	-10(5)
N(11)	48(4)	50(4)	38(3)	5(3)	6(3)	-6(3)
N(12)	43(4)	38(3)	41(3)	-1(3)	-2(3)	6(3)
C(11)	47(5)	47(5)	55(4)	-7(4)	0(3)	-4(4)
C(12)	43(5)	56(5)	54(4)	-1(4)	-2(3)	-6(4)
C(13)	40(4)	60(6)	62(5)	-7(4)	-3(4)	-2(4)
C(14)	61(6)	62(6)	102(8)	4(6)	-12(6)	-7(5)
C(15)	41(5)	64(6)	86(7)	5(5)	5(4)	-15(4)
C(16)	51(5)	54(5)	63(5)	-4(4)	14(4)	-9(4)
N(21)	42(4)	43(4)	42(3)	0(3)	-16(3)	3(3)
C(21)	45(5)	87(8)	73(6)	6(5)	-16(5)	-5(5)

Table 5a. Hydrogen coordinates ($\cdot 10^4$) and isotropic displacement parameters ($Å^2 \cdot 10^3$).

	x	y	z	U(eq)
H(1A)	1592	7280	5727	55
H(1B)	1968	7136	6828	55
H(2A)	670	7559	9088	47
H(2B)	237	7501	8037	47
H(1)	752	6760	6288	78
H(2)	1257	6739	8623	75
H(3A)	32	6316	7880	113
H(3B)	230	6406	9253	113
H(3C)	-37	6461	8232	113
H(3D)	410	6244	9320	113
H(4A)	1082	5640	8980	81
H(4B)	403	5317	8694	81
H(5A)	1117	5114	7076	81
H(5B)	543	5557	6618	81
H(6A)	1552	5957	6039	65
H(6B)	1741	6025	7411	65
H(4C)	874	5425	8237	110
H(4D)	150	5384	7830	110
H(5C)	874	5206	6237	106
H(5D)	392	5781	5957	106

Table 5b. Hydrogen coordinates ($\cdot 10^4$) and isotropic displacement parameters ($Å^2 \cdot 10^3$).

	x	y	z	U(eq)
H(6C)	1419	6129	5499	73
H(6D)	1673	5917	6789	73
H(11A)	1868	8573	5630	55
H(11B)	1754	9090	6521	55
H(12A)	1807	8159	9358	49
H(12B)	2140	7658	8652	49
H(11)	2656	8126	6671	60
H(12)	2309	8948	8561	61
H(13A)	3041	8428	9759	65
H(13B)	3245	7969	8683	65
H(14A)	4001	8772	8843	90
H(14B)	3461	9310	8784	90
H(15A)	3952	9224	6906	77
H(15B)	3794	8478	6857	77
H(16A)	3055	9031	5697	67
H(16B)	2868	9471	6812	67

Table 6. Hydrogen bonds with H..A < r(A) + 2.000 Angstroms and <DHA > 110 deg.

D-H	d(D-H)	d(H..A)	<DHA	d(D..A)	A
N1-H1A	0.920	2.676	159.63	3.553	S5 [y-1, -x+1, -z+1]
N1-H1B	0.920	2.926	153.23	3.770	S5 [-x+1/2, y-1/2, -z+3/2]
N2-H2A	0.920	2.569	160.06	3.448	S3 [y-1, -x+1, -z+2]
N2-H2B	0.920	2.890	136.95	3.617	S4 [y-1, -x+1, -z+2]
N11-H11A	0.920	2.816	155.94	3.675	S5 [y-1, -x+1, -z+1]
N12-H12A	0.920	2.808	141.82	3.577	S4
N12-H12B	0.920	2.677	168.98	3.585	S5 [-x+1/2, y-1/2, -z+3/2]

5.3.19 Messprotokoll der Verbindung $[Ni(tren)_2]_2[Sn_2S_6]\cdot 8H_2O$

Table 1. Crystal data and structure refinement for $[Ni(C_6H_{18}N_2)_2]_2[Sn_2S_6]\cdot 8H_2O$. ($C_6H_{18}N_2$, tren = Tris(2-aminoethyl)amin)

Identification code	jh1896	
Empirical formula	$[Ni(C_6H_{18}N_2)_2]_2[Sn_2S_6]\cdot 8H_2O$	
Crystal color, habitus	violet blocks	
Formula weight	1276.26	
Temperature	170(2) K	
Wavelength	0.71073 Å	
Crystal system	triclinic	
Space group	$P\bar{1}$	
Unit cell dimensions	a = 10.2878(4) Å	α= 84.740(3)°.
	b = 11.1100(4) Å	β= 84.395(3)°.
	c = 11.4206(4) Å	γ = 79.093(3)°.
Volume	1272.05(8) $Å^3$	
Z	1	
Density (calculated)	1.666 Mg/m^3	
Absorption coefficient	2.001 mm^{-1}	
F(000)	660	
Crystal size	0.08 x 0.10 x 0.12 mm^3	
Theta range for data collection	1.797 to 27.004°.	
Index ranges	-13<=h<=13, -14<=k<=14, -14<=l<=14	
Reflections collected	18612	
Independent reflections	5546 [R(int) = 0.0310]	
Completeness to theta = 25.242°	100.0 %	
Refinement method	Full-matrix least-squares on F^2	
Data / restraints / parameters	5546 / 0 / 266	
Goodness-of-fit on F^2	1.039	
Final R indices [I>2sigma(I)]	R1 = 0.0272, wR2 = 0.0625	
R indices (all data)	R1 = 0.0339, wR2 = 0.0641	
Extinction coefficient	0.0015(4)	
Largest diff. peak and hole	0.655 and -0.549 e.$Å^{-3}$	

Comments: All non-hydrogen atoms were refines anisotropic. The C-H and N-H H atoms of the coordinated amino groups were positioned with idealized geometry and refined isotropic with U_{iso}(H) = 1.2 Ueq (C,N) using a riding model. In the beginning the terminal N-H and water H atoms were located in difference map and refined isotropic but later their bond lengths were set to ideal values and they were refined isotropic with U_{iso}(H) = 1.5 Ueq (N,O) using a riding model refinement. A numerical absorption correction was performed ($T_{min/max}$: 0.6650/0.7948).

Table 2. Atomic coordinates ($\cdot 10^4$) and equivalent isotropic displacement parameters ($Å^2 \cdot 10^3$). U(eq) is defined as one third of the trace of the orthogonalized U_{ij} tensor.

	x	y	z	U(eq)
Sn(1)	4248(1)	45(1)	1402(1)	20(1)
S(1)	3837(1)	1826(1)	2415(1)	26(1)
S(2)	3571(1)	-1675(1)	2447(1)	26(1)
S(3)	3437(1)	354(1)	-568(1)	24(1)
Ni(1)	0	0	5000	19(1)
N(1)	1673(2)	190(2)	5920(2)	22(1)
C(1)	1119(3)	384(3)	7156(2)	33(1)
C(2)	129(3)	-427(3)	7609(2)	31(1)
N(2)	-799(2)	-451(2)	6714(2)	27(1)
C(3)	2667(3)	-953(3)	5803(3)	32(1)
C(4)	2064(3)	-2089(3)	5750(3)	31(1)
N(3)	1064(2)	-1847(2)	4889(2)	32(1)
C(5)	2268(3)	1266(2)	5433(2)	25(1)
C(6)	3466(3)	1470(3)	6034(2)	30(1)
N(4)	3950(2)	2537(2)	5411(2)	30(1)
Ni(2)	5000	5000	0	19(1)
N(11)	6679(2)	5160(2)	953(2)	23(1)
C(11)	6134(3)	5453(3)	2165(2)	33(1)
C(12)	4984(3)	4825(3)	2621(2)	33(1)
N(12)	4009(2)	4943(2)	1730(2)	26(1)
C(13)	7593(3)	3958(2)	897(3)	30(1)
C(14)	6900(3)	2864(2)	974(3)	31(1)
N(13)	5753(2)	3106(2)	247(2)	22(1)
C(15)	7389(3)	6136(2)	406(2)	26(1)
C(16)	8606(3)	6319(3)	990(3)	32(1)
N(14)	9260(2)	7278(2)	360(2)	32(1)
O(1)	520(2)	5377(2)	3490(2)	46(1)
O(2)	1242(2)	7066(2)	1846(2)	49(1)
O(3)	727(2)	3183(2)	2408(2)	48(1)
O(4)	1988(2)	4716(2)	5394(2)	49(1)

Table 3. Bond lengths [Å] and angles [°].

Sn(1)-S(1)	2.3317(6)	Sn(1)-S(3)	2.4487(6)
Sn(1)-S(2)	2.3422(6)	Sn(1)-S(3)#1	2.4511(7)
S(3)-Sn(1)#1	2.4510(6)	S(1)-Sn(1)-S(3)#1	110.18(2)
S(1)-Sn(1)-S(2)	115.24(2)	S(2)-Sn(1)-S(3)#1	113.51(2)
S(1)-Sn(1)-S(3)	113.56(2)	S(3)-Sn(1)-S(3)#1	91.48(2)
S(2)-Sn(1)-S(3)	110.57(2)	Sn(1)-S(3)-Sn(1)#1	88.52(2)
Ni(1)-N(2)	2.102(2)	Ni(2)-N(13)	2.103(2)
Ni(1)-N(2)#2	2.102(2)	Ni(2)-N(13)#3	2.103(2)
Ni(1)-N(3)	2.144(2)	Ni(2)-N(12)	2.134(2)
Ni(1)-N(3)#2	2.144(2)	Ni(2)-N(12)#3	2.134(2)
Ni(1)-N(1)	2.154(2)	Ni(2)-N(11)#3	2.172(2)
Ni(1)-N(1)#2	2.154(2)	Ni(2)-N(11)	2.172(2)
N(2)-Ni(1)-N(2)#2	180.00(5)	N(13)-Ni(2)-N(13)#3	180.0
N(2)-Ni(1)-N(3)	90.59(10)	N(13)-Ni(2)-N(12)	89.56(8)
N(2)#2-Ni(1)-N(3)	89.41(10)	N(13)#3-Ni(2)-N(12)	90.44(8)
N(2)-Ni(1)-N(3)#2	89.41(10)	N(13)-Ni(2)-N(12)#3	90.44(8)
N(2)#2-Ni(1)-N(3)#2	90.59(10)	N(13)#3-Ni(2)-N(12)#3	89.56(8)
N(3)-Ni(1)-N(3)#2	180.0	N(12)-Ni(2)-N(12)#3	180.0
N(2)-Ni(1)-N(1)	82.71(8)	N(13)-Ni(2)-N(11)#3	96.72(8)
N(2)#2-Ni(1)-N(1)	97.29(8)	N(13)#3-Ni(2)-N(11)#3	83.28(8)
N(3)-Ni(1)-N(1)	82.74(9)	N(12)-Ni(2)-N(11)#3	97.09(8)
N(3)#2-Ni(1)-N(1)	97.26(9)	N(12)#3-Ni(2)-N(11)#3	82.91(8)
N(2)-Ni(1)-N(1)#2	97.29(8)	N(13)-Ni(2)-N(11)	83.28(8)
N(2)#2-Ni(1)-N(1)#2	82.71(8)	N(13)#3-Ni(2)-N(11)	96.72(8)
N(3)-Ni(1)-N(1)#2	97.26(9)	N(12)-Ni(2)-N(11)	82.91(8)
N(3)#2-Ni(1)-N(1)#2	82.74(9)	N(12)#3-Ni(2)-N(11)	97.09(8)
N(1)-Ni(1)-N(1)#2	180.0	N(11)#3-Ni(2)-N(11)	180.0
N(1)-C(3)	1.480(3)	N(11)-C(15)	1.478(3)
N(1)-C(5)	1.483(3)	N(11)-C(13)	1.483(3)
N(1)-C(1)	1.489(3)	N(11)-C(11)	1.483(3)
C(1)-C(2)	1.509(4)	C(11)-C(12)	1.511(4)
C(2)-N(2)	1.470(3)	C(12)-N(12)	1.478(3)
C(3)-C(4)	1.516(4)	C(13)-C(14)	1.513(4)
C(4)-N(3)	1.464(3)	C(14)-N(13)	1.478(3)
C(5)-C(6)	1.531(3)	C(15)-C(16)	1.530(4)
C(6)-N(4)	1.469(4)	C(16)-N(14)	1.463(4)
C(3)-N(1)-C(5)	109.9(2)	C(15)-N(11)-C(13)	108.8(2)
C(3)-N(1)-C(1)	113.6(2)	C(15)-N(11)-C(11)	109.7(2)
C(5)-N(1)-C(1)	109.1(2)	C(13)-N(11)-C(11)	113.9(2)
N(1)-C(1)-C(2)	113.5(2)	N(11)-C(11)-C(12)	113.6(2)
N(2)-C(2)-C(1)	110.4(2)	N(12)-C(12)-C(11)	111.1(2)
N(1)-C(3)-C(4)	113.8(2)	N(11)-C(13)-C(14)	114.2(2)
N(3)-C(4)-C(3)	109.8(2)	N(13)-C(14)-C(13)	111.5(2)
N(1)-C(5)-C(6)	115.8(2)	N(11)-C(15)-C(16)	117.1(2)
N(4)-C(6)-C(5)	108.2(2)	N(14)-C(16)-C(15)	112.7(2)

Symmetry transformations used to generate equivalent atoms:
#1 -x+1,-y,-z #2 -x,-y,-z+1 #3 -x+1,-y+1,-z

Table 4. Anisotropic displacement parameters ($Å^2 \cdot 10^3$). The anisotropic displacement factor exponent takes the form: $-2\pi^2[h^2 a^{*2} U_{11} + ... + 2 h k a^* b^* U_{12}]$

	U_{11}	U_{22}	U_{33}	U_{23}	U_{13}	U_{12}
Sn(1)	19(1)	21(1)	18(1)	-2(1)	-1(1)	-4(1)
S(1)	32(1)	24(1)	23(1)	-6(1)	2(1)	-6(1)
S(2)	26(1)	27(1)	25(1)	1(1)	-2(1)	-9(1)
S(3)	19(1)	30(1)	21(1)	-3(1)	-3(1)	-1(1)
Ni(1)	18(1)	23(1)	18(1)	-1(1)	-2(1)	-3(1)
N(1)	18(1)	30(1)	20(1)	0(1)	-4(1)	-6(1)
C(1)	33(2)	54(2)	18(1)	-7(1)	-2(1)	-19(1)
C(2)	27(1)	45(2)	21(1)	2(1)	-3(1)	-11(1)
N(2)	24(1)	38(1)	21(1)	0(1)	1(1)	-9(1)
C(3)	21(1)	30(1)	44(2)	1(1)	-8(1)	-1(1)
C(4)	27(1)	28(1)	36(1)	2(1)	-9(1)	0(1)
N(3)	33(1)	27(1)	35(1)	-4(1)	-9(1)	1(1)
C(5)	23(1)	30(1)	25(1)	1(1)	-4(1)	-9(1)
C(6)	27(1)	36(2)	29(1)	0(1)	-7(1)	-11(1)
N(4)	26(1)	38(1)	29(1)	-3(1)	-3(1)	-12(1)
Ni(2)	19(1)	19(1)	19(1)	-1(1)	-3(1)	-2(1)
N(11)	20(1)	23(1)	26(1)	-3(1)	-6(1)	-3(1)
C(11)	32(2)	44(2)	26(1)	-10(1)	-5(1)	-10(1)
C(12)	36(2)	43(2)	20(1)	-3(1)	-4(1)	-8(1)
N(12)	23(1)	27(1)	26(1)	-1(1)	-3(1)	-4(1)
C(13)	24(1)	25(1)	42(2)	-3(1)	-12(1)	-1(1)
C(14)	28(1)	23(1)	41(2)	1(1)	-12(1)	-1(1)
N(13)	24(1)	19(1)	24(1)	-1(1)	-4(1)	-2(1)
C(15)	24(1)	25(1)	31(1)	1(1)	-7(1)	-7(1)
C(16)	27(1)	32(1)	37(1)	1(1)	-9(1)	-8(1)
N(14)	24(1)	28(1)	44(1)	-4(1)	-7(1)	-5(1)
O(1)	44(1)	51(1)	42(1)	11(1)	-11(1)	-8(1)
O(2)	48(1)	50(1)	55(1)	13(1)	-22(1)	-25(1)
O(3)	35(1)	38(1)	72(2)	-2(1)	-7(1)	-7(1)
O(4)	41(1)	53(1)	51(1)	-8(1)	-12(1)	-1(1)

Table 5. Hydrogen coordinates ($\cdot 10^4$) and isotropic displacement parameters ($Å^2 \cdot 10^3$).

	x	y	z	U(eq)
H(1A)	683	1255	7202	40
H(1B)	1859	225	7675	40
H(2A)	604	-1271	7807	37
H(2B)	-373	-112	8337	37
H(1N)	-1562	91	6879	33
H(2N)	-1006	-1215	6747	33
H(3A)	3220	-1078	6482	38
H(3B)	3259	-854	5078	38
H(4A)	2769	-2785	5521	37
H(4B)	1648	-2315	6538	37
H(3N)	492	-2385	5044	39
H(4N)	1465	-1946	4149	39
H(5A)	1572	2013	5484	30
H(5B)	2542	1170	4586	30
H(6A)	3204	1624	6872	36
H(6B)	4175	732	6001	36
H(5N)	4695	2617	5744	45
H(6N)	4192	2385	4643	45
H(11A)	5836	6353	2175	39
H(11B)	6851	5206	2704	39
H(12A)	5321	3944	2827	40
H(12B)	4542	5196	3345	40
H(11N)	3396	5643	1816	31
H(12N)	3577	4293	1836	31
H(13A)	8177	3857	1552	36
H(13B)	8164	3966	148	36
H(14A)	7537	2140	703	37
H(14B)	6590	2672	1806	37
H(13N)	5102	2716	606	27
H(14N)	6008	2797	-468	27
H(15A)	6749	6923	390	32
H(15B)	7673	5957	-423	32
H(16A)	8330	6540	1809	38
H(16B)	9250	5535	1026	38
H(15N)	8699	8018	361	48
H(16N)	9383	7139	-420	48
H(1O1)	715	5950	3013	69
H(2O1)	965	5199	4081	69
H(1O2)	690	7338	1346	73
H(2O2)	1685	7618	1900	73
H(1O3)	1511	2798	2422	72
H(2O3)	628	3832	2756	72
H(1O4)	2596	4094	5380	73
H(2O4)	1260	4564	5713	73

Table 6. Hydrogen bonds [Å and °].

D-H...A	d(D-H)	d(H...A)	d(D...A)	<(DHA)
C(1)-H(1B)...S(3)#4	0.99	2.73	3.689(3)	162.9
N(2)-H(1N)...S(2)#2	0.91	2.55	3.459(3)	173.1
N(2)-H(2N)...O(3)#2	0.91	2.29	3.097(3)	148.4
N(3)-H(4N)...S(2)	0.91	2.81	3.626(3)	150.4
C(5)-H(5B)...S(1)	0.99	2.80	3.711(3)	153.2
N(4)-H(5N)...S(2)#5	0.91	2.86	3.643(2)	145.4
N(4)-H(6N)...S(1)	0.91	2.75	3.599(2)	156.2
C(11)-H(11A)...S(2)#6	0.99	2.89	3.752(3)	145.4
C(11)-H(11B)...O(4)#7	0.99	2.59	3.516(4)	154.8
N(12)-H(11N)...O(2)	0.91	2.47	3.336(3)	160.0
N(12)-H(12N)...S(1)	0.91	2.73	3.514(2)	145.0
C(13)-H(13B)...O(2)#3	0.99	2.61	3.457(4)	143.5
N(13)-H(13N)...S(1)	0.91	2.56	3.392(2)	153.1
N(13)-H(14N)...S(2)#1	0.91	2.64	3.540(2)	170.3
C(15)-H(15A)...S(3)#3	0.99	3.02	3.848(3)	142.1
N(14)-H(15N)...S(3)#3	0.91	2.57	3.449(3)	161.3
N(14)-H(16N)...O(3)#3	0.91	2.35	3.247(4)	169.5
O(1)-H(1O1)...O(2)	0.84	1.85	2.685(3)	173.1
O(1)-H(2O1)...O(4)	0.84	1.90	2.734(3)	177.1
O(2)-H(1O2)...N(14)#8	0.84	1.95	2.741(3)	155.9
O(2)-H(2O2)...S(2)#6	0.84	2.38	3.151(2)	152.6
O(3)-H(1O3)...S(1)	0.84	2.43	3.270(2)	175.8
O(3)-H(2O3)...O(1)	0.84	1.96	2.796(4)	175.5
O(4)-H(1O4)...N(4)	0.84	2.00	2.843(4)	175.7
O(4)-H(2O4)...O(1)#9	0.84	1.96	2.780(3)	166.5

Symmetry transformations used to generate equivalent atoms:
#1 -x+1,-y,-z #2 -x,-y,-z+1 #3 -x+1,-y+1,-z
#4 x,y,z+1 #5 -x+1,-y,-z+1 #6 x,y+1,z #7 -x+1,-y+1,-z+1
#8 x-1,y,z #9 -x,-y+1,-z+1

5.3.20 Messprotokoll der Verbindung $[Ni(2amp)(tren)]_2[Sn_2S_6]$

Table 1. Crystal data and structure refinement for $[Ni(C_{12}H_8N_2)(C_6H_8N_2)]_2[Sn_2S_6]$ ($C_{12}H_8N_2$, tren = Tris(2-aminoethyl)amin; $C_6H_8N_2$, 2amp = 2-Aminomethylpyridin)

Identification code	jh1898n	
Empirical formula	$[Ni(C_{12}H_8N_2)(C_6H_8N_2)]_2[Sn_2S_6]$	
Crystal color, habitus	violet needles	
Formula weight	1055.93	
Temperature	170(2) K	
Wavelength	0.71073 Å	
Crystal system	tetragonal	
Space group	$P4_2/n$	
Unit cell dimensions	a = 26.1885(3) Å	α= 90°.
	b = 26.1885(3) Å	β= 90°.
	c = 11.11220(10) Å	γ = 90°.
Volume	7621.16(19) $Å^3$	
Z	8	
Density (calculated)	1.841 Mg/m^3	
Absorption coefficient	2.634 mm^{-1}	
F(000)	4256	
Crystal size	0.07 x 0.12 x 0.16 mm^3	
Theta range for data collection	1.555 to 26.005°.	
Index ranges	-32<=h<=32, -31<=k<=32, -13<=l<=13	
Reflections collected	71138	
Independent reflections	7498 [R(int) = 0.0363]	
Completeness to theta = 25.242°	99.9 %	
Refinement method	Full-matrix least-squares on F^2	
Data / restraints / parameters	7498 / 8 / 411	
Goodness-of-fit on F^2	1.150	
Final R indices [I>2sigma(I)]	R1 = 0.0389, wR2 = 0.0950	
R indices (all data)	R1 = 0.0411, wR2 = 0.0964	
Extinction coefficient	0.00043(5)	
Largest diff. peak and hole	0.836 and -0.568 $e.Å^{-3}$	

Comments: All non-hydrogen atoms except the disordered C atoms were refined anisotropic. The C-H and N-H H atoms were positioned with idealized geometry and refined isotropic using a riding model. A numerical absorption correction was performed ($T_{min/max}$: 0.5604/0.7503). Some atoms of one of the amp ligands is disordered in two orientations. In this case artificial short C-C distances occur to a neighbored ligand generated by symmetry. If the structure is refined, e.g. in space group P42, where both of these ligands are located in general positions the disorder remain constant and there are also no hints for super structure reflections.

Table 2. Atomic coordinates ($\cdot 10^4$) and equivalent isotropic displacement parameters ($Å^2 \cdot 10^3$). U(eq) is defined as one third of the trace of the orthogonalized U_{ij} tensor.

	x	y	z	U(eq)
Sn(1)	7533(1)	5106(1)	6118(1)	27(1)
Sn(2)	7184(1)	4925(1)	3209(1)	29(1)
S(1)	6988(1)	5521(1)	7462(1)	33(1)
S(2)	8312(1)	4857(1)	6930(1)	34(1)
S(3)	7093(1)	4410(1)	5054(1)	34(1)
S(4)	7655(1)	5601(1)	4263(1)	31(1)
S(5)	6412(1)	5206(1)	2413(1)	40(1)
S(6)	7723(1)	4514(1)	1847(1)	34(1)
Ni(1)	8984(1)	3708(1)	4258(1)	27(1)
N(1)	8376(1)	3185(1)	4472(4)	33(1)
C(1)	8139(2)	3315(2)	5637(5)	43(1)
C(2)	8544(2)	3386(2)	6597(5)	45(1)
N(2)	8940(2)	3748(2)	6167(4)	37(1)
C(3)	8030(2)	3272(2)	3448(5)	43(1)
C(4)	8318(2)	3272(2)	2282(5)	44(1)
N(3)	8774(2)	3612(2)	2372(3)	36(1)
C(5)	8589(2)	2657(2)	4489(5)	38(1)
C(6)	9103(2)	2618(2)	3863(5)	37(1)
N(4)	9429(1)	3042(1)	4288(4)	32(1)
N(11)	9582(1)	4213(2)	4019(4)	36(1)
C(11)	9446(2)	4684(2)	3653(5)	40(1)
C(12)	9812(2)	5046(2)	3352(8)	69(2)
C(13)	10318(3)	4927(3)	3443(9)	82(3)
C(14)	10459(2)	4446(2)	3872(7)	64(2)
C(15)	10084(2)	4103(2)	4139(5)	45(1)
C(16)	8888(2)	4801(2)	3574(5)	40(1)
N(12)	8574(1)	4407(1)	4151(3)	30(1)
Ni(2)	5916(1)	6511(1)	5088(1)	31(1)
N(21)	6592(2)	6957(2)	4973(4)	37(1)
C(21)	6857(2)	6768(2)	3895(5)	46(1)
C(22)	6500(2)	6735(2)	2818(5)	51(1)
N(22)	6014(2)	6489(2)	3158(4)	44(1)
C(23)	6876(2)	6855(2)	6093(5)	43(1)
C(24)	6520(2)	6878(2)	7168(5)	48(1)
N(23)	6089(2)	6525(2)	6957(4)	40(1)
C(25)	6450(2)	7503(2)	4893(5)	43(1)
C(26)	5913(2)	7588(2)	4432(5)	42(1)
N(24)	5566(2)	7230(2)	5038(4)	38(1)
N(31)	5240(4)	6122(4)	5501(11)	43(3)
C(31)	5317(6)	5658(6)	5730(20)	94(6)
C(32)	4887(7)	5348(7)	6058(19)	99(6)
C(33)	4397(7)	5576(8)	5970(20)	103(6)
C(36)	5852(5)	5447(6)	5800(17)	72(4)
C(34)	4352(4)	6008(4)	5281(9)	97(3)
C(35)	4776(2)	6230(4)	5052(6)	78(2)
N(32)	6236(1)	5761(1)	5107(3)	32(1)
N(31')	5252(3)	6086(3)	5113(9)	33(2)
C(31')	5303(5)	5589(5)	5214(16)	67(4)
C(32')	4881(6)	5242(6)	5196(18)	88(5)
C(33')	4388(7)	5449(8)	5187(19)	97(5)
C(36')	5830(6)	5351(7)	5250(20)	88(5)

Table 3. Bond lengths [Å] and angles [°].

Sn(1)-S(2)	2.3221(11)	Sn(2)-S(5)	2.3263(12)
Sn(1)-S(1)	2.3345(11)	Sn(2)-S(6)	2.3326(11)
Sn(1)-S(4)	2.4569(11)	Sn(2)-S(4)	2.4543(11)
Sn(1)-S(3)	2.4580(11)	Sn(2)-S(3)	2.4655(12)
S(2)-Sn(1)-S(1)	114.76(4)	S(5)-Sn(2)-S(6)	115.12(4)
S(2)-Sn(1)-S(4)	111.12(4)	S(5)-Sn(2)-S(4)	112.97(4)
S(1)-Sn(1)-S(4)	111.74(4)	S(6)-Sn(2)-S(4)	109.84(4)
S(2)-Sn(1)-S(3)	112.98(4)	S(5)-Sn(2)-S(3)	113.87(4)
S(1)-Sn(1)-S(3)	111.46(4)	S(6)-Sn(2)-S(3)	110.20(4)
S(4)-Sn(1)-S(3)	92.79(4)	S(4)-Sn(2)-S(3)	92.67(4)
Sn(1)-S(3)-Sn(2)	87.09(4)	Sn(2)-S(4)-Sn(1)	87.36(4)
Ni(1)-N(11)	2.066(4)	Ni(1)-N(12)	2.126(3)
Ni(1)-N(4)	2.099(4)	Ni(1)-N(2)	2.127(4)
Ni(1)-N(1)	2.116(4)	Ni(1)-N(3)	2.182(4)
N(11)-Ni(1)-N(4)	96.56(15)	N(1)-Ni(1)-N(2)	83.02(16)
N(11)-Ni(1)-N(1)	178.91(16)	N(12)-Ni(1)-N(2)	89.19(15)
N(4)-Ni(1)-N(1)	82.93(14)	N(11)-Ni(1)-N(3)	98.14(16)
N(11)-Ni(1)-N(12)	79.90(15)	N(4)-Ni(1)-N(3)	93.39(15)
N(4)-Ni(1)-N(12)	175.98(15)	N(1)-Ni(1)-N(3)	80.94(15)
N(1)-Ni(1)-N(12)	100.58(14)	N(12)-Ni(1)-N(3)	85.27(15)
N(11)-Ni(1)-N(2)	97.97(16)	N(2)-Ni(1)-N(3)	161.75(16)
N(4)-Ni(1)-N(2)	93.21(15)		
Ni(2)-N(31')	2.065(9)	Ni(2)-N(23)	2.127(4)
Ni(2)-N(31)	2.093(10)	Ni(2)-N(32)	2.135(4)
Ni(2)-N(24)	2.096(4)	Ni(2)-N(22)	2.161(4)
Ni(2)-N(21)	2.125(4)	N(31)-Ni(2)-N(32)	83.3(3)
N(31')-Ni(2)-N(24)	96.7(3)	N(24)-Ni(2)-N(32)	177.05(15)
N(31)-Ni(2)-N(24)	94.2(3)	N(21)-Ni(2)-N(32)	100.26(15)
N(31')-Ni(2)-N(21)	177.2(3)	N(23)-Ni(2)-N(32)	85.56(15)
N(31)-Ni(2)-N(21)	170.1(4)	N(31')-Ni(2)-N(22)	95.7(3)
N(24)-Ni(2)-N(21)	82.47(16)	N(31)-Ni(2)-N(22)	107.8(4)
N(31')-Ni(2)-N(23)	100.1(3)	N(24)-Ni(2)-N(22)	92.88(16)
N(31)-Ni(2)-N(23)	88.5(3)	N(21)-Ni(2)-N(22)	81.72(17)
N(24)-Ni(2)-N(23)	95.91(16)	N(23)-Ni(2)-N(22)	160.85(17)
N(21)-Ni(2)-N(23)	82.61(17)	N(32)-Ni(2)-N(22)	86.47(15)
N(31')-Ni(2)-N(32)	80.5(3)		
N(1)-C(3)	1.473(6)	C(3)-C(4)	1.501(8)
N(1)-C(1)	1.476(6)	C(4)-N(3)	1.491(6)
N(1)-C(5)	1.490(6)	C(5)-C(6)	1.520(7)
C(1)-C(2)	1.517(8)	C(6)-N(4)	1.478(6)
C(2)-N(2)	1.483(7)	N(2)-C(2)-C(1)	110.0(4)
C(3)-N(1)-C(1)	112.5(4)	N(1)-C(3)-C(4)	110.9(4)
C(3)-N(1)-C(5)	112.6(4)	N(3)-C(4)-C(3)	110.2(4)
C(1)-N(1)-C(5)	111.1(4)	N(1)-C(5)-C(6)	112.9(4)
N(1)-C(1)-C(2)	110.5(4)	N(4)-C(6)-C(5)	108.3(4)
N(11)-C(11)	1.345(6)	C(12)-C(13)	1.367(10)
N(11)-C(15)	1.352(6)	C(13)-C(14)	1.395(11)
C(11)-C(12)	1.387(7)	C(14)-C(15)	1.364(8)
C(11)-C(16)	1.496(7)	C(16)-N(12)	1.468(6)

C(11)-N(11)-C(15)	118.8(4)	C(12)-C(13)-C(14)	119.1(6)
N(11)-C(11)-C(12)	121.1(5)	C(15)-C(14)-C(13)	118.5(6)
N(11)-C(11)-C(16)	117.6(4)	N(11)-C(15)-C(14)	122.6(5)
C(12)-C(11)-C(16)	121.2(5)	N(12)-C(16)-C(11)	112.2(4)
C(13)-C(12)-C(11)	119.7(6)		
N(21)-C(21)	1.470(7)	C(23)-C(24)	1.517(8)
N(21)-C(23)	1.473(6)	C(24)-N(23)	1.476(7)
N(21)-C(25)	1.482(6)	C(25)-C(26)	1.512(7)
C(21)-C(22)	1.521(8)	C(26)-N(24)	1.469(7)
C(22)-N(22)	1.475(7)		
C(21)-N(21)-C(23)	112.9(4)	N(21)-C(23)-C(24)	110.3(4)
C(21)-N(21)-C(25)	113.3(4)	N(23)-C(24)-C(23)	108.8(4)
C(23)-N(21)-C(25)	110.6(4)	N(21)-C(25)-C(26)	113.3(4)
N(21)-C(21)-C(22)	111.8(4)	N(24)-C(26)-C(25)	109.1(4)
N(22)-C(22)-C(21)	110.7(4)		
N(31)-C(31)	1.259(14)	C(34)-C(33')	1.47(2)
N(31)-C(35)	1.343(12)	C(35)-N(31')	1.304(11)
C(31)-C(32)	1.436(18)	N(32)-C(36')	1.520(18)
C(31)-C(36)	1.507(16)	N(31')-C(31')	1.313(13)
C(32)-C(33)	1.419(19)	C(31')-C(32')	1.433(17)
C(33)-C(34)	1.37(2)	C(31')-C(36')	1.514(16)
C(36)-N(32)	1.510(16)	C(32')-C(33')	1.401(18)
C(34)-C(35)	1.278(11)		
C(31)-N(31)-C(35)	114.9(12)	C(34)-C(35)-N(31')	133.6(9)
N(31)-C(31)-C(32)	118.1(14)	C(34)-C(35)-N(31)	128.1(9)
N(31)-C(31)-C(36)	120.9(13)	C(35)-N(31')-C(31')	112.8(9)
C(32)-C(31)-C(36)	120.6(14)	N(31')-C(31')-C(32')	123.3(12)
C(33)-C(32)-C(31)	117.1(16)	N(31')-C(31')-C(36')	120.3(12)
C(34)-C(33)-C(32)	117.5(17)	C(32')-C(31')-C(36')	116.2(12)
C(31)-C(36)-N(32)	113.1(11)	C(33')-C(32')-C(31')	117.7(15)
C(35)-C(34)-C(33)	114.2(11)	C(32')-C(33')-C(34)	116.4(15)
C(35)-C(34)-C(33')	112.4(11)	C(31')-C(36')-N(32)	110.1(12)

Table 4. Anisotropic displacement parameters ($Å^2 \cdot 10^3$). The anisotropic displacement factor exponent takes the form: $-2\pi^2[h^2 a^{*2} U_{11} + ... + 2 h k a^* b^* U_{12}]$

	U_{11}	U_{22}	U_{33}	U_{23}	U_{13}	U_{12}
Sn(1)	25(1)	29(1)	26(1)	0(1)	0(1)	1(1)
Sn(2)	26(1)	33(1)	27(1)	-1(1)	-1(1)	1(1)
S(1)	32(1)	38(1)	29(1)	2(1)	4(1)	9(1)
S(2)	28(1)	38(1)	35(1)	-5(1)	-5(1)	6(1)
S(3)	38(1)	34(1)	32(1)	2(1)	0(1)	-10(1)
S(4)	33(1)	30(1)	31(1)	2(1)	1(1)	-4(1)
S(5)	28(1)	48(1)	46(1)	-2(1)	-7(1)	4(1)
S(6)	35(1)	39(1)	28(1)	-2(1)	0(1)	8(1)
Ni(1)	25(1)	26(1)	29(1)	1(1)	1(1)	2(1)
N(1)	30(2)	29(2)	41(2)	3(2)	0(2)	2(2)
C(1)	38(3)	38(3)	54(3)	7(2)	19(2)	6(2)
C(2)	58(3)	40(3)	37(3)	5(2)	12(2)	8(2)
N(2)	41(2)	38(2)	33(2)	3(2)	0(2)	8(2)
C(3)	35(2)	34(2)	60(3)	-2(2)	-10(2)	0(2)
C(4)	50(3)	38(3)	43(3)	-6(2)	-17(2)	0(2)
N(3)	46(2)	31(2)	30(2)	-1(2)	0(2)	5(2)
C(5)	38(2)	25(2)	50(3)	4(2)	3(2)	-1(2)
C(6)	42(3)	28(2)	41(3)	1(2)	2(2)	6(2)
N(4)	29(2)	31(2)	37(2)	4(2)	0(2)	4(2)
N(11)	28(2)	32(2)	47(2)	-6(2)	2(2)	-1(2)
C(11)	39(3)	28(2)	51(3)	-2(2)	5(2)	-4(2)
C(12)	54(4)	32(3)	120(6)	-2(3)	26(4)	-10(2)
C(13)	48(4)	51(4)	147(8)	-26(4)	28(4)	-24(3)
C(14)	33(3)	53(3)	105(5)	-33(4)	12(3)	-7(2)
C(15)	27(2)	42(3)	66(3)	-20(2)	2(2)	-1(2)
C(16)	41(3)	28(2)	53(3)	5(2)	2(2)	2(2)
N(12)	27(2)	30(2)	34(2)	-1(2)	0(2)	5(1)
Ni(2)	27(1)	33(1)	34(1)	-2(1)	-3(1)	4(1)
N(21)	31(2)	32(2)	49(2)	6(2)	-4(2)	3(2)
C(21)	36(3)	47(3)	57(3)	8(2)	11(2)	8(2)
C(22)	60(3)	54(3)	39(3)	7(2)	12(3)	15(3)
N(22)	53(3)	42(2)	36(2)	-6(2)	-10(2)	14(2)
C(23)	34(2)	39(3)	56(3)	5(2)	-15(2)	1(2)
C(24)	56(3)	43(3)	44(3)	-2(2)	-15(2)	7(2)
N(23)	41(2)	45(2)	34(2)	2(2)	4(2)	10(2)
C(25)	41(3)	35(3)	54(3)	6(2)	-8(2)	3(2)
C(26)	43(3)	35(2)	48(3)	-2(2)	-11(2)	11(2)
N(24)	33(2)	41(2)	41(2)	-7(2)	-7(2)	9(2)
C(34)	76(5)	112(7)	103(7)	26(6)	-14(5)	-4(5)
C(35)	32(3)	137(7)	63(4)	40(4)	2(3)	3(4)
N(32)	34(2)	30(2)	32(2)	3(2)	0(2)	6(2)

Table 5. Hydrogen coordinates ($\cdot 10^4$) and isotropic displacement parameters ($Å^2 \cdot 10^3$).

	x	y	z	U(eq)
H(1A)	7903	3038	5882	52
H(1B)	7938	3633	5552	52
H(2A)	8385	3520	7341	54
H(2B)	8704	3053	6786	54
H(1N)	9247	3667	6496	45
H(2N)	8858	4072	6398	45
H(3A)	7854	3604	3550	52
H(3B)	7767	3000	3429	52
H(4A)	8429	2920	2087	52
H(4B)	8093	3393	1625	52
H(3N)	8701	3922	2042	43
H(4N)	9039	3473	1959	43
H(5A)	8345	2424	4091	45
H(5B)	8627	2545	5335	45
H(6A)	9266	2286	4053	44
H(6B)	9057	2640	2980	44
H(5N)	9705	3078	3799	39
H(6N)	9541	2978	5048	39
H(12)	9710	5375	3085	83
H(13)	10572	5168	3216	98
H(14)	10809	4360	3975	77
H(15)	10179	3774	4422	54
H(16A)	8822	5134	3966	49
H(16B)	8790	4831	2717	49
H(7N)	8283	4360	3717	36
H(8N)	8484	4511	4903	36
H(21A)	7000	6425	4063	56
H(21B)	7144	6999	3701	56
H(22A)	6431	7082	2507	61
H(22B)	6666	6535	2169	61
H(9N)	6014	6159	2902	53
H(10N)	5750	6654	2795	53
H(23A)	7150	7112	6190	51
H(23B)	7037	6514	6049	51
H(24A)	6705	6777	7907	57
H(24B)	6391	7230	7276	57
H(11N)	5810	6631	7380	48
H(12N)	6173	6206	7212	48
H(25A)	6693	7679	4353	52
H(25B)	6481	7660	5701	52
H(26A)	5806	7943	4593	51
H(26B)	5903	7530	3551	51
H(13N)	5265	7212	4631	46
H(14N)	5500	7340	5800	46
H(32)	4929	5006	6323	119
H(33)	4110	5435	6379	123
H(36A)	5853	5094	5482	86
H(36B)	5957	5433	6655	86
H(34)	4033	6132	4998	116
H(34')	4047	6185	5489	116
H(35)	4761	6504	4495	93
H(35')	4736	6571	4780	93

Table 5. Hydrogen coordinates ($\cdot 10^4$) and isotropic displacement parameters ($Å^2 \cdot 10^3$).

	x	y	z	U(eq)
H(15N)	6275	5639	4346	38
H(16N)	6545	5760	5482	38
H(17N)	6410	5708	4410	38
H(18N)	6462	5737	5726	38
H(32')	4933	4883	5189	105
H(33')	4093	5240	5124	116
H(36C)	5862	5099	4586	106
H(36D)	5879	5169	6018	106

Table 6. Hydrogen bonds for [Å and °].

D-H...A	d(D-H)	d(H...A)	d(D...A)	<(DHA)
C(2)-H(2B)...S(6)#1	0.99	2.94	3.868(5)	156.9
N(2)-H(1N)...S(5)#1	0.91	2.72	3.618(4)	170.6
N(2)-H(2N)...S(2)	0.91	2.57	3.443(4)	159.9
N(3)-H(3N)...S(6)	0.91	3.00	3.673(4)	131.8
N(3)-H(4N)...S(3)#2	0.91	2.76	3.582(4)	150.6
C(5)-H(5B)...S(6)#1	0.99	2.95	3.704(5)	133.7
N(4)-H(5N)...S(1)#2	0.91	2.61	3.507(4)	170.0
N(4)-H(6N)...S(6)#1	0.91	2.72	3.486(4)	143.0
C(12)-H(12)...S(5)#3	0.95	2.78	3.679(6)	157.9
N(12)-H(7N)...S(6)	0.91	2.58	3.405(4)	151.9
N(12)-H(8N)...S(2)	0.91	2.47	3.376(4)	174.2
C(21)-H(21A)...S(4)	0.99	2.77	3.724(5)	163.2
C(22)-H(22A)...S(4)#4	0.99	3.01	3.666(6)	124.7
N(22)-H(9N)...S(5)	0.91	2.76	3.614(4)	156.9
N(22)-H(10N)...S(4)#4	0.91	2.94	3.665(4)	137.4
N(23)-H(11N)...S(2)#5	0.91	2.62	3.481(4)	158.8
N(23)-H(12N)...S(1)	0.91	2.80	3.576(4)	143.5
N(24)-H(13N)...S(6)#4	0.91	2.57	3.464(4)	167.8
N(24)-H(14N)...S(1)#5	0.91	2.61	3.452(4)	153.7
C(36)-H(36B)...S(1)	0.99	2.86	3.508(15)	124.2
C(35)-H(35)...S(6)#4	0.95	2.60	3.529(8)	167.2
N(32)-H(15N)...S(5)	0.91	2.46	3.360(4)	172.6
N(32)-H(18N)...S(1)	0.91	2.44	3.335(4)	169.4
N(32)-H(15N)...S(5)	0.91	2.46	3.360(4)	172.6
N(32)-H(18N)...S(1)	0.91	2.44	3.335(4)	169.4
C(32')-H(32')...N(31')#6	0.95	2.60	3.511(19)	159.7
C(36')-H(36C)...S(5)	0.99	2.83	3.52(2)	127.6

Symmetry transformations used to generate equivalent atoms:
#1 y+1/2,-x+1,z+1/2 #2 y+1/2,-x+1,z-1/2 #3 -y+3/2,x,-z+1/2
#4 y,-x+3/2,-z+1/2 #5 y,-x+3/2,-z+3/2 #6 -x+1,-y+1,-z+1

5.3.21 Messprotokoll der Verbindung $[Ni(en)(tren)]_2[Sn_2S_6]\cdot 2H_2O$

Table 1. Crystal data and structure refinement for $[Ni(C_6H_{18}N_4)(C_2H_8N_2)]_2[Sn_2S_6]\cdot 2H_2O$ ($C_6H_{18}N_4$, tren = Tris(2-aminoethyl)amin; $C_2H_8N_2$, en = Ethylendiamin)

Identification code	ds206	
Empirical formula	$[Ni(C_6H_{18}N_4)(C_2H_8N_2)]_2[Sn_2S_6]\cdot 2H_2O$	
Crystal color, habitus	purple, blocks	
Formula weight	995.89	
Temperature	293(2) K	
Wavelength	0.71073 Å	
Crystal system	monoclinic	
Space group	$P2_1/n$	
Unit cell dimensions	a = 12.7041(7) Å	α = 90°.
	b = 9.8000(3) Å	β = 108.843(4)°.
	c = 15.3989(8) Å	γ = 90°.
Volume	1814.42(15) $Å^3$	
Z	2	
Density (calculated)	1.823 Mg/m^3	
Absorption coefficient	2.764 mm^{-1}	
F(000)	1008	
Crystal size	0.14 x 0.11 x 0.08 mm^3	
Theta range for data collection	2.50 to 26.73°.	
Index ranges	-15<=h<=16, -12<=k<=12, -19<=l<=19	
Reflections collected	11637	
Independent reflections	3808 [R(int) = 0.0325]	
Completeness to theta = 26.73°	98.6 %	
Refinement method	Full-matrix least-squares on F^2	
Data / restraints / parameters	3808 / 0 / 181	
Goodness-of-fit on F^2	1.058	
Final R indices [I>2sigma(I)]	R1 = 0.0309, wR2 = 0.0596	
R indices (all data)	R1 = 0.0450, wR2 = 0.0627	
Largest diff. peak and hole	0.624 and -0.612 $e.Å^{-3}$	

Remarks:
All non-hydrogen were refined anisotropic. The C-H and N-H H atoms were positioned with idealized geometry and were refined using a riding model. The O-H H atoms were located in difference map, their bond lengths set to ideal values and finally they were refined using a riding model. A numerical absorption correction was performed ($T_{min}/_{max}$: 0.5461/0.7345).

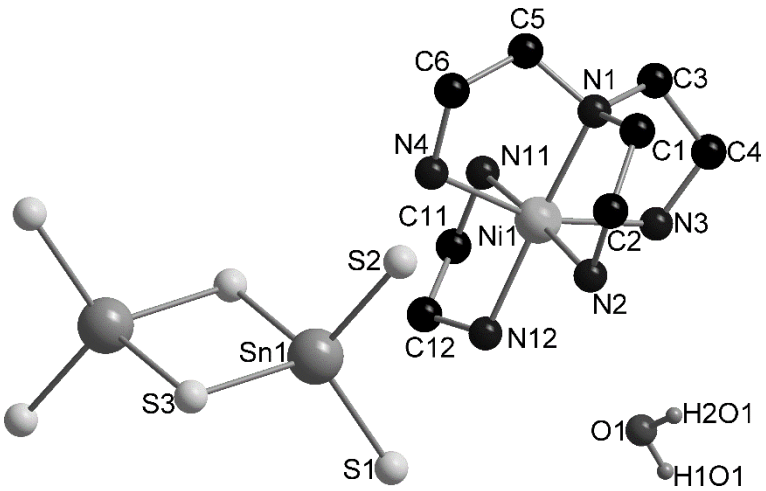

Figure 1: Part of the crystal structure of $[Ni(tren)(en)]_2[Sn_2S_6]\cdot 2H_2O$ with labelling of the crystallographic independent atoms.

Table 2. Atomic coordinates ($\cdot 10^4$) and equivalent isotropic displacement parameters ($Å^2\cdot 10^3$). U(eq) is defined as one third of the trace of the orthogonalized U_{ij} tensor.

	x	y	z	U(eq)
Sn(1)	8746(1)	4400(1)	5002(1)	31(1)
S(1)	7756(1)	5256(1)	5940(1)	48(1)
S(2)	7780(1)	2715(1)	3986(1)	42(1)
S(3)	10678(1)	3735(1)	5799(1)	44(1)
Ni(1)	5013(1)	6205(1)	2804(1)	32(1)
N(1)	4296(2)	4989(3)	1641(2)	38(1)
C(1)	4073(4)	3604(5)	1923(3)	53(1)
C(2)	4683(5)	3272(5)	2890(4)	71(1)
N(2)	4836(3)	4403(4)	3503(2)	59(1)
C(3)	3253(3)	5666(5)	1091(3)	49(1)
C(4)	2581(3)	6069(5)	1696(3)	55(1)
N(3)	3278(2)	6809(4)	2507(2)	46(1)
C(5)	5105(3)	4976(5)	1143(2)	47(1)
C(6)	6260(3)	4675(4)	1777(3)	48(1)
N(4)	6519(2)	5510(4)	2615(2)	48(1)
N(11)	5229(3)	8100(3)	2190(2)	40(1)
C(11)	5548(5)	9121(5)	2934(3)	66(1)
C(12)	6224(5)	8528(6)	3809(3)	74(2)
N(12)	5719(3)	7303(4)	4023(2)	47(1)
O(1)	3757(3)	7519(4)	4695(2)	76(1)

Table 3. Bond lengths [Å] and angles [°].

Sn(1)-S(2)	2.3319(9)	Sn(1)-S(3A)	2.4465(10)
Sn(1)-S(1)	2.3544(10)	Sn(1)-S(3)	2.4524(9)
S(3)-Sn(1A)	2.4465(10)		
S(2)-Sn(1)-S(1)	113.21(3)	S(2)-Sn(1)-S(3)	111.86(4)
S(2)-Sn(1)-S(3A)	111.65(4)	S(1)-Sn(1)-S(3)	115.74(4)
S(1)-Sn(1)-S(3A)	110.44(4	S(3A)-Sn(1)-S(3)	92.13(3)
Ni(1)-N(12)	2.097(3)	Ni(1)-N(4)	2.138(3)
Ni(1)-N(1)	2.099(3)	Ni(1)-N(11)	2.142(3)
Ni(1)-N(2)	2.117(4)	Ni(1)-N(3)	2.182(3)
N(12)-Ni(1)-N(1)	175.99(13)	N(2)-Ni(1)-N(11)	175.96(13)
N(12)-Ni(1)-N(2)	93.35(14)	N(4)-Ni(1)-N(11)	88.13(13)
N(1)-Ni(1)-N(2)	82.64(14)	N(12)-Ni(1)-N(3)	99.19(13)
N(12)-Ni(1)-N(4)	98.19(13)	N(1)-Ni(1)-N(3)	81.08(12)
N(1)-Ni(1)-N(4)	82.13(12)	N(2)-Ni(1)-N(3)	93.88(15)
N(2)-Ni(1)-N(4)	92.85(15)	N(4)-Ni(1)-N(3)	160.94(12)
N(12)-Ni(1)-N(11)	82.64(13)	N(11)-Ni(1)-N(3)	86.40(13)
N(1)-Ni(1)-N(11)	101.38(12)		
N(1)-C(5)	1.467(5)	C(3)-C(4)	1.506(6)
N(1)-C(3)	1.480(5)	C(4)-N(3)	1.468(5)
N(1)-C(1)	1.480(5)	C(5)-C(6)	1.506(6)
C(1)-C(2)	1.475(6)	C(6)-N(4)	1.473(5)
C(2)-N(2)	1.428(7)		
C(5)-N(1)-C(3)	110.7(3)	N(1)-C(3)-C(4)	110.2(3)
C(5)-N(1)-C(1)	112.2(3)	N(3)-C(4)-C(3)	110.4(3)
C(3)-N(1)-C(1)	111.0(3)	N(1)-C(5)-C(6)	111.3(3)
C(2)-C(1)-N(1)	114.3(4)	N(4)-C(6)-C(5)	110.7(3)
N(2)-C(2)-C(1)	114.3(4)		
N(11)-C(11)	1.476(5)	C(12)-N(12)	1.448(6)
C(11)-C(12)	1.465(7)		
C(12)-C(11)-N(11)	112.2(4)	N(12)-C(12)-C(11)	111.5(4)

Symmetry transformations used to generate equivalent atoms: A: -x+2,-y+1,-z+1

Table 4. Anisotropic displacement parameters ($Å^2 \cdot 10^3$). The anisotropic displacement factor exponent takes the form: $-2\pi^2[h^2 a^{*2} U_{11} + ... + 2 h k a^* b^* U_{12}]$

	U_{11}	U_{22}	U_{33}	U_{23}	U_{13}	U_{12}
Sn(1)	29(1)	32(1)	33(1)	2(1)	13(1)	-1(1)
S(1)	45(1)	54(1)	54(1)	-15(1)	28(1)	-6(1)
S(2)	42(1)	41(1)	46(1)	-9(1)	19(1)	-6(1)
S(3)	34(1)	43(1)	52(1)	19(1)	11(1)	1(1)
Ni(1)	32(1)	37(1)	29(1)	0(1)	10(1)	2(1)
N(1)	41(2)	36(2)	37(1)	-3(1)	13(1)	-1(1)
C(1)	57(2)	43(3)	62(2)	-2(2)	26(2)	-8(2)
C(2)	80(3)	46(3)	79(3)	18(2)	15(3)	-9(2)
N(2)	77(2)	56(2)	48(2)	16(2)	28(2)	11(2)
C(3)	44(2)	55(3)	39(2)	-4(2)	0(2)	-1(2)
C(4)	35(2)	65(3)	58(2)	4(2)	7(2)	1(2)
N(3)	39(2)	59(2)	44(2)	2(2)	19(1)	6(2)
C(5)	63(2)	46(2)	37(2)	-5(2)	26(2)	0(2)
C(6)	54(2)	39(3)	62(2)	0(2)	35(2)	9(2)
N(4)	38(2)	52(2)	52(2)	-1(2)	11(1)	9(2)
N(11)	42(2)	41(2)	41(2)	3(1)	17(1)	2(1)
C(11)	83(3)	40(3)	64(3)	-5(2)	11(2)	-8(2)
C(12)	83(3)	76(4)	60(3)	-17(2)	18(3)	-32(3)
N(12)	39(2)	63(2)	36(2)	-7(2)	12(1)	-5(2)
O(1)	63(2)	105(3)	73(2)	-10(2)	42(2)	-18(2)

Table 5. Hydrogen coordinates ($\cdot 10^4$) and isotropic displacement parameters ($Å^2 \cdot 10^3$).

	x	y	z	U(eq)
H(1A)	3282	3516	1822	63
H(1B)	4270	2941	1533	63
H(2A)	4281	2562	3090	85
H(2B)	5406	2908	2928	85
H(2C)	5448	4272	3992	70
H(2D)	4247	4479	3703	70
H(3A)	2822	5051	615	59
H(3B)	3426	6472	796	59
H(4A)	1965	6643	1354	65
H(4B)	2278	5258	1889	65
H(3C)	3054	6620	2992	55
H(3D)	3209	7714	2403	55
H(5A)	5100	5856	853	56
H(5B)	4891	4289	664	56
H(6A)	6317	3716	1941	57
H(6B)	6796	4865	1465	57
H(4C)	6936	6231	2568	58
H(4D)	6911	5012	3103	58
H(11A)	5765	8022	1928	48
H(11B)	4592	8347	1756	48
H(11A)	5963	9848	2766	79
H(11B)	4881	9516	3005	79
H(12A)	6957	8310	3780	89
H(12B)	6313	9192	4295	89
H(12C)	5191	7525	4272	56
H(12D)	6236	6792	4430	56
H(1O1)	3450	7819	5049	114
H(2O1)	3453	6777	4550	114

Table 6. Hydrogen bonds [Å and °].

D-H...A	d(D-H)	d(H...A)	d(D...A)	<(DHA)
N(2)-H(2C)…O1#1	0.900	2.621	3.353	139.03
N(2)-H(2C)…S1#1	0.900	2.784	3.677	171.90
N(3)-H(3C)…O1	0.900	2.634	3.299	131.36
N(3)-H(3C)…S1#1	0.900	2.870	3.684	151.11
N(3)-H(3D)…S1#2	0.900	2.921	3.675	142.40
N(4)-(H(4C)…S2#3	0.900	2.920	3.600	133.52
N(4)-(H(4D)…S2	0.900	2.677	3.514	155.08
N(11)-H(11A)…S2#3	0.900	2.677	3.574	174.97
N(11)-H(11B)…S1#2	0.900	2.647	3.503	159.26
N(12)-H(12C)…O1	0.900	2.124	2.999	163.94
N(12)-H(12D)…S1	0.900	2.915	3.808	171.69
O(1)-H(1O1)…S2#1	0.820	2.534	3.248	146.20

Symmetry transformations used to generate equivalent atoms:
-y+1, -z+1; #2: x-1/2, -y+3/2, z-1/2]; 3#: -x+3/2, y+1/2, -z+1/2 .55 3.290 S1 [-x+1, -y+1, -z+1]
#1: -x+1, -y+1, -z+1; 2#: x-1/2, -y+3/2, z-1/2; 3#: -x+3/2, y+1/2, -z+1/2

5.3.22 Messprotokoll der Verbindung $[Ni(en)(tren)]_2[Sn_2S_6]\cdot 6H_2O$

Table 1. Crystal data and structure refinement for $[Ni(C_6H_{18}N_4)(C_2H_8N_2)]_2[Sn_2S_6]\cdot 6H_2O$ ($C_6H_{18}N_4$, tren = Tris(2-aminoethyl)amin; $C_2H_8N_2$, en = Ethylendiamin)

Identification code	jh2338a	
Empirical formula	$[Ni(C_6H_{18}N_4)(C_2H_8N_2)]_2[Sn_2S_6]\cdot 6H_2O$	
Crystal color, habitus	purple, blocks	
Formula weight	1067.95	
Temperature	170(2) K	
Wavelength	0.71073 Å	
Crystal system	monoclinic	
Space group	$P2_1/c$	
Unit cell dimensions	a = 12.5580(3) Å	α= 90°.
	b = 9.7089(2) Å	β= 91.827(2)°.
	c = 16.0359(4) Å	γ = 90°.
Volume	1954.17(8) $Å^3$	
Z	2	
Density (calculated)	1.815 Mg/m^3	
Absorption coefficient	2.580 mm^{-1}	
F(000)	1088	
Crystal size	0.07 x 0.11 x 0.14 mm^3	
Theta range for data collection	1.622 to 27.908°.	
Index ranges	-16<=h<=15, -12<=k<=12, -21<=l<=21	
Reflections collected	24951	
Independent reflections	4673 [R(int) = 0.0335]	
Completeness to theta = 25.242°	100.0 %	
Refinement method	Full-matrix least-squares on F^2	
Data / restraints / parameters	4673 / 0 / 200	
Goodness-of-fit on F^2	1.073	
Final R indices [I>2sigma(I)]	R1 = 0.0357, wR2 = 0.0909	
R indices (all data)	R1 = 0.0404, wR2 = 0.0932	
Extinction coefficient	0.0049(5)	
Largest diff. peak and hole	0.978 and -0.870 e.$Å^{-3}$	

Comments: A numerical absorption correction was performed ($T_{min/max}$: 0.6007/0.7562). All non-hydrogen atoms were refined anisotropic. The C-H and N-H H atoms were positioned with idealized geometry and refined isotropic with $U_{iso}(H) = 1.2\ U_{eq}(C,N)$ using a rind model. The O-H H atoms were located in difference map, their bond lengths were set to ideal values and finally, they were refined isotropic with $U_{iso}(H) = 1.5\ U_{eq}(O)$ using a rind model.

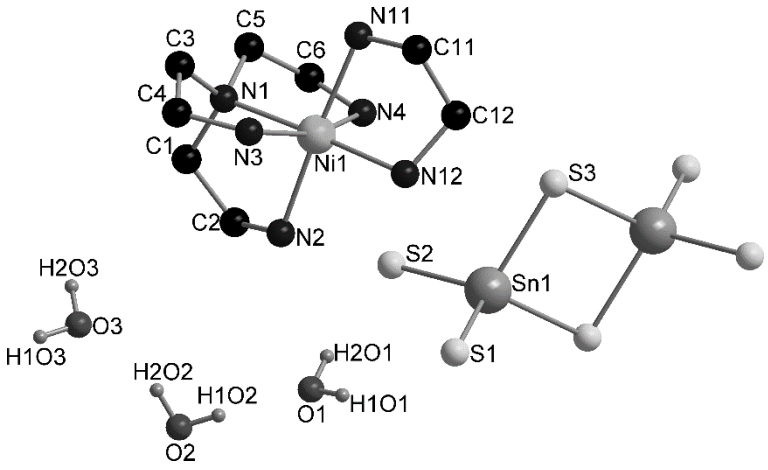

Figure 1: Part of the crystal structure of $[Ni(tren)(en)]_2[Sn_2S_6]\cdot 6H_2O$ with labelling of the crystallographic independent atoms.

Table 2. Atomic coordinates ($\cdot 10^4$) and equivalent isotropic displacement parameters ($Å^2\cdot 10^3$). U(eq) is defined as one third of the trace of the orthogonalized U_{ij} tensor.

	x	y	z	U(eq)
Sn(1)	3900(1)	4325(1)	9511(1)	23(1)
S(1)	2122(1)	4973(1)	9758(1)	31(1)
S(2)	4000(1)	2752(1)	8419(1)	28(1)
S(3)	4996(1)	6363(1)	9274(1)	28(1)
Ni(1)	2464(1)	6430(1)	6839(1)	22(1)
N(1)	2480(2)	5306(3)	5713(2)	26(1)
C(1)	2010(3)	3914(3)	5839(2)	32(1)
C(2)	2035(3)	3465(3)	6751(2)	33(1)
N(2)	1732(2)	4635(3)	7277(2)	29(1)
C(3)	1838(3)	6103(3)	5094(2)	31(1)
C(4)	807(3)	6580(4)	5469(2)	33(1)
N(3)	1031(2)	7292(3)	6270(2)	31(1)
C(5)	3613(3)	5236(4)	5506(2)	33(1)
C(6)	4292(3)	4770(3)	6255(2)	31(1)
N(4)	3998(2)	5520(3)	7023(2)	27(1)
N(11)	3269(2)	8260(3)	6457(2)	26(1)
C(11)	3153(3)	9319(3)	7110(2)	28(1)
C(12)	3181(3)	8629(3)	7958(2)	31(1)
N(12)	2363(2)	7532(3)	7962(2)	29(1)
O(1)	1575(2)	2035(3)	8723(2)	42(1)
O(2)	643(2)	-89(3)	7825(2)	40(1)
O(3)	286(3)	658(3)	6149(2)	55(1)

Table 3. Bond lengths [Å] and angles [°].

Sn(1)-S(2)	2.3297(7)	Sn(1)-S(3A)	2.4469(8)
Sn(1)-S(1)	2.3645(8)	Sn(1)-S(3)	2.4477(8)
S(3)-Sn(1A)	2.4469(8)	S(2)-Sn(1)-S(3)	111.68(3)
S(2)-Sn(1)-S(1)	111.98(3)	S(1)-Sn(1)-S(3)	110.46(3)
S(2)-Sn(1)-S(3A)	112.12(3)	S(3A)-Sn(1)-S(3)	92.10(2)
S(1)-Sn(1)-S(3A)	116.94(3)		
Sn(1A)-S(3)-Sn(1)	87.90(2)		
Ni(1)-N(2)	2.102(3)	Ni(1)-N(4)	2.131(3)
Ni(1)-N(12)	2.102(2)	Ni(1)-N(11)	2.143(2)
Ni(1)-N(1)	2.111(2)	Ni(1)-N(3)	2.160(3)
N(2)-Ni(1)-N(12)	95.54(10)	N(1)-Ni(1)-N(11)	99.58(10)
N(2)-Ni(1)-N(1)	82.73(10)	N(4)-Ni(1)-N(11)	87.17(10)
N(12)-Ni(1)-N(1)	177.05(11)	N(2)-Ni(1)-N(3)	95.45(11)
N(2)-Ni(1)-N(4)	90.75(11)	N(12)-Ni(1)-N(3)	95.32(11)
N(12)-Ni(1)-N(4)	99.87(11)	N(1)-Ni(1)-N(3)	82.48(10)
N(1)-Ni(1)-N(4)	82.58(10)	N(4)-Ni(1)-N(3)	162.96(10)
N(2)-Ni(1)-N(11)	176.66(11)	N(11)-Ni(1)-N(3)	87.27(10)
N(12)-Ni(1)-N(11)	82.25(10)		
N(1)-C(5)	1.472(4)	C(3)-C(4)	1.517(5)
N(1)-C(3)	1.477(4)	C(4)-N(3)	1.476(4)
N(1)-C(1)	1.491(4)	C(5)-C(6)	1.519(5)
C(1)-C(2)	1.526(4)	C(6)-N(4)	1.487(4)
C(2)-N(2)	1.472(4)	N(2)-C(2)-C(1)	109.4(3)
C(5)-N(1)-C(3)	112.5(3)	N(1)-C(3)-C(4)	110.4(2)
C(5)-N(1)-C(1)	112.2(3)	N(3)-C(4)-C(3)	110.3(3)
C(3)-N(1)-C(1)	110.9(3)	N(1)-C(5)-C(6)	110.9(3)
N(1)-C(1)-C(2)	113.1(2)	N(4)-C(6)-C(5)	111.2(2)
N(11)-C(11)	1.478(4)	C(12)-N(12)	1.479(4)
C(11)-C(12)	1.516(4)	N(12)-C(12)-C(11)	109.0(2)
N(11)-C(11)-C(12)	109.2(2)		

Symmetry transformations used to generate equivalent atoms: A: -x+1,-y+1,-z+2

Table 4. Anisotropic displacement parameters ($Å^2 x\ 10^3$). The anisotropic displacement factor exponent takes the form: $-2\pi^2[h^2\ a^{*2}U_{11} + ...\ + 2\ h\ k\ a^*\ b^*\ U_{12}]$

	U_{11}	U_{22}	U_{33}	U_{23}	U_{13}	U_{12}
Sn(1)	23(1)	21(1)	24(1)	0(1)	0(1)	0(1)
S(1)	25(1)	32(1)	34(1)	-5(1)	1(1)	3(1)
S(2)	28(1)	28(1)	29(1)	-6(1)	1(1)	1(1)
S(3)	31(1)	25(1)	28(1)	6(1)	-3(1)	-3(1)
Ni(1)	23(1)	21(1)	22(1)	0(1)	2(1)	0(1)
N(1)	31(1)	24(1)	25(1)	-3(1)	1(1)	-2(1)
C(1)	42(2)	22(1)	32(2)	-4(1)	-5(1)	-3(1)
C(2)	39(2)	26(2)	34(2)	2(1)	-1(1)	-4(1)
N(2)	30(1)	28(1)	29(1)	3(1)	0(1)	-5(1)
C(3)	41(2)	28(1)	23(1)	2(1)	-6(1)	-4(1)
C(4)	33(2)	35(2)	31(2)	3(1)	-10(1)	-2(1)
N(3)	26(1)	30(1)	35(1)	-3(1)	-4(1)	2(1)
C(5)	34(2)	34(2)	31(2)	-3(1)	10(1)	2(1)
C(6)	28(2)	28(2)	38(2)	-4(1)	6(1)	7(1)
N(4)	26(1)	24(1)	30(1)	1(1)	0(1)	1(1)
N(11)	26(1)	25(1)	27(1)	1(1)	3(1)	-1(1)
C(11)	30(2)	23(1)	33(2)	0(1)	3(1)	-1(1)
C(12)	33(2)	28(2)	31(1)	-6(1)	-2(1)	-1(1)
N(12)	35(1)	28(1)	24(1)	-1(1)	4(1)	1(1)
O(1)	40(1)	47(2)	41(1)	-9(1)	6(1)	-15(1)
O(2)	31(1)	44(1)	46(1)	-7(1)	3(1)	-3(1)
O(3)	45(2)	77(2)	42(2)	-8(1)	0(1)	-12(2)

Table 5. Hydrogen coordinates ($\cdot 10^4$) and isotropic displacement parameters ($Å^2 \cdot 10^3$).

	x	y	z	U(eq)
H(1A)	2408	3233	5510	38
H(1B)	1263	3917	5624	38
H(2A)	1533	2692	6825	40
H(2B)	2759	3146	6918	40
H(2C)	1944	4476	7817	35
H(2D)	1011	4739	7257	35
H(3A)	1676	5523	4599	37
H(3B)	2250	6912	4912	37
H(4A)	430	7214	5077	40
H(4B)	341	5777	5562	40
H(3C)	475	7178	6614	37
H(3D)	1120	8209	6180	37
H(5A)	3854	6155	5323	39
H(5B)	3701	4583	5039	39
H(6A)	4194	3769	6339	38
H(6B)	5052	4938	6146	38
H(4C)	4489	6186	7143	32
H(4D)	3990	4925	7461	32
H(11A)	3971	8077	6386	31
H(11B)	2981	8567	5963	31
H(11A)	2470	9814	7020	34
H(11B)	3740	9997	7081	34
H(12A)	3894	8228	8076	37
H(12B)	3037	9317	8397	37
H(12C)	1703	7908	8003	34
H(12D)	2483	6960	8405	34
H(1O1)	1487	2681	9062	64
H(2O1)	2215	2117	8592	64
H(1O2)	899	586	8090	61
H(2O2)	656	253	7344	61
H(1O3)	-312	509	5917	82
H(2O3)	743	671	5778	82

Table 6. Hydrogen bonds [Å and °].

D-H...A	d(D-H)	d(H...A)	d(D...A)	<(DHA)
C(2)-H(2B)...S(2)	0.99	2.85	3.647(4)	138.0
N(2)-H(2D)...O(2)#2	0.91	2.08	2.993(4)	177.6
N(3)-H(3C)...O(1)#2	0.91	2.62	3.283(4)	130.5
N(3)-H(3D)...O(3)#3	0.91	2.60	3.403(4)	148.0
C(6)-H(6A)...S(3)#4	0.99	2.74	3.537(3)	137.6
N(4)-H(4C)...S(2)#5	0.91	2.61	3.411(3)	146.7
N(4)-H(4D)...S(2)	0.91	2.61	3.498(3)	165.4
N(11)-H(11A)...S(2)#5	0.91	2.58	3.464(3)	165.2
N(11)-H(11B)...S(1)#6	0.91	2.60	3.491(3)	165.5
C(12)-H(12A)...S(3)	0.99	2.95	3.767(3)	140.2
N(12)-H(12C)...O(2)#3	0.91	2.37	3.166(4)	146.2
N(12)-H(12D)...S(1)	0.91	2.95	3.823(3)	161.4
O(1)-H(1O1)...S(1)	0.84	2.60	3.361(3)	150.5
O(1)-H(2O1)...S(2)	0.84	2.35	3.176(3)	167.8
O(2)-H(1O2)...O(1)	0.84	1.92	2.755(4)	175.5
O(2)-H(2O2)...O(3)	0.84	2.00	2.805(4)	161.4
O(3)-H(1O3)...S(1)#7	0.84	2.54	3.380(3)	177.9
O(3)-H(2O3)...S(1)#8	0.84	2.50	3.316(3)	164.5

Symmetry transformations used to generate equivalent atoms: #1 -x+1,-y+1,-z+2; #2 -x,y+1/2,-z+3/2; #3 x,y+1,z; #4 -x+1,y-1/2,-z+3/2; #5 -x+1,y+1/2,-z+3/2; #6 x,-y+3/2,z-1/2; #7 -x,y-1/2,-z+3/2; #8 x,-y+1/2,z-1/2

5.3.23 Messprotokoll der Verbindung $[Ni(1,2dach)(tren)]_2[Sn_2S_6]\cdot 3H_2O$

Table 1. Crystal data and structure refinement for $[Ni(C_6H_{18}N_4)(C_6H_{14}N_2)]_2[Sn_2S_6]\cdot 3H_2O$. ($C_6H_{18}N_4$, tren = Tris(2-aminoethyl)amin; $C_6H_{14}N_2$, 1,2-Diaminocyclohexan)

Identification code	jh1573	
Empirical formula	$[Ni(C_6H_{18}N_4)(C_6H_{14}N_2)]_2[Sn_2S_6]\cdot 3H_2O$	
Crystal color, habitus	violet blocks	
Formula weight	1122.08	
Temperature	200(2) K	
Wavelength	0.71073 Å	
Crystal system	triclinic	
Space group	$P\bar{1}$	
Unit cell dimensions	a = 9.8121(9) Å	α= 86.379(11)°.
	b = 10.0080(9) Å	β= 79.646(10)°.
	c = 12.4221(11) Å	γ = 65.715(10)°.
Volume	1093.72(19) $Å^3$	
Z	1	
Density (calculated)	1.704 Mg/m^3	
Absorption coefficient	2.304 mm^{-1}	
F(000)	574	
Crystal size	0.05 x 0.12 x 0.18 mm^3	
Theta range for data collection	2.474 to 27.996°.	
Index ranges	-12<=h<=12, -13<=k<=13, -16<=l<=16	
Reflections collected	9799	
Independent reflections	5183 [R(int) = 0.0339]	
Completeness to theta = 25.242°	99.5 %	
Refinement method	Full-matrix least-squares on F^2	
Data / restraints / parameters	5183 / 1 / 272	
Goodness-of-fit on F^2	0.994	
Final R indices [I>2sigma(I)]	R1 = 0.0399, wR2 = 0.1014	
R indices (all data)	R1 = 0.0505, wR2 = 0.1077	
Extinction coefficient	0.0342(18)	
Largest diff. peak and hole	0.944 and -1.698 e.$Å^{-3}$	

Comments: All non-hydrogen atoms were refined anisotropic. The C-H and N-H H atoms were positioned with idealized geometry and refined using a riding model. The O-H H atoms of O1 were located in difference map, their bond lengths set to ideal values and finally they were refined using a riding model. The O-H H atoms at O2 were not located but considered in the molecular formula. A numerical absorption correction was performed ($T_{min/max}$: 0.5249/0.8069). Some C atoms of the organic ligands are disordered and were refined using a split model. One of the two water H atoms are occupied only to 50%.

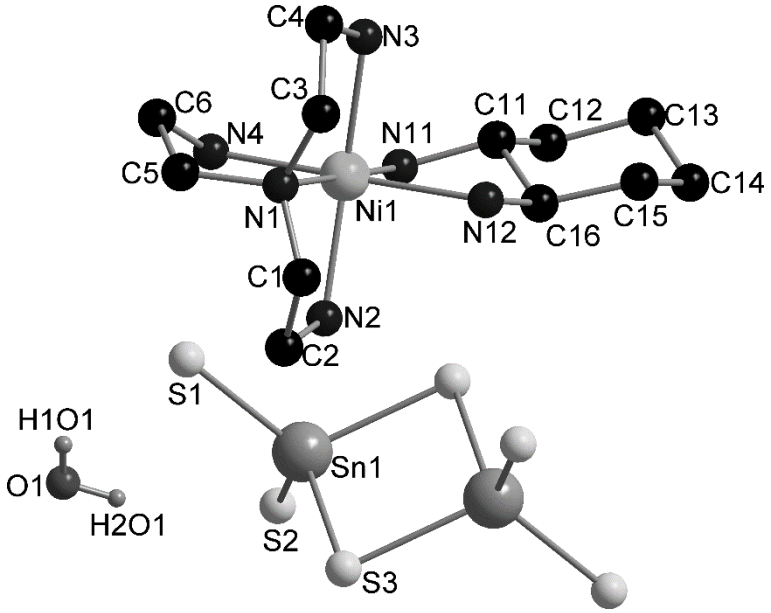

Figure 1: Part of the crystal structure of $[Ni(tren)(1,2\text{-dach})]_2[Sn_2S_6]\cdot 3H_2O$ with labelling of the crystallographic independent atoms.

Table 2. Atomic coordinates ($\cdot 10^4$) and equivalent isotropic displacement parameters ($Å^2 \cdot 10^3$). U(eq) is defined as one third of the trace of the orthogonalized U_{ij} tensor.

	x	y	z	U(eq)
Sn(1)	8682(1)	5170(1)	6135(1)	26(1)
S(1)	6122(1)	6738(1)	6221(1)	34(1)
S(2)	9263(1)	3802(1)	7718(1)	40(1)
S(3)	10302(1)	6472(1)	5465(1)	37(1)
Ni(1)	5640(1)	6779(1)	2696(1)	21(1)
N(1)	4723(3)	9005(3)	2276(3)	29(1)
C(1)	5962(5)	9488(5)	2259(4)	42(1)
C(2)	6675(5)	9005(5)	3277(5)	46(1)
N(2)	6996(3)	7451(4)	3493(3)	30(1)
C(3)	4306(5)	9060(5)	1188(3)	35(1)
C(4)	3424(5)	8135(5)	1154(3)	37(1)
N(3)	4224(4)	6654(4)	1589(3)	32(1)
C(5)	3375(4)	9842(5)	3118(4)	39(1)
C(6)	2644(8)	8796(10)	3774(7)	36(2)
C(6')	3428(10)	9156(11)	4157(7)	49(2)
N(4)	3818(4)	7499(4)	4032(3)	39(1)
N(11)	6448(4)	4629(4)	3204(3)	29(1)
C(11)	7306(7)	3651(6)	2243(5)	26(1)
C(11')	7904(13)	3733(12)	2460(10)	30(2)
C(12)	8127(5)	2071(4)	2520(4)	37(1)
C(13)	9011(10)	1140(8)	1505(6)	41(2)
C(14)	10164(10)	1722(10)	928(7)	47(2)
C(13')	9621(17)	1177(16)	1771(16)	62(5)
C(14')	9734(19)	1777(18)	615(13)	51(5)
C(15)	9367(5)	3347(5)	626(3)	42(1)

C(16)	8416(7)	4263(6)	1640(5)	24(1)
C(16')	7847(14)	4287(13)	1299(10)	32(3)
N(12)	7562(3)	5852(3)	1389(2)	27(1)
O(1)	6314(5)	6361(5)	9066(3)	65(1)
O(2)	439(12)	8842(12)	3717(11)	95(3)

Table 3. Bond lengths [Å] and angles [°].

Sn(1)-S(1)	2.3381(10)	Sn(1)-S(3A)	2.4483(10)
Sn(1)-S(2)	2.3424(11)	Sn(1)-S(3)	2.4512(11)
S(3)-Sn(1A)	2.4483(10)		
S(1)-Sn(1)-S(2)	114.57(4)	S(1)-Sn(1)-S(3)	110.67(4)
S(1)-Sn(1)-S(3A)	113.13(4)	S(2)-Sn(1)-S(3)	114.65(4)
S(2)-Sn(1)-S(3A)	109.55(4)	S(3A)-Sn(1)-S(3)	92.26(4)
Sn(1A)-S(3)-Sn(1)	87.74(4)		
Ni(1)-N(11)	2.065(3)	Ni(1)-N(2)	2.121(3)
Ni(1)-N(1)	2.102(3)	Ni(1)-N(3)	2.166(3)
Ni(1)-N(4)	2.120(3)	Ni(1)-N(12)	2.169(3)
N(11)-Ni(1)-N(1)	176.32(12)	N(4)-Ni(1)-N(3)	93.22(14)
N(11)-Ni(1)-N(4)	93.48(14)	N(2)-Ni(1)-N(3)	162.94(14)
N(1)-Ni(1)-N(4)	82.90(14)	N(11)-Ni(1)-N(12)	81.49(12)
N(11)-Ni(1)-N(2)	97.10(13)	N(1)-Ni(1)-N(12)	102.14(12)
N(1)-Ni(1)-N(2)	82.43(13)	N(4)-Ni(1)-N(12)	174.96(14)
N(4)-Ni(1)-N(2)	92.02(13)	N(2)-Ni(1)-N(12)	88.58(12)
N(11)-Ni(1)-N(3)	98.77(13)	N(3)-Ni(1)-N(12)	87.62(12)
N(1)-Ni(1)-N(3)	82.13(13)		
N(1)-C(3)	1.472(5)	C(4)-N(3)	1.483(5)
N(1)-C(1)	1.477(5)	C(5)-C(6')	1.422(11)
N(1)-C(5)	1.499(5)	C(5)-C(6)	1.604(10)
C(1)-C(2)	1.511(7)	C(6)-N(4)	1.402(9)
C(2)-N(2)	1.472(6)	C(6')-N(4)	1.552(12)
C(3)-C(4)	1.511(7)	N(1)-C(3)-C(4)	110.8(3)
C(3)-N(1)-C(1)	112.5(3)	N(3)-C(4)-C(3)	110.4(3)
C(3)-N(1)-C(5)	111.8(3)	C(6')-C(5)-N(1)	112.7(4)
C(1)-N(1)-C(5)	111.3(3)	N(1)-C(5)-C(6)	111.8(4)
N(1)-C(1)-C(2)	111.1(4)	N(4)-C(6)-C(5)	108.7(5)
N(2)-C(2)-C(1)	110.3(3)	C(5)-C(6')-N(4)	110.5(6)
N(11)-C(11)	1.484(6)	C(13)-C(14)	1.527(11)
N(11)-C(11')	1.509(11)	C(14)-C(15)	1.543(10)
C(11)-C(12)	1.500(7)	C(13')-C(14')	1.524(17)
C(11)-C(16)	1.522(9)	C(14')-C(15)	1.461(18)
C(11')-C(16')	1.514(18)	C(15)-C(16')	1.519(12)
C(11')-C(12)	1.585(12)	C(15)-C(16)	1.523(6)
C(12)-C(13)	1.517(8)	C(16)-N(12)	1.504(6)
C(12)-C(13')	1.534(16)	C(16')-N(12)	1.481(12)
N(11)-C(11)-C(12)	114.4(4)	C(15)-C(14')-C(13')	111.6(11)
N(11)-C(11)-C(16)	106.4(5)	C(14')-C(15)-C(16')	115.4(9)
C(12)-C(11)-C(16)	110.7(5)	C(16)-C(15)-C(14)	110.5(5)
N(11)-C(11')-C(16')	110.2(9)	N(12)-C(16)-C(11)	109.4(4)
N(11)-C(11')-C(12)	108.3(8)	N(12)-C(16)-C(15)	112.9(4)

C(16')-C(11')-C(12)	110.9(9)	C(11)-C(16)-C(15)	111.3(5)
C(11)-C(12)-C(13)	111.7(5)	N(12)-C(16')-C(11')	104.4(8)
C(13')-C(12)-C(11')	107.5(8)	N(12)-C(16')-C(15)	114.5(9)
C(12)-C(13)-C(14)	108.8(6)	C(11')-C(16')-C(15)	106.2(9)
C(13)-C(14)-C(15)	110.8(6)	C(16')-N(12)-Ni(1)	106.1(5)
C(14')-C(13')-C(12)	113.5(11)	C(16)-N(12)-Ni(1)	107.9(3)

Symmetry transformations used to generate equivalent atoms: A: -x+2,-y+1,-z+1

Table 4. Anisotropic displacement parameters ($Å^2 \cdot 10^3$). The anisotropic displacement factor exponent takes the form: $-2\pi^2 [h^2 a^{*2} U_{11} + ... + 2 h k a^* b^* U_{12}]$

	U_{11}	U_{22}	U_{33}	U_{23}	U_{13}	U_{12}
Sn(1)	18(1)	46(1)	15(1)	-2(1)	-1(1)	-13(1)
S(1)	20(1)	45(1)	35(1)	4(1)	-4(1)	-10(1)
S(2)	25(1)	66(1)	21(1)	8(1)	-5(1)	-12(1)
S(3)	32(1)	60(1)	26(1)	-14(1)	4(1)	-28(1)
Ni(1)	17(1)	24(1)	19(1)	0(1)	-2(1)	-6(1)
N(1)	21(1)	25(2)	34(2)	2(1)	-6(1)	-3(1)
C(1)	28(2)	28(2)	70(3)	5(2)	-10(2)	-11(2)
C(2)	34(2)	34(2)	73(3)	-11(2)	-20(2)	-11(2)
N(2)	22(1)	35(2)	30(2)	-5(1)	-4(1)	-8(1)
C(3)	32(2)	37(2)	28(2)	15(2)	-9(2)	-6(2)
C(4)	29(2)	45(2)	31(2)	3(2)	-17(2)	-5(2)
N(3)	26(2)	37(2)	35(2)	-3(1)	-10(1)	-10(1)
C(5)	26(2)	30(2)	50(2)	-13(2)	-3(2)	1(2)
C(6)	17(3)	48(5)	36(4)	-10(4)	5(3)	-7(3)
C(6')	37(5)	56(6)	29(4)	-18(4)	3(3)	6(4)
N(4)	29(2)	52(2)	29(2)	-2(2)	1(1)	-12(2)
N(11)	25(1)	28(2)	29(2)	5(1)	-2(1)	-8(1)
C(11)	22(3)	24(3)	31(3)	-2(2)	-7(2)	-8(2)
C(11')	16(5)	25(6)	45(7)	-8(5)	-11(5)	-3(4)
C(12)	31(2)	26(2)	52(2)	1(2)	-11(2)	-8(2)
C(13)	44(4)	27(3)	43(4)	-4(3)	-20(3)	-2(3)
C(14)	45(5)	42(4)	28(4)	-3(3)	-5(3)	9(4)
C(13')	26(7)	23(7)	122(18)	-2(9)	-17(9)	7(6)
C(14')	40(8)	35(8)	54(11)	-25(8)	-29(7)	19(6)
C(15)	39(2)	43(3)	24(2)	-8(2)	-2(2)	2(2)
C(16)	20(3)	25(3)	20(3)	-1(2)	-2(2)	-3(2)
C(16')	26(5)	30(6)	37(6)	-9(5)	-19(5)	-1(4)
N(12)	25(1)	27(2)	24(1)	2(1)	-2(1)	-8(1)
O(1)	62(2)	73(3)	35(2)	-15(2)	-1(2)	-4(2)
O(2)	80(7)	78(7)	128(9)	31(6)	-28(6)	-34(5)

Table 5. Hydrogen coordinates ($\cdot 10^4$) and isotropic displacement parameters ($Å^2 \cdot 10^3$).

	x	y	z	U(eq)
H(1A)	5555	10569	2211	50
H(1B)	6744	9070	1605	50
H(2A)	7630	9149	3179	55
H(2B)	5979	9612	3910	55
H(1N)	6802	7317	4226	36
H(2N)	7995	6892	3248	36
H(3A)	5236	8697	628	42
H(3B)	3682	10088	1015	42
H(4A)	2400	8615	1597	44
H(4B)	3305	8048	391	44
H(3N)	4806	6021	1028	39
H(4N)	3537	6317	1949	39
H(5A)	2601	10618	2753	47
H(5B)	3687	10322	3641	47
H(5C)	3322	10840	3197	47
H(5D)	2441	9938	2861	47
H(6A)	1969	9296	4453	44
H(6B)	2034	8569	3318	44
H(6C)	2433	9632	4638	59
H(6D)	4204	9277	4503	59
H(5N)	3460	6791	4201	47
H(6N)	4155	7657	4628	47
H(7N)	3008	7361	3888	47
H(8N)	4103	7009	4652	47
H(9N)	7064	4501	3704	35
H(10N)	5659	4406	3527	35
H(11N)	6618	4586	3904	35
H(12N)	5746	4258	3188	35
H(11)	6579	3717	1751	31
H(11')	8771	3820	2721	36
H(12A)	7383	1695	2904	45
H(12B)	8833	1992	3023	45
H(12C)	8167	1720	3282	45
H(12D)	7270	1966	2274	45
H(13A)	8310	1185	1008	49
H(13B)	9540	106	1712	49
H(14A)	10735	1135	256	57
H(14B)	10897	1621	1414	57
H(13C)	10476	1160	2100	74
H(13D)	9726	154	1730	74
H(14C)	10776	1251	212	61
H(14D)	9028	1598	225	61
H(15A)	10136	3717	288	50
H(15B)	8706	3437	85	50
H(15C)	9381	3697	-138	50
H(15D)	10173	3496	912	50
H(16)	9122	4212	2145	29
H(16')	7001	4189	1015	39
H(11N)	7236	5934	737	33
H(12N)	8176	6338	1346	33
H(13N)	7346	6319	749	33
H(14N)	8390	5939	1552	33
H(1O1)	5810	6757	8565	98
H(2O1)	7165	5724	8794	98

Table 6. Hydrogen bonds with H..A < r(A) + 2.000 Angströms and <DHA > 110 deg. Appropriate HTAB instructions appended to .res file for future use.

D-H	d(D-H)	d(H..A)	<DHA	d(D..A)	A
N2-H1N	0.910	2.543	173.16	3.448	S1
N2-H2N	0.910	2.563	159.68	3.431	S2 [-x+2, -y+1, -z+1]
N3-H4N	0.910	2.755	151.73	3.582	S2 [-x+1, -y+1, -z+1]
C5-H5C_b	0.990	2.853	163.06	3.811	S1 [-x+1, -y+2, -z+1]
C5-H5D_b	0.990	2.659	129.00	3.371	O2
C6_a-H6B_a	0.990	1.469	121.65	2.160	O2
O2-H6B_a	1.469	1.973	128.89	3.113	N4
N4-H6N_a	0.910	2.858	152.61	3.690	S1
N4-H7N_b	0.910	2.382	137.26	3.113	O2
N4-H8N_b	0.910	2.946	140.03	3.690	S1
N11-H9N_a	0.910	2.732	157.98	3.591	S3 [-x+2, -y+1, -z+1]
N11-H10N_a	0.910	2.422	158.82	3.287	S1 [-x+1, -y+1, -z+1]
N11-H11N_b	0.910	2.998	124.44	3.591	S3 [-x+2, -y+1, -z+1]
N11-H12N_b	0.910	2.413	161.23	3.287	S1 [-x+1, -y+1, -z+1]
C11'_b-H11'_b	1.000	2.535	135.68	3.325	S3 [-x+2, -y+1, -z+1]
C12-H12B_a	0.990	2.937	146.71	3.804	S3 [-x+2, -y+1, -z+1]
C15-H15B_a	0.990	2.920	129.09	3.627	S2 [x, y, z-1]
C15-H15C_b	0.990	2.681	160.02	3.627	S2 [x, y, z-1]
N12-H11N_a	0.910	2.358	175.22	3.265	O1 [x, y, z-1]
N12-H12N_a	0.910	2.903	138.82	3.638	S2 [-x+2, -y+1, -z+1]
N12-H13N_b	0.910	2.473	145.74	3.265	O1 [x, y, z-1]
N12-H14N_b	0.910	2.732	173.53	3.638	S2 [-x+2, -y+1, -z+1]
O1-H1O1	0.840	2.873	140.32	3.560	S1
O1-H2O1	0.840	2.409	166.25	3.231	S2

5.3.24 Messprotokoll der Verbindung $[Ni(1,2dach)(tren)]_2[Sn_2S_6]\cdot 4H_2O$

Table 1. Crystal data and structure refinement for $[Ni(C_6H_{18}N_4)(C_6H_{14}N_2)]_2[Sn_2S_6]\cdot 4H_2O$. ($C_6H_{18}N_4$, tren = Tris(2-aminoethyl)amin; $C_6H_{14}N_2$, 1,2-Diaminocyclohexan)

Identification code	jh2340	
Empirical formula	$[Ni(C_6H_{18}N_4)(C_6H_{14}N_2)]_2[Sn_2S_6]\cdot 4H_2O$	
Crystal color, habitus	violet blocks	
Formula weight	1140.09	
Temperature	170(2) K	
Wavelength	0.71073 Å	
Crystal system	monoclinic	
Space group	$P2_1/c$	
Unit cell dimensions	a = 10.7119(3) Å	α= 90°.
	b = 19.0797(4) Å	β= 104.803(2)°.
	c = 11.1005(3) Å	γ = 90°.
Volume	2193.42(10) $Å^3$	
Z	2	
Density (calculated)	1.726 Mg/m^3	
Absorption coefficient	2.301 mm^{-1}	
F(000)	1168	
Crystal size	0.06 x 0.09 x 0.12 mm^3	
Theta range for data collection	2.135 to 26.993°.	
Index ranges	-13<=h<=13, -24<=k<=24, -14<=l<=14	
Reflections collected	31432	
Independent reflections	4786 [R(int) = 0.0495]	
Completeness to theta = 25.242°	99.9 %	
Refinement method	Full-matrix least-squares on F^2	
Data / restraints / parameters	4786 / 12 / 251	
Goodness-of-fit on F^2	1.076	
Final R indices [I>2sigma(I)]	R1 = 0.0393, wR2 = 0.0998	
R indices (all data)	R1 = 0.0445, wR2 = 0.1031	
Extinction coefficient	0.0092(6)	
Largest diff. peak and hole	0.830 and -0.869 $e.Å^{-3}$	

Comments

A numerical absorption correction was performed ($T_{min/max}$: 0.6018/0.7690). All non-hydrogen atoms except the disordered C atoms of lower occupancy were refined anisotropic. The C-H and N-H H atoms were positioned with idealized geometry and refined isotropic with U_{iso}(H) = 1.2 U_{eq}(C,N) using a riding model. The O-H H atoms were located in difference map, their bond lengths were set to ideal values and finally, they were refined isotropic with U_{iso}(H) = 1.5 U_{eq}(O) using a riding model. The 6-membered ring of the 1,2-diaminocyclohexane molecule is disordered in two orientations and was refined using a split model with restraints and sof. 80:20. The site of lower occupancy was refined isotropic.

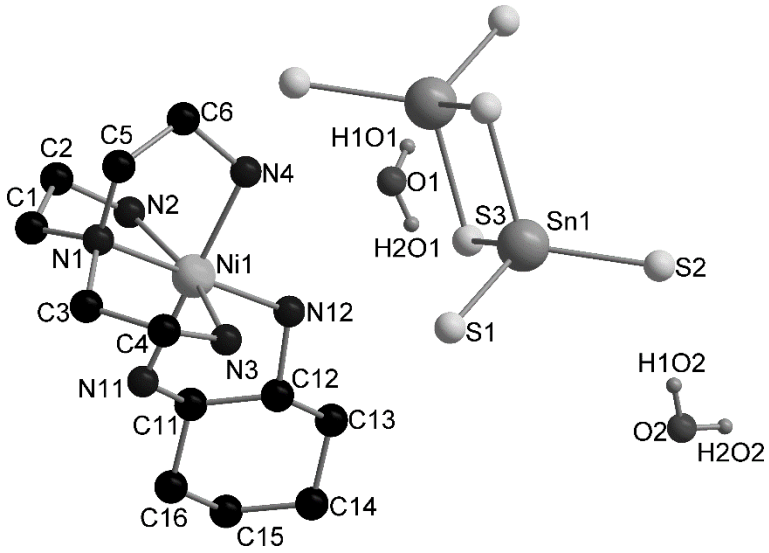

Figure 1: Part of the crystal structure of $[Ni(tren)(1,2\text{-dach})]_2[Sn_2S_6]\cdot 4H_2O$ with labelling of the crystallographic independent atoms.

Table 2. Atomic coordinates ($\cdot 10^4$) and equivalent isotropic displacement parameters ($Å^2 \cdot 10^3$). U(eq) is defined as one third of the trace of the orthogonalized U_{ij} tensor.

	x	y	z	U(eq)
Sn(1)	5713(1)	5609(1)	1067(1)	31(1)
S(1)	5146(1)	5685(1)	2959(1)	41(1)
S(2)	7240(1)	6415(1)	755(1)	38(1)
S(3)	6281(1)	4405(1)	629(1)	34(1)
Ni(1)	2655(1)	3772(1)	3076(1)	30(1)
N(1)	769(3)	3663(2)	3292(3)	34(1)
C(1)	478(3)	2908(2)	3164(4)	39(1)
C(2)	821(4)	2610(2)	2021(4)	40(1)
N(2)	2155(3)	2818(2)	2029(3)	37(1)
C(3)	854(4)	3940(2)	4560(4)	42(1)
C(4)	1524(4)	4648(2)	4742(4)	44(1)
N(3)	2729(3)	4626(2)	4327(3)	39(1)
C(5)	-150(3)	4083(2)	2333(4)	40(1)
C(6)	331(4)	4219(2)	1176(4)	42(1)
N(4)	1720(3)	4394(2)	1536(3)	37(1)
N(11)	3651(3)	3133(2)	4610(3)	34(1)
N(12)	4522(3)	3895(2)	2854(3)	40(1)
C(11)	4935(4)	2967(3)	4415(5)	34(1)
C(12)	5478(4)	3641(2)	4007(4)	36(1)
C(13)	6822(5)	3526(4)	3825(6)	44(1)
C(14)	7712(4)	3217(3)	4997(5)	50(1)
C(15)	7182(5)	2535(3)	5373(6)	46(1)
C(16)	5842(7)	2636(8)	5562(11)	39(3)
C(11')	5081(17)	3274(12)	4735(15)	34(4)
C(12')	5328(13)	3258(9)	3447(13)	27(3)
C(13')	6764(17)	3346(11)	3547(19)	35(7)
C(14')	7534(18)	2784(11)	4399(16)	44(4)
C(15')	7296(19)	2829(14)	5684(16)	45(6)
C(16')	5870(20)	2730(30)	5610(40)	32(13)
O(1)	2204(3)	6040(2)	1565(3)	57(1)
O(2)	10007(3)	5832(2)	2526(3)	58(1)

Table 3. Bond lengths [Å] and angles [°].

Sn(1)-S(1)	2.3344(9)	Sn(1)-S(3)#1	2.4599(9)
Sn(1)-S(2)	2.3347(9)	S(3)-Sn(1)#1	2.4599(9)
Sn(1)-S(3)	2.4561(9)		
S(1)-Sn(1)-S(2)	116.45(4)	S(1)-Sn(1)-S(3)#1	108.33(3)
S(1)-Sn(1)-S(3)	111.77(3)	S(2)-Sn(1)-S(3)#1	113.47(3)
S(2)-Sn(1)-S(3)	111.57(3)	S(3)-Sn(1)-S(3)#1	92.81(3)
Sn(1)-S(3)-Sn(1)#1	87.19(3)		
Ni(1)-N(12)	2.090(3)	Ni(1)-N(3)	2.130(3)
Ni(1)-N(1)	2.105(3)	Ni(1)-N(11)	2.145(3)
Ni(1)-N(4)	2.111(3)	Ni(1)-N(2)	2.153(3)
N(12)-Ni(1)-N(1)	179.20(13)	N(4)-Ni(1)-N(11)	178.19(12)
N(12)-Ni(1)-N(4)	96.43(12)	N(3)-Ni(1)-N(11)	89.35(12)
N(1)-Ni(1)-N(4)	82.96(12)	N(12)-Ni(1)-N(2)	98.33(13)
N(12)-Ni(1)-N(3)	96.52(13)	N(1)-Ni(1)-N(2)	82.21(12)
N(1)-Ni(1)-N(3)	83.00(12)	N(4)-Ni(1)-N(2)	92.16(12)
N(4)-Ni(1)-N(3)	91.65(12)	N(3)-Ni(1)-N(2)	164.15(12)
N(12)-Ni(1)-N(11)	81.95(12)	N(11)-Ni(1)-N(2)	87.28(12)
N(1)-Ni(1)-N(11)	98.67(11)		
N(1)-C(1)	1.474(5)	C(3)-C(4)	1.518(6)
N(1)-C(3)	1.484(5)	C(4)-N(3)	1.478(5)
N(1)-C(5)	1.486(4)	C(5)-C(6)	1.523(6)
C(1)-C(2)	1.520(5)	C(6)-N(4)	1.477(5)
C(2)-N(2)	1.480(5)	N(2)-C(2)-C(1)	109.5(3)
C(1)-N(1)-C(3)	113.6(3)	N(1)-C(3)-C(4)	110.8(3)
C(1)-N(1)-C(5)	111.9(3)	N(3)-C(4)-C(3)	110.8(3)
C(3)-N(1)-C(5)	110.8(3)	N(1)-C(5)-C(6)	113.0(3)
N(1)-C(1)-C(2)	110.9(3)	N(4)-C(6)-C(5)	110.2(3)
N(11)-C(11)	1.480(5)	C(14)-C(15)	1.520(7)
N(11)-C(11')	1.525(18)	C(15)-C(16)	1.515(8)
N(12)-C(12)	1.501(5)	C(11')-C(12')	1.519(15)
N(12)-C(12')	1.538(15)	C(11')-C(16')	1.528(18)
C(11)-C(16)	1.527(7)	C(12')-C(13')	1.523(16)
C(11)-C(12)	1.527(6)	C(13')-C(14')	1.526(17)
C(12)-C(13)	1.520(6)	C(14')-C(15')	1.514(17)
C(13)-C(14)	1.521(7)	C(15')-C(16')	1.521(18)
N(11)-C(11)-C(16)	112.5(5)	C(12')-C(11')-N(11)	108.9(12)
N(11)-C(11)-C(12)	107.5(4)	C(12')-C(11')-C(16')	112.7(19)
C(16)-C(11)-C(12)	112.8(6)	N(11)-C(11')-C(16')	108.5(15)
N(12)-C(12)-C(13)	113.4(4)	C(11')-C(12')-C(13')	110.2(13)
N(12)-C(12)-C(11)	107.3(3)	C(11')-C(12')-N(12)	100.0(11)
C(13)-C(12)-C(11)	111.3(4)	C(13')-C(12')-N(12)	112.9(12)
C(12)-C(13)-C(14)	110.5(4)	C(12')-C(13')-C(14')	110.1(14)
C(15)-C(14)-C(13)	111.7(5)	C(15')-C(14')-C(13')	110.4(15)
C(16)-C(15)-C(14)	111.3(7)	C(14')-C(15')-C(16')	111(2)
C(15)-C(16)-C(11)	111.1(6)	C(15')-C(16')-C(11')	109.2(19)

Symmetry transformations used to generate equivalent atoms: A: -x+1,-y+1,-z

Table 4. Anisotropic displacement parameters ($Å^2 \cdot 10^3$). The anisotropic displacement factor exponent takes the form: $-2\pi^2[h^2 a^{*2} U_{11} + ... + 2 h k a^* b^* U_{12}]$

	U_{11}	U_{22}	U_{33}	U_{23}	U_{13}	U_{12}
Sn(1)	30(1)	30(1)	31(1)	-1(1)	6(1)	-2(1)
S(1)	44(1)	47(1)	32(1)	-4(1)	9(1)	0(1)
S(2)	34(1)	33(1)	48(1)	0(1)	10(1)	-5(1)
S(3)	32(1)	33(1)	35(1)	-1(1)	3(1)	2(1)
Ni(1)	27(1)	31(1)	33(1)	1(1)	7(1)	0(1)
N(1)	29(1)	35(2)	39(2)	2(1)	8(1)	2(1)
C(1)	30(2)	37(2)	49(2)	5(2)	8(2)	-4(1)
C(2)	35(2)	35(2)	46(2)	-1(2)	0(2)	-3(2)
N(2)	36(2)	37(2)	36(2)	-2(1)	9(1)	0(1)
C(3)	37(2)	52(2)	40(2)	1(2)	14(2)	4(2)
C(4)	43(2)	45(2)	43(2)	-6(2)	10(2)	10(2)
N(3)	40(2)	34(2)	42(2)	-2(1)	6(1)	1(1)
C(5)	28(2)	41(2)	47(2)	4(2)	2(1)	4(2)
C(6)	37(2)	40(2)	42(2)	5(2)	-1(2)	1(2)
N(4)	38(2)	37(2)	35(2)	2(1)	7(1)	0(1)
N(11)	28(1)	37(2)	36(1)	2(1)	9(1)	-1(1)
N(12)	32(2)	45(2)	44(2)	9(1)	10(1)	2(1)
C(11)	26(2)	33(2)	43(2)	3(2)	7(2)	1(2)
C(12)	29(2)	39(2)	38(2)	3(2)	8(2)	0(2)
C(13)	33(3)	51(3)	52(3)	-1(3)	16(2)	-3(2)
C(14)	27(2)	65(3)	58(3)	11(3)	8(2)	0(2)
C(15)	32(2)	49(3)	54(3)	5(3)	5(2)	8(2)
C(16)	34(4)	33(5)	47(4)	7(4)	6(2)	2(2)
O(1)	48(2)	65(2)	62(2)	-3(2)	18(1)	-4(2)
O(2)	49(2)	54(2)	66(2)	9(2)	8(2)	8(2)

Table 5. Hydrogen coordinates ($\cdot 10^4$) and isotropic displacement parameters ($Å^2 \cdot 10^3$).

	x	y	z	U(eq)
H(1A)	-452	2833	3094	47
H(1B)	975	2659	3917	47
H(2A)	754	2092	2022	49
H(2B)	211	2789	1257	49
H(2C)	2214	2883	1233	44
H(2D)	2715	2471	2379	44
H(3A)	1339	3606	5190	51
H(3B)	-26	3989	4682	51
H(4A)	940	5008	4260	53
H(4B)	1726	4780	5633	53
H(3C)	3418	4574	4999	47
H(3D)	2827	5035	3941	47
H(5A)	-302	4538	2702	48
H(5B)	-986	3833	2086	48
H(6A)	188	3798	639	50
H(6B)	-162	4612	695	50
H(4C)	1826	4856	1741	45
H(4D)	2072	4313	885	45
H(11A)	3741	3368	5341	40
H(11B)	3201	2732	4640	40
H(11C)	3429	3256	5320	40
H(11D)	3463	2672	4451	40
H(12A)	4609	3645	2182	48
H(12B)	4671	4354	2722	48
H(12C)	4499	3922	2030	48
H(12D)	4880	4296	3232	48
H(11)	4809	2623	3715	41
H(12)	5539	4000	4676	43
H(13A)	7178	3978	3627	53
H(13B)	6772	3203	3116	53
H(14A)	8572	3130	4850	60
H(14B)	7819	3559	5687	60
H(15A)	7149	2179	4717	55
H(15B)	7768	2360	6155	55
H(16A)	5893	2940	6295	47
H(16B)	5491	2176	5730	47
H(11')	5302	3750	5105	41
H(12')	4989	2816	2996	32
H(13C)	7049	3816	3885	42
H(13D)	6922	3308	2709	42
H(14C)	7277	2315	4040	53
H(14D)	8466	2847	4463	53
H(15C)	7579	3293	6054	54
H(15D)	7809	2466	6229	54
H(16C)	5722	2776	6453	38
H(16D)	5599	2249	5301	38
H(1O1)	2272	5936	850	86
H(2O1)	2956	6054	2033	86
H(1O2)	9292	5949	2054	86
H(2O2)	10613	5933	2203	86

Table 6. Hydrogen bonds [Å and °].

D-H...A	d(D-H)	d(H...A)	d(D...A)	<(DHA)
C(1)-H(1B)...S(2)#2	0.99	3.01	3.746(4)	131.9
C(2)-H(2A)...O(2)#2	0.99	2.63	3.574(5)	159.9
N(2)-H(2C)...S(2)#1	0.91	2.77	3.625(3)	157.1
N(2)-H(2D)...S(2)#2	0.91	2.88	3.581(3)	134.7
C(4)-H(4A)...O(2)#3	0.99	2.49	3.428(5)	158.5
N(3)-H(3C)...S(1)#4	0.91	2.44	3.332(3)	165.5
C(5)-H(5A)...O(2)#3	0.99	2.51	3.345(5)	142.4
N(4)-H(4C)...O(1)	0.91	2.31	3.182(4)	159.8
N(4)-H(4D)...S(2)#1	0.91	2.54	3.397(3)	156.5
N(11)-H(11A)...S(1)#4	0.91	2.66	3.500(3)	153.0
N(11)-H(11D)...S(2)#2	0.91	2.51	3.410(3)	171.6
N(11)-H(11A)...S(1)#4	0.91	2.66	3.500(3)	153.0
N(11)-H(11D)...S(2)#2	0.91	2.51	3.410(3)	171.6
N(12)-H(12B)...S(1)	0.91	2.59	3.476(4)	165.1
N(12)-H(12C)...S(3)	0.91	2.90	3.603(3)	134.7
N(12)-H(12B)...S(1)	0.91	2.59	3.476(4)	165.1
C(12)-H(12)...S(1)#4	1.00	2.96	3.821(5)	144.5
C(11')-H(11')...S(1)#4	1.00	2.56	3.299(19)	130.7
O(1)-H(1O1)...S(3)#1	0.84	2.61	3.363(3)	149.6
O(1)-H(2O1)...S(1)	0.84	2.41	3.208(3)	158.2
O(2)-H(1O2)...S(2)	0.84	2.47	3.303(3)	174.0
O(2)-H(2O2)...O(1)#5	0.84	2.02	2.848(5)	171.0

Symmetry transformations used to generate equivalent atoms:
#1 -x+1,-y+1,-z #2 -x+1,y-1/2,-z+1/2 #3 x-1,y,z
#4 -x+1,-y+1,-z+1 #5 x+1,y,z

5.3.25 Messprotokoll der Verbindung $[Ni(1,2dap)(tren)]_2[Sn_2S_6]\cdot 4H_2O$

Table 1. Crystal data and structure refinement for $[Ni(C_6H_{18}N_4)(C_3H_{10}N_2)]_2[Sn_2S_6]\cdot 4H_2O$. ($C_6H_{18}N_4$, tren = Tris(2-aminoethyl)amin; $C_3H_{10}N_2$, 1,2-Diaminopropane)

Identification code	jh2341	
Empirical formula	$[Ni(C_6H_{18}N_4)(C_3H_{10}N_2)]_2[Sn_2S_6]\cdot 4H_2O$.	
Crystal color, habitus	violet blocks	
Formula weight	1059.97	
Temperature	170(2) K	
Wavelength	0.71073 Å	
Crystal system	monoclinic	
Space group	*C*2/*c*	
Unit cell dimensions	a = 14.3925(3) Å	α= 90°.
	b = 15.1550(4) Å	β= 99.108(2)°.
	c = 18.9307(4) Å	γ = 90°.
Volume	4077.07(16) $Å^3$	
Z	4	
Density (calculated)	1.727 Mg/m^3	
Absorption coefficient	2.469 mm^{-1}	
F(000)	2160	
Crystal size	0.07 x 0.11 x 0.13 mm^3	
Theta range for data collection	1.965 to 28.003°.	
Index ranges	-18<=h<=18, -20<=k<=20, -24<=l<=24	
Reflections collected	32085	
Independent reflections	4917 [R(int) = 0.0415]	
Completeness to theta = 25.242°	100.0 %	
Refinement method	Full-matrix least-squares on F^2	
Data / restraints / parameters	4917 / 0 / 201	
Goodness-of-fit on F^2	1.052	
Final R indices [I>2sigma(I)]	R1 = 0.0229, wR2 = 0.0528	
R indices (all data)	R1 = 0.0283, wR2 = 0.0545	
Extinction coefficient	n/a	
Largest diff. peak and hole	0.798 and -0.533 e.$Å^{-3}$	

Comments

A numerical absorption correction was performed ($T_{min/max}$: 0.5569/0.7169). All non-hydrogen atoms were refined anisotropic. The C-H and N-H H atoms were positioned with idealized geometry (methyl H atoms allowed to rotate but not to tip) and refined isotropic with $U_{iso}(H)$ = 1.2 $U_{eq}(C,N)$ (1.5 for methyl H atoms) using a rind model. The O-H H atoms were located in difference map, their bond lengths were set to ideal values and finally, they were refined isotropic with $U_{iso}(H)$ = 1.5 $U_{eq}(O)$ using a rind model.

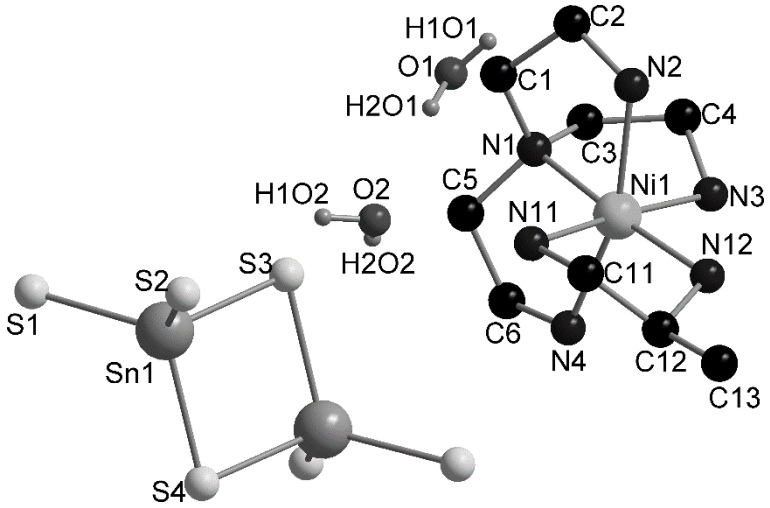

Figure 1: Part of the crystal structure of $[Ni(tren)(1,2\text{-dap})]_2[Sn_2S_6]\cdot 4H_2O$ with labelling of the crystallographic independent atoms.

Table 2. Atomic coordinates ($\cdot 10^4$) and equivalent isotropic displacement parameters ($Å^2 \cdot 10^3$). U(eq) is defined as one third of the trace of the orthogonalized U_{ij} tensor.

	x	y	z	U(eq)
Sn(1)	4440(1)	8580(1)	1641(1)	21(1)
S(1)	2806(1)	8556(1)	1375(1)	27(1)
S(2)	5234(1)	8562(1)	660(1)	29(1)
S(3)	5000	7394(1)	2500	25(1)
S(4)	5000	9744(1)	2500	27(1)
Ni(1)	7632(1)	5479(1)	3994(1)	21(1)
N(1)	6273(1)	4960(1)	3997(1)	26(1)
C(1)	6002(2)	4541(2)	3291(1)	31(1)
C(2)	6781(2)	3930(1)	3125(1)	32(1)
N(2)	7702(1)	4382(1)	3283(1)	26(1)
C(3)	6299(2)	4324(2)	4599(1)	33(1)
C(4)	7279(2)	3963(2)	4860(1)	33(1)
N(3)	7966(1)	4688(1)	4918(1)	29(1)
C(5)	5674(2)	5731(2)	4092(1)	32(1)
C(6)	6155(2)	6313(2)	4694(1)	33(1)
N(4)	7129(1)	6510(1)	4591(1)	28(1)
N(11)	7419(1)	6324(1)	3076(1)	25(1)
C(11)	8355(2)	6587(1)	2925(1)	30(1)
C(12)	9016(2)	6725(1)	3628(1)	31(1)
N(12)	9008(1)	5902(1)	4043(1)	28(1)
C(13)	9997(2)	7001(2)	3522(2)	45(1)
O(1)	6628(2)	5276(1)	1708(1)	49(1)
O(2)	6657(2)	7089(1)	1399(1)	53(1)

Table 3. Bond lengths [Å] and angles [°].

Sn(1)-S(1)	2.3250(5)	Sn(1)-S(4)	2.4474(5)
Sn(1)-S(2)	2.3296(5)	Sn(1)-S(3)	2.4715(5)
S(3)-Sn(1)#1	2.4715(5)	S(4)-Sn(1A)	2.4474(5)
S(1)-Sn(1)-S(2)	115.73(2)	S(1)-Sn(1)-S(3)	110.141(15)
S(1)-Sn(1)-S(4)	111.757(15)	S(2)-Sn(1)-S(3)	111.439(15)
S(2)-Sn(1)-S(4)	112.743(15)	S(4)-Sn(1)-S(3)	92.747(16)
Sn(1A)-S(3)-Sn(1)	86.72(2)	Sn(1A)-S(4)-Sn(1)	87.79(2)
Ni(1)-N(12)	2.0698(18)	Ni(1)-N(4)	2.1232(17)
Ni(1)-N(1)	2.1085(17)	Ni(1)-N(11)	2.1410(17)
Ni(1)-N(3)	2.1127(18)	Ni(1)-N(2)	2.1513(17)
N(12)-Ni(1)-N(1)	175.28(7)	N(3)-Ni(1)-N(11)	174.90(7)
N(12)-Ni(1)-N(3)	92.73(7)	N(4)-Ni(1)-N(11)	88.57(7)
N(1)-Ni(1)-N(3)	82.84(7)	N(12)-Ni(1)-N(2)	97.36(7)
N(12)-Ni(1)-N(4)	98.76(7)	N(1)-Ni(1)-N(2)	81.34(7)
N(1)-Ni(1)-N(4)	83.02(7)	N(3)-Ni(1)-N(2)	93.06(7)
N(3)-Ni(1)-N(4)	91.59(7)	N(4)-Ni(1)-N(2)	162.98(7)
N(12)-Ni(1)-N(11)	82.21(7)	N(11)-Ni(1)-N(2)	88.24(7)
N(1)-Ni(1)-N(11)	102.24(7)		
N(1)-C(1)	1.476(3)	C(3)-C(4)	1.520(3)
N(1)-C(5)	1.481(3)	C(4)-N(3)	1.470(3)
N(1)-C(3)	1.488(3)	C(5)-C(6)	1.519(3)
C(1)-C(2)	1.525(3)	C(6)-N(4)	1.476(3)
C(2)-N(2)	1.480(3)		
C(1)-N(1)-C(5)	111.93(17)	N(1)-C(3)-C(4)	113.07(17)
C(1)-N(1)-C(3)	112.74(17)	N(3)-C(4)-C(3)	109.46(17)
C(5)-N(1)-C(3)	111.24(17)	N(1)-C(5)-C(6)	110.11(17)
N(1)-C(1)-C(2)	110.44(18)	N(4)-C(6)-C(5)	110.41(17)
N(2)-C(2)-C(1)	109.97(17)		
N(11)-C(11)	1.475(3)	C(12)-N(12)	1.477(3)
C(11)-C(12)	1.522(3)	C(12)-C(13)	1.515(3)
N(11)-C(11)-C(12)	109.38(17)	N(12)-C(12)-C(11)	106.99(17)
N(12)-C(12)-C(13)	112.9(2)	C(13)-C(12)-C(11)	112.9(2)

Symmetry transformations used to generate equivalent atoms: A: -x+1,y,-z+1/2

Table 4. Anisotropic displacement parameters ($Å^2 \cdot 10^3$). The anisotropic displacement factor exponent takes the form: $-2\pi^2[h^2 a^{*2} U_{11} + ... + 2 h k a^* b^* U_{12}]$

	U_{11}	U_{22}	U_{33}	U_{23}	U_{13}	U_{12}
Sn(1)	24(1)	21(1)	19(1)	1(1)	2(1)	-1(1)
S(1)	24(1)	30(1)	27(1)	-1(1)	3(1)	0(1)
S(2)	30(1)	37(1)	21(1)	4(1)	5(1)	-4(1)
S(3)	34(1)	19(1)	20(1)	0	3(1)	0
S(4)	36(1)	19(1)	26(1)	0	0(1)	0
Ni(1)	23(1)	20(1)	18(1)	0(1)	3(1)	0(1)
N(1)	26(1)	28(1)	24(1)	-1(1)	6(1)	-1(1)
C(1)	30(1)	34(1)	29(1)	-6(1)	3(1)	-10(1)
C(2)	42(1)	27(1)	30(1)	-7(1)	9(1)	-9(1)
N(2)	32(1)	24(1)	24(1)	-1(1)	7(1)	1(1)
C(3)	37(1)	32(1)	32(1)	5(1)	15(1)	-3(1)
C(4)	46(1)	28(1)	28(1)	8(1)	15(1)	5(1)
N(3)	34(1)	32(1)	23(1)	4(1)	5(1)	7(1)
C(5)	25(1)	38(1)	32(1)	2(1)	7(1)	7(1)
C(6)	37(1)	34(1)	31(1)	-2(1)	11(1)	10(1)
N(4)	38(1)	23(1)	24(1)	-3(1)	5(1)	2(1)
N(11)	30(1)	23(1)	23(1)	1(1)	4(1)	3(1)
C(11)	34(1)	28(1)	30(1)	6(1)	9(1)	-1(1)
C(12)	35(1)	25(1)	34(1)	-3(1)	8(1)	-6(1)
N(12)	26(1)	28(1)	27(1)	-1(1)	1(1)	-1(1)
C(13)	43(1)	44(1)	51(2)	-4(1)	15(1)	-16(1)
O(1)	63(1)	41(1)	45(1)	-1(1)	15(1)	13(1)
O(2)	68(1)	50(1)	43(1)	9(1)	18(1)	25(1)

Table 5. Hydrogen coordinates ($\cdot 10^4$) and isotropic displacement parameters ($Å^2 \cdot 10^3$).

	x	y	z	U(eq)
H(1A)	5881	5003	2917	38
H(1B)	5415	4200	3287	38
H(2A)	6793	3388	3419	39
H(2B)	6657	3756	2615	39
H(2C)	7873	4578	2867	31
H(2D)	8148	3994	3487	31
H(3A)	5871	3826	4442	39
H(3B)	6064	4621	5002	39
H(4A)	7295	3679	5333	40
H(4B)	7441	3513	4521	40
H(3C)	8559	4469	4948	35
H(3D)	7934	5014	5318	35
H(5A)	5060	5527	4205	38
H(5B)	5554	6075	3642	38
H(6A)	5799	6871	4705	40
H(6B)	6162	6010	5158	40
H(4C)	7504	6561	5024	34
H(4D)	7145	7031	4354	34
H(11A)	7095	6033	2694	30
H(11B)	7083	6809	3165	30
H(11A)	8302	7139	2643	36
H(11B)	8609	6122	2642	36
H(12)	8749	7206	3897	37
H(12A)	9269	5999	4507	33
H(12B)	9352	5480	3860	33
H(13A)	10387	7094	3989	68
H(13B)	9961	7551	3246	68
H(13C)	10276	6537	3262	68
H(1O1)	7016	4914	1587	73
H(2O1)	6706	5759	1507	73
H(1O2)	6262	7301	1068	79
H(2O2)	6429	7125	1780	79

Table 6. Hydrogen bonds [Å and °].

D-H...A	d(D-H)	d(H...A)	d(D...A)	<(DHA)
N(2)-H(2D)...S(2)#2	0.91	2.70	3.5347(19)	153.5
C(4)-H(4A)...O(2)#3	0.99	2.62	3.557(3)	158.3
N(3)-H(3C)...S(2)#2	0.91	2.62	3.4250(19)	147.7
N(3)-H(3D)...S(1)#4	0.91	2.98	3.8653(19)	166.1
C(5)-H(5B)...S(3)	0.99	2.96	3.931(2)	166.9
C(6)-H(6A)...S(2)#1	0.99	2.99	3.954(2)	165.3
N(4)-H(4C)...S(1)#4	0.91	2.53	3.3650(19)	152.4
N(4)-H(4D)...S(1)#1	0.91	2.70	3.6088(18)	178.8
N(11)-H(11A)...O(1)	0.91	2.20	3.097(3)	167.1
N(11)-H(11B)...S(1)#1	0.91	2.78	3.5687(17)	145.1
C(11)-H(11B)...S(4)#5	0.99	2.93	3.828(2)	150.6
C(12)-H(12)...S(1)#1	1.00	3.02	3.817(2)	137.9
N(12)-H(12A)...S(2)#4	0.91	2.49	3.3811(19)	168.0
O(1)-H(1O1)...S(1)#5	0.84	2.42	3.2254(19)	162.2
O(1)-H(2O1)...O(2)	0.84	2.03	2.811(3)	155.1
O(2)-H(1O2)...S(2)	0.84	2.47	3.1978(19)	146.2
O(2)-H(2O2)...S(3)	0.84	2.67	3.4388(19)	152.2

Symmetry transformations used to generate equivalent atoms:
#1 -x+1,y,-z+1/2; #2 -x+3/2,y-1/2,-z+1/2; #3 x,-y+1,z+1/2; #4 x+1/2,-y+3/2,z+1/2; #5 x+1/2,y-1/2,z

5.3.26 Messprotokoll der Verbindung $[Ni(2amp)(tren)]_2[Sn_2S_6]\cdot 10H_2O$

Table 1. Crystal data and structure refinement for $[Ni(C_6H_{18}N_4)(C_6H_8N_2)]_2[Sn_2S_6]\cdot 10H_2O$ ($C_6H_{18}N_4$, tris = Tris(2-aminoethyl)amin; $C_6H_8N_2$, 2amp, 2-Aminomethylpyridin)

Identification code	jh2344	
Empirical formula	$[Ni(C_6H_{18}N_4)(C_6H_8N_2)]_2[Sn_2S_6]\cdot 10H_2O$	
Crystal color, habitus	violet blocks	
Formula weight	617.04	
Temperature	170(2) K	
Wavelength	0.71073 Å	
Crystal system	monoclinic	
Space group	$P2_1/n$	
Unit cell dimensions	a = 12.1933(4) Å	α= 90°.
	b = 13.4025(3) Å	β= 103.090(2)°.
	c = 14.8920(4) Å	γ = 90°.
Volume	2370.42(12) $Å^3$	
Z	4	
Density (calculated)	1.729 Mg/m^3	
Absorption coefficient	2.146 mm^{-1}	
F(000)	1260	
Crystal size	0.07 x 0.10 x 0.14 mm^3	
Theta range for data collection	1.955 to 27.004°.	
Index ranges	-15<=h<=15, -13<=k<=17, -19<=l<=19	
Reflections collected	23058	
Independent reflections	5166 [R(int) = 0.0302]	
Completeness to theta = 25.242°	99.7 %	
Refinement method	Full-matrix least-squares on F^2	
Data / restraints / parameters	5166 / 0 / 254	
Goodness-of-fit on F^2	1.059	
Final R indices [I>2sigma(I)]	R1 = 0.0311, wR2 = 0.0779	
R indices (all data)	R1 = 0.0383, wR2 = 0.0806	
Extinction coefficient	0.0027(3)	
Largest diff. peak and hole	0.793 and -0.704 e.$Å^{-3}$	

Comments

A numerical absorption correction was performed ($T_{min/max}$: 0.6906/0.7509). All non-hydrogen atoms were refined anisotropic. The C-H and N-H H atoms were positioned with idealized geometry and refined isotropic with Uiso(H) = 1.2 Ueq(C,N) using a riding model. The O-H H atoms were located in difference map, their bond lengths were set to ideal values and finally, they were refined isotropic with Uiso(H) = 1.5 Ueq(O) using a riding model.

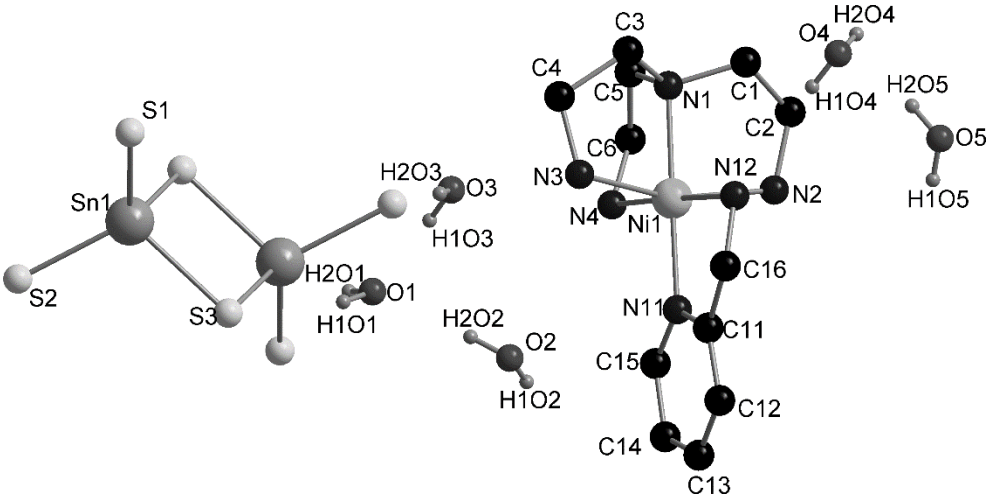

Figure 1: Part of the crystal structure of $[Ni(tren)(2amp)]_2[Sn_2S_6]\cdot 10H_2O$ with labelling of the crystallographic independent atoms.

Table 2. Atomic coordinates ($\cdot 10^4$) and equivalent isotropic displacement parameters ($Å^2\cdot 10^3$). U(eq) is defined as one third of the trace of the orthogonalized U_{ij} tensor.

	x	y	z	U(eq)
Sn(1)	725(1)	4278(1)	9383(1)	22(1)
S(1)	-25(1)	2847(1)	8580(1)	30(1)
S(2)	2602(1)	4666(1)	9387(1)	27(1)
S(3)	452(1)	4215(1)	10963(1)	26(1)
Ni(1)	6034(1)	3331(1)	7935(1)	21(1)
N(1)	6176(2)	4694(2)	7275(2)	25(1)
C(1)	7321(2)	4687(2)	7100(2)	29(1)
C(2)	7540(3)	3718(3)	6632(2)	32(1)
N(2)	7186(2)	2852(2)	7123(2)	28(1)
C(3)	6034(3)	5490(2)	7932(2)	28(1)
C(4)	5030(3)	5237(2)	8345(2)	31(1)
N(3)	5152(2)	4215(2)	8731(2)	28(1)
C(5)	5290(3)	4770(2)	6404(2)	30(1)
C(6)	4841(3)	3755(3)	6042(2)	30(1)
N(4)	4634(2)	3146(2)	6813(2)	27(1)
N(11)	5915(2)	1985(2)	8589(2)	24(1)
C(11)	6646(3)	1854(2)	9403(2)	28(1)
C(12)	6711(3)	962(3)	9883(2)	31(1)
C(13)	6006(3)	188(2)	9518(2)	32(1)
C(14)	5231(3)	327(3)	8693(2)	34(1)
C(15)	5212(3)	1235(2)	8254(2)	29(1)
C(16)	7337(3)	2743(3)	9789(2)	43(1)
N(12)	7458(2)	3464(2)	9070(2)	27(1)
O(1)	693(2)	2764(2)	6609(2)	36(1)
O(2)	2624(2)	1516(2)	7126(2)	43(1)
O(3)	2560(2)	4044(2)	7236(2)	44(1)
O(4)	7307(2)	3595(2)	3983(2)	48(1)
O(5)	8923(3)	2397(2)	5130(2)	55(1)

Table 3. Bond lengths [Å] and angles [°].

Sn(1)-S(1)	2.3348(8)	Sn(1)-S(3)#1	2.4637(7)
Sn(1)-S(2)	2.3453(7)	S(3)-Sn(1)#1	2.4637(7)
Sn(1)-S(3)	2.4511(7)		
S(1)-Sn(1)-S(2)	116.86(3)	S(1)-Sn(1)-S(3)#1	115.07(3)
S(1)-Sn(1)-S(3)	109.96(3)	S(2)-Sn(1)-S(3)#1	109.93(3)
S(2)-Sn(1)-S(3)	110.49(3)	S(3)-Sn(1)-S(3)#1	91.71(2)
Sn(1)-S(3)-Sn(1)#1	88.29(2)		
Ni(1)-N(11)	2.070(2)	Ni(1)-N(3)	2.131(2)
Ni(1)-N(1)	2.101(3)	Ni(1)-N(12)	2.139(2)
Ni(1)-N(4)	2.115(2)	Ni(1)-N(2)	2.149(2)
N(11)-Ni(1)-N(1)	179.27(9)	N(4)-Ni(1)-N(12)	178.05(10)
N(11)-Ni(1)-N(4)	98.04(10)	N(3)-Ni(1)-N(12)	86.34(10)
N(1)-Ni(1)-N(4)	82.51(10)	N(11)-Ni(1)-N(2)	97.40(10)
N(11)-Ni(1)-N(3)	97.18(9)	N(1)-Ni(1)-N(2)	82.11(10)
N(1)-Ni(1)-N(3)	83.23(10)	N(4)-Ni(1)-N(2)	91.94(10)
N(4)-Ni(1)-N(3)	94.95(10)	N(3)-Ni(1)-N(2)	162.83(10)
N(11)-Ni(1)-N(12)	80.33(10)	N(12)-Ni(1)-N(2)	87.22(10)
N(1)-Ni(1)-N(12)	99.11(10)		
N(1)-C(1)	1.477(3)	C(3)-C(4)	1.527(4)
N(1)-C(3)	1.484(4)	C(4)-N(3)	1.480(4)
N(1)-C(5)	1.492(4)	C(5)-C(6)	1.519(5)
C(1)-C(2)	1.525(5)	C(6)-N(4)	1.475(4)
C(2)-N(2)	1.488(4)	N(2)-C(2)-C(1)	109.9(2)
C(1)-N(1)-C(3)	112.2(2)	N(1)-C(3)-C(4)	109.3(2)
C(1)-N(1)-C(5)	112.0(2)	N(3)-C(4)-C(3)	110.0(2)
C(3)-N(1)-C(5)	110.8(2)	N(1)-C(5)-C(6)	112.3(2)
N(1)-C(1)-C(2)	110.9(2)	N(4)-C(6)-C(5)	109.3(2)
N(11)-C(15)	1.342(4)	C(12)-C(13)	1.378(5)
N(11)-C(11)	1.344(4)	C(13)-C(14)	1.383(5)
C(11)-C(12)	1.386(4)	C(14)-C(15)	1.378(5)
C(11)-C(16)	1.497(5)	C(16)-N(12)	1.475(4)
C(15)-N(11)-C(11)	118.3(3)	C(12)-C(13)-C(14)	119.2(3)
N(11)-C(11)-C(12)	121.8(3)	C(15)-C(14)-C(13)	118.4(3)
N(11)-C(11)-C(16)	116.3(3)	N(11)-C(15)-C(14)	123.0(3)
C(12)-C(11)-C(16)	121.9(3)	N(12)-C(16)-C(11)	112.5(3)
C(13)-C(12)-C(11)	119.3(3)		

Symmetry transformations used to generate equivalent atoms: A: -x,-y+1,-z+2

Table 4. Anisotropic displacement parameters ($Å^2 \cdot 10^3$). The anisotropic displacement factor exponent takes the form: $-2\pi^2[h^2 a^{*2} U_{11} + ... + 2 h k a^* b^* U_{12}]$

	U_{11}	U_{22}	U_{33}	U_{23}	U_{13}	U_{12}
Sn(1)	20(1)	23(1)	22(1)	-1(1)	4(1)	-1(1)
S(1)	24(1)	30(1)	35(1)	-9(1)	5(1)	-2(1)
S(2)	21(1)	30(1)	30(1)	-4(1)	7(1)	-2(1)
S(3)	28(1)	27(1)	24(1)	3(1)	6(1)	4(1)
Ni(1)	19(1)	22(1)	22(1)	0(1)	2(1)	0(1)
N(1)	21(1)	25(1)	27(1)	3(1)	3(1)	0(1)
C(1)	23(1)	34(2)	32(2)	1(1)	9(1)	-6(1)
C(2)	26(1)	40(2)	32(2)	-1(1)	12(1)	2(1)
N(2)	24(1)	30(1)	29(1)	-4(1)	4(1)	3(1)
C(3)	30(2)	19(1)	34(2)	-1(1)	6(1)	-1(1)
C(4)	30(2)	28(2)	35(2)	-4(1)	9(1)	4(1)
N(3)	24(1)	28(1)	31(1)	1(1)	9(1)	2(1)
C(5)	30(2)	31(2)	28(2)	6(1)	1(1)	0(1)
C(6)	27(2)	38(2)	23(1)	2(1)	0(1)	1(1)
N(4)	22(1)	29(1)	28(1)	0(1)	1(1)	-3(1)
N(11)	26(1)	22(1)	24(1)	0(1)	4(1)	2(1)
C(11)	30(1)	29(2)	25(1)	0(1)	5(1)	4(1)
C(12)	32(2)	36(2)	26(2)	5(1)	8(1)	5(1)
C(13)	33(2)	30(2)	38(2)	9(1)	17(1)	3(1)
C(14)	32(2)	30(2)	42(2)	1(1)	12(1)	-6(1)
C(15)	26(1)	31(2)	29(2)	2(1)	6(1)	-4(1)
C(16)	57(2)	33(2)	28(2)	6(1)	-15(2)	-4(2)
N(12)	22(1)	28(1)	28(1)	-4(1)	1(1)	0(1)
O(1)	31(1)	42(1)	36(1)	-4(1)	6(1)	0(1)
O(2)	36(1)	42(1)	47(1)	-7(1)	2(1)	3(1)
O(3)	35(1)	57(2)	39(1)	-12(1)	10(1)	-9(1)
O(4)	48(2)	50(2)	42(1)	4(1)	1(1)	-14(1)
O(5)	59(2)	40(2)	55(2)	-3(1)	-14(1)	-4(1)

Table 5. Hydrogen coordinates ($\cdot 10^4$) and isotropic displacement parameters ($Å^2 \cdot 10^3$).

	x	y	z	U(eq)
H(1A)	7883	4761	7691	35
H(1B)	7407	5260	6702	35
H(2A)	7114	3720	5982	38
H(2B)	8351	3663	6639	38
H(2A)	7802	2567	7496	33
H(2B)	6849	2386	6706	33
H(3A)	5905	6139	7608	33
H(3B)	6724	5545	8429	33
H(4A)	4985	5721	8838	37
H(4B)	4325	5285	7862	37
H(3A)	4461	3947	8710	33
H(3B)	5541	4232	9329	33
H(5A)	5608	5110	5930	36
H(5B)	4661	5182	6516	36
H(6A)	4131	3837	5570	37
H(6B)	5394	3416	5752	37
H(4A)	4555	2493	6645	33
H(4B)	3993	3351	6973	33
H(12)	7235	885	10457	38
H(13)	6052	-435	9830	39
H(14)	4724	-190	8434	41
H(15)	4678	1333	7689	35
H(16)	7661	2833	10426	52
H(12A)	8102	3337	8878	32
H(12B)	7499	4095	9300	32
H(1O1)	435	2862	7078	54
H(2O1)	148	2727	6150	54
H(1O2)	2604	1029	6767	64
H(2O2)	2067	1893	6945	64
H(1O3)	2024	3650	7038	65
H(2O3)	2625	4191	7794	65
H(1O4)	6747	3213	3897	72
H(2O4)	7418	3644	3448	72
H(1O5)	8604	1838	5050	83
H(2O5)	8532	2860	4841	83

Table 6. Hydrogen bonds [Å and °].

D-H...A	d(D-H)	d(H...A)	d(D...A)	<(DHA)
C(1)-H(1A)...S(3)#2	0.99	2.86	3.782(3)	155.4
N(2)-H(2A)...S(1)#3	0.91	2.80	3.595(3)	146.9
N(2)-H(2B)...S(3)#4	0.91	2.81	3.671(3)	159.0
C(3)-H(3A)...S(1)#5	0.99	2.94	3.912(3)	166.5
N(3)-H(3A)...S(2)	0.91	2.85	3.516(2)	131.3
N(3)-H(3B)...S(2)#2	0.91	3.00	3.759(3)	141.9
N(4)-H(4A)...S(3)#4	0.91	2.82	3.631(3)	148.6
N(4)-H(4B)...O(3)	0.91	2.09	2.994(4)	170.5
C(12)-H(12)...O(3)#6	0.95	2.59	3.421(4)	146.3
C(15)-H(15)...S(3)#4	0.95	3.02	3.541(3)	115.8
C(15)-H(15)...O(2)	0.95	2.47	3.244(4)	139.0
N(12)-H(12A)...S(1)#3	0.91	2.51	3.413(3)	171.2
N(12)-H(12B)...S(2)#2	0.91	2.59	3.413(3)	150.8
O(1)-H(1O1)...S(1)	0.84	2.42	3.249(2)	167.2
O(1)-H(2O1)...O(5)#7	0.84	1.92	2.756(4)	170.1
O(2)-H(1O2)...S(2)#8	0.84	2.48	3.319(3)	174.8
O(2)-H(2O2)...O(1)	0.84	2.01	2.849(4)	175.1
O(3)-H(1O3)...O(1)	0.84	2.00	2.834(4)	176.4
O(3)-H(2O3)...S(2)	0.84	2.46	3.299(3)	173.9
O(4)-H(1O4)...S(1)#4	0.84	2.54	3.378(3)	176.1
O(4)-H(2O4)...O(2)#4	0.84	2.05	2.881(4)	169.3
O(5)-H(1O5)...S(2)#4	0.84	2.45	3.264(3)	164.8
O(5)-H(2O5)...O(4)	0.84	1.99	2.803(4)	161.9

Symmetry transformations used to generate equivalent atoms:
#1 -x,-y+1,-z+2 #2 -x+1,-y+1,-z+2 #3 x+1,y,z
#4 x+1/2,-y+1/2,z-1/2 #5 -x+1/2,y+1/2,-z+3/2
#6 x+1/2,-y+1/2,z+1/2 #7 x-1,y,z #8 -x+1/2,y-1/2,-z+3/2

5.3.27 Messprotokoll der Verbindung $[Ni(2amp)_3]_2[Sn_2S_6]\cdot 9½\ H_2O$

Table 1. Crystal data and structure refinement for $[Ni(C_6H_8N_2)_3]_2[Sn_2S_6]\cdot 9½H_2O$. ($C_6H_8N_2$, 2amp = 2-Aminomethylpyridin)

Identification code	jh2260	
Empirical formula	$[Ni(C_6H_8N_2)_3]_2[Sn_2S_6]\cdot 9½H_2O$	
Crystal color, habitus	violet blocks	
Formula weight	1367.17	
Temperature	170(2) K	
Wavelength	0.71073 Å	
Crystal system	monoclinic	
Space group	$P2_1/n$	
Unit cell dimensions	a = 18.7021(3) Å	α= 90°.
	b = 14.6141(2) Å	β= 97.696(2)°.
	c = 20.2591(4) Å	γ = 90°.
Volume	5487.23(16) $Å^3$	
Z	4	
Density (calculated)	1.655 Mg/m^3	
Absorption coefficient	1.863 mm^{-1}	
F(000)	2780	
Crystal size	0.08 x 0.10 x 0.12 mm^3	
Theta range for data collection	1.392 to 26.005°.	
Index ranges	-23<=h<=23, -18<=k<=18, -24<=l<=24	
Reflections collected	71109	
Independent reflections	10763 [R(int) = 0.0356]	
Completeness to theta = 25.242°	99.7 %	
Refinement method	Full-matrix least-squares on F^2	
Data / restraints / parameters	10763 / 0 / 622	
Goodness-of-fit on F^2	1.083	
Final R indices [I>2sigma(I)]	R1 = 0.0294, wR2 = 0.0644	
R indices (all data)	R1 = 0.0368, wR2 = 0.0669	
Extinction coefficient	n/a	
Largest diff. peak and hole	0.435 and -0.429 e.$Å^{-3}$	

Comments

A numerical absorption correction was performed ($T_{min/max}$ = 0.5242/0.8331). All non-hydrogen atoms were refined isotropic. The C-H and N-H H atoms positioned with idealized geometry and refined isotropic with $U_{iso}(H) = 1.2\ U_{eq}(C,N)$ using a riding model. All O-H H atoms except those attached to O10/O10') were located in difference map, their bond lengths were set to ideal values and finally they were refined isotropic with $U_{iso}(H) = 1.5\ U_{eq}(O)$ using a riding model. O10 is disordered and was refined using a split model with sof 0.28:0.22.

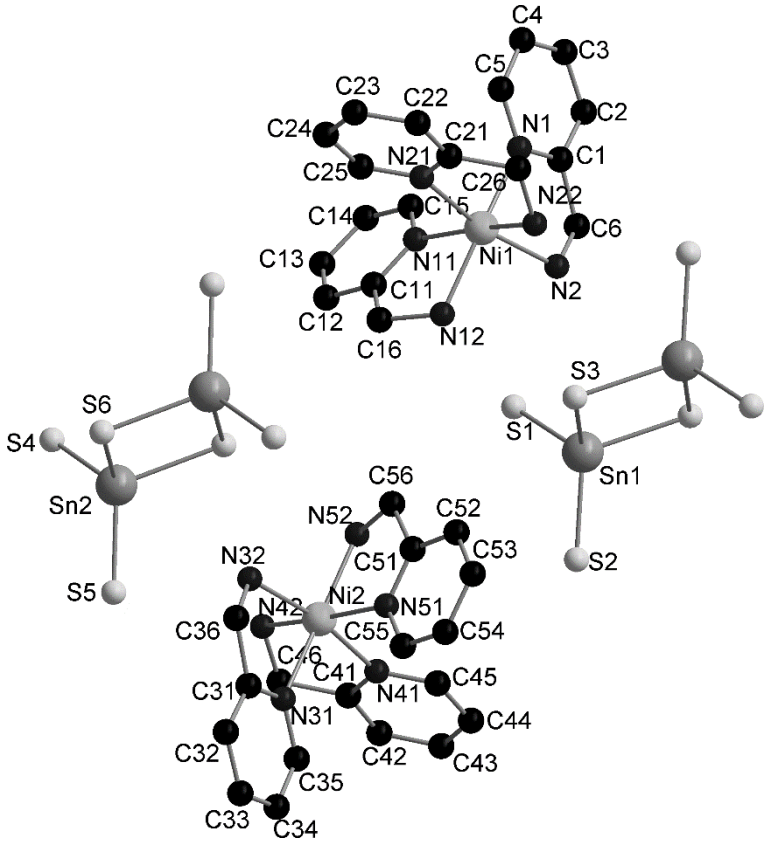

Figure 1: Part of the crystal structure of $[Ni(2amp)_3]_2[Sn_2S_6]\cdot 9.5H_2O$ with labelling of the crystallographic independent atoms.

Table 2. Atomic coordinates ($\cdot 10^4$) and equivalent isotropic displacement parameters ($Å^2\cdot 10^3$). U(eq) is defined as one third of the trace of the orthogonalized U_{ij} tensor.

	x	y	z	U(eq)
Sn(1)	5538(1)	4493(1)	9488(1)	23(1)
S(1)	6207(1)	5395(1)	8839(1)	37(1)
S(2)	5654(1)	2922(1)	9362(1)	30(1)
S(3)	4280(1)	5030(1)	9335(1)	28(1)
Sn(2)	5581(1)	4483(1)	4526(1)	22(1)
S(4)	6296(1)	5395(1)	3930(1)	30(1)
S(5)	5642(1)	2901(1)	4432(1)	28(1)
S(6)	4316(1)	4998(1)	4302(1)	25(1)
Ni(1)	4714(1)	7753(1)	8490(1)	24(1)
N(1)	5057(1)	8990(1)	8970(1)	25(1)
C(1)	5629(1)	8912(2)	9442(1)	27(1)
C(2)	5970(1)	9675(2)	9750(1)	31(1)
C(3)	5718(2)	10532(2)	9562(1)	34(1)
C(4)	5130(2)	10617(2)	9074(1)	33(1)
C(5)	4814(1)	9833(2)	8792(1)	30(1)
C(6)	5910(1)	7964(2)	9599(2)	36(1)
N(2)	5397(1)	7262(1)	9319(1)	28(1)
N(11)	5528(1)	7839(1)	7848(1)	28(1)
C(11)	5476(1)	7192(2)	7373(1)	27(1)

C(12)	5949(2)	7158(2)	6901(1)	35(1)
C(13)	6500(2)	7793(2)	6924(2)	40(1)
C(14)	6560(2)	8449(2)	7420(2)	40(1)
C(15)	6066(2)	8457(2)	7864(2)	35(1)
C(16)	4867(1)	6522(2)	7363(1)	31(1)
N(12)	4602(1)	6481(2)	8009(1)	29(1)
N(21)	3884(1)	8381(1)	7819(1)	27(1)
C(21)	3269(1)	8529(2)	8075(1)	28(1)
C(22)	2669(1)	8914(2)	7710(1)	34(1)
C(23)	2699(2)	9143(2)	7053(2)	38(1)
C(24)	3326(2)	8985(2)	6783(2)	39(1)
C(25)	3905(1)	8607(2)	7182(1)	33(1)
C(26)	3269(1)	8272(2)	8796(1)	34(1)
N(22)	3802(1)	7551(2)	8982(1)	29(1)
Ni(2)	5523(1)	2265(1)	6588(1)	28(1)
N(31)	5149(1)	1025(2)	6122(1)	32(1)
C(31)	4535(2)	1113(2)	5712(1)	33(1)
C(32)	4171(2)	359(2)	5412(2)	39(1)
C(33)	4448(2)	-506(2)	5549(2)	45(1)
C(34)	5079(2)	-600(2)	5977(2)	43(1)
C(35)	5415(2)	175(2)	6249(2)	38(1)
C(36)	4229(2)	2065(2)	5600(2)	37(1)
N(32)	4774(1)	2763(2)	5813(1)	30(1)
N(41)	6343(1)	1616(2)	7230(1)	31(1)
C(41)	6942(1)	1424(2)	6961(1)	32(1)
C(42)	7515(2)	963(2)	7315(1)	38(1)
C(43)	7473(2)	696(2)	7959(2)	38(1)
C(44)	6865(2)	905(2)	8241(1)	39(1)
C(45)	6312(2)	1367(2)	7863(1)	37(1)
C(46)	6939(2)	1701(2)	6242(2)	44(1)
N(42)	6409(1)	2419(2)	6051(1)	36(1)
N(51)	4741(1)	2217(2)	7242(1)	31(1)
C(51)	4643(1)	3011(2)	7548(1)	30(1)
C(52)	4131(2)	3099(2)	7982(2)	42(1)
C(53)	3706(2)	2363(2)	8092(2)	45(1)
C(54)	3801(2)	1546(2)	7772(2)	40(1)
C(55)	4323(1)	1500(2)	7357(2)	35(1)
C(56)	5095(2)	3812(2)	7397(2)	36(1)
N(52)	5705(1)	3533(2)	7054(1)	36(1)
O(1)	2863(1)	3952(2)	4698(1)	58(1)
O(2)	7463(1)	3965(2)	5730(1)	50(1)
O(3)	2640(1)	7231(2)	5411(1)	49(1)
O(4)	2788(2)	4091(2)	9681(1)	66(1)
O(5)	7406(1)	2867(2)	9831(1)	59(1)
O(6)	7599(1)	3966(2)	10976(2)	67(1)
O(7)	6819(2)	3510(2)	8213(1)	70(1)
O(8)	3022(1)	6311(2)	7812(2)	65(1)
O(9)	2471(2)	5956(2)	6441(2)	80(1)
O(10)	7734(6)	4664(9)	9354(6)	46(3)
O(10')	7861(9)	4410(12)	9143(9)	53(4)

Table 3. Bond lengths [Å] and angles [°].

Sn(1)-S(2)	2.3246(6)	Sn(2)-S(5)	2.3242(6)
Sn(1)-S(1)	2.3383(7)	Sn(2)-S(4)	2.3352(7)
Sn(1)-S(3)	2.4598(6)	Sn(2)-S(6)	2.4662(6)
Sn(1)-S(3)#1	2.4629(6)	Sn(2)-S(6)#2	2.4758(6)
S(3)-Sn(1)#1	2.4628(6)	S(6)-Sn(2)#2	2.4758(6)
S(2)-Sn(1)-S(1)	115.50(3)	S(5)-Sn(2)-S(4)	119.23(2)
S(2)-Sn(1)-S(3)	113.72(2)	S(5)-Sn(2)-S(6)	110.17(2)
S(1)-Sn(1)-S(3)	108.90(2)	S(4)-Sn(2)-S(6)	109.42(2)
S(2)-Sn(1)-S(3)#1	112.54(2)	S(5)-Sn(2)-S(6)#2	112.62(2)
S(1)-Sn(1)-S(3)#1	111.73(3)	S(4)-Sn(2)-S(6)#2	110.13(2)
S(3)-Sn(1)-S(3)#1	92.13(2)	S(6)-Sn(2)-S(6)#2	91.852(19)
Sn(1)-S(3)-Sn(1)#1	87.87(2)	Sn(2)-S(6)-Sn(2)#2	88.149(19)
Ni(1)-N(2)	2.095(2)	Ni(2)-N(52)	2.088(2)
Ni(1)-N(12)	2.097(2)	Ni(2)-N(32)	2.090(2)
Ni(1)-N(22)	2.109(2)	Ni(2)-N(41)	2.100(2)
Ni(1)-N(1)	2.111(2)	Ni(2)-N(51)	2.102(2)
Ni(1)-N(21)	2.129(2)	Ni(2)-N(42)	2.112(2)
Ni(1)-N(11)	2.134(2)	Ni(2)-N(31)	2.118(2)
N(2)-Ni(1)-N(12)	94.65(8)	N(52)-Ni(2)-N(32)	94.77(9)
N(2)-Ni(1)-N(22)	91.01(8)	N(52)-Ni(2)-N(41)	93.38(9)
N(12)-Ni(1)-N(22)	93.32(9)	N(32)-Ni(2)-N(41)	169.47(9)
N(2)-Ni(1)-N(1)	79.01(8)	N(52)-Ni(2)-N(51)	80.17(9)
N(12)-Ni(1)-N(1)	168.17(8)	N(32)-Ni(2)-N(51)	91.87(9)
N(22)-Ni(1)-N(1)	96.74(8)	N(41)-Ni(2)-N(51)	96.10(8)
N(2)-Ni(1)-N(21)	166.67(9)	N(52)-Ni(2)-N(42)	92.70(10)
N(12)-Ni(1)-N(21)	93.81(8)	N(32)-Ni(2)-N(42)	93.98(9)
N(22)-Ni(1)-N(21)	78.23(8)	N(41)-Ni(2)-N(42)	78.96(9)
N(1)-Ni(1)-N(21)	94.32(8)	N(51)-Ni(2)-N(42)	171.14(9)
N(2)-Ni(1)-N(11)	95.82(8)	N(52)-Ni(2)-N(31)	170.17(9)
N(12)-Ni(1)-N(11)	78.73(8)	N(32)-Ni(2)-N(31)	79.38(9)
N(22)-Ni(1)-N(11)	169.88(8)	N(41)-Ni(2)-N(31)	93.42(9)
N(1)-Ni(1)-N(11)	91.89(8)	N(51)-Ni(2)-N(31)	92.04(9)
N(21)-Ni(1)-N(11)	95.92(8)	N(42)-Ni(2)-N(31)	95.57(9)
N(1)-C(1)	1.341(3)	N(11)-C(11)	1.344(3)
N(1)-C(5)	1.345(3)	N(11)-C(15)	1.350(3)
C(1)-C(2)	1.390(4)	C(11)-C(12)	1.387(4)
C(1)-C(6)	1.501(4)	C(11)-C(16)	1.501(3)
C(2)-C(3)	1.374(4)	C(12)-C(13)	1.382(4)
C(3)-C(4)	1.382(4)	C(13)-C(14)	1.383(4)
C(4)-C(5)	1.378(4)	C(14)-C(15)	1.373(4)
C(6)-N(2)	1.466(3)	C(16)-N(12)	1.462(3)
C(1)-N(1)-C(5)	118.6(2)	C(11)-N(11)-C(15)	118.0(2)
N(1)-C(1)-C(2)	121.7(2)	N(11)-C(11)-C(12)	121.9(2)
N(1)-C(1)-C(6)	117.0(2)	N(11)-C(11)-C(16)	116.7(2)
C(2)-C(1)-C(6)	121.2(2)	C(12)-C(11)-C(16)	121.4(2)
C(3)-C(2)-C(1)	119.1(2)	C(13)-C(12)-C(11)	119.6(3)
C(2)-C(3)-C(4)	119.4(2)	C(12)-C(13)-C(14)	118.5(3)
C(5)-C(4)-C(3)	118.6(2)	C(15)-C(14)-C(13)	119.1(3)

N(1)-C(5)-C(4)	122.6(2)	N(11)-C(15)-C(14)	122.9(3)
N(2)-C(6)-C(1)	111.8(2)	N(12)-C(16)-C(11)	111.3(2)
N(21)-C(25)	1.338(3)	N(31)-C(31)	1.330(4)
N(21)-C(21)	1.342(3)	N(31)-C(35)	1.350(4)
C(21)-C(22)	1.378(4)	C(31)-C(32)	1.392(4)
C(21)-C(26)	1.508(4)	C(31)-C(36)	1.510(4)
C(22)-C(23)	1.381(4)	C(32)-C(33)	1.379(4)
C(23)-C(24)	1.379(4)	C(33)-C(34)	1.375(5)
C(24)-C(25)	1.376(4)	C(34)-C(35)	1.375(4)
C(26)-N(22)	1.465(3)	C(36)-N(32)	1.466(3)
C(25)-N(21)-C(21)	118.0(2)	C(31)-N(31)-C(35)	118.3(2)
N(21)-C(21)-C(22)	122.5(2)	N(31)-C(31)-C(32)	121.7(3)
N(21)-C(21)-C(26)	116.4(2)	N(31)-C(31)-C(36)	117.5(2)
C(22)-C(21)-C(26)	121.1(2)	C(32)-C(31)-C(36)	120.7(3)
C(21)-C(22)-C(23)	118.8(3)	C(33)-C(32)-C(31)	119.3(3)
C(24)-C(23)-C(22)	119.1(3)	C(34)-C(33)-C(32)	119.1(3)
C(25)-C(24)-C(23)	118.6(3)	C(35)-C(34)-C(33)	118.6(3)
N(21)-C(25)-C(24)	122.9(3)	N(31)-C(35)-C(34)	122.9(3)
N(22)-C(26)-C(21)	109.9(2)	N(32)-C(36)-C(31)	111.2(2)
N(41)-C(41)	1.340(3)	N(51)-C(51)	1.340(3)
N(41)-C(45)	1.343(4)	N(51)-C(55)	1.346(3)
C(41)-C(42)	1.382(4)	C(51)-C(52)	1.390(4)
C(41)-C(46)	1.509(4)	C(51)-C(56)	1.499(4)
C(42)-C(43)	1.375(4)	C(52)-C(53)	1.373(5)
C(43)-C(44)	1.374(4)	C(53)-C(54)	1.382(5)
C(44)-C(45)	1.377(4)	C(54)-C(55)	1.373(4)
C(46)-N(42)	1.460(4)	C(56)-N(52)	1.470(4)
C(41)-N(41)-C(45)	118.5(2)	C(51)-N(51)-C(55)	118.4(2)
N(41)-C(41)-C(42)	121.6(3)	N(51)-C(51)-C(52)	121.4(3)
N(41)-C(41)-C(46)	116.1(2)	N(51)-C(51)-C(56)	117.8(2)
C(42)-C(41)-C(46)	122.3(2)	C(52)-C(51)-C(56)	120.8(3)
C(43)-C(42)-C(41)	119.5(3)	C(53)-C(52)-C(51)	119.6(3)
C(44)-C(43)-C(42)	119.1(3)	C(52)-C(53)-C(54)	119.2(3)
C(43)-C(44)-C(45)	118.7(3)	C(55)-C(54)-C(53)	118.4(3)
N(41)-C(45)-C(44)	122.6(3)	N(51)-C(55)-C(54)	123.1(3)
N(42)-C(46)-C(41)	111.4(2)	N(52)-C(56)-C(51)	112.0(2)

Symmetry transformations used to generate equivalent atoms: #1 -x+1,-y+1,-z+2 #2 -x+1,-y+1,-z+1

Table 4. Anisotropic displacement parameters ($Å^2 \cdot 10^3$). The anisotropic displacement factor exponent takes the form: $-2\pi^2[h^2 a^{*2} U_{11} + ... + 2 h k a^* b^* U_{12}]$

	U_{11}	U_{22}	U_{33}	U_{23}	U_{13}	U_{12}
Sn(1)	26(1)	19(1)	26(1)	1(1)	6(1)	1(1)
S(1)	42(1)	25(1)	48(1)	6(1)	24(1)	2(1)
S(2)	41(1)	19(1)	30(1)	-1(1)	3(1)	2(1)
S(3)	26(1)	30(1)	27(1)	-2(1)	2(1)	2(1)
Sn(2)	24(1)	19(1)	25(1)	0(1)	6(1)	1(1)
S(4)	31(1)	27(1)	35(1)	4(1)	13(1)	1(1)
S(5)	36(1)	19(1)	30(1)	-2(1)	5(1)	3(1)
S(6)	24(1)	25(1)	25(1)	-2(1)	3(1)	1(1)
Ni(1)	26(1)	20(1)	25(1)	0(1)	4(1)	-1(1)
N(1)	28(1)	22(1)	25(1)	-1(1)	4(1)	0(1)
C(1)	30(1)	25(1)	26(1)	-2(1)	6(1)	-2(1)
C(2)	32(1)	31(1)	30(1)	-4(1)	6(1)	-5(1)
C(3)	40(1)	29(1)	34(1)	-8(1)	11(1)	-7(1)
C(4)	44(2)	22(1)	35(1)	1(1)	12(1)	0(1)
C(5)	36(1)	23(1)	30(1)	0(1)	6(1)	2(1)
C(6)	32(1)	27(1)	44(2)	0(1)	-7(1)	2(1)
N(2)	30(1)	22(1)	31(1)	0(1)	4(1)	-1(1)
N(11)	29(1)	24(1)	31(1)	-1(1)	6(1)	1(1)
C(11)	31(1)	24(1)	27(1)	2(1)	4(1)	1(1)
C(12)	38(1)	33(1)	35(1)	-5(1)	10(1)	2(1)
C(13)	36(1)	45(2)	42(2)	-4(1)	16(1)	-2(1)
C(14)	35(1)	36(2)	51(2)	-4(1)	15(1)	-10(1)
C(15)	37(1)	29(1)	41(2)	-6(1)	10(1)	-6(1)
C(16)	38(1)	27(1)	29(1)	-3(1)	8(1)	-5(1)
N(12)	32(1)	25(1)	31(1)	0(1)	5(1)	-4(1)
N(21)	29(1)	26(1)	28(1)	1(1)	5(1)	-1(1)
C(21)	30(1)	27(1)	29(1)	-2(1)	5(1)	-2(1)
C(22)	32(1)	34(1)	37(2)	0(1)	6(1)	4(1)
C(23)	34(1)	37(2)	40(2)	7(1)	0(1)	5(1)
C(24)	44(2)	43(2)	31(1)	11(1)	6(1)	3(1)
C(25)	33(1)	34(1)	34(1)	6(1)	9(1)	2(1)
C(26)	32(1)	42(2)	30(1)	1(1)	7(1)	5(1)
N(22)	31(1)	30(1)	27(1)	1(1)	5(1)	-3(1)
Ni(2)	32(1)	24(1)	30(1)	4(1)	10(1)	1(1)
N(31)	40(1)	23(1)	35(1)	0(1)	15(1)	1(1)
C(31)	38(1)	27(1)	36(1)	-1(1)	15(1)	-2(1)
C(32)	44(2)	33(2)	43(2)	-5(1)	17(1)	-9(1)
C(33)	59(2)	28(2)	51(2)	-8(1)	26(2)	-12(1)
C(34)	59(2)	24(1)	54(2)	1(1)	30(2)	1(1)
C(35)	48(2)	27(1)	41(2)	4(1)	17(1)	6(1)
C(36)	35(1)	28(1)	47(2)	0(1)	4(1)	-1(1)
N(32)	34(1)	23(1)	34(1)	3(1)	10(1)	0(1)
N(41)	33(1)	32(1)	30(1)	4(1)	10(1)	3(1)
C(41)	34(1)	32(1)	32(1)	-1(1)	10(1)	0(1)
C(42)	32(1)	44(2)	37(2)	-2(1)	9(1)	6(1)
C(43)	35(1)	40(2)	37(2)	1(1)	1(1)	6(1)

C(44)	41(2)	46(2)	30(1)	8(1)	6(1)	4(1)
C(45)	38(1)	41(2)	34(2)	7(1)	12(1)	5(1)
C(46)	41(2)	54(2)	39(2)	9(1)	16(1)	10(1)
N(42)	36(1)	42(1)	31(1)	5(1)	8(1)	-4(1)
N(51)	35(1)	28(1)	32(1)	4(1)	9(1)	5(1)
C(51)	32(1)	31(1)	26(1)	2(1)	0(1)	7(1)
C(52)	39(2)	48(2)	38(2)	-10(1)	6(1)	10(1)
C(53)	35(1)	62(2)	40(2)	0(2)	13(1)	7(1)
C(54)	31(1)	48(2)	42(2)	14(1)	10(1)	5(1)
C(55)	36(1)	30(1)	42(2)	6(1)	13(1)	2(1)
C(56)	42(2)	26(1)	39(2)	-3(1)	0(1)	4(1)
N(52)	44(1)	28(1)	36(1)	5(1)	6(1)	-4(1)
O(1)	51(1)	71(2)	47(1)	2(1)	-5(1)	-26(1)
O(2)	46(1)	46(1)	58(1)	-1(1)	9(1)	0(1)
O(3)	37(1)	47(1)	62(1)	0(1)	4(1)	10(1)
O(4)	73(2)	72(2)	54(2)	-10(1)	13(1)	-40(1)
O(5)	49(1)	50(1)	77(2)	1(1)	8(1)	8(1)
O(6)	58(2)	66(2)	78(2)	-13(1)	18(1)	0(1)
O(7)	71(2)	89(2)	52(2)	-4(1)	14(1)	32(2)
O(8)	41(1)	70(2)	82(2)	-3(1)	8(1)	-16(1)
O(9)	90(2)	77(2)	87(2)	28(2)	60(2)	42(2)
O(10)	41(6)	50(7)	42(6)	2(5)	-10(5)	-11(5)
O(10')	42(6)	49(9)	75(12)	3(7)	31(7)	10(6)

Table 5. Hydrogen coordinates ($\cdot 10^4$) and isotropic displacement parameters ($Å^2 \cdot 10^3$).

	x	y	z	U(eq)
H(2)	6372	9605	10087	37
H(3)	5945	11061	9766	40
H(4)	4948	11203	8936	40
H(5)	4408	9890	8458	36
H(6A)	6371	7882	9418	43
H(6B)	6006	7886	10089	43
H(1N)	5126	7078	9636	33
H(2N)	5644	6768	9196	33
H(12)	5894	6702	6564	42
H(13)	6830	7778	6606	48
H(14)	6937	8888	7452	48
H(15)	6105	8918	8197	42
H(16A)	4468	6706	7017	37
H(16B)	5034	5908	7246	37
H(3N)	4854	6050	8268	35
H(4N)	4129	6314	7950	35
H(22)	2243	9019	7907	41
H(23)	2292	9406	6790	45
H(24)	3358	9133	6332	47
H(25)	4338	8503	6996	40
H(26A)	3387	8815	9081	41
H(26B)	2784	8053	8865	41

H(5N)	3603	6995	8869	35
H(6N)	3937	7559	9431	35
H(32)	3737	438	5116	47
H(33)	4205	-1029	5351	54
H(34)	5279	-1188	6081	52
H(35)	5855	110	6540	45
H(36A)	4051	2148	5121	44
H(36B)	3814	2141	5852	44
H(7N)	4555	3271	5953	36
H(8N)	5005	2925	5463	36
H(42)	7935	832	7114	45
H(43)	7860	372	8207	45
H(44)	6826	735	8687	47
H(45)	5892	1514	8058	44
H(46A)	7424	1922	6177	52
H(46B)	6825	1160	5952	52
H(9N)	6254	2384	5606	43
H(10N)	6615	2977	6138	43
H(52)	4076	3664	8201	50
H(53)	3350	2416	8383	54
H(54)	3512	1027	7838	48
H(55)	4392	936	7141	42
H(56A)	4790	4252	7114	43
H(56B)	5282	4126	7818	43
H(11N)	6112	3503	7355	43
H(12N)	5777	3963	6744	43
H(1O)	3236	3639	4678	86
H(2O)	3006	4178	5073	86
H(3O)	7408	3635	5388	75
H(4O)	7403	4500	5580	75
H(5O)	3071	7197	5590	73
H(6O)	2550	7794	5410	73
H(7O)	3152	4150	9483	99
H(8O)	3008	4193	10063	99
H(9O)	7002	2834	9594	88
H(10O)	7509	2309	9813	88
H(11O)	7505	3685	10613	100
H(12O)	7533	4484	10800	100
H(13O)	6558	3286	8479	105
H(14O)	6762	4055	8327	105
H(15O)	2774	6200	7444	97
H(16O)	2811	6247	8150	97
H(17O)	2474	6375	6157	121
H(18O)	2798	5605	6345	121

Table 6. Hydrogen bonds [Å and °].

D-H...A	d(D-H)	d(H...A)	d(D...A)	<(DHA)
C(4)-H(4)...S(2)#3	0.95	2.91	3.534(3)	124.1
C(5)-H(5)...N(21)	0.95	2.68	3.239(3)	118.5
N(2)-H(1N)...S(2)#1	0.91	2.65	3.533(2)	162.6
N(2)-H(2N)...S(1)	0.91	2.42	3.329(2)	175.3
C(15)-H(15)...N(1)	0.95	2.67	3.213(4)	116.9
C(16)-H(16A)...S(5)#2	0.99	2.97	3.731(3)	134.2
N(12)-H(3N)...S(1)	0.91	2.81	3.606(2)	147.5
N(12)-H(3N)...S(3)	0.91	2.94	3.536(2)	124.2
N(12)-H(4N)...O(8)	0.91	2.05	2.937(3)	164.6
C(22)-H(22)...S(4)#4	0.95	3.03	3.928(3)	159.2
N(22)-H(5N)...O(8)	0.91	2.48	3.179(3)	134.0
N(22)-H(6N)...S(2)#1	0.91	2.56	3.442(2)	163.2
C(32)-H(32)...O(10)#5	0.95	2.27	3.207(11)	168.7
C(32)-H(32)...O(10')#5	0.95	2.40	3.32(2)	164.2
N(32)-H(7N)...S(4)#2	0.91	2.55	3.434(2)	164.8
N(32)-H(8N)...S(5)	0.91	2.54	3.423(2)	164.1
C(42)-H(42)...S(1)#6	0.95	2.75	3.655(3)	160.3
C(46)-H(46B)...O(10)#6	0.99	2.45	3.300(14)	144.2
C(46)-H(46B)...O(10')#6	0.99	2.64	3.469(19)	141.7
N(42)-H(9N)...S(5)	0.91	2.61	3.470(2)	158.2
N(42)-H(10N)...O(2)	0.91	2.37	3.124(3)	139.9
C(52)-H(52)...S(3)	0.95	3.03	3.918(3)	156.5
C(54)-H(54)...O(9)#7	0.95	2.50	3.156(4)	126.3
C(55)-H(55)...N(31)	0.95	2.66	3.187(4)	115.8
C(56)-H(56A)...S(4)#2	0.99	2.78	3.669(3)	150.2
N(52)-H(11N)...O(7)	0.91	2.04	2.923(4)	163.6
N(52)-H(12N)...S(6)#2	0.91	2.60	3.483(2)	165.3
O(1)-H(2O)...S(4)#2	0.84	2.34	3.154(2)	164.0
O(2)-H(3O)...O(3)#2	0.84	2.05	2.884(3)	174.7
O(2)-H(4O)...O(1)#2	0.84	2.37	3.201(4)	171.0
O(3)-H(5O)...S(5)#2	0.84	2.42	3.192(2)	153.6
O(3)-H(6O)...O(4)#8	0.84	2.00	2.832(3)	171.9
O(4)-H(7O)...S(3)	0.84	2.52	3.269(3)	148.7
O(4)-H(8O)...S(1)#1	0.84	2.57	3.404(3)	173.2
O(5)-H(9O)...S(2)	0.84	2.51	3.288(2)	155.3
O(5)-H(10O)...O(1)#9	0.84	1.98	2.817(3)	171.9
O(6)-H(11O)...O(5)	0.84	1.97	2.805(4)	170.0
O(6)-H(12O)...O(4)#1	0.84	2.34	3.179(4)	173.6
O(7)-H(13O)...S(2)	0.84	2.68	3.502(3)	168.5
O(7)-H(14O)...S(1)	0.84	2.51	3.300(3)	158.3
O(8)-H(15O)...O(9)	0.84	2.07	2.878(4)	162.3
O(8)-H(16O)...O(6)#1	0.84	2.05	2.882(4)	173.6
O(9)-H(17O)...O(3)	0.84	2.02	2.846(4)	168.5
O(9)-H(18O)...S(4)#2	0.84	2.36	3.200(3)	179.2

Symmetry transformations used to generate equivalent atoms:
#1 -x+1,-y+1,-z+2 #2 -x+1,-y+1,-z+1 #3 x,y+1,z; #4 x-1/2,-y+3/2,z+1/2 #5 x-1/2,-y+1/2,z-1/2
#6 -x+3/2,y-1/2,-z+3/2 #7 -x+1/2,y-1/2,-z+3/2; #8 -x+1/2,y+1/2,-z+3/2 #9 x+1/2,-y+1/2,z+1/2

5.4 Hintergrundinformationen zu Kap. 3.3.1

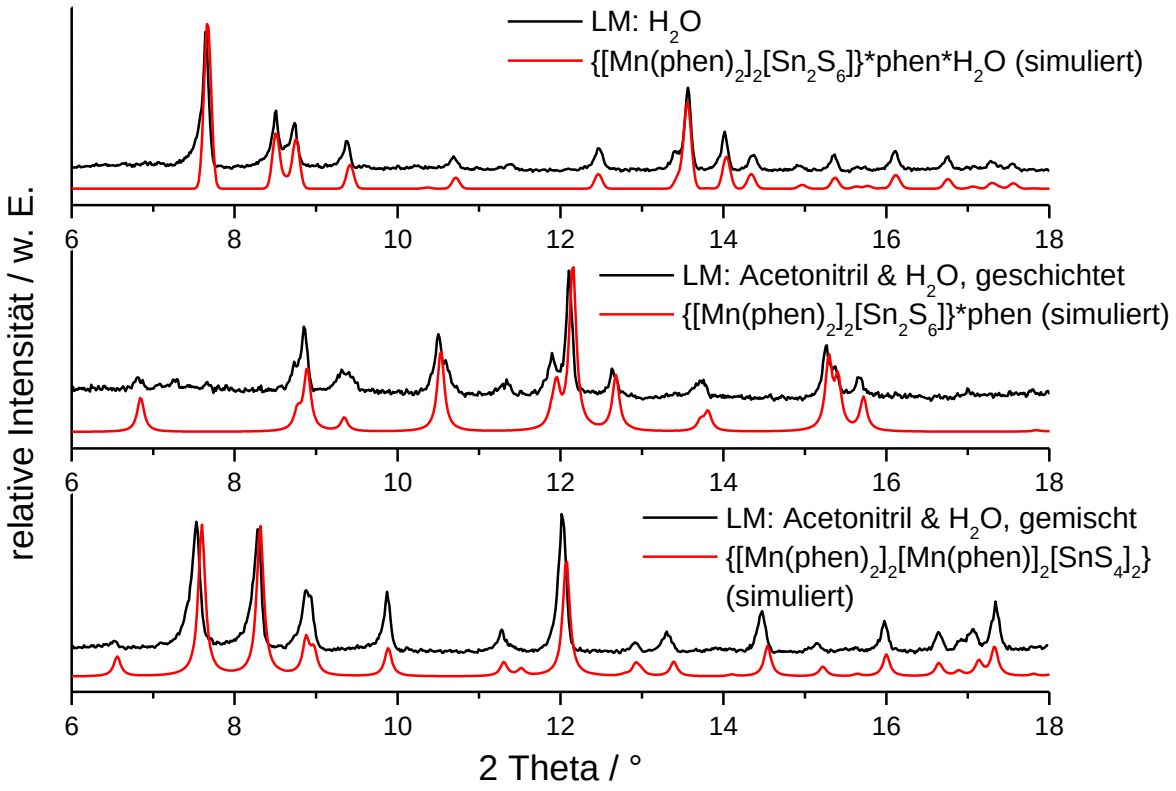

Abbildung A1: Pulverdiffraktogramme der Produkte erhalten bei Synthesen in verschiedenen LM(-Gemischen) bei 80°C.

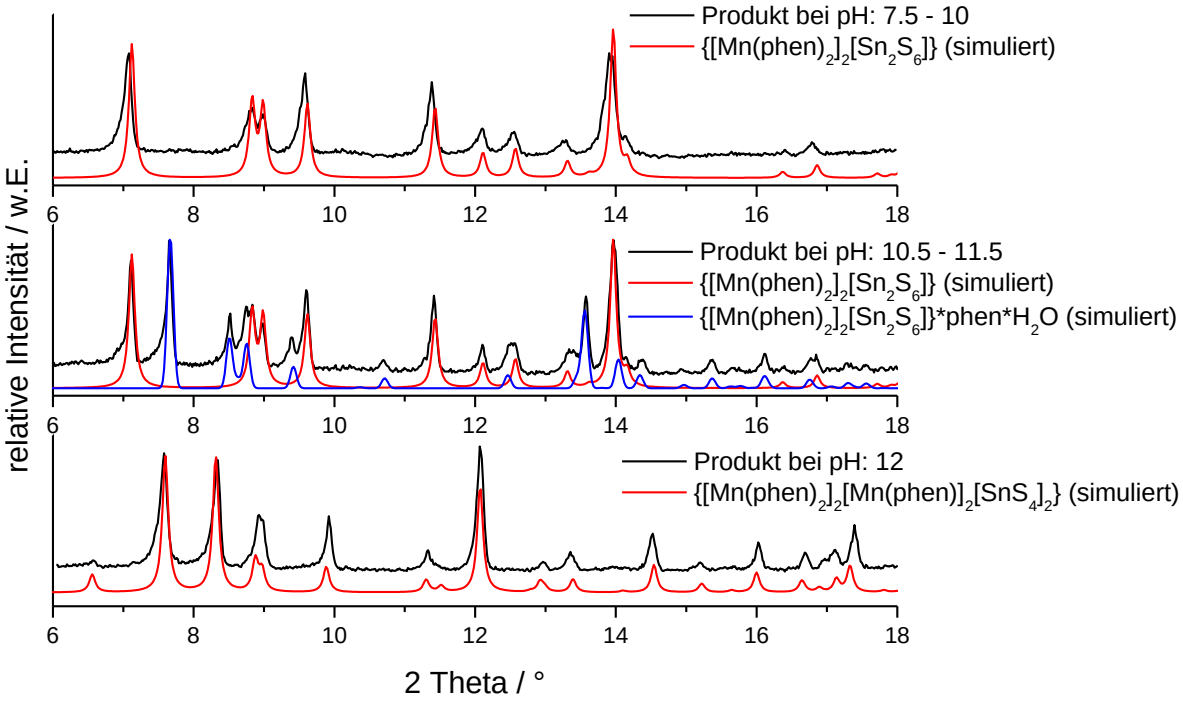

Abbildung A2: Pulverdiffraktogramme der Produkte erhalten bei Synthesen mit unterschiedlichen pH-Werten bei 80°C.

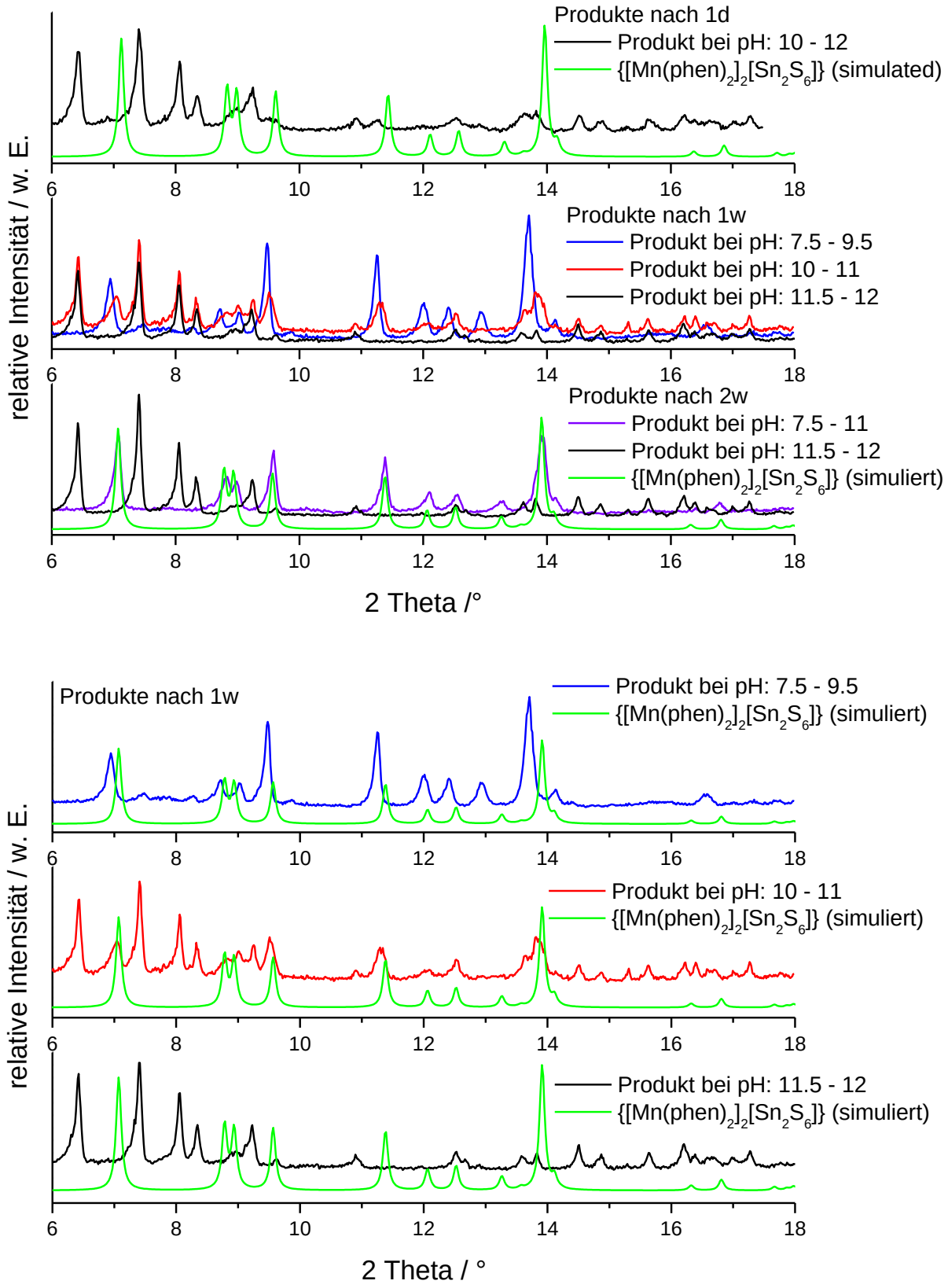

Abbildung A3: Pulverdiffraktogramme der Produkte bei Synthesen mit unterschiedlichen pH-Werten bei RT nach einen Tag (oben), einer Woche (oben und unten) und zwei Wochen (oben).

5.5 Hintergrundinformationen zu Kap. 3.3.2

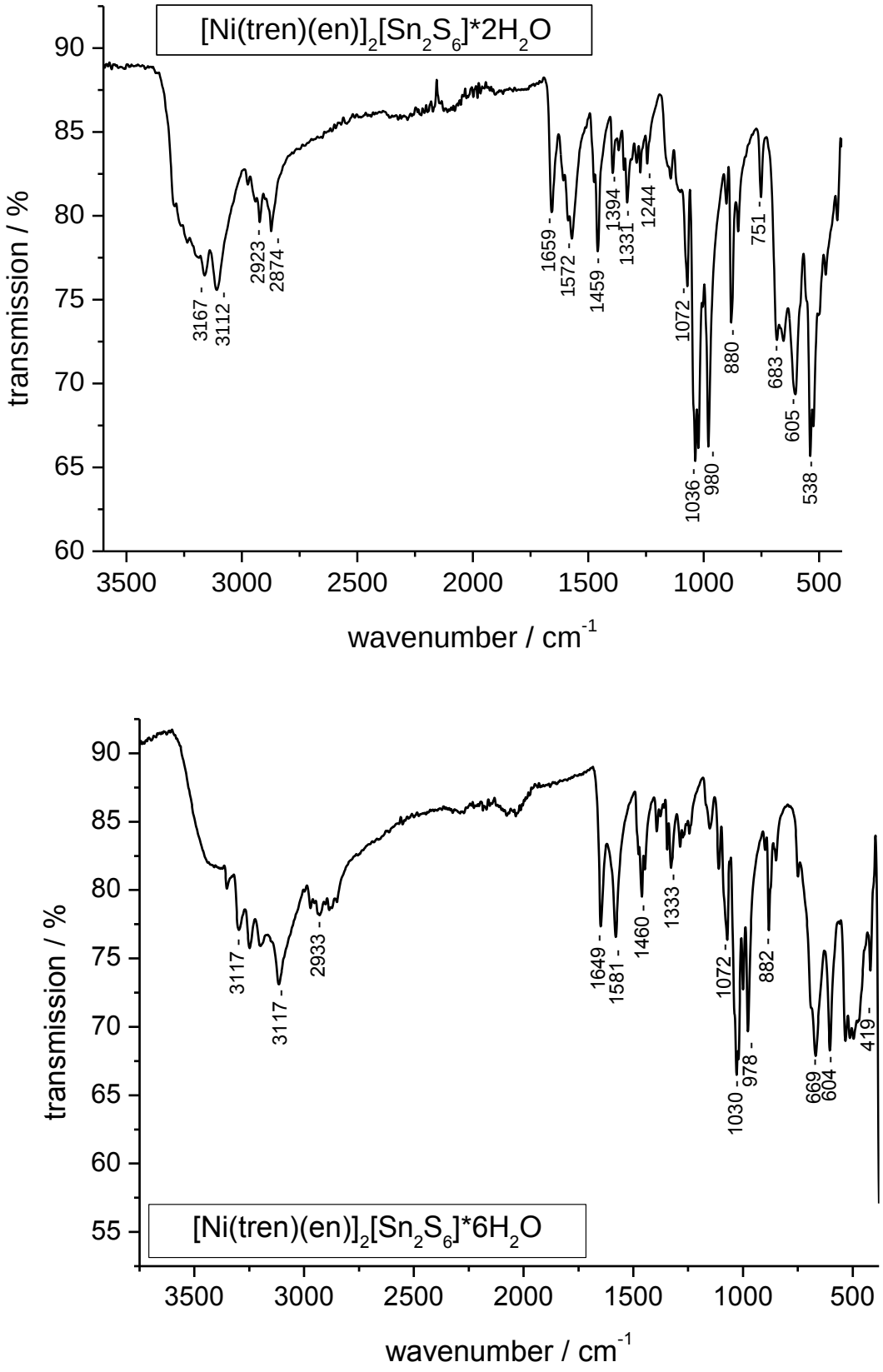

Abbildung A4: IR-Spektren der Verbindungen $[Ni(tren)(en)]_2[Sn_2S_6]\cdot 2H_2O$ (oben) und $[Ni(tren)(en)]_2[Sn_2S_6]\cdot 6H_2O$ (unten)

Tabelle A1: Zuordnung der Banden in den IR-Spektren von $[Ni(tren)(en)]_2[Sn_2S_6]\cdot 2H_2O$ und $[Ni(tren)(en)]_2[Sn_2S_6]\cdot 6H_2O$.

tren[110]	**en[111]]**	**$[Ni(tren)(en)]_2[Sn_2S_6]\cdot 2H_2O$**	**$[Ni(tren)(en)]_2[Sn_2S_6]\cdot 2H_2O$**	**Zuordnung**
3350, 3270, 3221, 3122	3246, 3171	3294w, 3269w, 3237w, 3164w, 3112m	3354w, 3300w, 3248w, 3201w, 3117m	ν (NH_2)
2970, 2924, 2886	2930, 2917, 2882	2975w, 2923m, 2874m	2971w, 2933w, 2884w	ν (CH_2)
---	---	1659m	1649m	δ(HOH)
1590	1598	1589m	1581m	δ (NH_2) + δ (CH_2)
1578	---	1572m	---	δ (NH_2) + δ (CH_2)
1477	1469	1475w	---	δ (NH_2) + δ (CH_2)
1457	1456	1459m	1460m	δ (NH_2) + δ (CH_2)
1390	---	1394w	1394w	δ (NH_2) + δ (CH_2)
---	1335	1331w	1333w	δ (C-C-H), δ (NH_2)
1270	---	1274w	1287w	ν (C-NH_2)+ ν (C-N)
1242	---	1244w	1243vw	ν (C-NH_2)+ ν (C-N)
---	1144	1143vw	1151w	ν (C-NH_2)
1108	1104	---	1109w	ν (C-NH_2)+ ν (C-N)
1070	1065	1072m	1072m	ρ (NH_2)
1035	1030	1036s	1030s	ρ (NH_2)
1020	---	1024s	---	ρ (NH_2)
---	980	980s	978s	ρ (NH_2)
902		902w		δ (NH_2)
---	880	880s	882m	δ (NH_2)
---	860	850m	849w	δ (NH_2)
---	761	751m	749w	δ (NH_2)
667	---	---	669s	δ (NH_2)
599	---	605m	604s	δ (C-C-C)
533	---	538s	533m	δ (C-C-C)
502	---	525m	---	δ (C-C-C)
470	468	471w	---	δ (C-C-C)
---	---	422w	419m	ν (TM-N)

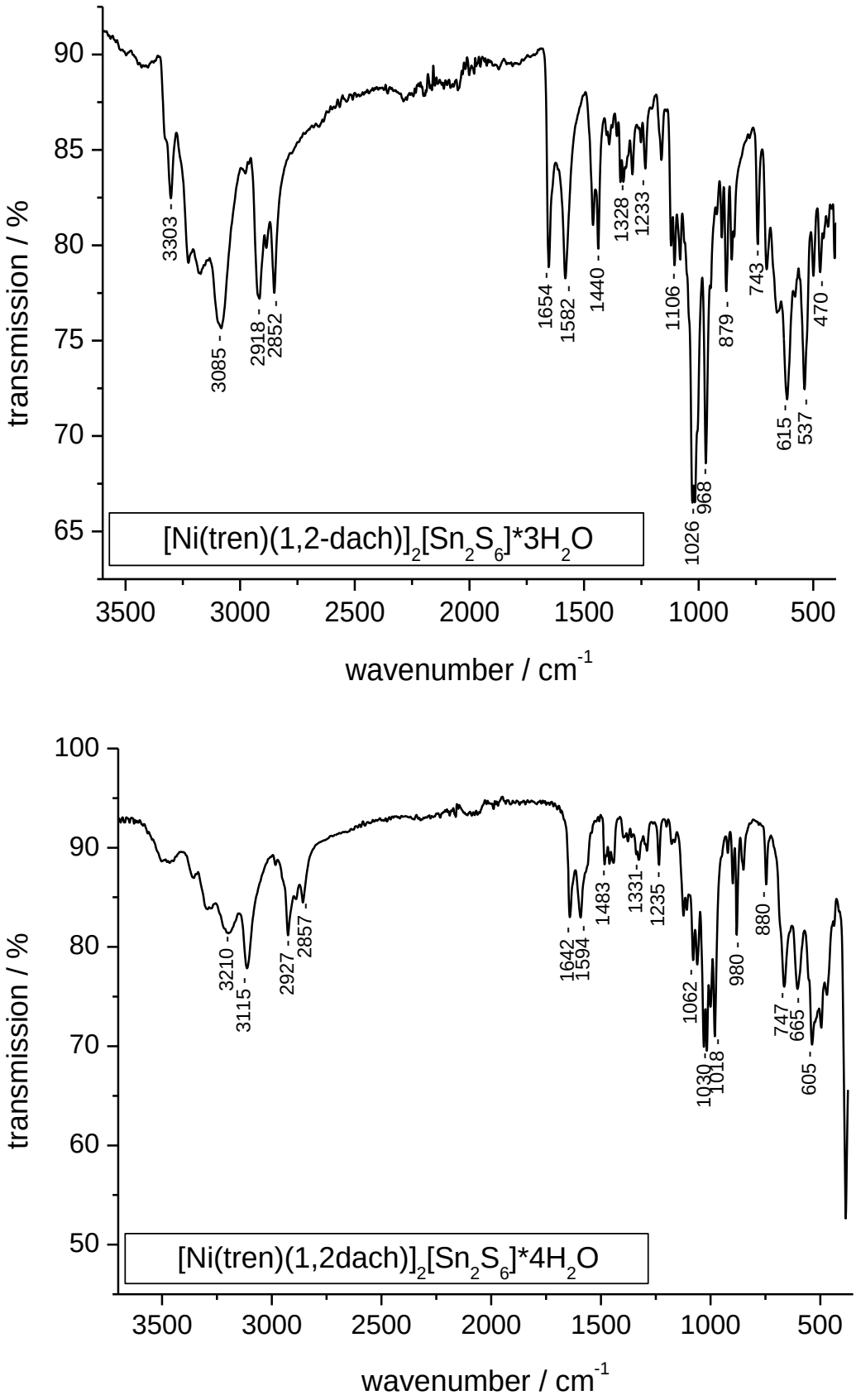

Abbildung A5: IR-Spektren der Verbindungen $[Ni(tren)(1,2\text{-dach})]_2[Sn_2S_6]\cdot 3H_2O$ (oben) und $[Ni(tren)(1,2\text{-dach})]_2[Sn_2S_6]\cdot 4H_2O$ (unten).

Tabelle A2: Zuordnung der Banden der IR-Spektren der Verbindungen $[Ni(tren)(1,2\text{-dach})]_2[Sn_2S_6]\cdot 3H_2O$ und $[Ni(tren)(1,2\text{-dach})]_2[Sn_2S_6]\cdot 4H_2O$.

tren[110]	**1,2-dach[112]**	**$[Ni(tren)(1,2\text{-dach})]_2[Sn_2S_6]\cdot 3H_2O$**	**$[Ni(tren)(1,2\text{-dach})]_2[Sn_2S_6]\cdot 4H_2O$**	**Zuordnung**
---	---	~3426	~3495	ν (O-H)
3270s	3255	3303m	3330 m	ν (NH_2)
---	3210	---	3210 m	ν (NH_2)
3180m	---	3228w, 3180w	---	ν (NH)
---	3120	---	3115 m	ν (NH_2)
---	---	3085s	---	ν (NH_2)
2930s, 2855s 2800s	---	2979vw, 2918m, 2888w, 2852m	2927 m, 2895 w, 2857 w	ν (CH_2)
---	---	1654m	1642 m	δ(HOH)
1590s 1445m	1591 1449	1582m, 1462m, 1440m	1594 m, 1483 w, 1460 w	δ (NH_2) + δ (CH_2)
1390w, 1365(sh)	1390	1391w, 1367w	---	δ (C-C-H), δ (NH_2)
---	1345	1341w	1331 w	δ (C-C-H), δ (NH_2)
1348m 1304m	---	1328w	---	δ (CH_2)
1270m 1230w	---	1289w, 1252w, 1233w	1235 m	ν (C-NH_2)+ ν (C-N)
---	---	1162m	---	ν (C-N)
1112vs	1112	1120w, 1106w,	1123 m	ν (C-NH_2)+ ν (C-N)
1090m, 1070m, 1035s, 1020(sh)	---	1080w, 1026s, 1016s	1079 m, 1030 s, 1018 s	δ (NH_2)
---	1062	---	1062m	ν (C-N)
---	---	968s	980 s	skeleton vib.
---	921	919vw	921 vw	δ (C-C-C), ν (C-N)
902s (br), 865s(br)	---	890w 879m,	899w 880 m,	δ (NH_2)
---	855	856w	852w	δ (C-C-C)
765(sh), 730w	---	743m, 659vw	747m, 665m	δ (NH_2)
625, 533, 502	---	615m, 577vw, 537m, 499w, 470w,	605m, 539m, 493w	δ (C-C-C)
---	---	407w	405w	ν (TM-N)

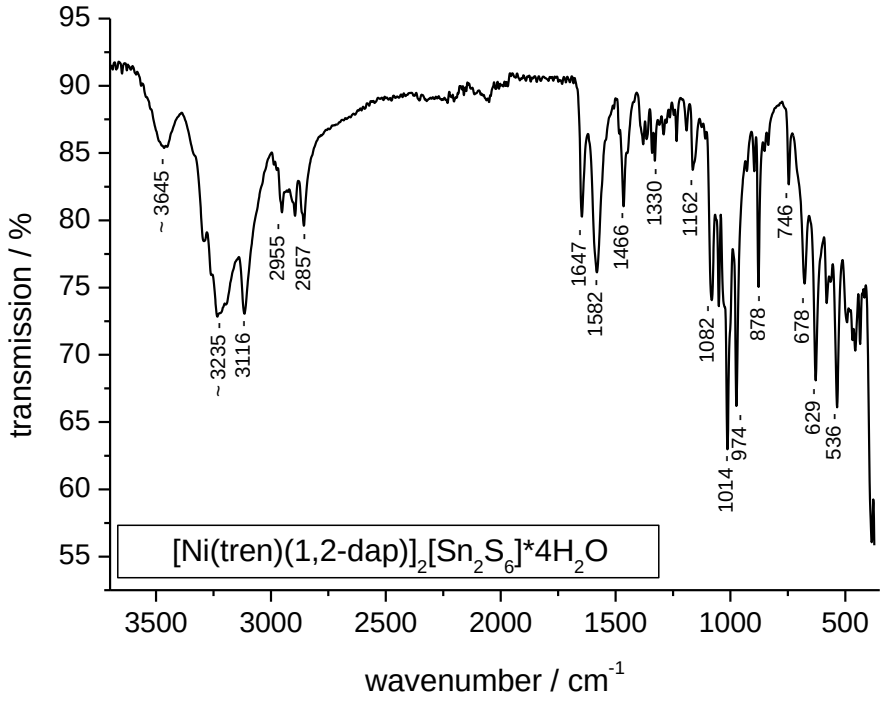

Abbildung A6: IR Spektrum der Verbindung $[Ni(tren)(1,2\text{-dap})]_2[Sn_2S_6]\cdot 4H_2O$.

Tabelle A3: Zuordnung der Banden des IR-Spektrums der Verbindung $[Ni(tren)(1,2\text{-dap})]_2[Sn_2S_6]\cdot 4H_2O$

tren[110]	**1,2-dap[113]**	**$[Ni(tren)(1,2\text{-dap})]_2[Sn_2S_6]\cdot 4H_2O$**	**Zuordnung**
---	---	~3645	ν (O-H)
3270	3284	3297w	ν (NH_2)
---	---	3235m	ν (NH_2)
---	---	3116m	ν (NH_2)
2930	2958	2955m	ν (CH_2)
2886	2890	2895m	ν (CH_2)
2855	2861	2857m	ν (CH_2)
---	---	1647s	δ(HOH)
1590	1585	1582s	δ (NH_2) + δ (CH_2)
1445	1455	1466s	δ (NH_2) + δ (CH_2)
1381	1375	1379w	δ (NH_2) + δ (CH_2)
---	1349	1330w	ρ (CH_2)
1230	---	1235w	ν (C-NH_2)+ ν (C-N)
---	1186	1191w	δ (NH_2)
1165	---	1162m	ν (C-NH_2)+ ν (C-N)
1090	---	1082s	ρ (NH_2)
1057	1061	1050m	ρ (NH_2), ν (C-N)
1020	1019	1014s	ρ (NH_2), ν (C-N)
---	970	974s	ρ (NH_2)
865	878	878m	δ (NH_2)
765	738	746m	δ (NH_2), ρ (CH_2)
667	---	678m	δ (NH_2)
625	---	629s	δ (C-C-C)
599	---	581w	δ (C-C-C)
533	---	536s	δ (C-C-C)
502	---	495w	δ (C-C-C)
---	---	437w	ν (TM-N)
---	---	401w	ν (TM-N)

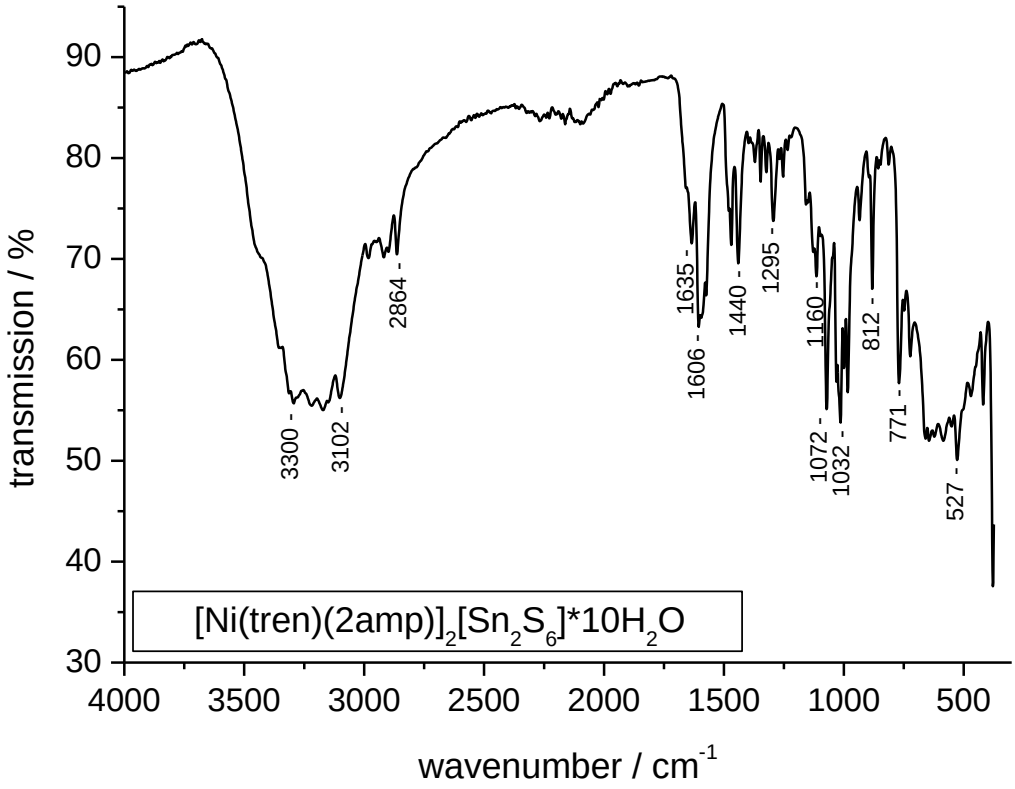

Abbildung A7: IR-Spektrum der Verbindung $[Ni(tren)(2amp)]_2[Sn_2S_6]\cdot 10H_2O$.

Tabelle A4: Zuordnung der Banden des IR-Spektrums von $[Ni(tren)(2amp)]_2[Sn_2S_6]\cdot 10H_2O$.

tren[110]	**2amp[119]**	**$[Ni(tren)(2amp)]_2[Sn_2S_6]\cdot 10H_2O$**	**Zuordnung**
3350, 3270, 3180	3291, 3258, 3171	3300m, 3228m, 3174m, 3102m	ν (NH_2)
2970, 2930, 2886	2902, 2856	2981w, 2920w, 2864w	ν (CH_2), ν $(NH)_{arom}$
---	---	1635w	δ(HOH)
1593	1604	1606m	δ (NH_2) + δ (CH_2)+ ν (C=C)
1477	1466	1470m	δ (NH_2) + δ (CH_2)+ ν (C=C)
1445	---	1440m	δ (NH_2) + δ (CH_2)+ ν (C=C)
1287	1291	1295m	ν (C-NH_2)+ ν (C-N)
1259	1253	1255w	ν (C-NH_2)+ ν (C-N)
1182	1161	1160w	ν (C-NH_2)+ ν (C-N)
1070	1086	1072s	ρ (NH_2)
1035	1032	1032s	ρ (NH_2)
---	---	983m	δ (NH_2)
---	818	812m	δ (CH_2)
765	767	771m	δ (NH_2), γ(C-H)
---	725	723w	δ(C- CH_2)
533	---	527w	δ (C-C-C)
---	---	420w	ν (M-N)

5.6 Hintergrundinformationen zu Kap. 3.3.3

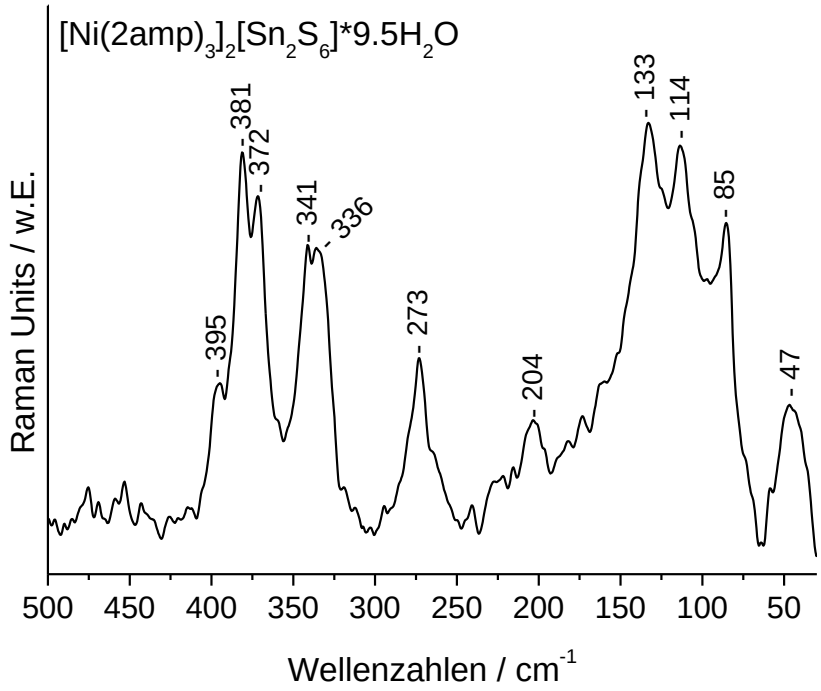

Abbildung A8: Raman-Spektrum der Verbindung $[Ni(2amp)_3]_2[Sn_2S_6]\cdot 9.5H_2O$.

Tabelle A5: Zuordnung der Banden des Raman-Spektrums von $[Ni(2amp)_3]_2[Sn_2S_6]\cdot 9.5H_2O$ (Wellenzahlen in cm^{-1}).

$Na_4Sn_2S_6$[88]	$[Ni(2amp)_3]_2[Sn_2S_6]\cdot 9.5H_2O$	Zuordnung
391	395	$\nu_{as}(SnS_2)$
377	381	$\nu_s(SnS_2)$
	372	
341	341	ν_{as}(Sn-S-Sn)
	336	
281	273	ν (Sn_2S_2)
190	204	Deformations- und Torsionsschwingungen
151		
136	133	
	85	

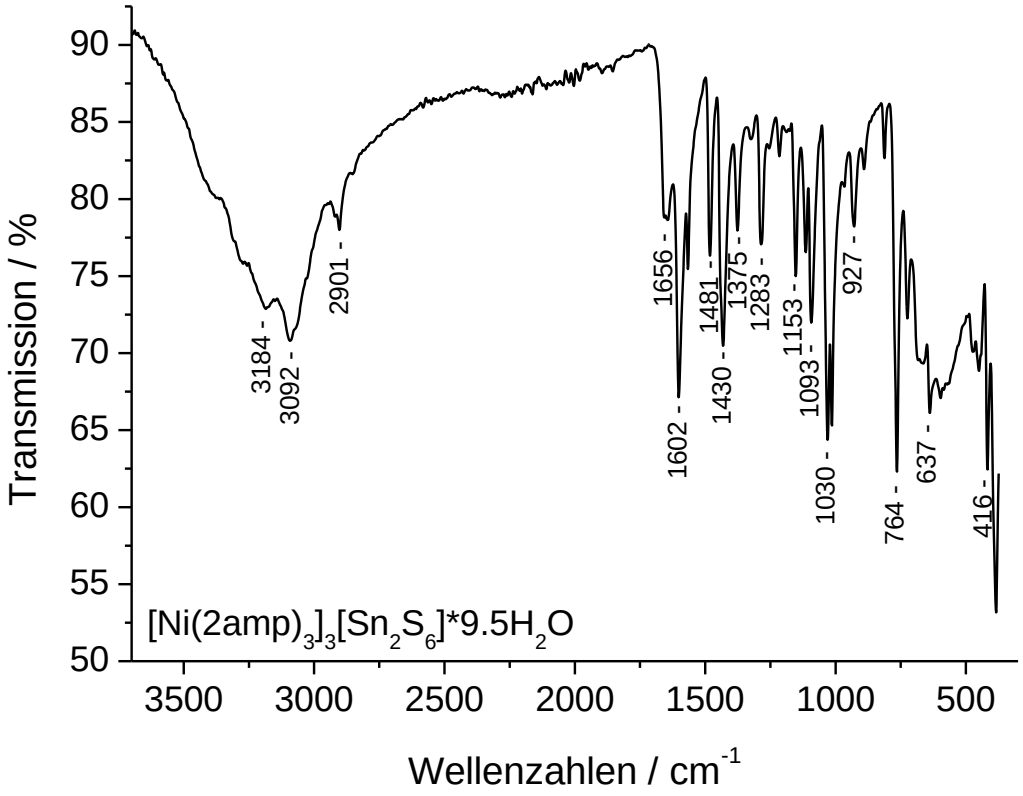

Abbildung A9: IR-Spektrum der Verbindung $[Ni(2amp)_3]_2[Sn_2S_6]\cdot 9.5H_2O$.

Tabelle A6: Zuordnung der Banden im IR-Spektrum von $[Ni(2amp)_3]_2[Sn_2S_6]\cdot 9.5H_2O$.

2amp[119]	$[Ni(2amp)_3]_2[Sn_2S_6]\cdot 9.5H_2O$	Zuordnung
3171	3184 (breit)	ν (NH_2), ν (HOH)
3079	3092 (breit)	ν (NH_2), ν (HOH)
2902	2901 w	ν (CH_2), ν $(NH)_{arom}$
---	1656 m	δ(HOH)
1604	1602s	ν (C-C), ν (C-N), δ (NH_2)
---	1567m	ν (C-C), ν (C-N), δ (NH_2)
1466	1481m	ν (C-C), ν (C-N), δ (NH_2)
---	1430s	ν (C-C), ν (C-N), δ (NH_2)
1375	1375m	δ (CH_2)
1325	1324w	δ (NH_2)
1291	1283m	ν (C-NH_2)
---	1216w	ν (C-NH_2)+
1161	1153m	ν (C-NH_2)+ ν (C-N)
1115	1114m	δ (CH)
1086	1093m	δ (CH_2)
1032	1030s	ν (C-N)
923	927s	δ (C-H)
---	890m	δ (NH_2)
818	812w	δ (C-H)
767	764s	δ (NH_2), δ (C-H)
725	724m	δ (C- CH_2)
638	637w	δ (C- CH_2)
455	447w	δ (C-C-N)
415	416m	δ (C-C-C)

s: stark, m: medium, w: schwach

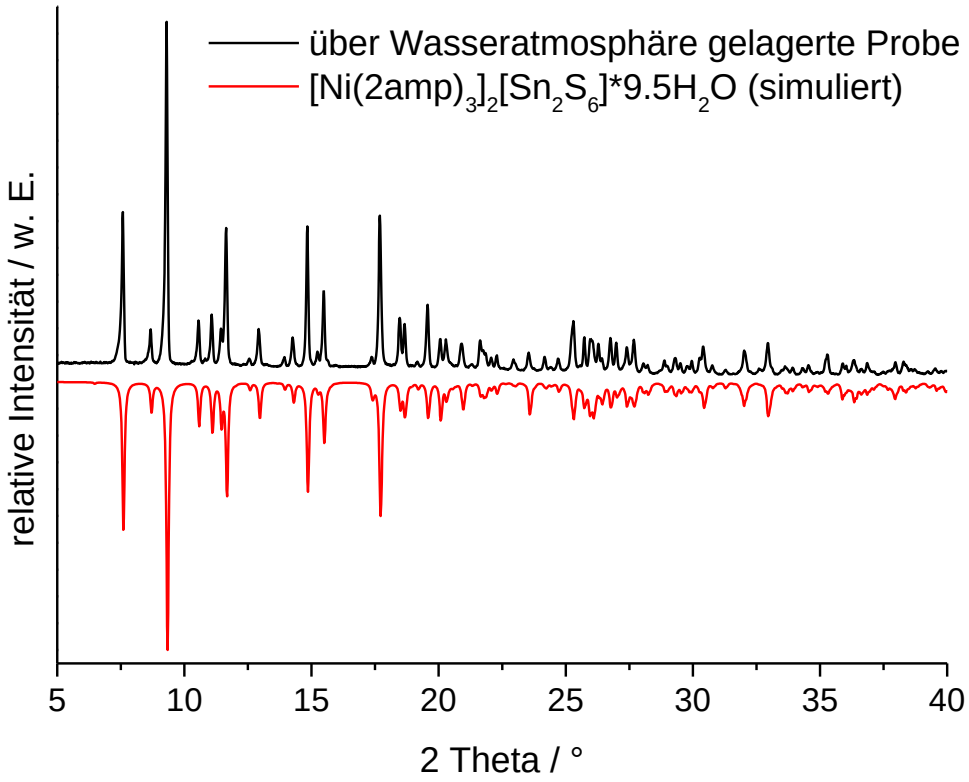

Abbildung A19: Pulverdiffraktogramm einer durch thermischen Abbau von $[Ni(2amp)_3]_2[Sn_2S_6]\cdot 9.5H_2O$ (100°C) erhaltenen Probe, in welche durch Lagern über einer Wasseratmosphäre das Kristallwasser wieder vollständig eingelagert werden konnte (schwarz). Mit Vergleich eines simulierten Pulverdiffraktogramms von $[Ni(2amp)_3]_2[Sn_2S_6]\cdot 9.5H_2O$ (rot).

5.7 Acta E Publikationen

5.7.1 Crystal structure of tris(N-methylsalicylaldiminato-κ²N,O)vanadium(III)

CRYSTALLOGRAPHIC COMMUNICATIONS

OPEN ACCESS

ISSN 2056-9890

Crystal structure of tris(*N*-methylsalicylaldiminato-κ^2N,O)vanadium(III)

Jessica Hilbert,* Sven Kabus, Christian Näther and Wolfgang Bensch

Institut für Anorganische Chemie, Christian-Albrechts-Universität zu Kiel, Max-Eyth-Strasse 2, 24118 Kiel, Germany. *Correspondence e-mail: jhilbert@ac.uni-kiel.de

Received 11 November 2015; accepted 12 November 2015

Edited by E. R. T. Tiekink, University of Malaya, Malaysia

The structure of the title complex, $[V(C_8H_8NO)_3]$, comprises neutral and discrete complexes, in which the V^{III} cation is coordinated by three anionic *N*-methylalicylaldiminate ligands within a slightly distorted *mer*-N_3O_3 octahedral geometry. In the crystal structure, the molecules are linked *via* C—H···O hydrogen bonds into supramolecular chains that extend along the *c* axis.

Keywords: crystal structure; vanadium(III); *N*-methylsalicylaldiminate.

CCDC reference: 1436532

1. Related literature

For structures of discrete complexes of Mo and V with *N*-methylsaldicylaldiminate as the ligand, see: Davies & Gatehouse (1974); Cornman *et al.* (1997). For the synthesis of the starting material, see: Bonadies & Carrano (1986).

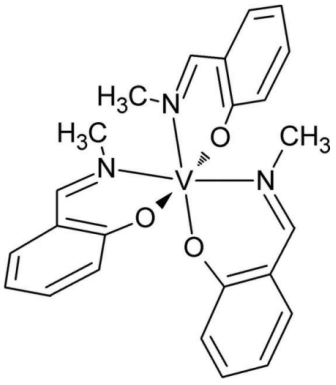

2. Experimental

2.1. Crystal data

$[V(C_8H_8NO)_3]$
M_r = 453.40
Monoclinic, $P2_1/c$
a = 7.7414 (3) Å
b = 26.0018 (7) Å
c = 11.1004 (4) Å
β = 103.265 (3)°
V = 2174.79 (13) Å^3
Z = 4
Mo $K\alpha$ radiation
μ = 0.49 mm^{-1}
T = 170 K
0.24 × 0.14 × 0.06 mm

2.2. Data collection

STOE IPDS-1 diffractometer
Absorption correction: numerical (*X-SHAPE* and *X-RED32*; Stoe, 2008)
T_{min} = 0.919, T_{max} = 0.974
18648 measured reflections
4741 independent reflections
4054 reflections with $I > 2\sigma(I)$
R_{int} = 0.030

2.3. Refinement

$R[F^2 > 2\sigma(F^2)]$ = 0.040
$wR(F^2)$ = 0.102
S = 1.07
4741 reflections
283 parameters
H-atom parameters constrained
$\Delta\rho_{max}$ = 0.30 e Å^{-3}
$\Delta\rho_{min}$ = −0.42 e Å^{-3}

Table 1
Hydrogen-bond geometry (Å, °).

D—H···A	D—H	H···A	D···A	D—H···A
C27—H27···O21^{i}	0.95	2.56	3.431 (2)	153

Symmetry code: (i) $x, -y+\frac{1}{2}, z+\frac{1}{2}$.

Data collection: *X-AREA* (Stoe, 2008); cell refinement: *X-AREA*; data reduction: *X-AREA*; program(s) used to solve structure: *SHELXS97* (Sheldrick, 2008); program(s) used to refine structure: *SHELXL2014* (Sheldrick, 2015); molecular graphics: *XP* in *SHELXTL* (Sheldrick, 2008) and *DIAMOND* (Brandenburg, 1999); software used to prepare material for publication: *publCIF* (Westrip, 2010).

Acknowledgements

This work was supported by the State of Schleswig-Holstein.

Supporting information for this paper is available from the IUCr electronic archives (Reference: TK5408).

References

Bonadies, J. A. & Carrano, C. J. (1986). *J. Am. Chem. Soc.* **108**, 4088–4095.
Brandenburg, K. (1999). *DIAMOND*. Crystal Impact GbR, Bonn, Germany.
Cornman, C. R., Geiser–Bush, K. M., Rowley, S. P. & Boyle, P. D. (1997). *CrystEngComm*, **36**, 6401–6408.
Davies, J. E. & Gatehouse, B. M. (1974). *J. Chem. Soc. Dalton Trans.* pp. 184–187.
Sheldrick, G. M. (2008). *Acta Cryst.* A**64**, 112–122.
Sheldrick, G. M. (2015). *Acta Cryst.* A**71**, 3–8.
Stoe (2008). *X-AREA*, *X-RED32* and *X-SHAPE*. Stoe & Cie, Darmstadt, Germany.
Westrip, S. P. (2010). *J. Appl. Cryst.* **43**, 920–925.

supporting information

Acta Cryst. (2015). E**71**, m225 [doi:10.1107/S2056989015021453]

Crystal structure of tris(*N*-methylsalicylaldiminato-κ^2N,O)vanadium(III)

Jessica Hilbert, Sven Kabus, Christian Näther and Wolfgang Bensch

S1. Synthesis and crystallization

Most of the chemicals are commercially available: Sn (Fluka, 99.9%), S (Alfa Aesar, 99.5%), and methylamine (abcr, 40% aqueous solution). (*N*,*N*′-Disalicylideneethylenediamine)oxovanadium(IV) was prepared following the procedure of Bonadies & Carrano (1986): (*N*,*N*′-disalicylideneethylenediamine)oxovanadium (IV) (83.8 mg, 0.25 mmol), Sn (29.7 mg, 0.25 mmol) and S (24.1 mg, 0.75 mmol) were reacted in a glass tube (inner volume 11 mL) with methylamine (1.5 mL) and H_2O (0.5 mL) under solvothermal conditions at 120 °C for 24 h. Afterwards, the solid residue was filtered off, washed with water and ethanol, and dried over silica gel. The product contains red blocks of the title complex and a small amount of brown blocks of bis(*N*-methylsaldicylaliminato)oxovanadium(IV) (Cornman *et al.* (1997)). Even if Sn and S are not contained in the final product, they are needed for product formation, as otherwise only (*N*,*N*′-disalicylideneethylenediamine)oxovanadium(IV) is isolated.

S2. Refinement

The C—H H atoms were positioned with idealized geometry (methyl H atoms allowed to rotate but not to tip) and were refined isotropically with U_{eq}(H) = 1.2 U_{eq}(C) (1.5 for methyl H atoms) using a riding model with C—H = 0.95 Å for aromatic H atoms and 0.98 Å for methyl H atoms.

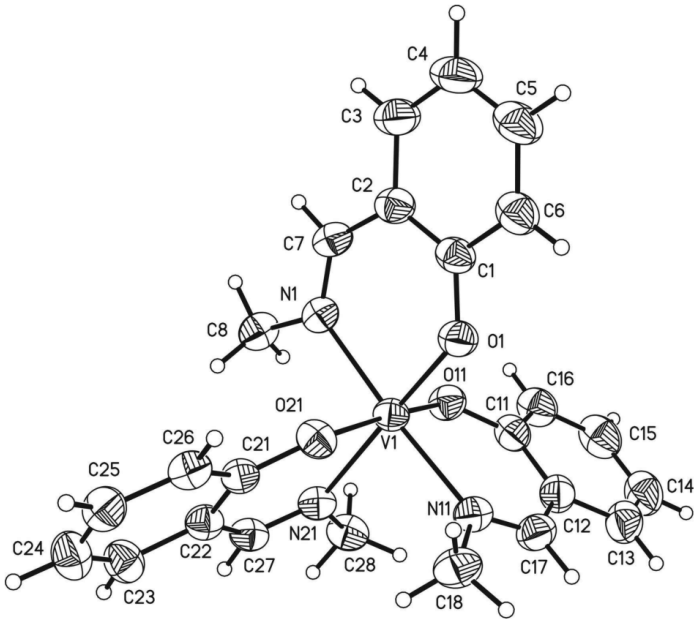

Figure 1

The molecular structure of the title complex with atom labelling. Displacement ellipsoids are drawn at the 50% probability level.

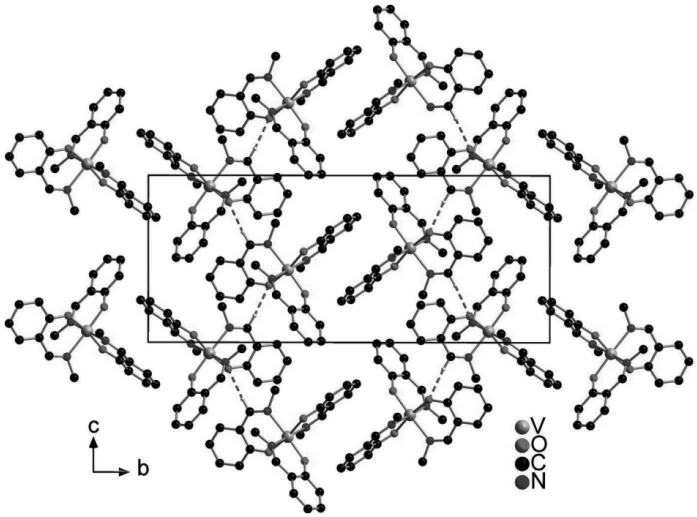

Figure 2

Unit cell contents of the crystal structure of the title complex viewed in projection down the *a* axis with hydrogen bonds shown as dashed lines. For clarity, all H atoms except those that participates in hydrogen bonding are omitted.

Tris(*N*-methylsalicylaldiminato-κ^2N,O)vanadium(III)

Crystal data

$[V(C_8H_8NO)_3]$	$F(000) = 944$
$M_r = 453.40$	$D_x = 1.385$ Mg m^{-3}
Monoclinic, $P2_1/c$	Mo $K\alpha$ radiation, $\lambda = 0.71073$ Å
$a = 7.7414$ (3) Å	Cell parameters from 18648 reflections
$b = 26.0018$ (7) Å	$\theta = 1.6$–$27.0°$
$c = 11.1004$ (4) Å	$\mu = 0.49$ mm^{-1}
$\beta = 103.265$ (3)°	$T = 170$ K
$V = 2174.79$ (13) Å^3	Block, red
$Z = 4$	0.24 × 0.14 × 0.06 mm

Data collection

STOE IPDS-1 diffractometer	4741 independent reflections
Radiation source: fine-focus sealed tube	4054 reflections with $I > 2\sigma(I)$
φ–scans	$R_{int} = 0.030$
Absorption correction: numerical (*X-SHAPE* and *X-RED32*; Stoe, 2008)	$\theta_{max} = 27.0°$, $\theta_{min} = 1.6°$
$T_{min} = 0.919$, $T_{max} = 0.974$	$h = -9 \rightarrow 9$
18648 measured reflections	$k = -30 \rightarrow 33$
	$l = -14 \rightarrow 14$

Refinement

Refinement on F^2	$S = 1.07$
Least-squares matrix: full	4741 reflections
$R[F^2 > 2\sigma(F^2)] = 0.040$	283 parameters
$wR(F^2) = 0.102$	0 restraints

Hydrogen site location: inferred from neighbouring sites	$w = 1/[\sigma^2(F_o^2) + (0.0523P)^2 + 0.6659P]$ where $P = (F_o^2 + 2F_c^2)/3$
H-atom parameters constrained	$(\Delta/\sigma)_{max} = 0.001$
	$\Delta\rho_{max} = 0.30$ e Å^{-3}
	$\Delta\rho_{min} = -0.42$ e Å^{-3}

Special details

Geometry. All esds (except the esd in the dihedral angle between two l.s. planes) are estimated using the full covariance matrix. The cell esds are taken into account individually in the estimation of esds in distances, angles and torsion angles; correlations between esds in cell parameters are only used when they are defined by crystal symmetry. An approximate (isotropic) treatment of cell esds is used for estimating esds involving l.s. planes.

Fractional atomic coordinates and isotropic or equivalent isotropic displacement parameters (Å^2)

	x	*y*	*z*	U_{iso}*/U_{eq}
V1	0.60947 (4)	0.34777 (2)	0.43424 (3)	0.03210 (10)
O1	0.58715 (17)	0.39024 (5)	0.28969 (12)	0.0400 (3)
C1	0.6728 (2)	0.39169 (7)	0.19994 (17)	0.0375 (4)
C2	0.8151 (3)	0.35824 (8)	0.19485 (18)	0.0390 (4)
C3	0.8995 (3)	0.36297 (9)	0.0951 (2)	0.0497 (5)
H3	0.9964	0.3410	0.0919	0.060*
C4	0.8448 (3)	0.39846 (10)	0.0029 (2)	0.0578 (6)
H4	0.9030	0.4010	−0.0634	0.069*
C5	0.7033 (3)	0.43068 (10)	0.0075 (2)	0.0550 (6)
H5	0.6646	0.4552	−0.0564	0.066*
C6	0.6186 (3)	0.42752 (9)	0.10360 (19)	0.0466 (5)
H6	0.5221	0.4499	0.1049	0.056*
C7	0.8789 (2)	0.31882 (8)	0.28513 (17)	0.0384 (4)
H7	0.9766	0.2989	0.2733	0.046*
N1	0.81716 (19)	0.30777 (6)	0.38049 (14)	0.0351 (3)
C8	0.9074 (3)	0.26689 (8)	0.46168 (18)	0.0423 (4)
H8A	0.9545	0.2808	0.5448	0.064*
H8B	1.0053	0.2533	0.4287	0.064*
H8C	0.8231	0.2392	0.4659	0.064*
O11	0.78967 (17)	0.38679 (5)	0.54398 (12)	0.0397 (3)
C11	0.7839 (3)	0.42940 (8)	0.60833 (18)	0.0402 (4)
C12	0.6228 (3)	0.45333 (8)	0.61828 (18)	0.0416 (4)
C13	0.6290 (3)	0.49804 (9)	0.6899 (2)	0.0510 (5)
H13	0.5211	0.5143	0.6952	0.061*
C14	0.7869 (4)	0.51892 (9)	0.7524 (2)	0.0580 (6)
H14	0.7882	0.5490	0.8012	0.070*
C15	0.9450 (4)	0.49555 (10)	0.7434 (2)	0.0587 (6)
H15	1.0549	0.5099	0.7863	0.070*
C16	0.9439 (3)	0.45159 (9)	0.6727 (2)	0.0501 (5)
H16	1.0533	0.4362	0.6676	0.060*
C17	0.4494 (3)	0.43340 (8)	0.56016 (18)	0.0430 (4)
H17	0.3499	0.4519	0.5740	0.052*
N11	0.4164 (2)	0.39324 (6)	0.49186 (15)	0.0378 (3)
C18	0.2295 (2)	0.37888 (9)	0.4467 (2)	0.0494 (5)

H18A	0.2020	0.3762	0.3562	0.074*
H18B	0.1538	0.4051	0.4715	0.074*
H18C	0.2079	0.3456	0.4822	0.074*
O21	0.42824 (16)	0.30065 (5)	0.34205 (11)	0.0370 (3)
C21	0.3734 (2)	0.25415 (7)	0.35945 (16)	0.0328 (4)
C22	0.4208 (2)	0.22876 (7)	0.47477 (17)	0.0352 (4)
C23	0.3555 (3)	0.17928 (8)	0.4881 (2)	0.0446 (5)
H23	0.3849	0.1630	0.5668	0.054*
C24	0.2496 (3)	0.15367 (9)	0.3894 (2)	0.0499 (5)
H24	0.2098	0.1197	0.3990	0.060*
C25	0.2023 (3)	0.17858 (8)	0.2756 (2)	0.0439 (5)
H25	0.1293	0.1613	0.2070	0.053*
C26	0.2596 (2)	0.22787 (8)	0.26080 (18)	0.0376 (4)
H26	0.2219	0.2445	0.1830	0.045*
C27	0.5263 (2)	0.25346 (7)	0.58385 (16)	0.0349 (4)
H27	0.5412	0.2352	0.6597	0.042*
N21	0.60191 (18)	0.29761 (6)	0.58834 (13)	0.0342 (3)
C28	0.6848 (3)	0.31610 (9)	0.71350 (17)	0.0426 (4)
H28A	0.6331	0.3493	0.7276	0.064*
H28B	0.8128	0.3201	0.7215	0.064*
H28C	0.6637	0.2912	0.7748	0.064*

Atomic displacement parameters (Å²)

	U^{11}	U^{22}	U^{33}	U^{12}	U^{13}	U^{23}
V1	0.03170 (16)	0.03642 (17)	0.02820 (16)	−0.00124 (12)	0.00694 (11)	−0.00003 (12)
O1	0.0416 (7)	0.0421 (7)	0.0386 (7)	0.0028 (6)	0.0140 (5)	0.0045 (6)
C1	0.0413 (9)	0.0401 (10)	0.0313 (9)	−0.0078 (8)	0.0092 (7)	−0.0013 (8)
C2	0.0401 (9)	0.0438 (11)	0.0339 (9)	−0.0078 (8)	0.0101 (7)	−0.0057 (8)
C3	0.0530 (12)	0.0571 (13)	0.0436 (11)	−0.0077 (10)	0.0207 (9)	−0.0064 (10)
C4	0.0709 (15)	0.0681 (15)	0.0409 (12)	−0.0128 (12)	0.0264 (11)	−0.0010 (11)
C5	0.0711 (14)	0.0583 (14)	0.0364 (11)	−0.0081 (11)	0.0141 (10)	0.0083 (10)
C6	0.0543 (11)	0.0454 (11)	0.0398 (10)	−0.0047 (9)	0.0105 (9)	0.0034 (9)
C7	0.0324 (8)	0.0467 (11)	0.0369 (10)	−0.0013 (8)	0.0098 (7)	−0.0075 (8)
N1	0.0322 (7)	0.0392 (8)	0.0325 (8)	−0.0001 (6)	0.0045 (6)	−0.0042 (7)
C8	0.0383 (9)	0.0494 (11)	0.0373 (10)	0.0086 (8)	0.0044 (8)	0.0007 (9)
O11	0.0380 (7)	0.0424 (7)	0.0389 (7)	−0.0036 (5)	0.0095 (5)	−0.0066 (6)
C11	0.0474 (10)	0.0388 (10)	0.0341 (9)	−0.0077 (8)	0.0084 (8)	−0.0013 (8)
C12	0.0548 (11)	0.0368 (10)	0.0343 (9)	0.0009 (8)	0.0121 (8)	0.0004 (8)
C13	0.0704 (14)	0.0423 (11)	0.0411 (11)	0.0029 (10)	0.0145 (10)	−0.0016 (9)
C14	0.0837 (17)	0.0436 (12)	0.0470 (12)	−0.0106 (11)	0.0156 (11)	−0.0081 (10)
C15	0.0691 (15)	0.0558 (14)	0.0484 (12)	−0.0224 (12)	0.0075 (11)	−0.0072 (11)
C16	0.0520 (11)	0.0516 (12)	0.0459 (11)	−0.0129 (10)	0.0095 (9)	−0.0056 (10)
C17	0.0460 (10)	0.0461 (11)	0.0393 (10)	0.0074 (8)	0.0148 (8)	0.0021 (9)
N11	0.0366 (8)	0.0424 (9)	0.0356 (8)	0.0021 (6)	0.0105 (6)	0.0010 (7)
C18	0.0337 (9)	0.0605 (13)	0.0550 (13)	0.0018 (9)	0.0120 (9)	−0.0024 (11)
O21	0.0391 (6)	0.0404 (7)	0.0296 (6)	−0.0041 (5)	0.0041 (5)	0.0024 (5)
C21	0.0287 (8)	0.0365 (9)	0.0333 (9)	0.0011 (7)	0.0076 (6)	−0.0002 (7)

C22	0.0317 (8)	0.0394 (10)	0.0345 (9)	0.0025 (7)	0.0074 (7)	0.0020 (8)
C23	0.0429 (10)	0.0417 (11)	0.0477 (11)	0.0003 (8)	0.0073 (8)	0.0075 (9)
C24	0.0461 (11)	0.0408 (11)	0.0605 (13)	−0.0048 (9)	0.0074 (10)	0.0008 (10)
C25	0.0375 (9)	0.0464 (11)	0.0463 (11)	−0.0026 (8)	0.0062 (8)	−0.0075 (9)
C26	0.0325 (8)	0.0456 (11)	0.0342 (9)	0.0005 (7)	0.0066 (7)	−0.0038 (8)
C27	0.0311 (8)	0.0431 (10)	0.0305 (8)	0.0038 (7)	0.0070 (6)	0.0070 (8)
N21	0.0318 (7)	0.0427 (9)	0.0271 (7)	0.0009 (6)	0.0045 (6)	0.0015 (6)
C28	0.0430 (10)	0.0553 (12)	0.0271 (9)	−0.0048 (9)	0.0032 (7)	0.0012 (9)

Geometric parameters (Å, º)

V1—O11	1.9183 (13)	C13—H13	0.9500
V1—O1	1.9227 (14)	C14—C15	1.390 (4)
V1—O21	1.9641 (13)	C14—H14	0.9500
V1—N1	2.1126 (15)	C15—C16	1.386 (3)
V1—N11	2.1163 (16)	C15—H15	0.9500
V1—N21	2.1625 (15)	C16—H16	0.9500
O1—C1	1.318 (2)	C17—N11	1.281 (3)
C1—C6	1.408 (3)	C17—H17	0.9500
C1—C2	1.415 (3)	N11—C18	1.467 (2)
C2—C3	1.414 (3)	C18—H18A	0.9800
C2—C7	1.439 (3)	C18—H18B	0.9800
C3—C4	1.371 (3)	C18—H18C	0.9800
C3—H3	0.9500	O21—C21	1.310 (2)
C4—C5	1.389 (4)	C21—C22	1.412 (3)
C4—H4	0.9500	C21—C26	1.414 (2)
C5—C6	1.376 (3)	C22—C23	1.402 (3)
C5—H5	0.9500	C22—C27	1.447 (3)
C6—H6	0.9500	C23—C24	1.379 (3)
C7—N1	1.290 (2)	C23—H23	0.9500
C7—H7	0.9500	C24—C25	1.392 (3)
N1—C8	1.463 (2)	C24—H24	0.9500
C8—H8A	0.9800	C25—C26	1.379 (3)
C8—H8B	0.9800	C25—H25	0.9500
C8—H8C	0.9800	C26—H26	0.9500
O11—C11	1.325 (2)	C27—N21	1.284 (2)
C11—C16	1.404 (3)	C27—H27	0.9500
C11—C12	1.420 (3)	N21—C28	1.471 (2)
C12—C13	1.403 (3)	C28—H28A	0.9800
C12—C17	1.446 (3)	C28—H28B	0.9800
C13—C14	1.371 (3)	C28—H28C	0.9800
O11—V1—O1	98.00 (6)	C14—C13—H13	119.2
O11—V1—O21	171.59 (6)	C12—C13—H13	119.2
O1—V1—O21	90.39 (6)	C13—C14—C15	119.2 (2)
O11—V1—N1	87.14 (6)	C13—C14—H14	120.4
O1—V1—N1	88.60 (6)	C15—C14—H14	120.4
O21—V1—N1	92.56 (6)	C16—C15—C14	120.7 (2)

O11—V1—N11	88.49 (6)	C16—C15—H15	119.7
O1—V1—N11	89.82 (6)	C14—C15—H15	119.7
O21—V1—N11	92.09 (6)	C15—C16—C11	121.1 (2)
N1—V1—N11	175.10 (6)	C15—C16—H16	119.4
O11—V1—N21	87.96 (6)	C11—C16—H16	119.4
O1—V1—N21	173.21 (6)	N11—C17—C12	126.48 (19)
O21—V1—N21	83.70 (5)	N11—C17—H17	116.8
N1—V1—N21	94.99 (6)	C12—C17—H17	116.8
N11—V1—N21	87.06 (6)	C17—N11—C18	117.16 (17)
C1—O1—V1	133.07 (12)	C17—N11—V1	125.15 (13)
O1—C1—C6	118.64 (18)	C18—N11—V1	117.65 (13)
O1—C1—C2	122.96 (17)	N11—C18—H18A	109.5
C6—C1—C2	118.39 (18)	N11—C18—H18B	109.5
C3—C2—C1	118.79 (19)	H18A—C18—H18B	109.5
C3—C2—C7	117.42 (19)	N11—C18—H18C	109.5
C1—C2—C7	123.78 (17)	H18A—C18—H18C	109.5
C4—C3—C2	121.6 (2)	H18B—C18—H18C	109.5
C4—C3—H3	119.2	C21—O21—V1	135.69 (11)
C2—C3—H3	119.2	O21—C21—C22	122.67 (16)
C3—C4—C5	119.3 (2)	O21—C21—C26	119.81 (16)
C3—C4—H4	120.3	C22—C21—C26	117.52 (17)
C5—C4—H4	120.3	C23—C22—C21	119.98 (17)
C6—C5—C4	120.8 (2)	C23—C22—C27	117.86 (17)
C6—C5—H5	119.6	C21—C22—C27	122.03 (17)
C4—C5—H5	119.6	C24—C23—C22	121.5 (2)
C5—C6—C1	121.1 (2)	C24—C23—H23	119.3
C5—C6—H6	119.5	C22—C23—H23	119.3
C1—C6—H6	119.5	C23—C24—C25	118.7 (2)
N1—C7—C2	126.67 (18)	C23—C24—H24	120.6
N1—C7—H7	116.7	C25—C24—H24	120.6
C2—C7—H7	116.7	C26—C25—C24	121.06 (19)
C7—N1—C8	116.91 (16)	C26—C25—H25	119.5
C7—N1—V1	124.86 (13)	C24—C25—H25	119.5
C8—N1—V1	118.07 (12)	C25—C26—C21	121.15 (18)
N1—C8—H8A	109.5	C25—C26—H26	119.4
N1—C8—H8B	109.5	C21—C26—H26	119.4
H8A—C8—H8B	109.5	N21—C27—C22	126.46 (17)
N1—C8—H8C	109.5	N21—C27—H27	116.8
H8A—C8—H8C	109.5	C22—C27—H27	116.8
H8B—C8—H8C	109.5	C27—N21—C28	115.14 (16)
C11—O11—V1	132.48 (12)	C27—N21—V1	127.10 (12)
O11—C11—C16	118.88 (19)	C28—N21—V1	117.71 (12)
O11—C11—C12	123.17 (17)	N21—C28—H28A	109.5
C16—C11—C12	117.93 (19)	N21—C28—H28B	109.5
C13—C12—C11	119.37 (19)	H28A—C28—H28B	109.5
C13—C12—C17	117.2 (2)	N21—C28—H28C	109.5
C11—C12—C17	123.40 (18)	H28A—C28—H28C	109.5
C14—C13—C12	121.7 (2)	H28B—C28—H28C	109.5

Hydrogen-bond geometry (Å, º)

D—H···*A*	*D*—H	H···*A*	*D*···*A*	*D*—H···*A*
C27—H27···O21^{i}	0.95	2.56	3.431 (2)	153

Symmetry code: (i) *x*, −*y*+1/2, *z*+1/2.

5.7.2 Crystal structure of tris(N-methylsalicylaldiminato-κ²N,O)chromium(III)

CRYSTALLOGRAPHIC COMMUNICATIONS

OPEN ACCESS

ISSN 2056-9890

Crystal structure of tris(*N*-methylsalicylaldiminato-κ^2N,O)chromium(III)

Jessica Hilbert,* Sven Kabus, Christian Näther and Wolfgang Bensch

Institute of Inorganic Chemistry, Christian-Albrechts-University of Kiel, Max-Eyth-Strasse 2, 24118 Kiel, Germany. *Correspondence e-mail: jhilbert@ac.uni-kiel.de

Received 25 November 2015; accepted 1 December 2015

Edited by M. Weil, Vienna University of Technology, Austria

The crystal structure of the title compound, $[Cr(C_8H_8NO)_3]$, is isotypic with the vanadium(III) analogue. The asymmetric unit consists of one Cr^{3+} cation and three *N*-methylsalicylaldiminate anions. The metal cation is octahedrally coordinated by three *N*,*O*-chelating *N*-methylsalicylaldiminate ligands, leading to discrete and neutral complexes. In the crystal, neighbouring complexes are linked *via* C—H···O hydrogen-bonding interactions into chains propagating parallel to the *c* axis.

Keywords: crystal structure; chromium(III); *N*-methylsalicylaldiminate; hydrogen bonding.

CCDC reference: 1439806

1. Related literature

This structure determination was undertaken as part of a project intending to synthesise chromium-containing thiostannates, for which no compounds are known to date. Instead, the title compound was isolated. Its structure is isotypic with the vanadium(III) analogue reported recently by us (Hilbert *et al.*, 2015). For the structures of similar discrete vanadium complexes with *N*-methylsalicylaldiminate as ligand, see: Cornman *et al.* (1997).

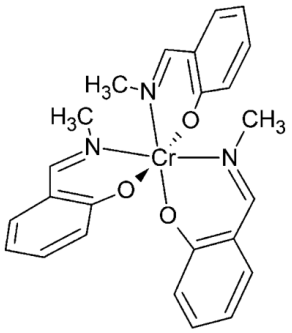

2. Experimental

2.1. Crystal data

$[Cr(C_8H_8NO)_3]$
M_r = 454.46
Monoclinic, $P2_1/c$
a = 7.7463 (2) Å
b = 25.4402 (8) Å
c = 11.1421 (3) Å
β = 102.659 (2)°
V = 2142.37 (11) Å^3
Z = 4
Mo $K\alpha$ radiation
μ = 0.57 mm^{-1}
T = 170 K
0.28 × 0.2 × 0.06 mm

2.2. Data collection

Stoe IPDS-1 diffractometer
Absorption correction: numerical (*X-SHAPE* and *X-RED32*; Stoe, 2008)
T_{min} = 0.841, T_{max} = 0.972
25422 measured reflections
4665 independent reflections
3991 reflections with $I > 2\sigma(I)$
R_{int} = 0.030

2.3. Refinement

$R[F^2 > 2\sigma(F^2)]$ = 0.033
$wR(F^2)$ = 0.092
S = 1.07
4665 reflections
283 parameters
H-atom parameters constrained
$\Delta\rho_{max}$ = 0.32 e Å^{-3}
$\Delta\rho_{min}$ = −0.41 e Å^{-3}

Table 1
Hydrogen-bond geometry (Å, °).

D—H···A	D—H	H···A	D···A	D—H···A
C17—H17···O11^{i}	0.95	2.44	3.3154 (19)	154

Symmetry code: (i) $x, -y+\frac{1}{2}, z+\frac{1}{2}$.

Data collection: *X-AREA* (Stoe, 2008); cell refinement: *X-AREA*; data reduction: *X-AREA*; program(s) used to solve structure: *SHELXS97* (Sheldrick, 2008); program(s) used to refine structure: *SHELXL2014* (Sheldrick, 2015); molecular graphics: *XP* in *SHELXTL* (Sheldrick, 2008) and *DIAMOND* (Brandenburg, 1999); software used to prepare material for publication: *publCIF* (Westrip, 2010).

Acknowledgements

This work was supported by the State of Schleswig–Holstein.

Supporting information for this paper is available from the IUCr electronic archives (Reference: WM5245).

References

Brandenburg, K. (1999). *DIAMOND*. Crystal Impact GbR, Bonn, Germany.
Cornman, C. R., Geiser-Bush, K. M., Rowley, S. P. & Boyle, P. D. (1997). *Inorg. Chem.* **36**, 6401–6408.
Hilbert, J., Kabus, S., Näther, C. & Bensch, W. (2015). *Acta Cryst.* E**71**, m225.
Sheldrick, G. M. (2008). *Acta Cryst.* A**64**, 112–122.
Sheldrick, G. M. (2015). *Acta Cryst.* A**71**, 3–8.
Stoe (2008). *X-AREA*, *X-RED32* and *X-SHAPE*. Stoe & Cie, Darmstadt, Germany.
Westrip, S. P. (2010). *J. Appl. Cryst.* **43**, 920–925.

supporting information

Acta Cryst. (2015). E**71**, m247–m248 [doi:10.1107/S2056989015023038]

Crystal structure of tris(*N*-methylsalicylaldiminato-κ^2N,O)chromium(III)

Jessica Hilbert, Sven Kabus, Christian Näther and Wolfgang Bensch

S1. Synthesis and crystallization

All chemicals were commercially available. The title compound was serendipitously obtained under solvothermal conditions. For the synthesis 66.6 mg (0.25 mmol) $CrCl_3 \cdot 6H_2O$ (Merck, 95%), 29.7 mg (0.25 mmol) Sn (Fluka, 99.9%), 24.1 mg (0.75 mmol) S (Alfa Aesar, 99.5%) and 134.2 mg (0.5 mol) *N*,*N*-ethylenebis(salicylimine) (Alfa Aesar, 99%) were mixed in a glass tube (inner volume 11 ml) with 1.5 ml methylamine (abcr, 40% aqueous solution) and 0.5 ml water. The reaction slurry was tempered at 398 K for one day. After cooling to room temperature the crystalline product (dark red blocks) was filtered off, washed with water and ethanol and dried over silica gel.

S2. Refinement

The C-bound H atoms were positioned with idealized geometry (methyl H atoms were allowed to rotate but not to tip) and were refined with $U_{iso}(H) = 1.2U_{eq}(C)$ (1.5 for methyl H atoms) using a riding model with C—H = 0.95 Å for aromatic H atoms and 0.98 Å for methyl H atoms.

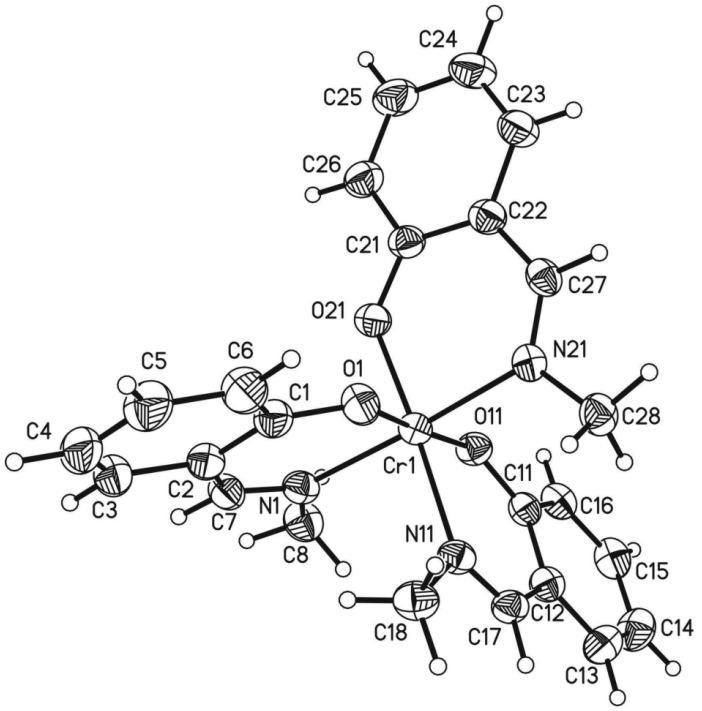

Figure 1

The molecular structure of the title compound. Displacement ellipsoids are drawn at the 50% probability level.

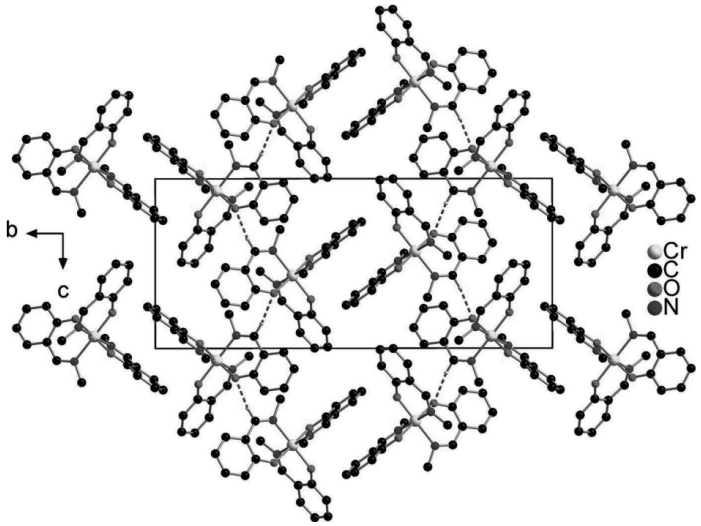

Figure 2

The crystal structure of the title compound in a view along [100]. C—H···O hydrogen bonds are shown as dashed lines. For clarity, all H atoms except those that participate in hydrogen bonding were omitted.

Tris(*N*-methylsalicylaldiminato-κ^2N,O)chromium(III)

Crystal data

$[Cr(C_8H_8NO)_3]$
$M_r = 454.46$
Monoclinic, $P2_1/c$
$a = 7.7463$ (2) Å
$b = 25.4402$ (8) Å
$c = 11.1421$ (3) Å
$\beta = 102.659$ (2)°
$V = 2142.37$ (11) Å^3
$Z = 4$
$F(000) = 948$
$D_x = 1.409$ Mg m^{-3}
Mo $K\alpha$ radiation, $\lambda = 0.71073$ Å
Cell parameters from 25422 reflections
$\theta = 1.6$–27.0°
$\mu = 0.56$ mm^{-1}
$T = 170$ K
Block, red
0.28 × 0.2 × 0.06 mm

Data collection

Stoe IPDS-1 diffractometer
Radiation source: fine-focus sealed tube
phi–scans
Absorption correction: numerical (*X-SHAPE* and *X-RED32*; Stoe, 2008)
$T_{min} = 0.841$, $T_{max} = 0.972$
25422 measured reflections
4665 independent reflections
3991 reflections with $I > 2\sigma(I)$
$R_{int} = 0.030$
$\theta_{max} = 27.0°$, $\theta_{min} = 1.6°$
$h = -9\rightarrow9$
$k = -32\rightarrow32$
$l = -14\rightarrow14$

Refinement

Refinement on F^2
Least-squares matrix: full
$R[F^2 > 2\sigma(F^2)] = 0.033$
$wR(F^2) = 0.092$
$S = 1.07$
4665 reflections

283 parameters	$w = 1/[\sigma^2(F_o^2) + (0.0557P)^2 + 0.4287P]$ where $P = (F_o^2 + 2F_c^2)/3$
0 restraints	$(\Delta/\sigma)_{max} < 0.001$
Hydrogen site location: inferred from neighbouring sites	$\Delta\rho_{max} = 0.32$ e Å^{-3}
H-atom parameters constrained	$\Delta\rho_{min} = -0.41$ e Å^{-3}

Special details

Geometry. All esds (except the esd in the dihedral angle between two l.s. planes) are estimated using the full covariance matrix. The cell esds are taken into account individually in the estimation of esds in distances, angles and torsion angles; correlations between esds in cell parameters are only used when they are defined by crystal symmetry. An approximate (isotropic) treatment of cell esds is used for estimating esds involving l.s. planes.

Fractional atomic coordinates and isotropic or equivalent isotropic displacement parameters (Å²)

	x	*y*	*z*	U_{iso}*/U_{eq}
Cr1	0.61749 (3)	0.34539 (2)	0.42884 (2)	0.02599 (9)
C1	0.7885 (2)	0.43007 (6)	0.59566 (15)	0.0326 (3)
C2	0.6253 (2)	0.45158 (6)	0.61013 (15)	0.0329 (3)
C3	0.6253 (3)	0.49641 (7)	0.68446 (16)	0.0392 (4)
H3	0.5156	0.5110	0.6925	0.047*
C4	0.7796 (3)	0.51944 (7)	0.74539 (18)	0.0455 (4)
H4	0.7771	0.5493	0.7962	0.055*
C5	0.9405 (3)	0.49834 (8)	0.73162 (19)	0.0468 (5)
H5	1.0482	0.5142	0.7730	0.056*
C6	0.9450 (3)	0.45480 (7)	0.65863 (18)	0.0415 (4)
H6	1.0561	0.4412	0.6506	0.050*
O1	0.80043 (15)	0.38808 (5)	0.52894 (11)	0.0343 (3)
C7	0.4555 (2)	0.42962 (7)	0.55375 (15)	0.0334 (3)
H7	0.3547	0.4475	0.5688	0.040*
N1	0.42562 (18)	0.38859 (5)	0.48548 (12)	0.0302 (3)
C8	0.2410 (2)	0.37274 (8)	0.43983 (18)	0.0387 (4)
H8A	0.1627	0.3983	0.4667	0.058*
H8B	0.2221	0.3379	0.4725	0.058*
H8C	0.2147	0.3714	0.3498	0.058*
C11	0.38538 (19)	0.25243 (6)	0.34655 (14)	0.0281 (3)
C12	0.4286 (2)	0.22699 (6)	0.46229 (15)	0.0302 (3)
C13	0.3594 (2)	0.17682 (7)	0.47646 (18)	0.0385 (4)
H13	0.3867	0.1605	0.5550	0.046*
C14	0.2529 (3)	0.15077 (7)	0.3791 (2)	0.0438 (4)
H14	0.2106	0.1164	0.3894	0.053*
C15	0.2085 (2)	0.17586 (7)	0.26552 (18)	0.0388 (4)
H15	0.1346	0.1584	0.1979	0.047*
C16	0.2704 (2)	0.22570 (7)	0.24959 (15)	0.0328 (3)
H16	0.2349	0.2424	0.1718	0.039*
O11	0.44612 (14)	0.29877 (4)	0.32539 (10)	0.0301 (2)
C17	0.5348 (2)	0.25136 (6)	0.57088 (14)	0.0294 (3)
H17	0.5476	0.2324	0.6458	0.035*
N11	0.61359 (17)	0.29600 (5)	0.57646 (12)	0.0287 (3)
C18	0.6981 (2)	0.31436 (7)	0.70060 (15)	0.0362 (4)

H18A	0.6770	0.2888	0.7616	0.054*
H18B	0.6480	0.3484	0.7160	0.054*
H18C	0.8258	0.3181	0.7070	0.054*
C21	0.6776 (2)	0.39336 (6)	0.19948 (15)	0.0305 (3)
C22	0.8195 (2)	0.35940 (6)	0.19177 (15)	0.0317 (3)
C23	0.9048 (3)	0.36486 (8)	0.09236 (17)	0.0408 (4)
H23	1.0024	0.3428	0.0888	0.049*
C24	0.8505 (3)	0.40106 (8)	0.00151 (18)	0.0493 (5)
H24	0.9083	0.4038	−0.0651	0.059*
C25	0.7087 (3)	0.43397 (8)	0.00799 (17)	0.0470 (5)
H25	0.6700	0.4592	−0.0550	0.056*
C26	0.6242 (3)	0.43040 (7)	0.10408 (16)	0.0384 (4)
H26	0.5281	0.4533	0.1064	0.046*
O21	0.59264 (15)	0.39170 (5)	0.28869 (11)	0.0342 (3)
C27	0.8836 (2)	0.31882 (6)	0.28005 (15)	0.0302 (3)
H27	0.9814	0.2989	0.2667	0.036*
N21	0.82298 (17)	0.30641 (5)	0.37540 (12)	0.0283 (3)
C28	0.9138 (2)	0.26427 (7)	0.45369 (15)	0.0351 (4)
H28A	1.0136	0.2516	0.4207	0.053*
H28B	0.8311	0.2353	0.4556	0.053*
H28C	0.9577	0.2777	0.5373	0.053*

Atomic displacement parameters (Å²)

	U^{11}	U^{22}	U^{33}	U^{12}	U^{13}	U^{23}
Cr1	0.02573 (14)	0.02790 (14)	0.02495 (14)	−0.00027 (9)	0.00689 (10)	−0.00001 (9)
C1	0.0375 (9)	0.0301 (8)	0.0303 (8)	−0.0046 (7)	0.0078 (7)	−0.0021 (6)
C2	0.0394 (9)	0.0311 (8)	0.0289 (8)	0.0008 (7)	0.0093 (7)	0.0010 (6)
C3	0.0511 (11)	0.0333 (9)	0.0344 (9)	0.0033 (8)	0.0121 (8)	−0.0010 (7)
C4	0.0645 (13)	0.0341 (9)	0.0382 (10)	−0.0060 (9)	0.0122 (9)	−0.0060 (7)
C5	0.0529 (11)	0.0411 (10)	0.0443 (10)	−0.0143 (9)	0.0062 (9)	−0.0079 (8)
C6	0.0386 (9)	0.0411 (10)	0.0449 (10)	−0.0073 (8)	0.0096 (8)	−0.0057 (8)
O1	0.0300 (6)	0.0348 (6)	0.0388 (6)	−0.0032 (5)	0.0096 (5)	−0.0074 (5)
C7	0.0347 (8)	0.0357 (9)	0.0321 (8)	0.0048 (7)	0.0122 (7)	0.0004 (7)
N1	0.0282 (7)	0.0336 (7)	0.0301 (7)	0.0001 (5)	0.0090 (5)	0.0017 (5)
C8	0.0268 (8)	0.0446 (10)	0.0448 (10)	−0.0004 (7)	0.0086 (7)	−0.0032 (8)
C11	0.0244 (7)	0.0308 (8)	0.0296 (8)	0.0010 (6)	0.0072 (6)	−0.0019 (6)
C12	0.0252 (7)	0.0328 (8)	0.0327 (8)	0.0007 (6)	0.0064 (6)	0.0007 (6)
C13	0.0360 (9)	0.0347 (9)	0.0439 (10)	−0.0008 (7)	0.0067 (7)	0.0060 (7)
C14	0.0397 (10)	0.0343 (9)	0.0565 (12)	−0.0079 (7)	0.0083 (9)	−0.0014 (8)
C15	0.0304 (8)	0.0398 (9)	0.0454 (10)	−0.0040 (7)	0.0068 (7)	−0.0102 (8)
C16	0.0269 (7)	0.0397 (9)	0.0315 (8)	−0.0003 (6)	0.0056 (6)	−0.0051 (7)
O11	0.0322 (6)	0.0318 (6)	0.0257 (5)	−0.0021 (4)	0.0049 (4)	0.0007 (4)
C17	0.0271 (7)	0.0338 (8)	0.0275 (7)	0.0038 (6)	0.0064 (6)	0.0058 (6)
N11	0.0270 (6)	0.0348 (7)	0.0240 (6)	0.0011 (5)	0.0046 (5)	0.0017 (5)
C18	0.0379 (9)	0.0432 (9)	0.0253 (8)	−0.0029 (7)	0.0021 (7)	0.0011 (7)
C21	0.0331 (8)	0.0304 (8)	0.0288 (8)	−0.0057 (6)	0.0086 (6)	−0.0009 (6)
C22	0.0324 (8)	0.0331 (8)	0.0305 (8)	−0.0056 (6)	0.0089 (7)	−0.0035 (6)

C23	0.0446 (10)	0.0431 (10)	0.0393 (10)	−0.0030 (8)	0.0192 (8)	−0.0038 (8)
C24	0.0616 (13)	0.0546 (12)	0.0380 (10)	−0.0041 (10)	0.0247 (9)	0.0027 (9)
C25	0.0630 (13)	0.0457 (11)	0.0337 (9)	−0.0023 (9)	0.0136 (9)	0.0093 (8)
C26	0.0440 (10)	0.0356 (9)	0.0359 (9)	−0.0003 (7)	0.0098 (7)	0.0050 (7)
O21	0.0364 (6)	0.0345 (6)	0.0348 (6)	0.0048 (5)	0.0145 (5)	0.0061 (5)
C27	0.0254 (7)	0.0330 (8)	0.0328 (8)	−0.0017 (6)	0.0076 (6)	−0.0063 (6)
N21	0.0261 (6)	0.0286 (6)	0.0298 (7)	0.0003 (5)	0.0050 (5)	−0.0026 (5)
C28	0.0330 (8)	0.0376 (9)	0.0338 (8)	0.0077 (7)	0.0052 (7)	0.0013 (7)

Geometric parameters (Å, º)

Cr1—O21	1.9318 (11)	C13—H13	0.9500
Cr1—O1	1.9337 (12)	C14—C15	1.391 (3)
Cr1—O11	1.9563 (11)	C14—H14	0.9500
Cr1—N1	2.0557 (13)	C15—C16	1.381 (3)
Cr1—N21	2.0705 (13)	C15—H15	0.9500
Cr1—N11	2.0752 (13)	C16—H16	0.9500
C1—O1	1.316 (2)	C17—N11	1.285 (2)
C1—C6	1.409 (2)	C17—H17	0.9500
C1—C2	1.419 (2)	N11—C18	1.471 (2)
C2—C3	1.410 (2)	C18—H18A	0.9800
C2—C7	1.440 (2)	C18—H18B	0.9800
C3—C4	1.370 (3)	C18—H18C	0.9800
C3—H3	0.9500	C21—O21	1.3077 (19)
C4—C5	1.396 (3)	C21—C26	1.413 (2)
C4—H4	0.9500	C21—C22	1.415 (2)
C5—C6	1.379 (3)	C22—C23	1.415 (2)
C5—H5	0.9500	C22—C27	1.437 (2)
C6—H6	0.9500	C23—C24	1.365 (3)
C7—N1	1.282 (2)	C23—H23	0.9500
C7—H7	0.9500	C24—C25	1.395 (3)
N1—C8	1.465 (2)	C24—H24	0.9500
C8—H8A	0.9800	C25—C26	1.375 (3)
C8—H8B	0.9800	C25—H25	0.9500
C8—H8C	0.9800	C26—H26	0.9500
C11—O11	1.3098 (19)	C27—N21	1.291 (2)
C11—C16	1.415 (2)	C27—H27	0.9500
C11—C12	1.416 (2)	N21—C28	1.462 (2)
C12—C13	1.407 (2)	C28—H28A	0.9800
C12—C17	1.445 (2)	C28—H28B	0.9800
C13—C14	1.380 (3)	C28—H28C	0.9800
O21—Cr1—O1	93.11 (5)	C12—C13—H13	119.2
O21—Cr1—O11	87.64 (5)	C13—C14—C15	118.72 (17)
O1—Cr1—O11	175.79 (5)	C13—C14—H14	120.6
O21—Cr1—N1	88.36 (5)	C15—C14—H14	120.6
O1—Cr1—N1	90.60 (5)	C16—C15—C14	120.98 (16)
O11—Cr1—N1	93.56 (5)	C16—C15—H15	119.5

O21—Cr1—N21	90.36 (5)	C14—C15—H15	119.5
O1—Cr1—N21	85.55 (5)	C15—C16—C11	121.43 (16)
O11—Cr1—N21	90.31 (5)	C15—C16—H16	119.3
N1—Cr1—N21	175.87 (5)	C11—C16—H16	119.3
O21—Cr1—N11	173.59 (5)	C11—O11—Cr1	131.59 (10)
O1—Cr1—N11	91.09 (5)	N11—C17—C12	126.65 (14)
O11—Cr1—N11	88.52 (5)	N11—C17—H17	116.7
N1—Cr1—N11	86.75 (5)	C12—C17—H17	116.7
N21—Cr1—N11	94.80 (5)	C17—N11—C18	115.80 (13)
O1—C1—C6	118.97 (16)	C17—N11—Cr1	125.89 (11)
O1—C1—C2	123.49 (15)	C18—N11—Cr1	118.19 (10)
C6—C1—C2	117.53 (15)	N11—C18—H18A	109.5
C3—C2—C1	119.56 (16)	N11—C18—H18B	109.5
C3—C2—C7	116.92 (16)	H18A—C18—H18B	109.5
C1—C2—C7	123.51 (15)	N11—C18—H18C	109.5
C4—C3—C2	121.68 (18)	H18A—C18—H18C	109.5
C4—C3—H3	119.2	H18B—C18—H18C	109.5
C2—C3—H3	119.2	O21—C21—C26	118.70 (15)
C3—C4—C5	118.94 (17)	O21—C21—C22	123.61 (15)
C3—C4—H4	120.5	C26—C21—C22	117.69 (15)
C5—C4—H4	120.5	C21—C22—C23	119.31 (16)
C6—C5—C4	120.81 (18)	C21—C22—C27	123.58 (14)
C6—C5—H5	119.6	C23—C22—C27	117.11 (16)
C4—C5—H5	119.6	C24—C23—C22	121.71 (18)
C5—C6—C1	121.47 (18)	C24—C23—H23	119.1
C5—C6—H6	119.3	C22—C23—H23	119.1
C1—C6—H6	119.3	C23—C24—C25	118.99 (17)
C1—O1—Cr1	130.42 (11)	C23—C24—H24	120.5
N1—C7—C2	127.12 (15)	C25—C24—H24	120.5
N1—C7—H7	116.4	C26—C25—C24	121.00 (18)
C2—C7—H7	116.4	C26—C25—H25	119.5
C7—N1—C8	117.74 (14)	C24—C25—H25	119.5
C7—N1—Cr1	124.64 (11)	C25—C26—C21	121.27 (17)
C8—N1—Cr1	117.55 (11)	C25—C26—H26	119.4
N1—C8—H8A	109.5	C21—C26—H26	119.4
N1—C8—H8B	109.5	C21—O21—Cr1	131.04 (11)
H8A—C8—H8B	109.5	N21—C27—C22	127.26 (15)
N1—C8—H8C	109.5	N21—C27—H27	116.4
H8A—C8—H8C	109.5	C22—C27—H27	116.4
H8B—C8—H8C	109.5	C27—N21—C28	117.13 (14)
O11—C11—C16	119.08 (14)	C27—N21—Cr1	124.09 (11)
O11—C11—C12	123.55 (14)	C28—N21—Cr1	118.66 (10)
C16—C11—C12	117.36 (15)	N21—C28—H28A	109.5
C13—C12—C11	119.80 (15)	N21—C28—H28B	109.5
C13—C12—C17	117.14 (15)	H28A—C28—H28B	109.5
C11—C12—C17	122.97 (15)	N21—C28—H28C	109.5
C14—C13—C12	121.63 (17)	H28A—C28—H28C	109.5
C14—C13—H13	119.2	H28B—C28—H28C	109.5

Hydrogen-bond geometry (Å, º)

D—H···*A*	*D*—H	H···*A*	*D*···*A*	*D*—H···*A*
C17—H17···O11^{i}	0.95	2.44	3.3154 (19)	154

Symmetry code: (i) *x*, −*y*+1/2, *z*+1/2.

6. Danksagung

Wie wäre eine solche Arbeit ohne tatkräftige Unterstützung möglich? Im Folgenden möchte ich den Personen danken die mich, sei es aktiv oder passiv, in den letzten Jahren unterstützt und letztendlich diese Arbeit möglich gemacht haben.

Ins besondere möchte ich mich bei Herrn Prof. Dr. Bensch für die Bereitstellung des interessanten Themas und seine Unterstützung bei wissenschaftlichen Fragestellungen sowie Anregungen und Diskussionen danken. Bei Herrn Prof. Dr. Näther bedanke ich mich für die vielen Einkristallstrukturlösungen und ebenfalls für zahlreiche Diskussionen und Anregungen. Ein besonderer Dank gilt an dieser Stelle natürlich auch Frau Inke Jess, ohne deren geschulter Blick für „den richtigen Kristall“ diese Messungen für die Einkristallstrukturlösungen oft gar nicht erst möglich gewesen wären. Bedanken möchte ich mich zudem bei den Mitarbeiterinnen der Spektroskopie (Uschi Cornelissen, Stefanie Pehlke und Jaqueline Pick) für die Aufnahme zahlreicher IR-, Raman- und UV/vis-Spektren sowie die Durchführung von sehr vielen CHNS Messungen. Und natürlich danke ich allen weiteren MitarbeiterInnen des Instituts deren Hilfe ich in den letzten Jahren in Anspruch genommen haben und die hier nicht namentlich aufgeführt wurden.

Sich auszutauschen unter „Gleichgesinnten“ gehört natürlich auch zum wissenschaftlichen Arbeiten: Für zahlreiche hilfreiche Diskussionen (größtenteils fachbezogen :P) möchten ich den „Solvos“ - alteingesessen wie neudazugekommen - danken. Ein besonderer Dank gilt Nicole Pienack, ohne die ich wohl nicht zu diesem Thema gekommen wäre und von der ich sehr viel lernen durfte.

Studenten und Kollegen - ohne sie wären die letzten Jahre mit Sicherheit weitaus langweiliger gewesen. Des Weiteren möchte ich daher dem gesamten Arbeitskreis für die angenehme Atmosphäre, sowie hilfreiche Anregungen und Austausch danken. Danken möchte ich zudem auch den Studenten, die meine Arbeit durch Praktika oder Bachelorarbeiten unterstützt haben.

Ein Assistent im ersten Semester sagte zu Anfang: “Die Leute, mit denen ihr zu Anfang in einem Labor zusammenarbeitet, werden euch durchs ganze Studium begleiten und sehr wahrscheinlich darüber hinaus.“ Teilweise hatte er Recht: Innerhalb der ersten zwei Semester hat sich eine Truppe gefunden, die es bis zum Ende geschafft hat. Danke an Carolin, Joanna, Melanie, Anne, Gernot, Claudia und Kim für die schöne Zeit.

Natürlich hat auch die Familie einen entscheidenden Beitrag geleistet. Einfach dadurch, dass sie alle für mich da waren. Vielen Dank dafür.

7. Eidesstattliche Erklärung

Hiermit versichere ich an Eides statt, dass ich die vorliegende Arbeit selbstständig (abgesehen von der Beratung durch meine wissenschaftlichen Lehrer) und nur unter Verwendung der angegebenen Hilfsmittel angefertigt habe. Des Weiteren versichere ich, das die Arbeit unter Einhaltung der Regeln guter wissenschaftlicher Praxis der Deutschen Forschungsgemeinschaft entstanden ist.

Die Dissertation wird ausschließlich an dieser Stelle zur Promotion vorgelegt.

Zusätzlich erkläre ich, dass ich noch keinen Promotionsversuch, weder an dieser noch an einer anderen Hochschule, unternommen habe.

---------- ----------

Kiel, 2016 Jessica Hilbert

8. Literaturverzeichnis

[1] R. L. Bedard, S. T. Wilson, L. D. Vail, J. M. Bennett and E. M. Flaningen, *Studies in Surface Science and Catalysis* **1989**, *49*, 375–387.

[2] B. Krebs, *Angew. Chem. Int. Ed. Engl.* **1983**, *95*, 113–134.

[3] J. B. Parise and Y. Ko, *Chem. Mater.* **1994**, *6*, 718–720.

[4] K. L. Geisinger and G. V. Gibbs, *Phys. Chem. Mineral.* **1981**, *7*, 204–210.

[5] G. V. Gibbs, *Am. Mineral.* **1982**, *67*, 421–450.

[6] W. S. Sheldrick and M. Wachhold, *Coord. Chem. Rev.* **1998**, *176*, 211–322.

[7] W. S. Sheldrick, *J. Chem. Soc., Dalton Trans.* **2000**, 3041–3052.

[8] A. Rabenau, *Angew. Chem.* **1985**, *97*, 1017–1032.

[9] A. K. Cheetham, G. Férey and T. Loiseau, *Angew. Chem.* **1999**, *111*, 3466–3492.

[10] X. Bu, N. Zheng and P. Feng, *Chem. Eur. J.* **2004**, *10*, 3356–3362.

[11] S. Dehnen and M. Melullis, *Coord. Chem. Rev.* **2007**, *251*, 1259–1280.

[12] J. Zhou, J. Dai, G.-Q. Bian and C.-Y. Li, *Coord. Chem. Rev.* **2009**, *253*, 1221–1247.

[13] B. Seidlhofer, N. Pienack and W. Bensch, *Z. Naturforsch.* **2010**, *65b*, 937–975.

[14] W.-W. Xiong, G. Zhang and Q. Zhang, *Inorg. Chem. Front.* **2014**, *1*, 292–301.

[15] S. Santner, J. Heine and S. Dehnen, *Angew. Chem. Int. Ed. Engl.* **2016**, *55*, 876–893.

[16] P. Feng, X. Bu and N. Zheng, *Acc. chem. res.* **2005**, *38*, 293–303.

[17] W. S. Sheldrick and M. Wachhold, *Angew. Chem.* **1997**, *109*, 214–234.

[18] G. Demazeau, *J. Mater. Sci.* **2008**, *43*, 2104–2114.

[19] G. Demazeau and A. Largeteau, *Z. Anorg. Allg. Chem.* **2015**, *641*, 159–163.

[20] J. B. Parise, Y. Ko, J. Rijssenbeek, D. M. Nellis, K. Tan and S. Koch, *J. Chem. Soc., Chem. Commun.* **1994**, 527.

[21] M.-L. Feng, D. Sarma, X. Qi, K.-Z. Du, X.-Y. Huang and M. G. Kanatzidis, *J. Am. Chem. Soc.* **2016**.

[22] T. Jiang, A. Lough and G. A. Ozin, *Adv. Mater.* **1998**, *10*, 42–46.

[23] N. Zheng, X. Bu, H. Vu and P. Feng, *Angew. Chem. Int. Ed. Engl.* **2005**, *44*, 5299–5303.

[24] X. Wang, T.-L. Sheng, S.-C. Xiang, S.-M. Hu, R.-B. Fu and X.-T. Wu, *Chinese J. Struct. Chem.* **2010**, *29*, 260–264.

[25] T. Jiang, A. Lough, G. A. Ozin, R. L. Bedard and R. Broach, *J. Mater. Chem.* **1998**, *8*, 721–732.

[26] Y. Ko, C. L. Cahill and J. B. Parise, *J. Chem. Soc., Chem. Commun.* **1994**, 69–70.

[27] Y. Ko, K. Tan, D. M. Nellis, S. Koch and J. B. Parise, *J. Solid State Chem.* **1995**, *114*, 506–511.

[28] P. Nørby, E. Eikeland, J. Overgaard, S. Johnsen and B. B. Iversen, *CrystEngComm* **2015**, *17*, 2413–2420.

[29] K. Tsamourtzi, J.-H. Song, T. Bakas, A. J. Freeman, P. N. Trikalitis and M. G. Kanatzidis, *Inorg. Chem.* **2008**, *47*, 11920–11929.

[30] M. Jansen and J. C. Schön, *Angew. Chem. Int. Ed. Engl.* **2006**, *45*, 3406–3412.

[31] X.-H. Qi, K.-Z. Du, M.-L. Feng, J.-R. Li, C.-F. Du, B. Zhang and X.-Y. Huang, *J. Mater. Chem. A* **2015**, *3*, 5665–5673.

[32] P. Enzel, G. S. Henderson, G. A. Ozin and R. L. Bedard, *Adv. Mater.* **1995**, *7*, 64–68.

[33] J. P. Yohannan and K. Vidyasagar, *J. Solid State Chem.* **2015**, *221*, 426–432.

[34] X.-M. Gu, J. Dai, D.-X. Jia, Y. Zhang and Q.-Y. Zhu, *Cryst. Growth Des.* **2005**, *5*, 1845–1848.
[35] Z. Wang, G. Xu, Y. Bi and C. Wang, *CrystEngComm* **2010**, *12*, 3703–3707.
[36] J. Zhou, G.-Q. Bian, J. Dai, Y. Zhang, A.-B. Tang and Q.-Y. Zhu, *Inorg. Chem.* **2007**, *46*, 1541–1543.
[37] G.-N. Liu, G.-C. Guo, F. Chen, S.-P. Guo, X.-M. Jiang, C. Yang, M.-S. Wang, M.-F. Wu and J.-S. Huang, *CrystEngComm* **2010**, *12*, 4035–4037.
[38] J. Hilbert, C. Näther and W. Bensch, *Inorg. Chem.* **2014**, *53*, 5619–5630.
[39] C.-Y. Yue, X.-W. Lei, L. Yin, X.-R. Zhai, Z.-R. Ba, Y.-Q. Niu and Y.-P. Li, *CrystEngComm* **2015**, *17*, 814–823.
[40] Zhang, Hui-Ping, Lei, Xiao-Wu, *Chin. J. Inorg. Chem.* **2014**, *30*, 1–7.
[41] N. Pienack, D. Schinkel, A. Puls, M.-E. Ordolff, H. Lühmann, C. Näther and W. Bensch, *Z. Naturforsch.* **2012**, *67b*, 1098–1106.
[42] N. Pienack, C. Näther and W. Bensch, *Eur. J. Inorg. Chem.* **2009**, 1575–1577.
[43] N. Pienack, H. Lühmann, B. Seidlhofer, J. Ammermann, C. Zeisler, F. Danker, C. Näther and W. Bensch, *Solid State Sci.* **2014**, *33*, 67–72.
[44] N. Pienack, C. Näther and W. Bensch, *Z. Naturforsch.* **2008**, *63b*, 1243–1251.
[45] J. Hilbert, N. Pienack, H. Lühmann, C. Näther and W. Bensch, *Z. Anorg. Allg. Chem.* **2016**, *accepted 24.10.16*.
[46] D.-X. Jia, Y. Zhang, J. Dai, Q.-Y. Zhu and X.-M. Gu, *Z. Anorg. Allg. Chem.* **2004**, *630*, 313–318.
[47] M.-L. Fu, G.-C. Guo, Liu, Bing, Wu, A-Qing and J.-S. Huang, *Chin. J. Inorg. Chem.* **2005**, *21*, 25–29.
[48] N. Pienack, S. Lehmann, H. Lühmann, M. El-Madani, C. Näther and W. Bensch, *Z. Anorg. Allg. Chem.* **2008**, *634*, 2323–2329.
[49] J. Hilbert, C. Näther and W. Bensch, *Z. Anorg. Allg. Chem.* **2014**, *640*, 2858–2863.
[50] M. Behrens, S. Scherb, C. Näther and W. Bensch, *Z. Anorg. Allg. Chem.* **2003**, *629*, 1367–1373.
[51] C. Zeisler, C. Näther and W. Bensch, *CrystEngComm* **2013**, *15*, 8874–8876.
[52] P. Polzin, *Masterarbeit* **2016**.
[53] J. Zhou, X. Liu, G.-Q. Chen, F. Zhang and L.-R. Li, *Z. Naturforsch.* **2010**, *65b*, 1229–1234.
[54] J. Hilbert, C. Näther, R. Weihrich and W. Bensch, *Inorg. Chem.* **2016**, *55*, 7859–7865.
[55] J. Hilbert, C. Näther and W. Bensch, *Dalton Trans.* **2015**, *44*, 11542–11550.
[56] A. Benkada, *Masterarbeit* **2016**.
[57] J. Hilbert, C. Näther and W. Bensch, *Current Inorg. Chem.* **2016**, *submitted 10.10.16*.
[58] D.-X. Jia, J. Dai, Q.-Y. Zhu, Y. Zhang and X.-M. Gu, *Polyhedron* **2004**, *23*, 937–942.
[59] J. Hilbert, C. Näther and W. Bensch, *Inorg. Chim. Acta* **2016**, *submitted 03.11.16*.
[60] J. Hilbert, D. Schinkel, C. Näther and W. Bensch, *to be published*.
[61] N. Pienack, K. Möller, C. Näther and W. Bensch, *Solid State Sci.* **2007**, *9*, 1110–1114.
[62] A. Puls, C. Näther and W. Bensch, *Z. Anorg. Allg. Chem.* **2006**, *632*, 1239–1243.
[63] M. Schaefer, D. Kurowski, A. Pfitzner, C. Näther, Z. Rejai, K. Möller, N. Ziegler and W. Bensch, *Inorg. Chem.* **2006**, *45*, 3726–3731.
[64] W. Bensch and M. Schur, *Eur. J. Solid State Inorg. Chem.* **1996**, *33*, 1149–1160.

[65] H. Irving and R. J. Williams, *J. Chem. Soc.* **1953**, 3192–3210.
[66] H. Irving and J. Mellor, *J. Chem. Soc.* **1962**, 5222–5237.
[67] G. Anderegg, *Helv. Chim. Acta* **1971**, *54*, 509–512.
[68] C. N. Reilley and J. H. Holloway, *J. Am. Chem. Soc.* **1958**, *80*, 2917–2919.
[69] G. A. Carlson, J. P. McReynolds and F. H. Verhoek, *J. Am. Chem. Soc.* **1945**, *67*, 1334–1339.
[70] G. Schwarzenbach and R. Baur, *Helv. Chim. Acta* **1956**, *86*, 722–728.
[71] A. Evers and R. D. Hancock, *Inorg. Chim. Acta* **1989**, *160*, 245–248.
[72] N. Pienack, C. Näther and W. Bensch, *Solid State Sci.* **2007**, *9*, 100–107.
[73] N. Pienack and W. Bensch, *Z. Anorg. Allg. Chem.* **2006**, *632*, 1733–1736.
[74] N. Pienack, C. Näther and W. Bensch, *Eur. J. Inorg. Chem.* **2009**, 937–946.
[75] N. Pienack, A. Puls, C. Näther and W. Bensch, *Inorg. Chem.* **2008**, *47*, 9606–9611.
[76] M. Behrens, M.-E. Ordolff, C. Näther, W. Bensch, K.-D. Becker, C. Guillot-Deudon, A. Lafond and J. A. Cody, *Inorg. Chem.* **2010**, *49*, 8305–8309.
[77] T. Jiang, A. Lough, G. A. Ozin and R. L. Bedard, *J. Mater. Chem.* **1998**, *8*, 733–741.
[78] C. Anderer, N. Delwa de Alarcón, C. Näther and W. Bensch, *Chem. Eur. J.* **2014**, *20*, 16953–16959.
[79] C. Anderer, C. Näther and W. Bensch, *Cryst. Growth Des.* **2016**.
[80] C. Anderer, C. Näther and W. Bensch, *Z. Naturforsch.* **2016**, *71b*, 395–401.
[81] Y.-H. Chi, J.-M. Shi, H.-N. Li, W. Wei, E. Cottrill, N. Pan, H. Chen, Y. Liang, L. Yu, Y.-Q. Zhang and C. Hou, *Dalton Trans.* **2013**, *42*, 15559–15569.
[82] S. Grimme, *Angew. Chem. Int. Ed. Engl.* **2008**, *47*, 3430–3434.
[83] C. A. Hunter, K. R. Lawson, J. Perkins and C. J. Urch, *J. Chem. Soc., Perkin Trans. 2* **2001**, 651–669.
[84] C. R. Martinez and B. L. Iverson, *Chem. Sci.* **2012**, *3*, 2191–2201.
[85] M. Schur, A. Gruhl, C. Näther, I. Jeß and W. Bensch, *Z. Naturforsch.* **1999**, *B54*.
[86] J. Li, B. Marler, H. Kessler, M. Soulard and S. Kallus, *Inorg. Chem.* **1997**, *36*, 4697–4701.
[87] J. W. Mullin, *Crystallization*, Butterworth-Heinemann, Oxford, Boston, 4th edn. **2001**.
[88] B. Krebs, S. Pohl and W. Schiwy, *Angew. Chem. Int. Ed. Engl.* **1970**, *9*, 897–898.
[89] A. Marzotto, D. A. Clemente and V. Giovanni, *Acta Cryst.* **1993**, *C49*, 1252–1255.
[90] F. Basolo, ed., *Inorganic Syntheses*, John Wiley & Sons, Inc, Hoboken, NJ, USA **1976**.
[91] E. K. Barefield, F. Wagner, A. W. Herlinger, A. R. Dahl and S. Holt, in *Inorganic Syntheses*, ed. F. Basolo, John Wiley & Sons, Inc, Hoboken, NJ, USA **1976**, vol. 16, pp. 220–225.
[92] Y. Oh, S. Bag, C. D. Malliakas and M. G. Kanatzidis, *Chem. Mater.* **2011**, *23*, 2447–2456.
[93] C. Ruiz-Pérez, Lorenzo Luis, Pablo A, F. Lloret and M. Julve, *Inorg. Chim. Acta* **2002**, *336*, 131–136.
[94] W. Schiwy and B. Krebs, *Angew. Chem.* **1975**, *87*, 451–452.
[95] T. Kaib, M. Kapitein and S. Dehnen, *Z. anorg. allg. Chem.* **2011**, *637*, 1683–1686.
[96] F. A. Cotton and F. E. Harris, *J. Phys. Chem.* **1955**, *59*, 1203–1208.
[97] H. A. Laitinen, E. I. Onstott, J. C. Bailar and S. Swann, *J. Am. Chem. Soc.* **1945**, *67*, 1334–1339.
[98] H. B. Jonassen and Schaafsma, Westerman, L., *J. Phys. Chem.* **1958**, *62*, 1022–1024.

[99] K. M. Mackay, R. A. Mackay and W. Henderson, *Introduction to modern inorganic chemistry*, Nelson Thornes, Cheltenham, 6th edn. **2002**.
[100] T. J. Hubin, J. M. McCormick, S. R. Collinson, M. Buchalova, C. M. Perkins, N. W. Alcock, P. K. Kahol, A. Raghunathan and D. H. Busch, *Journal of the American Chemical Society* **2000**, *122*, 2512–2522.
[101] R. M. Kierat, *Dissertation*, Rubrechts-Karls-Universität Heidelberg **2008**.
[102] F. Sêby, M. Point-Gautier, E. Giffaut and O. F. Donard, *Geochim. Cosmochim. Acta* **2001**, *65*, 3041–3053.
[103] D. M. Sherman, K. V. Ragnarsdottir, E. H. Oelkers and C. R. Collins, *Chem. Geol.* **2000**, *167*, 169–176.
[104] E. Riedel, *Anorganische Chemie*, de Gruyter, Berlin, New York, 4th edn. **1999**.
[105] A. F. Holleman, E. Wiberg and N. Wiberg, *Lehrbuch der anorganischen Chemie*, de Gruyter, Berlin, New York, 102nd edn. **2007**.
[106] J. Strähle and E. Schweda, *Lehrbuch der analytischen und präparativen anorganischen Chemie*, S. Hirzel, Stuttgart, 14th edn. **1995**.
[107] L. Infantes, J. Chisholm and S. Motherwell, *CrystEngComm* **2003**, *5*, 480.
[108] L. Infantes and S. Motherwell, *CrystEngComm* **2002**, *4*, 454.
[109] R. P. Sharma, A. Singh, P. Venugopalan, P. Brandão and V. Félix, *Polyhedron* **2012**, *40*, 175–184.
[110] A. Marzotto, A. Ciccarese, D. A. Clemente and G. Valle, *J. Chem. Soc., Dalton Trans.* **1995**, 1461–1468.
[111] K. Krishnan and R. A. Plane, *Inorg. Chem.* **1966**, *5*, 852–857.
[112] G. Borch, P. Klaeboe and P. H. Nielsen, *Acta Chem. Scan.* **1979**, *A33*.
[113] L. Trišč́íková, I. Potočňák, J. Chomič and T. Müller, *Thermochim. Acta* **2004**, *419*, 231–237.
[114] S. Bruda, M. M. Turnbull, C. P. Landee and Q. Xu, *Inorg Chim Acta* **2006**, *359*, 298–308.
[115] S. P. Roe, J. O. Hill and R. J. Magee, *Monatsh. Chem.* **1991**, *122*, 467–478.
[116] A. L. Ringer, M. O. Sinnokrot, R. P. Lively and C. D. Sherrill, *Chem. Eur. J.* **2006**, *12*, 3821–3828.
[117] B.-Q. Ma, H.-L. Sun and S. Gao, *Chem. Commun.* **2004**, 2220–2221.
[118] X. Li, H.-L. Sun, X.-S. Wu, X. Qiu and M. Du, *Inorg. Chem.* **2010**, *49*, 1865–1871.
[119] Niven, Margaret L., Percy, Gordon C., *Trans. Met. Chem* **1978**, *3*, 267–271.
[120] E. González, A. Rodrigue-Witchel and C. Reber, *Coord. Chem. Rev.* **2007**, *251*, 351–363.
[121] L. Galicia, I. Gonzalez, Y. Meas and J. G. Ibanez, *Electrochim. Acta* **1990**, *35*, 209–213.